

VINEYARD MID-ATLANTIC

CONSTRUCTION AND OPERATIONS PLAN VOLUME II APPENDIX

JANUARY 2025

PREPARED BY:

Epsilon
ASSOCIATES INC.

SUBMITTED BY:

VINEYARD MID-ATLANTIC LLC

VINEYARD
MID-ATLANTIC

VINEYARD  OFFSHORE

PUBLIC VERSION

Vineyard Mid-Atlantic COP

Appendix II-C Lease Area OCS-A 0544 Avian Assessment

Prepared by:
Biodiversity Research Institute

Prepared for:
Vineyard Mid-Atlantic LLC



January 2025

Revision	Date	Description
0	January 2024	Initial submission.
1	September 2024	Updated to incorporate new MDAT models (v3) and to incorporate revisions to the Project Design Envelope (PDE).
2	November 2024	Updated to incorporate revisions to the PDE.
2	January 2025	Resubmitted without revisions.

Appendix II-C

Lease Area OCS-A 0544 Avian Assessment

November 2024 (v2.0)

Prepared by:

Biodiversity Research Institute

276 Canco Road

Portland, ME 04103



Table of Contents

1	Summary	12
2	Introduction	13
2.1	Description of Vineyard Mid-Atlantic	13
2.2	Climate Change and Birds	16
2.3	Methods Overview	17
2.3.1	Onshore	17
2.3.2	Offshore	18
3	Onshore Assessment	21
3.1	Introduction	21
3.2	Methods	23
3.2.1	Assessment of Co-location with Development and Habitats	23
3.2.2	Avian Data Sources and Methods	24
3.3	Results	24
3.3.1	Co-Location with Existing Development and Habitats	24
3.3.2	Species Potentially Present in the Onshore Development Area.....	36
3.4	Summary and Conclusions	48
4	Offshore Assessment: Results	65
4.1	Regional Context	65
4.2	Non-Marine Migratory Birds	71
4.2.1	Grebes and Waterfowl	71
4.2.2	Shorebirds	73
4.2.3	Wading Birds	80
4.2.4	Raptors	84
4.2.5	Songbirds.....	92
4.3	Marine Birds	96
4.3.1	Sea Ducks	96
4.3.2	Phalaropes.....	107
4.3.3	Auks.....	113
4.3.4	Gulls, Skuas, and Jaegers	120
4.3.5	Terns.....	134
4.3.6	Loons	145
4.3.7	Shearwaters, Petrels, and Storm-Petrels.....	152
4.3.8	Gannets	160
4.3.9	Cormorants and Pelicans.....	167
4.4	Protected Species and Species of Concern	174
4.4.1	Roseate Tern, Northeastern Population (<i>Endangered</i>)	175
4.4.2	Piping Plover, Atlantic Coast Population (<i>Threatened</i>).....	181
4.4.3	Red Knot, rufa subspecies (<i>Threatened</i>).....	185
4.4.4	Black-capped Petrel (<i>Endangered</i>)	189

4.4.5	Bald Eagle (Protected by the Bald and Golden Eagle Protection Act)	195
4.5	Conclusions	196
4.6	Supplemental Information: Seasonal Densities in the Lease Area	202
5	Detailed Offshore Avian Assessment Methods	207
5.1	Exposure Framework.....	207
5.1.1	Exposure Assessment Data Sources and Coverage	207
5.1.2	NYSERDA Digital Aerial Baseline Survey of Marine Wildlife	208
5.1.3	Digital Aerial Wildlife Survey of BOEM Lease Area OCS-a 0512	208
5.1.4	MDAT Marine Bird Abundance and Occurrence Models	212
5.1.5	Supplemental Data Sources	215
5.1.6	Digital Aerial Survey Density Modeling	218
5.1.7	Exposure Mapping.....	226
5.1.8	Exposure Assessment Metrics.....	227
5.2	Vulnerability Framework	231
5.2.1	Population Vulnerability.....	232
5.2.2	Collision Vulnerability.....	235
5.2.3	Displacement Vulnerability	237
5.3	Uncertainty.....	238
6	Literature Cited.....	240
Attachment A: Maps of Exposure for Marine Birds.....		262

List of Figures

Figure 2-1: Overview of Vineyard Mid-Atlantic’s offshore and onshore facilities in Lease OCS-A 0544 and on Long Island.....	15
Figure 2-2: BRI's risk assessment process overview. An exposure and behavioral vulnerability assessment are combined using expert opinion to estimate relative risk.	20
Figure 3-1: Onshore facilities of Vineyard Mid-Atlantic, located in Queens County, Suffolk County, and Nassau County, New York.....	22
Figure 3-2: Onshore Facilities and their associated National Landcover Database habitat types.....	27
Figure 3-3: A potential landfall site in a portion of a previously disturbed area adjacent to Rockaway Beach in Queens, New York.....	28
Figure 3-4: A potential landfall site in a paved parking area near Atlantic Beach in the Town of Hempstead, New York.....	29
Figure 3-5: A potential landfall site in a paved parking area at Jones Beach State Park in the Town of Hempstead, New York.....	30
Figure 3-6: Potential POI in Uniondale, New York on Long Island.....	31
Figure 3-7: Potential Ruland Road POI and Onshore Substation Site Envelope D.	32
Figure 3-8: Onshore Substation Site Envelopes B and C.....	33
Figure 3-9: Onshore Substation Site Envelope A.....	34
Figure 3-10: Potential Eastern Queens POI in Queens, New York on Long Island.	35
Figure 3-11: Monthly average of Roseate Tern observations in the Onshore Development Area over ten years, derived from the eBird database (total detections, with duplicate list postings removed).	40
Figure 3-12: Piping Plover nesting sites on Long Island, figure replicated from NYSDEC 2018.....	42
Figure 3-13: Monthly average of Piping Plover observations in the Onshore Development Area over ten years, derived from the eBird database (total detections, with duplicate list postings removed).	43
Figure 3-14: Monthly average of Red Knot observations in the Onshore Development Area over ten years, derived from the eBird database (total detections, with duplicate list postings removed).....	44
Figure 3-15: Critical Red Knot habitat proposed by the USFWS. Proposed Critical Habitat is adjacent to or overlaps with one potential landfall site.....	45
Figure 3-16: Monthly Average of Saltmarsh Sparrows observed in the Onshore Development Area over ten years, derived from the eBird database (total detections, with duplicate list postings removed).	47
Figure 3-17: Monthly Average of Bald Eagles observed in the Onshore Development Area over ten years, derived from the eBird database (total detections, with duplicate list postings removed).....	48
Figure 4-1: All-bird abundance estimates from the MDAT models.....	67
Figure 4-2: Modeled flight paths of migratory shorebirds equipped with nanotags, based on data from Loring et al. (2021).....	77
Figure 4-3: Modeled flight paths of migratory shorebirds equipped with nanotags, based on data from Loring et al. (2021).....	78
Figure 4-4: Modeled flight paths of migratory shorebirds equipped with nanotags, based on data from Loring et al. (2021).....	79

Figure 4-5: Track lines of Great Blue Herons captured in Maine and equipped with satellite transmitters provided by Maine Department of Inland Fisheries and Wildlife.	83
Figure 4-6: Flight heights (m) of Great Blue Herons satellite-tagged in Maine, flying over the Atlantic OCS.	84
Figure 4-7: Location estimates from satellite transmitters on Merlins (n=11) tracked from three raptor research stations along the Atlantic coast, 2010–2018 (DeSorbo et al. 2018).....	89
Figure 4-8: Location estimates from satellite transmitters on Peregrine Falcons (n=33) tracked from three raptor research stations along the Atlantic coast, 2010–2018 (DeSorbo et al. 2018).	90
Figure 4-9: Dynamic Brownian bridge movement models for Osprey (n=127) that were tracked with satellite transmitters by Rob Bierregaard and detailed at www.ospreytrax.com	91
Figure 4-10: Flight heights of songbirds (n=333) derived from Northwest Atlantic Seabird Catalog, showing the number of birds of each species or grouping (and the proportion of the total for that survey) in each flight band. ..	95
Figure 4-11: Modeled APEM digital aerial surveys for sea ducks in the NY Bight survey area and Lease Area OCS-A 0544.	100
Figure 4-12: Dynamic Brownian Bridge movement models for Surf Scoter (n= 8 in winter, 87 in spring, 83 in fall) that were tracked with satellite transmitters.....	101
Figure 4-13: Dynamic Brownian Bridge movement models for Black Scoter (n=61 in winter, 76 in spring, 80 in fall) that were tracked with satellite transmitters.....	102
Figure 4-14: Dynamic Brownian Bridge movement models for White-winged Scoter (n=66 in winter, 45 in spring, 62 in fall) that were tracked with satellite transmitters.	103
Figure 4-15: Dynamic Brownian Bridge movement models for Long-tailed Duck (n=49 in winter, 60 in spring, 37 in fall) that were tracked with satellite transmitters.	104
Figure 4-16: Monthly relative densities of sea ducks in the Lease Area from digital aerial surveys.	105
Figure 4-17: Sea duck key habitat sites as defined by Sea Duck Joint Venture in relation to the Lease Area and Offshore Export Cable Corridor.....	106
Figure 4-18: Flight heights of sea ducks (n=2,225) derived from the Northwest Atlantic Seabird Catalog.....	107
Figure 4-19: Modeled APEM digital aerial surveys for phalaropes in the NY Bight survey area and Lease Area OCS-A 0544.	111
Figure 4-20: Monthly relative densities of phalaropes in the Lease Area from digital aerial surveys.	112
Figure 4-21: Flight heights of phalaropes (n=198) derived from the Northwest Atlantic Seabird Catalog.	113
Figure 4-22: Modeled APEM digital aerial surveys for auks in the NY Bight survey area and Lease Area OCS-A 0544.	117
Figure 4-23: Monthly relative densities of auks in the Lease Area from digital aerial surveys.	119
Figure 4-24: Flight heights of auks (n=923) derived from the Northwest Atlantic Seabird Catalog.	120
Figure 4-25: Modeled APEM digital aerial surveys for small gulls in the NY Bight survey area and Lease Area OCS-A 0544.	124
Figure 4-26: Modeled APEM digital aerial surveys for medium gulls in the NY Bight survey area and Lease Area OCS-A 0544.	125
Figure 4-27: Modeled APEM digital aerial surveys for large gulls in the NY Bight survey area and Lease Area OCS-A 0544.	126

Figure 4-28: Modeled APEM digital aerial surveys for all gulls in the NY Bight survey area and Lease Area OCS-A 0544.	127
Figure 4-29: Modeled APEM digital aerial surveys for skuas and jaegers in the NY Bight survey area and Lease Area OCS-A 0544.	128
Figure 4-30: Monthly relative densities of gulls, jaegers, and skuas in the Lease Area from digital aerial surveys.	130
Figure 4-31: Flight heights of small gulls ($n=499$) derived from the Northwest Atlantic Seabird Catalog.	131
Figure 4-32: Flight heights of medium gulls ($n=4,848$) derived from the Northwest Atlantic Seabird Catalog.	132
Figure 4-33: Flight heights of large gulls ($n=10,705$) derived from the Northwest Atlantic Seabird Catalog.	133
Figure 4-34: Flight heights of jaegers ($n=381$) derived from the Northwest Atlantic Seabird Catalog.	134
Figure 4-35: Modeled APEM digital aerial surveys for small terns in the NY Bight survey area and Lease Area OCS-A 0544.	139
Figure 4-36: Modeled APEM digital aerial surveys for medium terns in the NY Bight survey area and Lease Area OCS-A 0544.	140
Figure 4-37: Modeled APEM digital aerial surveys for all terns in the NY Bight survey area and Lease Area OCS-A 0544.	141
Figure 4-38: Monthly relative densities of terns in the Lease Area from digital aerial surveys.	143
Figure 4-39: Common Tern ($n=30$) track locations and density from the Loring et al. (2019) radio telemetry study.	144
Figure 4-40: Flight heights of medium terns ($n=3,020$) derived from the Northwest Atlantic Seabird Catalog.	145
Figure 4-41: Modeled APEM digital aerial surveys for loons in the NY Bight survey area and Lease Area OCS-A 0544.	149
Figure 4-42: Monthly relative densities of loons in the Lease Area from digital aerial surveys.	150
Figure 4-43: Dynamic Brownian bridge movement models for Red-throated Loons ($n=46$ in winter, 46 in spring, and 31 in fall) that were tracked with satellite transmitters. The models indicate the birds stay close to shore in the winter and during fall migration, but may pass through the Lease Area during spring migration.	151
Figure 4-44: Flight heights of loons ($n=3,957$) derived from the Northwest Atlantic Seabird Catalog.	152
Figure 4-45: Modeled APEM digital aerial surveys for petrels and shearwaters in the NY Bight survey area and Lease Area OCS-A 0544.	156
Figure 4-46: Modeled APEM digital aerial surveys for storm-petrels in the NY Bight survey area and Lease Area OCS-A 0544.	157
Figure 4-47: Monthly relative densities of shearwaters, petrels, and storm-petrels in the Lease Area from digital aerial surveys.	159
Figure 4-48: Flight heights of shearwaters and petrels ($n=9,510$) derived from the Northwest Atlantic Seabird Catalog.	159
Figure 4-49: Flight heights of storm-petrels ($n=7,878$) derived from the Northwest Atlantic Seabird Catalog.	160
Figure 4-50: Modeled APEM digital aerial surveys for gannets in the NY Bight survey area and Lease Area OCS-A 0544.	164
Figure 4-51: Monthly relative densities of Northern Gannets in the Lease Area from digital aerial surveys.	165

Figure 4-52: Dynamic Brownian bridge movement models for Northern Gannets ($n=34$ in winter, 35 in spring, 36 in fall) that were tracked with satellite transmitters. The models indicate the Lease Area is used by Northern Gannets during the winter, spring, and fall.	166
Figure 4-53: Flight heights of Northern Gannets ($n=11,654$) derived from the Northwest Atlantic Seabird Catalog.	167
Figure 4-54: Modeled APEM digital aerial surveys for cormorants in the NY Bight survey area and Lease Area OCS-A 0544.	171
Figure 4-55: Monthly relative densities of cormorants and pelicans in the Lease Area from digital aerial surveys.	172
Figure 4-56: Flight heights of cormorants ($n=512$) derived from the Northwest Atlantic Seabird Catalog.	173
Figure 4-57: Flight heights of pelicans ($n=90$) derived from the Northwest Atlantic Seabird Catalog.	174
Figure 4-58: Spring Roseate Tern density proportions in the NY Bight survey data (A) and the MDAT model outputs at local (B) and regional scales (C). The scale for all maps is representative of relative spatial variation in the sites within the season for each data source.	179
Figure 4-59: Roseate Tern observations from NY Bight surveys (“APEM Observations 2017-2019”); and from the Northwest Atlantic Seabird Catalog. Data provided by National Oceanic and Atmospheric Administration and used with permission.	180
Figure 4-60: Roseate Tern ($n=149$) track locations and density from the Loring <i>et al.</i> (2019) radio telemetry study.	181
Figure 4-61: Modeled flight paths of migratory Piping Plovers equipped with nanotags ($n=70$), based on data from Loring <i>et al.</i> (2019).	185
Figure 4-62: Modeled flight paths of migratory Red Knots equipped with nanotags based on data from Loring <i>et al.</i> (2020). Spring migration ($n=31$) and fall migration ($n=146$) in 2014-2017.	189
Figure 4-63: Black-capped Petrel observations from the Northwest Atlantic Seabird Catalog and APEM. Data provided by NOAA and used with permission.	193
Figure 4-64: Export from Northeast Ocean Data Portal showing track lines of three Black-capped Petrels (purple, yellow, and blue lines each show a different individual) tagged with satellite transmitters. Offshore wind BOEM lease areas are also shown in colored polygons.	194
Figure 5-1: Location of digital aerial surveys conducted in the NYSERDA Digital Aerial Baseline Survey (Normandeau Associates and APEM 2021a, b) and the Digital Aerial Wildlife Survey of BOEM Lease Area OCS-A 0512 (Normandeau Associates and APEM 2019, 2021c) in relation to the Lease Area.	210
Figure 5-2: Overall survey effort by season. While effort varied by OCS lease block and season, the entire study area, including the Lease Area, was thoroughly surveyed each season.	211
Figure 5-3: Example MDAT abundance model, in this case for the Northern Gannet in the fall.	214
Figure 5-4: Example map of relative density proportions locally and regionally for Northern Gannet in the summer.	227

List of Tables

Table 2-1: BRI’s risk evaluation matrix. An initial risk determination is made based on vulnerability and exposure, and then the population vulnerability (PV) score is used to either keep the score the same, adjust the score up or down, or with a risk range eliminate the lower or upper portion of the range.....	21
Table 3-1: NLCD habitat types associated with the footprint of onshore facilities.	25
Table 3-2: Listed bird species observed within a 15 km (9.3 mi) buffer of the onshore facilities.	37
Table 3-3: Number of individual Piping Plovers, Red Knots, Roseate Terns, Saltmarsh Sparrows, and Bald Eagles observed in the immediate area of landfall sites, 2013-2023.	39
Table 3-4. Top five Piping Plover breeding sites on Long Island, table adapted from NYSDEC 2018.	42
Table 3-5: Species observed by eBird users within 15 km (9.3 mi) of onshore facilities in the last 10 years, along with their primary and general breeding habitats, as well as state and federal conservation listing statuses.	49
Table 4-1: Avian species recorded offshore of New York in the NY Bight survey area, cross-referenced with the US Fish and Wildlife Service (USFWS) Information for Planning and Consultation (IPaC) database.	68
Table 4-2: Summary of shorebird vulnerability.	80
Table 4-3: Summary of wading bird vulnerability.	84
Table 4-4: Summary of raptor vulnerability.....	92
Table 4-5: Summary of songbird vulnerability.....	95
Table 4-6: Seasonal exposure rankings for the sea duck group.	101
Table 4-7: Vulnerability assessment rankings by species for the sea duck group.	107
Table 4-8: Seasonal exposure rankings for the phalaropes group.	112
Table 4-9: Vulnerability assessment rankings by species for the phalaropes group.....	113
Table 4-10: Seasonal exposure rankings for the auks group.	118
Table 4-11: Vulnerability assessment rankings by species for the auks group.....	120
Table 4-12: Seasonal exposure scores for the gulls, skuas, and jaegers group.	129
Table 4-13: Vulnerability assessment rankings by species for the gulls and jaegers group.	134
Table 4-14: Seasonal exposure rankings for the terns group.	142
Table 4-15: Vulnerability assessment rankings by species for the terns group.....	145
Table 4-16: Seasonal exposure rankings for the loons group.....	150
Table 4-17: Vulnerability assessment rankings by species for the loon group.	152
Table 4-18: Seasonal exposure rankings for the shearwaters, petrels, and storm-petrels group.	158
Table 4-19: Vulnerability assessment rankings by species for the shearwaters, petrels, and storm-petrels group. ..	160
Table 4-20: Seasonal exposure scoring and categories for Northern Gannets.	165
Table 4-21: Vulnerability assessment rankings for Northern Gannets.	167
Table 4-22: Seasonal exposure rankings for cormorants and pelicans.....	172
Table 4-23: Vulnerability assessment rankings by species for cormorants and pelicans.	174

Table 4-24: Vulnerability assessment rankings for the Roseate Tern. Based on the literature, displacement vulnerability was adjusted to include a lower range limit.	178
Table 4-25: Overall summary of the assessment of potential effects on birds.	199
Table 4-26: Information sources available, uncertainty scores, and uncertainty levels in exposure assessments.	200
Table 4-27: Uncertainty scores for BRI's vulnerability assessment (for collision vulnerability and displacement vulnerability).....	201
Table 4-28: Seasonal species naive densities (uncorrected count per square kilometer of survey transect) within Lease Area OCS-A 0544 and the NY Bight survey area.	202
Table 5-1: Summary of integrated density models.	222
Table 5-2: Definitions of exposure levels developed for the avian assessment for each species and season.	229
Table 5-3: Assessment criteria used for assigning species to final (annual) exposure levels.	230
Table 5-4: Assessment criteria used for assigning species to each behavioral vulnerability level.	232
Table 5-5: Data sources and scoring of factors used in the vulnerability assessment.	233
Table 5-6: WTG specifications used in the vulnerability analysis. Mean sea level is the average hourly tidal height over 19 years.	236
Table 5-7: Description of data sources and their contribution to uncertainty scores.	239

List of Acronyms and Abbreviations

ad.	adult
AS	adult survival score
AWWI	American Wind Wildlife Institute
BGEPA	Bald and Golden Eagle Protection Act
BMP	best management practice
BOEM	Bureau of Ocean Energy Management
BRI	Biodiversity Research Institute
CCSmax	continental combined score
CFA	New Jersey Conservation Focal Area
COP	Construction and Operations Plan
CV	collision vulnerability
CWF	Conservation Wildlife Foundation New Jersey
dBMM	dynamic Brownian-bridge movement model
DFA	diurnal flight activity
DV	displacement vulnerability
ESA	Endangered Species Act
ESP	electrical service platform
ft	feet
GF	Gaussian Field
GMRF	Gaussian Markov Random Field
GPS	Global Positioning System
GSD	ground sampling distance
HY	hatch year
INLA	integrated nested Laplace approximation
IPaC	Information for Planning and Consultation
IPF	impact producing factors
km	kilometer
km ²	square kilometer
kW	kilowatt
LGCP	log Gaussian Cox Poisson
m	meter
MDAT	Marine-life Data and Analysis Team
MDIFW	Maine Department of Inland Fisheries and Wildlife
mi	statute mile
MW	megawatt
n	number of observations/data points
NFA	nocturnal flight activity
NLCD	National Land Cover Database
nm	nautical mile
NOAA	National Oceanic and Atmospheric Administration
NYSERDA	New York State Energy Research and Development Authority

OCS	Outer Continental Shelf
OECC	offshore export cable corridor
PC	penalized complexity
PiF	Partners in Flight
POI	point of interconnection
PTT	Argos platform terminal transmitter
PV	population vulnerability
RSZ	rotor swept zone
SGCN	species of greatest conservation need
SPDE	stochastic partial differential equation
SSmax	state status
SDJV	Sea Duck Joint Venture
SWAP	State Wildlife Action Plan
UD	Utilization distribution
USACE	United States Army Corps of Engineers
USFWS	United States Fish and Wildlife Service
VHF	very high frequency
WEA	wind energy area
WTG	wind turbine generator

1 Summary

Vineyard Mid-Atlantic LLC (the “Proponent”) proposes to develop, construct, and operate offshore renewable wind energy facilities in Bureau of Ocean Energy Management (BOEM) Lease Area OCS-A 0544 (the “Lease Area”) along with associated offshore and onshore transmission systems. This proposed development is referred to as “Vineyard Mid-Atlantic.” Vineyard Mid-Atlantic includes 118 total wind turbine generator (WTG) and electrical service platform (ESP) positions within the Lease Area. One or two of those positions will be occupied by ESPs and the remaining positions will be occupied by WTGs. Offshore export cables installed within an Offshore Export Cable Corridor (OECC) will transmit power from the renewable wind energy facilities to onshore transmission systems on Long Island, New York. This appendix to the Construction and Operations Plan (COP) assesses the potential effects on birds from onshore and offshore components of Vineyard Mid-Atlantic.

Onshore, potential effects on birds were assessed in several ways. First, BRI conducted a co-occurrence analysis to determine the degree to which the footprint of Vineyard Mid-Atlantic’s onshore facilities overlap with existing development and any bird habitats that have the potential to be disturbed. Then, BRI used publicly available data sources such as the eBird database to determine which bird species are likely occupy any impacted habitats or the vicinity, and to analyze the potential impacts on those species, including protected species.

Offshore, BRI’s assessment evaluated exposure, vulnerability, and risk for all avian groups and species likely to occur in the Lease Area. Exposure (i.e., the likelihood of occurrence) was first assessed using multiple data sources, including digital aerial surveys, integrated density models created by BRI, marine bird distribution models, individual tracking data, and relevant current literature. Vulnerability (i.e., the degree to which a group or species could be affected) was then assessed using a suite of behavioral variables to calculate scores for relative collision vulnerability and relative displacement vulnerability. Uncertainty was formally evaluated for exposure and vulnerability using a separate scoring process for each. Finally, exposure and vulnerability were combined to produce a final risk determination via a weight-of-evidence approach.

Onshore, Vineyard Mid-Atlantic’s activities will nearly completely be co-located with existing areas of development. The most sensitive areas expected to be disturbed are the landfall site(s), where transmission infrastructure will be installed at beaches known to provide habitat for federally-listed shorebirds: both beach-nesting Piping Plovers (*Charadrius melodus*) and migratory Red Knots of the Atlantic flyway subpopulation (*Calidris canutus rufa*).

Offshore, BRI’s final risk determinations for collision and displacement were minimal, minimal-low, or low for all avian groups and for the protected species considered individually. In general, the minimal and low risk determinations were mostly driven by a lack of exposure to the Lease Area. Exposure of non-marine birds is expected to be limited to migratory periods, while marine bird exposure is more variable according to different life histories among marine bird groups. For example, exposure of auks was minimal in summer and fall, when these colony-breeding birds are nesting farther north, and low in winter and spring when auks use the New York Bight as a winter foraging habitat. Exposure uncertainty was generally lower for marine birds, owing to higher quality information from digital aerial surveys and models. Uncertainty was high for exposure of shorebirds and songbirds, high for the two federally listed shorebirds, Red Knots and Piping Plovers, and medium for Bald Eagles (*Haliaeetus leucocephalus*).

2 Introduction

This avian risk appendix provides support for the avian assessment summary provided in Section 4.2 of COP Volume II, as well as the onshore avian information in Section 4.1 of COP Volume II. In this Appendix, Section 3 focuses on the onshore avian assessment and risk to birds in the onshore environment. Section 4 focuses on risk to birds in the offshore environment and includes the results of BRI's exposure and vulnerability assessments for all birds exposed to Lease Area OCS-A 0544 (the Lease Area). For methods, Section 2.3 provides a brief overview, and Section 5 is a detailed discussion of data sources and assessment methods. Section 6 lists literature cited, and Attachment A provides seasonal exposure maps, where available, for birds offshore.

2.1 Description of Vineyard Mid-Atlantic

Vineyard Mid-Atlantic LLC (the "Proponent") proposes to develop, construct, and operate offshore renewable wind energy facilities in Bureau of Ocean Energy Management (BOEM) Lease Area OCS-A 0544 (the "Lease Area") along with associated offshore and onshore transmission systems. This proposed development is referred to as "Vineyard Mid-Atlantic."

Vineyard Mid-Atlantic includes 118 total positions for wind turbine generators (WTGs) and electrical service platform (ESPs) within the Lease Area¹. One or two of the positions will be occupied by ESPs and the remainder will be occupied by WTGs. Offshore export cables installed within an offshore export cable corridor (OECC) will connect the renewable wind energy facilities to onshore transmission systems in New York, branching to reach landfall site(s) on coastal Long Island (Figure 2-1).

The WTGs, ESP(s), and their foundations, as well as the inter-array cables, inter-link cables (if used), and a portion of the offshore export cables, will be located in Lease Area OCS-A 0544. The Lease Area is one of six New York Bight Lease Areas identified by BOEM as suitable for offshore wind energy development, following a public process and environmental review. At its closest point, the 174 square kilometer (km² [43,056 acre]) Lease Area is approximately 38 km (24 miles [mi]) south of Fire Island, New York.

Between the Lease Area and shore, the offshore export cables will be installed within an Offshore Export Cable Corridor (OECC). Up to six high voltage alternating current (HVAC) cables, two high voltage direct current (HVDC) cable bundles, or a combination of up to four HVAC cables/HVDC cable bundles will be installed within the OECC. The OECC extends from the northern end of the Lease Area, continuing west along the boundary of neighboring Lease Area OCS-A 0512, and then proceeds northwest across the Ambrose to Nantucket and Nantucket to Ambrose Traffic Lanes towards the southern shore of Long Island, New York. As the OECC approaches shore, it splits into three variations to connect to three potential landfall sites (of

¹ As further described in Section 2.3 of COP Volume I, six WTG/ESP positions along the northwestern boundary of Lease Area OCS-A 0544 are contingent upon the final layout of the neighboring Empire Wind 2 project. Vineyard Mid-Atlantic will not develop these contingent WTG/ESP positions if the final Empire Wind 2 layout includes WTGs at immediately adjacent positions within Lease Area OCS-A 0512.

which, up to two will be used): the Rockaway Beach Landfall Site, the Atlantic Beach Landfall Site, and the Jones Beach Landfall Site. The Proponent has also identified a “Western Landfall Sites OECC Variant” that may be used for routing offshore export cables to the Rockaway Beach and Atlantic Beach Landfall Sites.

Onshore export cables will connect up to two of the three potential landfall sites to two new onshore substations in Nassau County and/or Suffolk County, New York. If HVAC cables are used, depending upon numerous technical considerations, an onshore reactive compensation station (RCS) may be located along each onshore export cable route to manage the export cables’ reactive power (unusable electricity), increase the transmission system’s operational efficiency, reduce conduction losses, and minimize excess heating. Grid interconnection cables will connect the new onshore substations to the existing East Garden City Substation (Uniondale) Point of Interconnection (POI) in Uniondale, New York, the Ruland Road Substation POI in Melville, New York, or the proposed Eastern Queens Substation POI in Queens, New York.

2.2 Climate Change and Birds

While it is important to weigh the risks that Vineyard Mid-Atlantic may pose to bird species, it is also worth considering the current and projected risks to birds from climate change and how Vineyard Mid-Atlantic may help offset those risks. A recent report details that since 1970, three billion birds have been lost across the United States (US) and Canada, and 70 species listed as *Birds of Conservation Concern* (BCC) have seen a collective two-thirds reduction in population size, driven in part by the stressors of anthropogenic climate change (North American Bird Conservation Initiative 2022). Warming global temperatures may reduce reproductive success and increase mortality through a variety of pathways, such as creating a mismatch between spring phenology and food availability (Saino et al. 2011; Both et al. 2009) and chronic body mass loss (du Plessis et al. 2012). For migratory birds, changes in range, earlier migration, and early breeding are all extensively documented changes (Weiskopf et al. 2020). Secondary consequences of climate change, such as sea level rise and increasing sea surface temperatures (SSTs), are also projected to reduce the populations of various species, leading to possible extirpations and extinctions under certain climatic scenarios as well (Bonnot et al. 2017; Barbraud et al. 2011; Ballerini et al. 2015; Aiello-Lammens et al. 2011).

One taxonomic group that may be particularly vulnerable to the impacts of climate change is seabirds (Dias et al. 2019). Warming-induced reductions in prey availability is considered one of the leading causes in the decline of seabird populations over the last two decades (Mitchell et al. 2020). Other high-priority threats posed by climate change to seabirds include loss of nesting habitat with sea level rise, increased nest failures due to extreme weather events, and increased disease exposure (Hakkinen et al. 2022, Olin et al. 2023).

A seabird species of critical concern is the Roseate Tern, which is listed as *Endangered* under the Endangered Species Act (ESA). The species breeds in colonies situated on coastal islands and barrier beaches and thus is at risk of habitat loss from sea level rise, particularly at low-lying colonies (US Fish and Wildlife Service 2010). With the Northeast US Atlantic Coast currently experiencing sea level rise greater than global mean sea levels (Dupigny-Giroux et al. 2018), some Roseate Tern breeding areas along the Northeast US coast are likely to lose the majority of nesting habitat within 40 to 60 years (US Fish and Wildlife Service 2020b). In turn, this could reduce the genetic diversity of certain populations, further endangering this listed species.

Shorebirds are another taxonomic group considered highly vulnerable to climate change (Galbraith et al. 2014). This is due to several migration-related factors. For example, shorebirds may experience climate-induced ecological mismatches at multiple life-history stages along their migratory paths (Galbraith et al. 2014; Galbraith et al. 2002; Hedenström et al. 2007). In addition, changing weather patterns, such as more extreme storms, may compound the already compromised condition of shorebirds undertaking migrations (Galbraith et al. 2014; Klaassen et al. 2012).

Rapidly changing environmental conditions may especially affect two ESA-listed shorebird species, the Red Knot (*Calidris canutus rufa*) and the Piping Plover (*Charadrius melodus*). As

detailed in the recent Species Status Assessment for Red Knot (US Fish and Wildlife Service 2020c), climate change is currently impacting or projected to impact, Red Knots through a variety of pathways. Harmful algal blooms, which cause sickness and mortality in the species (US Fish and Wildlife Service 2014), have increased in frequency and extent in part due to warming ocean temperatures (Pörtner et al. 2019). Increasing ocean acidification and SST resulting from climate change also reduces the availability of certain mollusk species, which serve as important prey for Red Knots at migration stopovers (US Fish and Wildlife Service 2014). For Piping Plovers, accelerated sea level rise in the Atlantic Ocean may reduce the extent of suitable breeding habitat, while more extreme coastal flooding may increase nest flooding and chick mortality (US Fish and Wildlife Service 2020a).

Global warming may also severely impact species that forage, breed and/or nest in coastal wetland ecosystems, and in combination with human development, is responsible for the loss of nearly 50% of coastal wetlands in the last 100 years (Pörtner et al. 2019). Two marsh birds of critical conservation concern with narrow habitat requirements are the Eastern Black Rail (*Laterallus jamaicensis jamaicensis*), listed as *Threatened* under the ESA, and the Saltmarsh Sparrow (*Ammodramus caudacutus*), which may be proposed for ESA listing in 2023. Effects of global warming on coastal wetlands, including increased extreme weather events and wave heights, increased precipitation, and inundation from sea level rise (Pörtner et al. 2019), may lead to nest failure and direct mortality of individuals (US Fish and Wildlife Service 2018). Indirect impacts may also be incurred, such as increased predation exposure of rails due to flooding events (e.g., Thorne et al. 2019) and reduced reproductive success due to loss of critical nesting substrate from sea level rise, and reduced availability of invertebrates with increasing drought and flooding (US Fish and Wildlife Service 2018; Hartley and Weldon 2020). The interaction of these effects has likely largely contributed to the 50% decline of Saltmarsh Sparrows in the last 10 years (Hartley and Weldon 2020) and will likely lead to the extirpation of Eastern Black Rails by 2068 (US Fish and Wildlife Service 2018).

2.3 Methods Overview

This section provides a brief description of the assessment methodology. More information on onshore and offshore methodology is presented in Sections 3.2 and 5.0, respectively.

2.3.1 Onshore

The potential effects on birds from activities in the footprint of the onshore facilities (i.e., transition vaults, splice vaults, duct bank, onshore export cables, grid interconnection cables, onshore substations, onshore RCSs [if used], points of interconnection [POIs] plus the broader region that could be affected (Onshore Development Area) were evaluated in a desktop study by assessing the degree that the onshore facilities were co-occurring with existing development, the habitat that has the potential to be disturbed, and the birds that may occupy the habitat. Co-occurrence of the onshore cable route options with existing developed areas and linear infrastructure was assessed in ArcGIS by calculating the percentage of the onshore cable routes that aligned with existing roads. The habitat potentially to be disturbed in the Onshore

Development Area was assessed by calculating the overlap of the onshore cable routes, within a 50 meter (m; 164 feet [ft]) buffer, with local habitat types. Species that are known to occur around the Onshore Development Area were evaluated using the eBird database (Sullivan et al. 2009).

2.3.2 Offshore

For the marine bird groups, a semi-quantitative approach was taken that describes the species that would potentially be exposed to the Lease Area, examines the vulnerability of the species exposed, and then performs a final risk assessment (Figure 2-2). For each marine bird group addressed under this assessment, species occurrence and area use were identified and evaluated using multiple data sources, including but not limited to:

- the New York State Energy Research & Development (NYSERDA) Digital Aerial Baseline Surveys of Marine Life (Normandeau Associates and APEM 2021b) and the Digital Aerial Wildlife Survey of BOEM Lease Area OCS-A 0512 (also referred to as the Empire Wind digital aerial surveys; Normandeau Associates and APEM 2019, 2021c), collectively referred to throughout as “digital aerial surveys” or “NY Bight surveys”;
- integrated density models (INLA) created by BRI;
- National Oceanic and Atmospheric Administration (NOAA) Marine-life Data and Analysis Team (MDAT) bird distribution models;
- the Northwest Atlantic Seabird Catalog;
- individual tracking studies;
- relevant current literature;
- and published species accounts.

These information sources and BRI’s application of them are further described in Section 5. For non-marine migratory birds, the available data was not sufficient for the semi-quantitative approach applied to marine birds, so a qualitative approach was used instead.

The results section of this Appendix addresses exposure and vulnerability separately for non-marine migratory birds; marine birds; and species listed (or proposed for listing) under the ESA or protected by the Bald and Golden Eagle Protection Act (BGEPA), collectively referred to throughout as “protected species.” The results section includes maps, tables, and figures for each major avian group and each protected species.

Most species were assessed within general avian taxonomic groups (e.g., wading birds), following groupings that are practical for offshore assessment rather than strict taxonomic divisions (e.g., phalaropes, while technically shorebirds, have a far more pelagic life history than their fellow shorebirds and are thus assessed with the other marine bird groups). The protected species that were individually assessed are: Piping Plover (*Charadrius m. melodus*), Red Knot (*Calidris canutus rufa*), Roseate Tern (*Sterna dougallii*), Bald Eagle (*Haliaeetus leucocephalus*), and Black-capped Petrel (*Pterodroma hasitata*).

The assessment process was as follows (with additional details provided in Section 5):

- *Exposure* – The first step in the process was to assess exposure for each species and each taxonomic group, with “exposure” defined as the extent of overlap between a species’ seasonal or annual distribution and the Lease Area. For species where site-specific data were available, a semi-quantitative exposure assessment was conducted. This exposure assessment focused exclusively on the horizontal, or two-dimensional, likelihood that a bird would use the Lease Area. Exposure was evaluated by comparing the modeled bird density within the Lease Area to surrounding areas, on a local and regional scale, to assign a categorical exposure score of minimal, low, medium, or high. Local density estimates were derived from modeled density outputs of the NYSERDA 2016-2019 digital aerial surveys and Empire Wind digital aerial surveys. Regional estimates came from Version 3 of the MDAT marine bird relative density and distribution models (hereafter MDAT models; Curtice et al. 2019, Winship et al. 2023). Analysis of individual tracking studies and records in the Northwest Atlantic Seabird Catalog were used to augment the exposure analysis. Details on each of the datasets and detailed methods used in the exposure assessment are found in Section 5. Due to gaps in knowledge on the relationship between the number of WTGs and risk, this assessment analyzes the exposure of birds to the total area of development rather than to a specific number of WTGs.²
- *Vulnerability* – Vulnerability was then assessed for marine birds using a scoring process. For the purposes of this analysis, relative behavioral vulnerability (hereafter, “vulnerability”) is defined as the degree to which a species is expected to be affected by WTGs in the Lease based on known behavioral responses to similar offshore developments. The relative collision vulnerability score (CV) includes proportion of time within the rotor swept zone (RSZ), a measure of avoidance, and flight activity; the displacement vulnerability score (DV) includes two factors—disturbance and habitat flexibility. Flight heights used in the assessment were gathered from the non-digital aerial survey datasets in the Northwest Atlantic Seabird Catalog. For each score, the factors were combined to create a score that was translated into four vulnerability categories: minimal, low, medium, and high (see Section 5 for details). The results provide a categorical vulnerability score for each group and species relative to the others exposed to the Lease Area and are not intended to provide an absolute likelihood of collision or displacement. In other words, minimal collision vulnerability means a group or species that is less likely to collide with WTGs if exposed than the other assessed groups and species.
- *Risk* – The likelihood that the presence of WTGs in the Lease Area would impact birds was then evaluated using a weight-of-evidence approach, by combining the results of the

² Risk may not increase in a linear manner as the number of WTGs increases because birds’ avoidance response may change as the numbers of WTGs increase. Risk is also likely affected by the size and spacing of WTGs: larger WTGs have fewer revolutions than smaller WTGs, may have a greater airgap between the water and the lowest blade position, and may be spaced much farther apart. Thus, fewer larger WTGs may pose a lower risk than many smaller WTGs (Johnston et al. 2014).

exposure and vulnerability assessments (Table 2-1). The additional factor of population vulnerability (PV) was considered in assigning a final risk category, where a risk score was adjusted up or down based on the overall conservation status of the population. For non-listed species, the assessment provides information for BOEM to make its impact determination at a population level, as has been done for assessments of Wind Energy Areas (WEAs). For federally listed species, this assessment provides information on an individual level because the loss of one individual from the breeding population has a greater likelihood of affecting a population than for non-listed species.

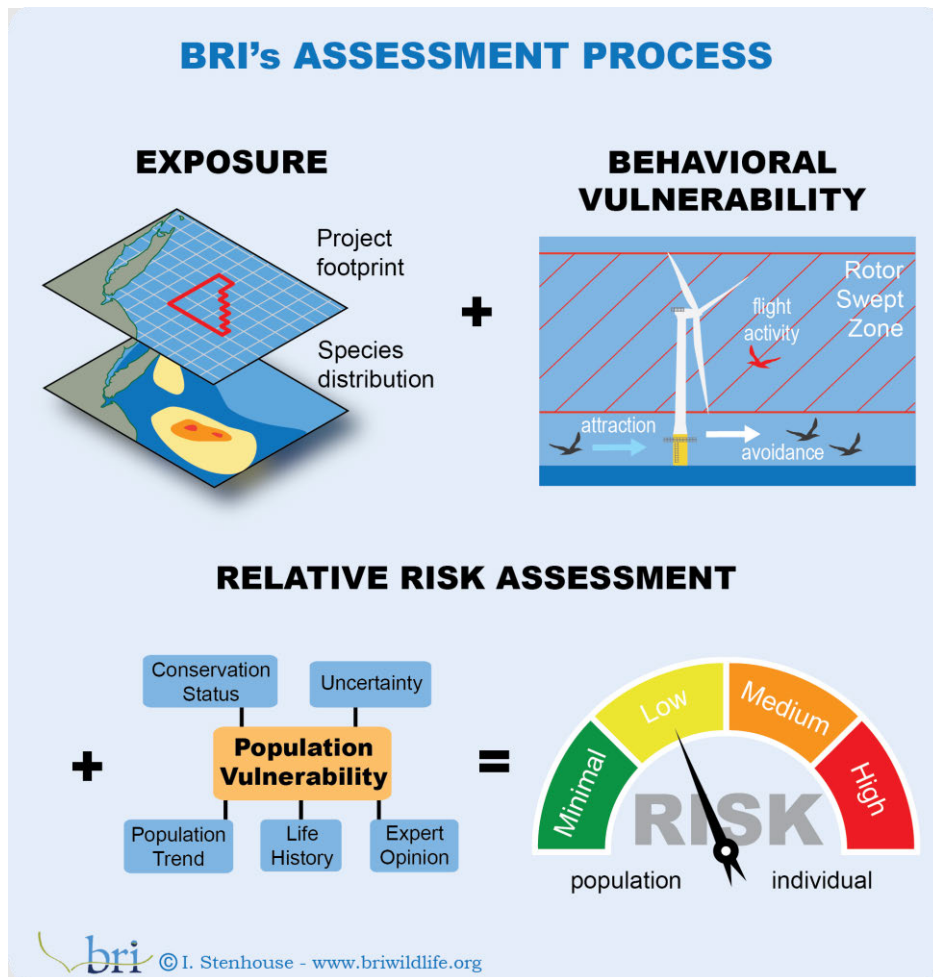


Figure 2-2: BRI's risk assessment process overview. An exposure and behavioral vulnerability assessment are combined using expert opinion to estimate relative risk.

Table 2-1: BRI’s risk evaluation matrix. An initial risk determination is made based on vulnerability and exposure, and then the population vulnerability (PV) score is used to either keep the score the same, adjust the score up or down, or with a risk range eliminate the lower or upper portion of the range.

Exposure	Vulnerability (CV & DV)				PV
	Minimal	Low	Medium	High	
Minimal	Minimal	Minimal	Minimal	Minimal	
Low	Minimal	Low	Low	Low	
Medium	Minimal	Low	Medium	Medium	
High	Minimal	Low	Medium	High	
PV	←			→	

3 Onshore Assessment

3.1 Introduction

This section discusses the birds that may be impacted by construction and operation of Vineyard Mid-Atlantic’s onshore facilities, including potential landfall sites: Rockaway Beach Landfall Site, Atlantic Beach Landfall Site, Jones Beach Landfall Site; onshore export cable routes; points of interconnection (POI): East Garden City Substation (Uniondale) POI, Ruland Road Substation POI, and Eastern Queens Substation POI; two substations to be constructed; and if necessary, up to two reactive compensations stations (RCSs). This section includes supporting tables, maps, and figures for the assessment of proposed onshore facilities development. See Figure 3-1 for a general schematic of the onshore facilities.

Onshore facilities are located within Queens, Nassau, and Suffolk Counties, New York. The landfall sites are situated on a peninsula (Rockaway Beach Landfall Site) and two barrier islands that separate the Atlantic Ocean from Reynolds Channel (Long Beach Island) and Jones Bay (Jones Beach Island). The Atlantic Beach Landfall Site is located in Atlantic Beach on Long Beach Island, while the Jones Beach Landfall Site is found on Jones Beach Island. The onshore facilities are approximately 32 km (20 mi) east of Manhattan, making the beaches on which the landfall sites are located a popular destination for visitors and residents of the surrounding communities and New York City.

The densely populated area is inhabited year-round and is known for its beaches, boardwalks, shops, restaurants, and entertainment venues. The surrounding natural landscape is characterized by salt marshes, sand dunes, beaches, and several parks and wildlife areas including Jones Beach State Park, Lido Beach Wildlife Management Area, and Jamaica Bay Wildlife Refuge.

3.2 Methods

This desktop study includes an assessment of the degree that the onshore facilities co-occur with existing development, the habitat that has the potential to be disturbed, and the birds that may occupy the habitat. Additional information is provided on federally listed species. Co-occurrence of the onshore facilities options with existing linear infrastructure was assessed in ArcGIS by calculating the percentage of the onshore facilities that aligned with existing roads. The habitat potentially to be disturbed by onshore facilities was assessed by calculating the overlap of local habitat types with the onshore facilities, including a 50 m (164 ft) buffer around the footprint. For the purposes of this assessment, the Onshore Development Area was defined as the geographic footprint of all onshore facilities plus the 50 m (164 ft) buffer. Species that occurred within the Onshore Development Area were identified using the eBird database (Sullivan et al. 2009).

3.2.1 Assessment of Co-location with Development and Habitats

Co-location of the onshore export cable routes with existing linear infrastructure was assessed in ArcGIS Pro (ESRI v3.1.3). Road centerlines for the State of New York were downloaded from the New York State GIS Clearing House. The centerlines were then clipped to the buffered onshore export cable route layer. All road features that ran parallel to the onshore export cable routes were manually selected and summed for total road length and percentage of total route length.

The habitat to be potentially disturbed by onshore facilities was assessed by calculating the overlap of the onshore export cable routes with local habitat types, and then by calculating the percentage of each route that was co-located with existing development as well as overlapping other landcover (habitat) types. The habitat types were determined for each cable route using the NLCD.³ A 50 m (164 ft) buffer was applied to either side of each onshore export cable route. This buffer width was expected to account for potential disturbance across the construction right-of-way. The area of each landscape type within each buffered onshore cable export route was calculated by first intersecting the NLCD raster with the buffered onshore cable export route using the crop function from the package “Raster” (Hijmans 2020) in R version 4.4.0 (R Core Team 2021) and then summarizing the area covered by each landcover type in each onshore export cable route. Exposure was determined based upon available data, existing literature, and species accounts.

BRI’s assessment of co-location with development and habitat was done for the entire Onshore Development Area collectively and does not assess onshore facilities independently from each other.

³ <https://www.mrlc.gov/data/nlcd-2019-land-cover-conus>

3.2.2 Avian Data Sources and Methods

Data on possible bird species present, including Piping Plover, Red Knot, and Roseate Tern, were primarily compiled from eBird citizen science data (Sullivan et al. 2009) from within a 15 km (9.3 mi) buffer of the centroid of the onshore facilities, and were temporally constrained to the prior 10 years of data (2013–2023). Due to inconsistencies in eBird effort and the mobility of birds, the buffer was used to include more sites where birds were observed to ensure that most species using the general area were recorded.

To more closely examine the presence of, and potential impact to, federally listed species at each landfall site, eBird observations in the immediate area of each site were examined. As there were no eBird observations of Eastern Black Rail in the entirety of the Onshore Development Area, eBird data is not provided. Saltmarsh Sparrows were included in this examination due to presence in the eBird database within the Onshore Development Area and because the US Fish and Wildlife Service (USFWS) may decide to list the species (Gifford 2019). Localities of eBird observations that were nearest each landfall site were used to filter the dataset. The dataset was then further filtered to only show observations of the species of interest within each landfall site/landfall site area: Piping Plover, Red Knot, Roseate Tern, Bald Eagle, and Saltmarsh Sparrow.

In addition, the USFWS IPaC database (USFWS 2022) and the New York Natural Heritage Bureau were queried using a polygon encompassing the entire Onshore Development Area.

3.3 Results

3.3.1 Co-Location with Existing Development and Habitats

The onshore facilities are located in the New York North Atlantic Coast Ecoregion. The region is characterized by shrublands, grasslands, coastal plain ponds and dunes, vast pine barrens, and extensive salt marshes that cover Long Island and Staten Island (NYSDEC 2023). The New York State Wildlife Action Plan (NYSWAP) terrestrial habitats intersected by the onshore facilities include, but are not limited to, commercial/industrial and residential, urban and recreational grasses, as well as salt marsh.

Based on the co-location analysis, the onshore export cable routes are approximately 99% co-located with existing linear infrastructure. Areas not co-located with existing infrastructure include open water crossings and undeveloped vegetated areas.

The Onshore Development Area was examined using NLCD habitat types summarized into eight categories (Table 3-1). Developed habitat accounted for 93.4% of the 17.6 km² (6.8 mi²) Onshore Development Area. After developed habitat, the next three most prevalent habitat types co-located with the Onshore Development Area were wetlands (1.9%), open water (1.3%), and

forested habitat (2.5%) (Table 3-1). The remaining <1% was made up of barren land, grassland, shrub, and agricultural land (Figure 3-2).

Table 3-1: NLCD habitat types associated with the footprint of onshore facilities.

Total Area (km ²)	Habitat Type (% of Total Area)							
	Open Water	Developed	Barren Land ¹	Forested	Shrub	Grassland	Agricultural	Wetland
17.6	1.3	93.4	0.4	2.5	0.2	0.1	0.2	1.9
¹ Barren Land includes classifications of Dry Salt Flats, Beaches, Sandy Areas other than Beaches, Bare Exposed Rock, Strip Mines, Quarries, Gravel Pits, Transitional Areas, and Mixed Barren Land.								

Three potential landfall sites have been identified along the New York coast. The Rockaway Beach Landfall Site is located in a previously disturbed area adjacent to Rockaway Beach in Queens, New York (Figure 3-3). The Atlantic Beach Landfall Site is located in a paved parking area near Atlantic Beach in the Town of Hempstead, New York (Figure 3-4). The Jones Beach Landfall Site is located in a paved parking area at Jones Beach State Park in the Town of Hempstead, New York (Figure 3-5). All landfall sites are in, or adjacent to, beach areas that have substantial existing development. Portions of Jones Beach, including the Jones Beach Landfall Site, overlap with proposed Red Knot Critical Habitat (USFWS 2021) (Figure 3-15). Additionally, Jones Beach State Park has documented Piping Plover nests (NYSDEC 2018). Exact locations of known nesting sites or areas on Jones Beach are not available at this time. Vineyard Mid-Atlantic submitted a Project Screening request to the New York Natural Heritage Program (NYNHP) for information on rare or listed plant and animals or of significant natural communities that may be impacted by Vineyard Mid-Atlantic.

The Uniondale POI, Ruland Road Substation POI, and Eastern Queens Substation POI occur in highly developed areas. The Uniondale POI footprint consists mostly of impervious surfaces, buildings, and electrical infrastructure, with very limited vegetation in the immediate vicinity (Figure 3-6). The surrounding area is comprised of commercial and residential development. The Ruland Road Substation POI also consists mostly of impervious surfaces, buildings, and electrical infrastructure (Figure 3-7). While there are fragmented forested areas adjacent to the Ruland Road Substation POI, there is very little to no vegetation within the footprint of the Ruland Road Substation POI. Overall, the surrounding area has been considerably impacted by human activities and consists of commercial and residential development. The proposed Eastern Queens Substation POI is located in a mixed residential and industrial area of Queens, consisting mostly of impervious surfaces. It is adjacent to the Hillside Support Facility, a major maintenance complex for the Long Island Railroad in the Jamaica neighborhood of Queens (Figure 3-10).

Four onshore substation site envelopes are proposed; [REDACTED]
 [REDACTED]
 [REDACTED]

[REDACTED]



Figure 3-3: A potential landfall site in a portion of a previously disturbed area adjacent to Rockaway Beach in Queens, New York.



Figure 3-4: A potential landfall site in a paved parking area near Atlantic Beach in the Town of Hempstead, New York.



Figure 3-5: A potential landfall site in a paved parking area at Jones Beach State Park in the Town of Hempstead, New York.



Figure 3-6: Potential POI in Uniondale, New York on Long Island.



Figure 3-10: Potential Eastern Queens POI in Queens, New York on Long Island.

3.3.2 Species Potentially Present in the Onshore Development Area

Due to the mobility of birds, many species have the potential to pass through habitats within or adjacent to the Onshore Development Area. Table 3-5 lists all species detected in the eBird database over the last ten years (2013–2023) within 15 km (9.3 mi) of Onshore Facilities. Habitat associations for each species in Table 3-5 are obtained from BirdLife International Data Zone fact sheets⁴. Inclusion of each species on state, federal, and global conservation lists is noted, as appropriate. Protected species and species of concern are identified in Section 3.3.2.1, and federally protected species Roseate Tern, Piping Plover, Red Knot, Eastern Black Rail, and Bald Eagle, are discussed in further detail. Saltmarsh Sparrow is also discussed in more detail due to its presence in the eBird database within the onshore facilities area, and because the USFWS may decide to list the species in 2024.

3.3.2.1 *Protected Species and Species of Concern*

Table 3-2 provides all bird species identified in the NYSWAP, along with the number of days each species was observed within 15 km (9.3 mi) of onshore facilities between 2013 and 2023 according to the eBird database. The state and federal listing status and IPaC result of each species is also included. There are three federally listed, one federally protected, and 11 state-listed (*Endangered* or *Threatened*) species that may occur in the vicinity of the onshore facilities. An additional 25 species are listed as *Special Concern* or *High Priority Species of Greatest Need (SGCN)* by New York State.

Four species of birds (Cerulean Warbler, Cory’s Shearwater, Long-eared Owl, and Manx Shearwater) were identified by the IPaC results as potentially present BCC but were not observed within the buffer of the onshore facilities within the last 10 years. An additional nine non-BCC vulnerable species (Black-legged Kittiwake, Common Murre, Dovekie, Golden Eagle, Great Shearwater, Pomarine Jaeger, Red Phalarope, Red-necked Phalarope, and Thick-billed Murre) were identified as potentially present by the IPaC results, but were not observed within the buffer of the onshore facilities within the last 10 years. Moreover, Cory’s Shearwater, Manx Shearwater, Black-legged Kittiwake, Common Murre, Dovekie, Great Shearwater, Pomarine Jaeger, Red Phalarope, Red-necked Phalarope, and Thick-billed Murre are extremely unlikely to be observed from shore or over land because these species are marine birds and spend most of their lives offshore, except during breeding which does not occur in the region. Due to the lack of observations these species are not included in the table. The New York Natural Heritage Bureau database documents the presence of ESA-listed birds (Roseate Tern, Piping Plover) and state-listed birds (Black Skimmer [*Rynchops niger*], Common Tern [*Sterna hirundo*], Least Tern [*Sternula antillarum*], and Short-eared Owl [*Asio flammeus*]) “at or in the vicinity of” each landfall

⁴ <http://datazone.birdlife.org/species/search>

site, all of which are documented in the eBird analysis. The Natural Heritage Bureau report also notes Peregrine Falcon (*Falco peregrinus*; New York *Endangered*; also detected by the eBird analysis) nesting sites at the Jones Beach water tower and Nassau County Medical Center, both locations adjacent to the Onshore Export Cable Route.

Table 3-3 displays the number of each federally protected species and Saltmarsh Sparrow observed by eBird users in the immediate area of the landfall sites. eBird users reported over 10 times more endangered and threatened species observations at eBird’s “Jones Beach” location (which encompasses Jones Beach State Park) than the other landfall site areas. Although the eBird “Jones Beach” location island encompasses the largest combined area for this analysis, Jones Beach State Park, within which the Jones Beach Landfall Site is located, appears to be an important area for breeding and migratory birds, especially Piping Plovers and Red Knots (NYSDEC 2018; USFWS 2021). Across landfall sites, Piping Plover was the most common.

Table 3-2: Listed bird species observed within a 15 km (9.3 mi) buffer of the onshore facilities.

NOTE: Species with zero observations within this area over the last 10 years have been excluded from this list.

Common Name	Latin Name	Days observed by eBirders ¹	New York Status ²	Federal Listing	IPaC ³
American Black Duck	<i>Anas rubripes</i>	3318	High SGCN	-	-
Common Eider	<i>Somateria mollissima</i>	1181	-	-	V
Long-tailed Duck	<i>Clangula hyemalis</i>	1515	-	-	V
Red-breasted Merganser	<i>Mergus serrator</i>	1897	-	-	V
Northern Bobwhite	<i>Colinus virginianus</i>	42	High SGCN	-	-
Pied-billed Grebe	<i>Podilymbus podiceps</i>	1595	T	-	-
Black-billed Cuckoo	<i>Coccyzus erythrophthalmus</i>	178	-	-	BCC
Common Nighthawk	<i>Chordeiles minor</i>	248	SC	-	-
Eastern Whip-poor-will	<i>Antrostomus vociferus</i>	36	SC	-	BCC
Chimney Swift	<i>Chaetura pelagica</i>	1621	-	-	BCC
American Oystercatcher	<i>Haematopus palliatus</i>	2741	-	-	BCC
Piping Plover	<i>Charadrius melodus</i>	1307	E	T	-
Whimbrel	<i>Numenius phaeopus</i>	205	High SGCN	-	-
Hudsonian Godwit	<i>Limosa haemastica</i>	149	-	-	BCC
Red Knot	<i>Calidris canutus</i>	966	T	T	-
Purple Sandpiper	<i>Calidris maritima</i>	690	-	-	BCC
Semipalmated Sandpiper	<i>Calidris pusilla</i>	1369	High SGCN	-	
Short-billed Dowitcher	<i>Limnodromus griseus</i>	1241	High SGCN	-	BCC
Willet	<i>Tringa semipalmata</i>	1418	-	-	BCC
Lesser Yellowlegs	<i>Tringa flavipes</i>	1347	-	-	BCC
Ring-billed Gull	<i>Larus delawarensis</i>	3650	-	-	V
Least Tern	<i>Sternula antillarum</i>	1115	T	-	-
Gull-billed Tern	<i>Gelochelidon nilotica</i>	489	-	-	BCC

Common Name	Latin Name	Days observed by eBirders ¹	New York Status ²	Federal Listing	IPaC ³
Black Tern	<i>Chlidonias niger</i>	151	E	-	-
Roseate Tern	<i>Sterna dougallii</i>	202	E	E	V
Common Tern	<i>Sterna hirundo</i>	1542	T	-	-
Royal Tern	<i>Thalasseus maximus</i>	735	-	-	V
Black Skimmer	<i>Rynchops niger</i>	1359	SC	-	BCC
Red-throated Loon	<i>Gavia stellata</i>	1631	-	-	V
Common Loon	<i>Gavia immer</i>	2299	SC	-	V
Brown Pelican	<i>Pelecanus occidentalis</i>	48	-	-	BCC
American Bittern	<i>Botaurus lentiginosus</i>	134	SC	-	-
Least Bittern	<i>Ixobrychus exilis</i>	34	T	-	-
Northern Harrier	<i>Circus hudsonius</i>	2105	T	-	-
Bald Eagle	<i>Haliaeetus leucocephalus</i>	1571	T	BGEPA	V
Red-shouldered Hawk	<i>Buteo lineatus</i>	433	SC	-	-
Red-headed Woodpecker	<i>Melanerpes erythrocephalus</i>	255	SC	-	BCC
Peregrine Falcon	<i>Falco peregrinus</i>	3226	E	-	-
Short-eared Owl	<i>Asio flammeus</i>	58	E	-	-
Horned Lark	<i>Eremophila alpestris</i>	1525	SC	-	-
Brown Thrasher	<i>Toxostoma rufum</i>	1834	High SGCN	-	-
Wood Thrush	<i>Hylocichla mustelina</i>	949	-	-	BCC
Vesper Sparrow	<i>Pooecetes gramineus</i>	191	SC	-	-
Seaside Sparrow	<i>Ammospiza maritima</i>	554	SC	-	-
Saltmarsh Sparrow	<i>Ammospiza caudacuta</i>	1196	High SGCN	-	-
Yellow-breasted Chat	<i>Icteria virens</i>	124	SC	-	-
Bobolink	<i>Dolichonyx oryzivorus</i>	369	High SGCN	-	BCC
Eastern Meadowlark	<i>Sturnella magna</i>	344	High SGCN	-	-
Rusty Blackbird	<i>Euphagus carolinus</i>	1014	High SGCN	-	BCC
Prothonotary Warbler	<i>Protonotaria citrea</i>	66	High SGCN	-	BCC
Kentucky Warbler	<i>Geothlypis formosa</i>	44	High SGCN	-	-
Bay-breasted Warbler	<i>Setophaga castanea</i>	278	High SGCN	-	-
Prairie Warbler	<i>Setophaga discolor</i>	522	-	-	BCC
Canada Warbler	<i>Cardellina canadensis</i>	327	High SGCN	-	BCC
<p>E = Endangered, T = Threatened, SC = Special Concern, BCC = USFWS Bird of Conservation Concern, V = non-BCC vulnerable, - = not applicable, BGEPA = Bald and Golden Eagle Protection Act, High SGCN= High Priority Species of Greatest Conservation Need</p> <p>¹ Days observed over 10 years within 15 km (9.3 mi) of the Onshore Facilities area.</p> <p>² Data from New York's Endangered, Threatened, and Special Concern Fish and Wildlife Species https://www.dec.ny.gov/animals/7494.html</p> <p>³ IPaC is a project planning tool that streamlines the USFWS environmental review process by providing information to assist in determining how proposed activities may impact sensitive natural resources. Data from the online USFWS IPaC tool, available at: https://ipac.ecosphere.fws.gov.</p>					

Table 3-3: Number of individual Piping Plovers, Red Knots, Roseate Terns, Saltmarsh Sparrows, and Bald Eagles observed in the immediate area of landfall sites, 2013-2023.

Landfall Site	Number of individuals observed in the eBird database ¹				
	Piping Plovers observed	Red Knots observed	Roseate Terns observed	Saltmarsh Sparrows observed	Bald Eagles observed
Rockaway Beach Landfall Site	196	12	1	0	0
Atlantic Beach Landfall Site	3	0	0	0	0
Jones Beach Landfall Site	1365	1450	18	15	117
¹ Individuals observed over 10 years (2013-2023) within Landfall Site areas					

3.3.2.1.1 Roseate Tern

Although Roseate Terns have a broader global distribution, the USFWS listed the North Atlantic breeding population as *Endangered* in 1987.⁵ Roseate Terns are also listed as *Endangered* by the New York Department of Environmental Protection. The largest breeding colony of Roseate Terns in New York is on Great Gull Island off eastern Long Island, with 99% of breeding pairs in New York State nesting at Great Gull Island in 2010 (NYSDEC 2015). Great Gull Island is located approximately 134 km (83 mi) from the closest potential landfall site. Individual migrating Roseate Terns may pass through the landfall sites during spring and fall migration but are unlikely to linger there or use any other non-coastal areas of the onshore facilities. The eBird database contains Roseate Tern detections on 202 days within the 15 km (9.3 mile) buffer of the onshore facilities from 2013–2023 (Table 3-2), with most observations occurring in June (Figure 3-11). The New York Natural Heritage Bureau database documents Roseate Terns “at or in the vicinity of” the West Jones Beach Landfall Site, confirming what is shown by the eBird analysis.

⁵ <https://www.nj.gov/dep/fgw/ensp/pdf/end-thrtened/roseatetern.pdf>

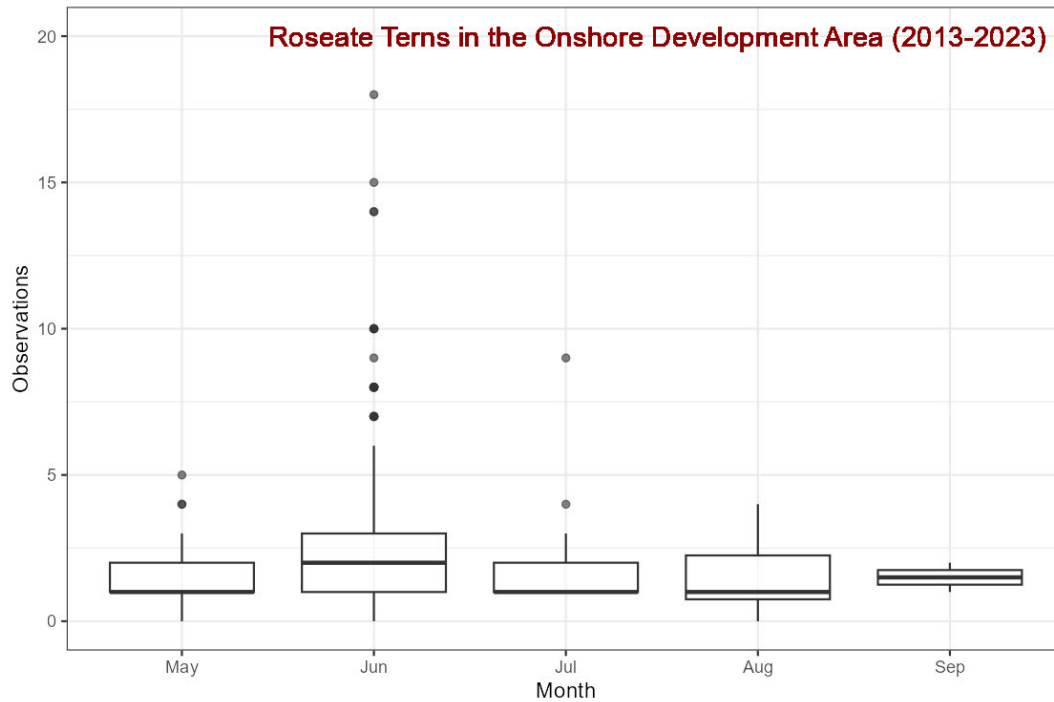


Figure 3-11: Monthly average of Roseate Tern observations in the Onshore Development Area over ten years, derived from the eBird database (total detections, with duplicate list postings removed).

3.3.2.1.2 Piping Plover

The Atlantic Coast population of the Piping Plover was federally listed as *Threatened* in 1986 and is also listed as *Threatened* by the State of New York, with approximately 1,698 nesting pairs in the US, as of 2018 (USFWS 2022). Piping Plovers nest on coastal beaches, sandflats at the ends of sand spits and barrier islands, gently sloped foredunes, sparsely vegetated dunes, and washover areas cut into or between dunes. Breeding Piping Plovers feed at areas of exposed wet sand in wash zones, intertidal ocean beach, wrack lines, washover passes, mud, sand, algal flats, shorelines of streams, ephemeral ponds, lagoons, and salt marshes by probing for invertebrates at or just below the surface. They use beaches adjacent to foraging areas for roosting and preening. Small sand dunes, debris, and sparse vegetation within adjacent beaches provide shelter from wind and extreme temperatures.

Piping Plovers are sensitive to disturbance during breeding. The presence of people is stressful for adults and chicks, forcing them to spend significantly less time foraging, which may result in decreased overall reproductive success (Burger 1990). Excessive disturbance may cause adults to desert the nest, exposing eggs or chicks to the summer sun and predators. Interrupted feedings may stress juvenile birds during critical periods in their development, and foot and vehicle traffic may crush eggs or chicks (USFWS 2001). Examples of actions that may affect this species include construction of any new permanent or temporary structure, grading, vegetation removal, equipment storage, any new or expanded human activity during the nesting season of March 15

to August 31; this includes activities involving motorized vehicles, permanent or temporary increases in noise or disturbance during the nesting season, including, but not limited to, construction work. Best management practices for protecting Piping Plovers include avoiding permanent or temporary modification of nest habitat and avoiding noise and disturbance during the nesting season, particularly work involving use of motorized vehicles (USFWS 2019).

Onshore in New York, approximately 385 breeding pairs of Piping Plovers nest exclusively on Long Island, including the eastern bays and harbors of northern Suffolk County. The top 5 breeding sites for Piping Plovers on Long Island, according to the New York State Department of Environmental Conservation (NYSDEC), include Jones Beach Island West and Long Beach Island Lido Beach (Table 3-4; NYSDEC 2018). While the exact locations of the nesting sites are not available at this time, Figure 3-11 created by NYSDEC provides approximate locations of 82 active nesting sites on Long Island as of 2018. Vineyard Mid-Atlantic submitted a Project Screening request to the NYNHP for information on rare or listed plant and animals or of significant natural communities that may be impacted by the development.

Piping plovers arrive on the breeding grounds during mid-March through mid-May and remain for 3 to 4 months per year and depart for the wintering grounds from mid-July through late October (Elliott-Smith and Haig 2004, USFWS 2019), with most having departed by early September (NYSDEC 2019).

The eBird database contains Piping Plover detections on 1,307 days within the 15 km (9.3 mi) buffer of the onshore facilities from 2013–2023 (Table 3-2), with most observations occurring in June (Figure 3-13). The New York Natural Heritage Bureau database documents Piping Plovers at or in the vicinity of all the landfall sites, confirming what is shown by the eBird analysis. Although the buffer encompasses non-coastal areas, it is unlikely that Piping Plovers would be observed outside of beaches and estuaries.

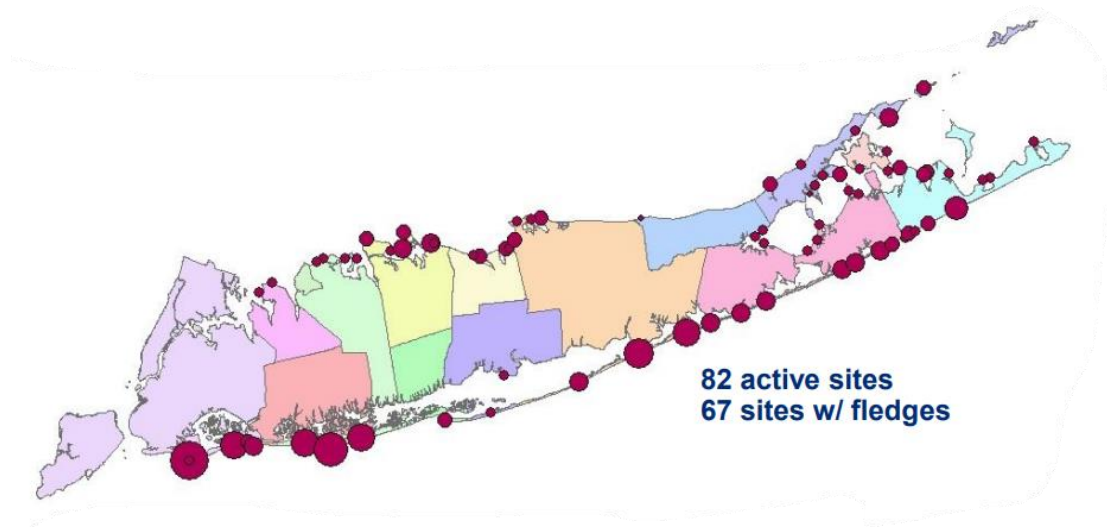


Figure 3-12. Piping Plover nesting sites on Long Island, figure replicated from NYSDEC 2018.

Table 3-4. Top five Piping Plover breeding sites on Long Island, table adapted from NYSDEC 2018.

Location	Total Breeding Pairs
Jones Beach Island West	30
Fire Island East aka Smith Point	25
Breezy Point (Park Service Property)	15
Arverne by the Sea	15
Long Beach Island Lido Beach	14

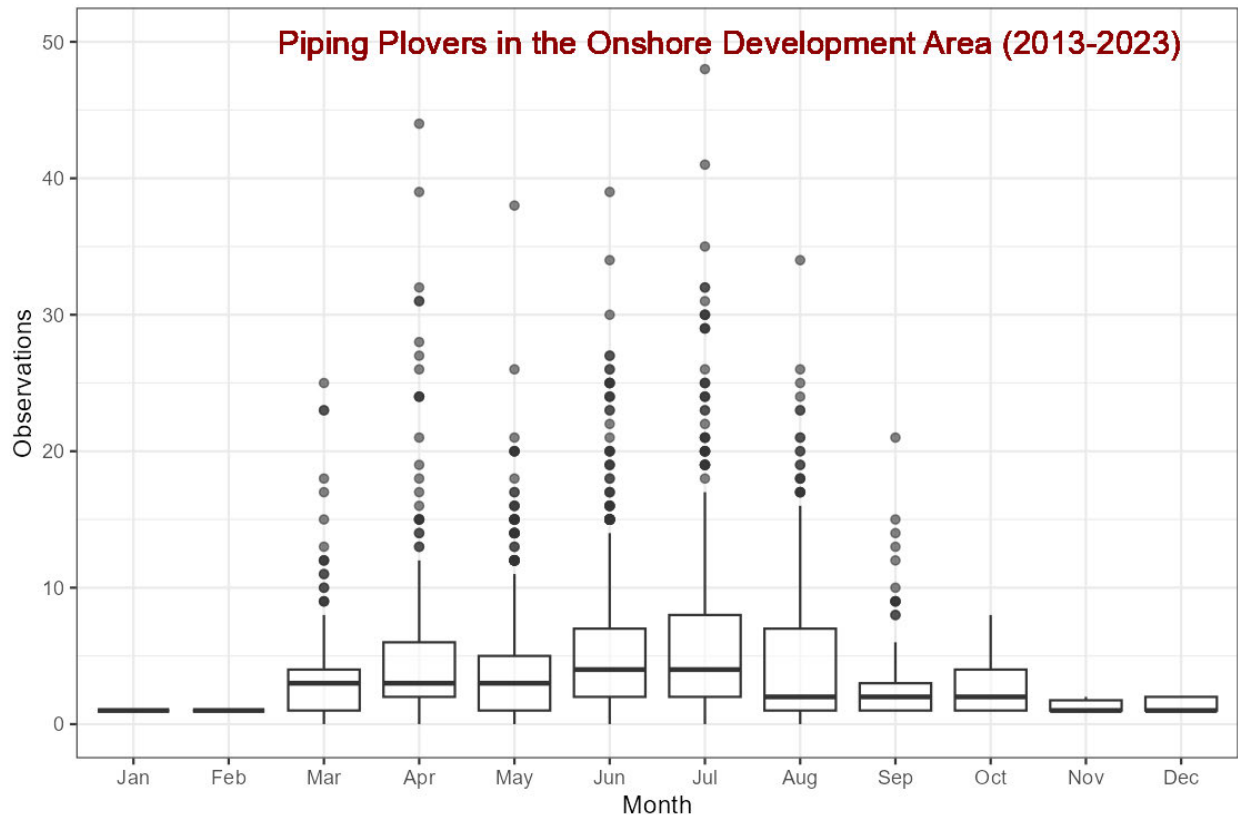


Figure 3-13: Monthly average of Piping Plover observations in the Onshore Development Area over ten years, derived from the eBird database (total detections, with duplicate list postings removed).

3.3.2.1.3 Red Knot

In 2014, USFWS listed the North Atlantic subspecies of Red Knot as *Threatened* under the ESA of 1973 (USFWS 2015). It is also listed as *Threatened* by New York State. The *rufa* subspecies breeds in the central and eastern Canadian Arctic and winters at sites as far south as Tierra del Fuego, Argentina. During both migrations, Red Knots use key staging and stopover areas to rest and feed where they utilize habitats including sandy coastal beaches, at or near tidal inlets, or the mouths of bays and estuaries, salt marshes, tidal mudflats, and sandy/gravel beaches where they feed on clams, crustaceans, and invertebrates.

The south shore of Long Island is an important stopover location during spring and fall Red Knot migration in New York. Red Knots are known to use Jamaica Bay, Far Rockaway, Long Beach, and Jones Beach (NYSDEC 2015a). The eBird database contains Red Knot detections on 966 days within the 15 km (9.3 mi) buffer of onshore facilities from 2013–2023 (Table 3-2), with most observations occurring in August (Figure 3-14). Although the buffer encompasses non-coastal areas, it is unlikely that Red Knots would be observed outside of beaches and estuaries. The Jones Beach Landfall Site overlaps with proposed Red Knot Critical Habitat, designated by the USFWS and referred to as the Jones Inlet unit. In addition, the USFWS Jamaica Bay unit is

southwest of Rockaway Beach Landfall Site within the Gateway National Recreation Area (Figure 3-15). Proposed Red Knot Critical Habitat units are specific areas that contain physical and or biological features that are essential to the conservation of Red Knots due to features such as, but not limited to, cover or shelter, and nutritional or physiological requirements (USFWS 2021). The New York Natural Heritage Bureau does not contain records of Red Knots in the Onshore Development Area.

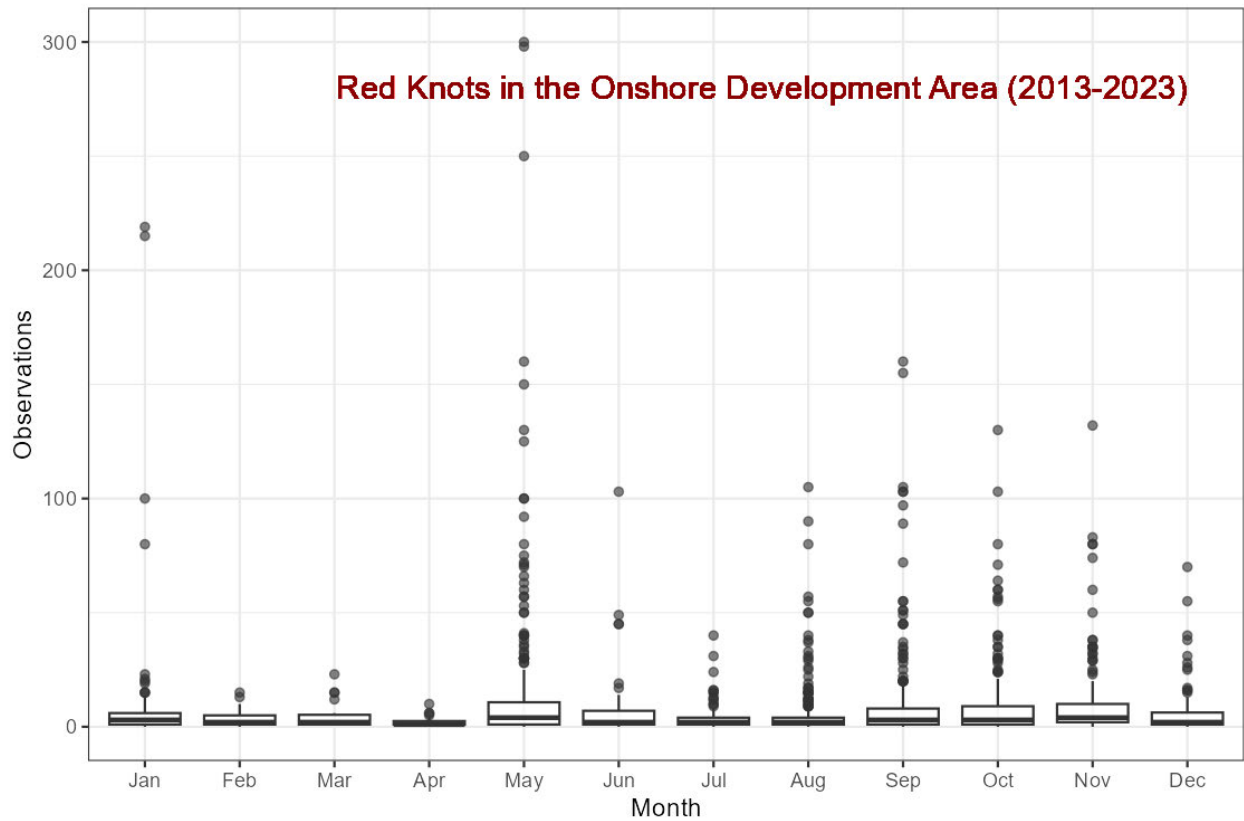


Figure 3-14: Monthly average of Red Knot observations in the Onshore Development Area over ten years, derived from the eBird database (total detections, with duplicate list postings removed).

3.3.2.1.4 Eastern Black Rail

The Eastern Black Rail is state-listed as *Endangered*, designated a *High Priority SGCN* (NYSWAP 2015), and is listed as *Threatened* under the ESA (USFWS 2020).

Multiple environmental stressors including development, predation, pollution, and invasive species are suspected to have contributed to the population decline in the eastern US over the past 20 years (NYSDEC Black Rail 2023). Eastern Black Rails are habitat specialists and have an extremely narrow suitability range. Suitable habitat consists of coastal wetlands characterized by shallow fresh to brackish water and dense emergent vegetation (USFWS 2020). While the extent of their migration is not well known, it is likely that most east coast populations migrate south in the fall (NYSDEC Black Rail 2023).

No Eastern Black Rail detections were reported in the vicinity of the onshore facilities in the eBird database between 2013 and 2023. Eastern Black Rails have historically bred on the south shore of Long Island at Oak Beach marsh, Long Beach and Lido Beach. The last confirmed breeding pair was recorded in 1968 at Oak Beach marsh and one individual was identified by sound during the second New York State Breeding Bird Atlas (2000-2005) at the same location (NYSDEC Black Rail 2023). The New York Natural Heritage Bureau does not contain records of Black Rails in the Onshore Development Area. Therefore, exposure of the Eastern Black Rail to onshore activities is highly unlikely.

3.3.2.1.5 Saltmarsh Sparrow

USFWS is currently reviewing the status of the Saltmarsh Sparrow and is expected to decide on whether or not the species warrants protection under the ESA by the end of 2024 (Gifford 2019). Saltmarsh Sparrow is listed as a *High Priority SGCN* by New York State. Saltmarsh Sparrows are habitat specialists and have an extremely narrow suitability range. Suitable habitat consists of high marsh vegetation with dense layers of thatch for nest construction and protection from tides (Hartley and Weldon 2020). The eBird database contains Saltmarsh Sparrow detections on 1,196 days within the 15 km (9.3 mi) buffer of the onshore facilities between 2013 and 2023 (Table 3-2), with the most frequent observations occurring in July (Figure 3-16). The New York Natural Heritage Bureau does not contain records of Saltmarsh Sparrows in the Onshore Development Area. During New York's Breeding Bird Atlas in 2000-2005 breeding saltmarsh sparrows were confirmed on the South Shore of Long Island (NYSDEC 2014). The Atlantic Coast Joint Venture has partnered with USFWS and NYSDEC to conserve Saltmarsh Sparrows and coastal marshes (ACJV 2022). The landfall sites are located on the south side of Rockaway Beach, Atlantic Beach, and Jones Beach Island, in highly developed areas. Suitable habitat for Saltmarsh Sparrow exists on the north side of these areas in the waters and marshes between Long Island and the barrier islands.

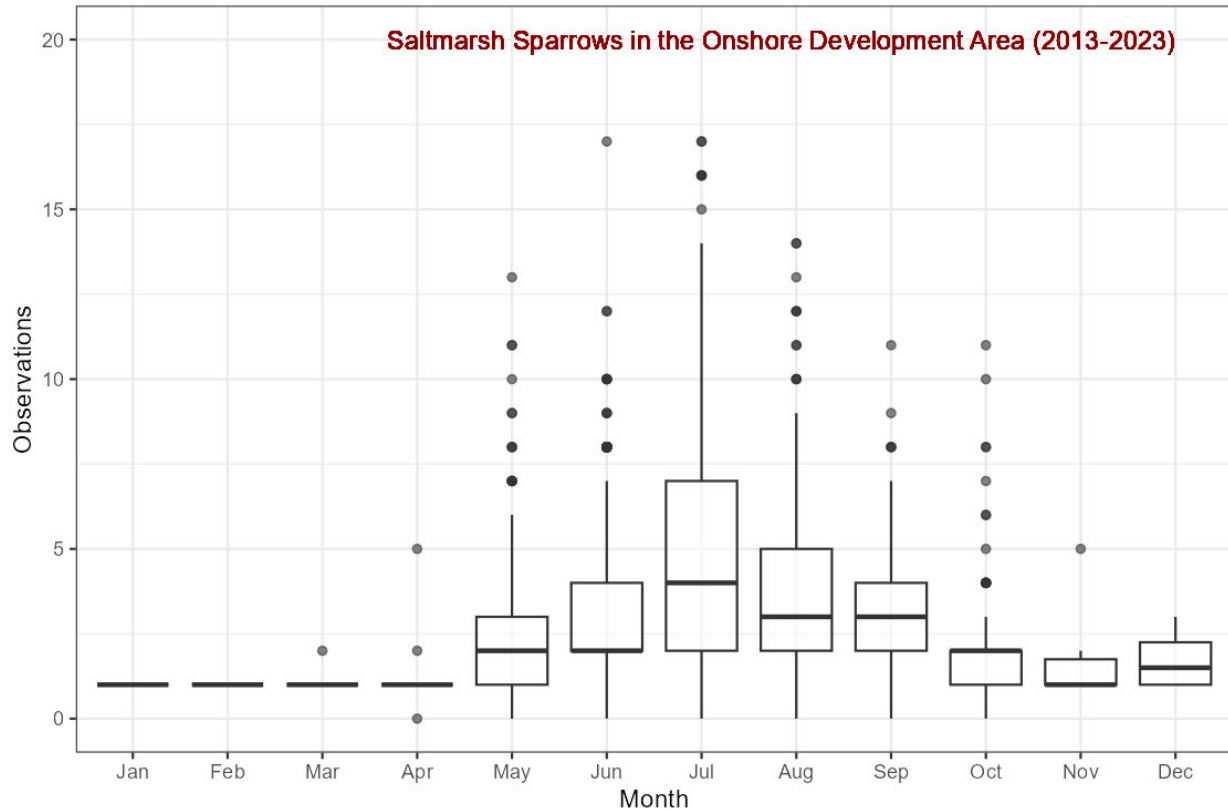


Figure 3-16: Monthly Average of Saltmarsh Sparrows observed in the Onshore Development Area over ten years, derived from the eBird database (total detections, with duplicate list postings removed).

3.3.2.1.6 Bald Eagle

Bald Eagles are federally protected under the BGEPA. Additionally, Bald Eagles are listed as *Threatened* in New York State. In the late 1960s Bald Eagles were nearly extirpated from New York. However, the population of Bald Eagles in New York is now on the rise as a result of protection and restoration measures that have been taken since the 1970s (NYSDEC 2015b). Onshore in New York, Bald Eagles are year-round residents, frequently nest in coastal hardwood forests, and congregate in larger rivers and estuaries in the winter, where water remains open and food sources are available year-round (NYSDEC 2015b). According to the NYSDEC, as of 2018, there were 8 known Bald Eagle nests on Long Island including a nest at Mill Pond in Centerport (Boyle 2018). The eBird database contains Bald Eagle detections on 1,571 days within the 15 km buffer of the onshore facilities from 2013–2023 (Table 3-2), with most observations occurring in spring and summer (Figure 3-17). The New York Natural Heritage Bureau database documents Bald Eagles “in the vicinity of” the Onshore Export Cable Route, confirming what is

shown by the eBird analysis.

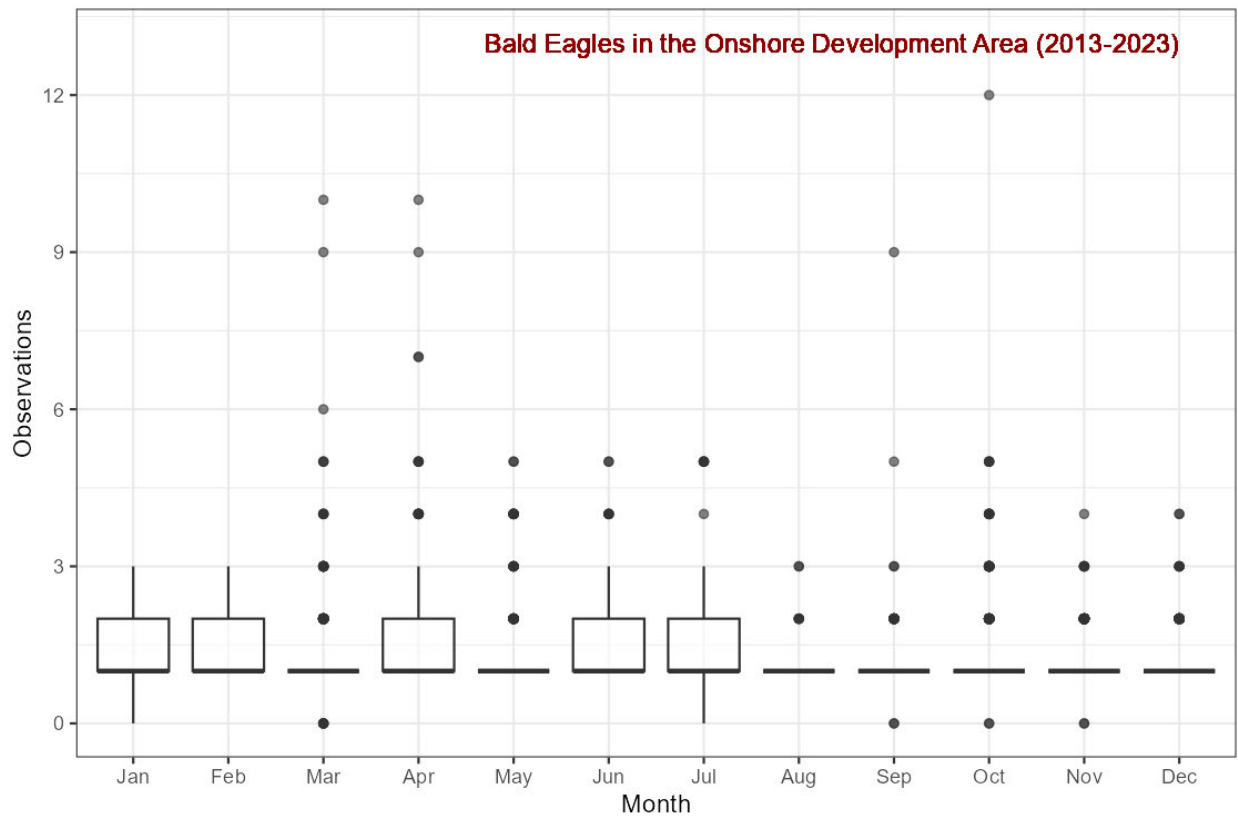


Figure 3-17: Monthly Average of Bald Eagles observed in the Onshore Development Area over ten years, derived from the eBird database (total detections, with duplicate list postings removed).

3.4 Summary and Conclusions

The co-location analysis found that, of the 17.6 km² Onshore Development Area (the onshore facilities plus the 50-m buffer), 93.4% was located in already developed areas. Where open water or wetland areas are crossed by proposed onshore cable routes, developed corridors along roadways are already present. Little to no vegetation is present at the POI locations. The landfall site(s) are proposed in existing developed areas such as parking lots. The available data on species potentially present in the Onshore Development Area indicate that federally protected birds (Roseate Tern, Piping Plover, Red Knot, and Bald Eagle) and state protected birds do occur. Because Vineyard Mid-Atlantic's proposed activities onshore are nearly completely co-located with existing areas of development, disturbance of important bird habitat will be very limited; therefore, exposure of birds to the onshore activities will be similarly limited.

Table 3-5: Species observed by eBird users within 15 km (9.3 mi) of onshore facilities in the last 10 years, along with their primary and general breeding habitats, as well as state and federal conservation listing statuses.

Common Name	Latin Name	Primary Habitat	General Breeding Habitat	New York Status ¹	Federal Listing	IPaC ²
Snow Goose	<i>Anser caerulescens</i>	Terrestrial	Grassland	-	-	-
Greater White-fronted Goose	<i>Anser albifrons</i>	Artificial, Terrestrial	Arable Land	-	-	-
Pink-footed Goose	<i>Anser brachyrhynchus</i>	Artificial, Terrestrial	Arable Land	-	-	-
Brant	<i>Branta bernicla</i>	Terrestrial	Grassland	-	-	-
Cackling Goose	<i>Branta hutchinsii</i>	Terrestrial	Grassland	-	-	-
Canada Goose	<i>Branta canadensis</i>	Terrestrial, Aquatic	Grassland, Wetland	-	-	-
Mute Swan	<i>Cygnus olor</i>	Aquatic	Coastal/Supratidal, Wetland	-	-	-
Wood Duck	<i>Aix sponsa</i>	Terrestrial, Aquatic	Forest, Wetland	-	-	-
Blue-winged Teal	<i>Spatula discors</i>	Freshwater	Wetland	-	-	-
Northern Shoveler	<i>Spatula clypeata</i>	Freshwater	Wetland	-	-	-
Gadwall	<i>Mareca strepera</i>	Freshwater	Wetland	-	-	-
Eurasian Wigeon	<i>Mareca penelope</i>	Freshwater	Wetland	-	-	-
American Wigeon	<i>Mareca americana</i>	Freshwater	Wetland	-	-	-
Mallard	<i>Anas platyrhynchos</i>	Aquatic	Marine, Wetland	-	-	-
American Black Duck	<i>Anas rubripes</i>	Freshwater	Wetland	High SGCN	-	-

Common Name	Latin Name	Primary Habitat	General Breeding Habitat	New York Status ¹	Federal Listing	IPaC ²
Northern Pintail	<i>Anas acuta</i>	Freshwater	Wetland	-	-	-
Green-winged Teal	<i>Anas crecca</i>	Freshwater	Wetland	-	-	-
Canvasback	<i>Aythya valisineria</i>	Freshwater	Wetland	-	-	-
Redhead	<i>Aythya americana</i>	Freshwater	Wetland	-	-	-
Ring-necked Duck	<i>Aythya collaris</i>	Freshwater	Wetland	-	-	-
Greater Scaup	<i>Aythya marila</i>	Marine	Marine	-	-	-
Lesser Scaup	<i>Aythya affinis</i>	Freshwater	Wetland	-	-	-
King Eider	<i>Somateria spectabilis</i>	Freshwater, Marine	Marine, Wetland	-	-	-
Common Eider	<i>Somateria mollissima</i>	Marine	Intertidal	-	-	V
Harlequin Duck	<i>Histrionicus histrionicus</i>	Marine	Maine, Intertidal	-	-	-
Surf Scoter	<i>Melanitta perspicillata</i>	Freshwater	Wetland	-	-	V
White-winged Scoter	<i>Melanitta deglandi</i>	Freshwater	Wetland	-	-	V
Black Scoter	<i>Melanitta americana</i>	Freshwater	Wetland	-	-	V
Long-tailed Duck	<i>Clangula hyemalis</i>	Terrestrial	Grassland	-	-	V
Bufflehead	<i>Bucephala albeola</i>	Terrestrial, Aquatic	Forest, Wetland	-	-	-
Common Goldeneye	<i>Bucephala clangula</i>	Terrestrial	Forest	-	-	-
Hooded Merganser	<i>Lophodytes cucullatus</i>	Terrestrial, Aquatic	Forest, Wetland	-	-	-
Common Merganser	<i>Mergus merganser</i>	Freshwater	Wetland	-	-	-

Common Name	Latin Name	Primary Habitat	General Breeding Habitat	New York Status ¹	Federal Listing	IPaC ²
Red-breasted Merganser	<i>Mergus serrator</i>	Freshwater	Wetland	-	-	V
Ruddy Duck	<i>Oxyura jamaicensis</i>	Freshwater	Wetland	-	-	-
Northern Bobwhite	<i>Colinus virginianus</i>	Terrestrial	Grassland	High SGCN	-	-
Pied-billed Grebe	<i>Podilymbus podiceps</i>	Freshwater	Wetland	T	-	-
Horned Grebe	<i>Podiceps auritus</i>	Freshwater	Wetland	-	-	-
Red-necked Grebe	<i>Podiceps grisegena</i>	Freshwater	Wetland	-	-	-
Rock Pigeon	<i>Columba livia</i>	Terrestrial	Artificial	-	-	-
Mourning Dove	<i>Zenaida macroura</i>	Terrestrial	Forest, Grassland, Shrubland I	-	-	-
Yellow-billed Cuckoo	<i>Coccyzus americanus</i>	Terrestrial	Forest	-	-	-
Black-billed Cuckoo	<i>Coccyzus erythrophthalmus</i>	Terrestrial	Forest, Shrubland	-	-	BCC
Common Nighthawk	<i>Chordeiles minor</i>	Terrestrial	Grassland	SC	-	-
Eastern Whip-poor-will	<i>Antrostomus vociferus</i>	Terrestrial	Grassland, Forest	SC	-	BCC
Chimney Swift	<i>Chaetura pelagica</i>	Terrestrial	Artificial, Forest	-	-	BCC
Ruby-throated Hummingbird	<i>Archilochus colubris</i>	Terrestrial	Forest	-	-	-
Clapper Rail	<i>Rallus crepitans</i>	Freshwater	Wetland	-	-	-
Common Gallinule	<i>Gallinula galeata</i>	Freshwater	Wetland	-	-	-
American Coot	<i>Fulica americana</i>	Freshwater	Wetland	-	-	-

Common Name	Latin Name	Primary Habitat	General Breeding Habitat	New York Status ¹	Federal Listing	IPaC ²
American Oystercatcher	<i>Haematopus palliatus</i>	Marine Intertidal	Intertidal	-	-	BCC
Black-bellied Plover	<i>Pluvialis squatarola</i>	Terrestrial	Grassland	-	-	-
Semipalmated Plover	<i>Charadrius semipalmatus</i>	Marine Intertidal	Intertidal	-	-	-
Piping Plover	<i>Charadrius melodus</i>	Coastal	Coastal/Supratidal, Wetland	E	T	-
Killdeer	<i>Charadrius vociferus</i>	Freshwater	Wetland	-	-	-
Whimbrel	<i>Numenius phaeopus</i>	Terrestrial, Aquatic	Coastal/Supratidal, Wetland	High SGCN	-	-
Hudsonian Godwit	<i>Limosa haemastica</i>	Terrestrial	Tundra	-	-	BCC
Ruddy Turnstone	<i>Arenaria interpres</i>	Terrestrial, Aquatic	Grassland, Wetland	-	-	BCC
Red Knot	<i>Calidris canutus</i>	Marine Intertidal	Tundra	T	T	-
Sanderling	<i>Calidris alba</i>	Terrestrial	Grassland	-	-	-
Dunlin	<i>Calidris alpina</i>	Intertidal, Freshwater	Intertidal, Wetland	-	-	-
Purple Sandpiper	<i>Calidris maritima</i>	Intertidal, Freshwater	Grassland, Marine, Wetland	-	-	BCC
Least Sandpiper	<i>Calidris minutilla</i>	Terrestrial, Freshwater	Forest, Grassland, Shrubland, Wetland	-	-	-
Pectoral Sandpiper	<i>Calidris melanotos</i>	Artificial, Marine	Tundra	-	-	-
Semipalmated Sandpiper	<i>Calidris pusilla</i>	Terrestrial, Aquatic	Grassland, Wetland	High SGCN	-	-

Common Name	Latin Name	Primary Habitat	General Breeding Habitat	New York Status ¹	Federal Listing	IPaC ²
Short-billed Dowitcher	<i>Limnodromus griseus</i>	Intertidal	Intertidal	High SGCN	-	BCC
American Woodcock	<i>Scolopax minor</i>	Terrestrial	Forest	-	-	-
Wilson's Snipe	<i>Gallinago delicata</i>	Terrestrial, Aquatic	Forest, Wetland	-	-	-
Spotted Sandpiper	<i>Actitis macularius</i>	Freshwater	Wetland	-	-	-
Solitary Sandpiper	<i>Tringa solitaria</i>	Terrestrial	Grassland	-	-	-
Greater Yellowlegs	<i>Tringa melanoleuca</i>	Terrestrial, Aquatic	Forest, Shrubland, Wetland	-	-	-
Willet	<i>Tringa semipalmata</i>	Coastal	Intertidal, Wetland	-	-	BCC
Lesser Yellowlegs	<i>Tringa flavipes</i>	Terrestrial, Aquatic	Shrubland, Wetland	-	-	BCC
Razorbill	<i>Alca torda</i>	Marine	Intertidal	-	-	V
Bonaparte's Gull	<i>Chroicocephalus philadelphia</i>	Marine	Intertidal	-	-	-
Black-headed Gull	<i>Chroicocephalus ridibundus</i>	Marine	Intertidal	-	-	-
Laughing Gull	<i>Leucophaeus atricilla</i>	Marine	Intertidal	-	-	-
Ring-billed Gull	<i>Larus delawarensis</i>	Terrestrial, Aquatic	Grassland, Wetland	-	-	V
Herring Gull	<i>Larus argentatus</i>	Terrestrial, Aquatic	Coastal, Intertidal	-	-	-
Iceland Gull	<i>Larus glaucoides</i>	Coastal	Coastal, Intertidal	-	-	-
Lesser Black-backed Gull	<i>Larus fuscus</i>	Coastal	Coastal, Intertidal	-	-	-
Glaucous Gull	<i>Larus hyperboreus</i>	Coastal	Coastal, Intertidal	-	-	-

Common Name	Latin Name	Primary Habitat	General Breeding Habitat	New York Status ¹	Federal Listing	IPaC ²
Great Black-backed Gull	<i>Larus marinus</i>	Coastal	Coastal, Marine	-	-	-
Least Tern	<i>Sternula antillarum</i>	Marine	Marine	T	-	-
Gull-billed Tern	<i>Gelochelidon nilotica</i>	Terrestrial, Aquatic	Coastal, Intertidal	-	-	BCC
Caspian Tern	<i>Hydroprogne caspia</i>	Marine	Marine	-	-	-
Roseate Tern	<i>Sterna dougallii dougalli</i>	Marine, Coastal	Intertidal	E	E	V
Common Tern	<i>Sterna hirundo</i>	Marine	Marine	T	-	-
Forster's Tern	<i>Sterna forsteri</i>	Marine	Marine	-	-	-
Royal Tern	<i>Thalasseus maximus</i>	Marine	Marine	-	-	V
Black Skimmer	<i>Rynchops niger</i>	Marine, Coastal	Supratidal, Brackish	SC	-	BCC
Red-throated Loon	<i>Gavia stellata</i>	Freshwater	Marine, Wetland	-	-	V
Common Loon	<i>Gavia immer</i>	Freshwater	Marine, Wetland	SC	-	V
Wilson's Storm-Petrel	<i>Oceanites oceanicus</i>	Marine	Coastal, Marine, Oceanic	-	-	V
Northern Gannet	<i>Morus bassanus</i>	Marine	Coastal, Marine, Oceanic	-	-	-
Great Cormorant	<i>Phalacrocorax carbo</i>	Aquatic	Forest, Marine, Wetland	-	-	-
Double-crested Cormorant	<i>Nannopterum auritum</i>	Marine	Marine	-	-	V
Brown Pelican	<i>Pelecanus occidentalis</i>	Marine	Marine	-	-	BCC

Common Name	Latin Name	Primary Habitat	General Breeding Habitat	New York Status ¹	Federal Listing	IPaC ²
American Bittern	<i>Botaurus lentiginosus</i>	Terrestrial, Aquatic	Wetland	SC	-	-
Least Bittern	<i>Ixobrychus exilis</i>	Freshwater	Wetland	T	-	-
Great Blue Heron	<i>Ardea herodias</i>	Freshwater	Wetland	-	-	-
Great Egret	<i>Ardea alba</i>	Terrestrial, Aquatic	Grassland, Wetland	-	-	-
Snowy Egret	<i>Egretta thula</i>	Freshwater	Wetland	-	-	-
Little Blue Heron	<i>Egretta caerulea</i>	Freshwater	Wetland	-	-	-
Green Heron	<i>Butorides virescens</i>	Freshwater	Wetland	-	-	-
Black-crowned Night-Heron	<i>Nycticorax nycticorax</i>	Terrestrial, Aquatic	Forest, Intertidal, Wetland	-	-	-
Yellow-crowned Night-Heron	<i>Nyctanassa violacea</i>	Terrestrial, Aquatic	Forest, Intertidal, Wetland	-	-	-
Glossy Ibis	<i>Plegadis falcinellus</i>	Freshwater	Wetland	-	-	-
Black Vulture	<i>Coragyps atratus</i>	Terrestrial	Artificial	-	-	-
Turkey Vulture	<i>Cathartes aura</i>	Terrestrial	Forest, Grassland, Shrubland	-	-	-
Osprey	<i>Pandion haliaetus</i>	Terrestrial, Aquatic	Forest, Coastal, Wetland	-	-	-
Northern Harrier	<i>Circus hudsonius</i>	Terrestrial	Forest, Grassland, Shrubland	T	-	-
Sharp-shinned Hawk	<i>Accipiter striatus</i>	Terrestrial	Forest, Grassland, Shrubland	-	-	-

Common Name	Latin Name	Primary Habitat	General Breeding Habitat	New York Status ¹	Federal Listing	IPaC ²
Cooper's Hawk	<i>Accipiter cooperii</i>	Terrestrial	Forest	-	-	-
Bald Eagle	<i>Haliaeetus leucocephalus</i>	Freshwater	Wetland	T	BGEPA	V
Red-shouldered Hawk	<i>Buteo lineatus</i>	Terrestrial	Forest	SC	-	-
Broad-winged Hawk	<i>Buteo platypterus</i>	Terrestrial	Forest	-	-	-
Red-tailed Hawk	<i>Buteo jamaicensis</i>	Terrestrial	Forest, Grassland, Shrubland	-	-	-
Eastern Screech-Owl	<i>Megascops asio</i>	Terrestrial	Forest	-	-	-
Great Horned Owl	<i>Bubo virginianus</i>	Terrestrial	Forest, Shrubland	-	-	-
Short-eared Owl	<i>Asio flammeus</i>	Terrestrial	Grassland	E	-	-
Belted Kingfisher	<i>Megaceryle alcyon</i>	Freshwater	Wetland	-	-	-
Yellow-bellied Sapsucker	<i>Sphyrapicus varius</i>	Terrestrial	Forest	-	-	-
Red-headed Woodpecker	<i>Melanerpes erythrocephalus</i>	Terrestrial	Forest	SC	-	BCC
Red-bellied Woodpecker	<i>Melanerpes carolinus</i>	Terrestrial	Forest	-	-	-
Downy Woodpecker	<i>Dryobates pubescens</i>	Terrestrial	Forest	-	-	-
Hairy Woodpecker	<i>Dryobates villosus</i>	Terrestrial	Forest	-	-	-
Pileated Woodpecker	<i>Dryocopus pileatus</i>	Terrestrial	Forest	-	-	-
Northern Flicker	<i>Colaptes auratus</i>	Terrestrial	Forest	-	-	-
American Kestrel	<i>Falco sparverius</i>	Terrestrial	Forest, Grassland, Shrubland	-	-	-

Common Name	Latin Name	Primary Habitat	General Breeding Habitat	New York Status ¹	Federal Listing	IPaC ²
Merlin	<i>Falco columbarius</i>	Terrestrial	Forest, Grassland, Shrubland	-	-	-
Peregrine Falcon	<i>Falco peregrinus</i>	Terrestrial	Rocky Cliffs	E	-	-
Eastern Wood-Pewee	<i>Contopus virens</i>	Terrestrial	Forest	-	-	-
Acadian Flycatcher	<i>Empidonax virescens</i>	Terrestrial	Forest	-	-	-
Alder Flycatcher	<i>Empidonax alnorum</i>	Terrestrial	Shrubland	-	-	-
Willow Flycatcher	<i>Empidonax traillii</i>	Terrestrial	Shrubland	-	-	-
Least Flycatcher	<i>Empidonax minimus</i>	Terrestrial	Forest	-	-	-
Eastern Phoebe	<i>Sayornis phoebe</i>	Terrestrial	Forest	-	-	-
Great Crested Flycatcher	<i>Myiarchus crinitus</i>	Terrestrial	Forest	-	-	-
Eastern Kingbird	<i>Tyrannus tyrannus</i>	Terrestrial	Forest, Shrubland	-	-	-
White-eyed Vireo	<i>Vireo griseus</i>	Terrestrial	Shrubland	-	-	-
Yellow-throated Vireo	<i>Vireo flavifrons</i>	Terrestrial	Forest	-	-	-
Blue-headed Vireo	<i>Vireo solitarius</i>	Terrestrial	Forest	-	-	-
Warbling Vireo	<i>Vireo gilvus</i>	Terrestrial, Aquatic	Forest, Wetland	-	-	-
Red-eyed Vireo	<i>Vireo olivaceus</i>	Terrestrial	Forest	-	-	-
Blue Jay	<i>Cyanocitta cristata</i>	Terrestrial	Forest	-	-	-
American Crow	<i>Corvus brachyrhynchos</i>	Terrestrial	Forest, Grassland, Shrubland	-	-	-

Common Name	Latin Name	Primary Habitat	General Breeding Habitat	New York Status ¹	Federal Listing	IPaC ²
Fish Crow	<i>Corvus ossifragus</i>	Terrestrial, Aquatic	Grassland, Wetland	-	-	-
Common Raven	<i>Corvus corax</i>	Terrestrial	Forest, Rocky Cliffs	-	-	-
Tufted Titmouse	<i>Baeolophus bicolor</i>	Terrestrial	Forest	-	-	-
Horned Lark	<i>Eremophila alpestris</i>	Terrestrial	Grassland, Shrubland	SC	-	-
Northern Rough-winged Swallow	<i>Stelgidopteryx serripennis</i>	Terrestrial	Rocky Cliffs, Wetland	-	-	-
Purple Martin	<i>Progne subis</i>	Terrestrial	Forest	-	-	-
Tree Swallow	<i>Tachycineta bicolor</i>	Freshwater	Wetland	-	-	-
Bank Swallow	<i>Riparia riparia</i>	Terrestrial, Aquatic	Grassland, Wetland	-	-	-
Barn Swallow	<i>Hirundo rustica</i>	Terrestrial, Aquatic	Grassland, Wetland	-	-	-
Cliff Swallow	<i>Petrochelidon pyrrhonota</i>	Artificial, Terrestrial	Arable Land	-	-	-
Ruby-crowned Kinglet	<i>Corthylio calendula</i>	Terrestrial	Forest	-	-	-
Golden-crowned Kinglet	<i>Regulus satrapa</i>	Terrestrial	Forest	-	-	-
Red-breasted Nuthatch	<i>Sitta canadensis</i>	Terrestrial	Forest	-	-	-
White-breasted Nuthatch	<i>Sitta carolinensis</i>	Terrestrial	Forest	-	-	-
Brown Creeper	<i>Certhia americana</i>	Terrestrial	Forest	-	-	-
Blue-gray Gnatcatcher	<i>Polioptila caerulea</i>	Terrestrial	Forest	-	-	-
House Wren	<i>Troglodytes aedon</i>	Terrestrial	Forest, Shrubland	-	-	-

Common Name	Latin Name	Primary Habitat	General Breeding Habitat	New York Status ¹	Federal Listing	IPaC ²
Winter Wren	<i>Troglodytes hiemalis</i>	Terrestrial	Forest	-	-	-
Marsh Wren	<i>Cistothorus palustris</i>	Freshwater	Wetland	-	-	-
Carolina Wren	<i>Thryothorus ludovicianus</i>	Terrestrial	Forest	-	-	-
European Starling	<i>Sturnus vulgaris</i>	Terrestrial	Forest, Grassland, Shrubland	-	-	-
Gray Catbird	<i>Dumetella carolinensis</i>	Terrestrial	Shrubland	-	-	-
Brown Thrasher	<i>Toxostoma rufum</i>	Terrestrial	Shrubland	High SGCN	-	-
Northern Mockingbird	<i>Mimus polyglottos</i>	Terrestrial	Shrubland	-	-	-
Eastern Bluebird	<i>Sialia sialis</i>	Terrestrial	Forest	-	-	-
Veery	<i>Catharus fuscescens</i>	Terrestrial	Forest	-	-	-
Swainson's Thrush	<i>Catharus ustulatus</i>	Terrestrial	Forest	-	-	-
Hermit Thrush	<i>Catharus guttatus</i>	Terrestrial	Forest	-	-	-
Wood Thrush	<i>Hylocichla mustelina</i>	Terrestrial	Forest	-	-	BCC
American Robin	<i>Turdus migratorius</i>	Terrestrial	Forest	-	-	-
Cedar Waxwing	<i>Bombycilla cedrorum</i>	Terrestrial	Forest	-	-	-
House Sparrow	<i>Passer domesticus</i>	Terrestrial	Forest, Grassland, Shrubland	-	-	-
American Pipit	<i>Anthus rubescens</i>	Terrestrial	Grassland, Rocky Cliffs	-	-	-

Common Name	Latin Name	Primary Habitat	General Breeding Habitat	New York Status ¹	Federal Listing	IPaC ²
House Finch	<i>Haemorhous mexicanus</i>	Terrestrial	Shrubland	-	-	-
Purple Finch	<i>Haemorhous purpureus</i>	Terrestrial	Forest	-	-	-
Common Redpoll	<i>Acanthis flammea</i>	Terrestrial	Forest	-	-	-
Red Crossbill	<i>Loxia curvirostra</i>	Terrestrial	Forest	-	-	-
Pine Siskin	<i>Spinus pinus</i>	Terrestrial	Forest	-	-	-
American Goldfinch	<i>Spinus tristis</i>	Terrestrial	Forest, Grassland, Shrubland	-	-	-
Snow Bunting	<i>Plectrophenax nivalis</i>	Terrestrial	Grassland	-	-	-
Chipping Sparrow	<i>Spizella passerina</i>	Terrestrial	Forest, Grassland, Shrubland	-	-	-
Field Sparrow	<i>Spizella pusilla</i>	Terrestrial	Forest, Grassland, Shrubland	-	-	-
American Tree Sparrow	<i>Spizelloides arborea</i>	Terrestrial, Aquatic	Grassland, Shrubland, Wetland	-	-	-
Fox Sparrow	<i>Passerella iliaca</i>	Terrestrial	Forest	-	-	-
Dark-eyed Junco	<i>Junco hyemalis</i>	Terrestrial	Forest	-	-	-
White-crowned Sparrow	<i>Zonotrichia leucophrys</i>	Terrestrial	Forest, Grassland, Shrubland	-	-	-
White-throated Sparrow	<i>Zonotrichia albicollis</i>	Terrestrial	Forest, Shrubland	-	-	-
Vesper Sparrow	<i>Pooecetes gramineus</i>	Terrestrial	Grassland	SC	-	-

Common Name	Latin Name	Primary Habitat	General Breeding Habitat	New York Status ¹	Federal Listing	IPaC ²
Seaside Sparrow	<i>Ammospiza maritima</i>	Marine Intertidal	Salt Marshes	SC	-	-
Saltmarsh Sparrow	<i>Ammodramus caudacutus</i>	Marine Intertidal	Salt Marshes	High SGCN	-	-
Savannah Sparrow	<i>Passerculus sandwichensis</i>	Terrestrial	Artificial, Terrestrial	-	-	-
Song Sparrow	<i>Melospiza melodia</i>	Terrestrial	Artificial, Terrestrial	-	-	-
Lincoln's Sparrow	<i>Melospiza lincolnii</i>	Terrestrial	Grassland, Temperate	-	-	-
Swamp Sparrow	<i>Melospiza georgiana</i>	Freshwater	Wetland	-	-	-
Eastern Towhee	<i>Pipilo erythrophthalmus</i>	Terrestrial	Forest	-	-	-
Yellow-breasted Chat	<i>Icteria virens</i>	Terrestrial	Forest, Grassland, Shrubland	SC	-	-
Bobolink	<i>Dolichonyx oryzivorus</i>	Terrestrial	Grassland	High SGCN	-	BCC
Eastern Meadowlark	<i>Sturnella magna</i>	Terrestrial	Grassland, Shrubland	High SGCN	-	-
Orchard Oriole	<i>Icterus spurius</i>	Terrestrial	Forest, Savanna	-	-	-
Baltimore Oriole	<i>Icterus galbula</i>	Terrestrial	Forest, Grassland	-	-	-
Red-winged Blackbird	<i>Agelaius phoeniceus</i>	Freshwater	Wetland	-	-	-
Brown-headed Cowbird	<i>Molothrus ater</i>	Terrestrial	Forest, Grassland	-	-	-
Rusty Blackbird	<i>Euphagus carolinus</i>	Freshwater	Wetland	High SGCN	-	BCC

Common Name	Latin Name	Primary Habitat	General Breeding Habitat	New York Status ¹	Federal Listing	IPaC ²
Common Grackle	<i>Quiscalus quiscula</i>	Terrestrial	Forest, Shrubland, Wetland	-	-	-
Boat-tailed Grackle	<i>Quiscalus major</i>	Marine Coastal	Supratidal	-	-	-
Ovenbird	<i>Seiurus aurocapilla</i>	Terrestrial	Forest	-	-	-
Worm-eating Warbler	<i>Helmitheros vermivorum</i>	Terrestrial	Forest	-	-	-
Louisiana Waterthrush	<i>Parkesia motacilla</i>	Terrestrial, Aquatic	Forest, Wetland	-	-	-
Northern Waterthrush	<i>Parkesia noveboracensis</i>	Freshwater	Wetland	-	-	-
Blue-winged Warbler	<i>Vermivora cyanoptera</i>	Terrestrial	Grassland	-	-	BCC
Black-and-white Warbler	<i>Mniotilta varia</i>	Terrestrial	Forest	-	-	-
Prothonotary Warbler	<i>Protonotaria citrea</i>	Terrestrial	Forest	High SGCN	-	BCC
Tennessee Warbler	<i>Leiothlypis peregrina</i>	Terrestrial	Forest, Shrubland	-	-	-
Orange-crowned Warbler	<i>Leiothlypis celata</i>	Terrestrial	Shrubland	-	-	-
Nashville Warbler	<i>Leiothlypis ruficapilla</i>	Terrestrial	Forest	-	-	-
Connecticut Warbler	<i>Oporornis agilis</i>	Terrestrial	Forest	-	-	-
Kentucky Warbler	<i>Geothlypis formosa</i>	Freshwater	Wetland	High SGCN	-	BCC
Common Yellowthroat	<i>Geothlypis trichas</i>	Freshwater	Wetland	-	-	-
Hooded Warbler	<i>Setophaga citrina</i>	Terrestrial	Forest	-	-	-

Common Name	Latin Name	Primary Habitat	General Breeding Habitat	New York Status ¹	Federal Listing	IPaC ²
American Redstart	<i>Setophaga ruticilla</i>	Terrestrial	Forest	-	-	-
Cape May Warbler	<i>Setophaga tigrina</i>	Terrestrial	Forest	-	-	-
Northern Parula	<i>Setophaga americana</i>	Terrestrial	Forest	-	-	-
Magnolia Warbler	<i>Setophaga magnolia</i>	Terrestrial	Forest	-	-	-
Bay-breasted Warbler	<i>Setophaga castanea</i>	Terrestrial	Forest	High SGCN	-	-
Blackburnian Warbler	<i>Setophaga fusca</i>	Terrestrial	Forest	-	-	-
Yellow Warbler	<i>Setophaga petechia</i>	Terrestrial	Forest, Shrubland	-	-	-
Chestnut-sided Warbler	<i>Setophaga pensylvanica</i>	Terrestrial	Forest, Shrubland	-	-	-
Blackpoll Warbler	<i>Setophaga striata</i>	Terrestrial	Forest	-	-	-
Black-throated Blue Warbler	<i>Setophaga caerulescens</i>	Terrestrial	Forest	-	-	-
Palm Warbler	<i>Setophaga palmarum</i>	Freshwater	Wetland	-	-	-
Pine Warbler	<i>Setophaga pinus</i>	Terrestrial	Forest	-	-	-
Yellow-rumped Warbler	<i>Setophaga coronata</i>	Terrestrial	Forest	-	-	-
Prairie Warbler	<i>Setophaga discolor</i>	Terrestrial	Shrubland	-	-	BCC
Black-throated Green Warbler	<i>Setophaga virens</i>	Terrestrial	Forest	-	-	-
Canada Warbler	<i>Cardellina canadensis</i>	Terrestrial	Forest	High SGCN	-	BCC
Wilson's Warbler	<i>Cardellina pusilla</i>	Terrestrial	Forest, Grassland,	-	-	-

Common Name	Latin Name	Primary Habitat	General Breeding Habitat	New York Status ¹	Federal Listing	IPaC ²
			Shrubland			
Scarlet Tanager	<i>Piranga olivacea</i>	Terrestrial	Forest	-	-	-
Northern Cardinal	<i>Cardinalis cardinalis</i>	Terrestrial	Shrubland	-	-	-
Rose-breasted Grosbeak	<i>Pheucticus ludovicianus</i>	Terrestrial	Forest	-	-	-
Blue Grosbeak	<i>Passerina caerulea</i>	Terrestrial	Forest	-	-	-
Indigo Bunting	<i>Passerina cyanea</i>	Terrestrial	Forest	-	-	-
<p>E = Endangered, T = Threatened, SC = Special Concern, BCC = USFWS Bird of Conservation Concern, V = non-BCC vulnerable, () = candidate species for Federal listing, - = not applicable, BGEPA = Bald and Golden Eagle Protection Act, High SGCN= High Priority Species of Greatest Conservation Need ¹ Data from New York's Endangered, Threatened, and Special Concern Fish and Wildlife Species https://www.dec.ny.gov/animals/7494.html ² IPaC is a project planning tool that streamlines the USFWS environmental review process by providing information to assist in determining how proposed activities may impact sensitive natural resources. Data from the online USFWS IPaC tool, available at: https://ipac.ecosphere.fws.gov.</p>						

4 Offshore Assessment: Results

BRI's assessment of risk to avian resources in the offshore environment considers the risks that are posed during the construction, operations and maintenance, and decommissioning phases of Vineyard Mid-Atlantic.

Regional context is crucial for understanding how birds may be affected by Vineyard Mid-Atlantic's offshore activities. This regional context is provided in Section 4.1.

The results of BRI's offshore assessment are presented first for non-marine migratory birds (Section 4.2), then for marine birds (Section 4.3), and lastly for protected species (Section 4.4). Non-marine migratory birds and marine birds are assessed by taxonomic group, while federally listed and candidate species are assessed individually. Each assessment includes an overview of relevant life history and conservation status; an exposure assessment and determination; a behavioral vulnerability assessment and determination (including vulnerability to collision and displacement); and a final risk determination.

A summary table of the results of BRI's avian offshore risk assessment (Table 4-25) is provided in Section 4.5. A detailed description and explanation of avian offshore assessment methods is provided in Section 5.

4.1 Regional Context

The New York Bight is a geographic region of the Mid-Atlantic US coast that spans a roughly triangular area from Long Island in the northeast, to the Hudson River and Raritan River estuaries in the northwest, to Cape May in the southwest. The seafloor in this region is characterized by a broad expanse of gently sloping, sandy-bottomed continental shelf. Beyond the shelf edge, the continental slope descends rapidly to the deeper Atlantic basin around 2,600 m (8,530 ft) below sea level (GEBCO 2021). This gentle, uniform shelf is notably interrupted by the Hudson Canyon, a submarine canyon that begins as a shallow depression in the seafloor and eventually deepens and broadens to form a break in the continental slope 2 km (3.2 mi) deep. Hudson Canyon's complex bathymetry, freshwater inputs, upwelling, and nutrient cycling make it an important marine biodiversity hotspot that attracts birds with the presence of forage fish. The canyon begins approximately 160 km (100 mi) southeast of New York City.

Taking a broader geographic view, the New York Bight is situated within the larger Mid-Atlantic Bight from Cape Cod, MA, to Cape Hatteras, NC. Most of this Mid-Atlantic coastal region is bathed in cool Arctic waters introduced by the Labrador Current. At the southern end of this region, around Cape Hatteras, these cool waters collide with the warmer waters of the Gulf Stream. The Mid-Atlantic region experiences a strong seasonal cycle in temperature, with SSTs spanning a wide range of 3 to 30 °C (37 to 86 °F; Williams et al. 2015).

Migrant terrestrial birds may follow the coastline during migration or choose more direct flight routes over expanses of open water. Many marine birds, such as sea ducks, make annual migrations up and down the US Atlantic coast, taking them directly through the New York Bight in spring and/or fall on their way to and from breeding sites farther north, while other species groups, notably gulls and terns, breed in the area during spring and summer. Other summer residents, such as shearwaters and storm-petrels, visit from the Southern Hemisphere (where they breed during the austral summer). In the fall, many of the summer residents leave the area and migrate south to warmer regions and are replaced by species that breed farther north and winter in the Mid-Atlantic. This interplay of migratory birds arriving, departing, or merely passing through results in a complex ecosystem where the community composition shifts regularly and temporal and geographic patterns are highly variable. According to the MDAT model outputs, the modeled abundance of birds in general indicates that they are mostly concentrated along the shores of Long Island and New Jersey (Figure 4-1).

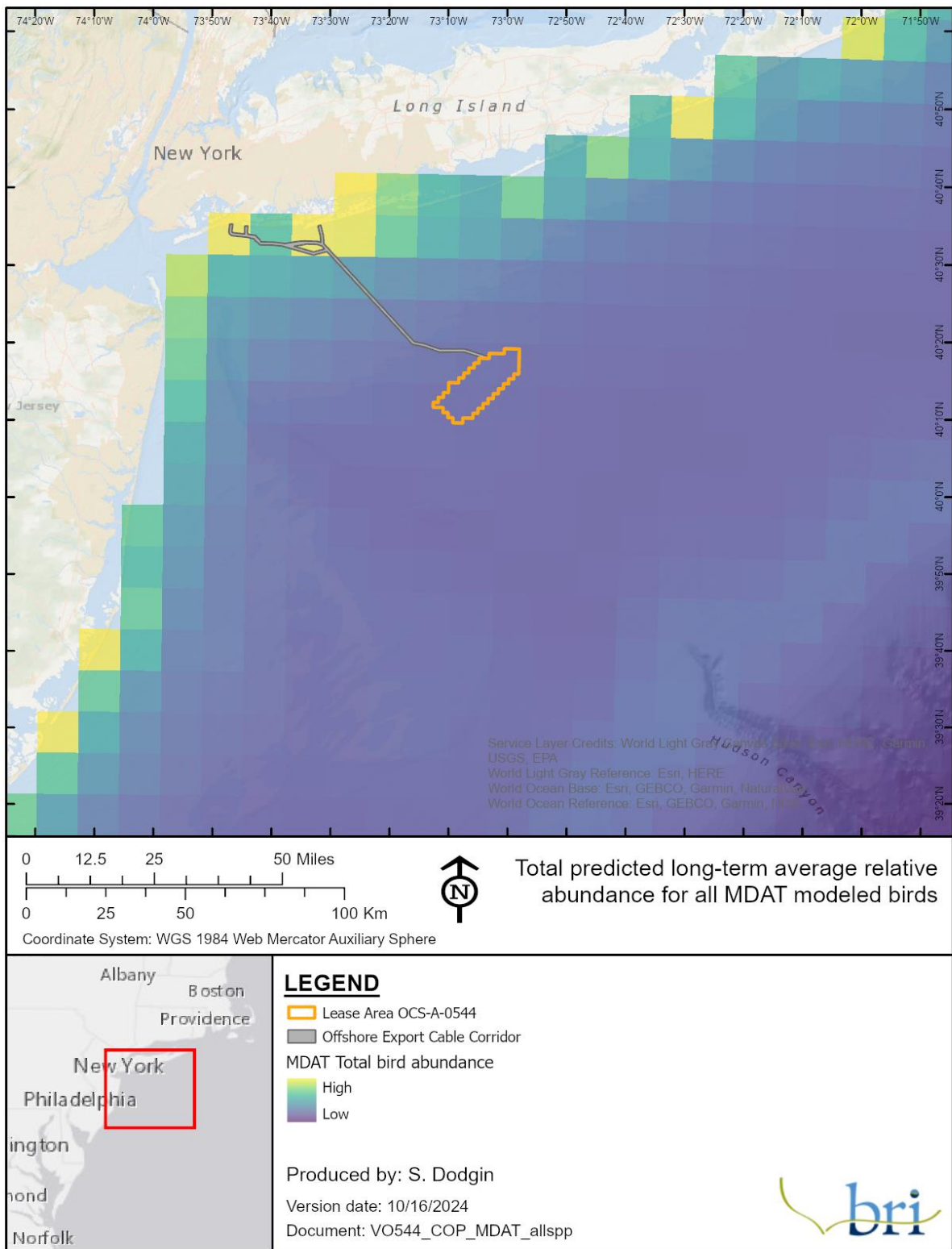


Figure 4-1: All-bird abundance estimates from the MDAT models.

The NY Bight surveys resulted in observations of 66 bird species in the survey area (Table 4-1). An additional five protected species that were not detected in the surveys, but are known to occur in the area, are included at the bottom of Table 4-1.

Four bird species listed under the ESA are present in the region (the Piping Plover, Red Knot, Black-capped Petrel, and Roseate Tern). Piping Plovers nest on beaches along the Long Island and New Jersey coasts in summer and also migrate through the area to and from more northern breeding sites in the spring and fall. Red Knots pass through the region during migration in transit to and from far northern breeding sites or South American overwintering areas, and Long Island is an important stopover location with critical habitat designated by USFWS. Just southwest of the New York Bight, Delaware Bay is a critical staging area for Red Knots during northbound migration. Roseate Terns migrate through the New York Bight and have important breeding sites east of Long Island (e.g., Great Gull Island in New York and Ram Island in Massachusetts). Black-capped Petrels breed in the Caribbean, but, during their non-breeding season, individuals occur along the shelf edge of the southeastern US Atlantic coast, commonly ranging as far north as Cape Hatteras and occasionally to the New York Bight.

Two eagle species are protected under the BGEPA, the Bald Eagle (*Haliaeetus leucocephalus*) and the Golden Eagle (*Aquila chrysaetos*). Bald Eagles are broadly distributed across North America, including the entire US Atlantic coast, and are present year-round in New Jersey. Golden Eagles are comparatively rare in the eastern US and those that are resident are concentrated in inland and coastal states of the southeastern US, generally using inland migration routes to reach breeding areas in eastern Canada. As such, Golden Eagles are not discussed further in the offshore assessment.

Table 4-1: Avian species recorded offshore of New York in the NY Bight survey area, cross-referenced with the US Fish and Wildlife Service (USFWS) Information for Planning and Consultation (IPaC) database.

Common Name	Latin Name	New York Listing ¹	Federal Listing	IPaC ²
Non marine Migratory Birds				
Grebes and Waterfowl				
American Black Duck	<i>Anas rubripes</i>	High SGCN	-	-
Canada Goose	<i>Branta canadensis</i>	-	-	-
Gadwall	<i>Mareca strepera</i>	-	-	-
Mallard	<i>Anas platyrhynchos</i>	-	-	-
Tundra Swan	<i>Cygnus columbianus</i>	-	-	-
Bufflehead	<i>Bucephala albeola</i>	-	-	-
Common Goldeneye	<i>Bucephala clangula</i>	-	-	-
Lesser Scaup	<i>Aythya affinis</i>	-	-	-
Horned Grebe	<i>Podiceps auritus</i>	-	-	-
Shorebirds				
Black-bellied Plover	<i>Pluvialis squatarola</i>	-	-	-

Common Name	Latin Name	New York Listing ¹	Federal Listing	IPaC ²
Semipalmated Sandpiper	<i>Calidris pusilla</i>	High SGCN	-	-
Wading Birds				
Great Blue Heron	<i>Ardea herodias</i>	-	-	-
Raptors				
Osprey	<i>Pandion haliaetus</i>	SC	-	-
Nightjars and allies				
Common Nighthawk	<i>Chordeiles minor</i>	SC	-	-
Marine Birds				
Sea Ducks				
Black Scoter	<i>Melanitta americana</i>	-	-	V
Common Eider	<i>Somateria mollissima</i>	-	-	V
Common Merganser	<i>Mergus Merganser</i>	-	-	-
Long-tailed Duck	<i>Clangula hyemalis</i>	-	-	V
Red-breasted Merganser	<i>Mergus serrator</i>	-	-	V
Surf Scoter	<i>Melanitta perspicillata</i>	-	-	V
White-winged Scoter	<i>Melanitta deglandi</i>	-	-	V
Phalaropes				
Red Phalarope	<i>Phalaropus fulicarius</i>	-	-	-
Red-necked Phalarope	<i>Phalaropus lobatus</i>	-	-	V
Auks				
Atlantic Puffin	<i>Fratercula arctica</i>	-	-	-
Black Guillemot	<i>Cephus grylle</i>	-	-	-
Common Murre	<i>Uria aalge</i>	-	-	V
Dovekie	<i>Alle alle</i>	-	-	V
Razorbill	<i>Alca torda</i>	-	-	V
Gulls, Jaegers, and Skuas				
Bonaparte's Gull	<i>Chroicocephalus philadelphia</i>	-	-	-
Little Gull	<i>Hydrocoloeus minutus</i>	-	-	-
Black-legged Kittiwake	<i>Rissa tridactyla</i>	-	-	V
Laughing Gull	<i>Leucophaeus atricilla</i>	-	-	-
Ring-billed Gull	<i>Larus delawarensis</i>	-	-	-
Glaucous Gull	<i>Larus hyperboreus</i>	-	-	-
Great Black-backed Gull	<i>Larus marinus</i>	-	-	-
Herring Gull	<i>Larus argentatus</i>	-	-	-
Iceland Gull	<i>Larus glaucoides</i>	-	-	-
Lesser Black-backed Gull	<i>Larus fuscus</i>	-	-	-
Great Skua	<i>Stercorarius skua</i>	-	-	-
Parasitic Jaeger	<i>Stercorarius parasiticus</i>	-	-	-

Common Name	Latin Name	New York Listing ¹	Federal Listing	IPaC ²
Pomarine Jaeger	<i>Stercorarius pomarinus</i>	-	-	V ⁴
South Polar Skua	<i>Stercorarius maccormicki</i>	-	-	-
Terns				
Black Tern	<i>Chlidonias niger</i>	-	-	-
Least Tern	<i>Sternula antillarum</i>	T	-	-
Artic Tern	<i>Sterna paradisaea</i>	-	-	-
Common Tern	<i>Sterna hirundo</i>	T	-	-
Forster's Tern	<i>Sterna forsteri</i>	-	-	-
Roseate Tern	<i>Sterna dougallii</i>	E	E	E
Royal Tern	<i>Thalasseus maximus</i>	-	-	-
Loons				
Common Loon	<i>Gavia immer</i>	SC	-	V
Red-throated Loon	<i>Gavia stellata</i>	-	-	V
Shearwaters, Petrels, and Storm-petrels				
Audubon's Shearwater	<i>Puffinus lherminieri</i>	-	-	-
Cory's Shearwater	<i>Calonectris diomedea</i>	-	-	BCC
Great Shearwater	<i>Ardenna gravis</i>	-	-	-
Manx Shearwater	<i>Puffinus puffinus</i>	-	-	-
Northern Fulmar	<i>Fulmarus glacialis</i>	-	-	-
Sooty Shearwater	<i>Ardenna grisea</i>	-	-	-
Trindade Petrel	<i>Pterodroma arminjoniana</i>	-	-	-
Band-rumped Storm-Petrel	<i>Hydrobates castro</i>	-	-	-
Leach's Storm-Petrel	<i>Hydrobates leucorhous</i>	-	-	-
White-faced Storm-Petrel	<i>Pelagodroma marina</i>	-	-	-
Wilson's Storm-Petrel	<i>Oceanites oceanicus</i>	-	-	V
Black-capped Petrel	<i>Pterodroma hasitata</i>	-	E	-
Gannets, Cormorants, and Pelicans				
Northern Gannet	<i>Morus bassanus</i>	-	-	-
Double-crested Cormorant	<i>Phalacrocorax auritus</i>	-	-	-
Brown Pelican	<i>Pelecanus occidentalis</i>	-	-	-
Potentially Occurring Protected Species and Species of Concern³				
Piping Plover	<i>Charadrius m. melodus</i>	E	T	-
Red Knot	<i>Calidris canutus rufa</i>	T	T	-
Eastern Black Rail	<i>Laterallus jamaicensis</i>	E	T	-
Saltmarsh Sparrow	<i>Ammodramus caudacutus</i>	High SGCN	. ⁵	-
Bald Eagle	<i>Haliaeetus leucocephalus</i>	T	BGEPA	-

Common Name	Latin Name	New York Listing ¹	Federal Listing	IPaC ²
<p>E = Endangered, T = Threatened, SC = Special Concern, BCC = USFWS Bird of Conservation Concern, V = non-BCC vulnerable, - = not applicable, BGEPA = Bald and Golden Eagle Protection Act, SGCN = Species of Greatest Conservation Need</p> <p>¹ Data from New York's List of Endangered, Threatened and Special Concern Fish and Wildlife Species, available at: https://www.dec.ny.gov/animals/7494.html</p> <p>² IPaC is a project planning tool that streamlines the USFWS environmental review process by providing information to assist in determining how proposed activities may impact sensitive natural resources. Data from the online USFWS IPaC tool, available at: https://ipac.ecosphere.fws.gov.</p> <p>³ These protected species were not detected in the NY Bight survey area, but they are included in this list as species of particular concern for the development of Vineyard Mid-Atlantic.</p> <p>⁴ Pomarine Jaeger was not included on the IPaC report for the Offshore Development Area but was included in the IPaC for the Onshore Development Area.</p> <p>⁵ The USFWS is reviewing the status of Saltmarsh Sparrow and will make a determination of whether or not to propose the species for protection under the ESA.</p>				

4.2 Non-Marine Migratory Birds

4.2.1 Grebes and Waterfowl

Minor Taxa Groups: Grebes (Podicipediformes: Podicipedidae); Waterfowl (Anseriformes: Anatidae, subgroups Anatini (dabbling), Aythyini (pochards), Anserini (geese), and Cygnini (swans); Mergini (sea ducks) are discussed separately, below)

Collision Risk Determination: **Minimal**

Displacement Risk Determination: **Minimal**

4.2.1.1 Overview

Distribution and Habitat Preferences: Grebes are present in the New York Bight region only during winter, as eastern North American species breed primarily in Canada (Winkler et al. 2020), aside from Pied-billed Grebes (*Podilymbus podiceps*) that may breed in freshwater wetlands similar to waterfowl. Grebes are adept diving birds that use relatively shallow freshwater lakes and rivers and nearshore marine habitats (≤ 20 m [66 ft] depth), although some grebe species are capable of diving to greater depths (Muller and Storer 2020; Stedman 2020; Stout and Neuchterlein 2020). Grebes are very efficient swimmers, and rarely located outside of wetlands or estuarine waters.

Dabbling ducks, geese, and swans are coastal or inland breeding species with broad spatial distributions that generally breed far north of the New York Bight region, aside from American Black Ducks, Mallards, and Mute Swans (Baldassarre 2014). These three species may breed in coastal wetlands of the New York Bight region, and some species of waterfowl (including sea ducks, which we discuss separately in section 4.3.1) can be found in coastal regions during winter. All feed primarily in freshwater or brackish habitats on vegetation and invertebrates accessible from the surface of the water, and, as such, are rarely located in open marine habitats (Baldassarre 2014). Dabbling ducks, geese, and swans are all capable of walking well on land and may feed far from water. Diving ducks (such as Pochards) feed in shallow habitats generally <10

m deep (Baldassarre 2014) and are unlikely to be present in the Lease Area at any time of the year.

Behavior and Ecology: Grebes and waterfowl feed in nearshore habitats on vegetation and aquatic invertebrates, often from the water’s surface, but also by diving. Waterfowl are highly gregarious, forming large flocks, and are the focus of extensive management efforts due to hunting. Grebes, however, are more solitary and rarely form large flocks, although some species are loosely colonial during the breeding season.

Reproduction: Grebes build nests in protected wetlands by piling aquatic vegetation into mounds that are barely higher than the surface of the water. They lay 2–3 eggs on the top of the mound, and adults trade off during incubation. Young are well-insulated at hatch, yet both adults will carry them on their backs and feed them until they become capable of feeding themselves.

Waterfowl and grebes breed in freshwater wetlands, north and west of the New York Bight region. Waterfowl build nests of down and feather plucked from the bodies of females that they mix in with vegetation; smaller species lay more eggs (10–14), while the larger species, such as swans, may lay only a few (3–5; Baldassarre 2014). Nests are generally dry and of variable distance from wetlands. Females generally incubate eggs alone through hatch, and only for geese and swans do males assist; female ducks are independent of males from early incubation throughout incubation and brood-rearing. Young are well-insulated and able to feed themselves shortly after hatch.

Conservation Status: Waterfowl are arguably the most studied avian taxa in the world, as they are widely hunted and, therefore, the focus of extensive habitat and population management. All waterfowl species in the New York Bight region have robust populations and are open to hunting, aside from the introduced Mute Swan. Grebes, however, are neither well-studied nor do they have robust populations, with one third of grebe species imperiled worldwide. The three grebe species likely to be present in the New York Bight region are not currently of widespread conservation concern, although the Pied-billed Grebe is listed as *Threatened* in New York, and as *Endangered* in New Jersey (NJDFW 2023, NYSDEC 2023).

4.2.1.2 Exposure Assessment

Group Exposure Determination: **Minimal**

Assessment Method: **Qualitative**

Information Sources: Baseline, MDAT, site-specific, literature

Exposure Uncertainty: **Low**

Based on BRI’s exposure assessment, the group exposure determination for grebes and waterfowl was **minimal**. As described above in the overview, grebes and waterfowl breed well to the north of the New York Bight and thus would not be expected to occur there at all in summer. Digital aerial surveys show no use of the Lease Area by any members of this group—except for some limited observations of ‘unknown duck’ that could be sea ducks—and there are very few

observations of this group across the entire NY Bight survey area. The literature indicates that the species in this group spend most of the year in freshwater aquatic systems and near-shore marine systems and are unlikely to extensively use areas as far offshore as the Lease Area. Uncertainty is **low** because site-specific baseline data and model outputs are available; however, no tracking data are available.

4.2.1.3 Behavioral Vulnerability Assessment

No vulnerability assessment was conducted for grebes and waterfowl (excluding sea ducks) due to their minimal expected exposure.

4.2.1.4 Risk Determination

Grebes and waterfowl received a final exposure determination of minimal. The relative collision vulnerability determination and relative displacement vulnerability determination were not conducted due to the minimal exposure. Based on BRI's risk assessment matrix (Table 2-1), final collision risk and displacement risk were assessed as **minimal**.

4.2.1.5 Tables and Figures

Maps for this group are contained in Attachment A.

4.2.2 Shorebirds

Minor Taxa Groups: Charadriiformes: suborders Charadrii, (includes Charadriidae [plovers], Recurvirostridae [stilts and avocets], and Haematopodidae [oystercatchers]), and Scolopaci (includes Scolopacidae [sandpipers]). Discussed separately are phalaropes (Scolopacidae, subfamily Phalaropinae; Section 4.3.2), and ESA-listed Piping Plovers (Section 4.4.2) and Red Knots of the *rufa* subspecies (Section 4.4.3).

Collision Risk Determination: **Minimal to Low**

Displacement Risk Determination: **Minimal**

4.2.2.1 Overview

Distribution and Habitat Preferences: Most shorebirds are long-distance migrants that breed in the Arctic or Subarctic and overwinter in the Southern Hemisphere (Winkler et al. 2020a, b, c, d). However, some species breed in freshwater wetlands and along coasts on both rocky and sandy beaches. During breeding, shorebirds may use a variety of habitats, but during migration and in winter, they are primarily distributed immediately adjacent to water on sandbars, mudflats, or beaches. Migration may follow coastlines or cross large expanses of open water, therefore multiple shorebird species may fly through lease areas in the New York Bight region, especially during southward fall migrations. However, shorebirds are present year-round on coastlines of the New York Bight region.

Behavior and Ecology: Outside the breeding season, shorebirds are highly gregarious and can form large flocks during migrations and in winter, sometimes of thousands of individuals (Winkler et al. 2020a, b, c, d). Feeding on invertebrate prey occurs by probing in soft sediments along the edges of wetlands, mudflats, or beaches; variation in bill morphology and body size in shorebirds is associated with segregation in microhabitat use, such that multiple species may forage on different prey in the same general area.

Reproduction: Shorebirds use a wide range of reproductive strategies, with both parents sharing incubation and brood-rearing in some species, and only by one parent in others. Nests are built on the ground in small cups, into which a maximum of four eggs are laid. Materials used to line nests vary widely, with some species reliant on vegetation, while others line the nests with bivalve shells (oystercatchers). Nests may be in vegetation (e.g., Spotted Sandpipers nest in forests near ponds) or fully exposed (e.g., Killdeer often nest in gravel parking lots; Reed et al. 2020; Jackson and Jackson 2020).

Conservation Status: Shorebirds in general are species of concern, due to long-term declines and high susceptibility to threats in coastal habitats. Two species are ESA-listed: Piping Plovers (section 4.4.2) and Red Knots of the *rufa* subspecies (section 4.4.3). In New York, Upland Sandpipers are considered *Threatened* (NYSDEC 2023). In New Jersey, Upland Sandpipers are state *Endangered*, while American Oystercatchers, Whimbrels, Sanderlings, and Semipalmated Sandpipers, and Spotted Sandpipers are listed as *Special Concern* (NJDFW 2023).

4.2.2.2 Exposure Assessment

Group Exposure Determination: **Minimal to Low**

Assessment Method: **Qualitative**

Information Sources: tracking, literature

Exposure Uncertainty: **High**

Based on BRI's exposure assessment, the group exposure determination for shorebirds was **minimal to low**. As indicated in the overview above, some shorebird species are present year-round in the New York Bight while others only pass through on migration. The literature indicates that shorebirds often migrate at night, and thus their movements may not be captured in diurnal survey efforts. Shorebirds mostly use nearshore areas, but some undertake migratory flights that cross the outer continental shelf; considerable uncertainty remains on shorebird offshore migratory patterns. While not designed to detect nocturnal migrants, the digital aerial surveys contain no observations of any members of this group within the Lease Area; 385 total observations of this group were recorded over the entire NY Bight survey area (Table 4-28). A Motus tagging study tracked shorebirds with land-based receiver towers with incomplete coverage of the OCS, meaning that any movements in the vicinity of the Lease Area should be interpreted with this caveat, and not all movements are expected to be captured. (Loring et al.

2020). Modeled flight paths (i.e., straight lines connecting the locations of detected tagged birds) indicated movements both along the coast and potentially crossing the New York Bight (Figure 4-2, Figure 4-3, Figure 4-4), some of which had the potential to traverse the Lease Area: Dunlin (*Calidris alpina*), White-rumped Sandpiper (*Calidris fuscicollis*), Least Sandpiper (*Calidris minutilla*). Uncertainty is high because the site-specific baseline digital aerial survey data are not suitable for detecting shorebirds, and no MDAT models are available (though tracking studies are available).

4.2.2.3 Behavioral Vulnerability Assessment

Collision Vulnerability Determination: **Low**

Assessment Method: **Qualitative**

Collision Uncertainty: **Medium**

Based on BRI's vulnerability assessment, the collision vulnerability determination for shorebirds was **low** (Table 4-2). This determination is based on species accounts in the scientific literature and data from tracking studies. Shorebirds often migrate at heights above the RSZ and fly during fair weather conditions. The tracked shorebird flights in the Loring et al. (2020) study occurred generally when there was low precipitation. Model-estimated shorebird flight altitudes of non-stop flights over federal waters ranged (5–95%) from 92–9,646 ft (28–2,940 m), with a mean of 2,999 ft (914 m) in spring, and 1,788 ft (545 m) in fall (Loring et al. 2020).

Another tracking study conducted in inland Canada indicated that shorebirds needed a distance of 2–14 km (1.2–8.7 mi) to climb above a 165 m (541.3 ft) WTG (Howell et al. 2019) and are expected to fly at high altitudes during migration (for additional detail, see discussion of Piping Plover and Red Knot in Section 4.4). With the distance from shore to the Lease Area, shorebirds migrating during fair weather conditions are likely flying above the RSZ, which reduces collision vulnerability. Shorebirds may reduce flight heights during periods of poor visibility, however.

A third recent tracking study focused on Eurasian Curlews (*Numenius arquata*; a shorebird species not found in the New York Bight but related to local species) found that while they demonstrated a broad-front migration across the Baltic Sea, core migration areas overlapped with offshore wind farms currently in operation (Schwemmer et al. 2022). Results from the study also showed that birds generally flew at sea at altitudes below 300 m and that altitudes were significantly lower at sea than over land. This recent data suggests that at least some migrating shorebirds may have greater potential to fly through the RSZ than previously thought. Uncertainty is **medium** due to the availability of flight height and activity information and the lack of avoidance information.

Displacement Vulnerability Determination: **Minimal to Low**

Assessment Method: **Qualitative**

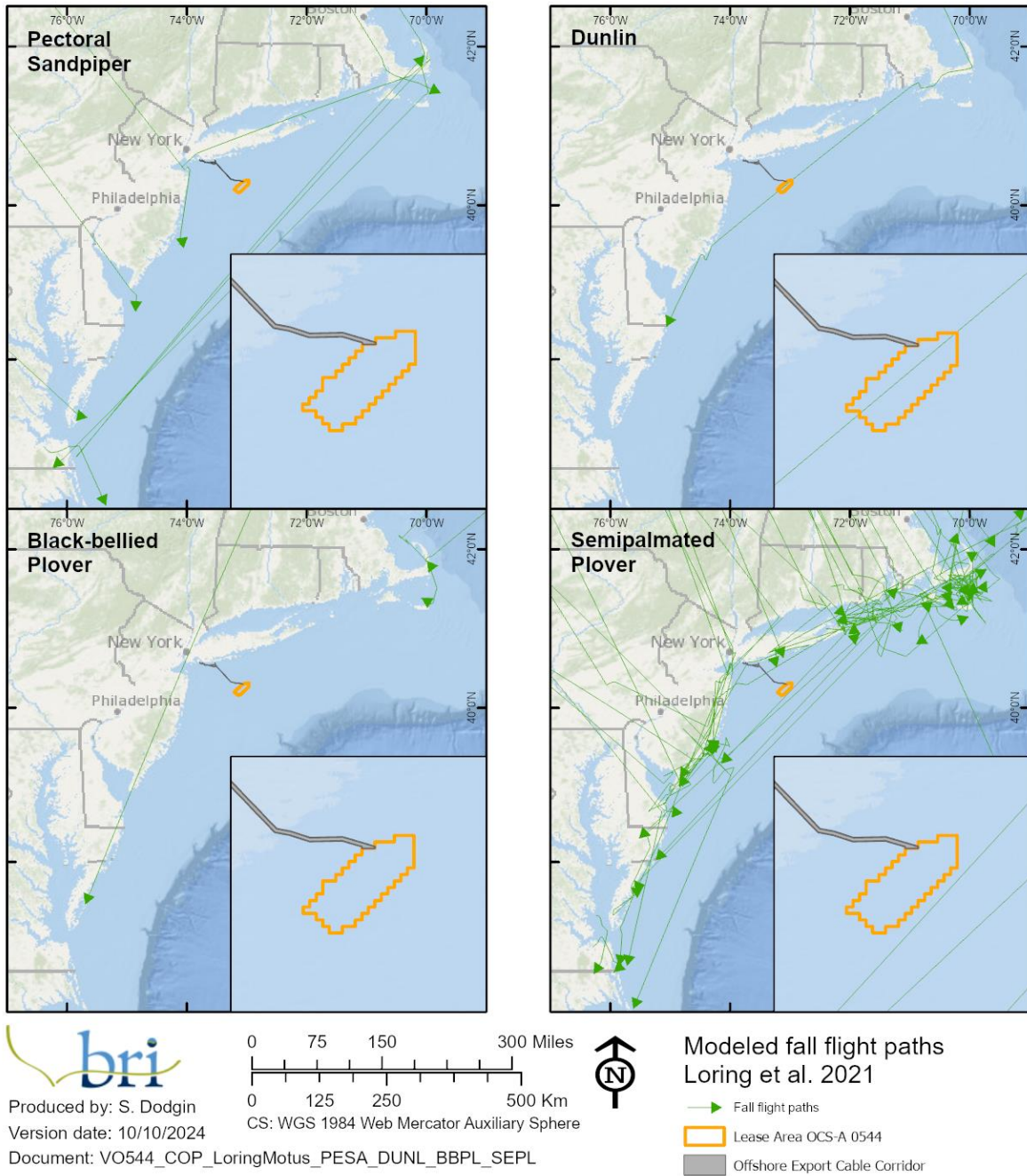
Displacement Uncertainty: **Medium**

Based on BRI's vulnerability assessment, the displacement vulnerability determination for shorebirds was **minimal to low** (Table 4-2). This determination is based on species accounts in the scientific literature and on tracking studies. Shorebirds are not expected to be vulnerable to displacement because they are not provided primary foraging habitat by the offshore environment, with the exception of phalaropes, which are technically shorebirds, but due to their pelagic foraging, are treated as marine birds here (see Section 4.3.2). Furthermore, any avoidance of the Lease Area is unlikely to impact overall individual fitness due to the size of the Lease Area in relation to the entire migratory trip (BOEM 2021). Uncertainty is **medium** due to the lack of information about avoidance.

4.2.2.4 Risk Determination

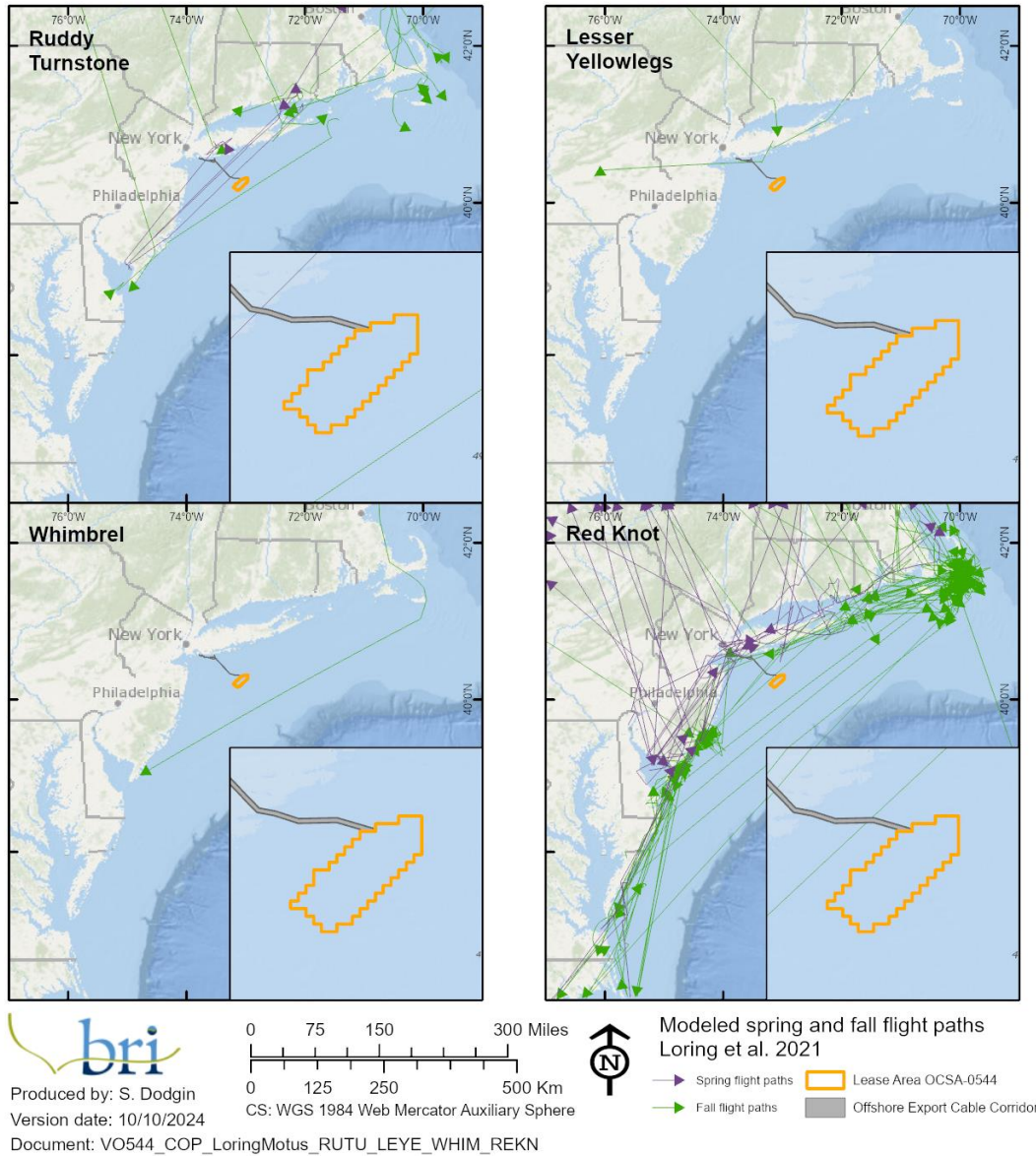
Shorebirds received a final exposure determination of minimal to low, a relative collision vulnerability determination of low, and a relative displacement vulnerability determination of minimal. Based on BRI's risk assessment matrix (Table 2-1), final collision risk was assessed as **minimal to low** and displacement risk was assessed as **minimal**.

4.2.2.5 Tables and Figures



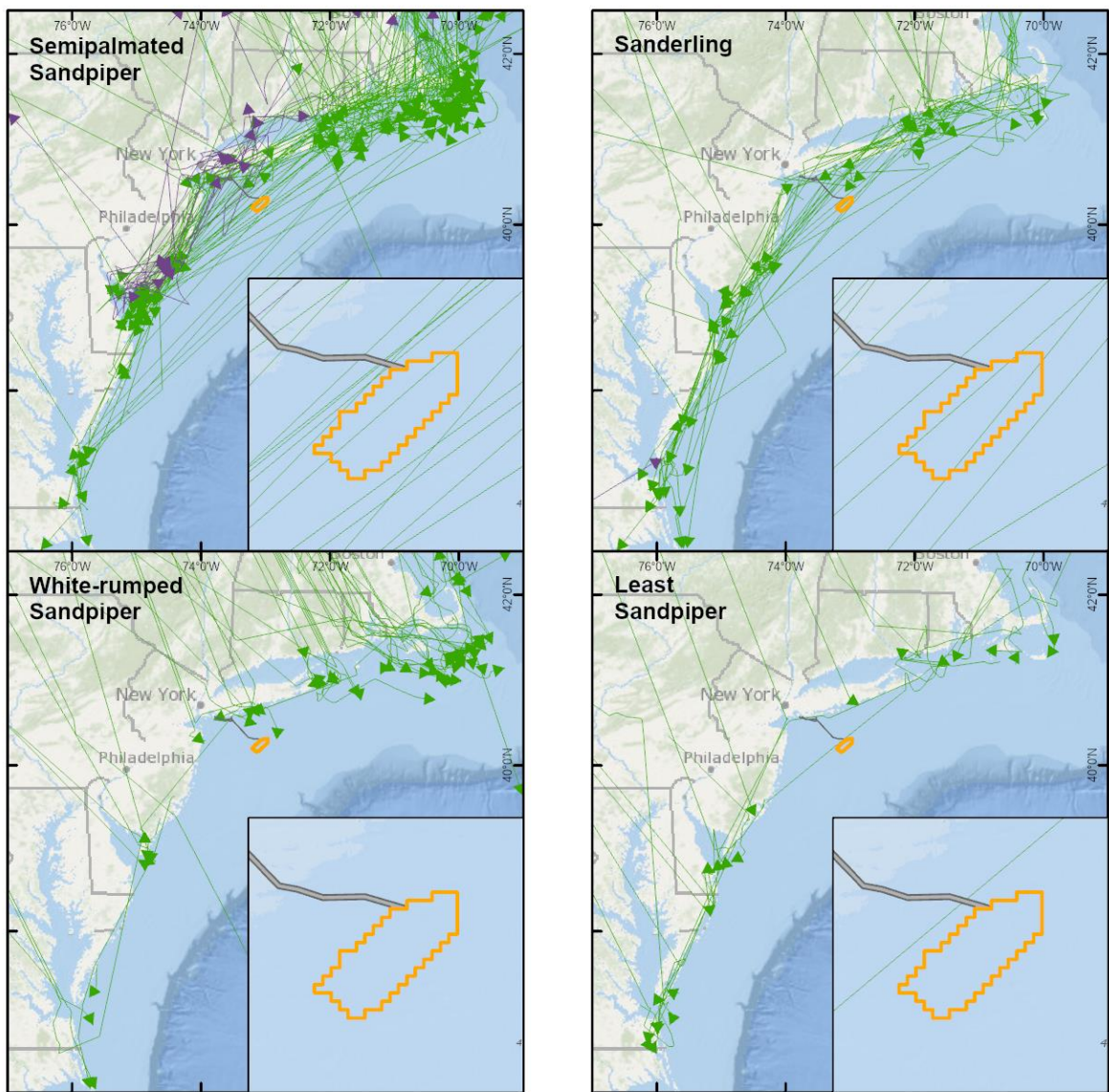
NOTE: All data are not actual flight paths but interpolated (model-generated) flight paths. Flight paths were modeled by detections of movements between land-based towers. Towers had a typical detection range <15 km (9.3 mi)), so birds were only detected when flying within approximately 15 km (9.3 mi) of one of the towers. See Loring et al. (2021) for tower locations and detection probability. Data provided by USFWS and used with permission.

Figure 4-2: Modeled flight paths of migratory shorebirds equipped with nanotags, based on data from Loring et al. (2021).



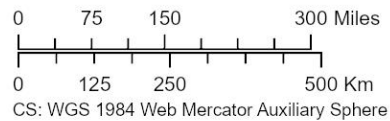
NOTE: All data are not actual flight paths but interpolated (model-generated) flight paths. Flight paths were modeled by detections of movements between land-based towers. Towers had a typical detection range <9.3 mi (15 km), so birds were only detected when flying within approximately 9.3 mi (15 km) of one of the towers. See Loring *et al.* (2021) for tower locations and detection probability. Data provided by USFWS and used with permission.

Figure 4-3: Modeled flight paths of migratory shorebirds equipped with nanotags, based on data from Loring *et al.* (2021).



Produced by: S. Dodgins
Version date: 10/10/2024

Document: VO544_COP_LoringMotus_SESA_SAND_WRSA_LESA



Modeled spring and fall flight paths
Loring et al. 2021

- Spring flight paths
- Fall flight paths
- Lease Area OCSA-0544
- Offshore Export Cable Corridor

NOTE: All data are not actual flight paths but interpolated (model-generated) flight paths. Flight paths were modeled by detections of movements between land-based towers. Towers had a typical detection range <9.3 mi (15 km), so birds were only detected when flying within approximately 9.3 mi (15 km) of one of the towers. See Loring et al. (2021) for tower locations and detection probability. Data provided by USFWS and used with permission.
Figure 4-4: Modeled flight paths of migratory shorebirds equipped with nanotags, based on data from Loring et al. (2021).

Table 4-2: Summary of shorebird vulnerability.

Effect	Description	Qualitative Evidence	
		Construction	Operation
Collision	Fatality and injury caused by collision with structures	low	low
Displacement	Temporary or permanent disturbance, avoidance and/or displacement resulting in effective habitat loss	minimal	minimal

4.2.3 Wading Birds

Minor Taxa Groups: Pelecaniformes: Ardeidae (herons and egrets) and Threskiornithidae (ibises and spoonbills)

Collision Risk Determination: **Minimal to Low**

Displacement Risk Determination: **Minimal**

4.2.3.1 Overview

Distribution and Habitat Preferences: Herons, egrets, and ibises are wetland-obligate species, rarely found far from water (Winkler et al. 2020e, f). During their breeding season, most species are found in temperate regions, rarely migrating farther north than southern Canada. Farther south, wading birds are often found in the same regions year-round, although individuals may still undergo short-distance migrations. Migrations may take some species far overwater. For example, Great Blue Herons (*Ardea herodias*) may fly directly over water from New England to the Caribbean or follow the US Atlantic coastline south.

Behavior and Ecology: Wading birds are highly predatory, with diverse diets of primarily amphibians, fish, and invertebrates, but also small birds, mammals, and reptiles (Winkler et al. 2020e, f). These long-legged birds feed by wading slowly through waters as deep as they can walk without submerging their body, or by ambushing prey while waiting in place. Flight is slow and direct, with heads tucked back tightly against the body and legs extended.

Reproduction: Herons and egrets primarily build nests in trees, over or adjacent to water, and often in colonies. However, some species (such as bitterns) are more secretive and will build solitary nests in cattails or other wetland vegetation (Winkler et al. 2020e). Both adults assist with nest-building, incubation, and rearing of young. Young are unable to thermoregulate or feed themselves at hatch, requiring brooding and feeding by adults in the nest until fledged.

Conservation Status: Herons and egrets, and to a lesser degree, ibises, are recovering from severe population declines in the early 20th century. Most populations are now stable, although many species are a conservation concern at the state level (Winkler et al. 2023e, f). In New York, Least Bitterns are listed as *Endangered*, and American Bitterns (*Botaurus lentiginosus*) as *Special Concern* (NY DEC 2023). In New Jersey, American Bitterns are listed as *Endangered*; Cattle Egrets

(*Bubulcus ibis*), Black-crowned Night Herons (*Nycticorax nycticorax*), and Yellow-crowned Night Herons (*Nyctanassa violacea*) are *Threatened*; and Great Blue Herons, Little Blue Herons (*Egretta caerulea*), Tricolored Herons (*Egretta tricolor*), and Glossy Ibises (*Plegadis falcinellus*) are of *Special Concern* (NJDFW 2023). Despite these state level concerns, no species in this group is currently listed at the federal level.

4.2.3.2 Exposure Assessment

Group Exposure Determination: **Minimal to Low**

Information Sources: Baseline, site-specific, literature, tracking

Assessment Method: **Qualitative**

Exposure Uncertainty: **Low**

Based on BRI's exposure assessment, the group exposure determination for wading birds was **minimal to low**. There were no observations of species in this group within the Lease Area, and there were only three total observations in the entire NY Bight survey area, all Great Blue Herons. Their low use of the offshore environment is expected from their requirement for shallow, wadable water for foraging. Despite the very low number of observations in the digital aerial survey data, the available tracking data indicate that migrating Great Blue Herons do traverse the New York Bight in the vicinity of the Lease Area over the Atlantic OCS (Brzord 2023; Figure 4-5). While little is known about the migratory behavior of herons, recent studies have documented long-distance migratory flights and use of the offshore environment during these periods. In a study of a related species in Europe, Purple Herons (*Ardea purpurea*) were satellite-tagged prior to fledging in Europe and were seen to migrate over 4,000 km (2,486 mi) in less than a week, including one individual that made a 5,600 km (3,480 mi) non-stop flight over mostly ocean (van der Winden et al. 2010). Uncertainty about this exposure assessment is **low** due to the presence of site-specific baseline data and tracking studies are available; however, there are no MDAT model outputs for species in this group.

4.2.3.3 Behavioral Vulnerability Assessment

Collision Vulnerability Determination: **Low**

Assessment Method: **Qualitative**

Collision Uncertainty: **Medium**

Based on BRI's vulnerability assessment, the collision vulnerability assessment for wading birds was **low** (Table 4-3). This determination is based on a review of the scientific literature. A recent telemetry study found that 43% of flight altitudes of Great Blue Herons occurred within the height range of terrestrial WTGs in Maine (Dolinski 2019; Figure 4-6). Birds migrating offshore, however, may fly at higher altitudes to take advantage of favorable tail winds. For example, herons tracked via radar migrating over the Strait of Messina in southern Italy had mean flight

heights of 821 m (2,694 ft; Mateos-Rodríguez and Liechti 2012). While there remains uncertainty on heron vulnerability, they have been identified as having a potential for collision sensitivity (Willmott et al. 2013); tracking data indicates that within the Atlantic OCS, they have the potential to fly within the RSZ (Figure 4-6); and there have been some individual mortalities detected at terrestrial wind projects (American Wind Wildlife Institute [AWWI] 2016). There do not, however, appear to be many records of wading birds colliding with WTGs at terrestrial wind farms. Uncertainty is **medium** because of a lack of information on avoidance rates.

Displacement Vulnerability Determination: **Minimal**

Assessment Method: **Qualitative**

Displacement Uncertainty: **Medium**

Based on BRI's vulnerability assessment, the displacement vulnerability assessment for wading birds was **minimal**. This determination is based on chiefly on the scientific literature, which indicates that the offshore environment is not providing primary foraging habitat. Uncertainty is **medium** because of a lack of information on avoidance rates.

4.2.3.4 Risk Determination

Wading birds received a final exposure determination of minimal to low, a relative collision vulnerability determination of low, and a relative displacement vulnerability determination of minimal. Based on BRI's risk assessment matrix (Table 2-1), final collision risk was assessed as **minimal to low** and displacement risk was assessed as **minimal**.

4.2.3.5 Tables and Figures

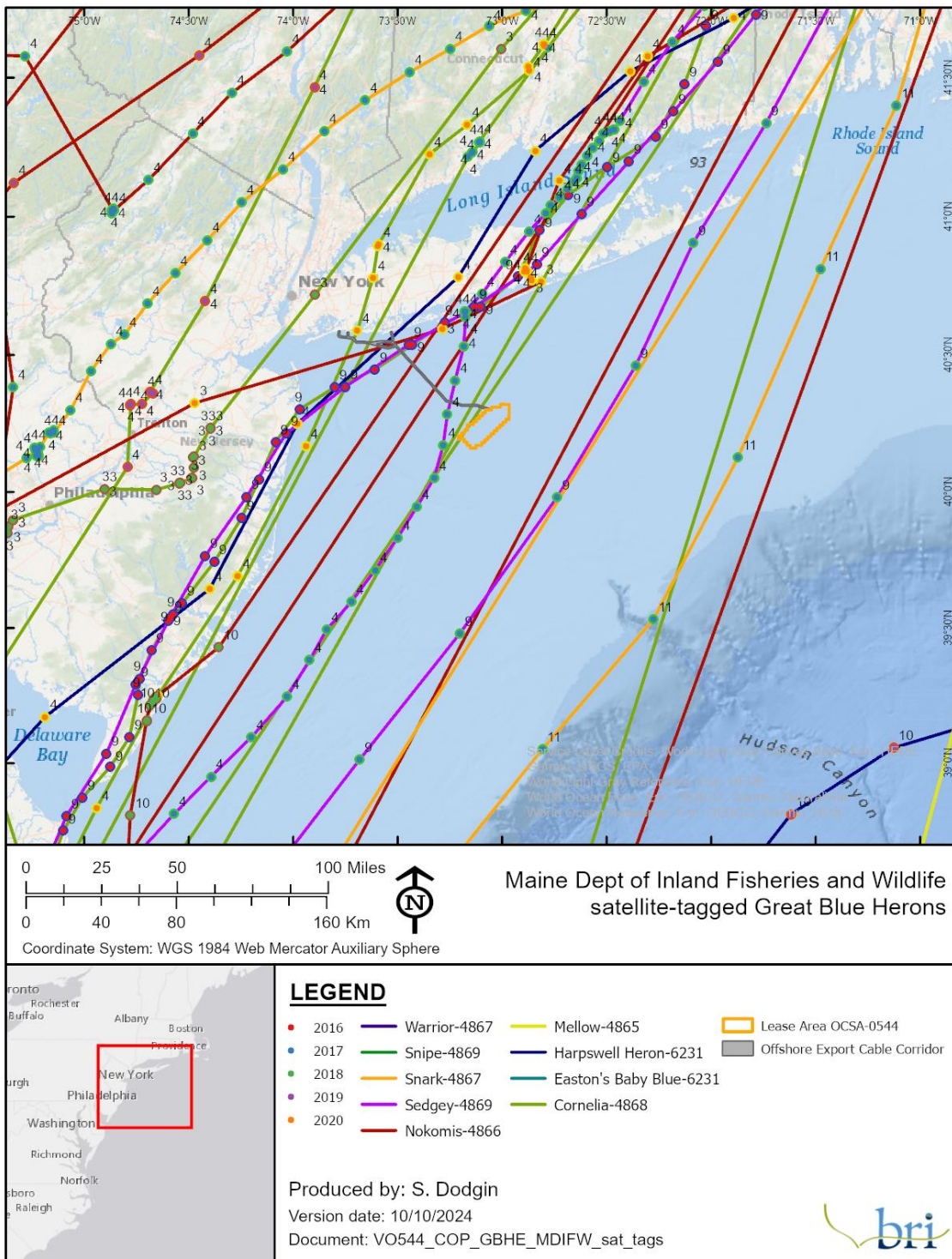
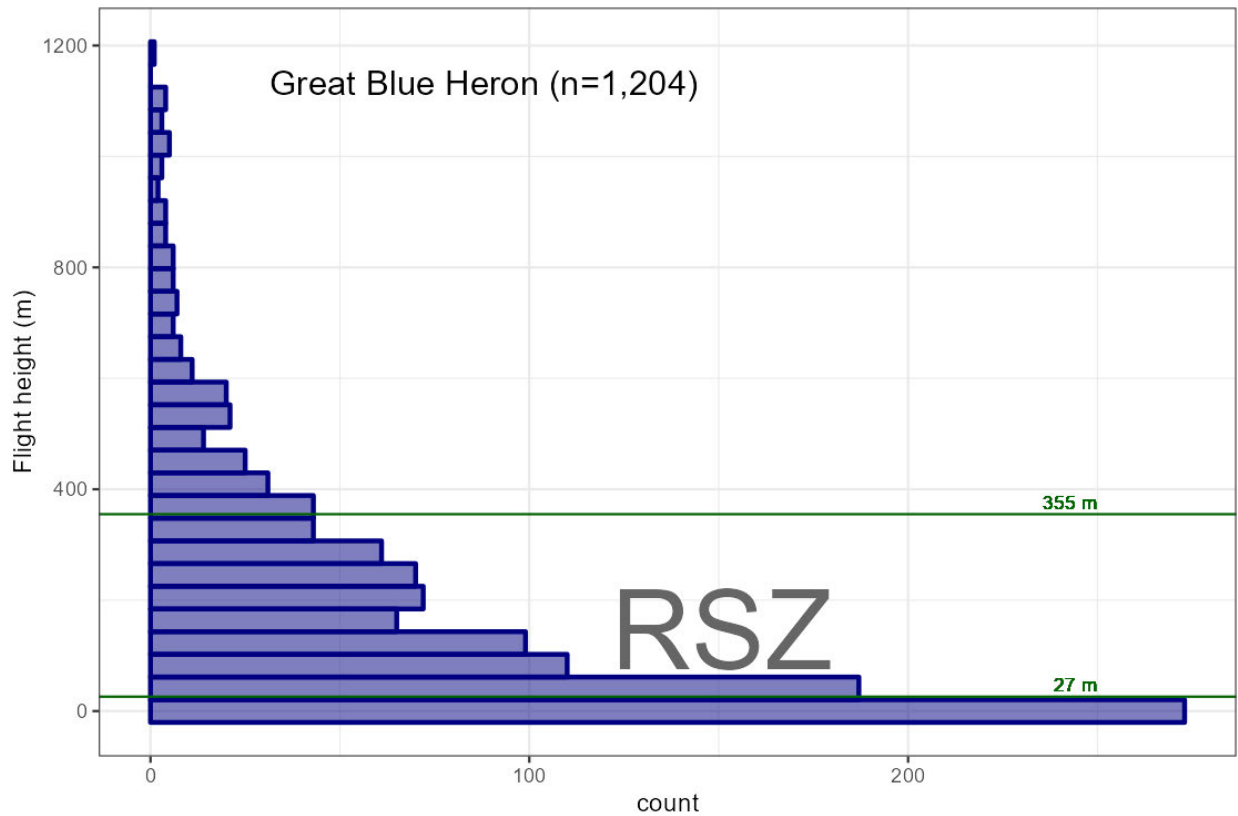


Figure 4-5: Track lines of Great Blue Herons captured in Maine and equipped with satellite transmitters provided by Maine Department of Inland Fisheries and Wildlife.



NOTE: Figure shows the actual number of birds in 5 m (16 ft) intervals (blue bars) in relation to the upper and lower limits of the RSZ (27-355 m; green lines).

Figure 4-6: Flight heights (m) of Great Blue Herons satellite-tagged in Maine, flying over the Atlantic OCS.

Table 4-3: Summary of wading bird vulnerability.

Effect	Description	Qualitative Evidence	
		Construction	Operation
Collision	Fatality and injury caused by collision with structures	low	low
Displacement	Temporary or permanent disturbance, avoidance, and/or displacement resulting in effective habitat loss	minimal	minimal

4.2.4 Raptors

Minor Taxa Groups: Accipitriformes: Accipitridae (eagles and hawks), Cathartidae (vultures), Pandionidae (Osprey); Falconiformes: Falconidae (falcons); Strigiformes: Tytonidae (barn owls), Strigidae (other owls)

Note: The Bald Eagle risk assessment is found separately in 4.4.5.

Collision Risk Determination: **Minimal to Low**

Displacement Risk Determination: **Minimal to Low**

4.2.4.1 Overview

Distribution and Habitat Preferences: Raptors as a group are broadly distributed and highly mobile. These birds can occupy a wide range of habitats ranging from open grasslands and beaches to dense forests. Some species are migratory, while others remain in the same areas year-round. Of this suite of birds, only falcons that primarily use flapping flight are likely to be found in marine areas, as the thermals required for soaring flight used by many raptor species are present only over land.

Behavior and Ecology: Raptors are generally large birds that feed on other animals. Some species may be scavengers, but most are predatory. This range of foraging modes is associated with various flight strategies and habitat preferences. Larger eagles and hawks that use warm air thermals to soar are typically found over land in open areas, where they hunt by sight (Winkler et al. 2020g). Vultures also use thermals to soar and locate carrion (Winkler et al. 2020h). Thermals are formed by warming land creating pockets of rising air, and therefore are only present over land, restricting most soaring species to overland migratory routes. Ospreys are wetland-obligates, primarily located near water in both coastal and inland areas (Bierregaard et al. 2020). Falcons, which feed primarily on other birds or flying insects they catch in the air, are highly rapid fliers and can be found in any habitat type, including hunting and migrating over water (Winkler et al. 2020i). Smaller hawks that pursue prey through rapid, powered flight may be found in forests or more restricted, mixed habitats (Winkler et al. 2020g). Owls are mostly non-migratory, mostly found in forested areas, and feed primarily on rodents captured at night (Winkler et al. 2020j).

Reproduction: Most raptors build nests of sticks and leaves in trees or on cliff faces, although some species will nest in cavities (small caves in rock faces or tree cavities). Peregrine Falcons will nest on tall buildings in cities, although most nest on remote cliffs (White et al. 2020). Eagles, hawks, Osprey, and falcons will lay 2–4 eggs in each nest which they then incubate and feed until fledge (Winkler et al. 2020 g, h, i; Bierregaard et al. 2023). Owls may regulate the number of eggs they lay based on food availability, so the number of eggs and survival of young depend on prey abundance (Winkler et al. 2020j). For most raptor species, both adults are highly involved with incubation and brood-rearing.

Conservation Status: Raptor populations are generally stable. However, given their high trophic status, raptors are highly sensitive to human land use and contaminants such as Dichlorodiphenyltrichloroethane (DDT) (now banned in the US) and lead. Regulations to reduce these threats have resulted in generally recovered populations. No raptors likely to be present in the New York Bight region are listed on the ESA, although Bald Eagles and Peregrine Falcons were removed from the federal list in recent decades (White et al. 2020; Buehler 2022). Many raptors are at risk at the state level, however. In New York, Golden Eagles, Peregrine Falcons, and Short-eared Owls (*Asio flammeus*) are listed as *Endangered*; Bald Eagles and Northern Harriers are *Threatened*; and Osprey, Sharp-shinned Hawks, Cooper's Hawks, Northern Goshawks, and

Red-shouldered Hawks are *Special Concern* (NYSDEC 2023). In New Jersey, Bald Eagles, Peregrine Falcons, Northern Goshawks, Northern Harriers, Red-shouldered Hawks, and Short-eared Owls are listed as *Endangered*; American Kestrels, Osprey, Barred Owls, and Long-eared Owls are *Threatened*; and Broad-winged Hawks, Cooper’s Hawks, and Sharp-shinned Hawks are *Special Concern* (NJDFW 2023).

4.2.4.2 Exposure Assessment

Group Exposure Determination: **Minimal to Low**

Assessment Method: **Qualitative**

Information Sources: Baseline, site-specific, tracking, literature

Exposure Uncertainty: **Low**

Discussion: Based on BRI’s exposure assessment, the group exposure determination for raptors was **minimal to low**. In the digital aerial surveys, there were no observations of species in this group within the Lease Area and only one observation in the entire NY Bight survey area (an Osprey). The literature indicates that the species in this group are unlikely to extensively use offshore areas, but some may pass through on migratory flights. Available tracking data indicate that Ospreys, Merlins, and Peregrine Falcons may occasionally use offshore areas in the vicinity of the Lease Area (Figure 4-7, Figure 4-8, and Figure 4-9). Uncertainty is **low** because site-specific and regional baseline data are available, as are tracking studies, but there are no MDAT model outputs available.

4.2.4.3 Behavioral Vulnerability Assessment

Collision Vulnerability Determination: **Low to Medium**

Assessment Method: **Qualitative**

Collision Uncertainty: **Low**

Based on BRI’s vulnerability assessment, the collision vulnerability determination for raptors was **low to medium** (Table 4-4). There is little information on how Ospreys respond to WTGs, but falcons may be attracted to WTGs as perching sites. In Europe, Peregrine Falcons and kestrels have been observed landing on the platform deck of offshore WTGs (Hill et al. 2014; Skov et al. 2016). A radar and laser rangefinder study found evidence indicating that multiple migrating raptor species were attracted to offshore WTGs in Denmark (Skov et al. 2016), and satellite-tagged Ospreys and Peregrine Falcons have been confirmed perching on offshore barges and structures. In a recent report summarizing findings from one year of post-construction monitoring at the Coastal Virginia Offshore Wind Pilot Project, Peregrine Falcons were observed patrolling the air space and perching on turbines. Additionally, video evidence and the physical remains of a

songbird show that a Peregrine Falcon successfully foraged from a turbine platform on at least one occasion (Normandeau Associates 2022).

Little information exists documenting Peregrine Falcon fatalities from collision, especially in offshore settings. No Peregrine Falcon fatalities have been documented at European offshore wind developments, such as during the monitoring effort at the Thanet Offshore Wind Farm (Skov et al. 2018). While Peregrine Falcon collisions with transmission lines have been documented (Olsen and Olsen 1980; White et al. 2002), only a few accounts of mortalities are associated with terrestrial-based WTGs in Europe (Meek et al. 1993; Hötter et al. 2006; Dürr 2011) and one in New Jersey (Mizrahi et al. 2009). In 2020, a total of eight nationwide fatalities of Peregrine Falcons associated with terrestrial-based WTGs were reported by the American Wind Wildlife Institute (AWWI 2020). Breeding adults and several young Peregrine Falcons were killed after colliding with a three-WTG terrestrial wind energy facility located close to their urban nest site in Massachusetts (MassWildlife 2018). However, no carcasses were detected in post-construction fatality studies at several terrestrial projects where falcons were present in the US (West Virginia and California) and New Zealand (Bull et al. 2013; Hein et al. 2013; DiGaudio and Geupel 2014).

American Kestrels (*Falco sparverius*) have been found to collide with terrestrial WTGs; their carcasses have been found during post-construction monitoring of much smaller terrestrial WTGs (Erickson et al. 2008; AWWI 2019). American Kestrel fatality has been demonstrated to decrease as WTG size increases (Smallwood 2013), though the species still ranks among the top 10 most reported fatalities in the Pacific, Northern Rockies, and Prairie avifaunal biomes (AWWI 2019). Evidence of nocturnal soaring, perching, and feeding under lighted structures in terrestrial and offshore settings has been noted in Peregrine Falcons (Voous 1961; Cochran 1985; Johnson et al. 2011; Kettel et al. 2016), and these behaviors increase the exposure risk in this species. While terrestrial habitats provide foraging and nesting opportunities onshore, these are generally not present offshore, which would limit exposure compared with onshore wind farms. Uncertainty is **low** because there is some information on flight height, avoidance, and flight activity.

Displacement Vulnerability Determination: **Minimal to Low**

Assessment Method: **Qualitative**

Displacement Uncertainty: **Low**

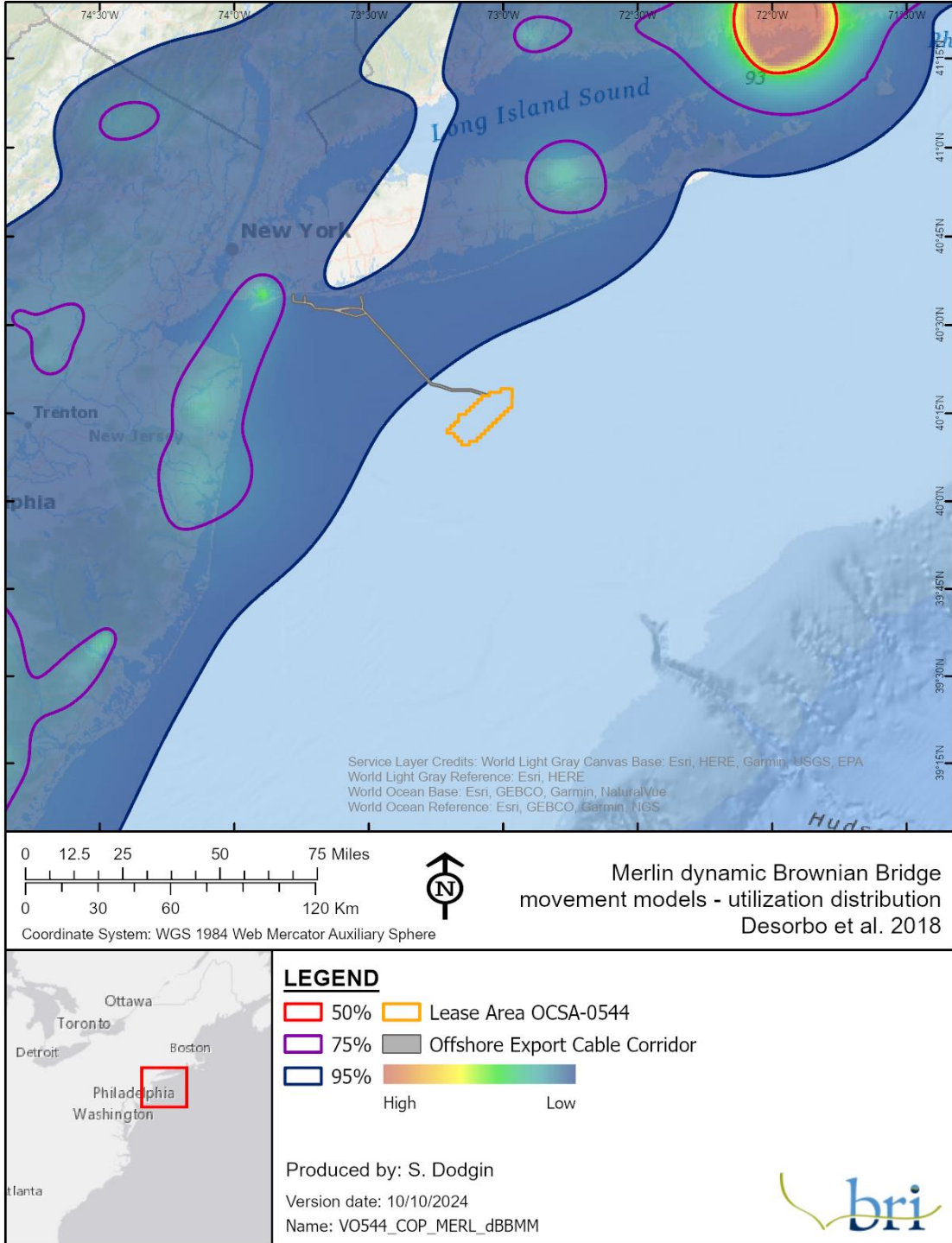
Based on BRI's vulnerability assessment, the displacement vulnerability determination for raptors was **minimal to low** (Table 4-4). Observations of raptors at the Anholt Offshore Wind Farm in the Baltic Sea, 20 km (12.4 mi) from the coast, indicate macro-avoidance behavior (i.e., avoiding entire wind farm; 13–59% of birds observed, depending on the species), which has the potential to cause a barrier for migrants in some locations, but may also reduce collision risk.

Birds may also exhibit meso-avoidance, which involves significant changes in flight height prior to entering a wind farm. The percentage of Merlins and kestrels showing macro-/meso-avoidance behavior was 14/36% and 46/50%, respectively (Jacobsen et al. 2019). Uncertainty is **low** because there is some available information on avoidance and flight height.

4.2.4.4 Risk Determination

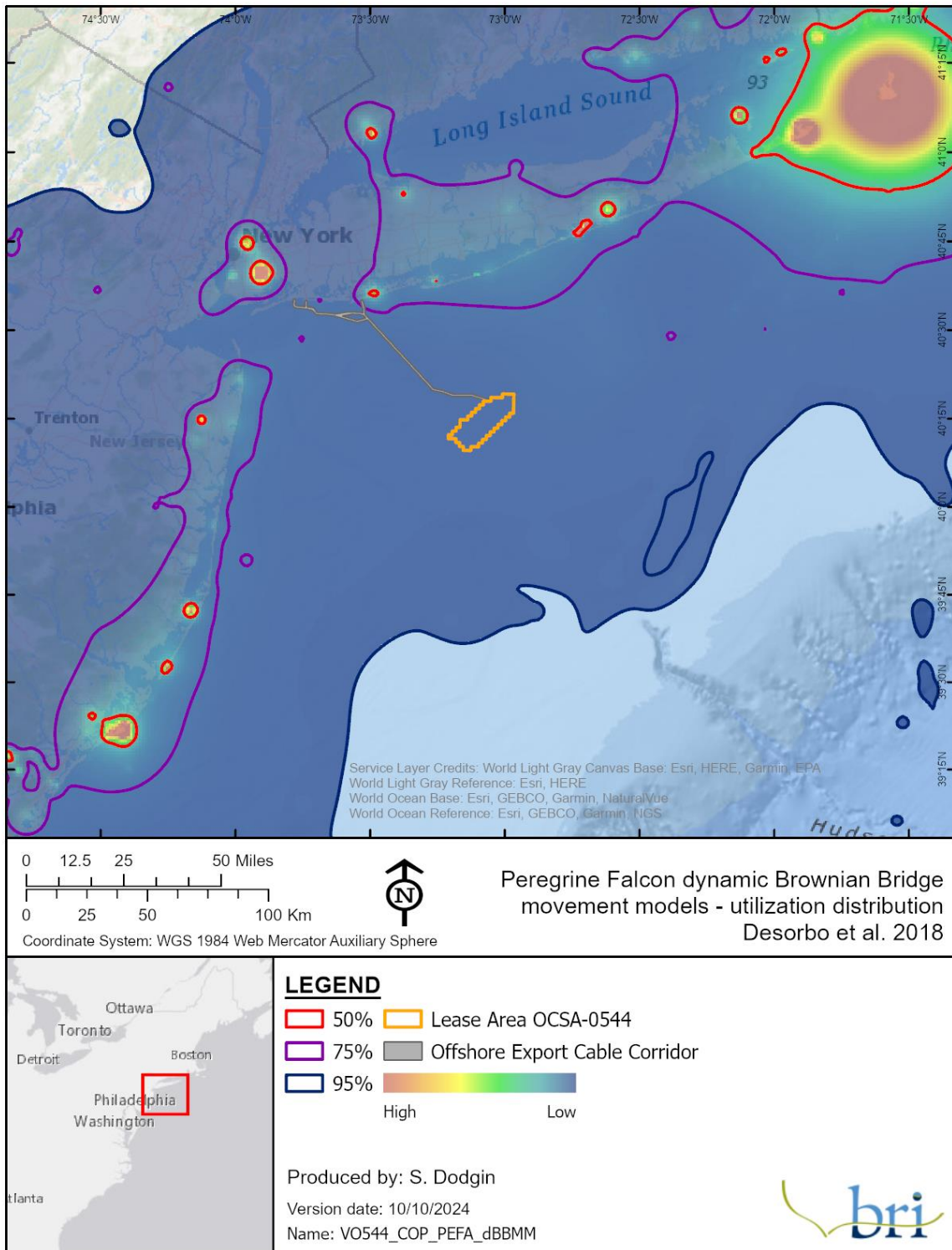
Raptors received a final exposure determination of minimal to low, a relative collision vulnerability determination of low to medium, and a relative displacement vulnerability determination of minimal to low. Based on BRI's risk assessment matrix (Table 2-1), final collision risk and final displacement risk were both assessed as **minimal to low**.

4.2.4.5 Tables and Figures

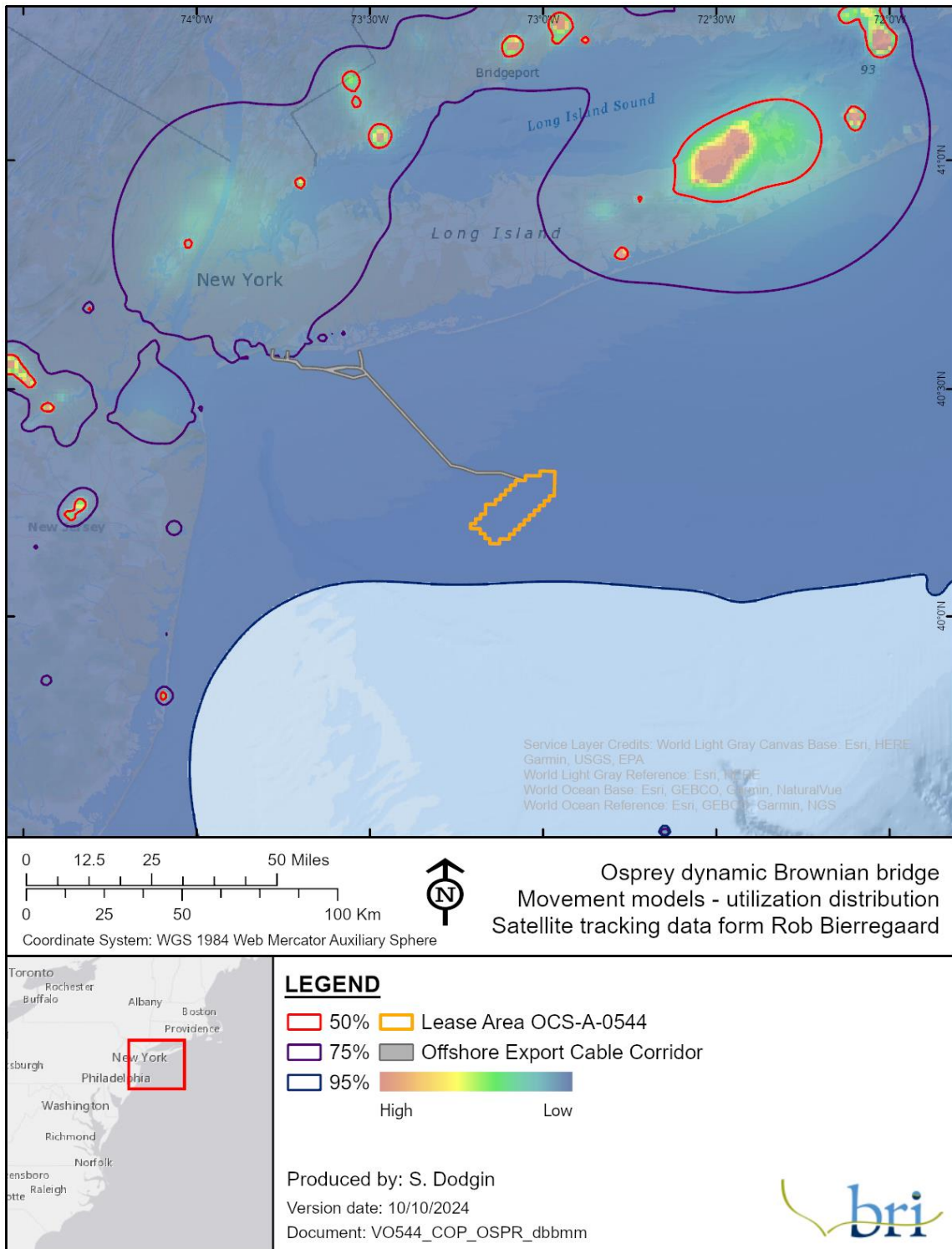


NOTE: Contours represent various levels of use, from 50% (core use) to 95% (home range).

Figure 4-7: Location estimates from satellite transmitters on Merlins (n=11) tracked from three raptor research stations along the Atlantic coast, 2010–2018 (DeSorbo et al. 2018).



NOTE: Contours represent various levels of use, from 50% (core use) to 95% (home range).
 Figure 4-8: Location estimates from satellite transmitters on Peregrine Falcons (n=33) tracked from three raptor research stations along the Atlantic coast, 2010–2018 (DeSorbo et al. 2018).



NOTE: Contours represent various levels of use, from 50% (core use) to 95% (home range).

Figure 4-9: Dynamic Brownian bridge movement models for Osprey ($n=127$) that were tracked with satellite transmitters by Rob Bierregaard and detailed at www.ospreytrax.com.

Table 4-4: Summary of raptor vulnerability.

Effect	Description	Qualitative Evidence	
		Construction	Operation
Collision	Fatality and injury caused by collision with structures	low - medium	low - medium
Displacement	Temporary or permanent disturbance, avoidance, and/or displacement resulting in effective habitat loss	minimal - low	minimal - low

4.2.5 Songbirds

Minor Taxa Groups: Passeriformes (entire order)

Collision Risk Determination: **Minimal to Low**

Displacement Risk Determination: **Minimal to Low**

4.2.5.1 *Overview*

Distribution and Habitat Preferences: Passerines are highly abundant, with far greater diversity than any other avian order. As such, they are found in all habitat types, and across the globe, except Antarctica. Most passerines are small-bodied, and therefore feed frequently during migrations; a few species, however, do undergo long-distance overwater migrations along the Atlantic coastline, including Blackpoll Warblers (*Setophaga striata*; DeLuca et al. 2020) and Bobolinks (*Dolichonyx oryzivorus*; Renfrew et al. 2020). Many species are long-distance migrants, although some are resident, remaining in the same locations year-round, and a range of intermediate migration strategies exist for this group of birds.

Behavior and Ecology: Usually solitary nesters, but gregarious otherwise, passerines are the most frequently observed birds. Generally, passerines eat vegetation, seeds, or invertebrates, although some species are highly predatory and feed on other birds, small mammals, amphibians, and reptiles.

Reproduction: Passerines are generally territorial during breeding, with males singing throughout the season to defend territories, while females incubate eggs. Clutches are highly variable, but a typical clutch is 2–6 eggs. Generally, both sexes assist with feeding and brooding of young, which are unable to feed themselves or thermoregulate at hatch, and feeding of young may continue until after the young fledge. Some species are able to have multiple clutches of young each year, although for most species that have long-distance migrations, only a single breeding attempt is possible.

Conservation Status: As passerines are highly diverse, many species are of conservation concern. In the New York Bight region, however, a select few are of particular concern. In New York, Loggerhead Shrikes (*Lanius ludovicianus*) are listed as *Endangered*; Sedge Wrens (*Cistothorus*

stellaris) and Henslow's Sparrows (*Ammodramus henslowii*) are *Threatened*; and Horned Larks (*Eremophila alpestris*), Bicknell's Thrushes (*Catharus bicknelli*), Golden-winged Warblers (*Vermivora chrysoptera*), Cerulean Warblers (*Setophaga cerulea*), Yellow-breasted Chats (*Icteria virens*), and Vesper Sparrow (*Pooecetes gramineus*), Grasshopper Sparrows (*Ammodramus savannarum*), and Seaside Sparrows (*Ammodramus maritima*) are *Special Concern* (NYSDEC 2023). In New Jersey, Loggerhead Shrikes, Henslow's Sparrows, Vesper Sparrows, Golden-winged Warblers, and Sedge Wrens are listed as *Endangered*; Bobolinks, Horned Larks, Grasshopper Sparrows, and Savannah Sparrows (*Passerculus sandwichensis*) are *Threatened*; and Bobolinks, Least Flycatchers (*Empidonax minimus*), Eastern Meadowlarks (*Sturnella magna*), Northern Parulas (*Setophaga americana*), Ipswich Sparrows (*Passerculus princeps*), Saltmarsh Sparrows (*Ammodramus caudacuta*), Cliff Swallows (*Petrochelidon pyrrhonota*), Brown Thrashers (*Toxostoma rufum*), Gray-cheeked Thrushes (*Catharus minimus*), Wood Thrushes (*Hylocichla mustelina*), Winter Wrens (*Troglodytes hiemalis*), Veeries (*Catharus fuscescens*), Blue-headed Vireos (*Vireo solitarius*), and ten species of warblers are *Special Concern* (NJDFW 2023). No federally listed Passerines are likely to be present in the New York Bight region, however.

4.2.5.2 Exposure Assessment

Group Exposure Determination: **Minimal to Low**

Assessment Method: **Qualitative**

Information Sources: Literature

Exposure Uncertainty: **High**

Based on BRI's exposure assessment, the group exposure determination for songbirds was **minimal to low**. The literature indicates that songbirds do not use the outer continental shelf as habitat, but they may pass through during migratory flights. There is considerable uncertainty around the timing and location of these migratory flights. In the NY Bight survey data, there are no observations of species in this group within the Lease Area, and there are very few observations of songbirds over the entire NY Bight survey area. Due to their small size, songbirds are less likely than the other taxonomic groups to be captured in the NY Bight surveys. Furthermore, the literature indicates that many species migrate at night, rendering diurnal surveys unlikely to capture such flights. Uncertainty is **high** due to the lack of MDAT models and tracking data, and due to the lack of suitable regional and local baseline data.

4.2.5.3 Behavioral Vulnerability Assessment

Collision Vulnerability Determination: **Low to Medium**

Assessment Method: **Qualitative**

Collision Uncertainty: **High**

Based on BRI's vulnerability assessment, the collision vulnerability determination for songbirds was **low** to **medium** (Table 4-5). Fatalities of songbirds have been documented at terrestrial WTGs (Erickson et al. 2014; Choi et al. 2020). In some instances, songbirds may be able to avoid colliding with offshore WTGs (Petersen et al. 2006) but are known to collide with illuminated terrestrial and marine structures (Fox et al. 2006). Movement during low visibility periods creates the highest collision risk conditions; at an offshore research station with substantial lighting, songbird fatalities have been documented during poor weather conditions (Hüppop et al. 2006). While avian fatality rates associated with terrestrial WTGs range from 3–5 birds per megawatt (MW) per year (AWWI 2016), direct comparisons between fatality rates recorded at terrestrial and offshore wind developments should be made with caution because collisions with offshore WTGs could be lower due to differing behaviors or lower exposure (NYSERDA 2015). At the Thanet Offshore Wind Farm, thermal imaging did not detect any songbird collisions (Skov et al. 2018). At Nysted, Denmark, in 2,400 hours of monitoring with an infrared video camera, only one collision of an unidentified small bird was detected (Petersen et al. 2006). In a report summarizing findings from one year of post-construction monitoring at the Coastal Virginia Offshore Wind Pilot Project, there were 975 bird detections, 71% of which were passerines, and no bird collisions were observed (Normandeau Associates 2022). Passerines were observed foraging, with most observations occurring when the turbine blades were stationary. Conversely, most observations of flyover occurred while the turbine blades were moving. Additionally micro-avoidance behaviors were observed in passerines while the blades were moving.

Songbirds typically migrate at 90–600 m (295–1,968 ft; NYSERDA 2010) but can fly lower during inclement weather or with headwinds. In a study in Sweden, nocturnal migrating songbirds flew on average at 330 m (1,083 ft) above the ocean during the fall and 529 m (1,736 ft) during the spring (Pettersson 2005). Given the limited understanding of songbird migration, exposure of migratory songbirds to the Lease Area is uncertain, but some birds will likely cross the Lease Area during fall migration. Under poor weather conditions, individual vulnerability to collision may increase as birds fly at lower altitudes and may be more likely to fly through RSZs. Fatality is likely to be stochastic and infrequent. However, the fatalities from all terrestrial WTGs in the US and Canada combined are predicted to have only a small effect on passerine populations, at most (Erickson et al. 2014).

Flight heights recorded during the New Jersey Department of Environmental Protection Ecological Baseline Studies survey showed that songbirds generally flew below the RSZ during the day (Geo-Marine 2010). In a study in Sweden, nocturnal migrating songbirds flew on average at 330 m (1,083 ft) above the ocean during the fall and 529 m (1,736 ft) during the spring (Pettersson 2005). Uncertainty is **high** because there is little to no information on the birds' flight heights and avoidance rates offshore during migration.

Displacement Vulnerability Determination: **Minimal to Low**

Assessment Method: **Qualitative**

Displacement Uncertainty: **Medium**

Based on BRI's vulnerability assessment, songbirds have a displacement vulnerability determination of **minimal to low**. Species accounts in the literature indicate that songbirds do not use the Atlantic OCS as habitat, so there is little concern about displacement from foraging or other primary habitat uses, but little is known about the vulnerability of songbirds to displacement from migratory routes over the Atlantic OCS. Hence, the uncertainty is **medium**.

4.2.5.4 Risk Determination

Songbirds received an exposure determination of minimal to low, a relative collision vulnerability determination of low to medium, and a relative displacement vulnerability determination of minimal to low. Based on BRI's risk assessment matrix (Table 2-1), final collision risk and final displacement risk were both assessed as **minimal to low**.

4.2.5.5 Tables and Figures

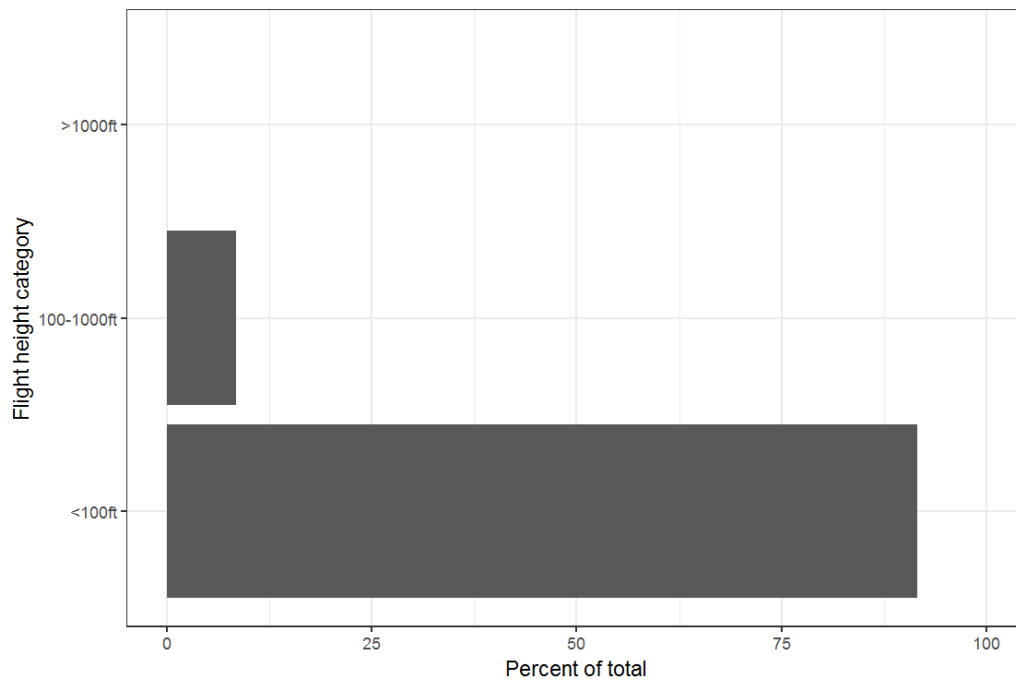


Figure 4-10: Flight heights of songbirds (n=333) derived from Northwest Atlantic Seabird Catalog, showing the number of birds of each species or grouping (and the proportion of the total for that survey) in each flight band.

Table 4-5: Summary of songbird vulnerability.

Effect	Description	Qualitative Evidence	
		Construction	Operation
Collision	Fatality and injury caused by collision with structures	low - medium	low - medium
Displacement	Temporary or permanent disturbance, avoidance and/or displacement resulting in effective habitat loss	minimal	minimal

4.3 Marine Birds

Marine bird distributions are generally more pelagic and widespread than coastal birds. A total of 83 marine bird species are known to regularly occur off the US Atlantic coast (Nisbet et al. 2013), and 52 of these species were observed in the NY Bight surveys.

Many of these marine bird species use the Lease Area during multiple time periods, either seasonally or year-round, including sea ducks, phalaropes, auks, gulls and jaegers, terns, loons, shearwaters, petrels, storm-petrels, gannets, and cormorants. In general, marine birds are also considered particularly vulnerable to the impacts of climate change (Dias et al. 2019), as warming-induced reductions in prey availability is considered one of the leading causes in the declines of seabird populations over the last two decades (Mitchell et al. 2020).

The IPaC database indicates that some “non-BCC vulnerable” marine birds may be present in the Lease Area and adjacent waters, including the Red-throated Loon (*Gavia stellate*), Common Loon (*Gavia immer*), Wilson’s Storm-petrel (*Oceanites oceanicus*), Black-legged Kittiwake (*Rissa tridactyla*), Common Eider (*Somateria mollissima*), Common Murre (*Uria aalge*), and Razorbill (*Alca torda*). Tracking data suggest that the Roseate Tern (a federally listed species) may pass near the Lease Area during migration. The Roseate Tern is discussed in detail in Section 4.4. In the following sections, BRI’s assessments for major taxonomic groups of marine birds are reported, including discussion of their exposure and their densities inside and outside of the Lease Area (summarized in Table 4-28). Section 4.6 of this assessment provides seasonal densities as supplemental data.

4.3.1 Sea Ducks

Minor Taxa Groups: Anseriformes: Mergini (sea ducks), including eiders, scoters, mergansers, and Long-tailed Ducks. Note, we exclude Bufflehead (*Bucephala albeola*), Barrow’s Goldeneye (*Bucephala islandica*), and Common Goldeneye (*Bucephala clangula*), as they remain in shallow waters and their exposure and vulnerability likely mimic those of other waterfowl species (described in Section 4.2.1).

Collision Risk Determination: **Minimal**

Displacement Risk Determination: **Minimal**

4.3.1.1 Overview

Distribution and Habitat Preferences: The sea ducks (eiders, scoters, mergansers, and Long-tailed Ducks), considered marine birds for this assessment, breed in northern regions in the summer and migrate to southerly coastal areas during the non-breeding season. During winter, sea ducks can gather in large flocks in both coastal and offshore habitats, sometimes in mixed species groups (Anderson et al. 2020; Goudie et al. 2020). Depending on whether they are foraging or resting, sea ducks may use a variety of habitat types during the non-breeding season, when they are likely to be present in the New York Bight region, but generally they prefer to winter in shallower inshore waters or out over large offshore shoals, where they can access their benthic prey.

Behavior and Ecology: Most sea ducks forage on mussels, other shellfish, and benthic invertebrates. Sea ducks in the north Atlantic generally forage on benthic prey in depths of 5–20 m (17–66 ft), with some species feeding at depths up to 30 m (98 ft ; Meattey et al. 2019; Zydalis and Richman 2015). Some species (mergansers, scoters, and Long-tailed Ducks) may also forage on pelagic fish or amphipods in the water column at any water depth (Zydalis and Richman 2015), including up to 60 m (197 ft ; Cottam 1939; Schorger 1947) in Long-tailed Ducks. Most benthic-foraging sea ducks will use foraging habitats in shallow areas closer to shore or on offshore shoals, whereas pelagic-feeding sea ducks will use a wider range of habitats and water depths based on prey distributions and oceanographic factors (Zydalis and Richman 2015; White and Veit 2020).

Reproduction: Sea ducks breed in northern regions, all outside of the New York Bight region (Eadie and Savard 2015). Females nest either on the ground (eiders, scoters, and Long-tailed Ducks) or in tree cavities (mergansers; Eadie and Savard 2015). Nests are constructed of down and body feathers mixed with vegetation around nest sites, in which 4–10 eggs are laid and then incubated for roughly 25–30 days (Alisauskas and Devink 2015). After hatch, broods are typically reared in habitats near nest sites, although substantial movements away from nest sites are not uncommon (Mallory 2015). Young sea ducks fledge at 35–60 days of age (Anderson et al. 2020; Goudie et al. 2020) and may return to breed as 2 or 3-year-olds (Eadie and Savard 2015).

Conservation Status: Sea duck population trajectories are not well documented in some regions, and common use of wintering areas by multiple breeding populations poses challenges for determining breeding population sizes. Few large-scale surveys have been achieved, although finer-scale surveys by state and federal agencies have been completed. Some analyses in recent decades have indicated population declines in some species, and unknown trends in others, due to a paucity of data (Bowman et al. 2015). There are no observations of federally or state-listed sea duck species in the New York Bight region.

4.3.1.2 Exposure Assessment

Group Exposure Determination: **Minimal**

Assessment Method: **Semi-quantitative**

Main Information Sources: MDAT, baseline, site-specific

Supplemental Information Sources: Literature, tracking

Exposure Uncertainty: **Minimal**

Based on BRI's exposure assessment, the group exposure determination for sea ducks was **minimal** (Table 4-6). The mapped outputs of the spatial density model for sea ducks show that the Lease Area is outside predicted areas of higher density along the coast (Figure 4-11). No sea ducks were observed in the NY Bight surveys during summer, which is reflective of their far northern breeding locations. Local exposure scores for sea ducks for all seasons with models available were 0, and regional exposure scores for seasons with models available ranged from 0 to 1. All total exposure scores ranged from 0 to 1, corresponding to three minimal categories and one low category, all equating to a minimal exposure determination. Tracking data indicate that some species may infrequently use offshore areas in the vicinity of the Lease Area during spring and fall migration periods (Figure 4-12, Figure 4-13, Figure 4-14, and Figure 4-15). Within the Lease Area, the only sea duck observations were of Surf Scoters in fall (as shown by density values of 0.008 counts/km² in Table 4-28). Within the Lease Area, seasonal densities of the sea duck taxa group were greatest in the fall and winter, which generally corresponds to the non-breeding season for this taxa group (Figure 4-16). Habitat maps provided by the Sea Duck Joint Venture (SDJV; SDJV 2022) indicate that the Lease Area is in proximity to, but outside of, mapped Key Habitat Areas, though the OECC crosses one such mapped area (Figure 4-17). Uncertainty is minimal for the exposure assessment due to the availability of regional and site-specific digital aerial surveys, MDAT models, and tracking studies.

4.3.1.3 Behavioral Vulnerability Assessment

Collision Vulnerability Determination: **Low**

Assessment Method: **Semi-quantitative**

Collision Uncertainty: **Low**

Based on BRI's vulnerability assessment, the collision vulnerability determination for sea ducks was **low** (Table 4-7). This determination was based on the proportion of time spent flying in the RSZ, avoidance, and flight activity, all of which were derived from the scientific literature. Sea ducks primarily fly low over the sea surface, below the RSZ 96% of the time and within the RSZ the remaining 4% (Figure 4-18), and the literature has documented strong avoidance behavior for Black Scoter (*Melanitta americana*), Common Eider (Desholm and Kahlert 2005; Larsen and Guillemette 2007), and Greater Scaup (*Aythya marila*) (Dirksen and van der Winden 1998 in Langston 2013). Uncertainty is **low** in the collision determination due to the availability of quality data on all parameters.

Displacement Vulnerability Determination: **Low to High**

Assessment Method: **Semi-quantitative**

Displacement Uncertainty: **Low**

Based on BRI's vulnerability assessment, the displacement vulnerability determination for sea ducks was **low** to **high** (Table 4-6). This determination is based on measures of sea duck avoidance behavior and habitat flexibility, which are derived from species accounts in the scientific literature and from tracking studies. Avoidance occurs through macro-avoidance (Langston 2013) and has been demonstrated by a 4.5-fold reduction in waterfowl flocks entering an offshore development post-construction (Desholm and Kahlert 2005). Sea ducks, particularly scoters, are considered to have greater displacement vulnerability than all other seabirds, except loons (Furness et al. 2013). Avoidance behavior can lead to permanent or semi-permanent displacement, resulting in effective habitat loss (Petersen and Fox 2007; Percival 2010; Langston 2013). Avoidance of individual wind arrays is not expected to significantly increase energy expenditure (Masden et al. 2009). However, it is important to note that these avoidance studies were conducted on smaller WTGs, which were spaced closer together than those being considered for the Lease Area, and so may not accurately reflect the future behavior of sea ducks around the Lease Area. For some species, this displacement may cease several years after construction, as food resources, behavioral responses, and/or other factors change (Petersen and Fox 2007; Leonhard et al. 2013). Overall, displacement from individual wind facilities is unlikely to affect populations because relatively few individuals are affected, and there is evidence of birds returning to wind facilities once they become operational (Fox and Petersen 2019). While the OECC will pass through roughly 50 km (31 mi) of mapped key habitat for sea ducks (Figure 4-17), the temporary effects of sediment suspension and deposition will quickly abate. Vulnerability to long-term displacement will vary by species; the range is low-medium for Red-breasted Mergansers (*Mergus serrator*), but medium-high for the other five species considered. Uncertainty in the displacement vulnerability determination is **low** due to the availability of quality information on avoidance and habitat flexibility.

Population Vulnerability Determination: **Low** to **Medium**

Assessment Method: **Semi-quantitative**

Based on BRI's vulnerability assessment, the population vulnerability determination for sea ducks was **low** to **medium**. This determination is based on the continental combined score, the state listing status, and adult survival (see methods in Section 3.8.2). Sea ducks are not listed at the federal or state level, but their adult survival is high relative to other taxa, making sea duck populations in general more sensitive to mortality of adult individuals (Koneff et al. 2017).

4.3.1.4 Risk Determination

Sea ducks received a final exposure determination of minimal, a relative collision vulnerability determination of low, a relative displacement vulnerability determination of low to high, and a

population vulnerability determination of low to medium. Based on BRI's risk assessment matrix (Table 2-1), final collision and displacement risk were both assessed as **minimal**.

4.3.1.5 Tables and Figures

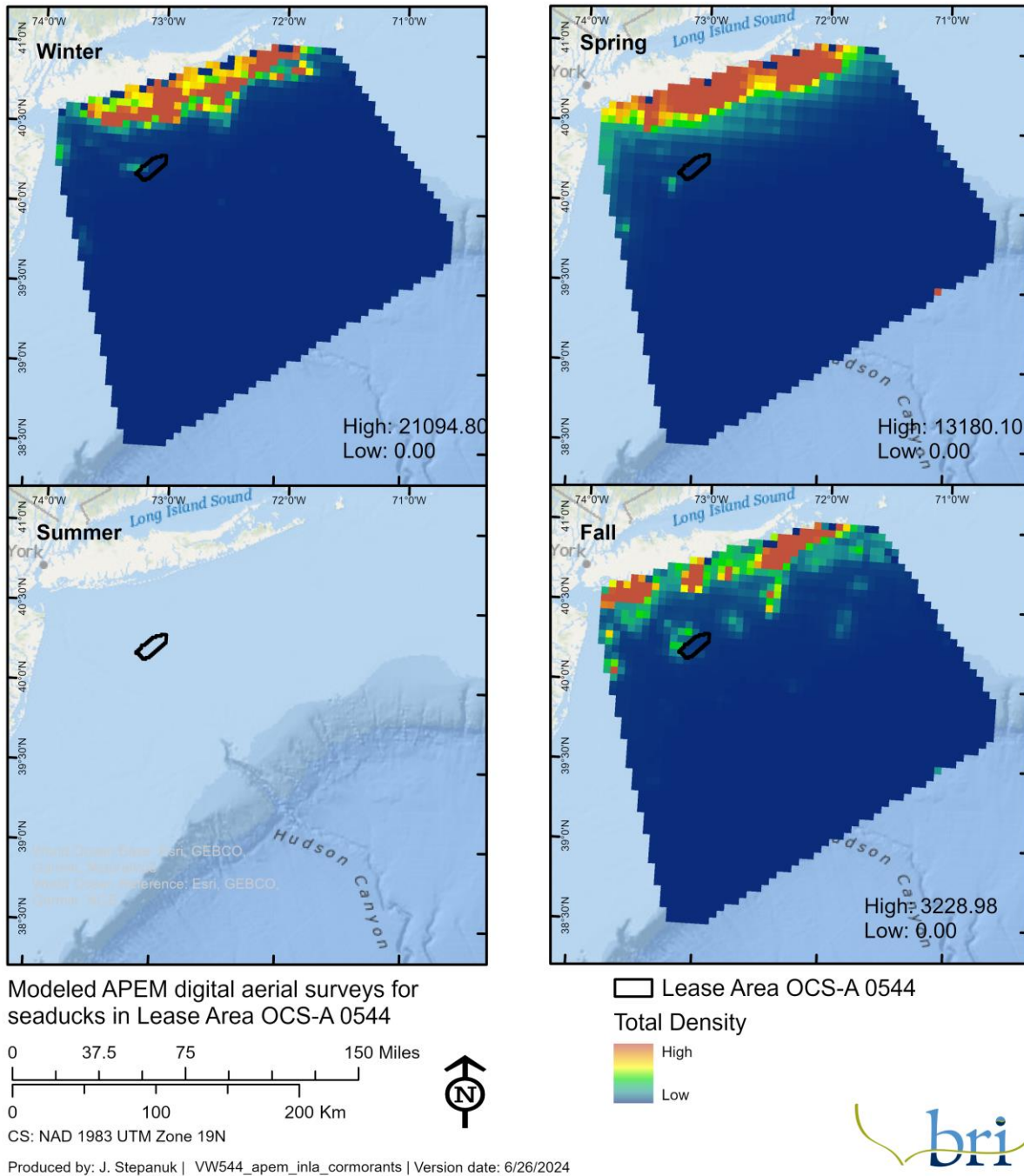
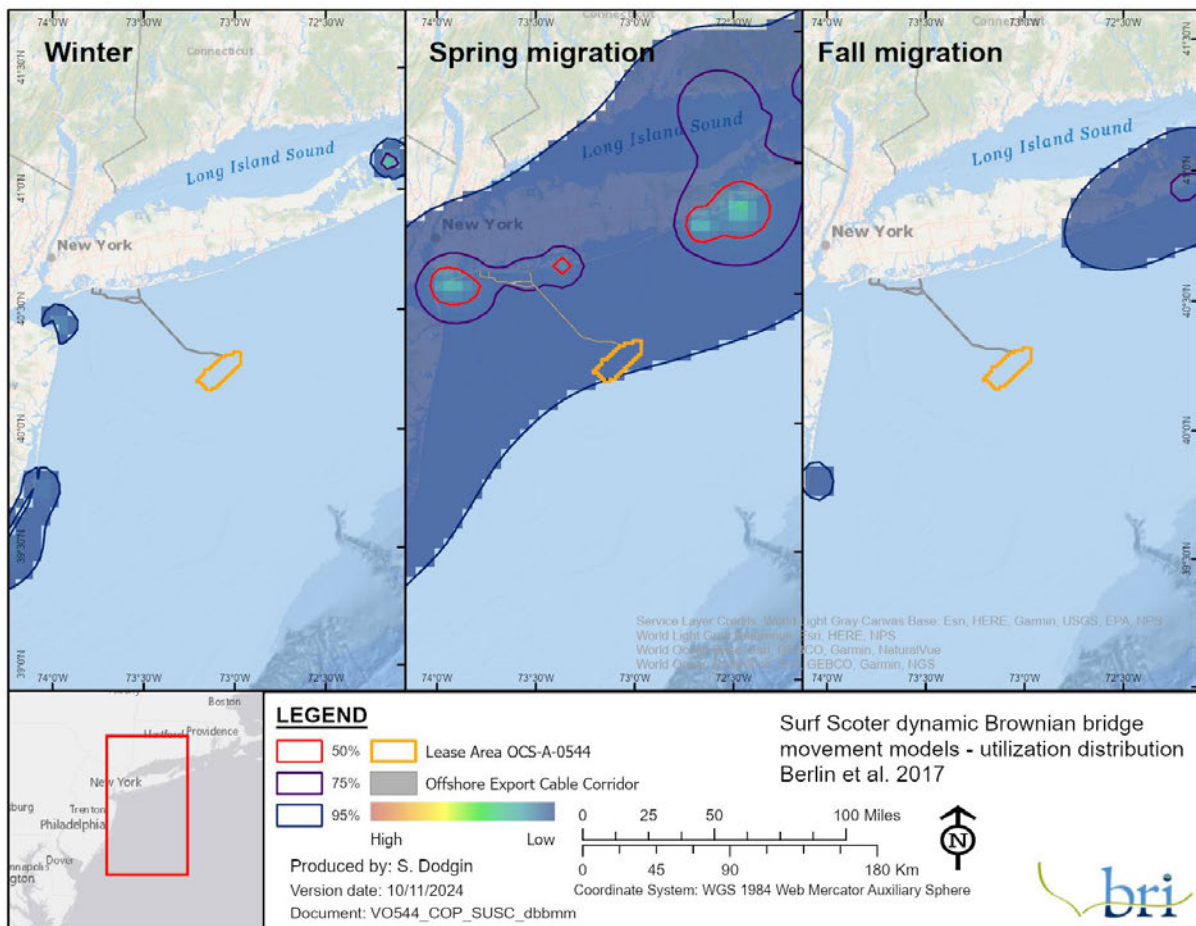


Figure 4-11: Modeled APEM digital aerial surveys for sea ducks in the NY Bight survey area and Lease Area OCS-A 0544.

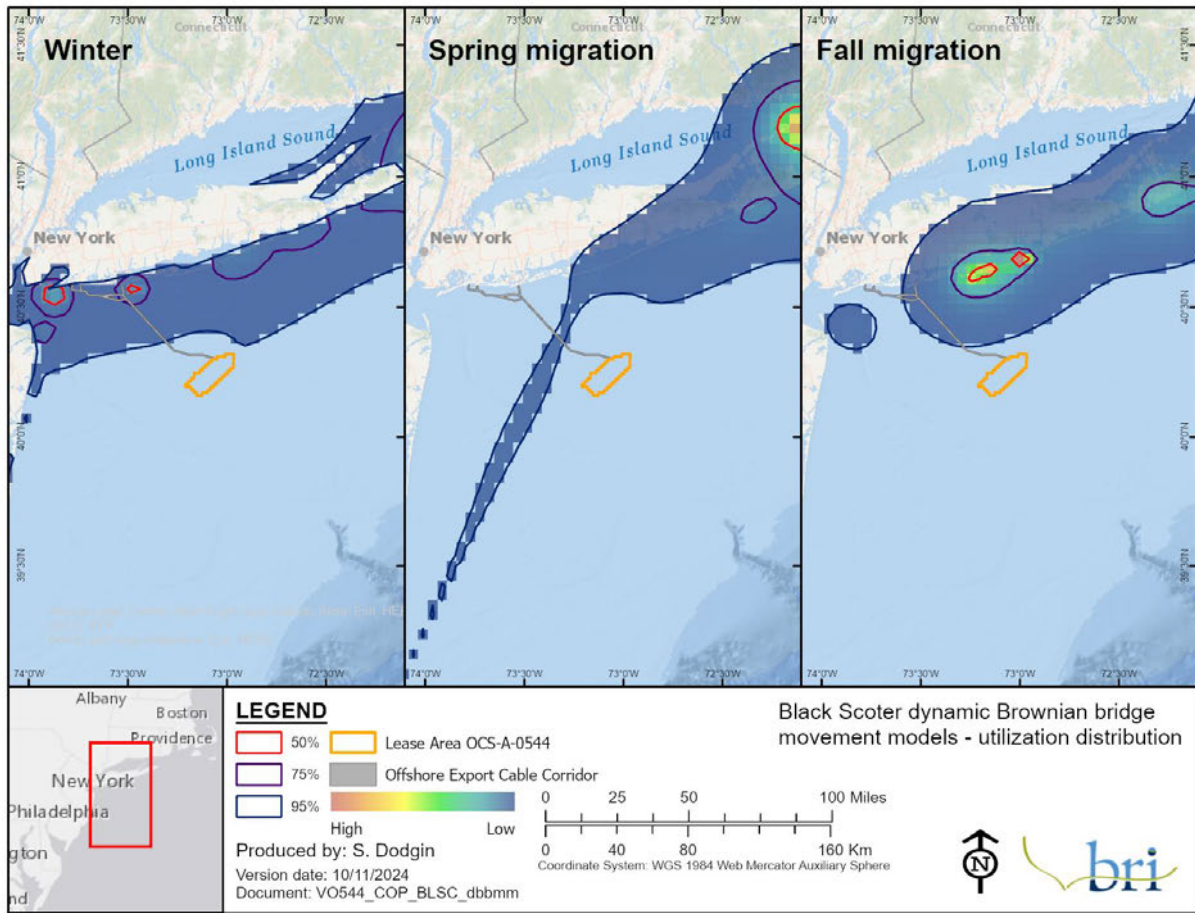
Table 4-6: Seasonal exposure rankings for the sea duck group.

Taxa Group	Season	Local Score	Regional Score	Total Score	Exposure Category
Sea ducks	Winter	0	0	0	minimal
	Spring	0	1	1	low
	Summer	-	-	-	minimal
	Fall	0	0	0	minimal

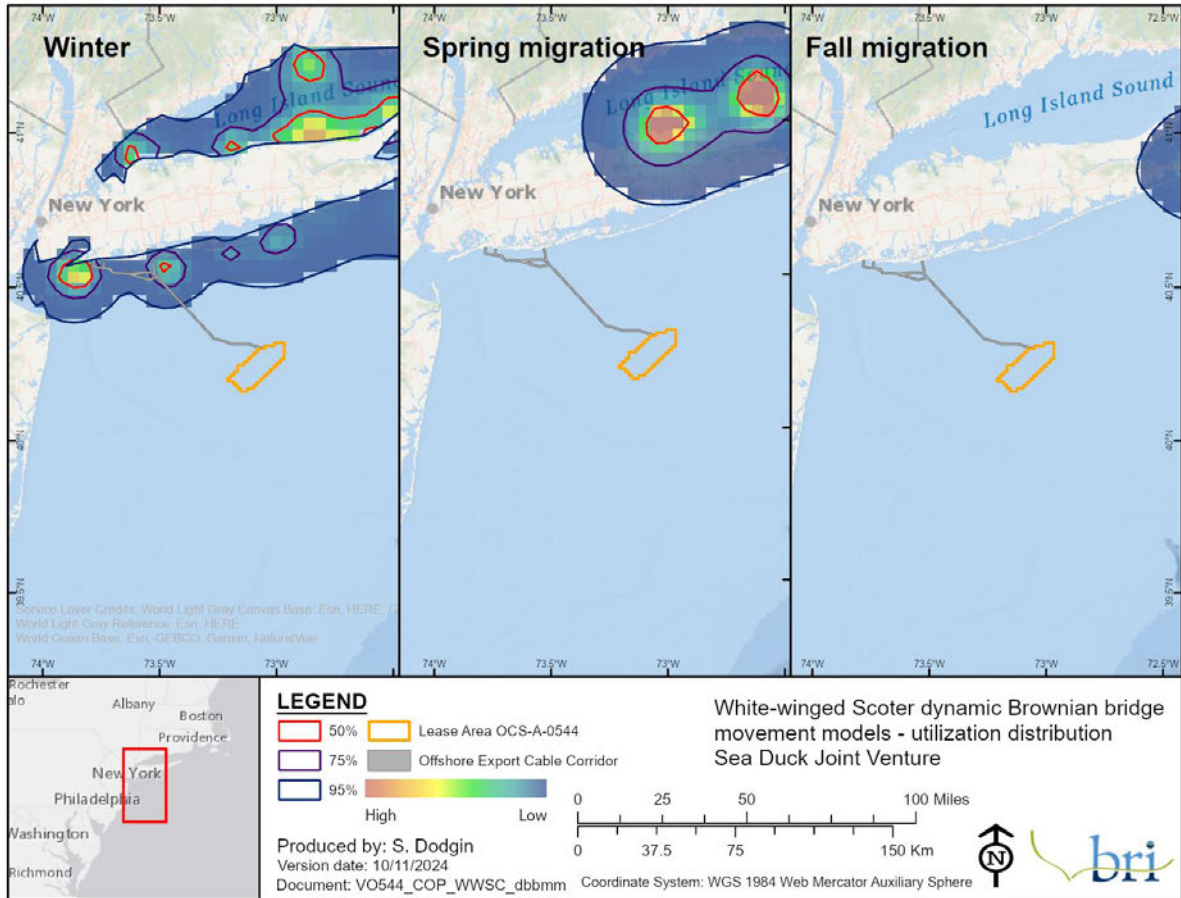


NOTE: Contours represent various levels of use, from 50% (core use) to 95% (home range).

Figure 4-12: Dynamic Brownian Bridge movement models for Surf Scoter ($n=8$ in winter, 87 in spring, 83 in fall) that were tracked with satellite transmitters.

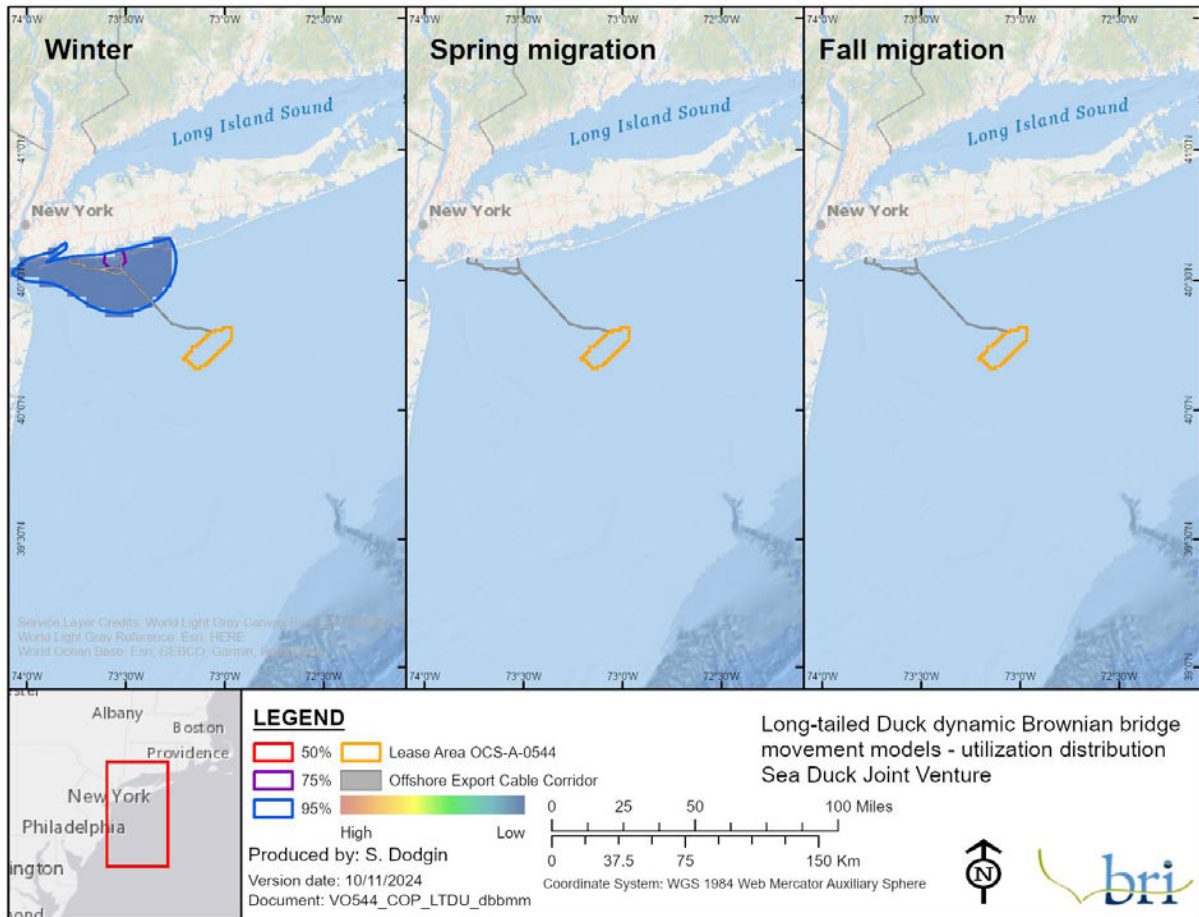


NOTE: Contours represent various levels of use, from 50 % (core use) to 95 % (home range).
 Figure 4-13: Dynamic Brownian Bridge movement models for Black Scoter (n=61 in winter, 76 in spring, 80 in fall) that were tracked with satellite transmitters.



NOTE: Contours represent various levels of use, from 50 % (core use) to 95 % (home range).

Figure 4-14: Dynamic Brownian Bridge movement models for White-winged Scoter ($n=66$ in winter, 45 in spring, 62 in fall) that were tracked with satellite transmitters.



NOTE: Contours represent various levels of use, from 50 % (core use) to 95 % (home range).
 Figure 4-15: Dynamic Brownian Bridge movement models for Long-tailed Duck ($n=49$ in winter, 60 in spring, 37 in fall) that were tracked with satellite transmitters.

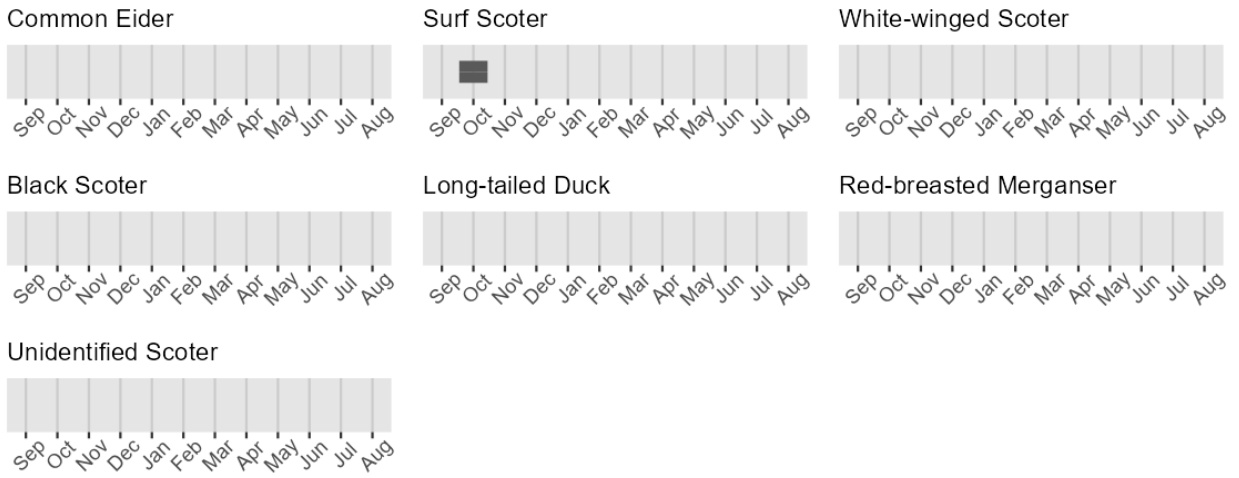


Figure 4-16: Monthly relative densities of sea ducks in the Lease Area from digital aerial surveys.

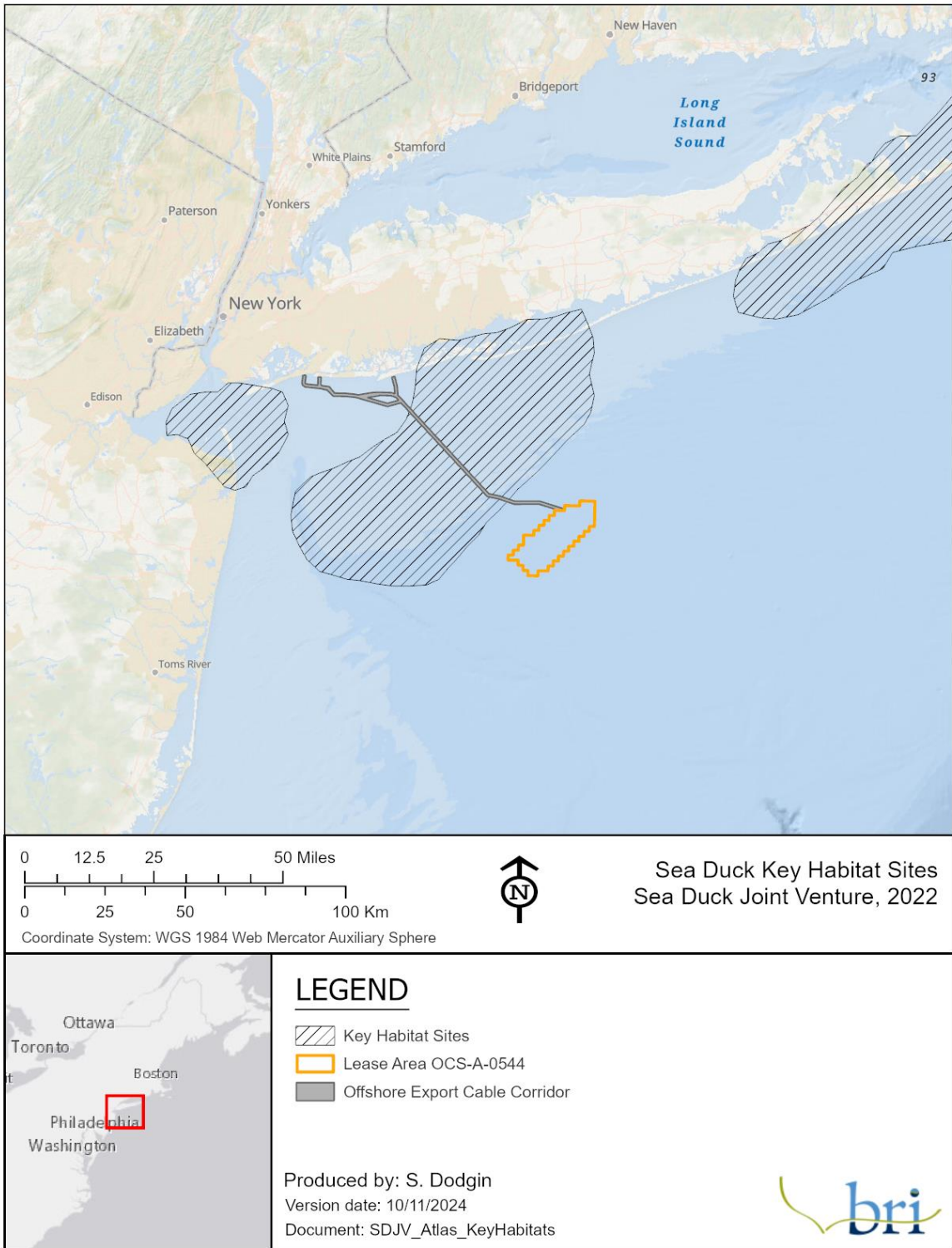
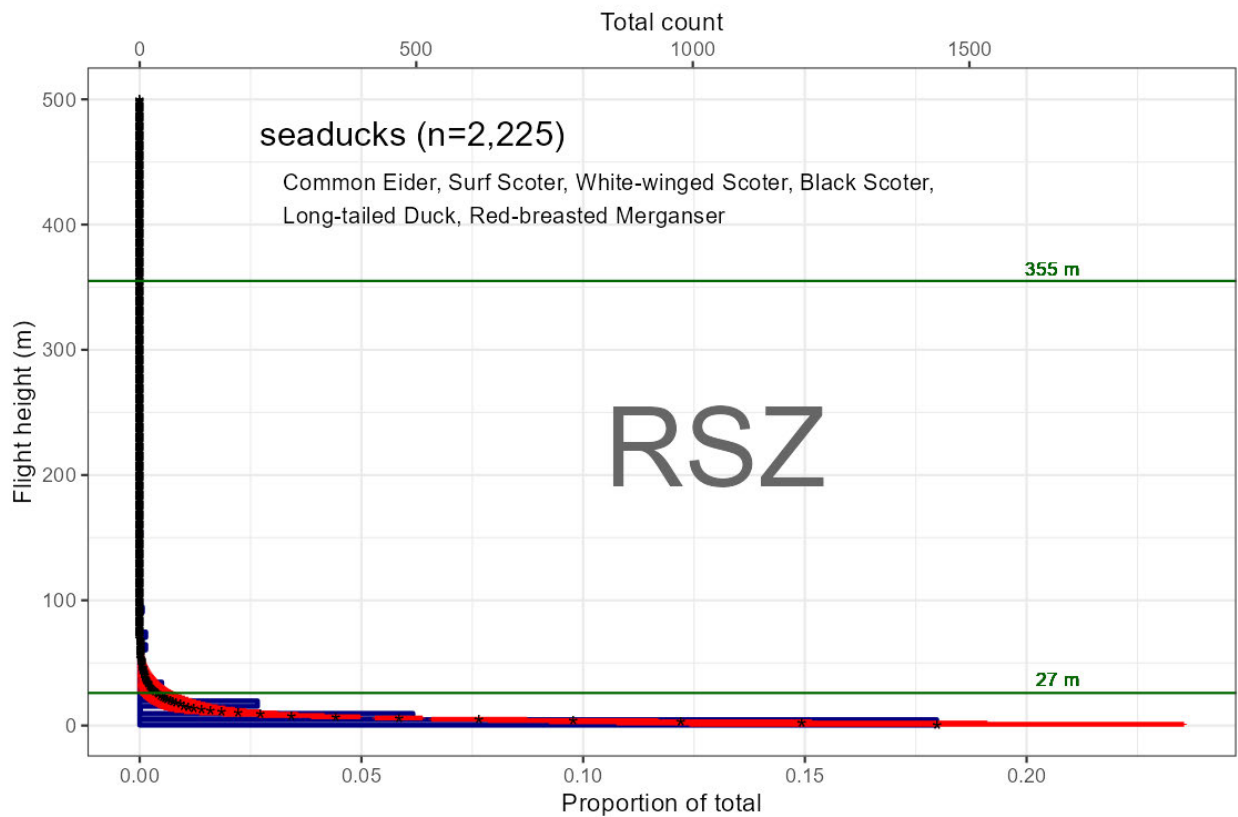


Figure 4-17: Sea duck key habitat sites as defined by Sea Duck Joint Venture in relation to the Lease Area and Offshore Export Cable Corridor.



NOTE: Figure shows the actual number of birds in 5 m (16 ft) intervals (blue bars), the modeled average flight height in 1 m (3 ft) intervals (black asterisks), and the standard deviation (red lines), in relation to the upper and lower limits of the RSZ (27–355 m; green lines).

Figure 4-18: Flight heights of sea ducks (n=2,225) derived from the Northwest Atlantic Seabird Catalog.

Table 4-7: Vulnerability assessment rankings by species for the sea duck group.

NOTE: A lower range is added in green font to the Displacement Vulnerability (DV) score because there is evidence in the literature that some sea ducks will return to offshore wind farms several years after operation.

Species	Collision Vulnerability (CV)	Displacement Vulnerability (DV)	Population Vulnerability (PV)
Black Scoter	low (0.3)	medium-high (0.9)	low (0.4)
Common Eider	low (0.27)	medium-high (0.9)	low (0.47)
Long-tailed Duck	low (0.33)	medium-high (0.9)	low (0.27)
Red-breasted Merganser	low (0.4)	low-medium (0.5)	low (0.27)
Surf Scoter	low (0.3)	medium-high (0.9)	medium (0.53)
White-winged Scoter	low (0.27)	medium-high (0.8)	medium (0.53)

4.3.2 Phalaropes

Minor Taxa Groups: Charadriiformes: Scolopacidae, genus Phalaropus

Collision Risk Determination: **Minimal**

Displacement Risk Determination: **Minimal**

4.3.2.1 *Overview*

Distribution and Habitat Preferences: Phalaropes are Arctic and Subarctic breeding shorebirds that, unlike other shorebirds, use offshore marine habitats during the non-breeding period. They migrate long distances over water, stopping to feed in marine areas before proceeding. Non-breeding birds may overwinter 40–80 km (25-50 mi) offshore, with concentrations along oceanographic fronts (Haney 1985). Phalaropes may also aggregate near Sargassum mats that presumably concentrate invertebrate prey at depths accessible by these small surface-feeding birds (Haney 1986). Migratory routes are largely unknown but appear associated with upwelling areas and fronts with concentrated prey (Rubega et al. 2020; Tracy et al. 2020).

Behavior and Ecology: Phalaropes feed on zooplankton and other prey at the surface of the water, regardless of water depth. By spinning in tight circles, individual phalaropes may concentrate prey which they then pluck from the water. Phalaropes have webbed feet which allow them to swim effectively.

Reproduction: Phalaropes do not occur in the New York Bight region during the breeding season of May to September, as they are farther north at breeding areas. Phalaropes have reverse sexual dichromatism, where females have bright and showy plumage and males are more subdued and less conspicuous. Females compete for breeding males, and lay eggs in a nest built by the male before departing to potentially find another mate and lay another clutch of eggs. The male then incubates the eggs and raises the chicks without assistance from the female. Chicks develop rapidly and become flight capable at roughly 15 days of age.

Conservation Status: Phalaropes, like other shorebirds, are highly sensitive to broad-scale changes in the marine environment (e.g., localized population declines in a staging area in the Bay of Fundy perhaps related to conditions in coastal Ecuador and Peru) (Rubega et al. 2020; Tracy et al. 2020). Populations have declined from historic levels, but the magnitude of change is poorly documented (Rubega et al. 2020; Tracy et al. 2020). Mortality associated with power line collisions does occur (Rubega et al. 2020; Tracy et al. 2020). Two species, the Red Phalarope and the Red-necked Phalarope, migrate along the US Atlantic coast; however, neither species is federally listed.

4.3.2.2 *Exposure Assessment*

Group Exposure Determination: **Minimal**

Assessment Method: **Semi-quantitative**

Main Information Sources: MDAT, baseline, site-specific

Supplemental Information Sources: Literature

Exposure Uncertainty: **Low**

Based on BRI's exposure assessment, the group exposure determination for phalaropes was minimal (Table 4-8). The mapped outputs of the spatial density model for phalaropes show that

the Lease Area is outside predicted core areas of phalarope density along the coast in fall and spring, while higher densities are farther offshore in winter (Figure 4-19). In summer, the mapped outputs show the Lease Area to be within an area of higher density, but overall density is much lower than in the other seasons; as noted above, phalaropes are not in the New York Bight during the breeding season save for a few scattered individuals arriving late or departing early. Local exposure scores for this group for winter, spring, and fall were 0, which corresponds to minimal exposure categories. The local exposure score for summer was 1, which corresponds to a low total exposure category for summer, but this is largely due to a low sample size of observations in summer, as seen in very low density overall. In the Lease Area, there were observations of Red Phalaropes (*Phalaropus fulicarius*) and “Unidentified phalarope” (as shown by density counts/km² in Table 4-28) primarily during winter and fall. Within the Lease Area, seasonal densities of phalaropes were greatest in the fall and spring (Figure 4-20). Uncertainty is low due to the availability of local and regional digital aerial survey data and MDAT models. Tracking data are not available for either phalarope species present on the US Atlantic coast.

4.3.2.3 Behavioral Vulnerability Assessment

Collision Vulnerability Determination: **Low**

Assessment Method: **Semi-quantitative**

Collision Uncertainty: **High**

Based on BRI’s vulnerability assessment, the collision vulnerability determination for phalaropes was **low** (Table 4-9). Little is known about how phalaropes respond to offshore WTGs in terms of avoidance behavior, and their flight activity is not well studied. The available flight height data from the Northwest Atlantic Seabird Catalog indicate that phalaropes fly very low over the sea surface, well below the RSZ (Figure 4-21), 99.9% of the time. Uncertainty about this determination is **high** due to the lack of quality information about flight activity and avoidance for phalaropes.

Displacement Vulnerability Determination: **Medium**

Assessment Method: **Semi-quantitative**

Displacement Uncertainty: **Medium**

Based on BRI’s vulnerability assessment, the displacement vulnerability determination for phalaropes was **medium** (Table 4-9). As noted above for collision vulnerability, little is known about the potential for phalarope avoidance of offshore WTGs. In their non-breeding marine habitat, phalaropes are surface feeders regardless of water depth, and have some habitat flexibility as a result. Uncertainty about phalaropes’ vulnerability to displacement is **medium**, due to their unknown avoidance rates, factors affecting their habitat flexibility, and their migratory routes over the offshore environment.

Population Vulnerability Determination: **Low**

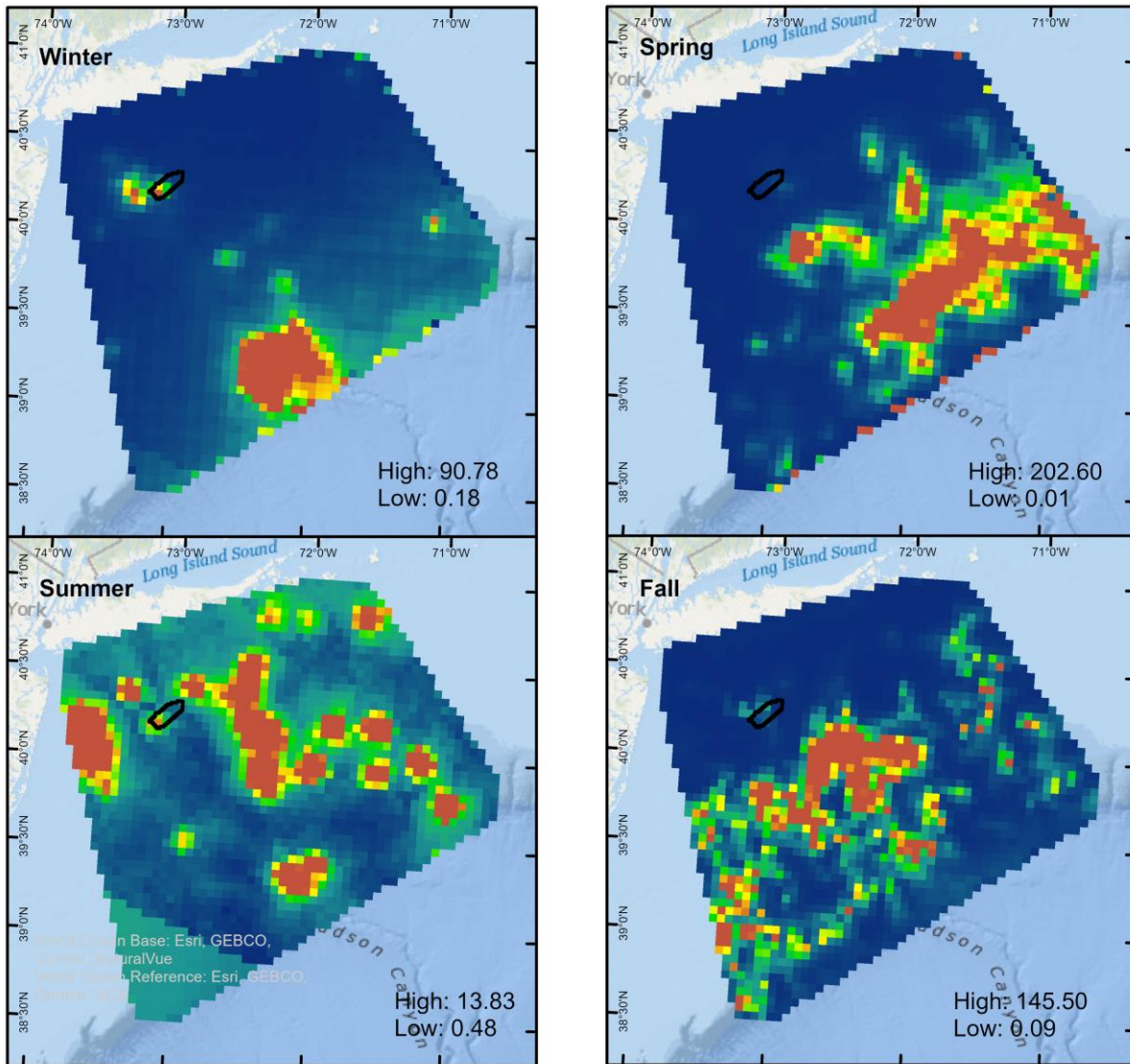
Assessment Method: **Semi-quantitative**

Based on BRI's vulnerability assessment, the population vulnerability determination for phalaropes was **low** (Table 4-9). Phalarope species are not considered to have high priority conservation status.

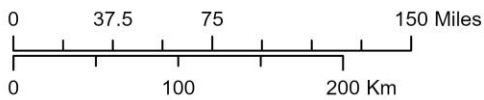
4.3.2.4 Risk Determination

Phalaropes received an exposure determination of minimal, a relative collision vulnerability determination of low, a relative displacement vulnerability determination of medium, and a population vulnerability determination of low. Based on BRI's risk assessment matrix (Table 2-1), final collision and displacement risk were both assessed as **minimal**.

4.3.2.5 Tables and Figures



Modeled APTEM digital aerial surveys for phalaropes in Lease Area OCS-A 0544



CS: NAD 1983 UTM Zone 19N

Produced by: J. Stepanuk | VW544_apem_inla_cormorants | Version date: 6/26/2024



Figure 4-19: Modeled APTEM digital aerial surveys for phalaropes in the NY Bight survey area and Lease Area OCS-A 0544.

Table 4-8: Seasonal exposure rankings for the phalaropes group.

Taxa Group	Season	Local Score	Regional Score	Total Score	Exposure Category
Phalaropes	Winter	0	0	0	minimal
	Spring	0	0	0	minimal
	Summer	1	0	1	low
	Fall	0	0	0	minimal

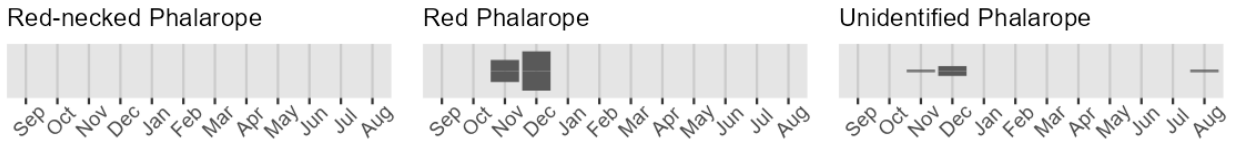
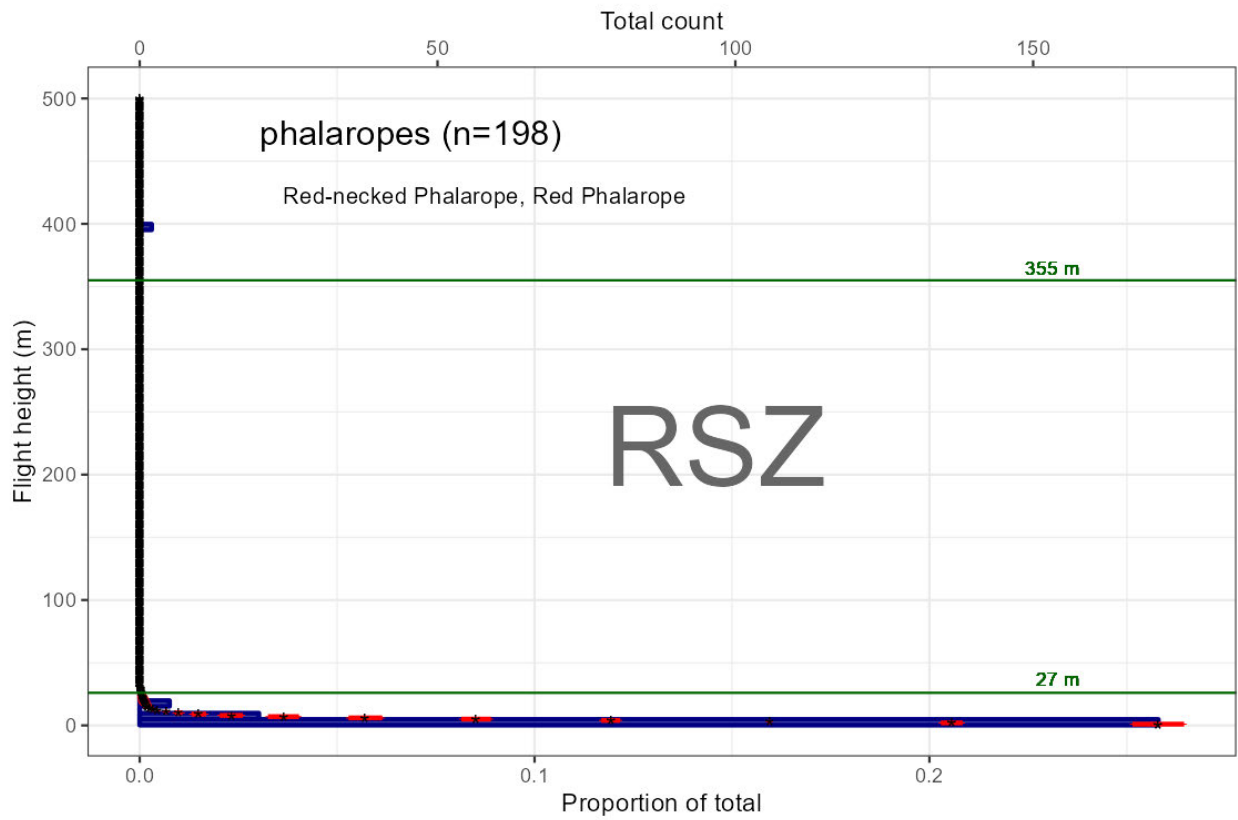


Figure 4-20: Monthly relative densities of phalaropes in the Lease Area from digital aerial surveys.



NOTE: Figure shows the actual number of birds in 5 m (16-ft) intervals (blue bars), the modeled average flight height in 1 m (3 ft) intervals (black asterisks), and the standard deviation (red lines), in relation to the upper and lower limits of a minimum and maximum RSZ scenario (27–355 m; green lines).

Figure 4-21: Flight heights of phalaropes (n=198) derived from the Northwest Atlantic Seabird Catalog.

Table 4-9: Vulnerability assessment rankings by species for the phalaropes group.

Species	Collision Vulnerability (CV)	Displacement Vulnerability (DV)	Population Vulnerability (PV)
Red-necked Phalarope	low (0.37)	medium (0.5)	low (0.27)
Red Phalarope	low (0.43)	medium (0.5)	low (0.27)

4.3.3 Auks

Minor Taxa Groups: Charadriiformes: Alcidae (auks)

Collision Risk Determination: **Minimal**

Displacement Risk Determination: **Low**

4.3.3.1 Overview

Distribution and Habitat Preferences: The auks are a group of marine-obligate species that spend their entire lives at sea aside from the breeding season (Winkler et al. 2020k). On land, auks are generally restricted to breeding colonies on cliffs or offshore islands, but at sea they range broadly. Most species breed far north of the New York Bight but use the region to some degree during winter.

Behavior and Ecology: Auks feed exclusively on small fish and marine invertebrates that they capture at sea by diving and pursuing prey underwater (Winkler et al. 2020k). Dives may reach substantial depths, facilitated by flying underwater, meaning that auks use their wings to assist with diving and chasing prey. Auks may occur in very large, mobile flocks that are largely nomadic during the non-breeding season, following congregations of ephemeral prey species.

Reproduction: Auks either nest on cliff faces or in shallow cavities, generally in large colonies (Winkler et al. 2020k). Of the species likely to be present in the New York Bight during the non-breeding season, most breeding takes place in the Gulf of Maine and farther north to Subarctic and Arctic regions (Gaston and Jones 1998). Clutches of 1-2 eggs are raised by both adults, with each adult provisioning young between hatch and fledge with small fish the adults carry in their bills (Winkler et al. 2020k).

Conservation Status: None of the auks present in the US Atlantic are federally listed, although all species are highly sensitive to changes in marine conditions and are of particular concern regarding the impacts of climate change. Historic extirpations in the southern reaches of their breeding grounds were associated with overharvest by humans (Winkler et al. 2020k), which no longer occurs in the US, although legal harvest of auks continues in the Canadian provinces of Newfoundland and Labrador and across the eastern Canadian Arctic. Given their highly mobile nature and lack of broad-scale population surveys, conservation status of auks is somewhat uncertain. No auks are listed in either New York or New Jersey.

4.3.3.2 Exposure Assessment

Group Exposure Determination: **Low**

Assessment Method: **Semi-quantitative**

Main Information Sources: Baseline, MDAT, site-specific

Supplemental Information Sources: Literature

Exposure Uncertainty: **Low**

Based on BRI's exposure assessment, the group exposure determination for auks was low (Table 4-10). The mapped outputs of the spatial density model for auks show that the Lease Area is outside the areas of highest predicted density, which for auks are dispersed throughout the NY Bight survey area (Figure 4-22). Auks in summer were too infrequently observed to model, as is expected from their northern breeding locations. Local exposure scores for the auks were 1 for winter, 2 for spring, and 0 for all remaining seasons, meaning that all total exposure scores range from minimal to low exposure categories. In the Lease Area, there were observations of

Razorbills as well as observations APEM termed “Unidentified Alcid and “Unidentified Murre” (as shown by density values counts/km² provided in Table 4-28). Within the Lease Area, seasonal densities of auks were greatest in the fall, winter, and spring (Figure 4-23). Uncertainty is low for the exposure assessment due to the availability of regional and site-specific digital aerial surveys, and MDAT models. Tracking data are not available for any of the auks.

4.3.3.3 Behavioral Vulnerability Assessment

Collision Vulnerability Determination: **Minimal**

Assessment Method: **Semi-quantitative**

Collision Uncertainty: **Low**

Based on BRI’s vulnerability assessment, the collision vulnerability determination for auks was **minimal** (Table 4-11). The available flight height data from the Northwest Atlantic Seabird Catalog indicate that auks fly low over the sea surface, below the RSZ under consideration (Figure 4-24), more than 99% of the time. At considerably smaller WTGs than those being considered for the Lease Area, Atlantic Puffins (*Fratercula arctica*), Razorbills, and Common Murres were estimated to fly between 20–150 m (66–492 ft) 0.1%, 0.4 %, and 0.01 % of the time, respectively (Cook et al. 2012). Uncertainty about this determination is **low** due to the availability of quality information about flight height, avoidance, and flight activity.

Displacement Vulnerability Determination: **Medium to High**

Assessment Method: **Semi-quantitative**

Displacement Uncertainty: **Low**

Based on BRI’s vulnerability assessment, the displacement vulnerability determination for auks was **medium to high** (Table 4-11). Due to their sensitivity to disturbance from boat traffic and habitat/prey specialization, many auks rank high in displacement vulnerability assessments (Furness et al. 2013; Dierschke et al. 2016; Wade et al. 2016). Studies in Europe have documented varying levels of displacement with rates ranging from no apparent displacement to 70% (Ørsted 2018). Auks have a total avoidance rate of 99.2% (Cook et al. 2012). The abundance of Common Murres and Razorbills decreased in wind farm areas by 71% and 64%, respectively (Vanermen et al. 2015). Auks have been shown to have a 75% lower abundance inside offshore wind farms than in adjacent waters and are estimated to start avoidance behaviors at 1.2–2.5 km (0.7–1.6 mi) (Welcker and Nehls 2016). Uncertainty about the displacement vulnerability determination is **low** due to the high-quality information available on auk avoidance of WTGs and habitat flexibility.

Population vulnerability determination: **Low to Medium**

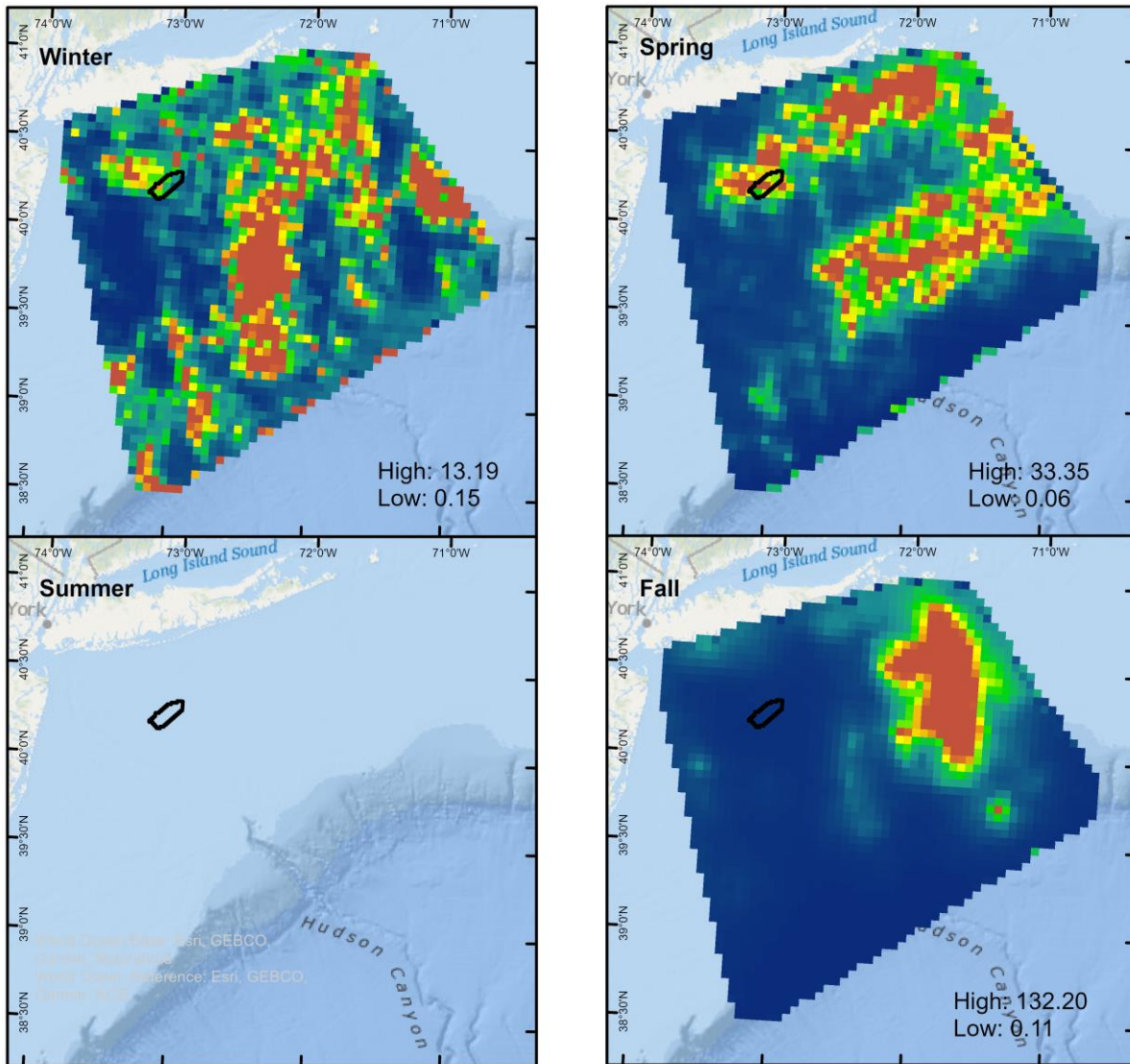
Assessment Method: **Semi-quantitative**

Based on BRI's vulnerability assessment, the population vulnerability determination for auks was **low to medium** (Table 4-11). Atlantic Puffins and Razorbills were assessed as medium, which is attributable to these species' higher adult survival than the other four auk species assessed. Auk populations are generally stable (Ainley et al. 2021; Lowther et al. 2020; Lavers et al. 2020) and the group does not have a high priority conservation status.

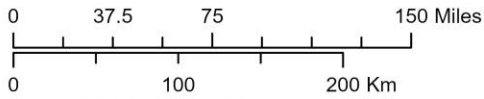
4.3.3.4 Risk Determination

Auks received an exposure determination of low, a relative collision vulnerability determination of minimal, a relative displacement vulnerability determination of medium to high, and a population vulnerability determination of low to medium. Based on BRI's risk assessment matrix (Table 2-1), final collision risk was assessed as **minimal**, and displacement risk was assessed as **low**.

4.3.3.5 Tables and Figures



Modeled APEM digital aerial surveys for auks in Lease Area OCS-A 0544



CS: NAD 1983 UTM Zone 19N

Produced by: J. Stepanuk | VW544_apem_inla_cormorants | Version date: 6/26/2024



□ Lease Area OCS-A 0544

Total Density



Figure 4-22: Modeled APEM digital aerial surveys for auks in the NY Bight survey area and Lease Area OCS-A 0544.

Table 4-10: Seasonal exposure rankings for the auks group.

Taxa Group	Season	Local Score	Regional Score	Total Score	Exposure Category
Auks	Winter	1	0	1	low
	Spring	2	0	2	low
	Summer	-	-	-	minimal
	Fall	0	0	0	minimal

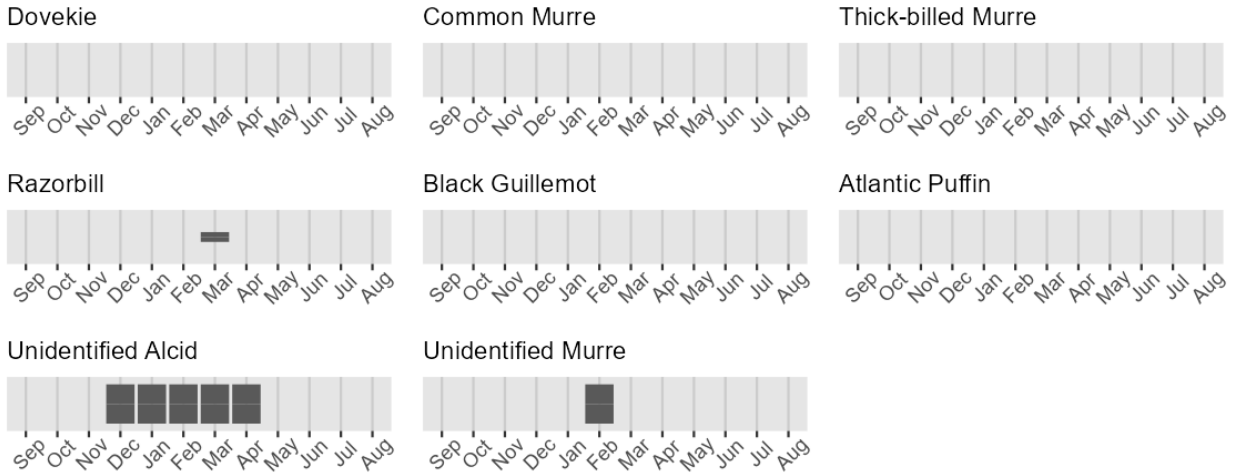
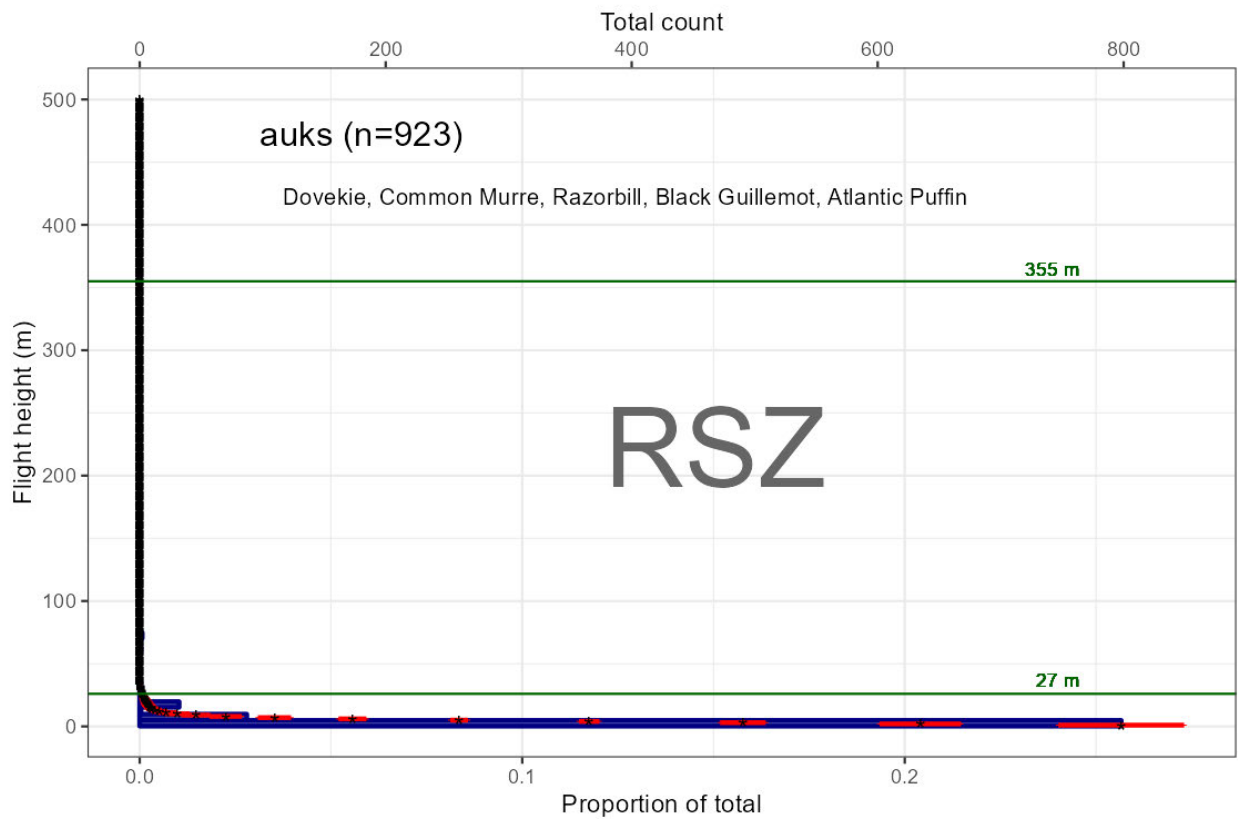


Figure 4-23: Monthly relative densities of auks in the Lease Area from digital aerial surveys.



NOTE: Figure shows the actual number of birds in 5 m (16 ft) intervals (blue bars), the modeled average flight height in 1 m (3 ft) intervals (black asterisks), and the standard deviation (red lines), in relation to the upper and lower limits of a minimum and maximum RSZ scenario (27–355 m; green lines).

Figure 4-24: Flight heights of auks (n=923) derived from the Northwest Atlantic Seabird Catalog.

Table 4-11: Vulnerability assessment rankings by species for the auks group.

Species	Collision Vulnerability (CV)	Displacement Vulnerability (DV)	Population Vulnerability (PV)
Atlantic Puffin	minimal (0.2)	high (0.8)	medium (0.53)
Black Guillemot	minimal (0.2)	high (0.9)	low (0.4)
Common Murre	minimal (0.23)	high (0.8)	low (0.4)
Dovekie	minimal (0.2)	medium (0.7)	low (0.4)
Razorbill	minimal (0.2)	high (0.8)	medium (0.6)

4.3.4 Gulls, Skuas, and Jaegers

Minor Taxa Groups: Charadriiformes: Laridae: subfamily Larinae (gulls), Charadriiformes: Stercorariidae (jaegers and skuas)

Collision Risk Determination: **Minimal to Low**

Displacement Risk Determination: **Minimal to Low**

4.3.4.1 *Overview*

Distribution and Habitat Preferences: Gulls are largely coastal species year-round, although some species are broadly distributed inland as well (Winkler et al. 2020l). Jaegers and skuas are pelagic, remaining at sea during most of the non-breeding season (Winkler et al. 2020m). Gulls are found in coastal habitats foraging on a wide range of prey, including scavenging of anthropogenic and natural foods. Jaegers and skuas tend to breed at high latitudes, while gulls breed throughout the Atlantic coast of North America (Winkler et al. 2020l, m).

Behavior and Ecology: Both predatory and scavenging, these birds are locally abundant, especially near humans. Jaegers and skuas feed on any prey they can capture, often doing so by stealing captured fish from other predatory birds, such as auks (Winkler et al. 2020m). Gulls are highly adept predators, often consuming eggs and chicks of other seabird species in coastal breeding areas (Winkler et al. 2020l). Depending on the species, gulls become sexually mature at 2, 3, or 4 years of age, consistent with respectively small, medium, and large body size.

Reproduction: Both adults are involved at all stages of reproduction, with males helping females to build nests, incubate eggs, and provision young. Precocial young grow quickly and become mature in 2–4 years, depending on the species. Nests are shallow scrapes in the ground, which gulls build up by piling vegetation around eggs as they are laid. Gulls lay 2–3 eggs, while skuas and jaegers typically lay 1–2 (Winkler et al. 2020l, m).

Conservation Status: None of the species in the gulls, skuas, and jaegers group are federally listed, nor are any listed at the state level in New York or New Jersey. However, all species are data-deficient and lack information regarding population trajectories and distributions at sea.

4.3.4.2 Exposure Assessment

Group Exposure Determination: **Minimal to Low**

Assessment Method: **Semi-quantitative**

Main Information Sources: MDAT, baseline, site-specific

Supplemental Information Sources: Literature

Exposure Uncertainty: **Low**

Based on BRI's exposure assessment, the group exposure determination for gulls, jaegers, and skuas was **minimal to low** (Table 4-12). Mapping and exposure scoring were done for five sub-groups: small gulls; medium gulls; large gulls; all gulls; and skuas and jaegers. The mapped outputs of the spatial density model for gulls, jaegers, and skuas show that the Lease Area is within areas of medium or higher predicted density for small gulls, especially in winter and spring (Figure 4-25), and within areas of lower density for medium gulls, large gulls, all gulls, and skuas and jaegers (Figure 4-26, Figure 4-27, Figure 4-28, and Figure 4-29). In local exposure scoring, small gulls were the most exposed, with medium exposure in winter. Supporting this determination, the Bonaparte's Gull (*Chroicocephalus philadelphia*, a small gull) had the highest annual density of any bird species observed in the Lease Area (Table 4-28) and was present in its highest densities in winter. Medium gulls had local exposure scores of 2 in winter, 1 in spring and 0 for all remaining seasons. Large gulls had local exposure scores of 2 in fall, and 0 for all other seasons. Skuas and jaegers had local exposure scores of 0 in spring and fall, and observations were too few for INLA models in winter and summer. No jaegers or skuas were identified within the Lease Area, and in the NY Bight survey area they were present in much lower densities and total counts than the gulls (Table 4-28). Uncertainty is **low** for the exposure assessment due to the availability of regional and site-specific digital aerial surveys, as well as MDAT models. Tracking data are not available for any species in this group.

4.3.4.3 Behavioral Vulnerability Assessment

Collision Vulnerability Determination: **Low to Medium**

Assessment Method: **Semi-quantitative**

Collision Uncertainty: **Low**

Based on BRI's vulnerability assessment, the collision vulnerability determination for gulls, skuas, and jaegers was **low to medium** (Table 4-13). The available flight height data from the Northwest Atlantic Seabird Catalog indicate that small gulls fly within the RSZ 2% of the time (Figure 4-31), medium gulls 7% of the time (Figure 4-32), large gulls 22% of the time (Figure 4-33), and skuas and jaegers 6% of the time (Figure 4-34); virtually all the rest of the flights are below the RSZ.

Among marine bird groups, gulls have typically ranked at the top of collision vulnerability assessments because they can fly within the RSZ (Johnston et al. 2014), have a documented attraction to WTGs (Vanermen et al. 2015), and individual birds have been documented to collide with WTGs (Skov et al. 2018). However, many recent studies have documented meso-avoidance and micro-avoidance behavior that indicate a lower collision risk than previously thought. A recent study at an offshore wind farm near Aberdeen, Scotland, studied the flight behavior of Black-legged Kittiwakes and several large gull species, as well as Northern Gannets (*Morus bassanus*), and documented no collisions or even near misses in over 10,000 bird videos and over 3,000 combined video-radar tracks (Tjørnløv et al. 2023). Recent GPS tracking studies in the UK showed that Lesser Black-backed Gulls (*Larus fuscus*) do not exhibit macro-avoidance of offshore wind farms but will preferentially fly between the WTG rows in a meso-avoidance pattern (Green et al. 2023). In the 2023 Green et al. study, the GPS-tracked Lesser Black-backed Gulls had a mean flight height below 14 m and flew higher during the day than at night within the wind farm. Other recent research shows that the attraction response in gulls may be mostly confined to certain WTGs at the edge of a wind farm array, potentially limiting collision risk to a small subset of WTGs (Vanermen et al. 2019). The Aberdeen study (Tjørnløv et al. 2023) recorded very strong micro-avoidance behavior near rotor blades. Uncertainty about this determination is **low** due to the quality information available for flight height, avoidance, and flight activity.

Displacement Vulnerability Determination: **Low to Medium**

Assessment Method: **Semi-quantitative**

Displacement Uncertainty: **Low**

Based on BRI's vulnerability assessment, the displacement vulnerability determination for gulls, skuas, and jaegers was **low to medium** (Table 4-13). Gulls rank low in displacement vulnerability assessments (Furness et al. 2013), and research suggests that distribution and abundance is either not affected by the presence of wind farms or, in the case of gulls, that the birds may be attracted to them (Krijgsveld et al. 2011; Lindeboom et al. 2011). At European offshore wind developments, gulls have been documented to be attracted to WTGs, which may be due to increased boat traffic, new food resources, or new loafing habitat (i.e., perching areas; Fox et al. 2006; Vanermen et al. 2015), but interaction with offshore wind developments varies by season (Thaxter et al. 2015). Less is known about how jaegers (or skuas) will respond to offshore wind farms, but jaegers rank low in vulnerability-to-displacement assessments (Furness et al. 2013) and there is no evidence in the literature that they are displaced from projects. Uncertainty about this determination is **low** due to the quality information available (for many of the species in the group) on avoidance and habitat flexibility.

Population Vulnerability Determination: **Minimal to Medium**

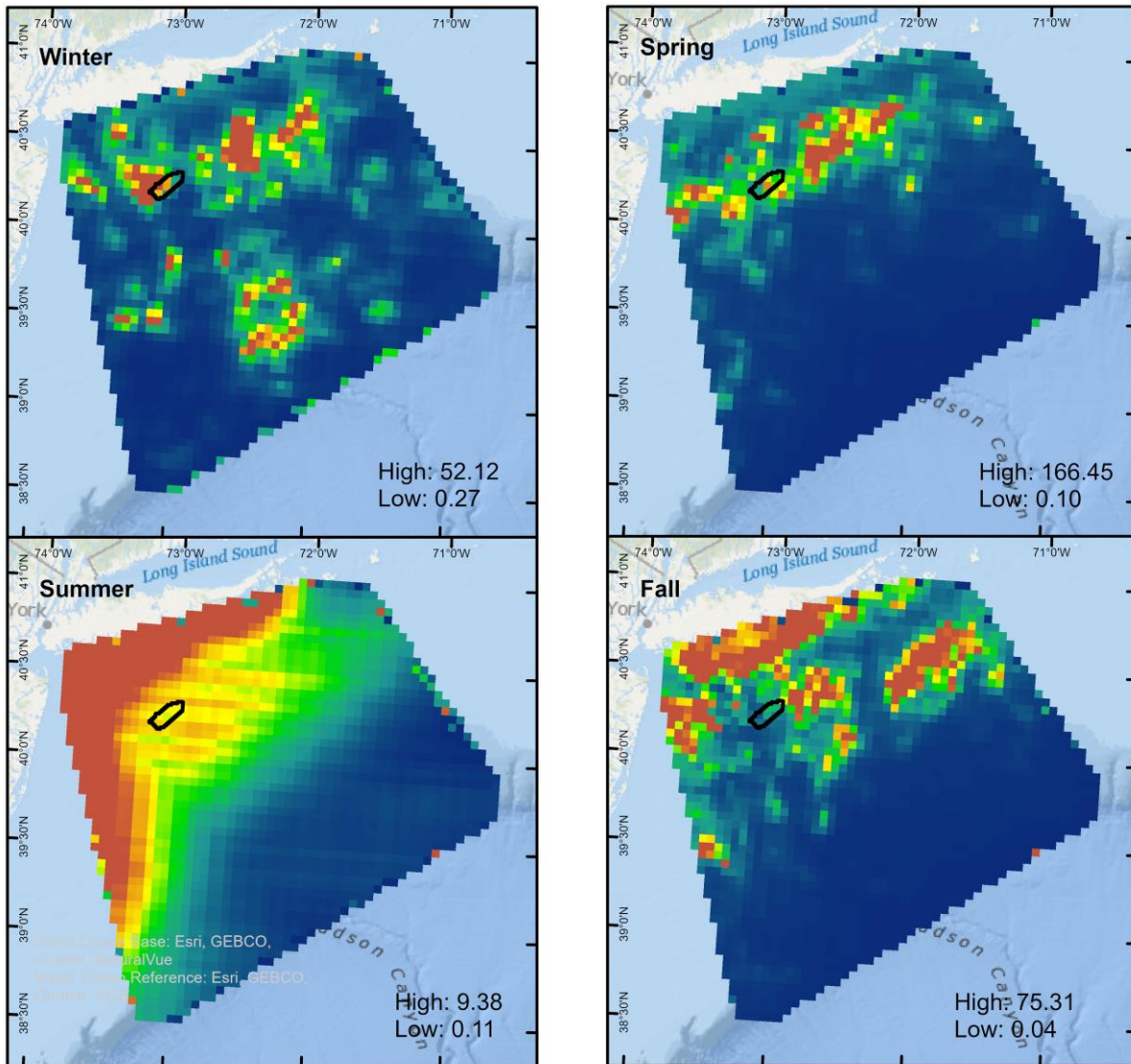
Assessment Method: **Semi-quantitative**

Based on BRI's vulnerability assessment, the population vulnerability determination for gulls, skuas, and jaegers was **minimal to medium** (Table 4-13). Two species, the Herring Gull and South Polar Skua, have medium population vulnerability, which is attributable to their higher adult survival compared with other species in this group.

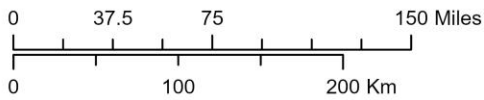
4.3.4.4 Risk Determination

Gulls, jaegers, and skuas received an exposure determination of minimal to low, a relative collision vulnerability determination of low to medium, a relative displacement vulnerability determination of low to medium, and a population vulnerability determination of minimal to medium. Based on BRI's risk assessment matrix (Table 2-1), final collision and displacement risk were both assessed as **minimal to low**.

4.3.4.5 Table and Figures



Modeled APem digital aerial surveys for small gulls in Lease Area OCS-A 0544



Produced by: J. Stepanuk | VW544_apem_inla_cormorants | Version date: 6/26/2024

Lease Area OCS-A 0544

Total Density

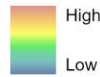
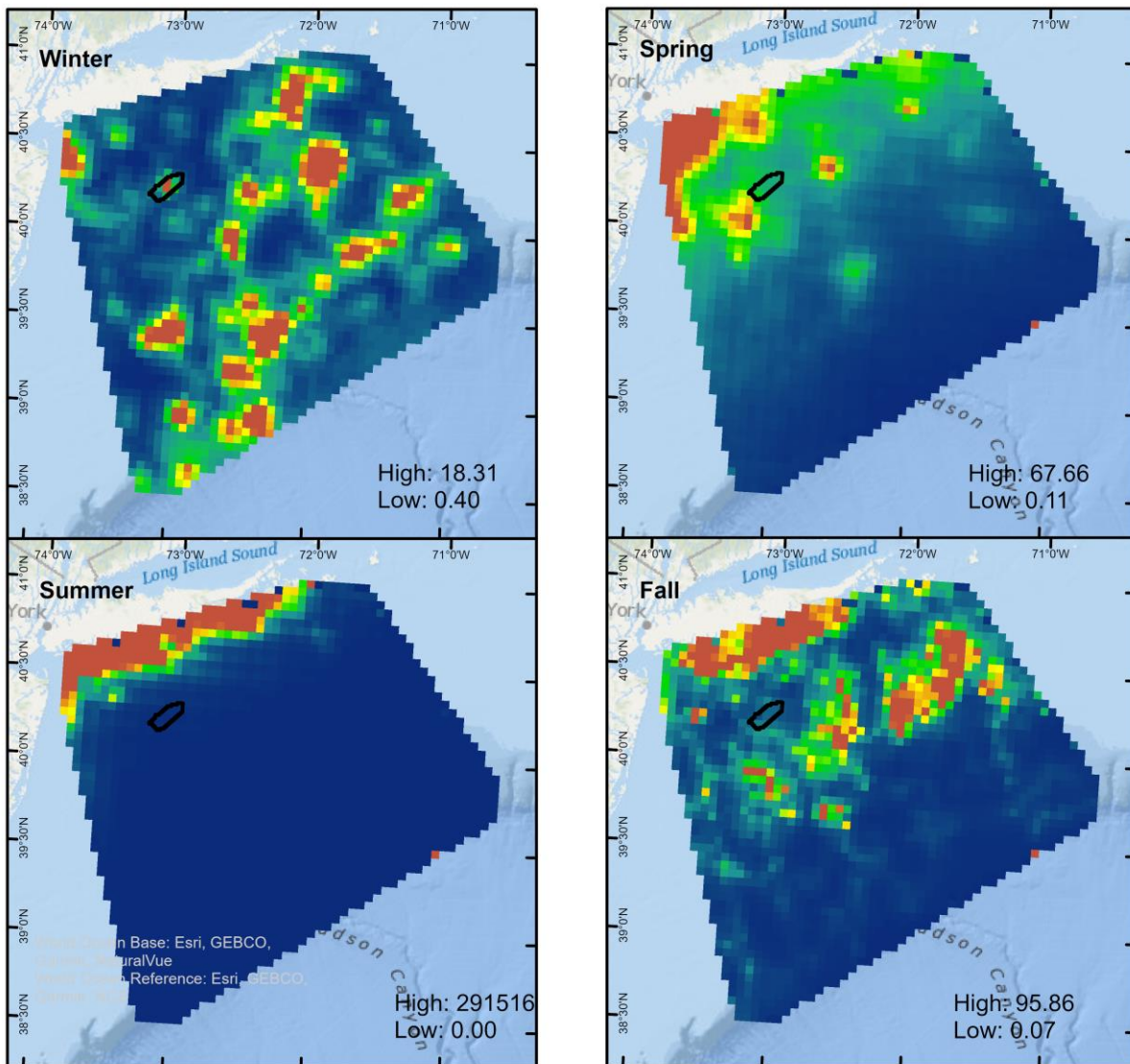
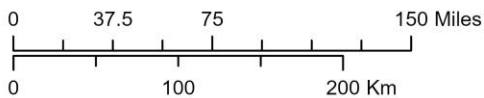


Figure 4-25: Modeled APem digital aerial surveys for small gulls in the NY Bight survey area and Lease Area OCS-A 0544.



Modeled APEM digital aerial surveys for medium gulls in Lease Area OCS-A 0544

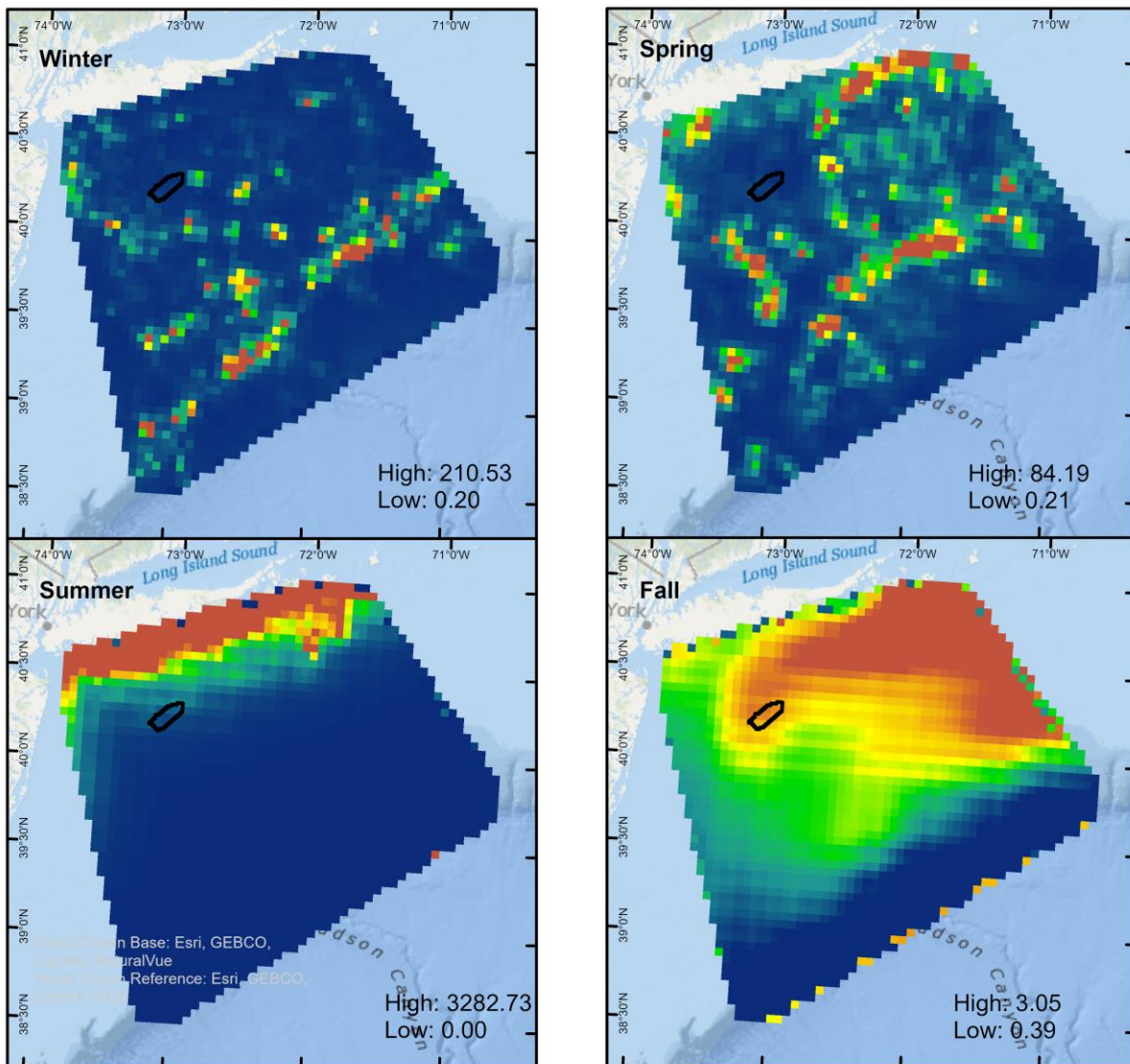


CS: NAD 1983 UTM Zone 19N

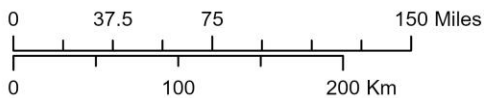
Produced by: J. Stepanuk | VW544_apem_inla_cormorants | Version date: 6/26/2024



Figure 4-26: Modeled APEM digital aerial surveys for medium gulls in the NY Bight survey area and Lease Area OCS-A 0544.



Modeled APEM digital aerial surveys for large gulls in Lease Area OCS-A 0544



CS: NAD 1983 UTM Zone 19N

Produced by: J. Stepanuk | VW544_apem_inla_cormorants | Version date: 6/26/2024



□ Lease Area OCS-A 0544

Total Density

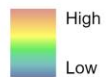
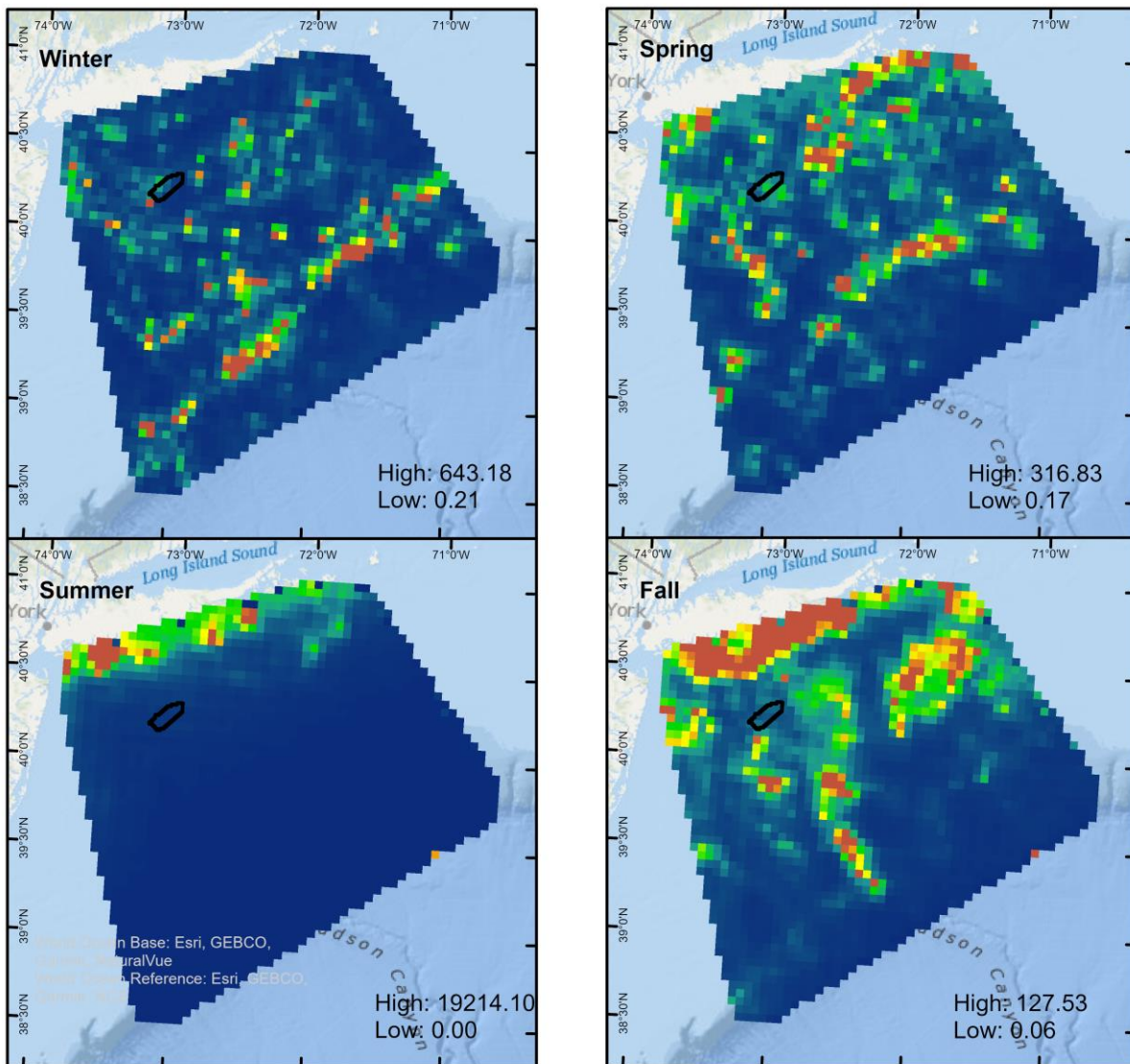
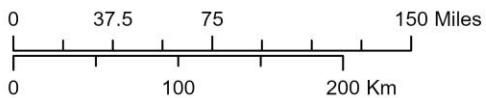


Figure 4-27: Modeled APEM digital aerial surveys for large gulls in the NY Bight survey area and Lease Area OCS-A 0544.



Modeled APEM digital aerial surveys for all gulls in Lease Area OCS-A 0544



CS: NAD 1983 UTM Zone 19N

Produced by: J. Stepanuk | VW544_apem_inla_cormorants | Version date: 6/26/2024

□ Lease Area OCS-A 0544

Total Density

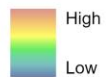
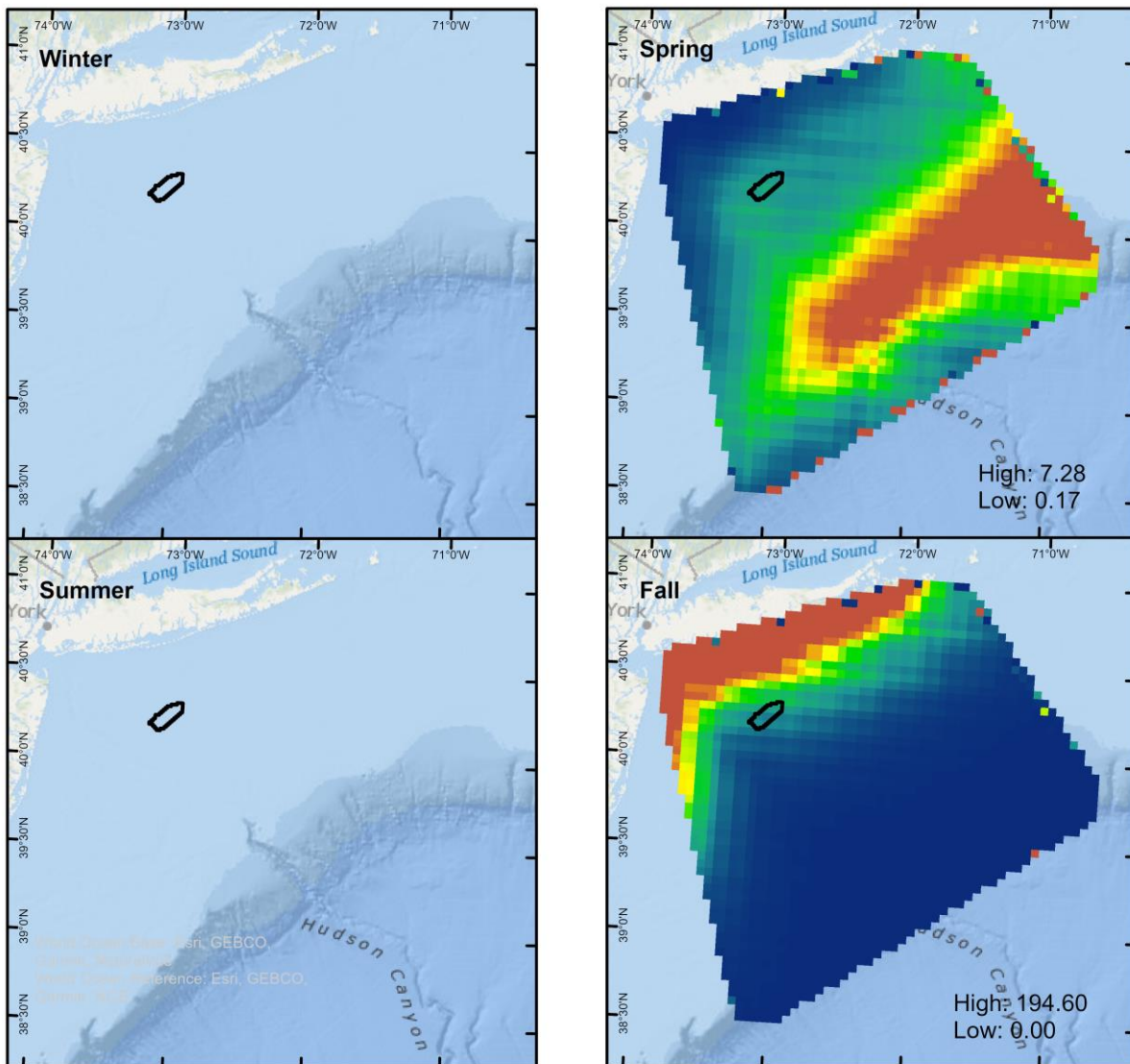
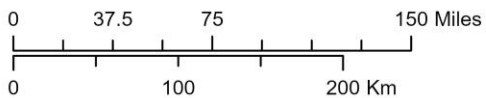


Figure 4-28: Modeled APEM digital aerial surveys for all gulls in the NY Bight survey area and Lease Area OCS-A 0544.



Modeled APPEM digital aerial surveys for skuas and jaegers in Lease Area OCS-A 0544



CS: NAD 1983 UTM Zone 19N

Produced by: J. Stepanuk | VW544_apem_inla_cormorants | Version date: 6/26/2024

□ Lease Area OCS-A 0544

Total Density

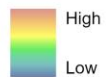


Figure 4-29: Modeled APPEM digital aerial surveys for skuas and jaegers in the NY Bight survey area and Lease Area OCS-A 0544.

Table 4-12: Seasonal exposure scores for the gulls, skuas, and jaegers group.

Taxa Group	Season	Local Score	Regional Score	Total Score	Exposure Category
Small Gulls	Winter	3	0	3	medium
	Spring	2	0	2	low
	Summer	1	-	2	low
	Fall	0	2	2	low
Medium Gulls	Winter	2	0	2	low
	Spring	1	0	1	low
	Summer	0	0	0	minimal
	Fall	0	0	0	minimal
Large Gulls	Winter	0	0	0	minimal
	Spring	0	0	0	minimal
	Summer	0	0	0	minimal
	Fall	2	0	2	low
All Gulls	Winter	1	0	1	low
	Spring	1	0	1	low
	Summer	0	0	0	minimal
	Fall	0	0	0	minimal
Skuas and Jaegers	Winter	-	2	-	minimal
	Spring	0	1	1	low
	Summer	-	1	-	minimal
	Fall	0	1	1	low

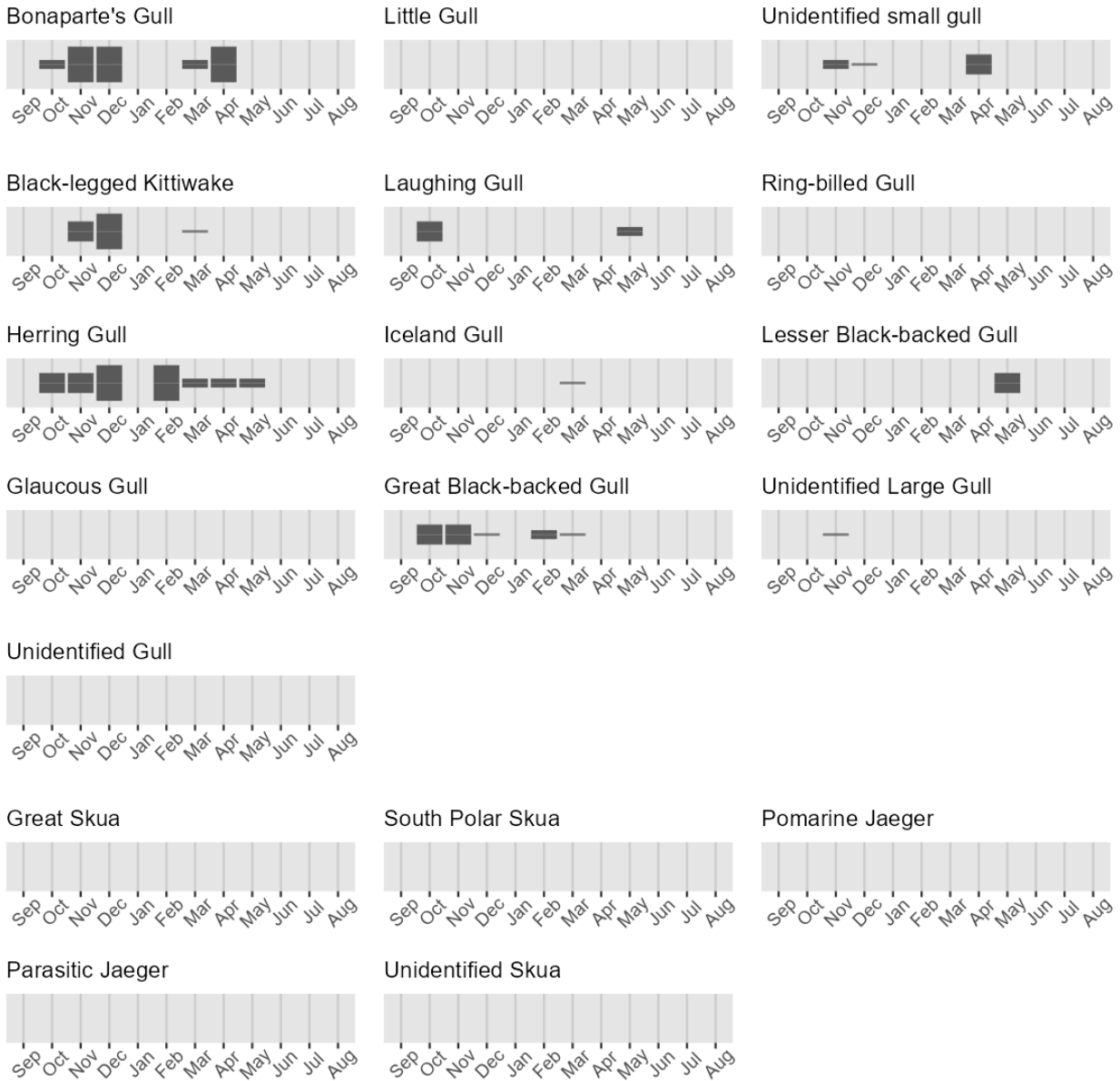
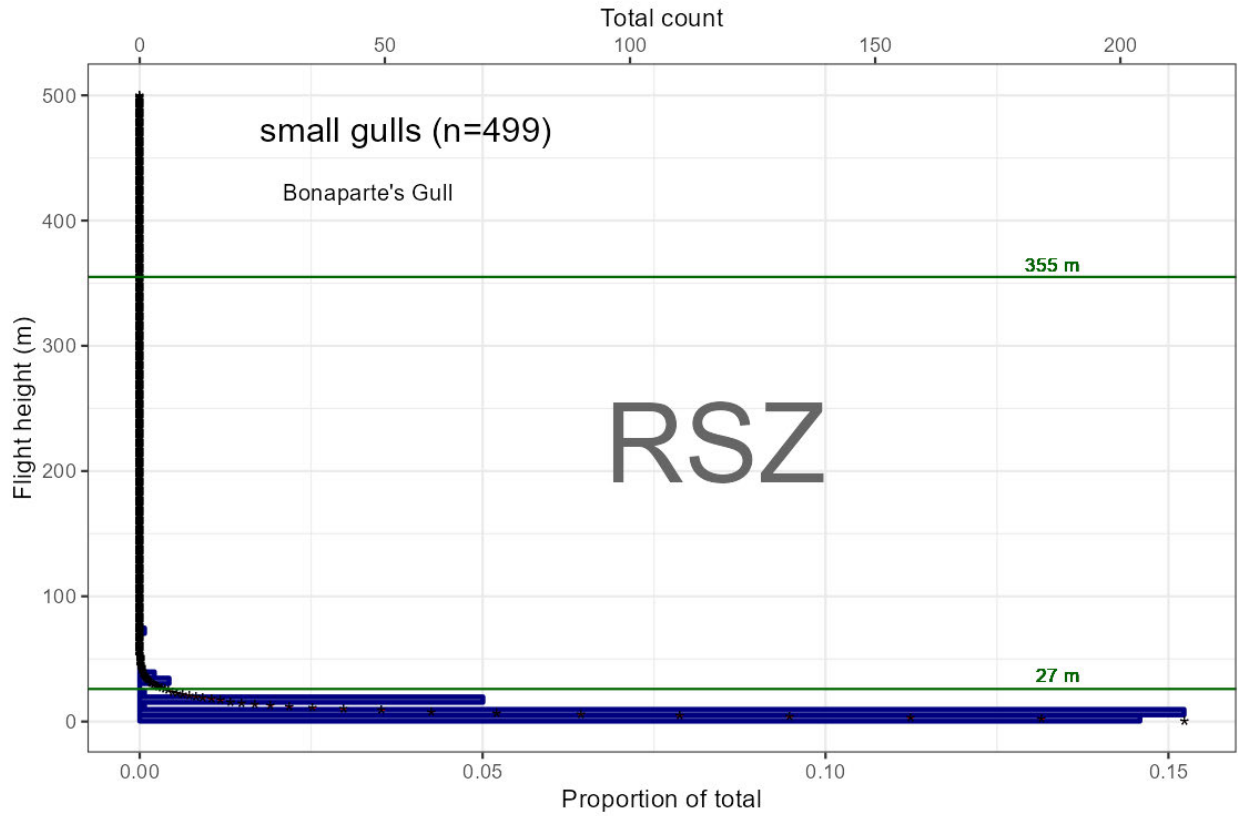
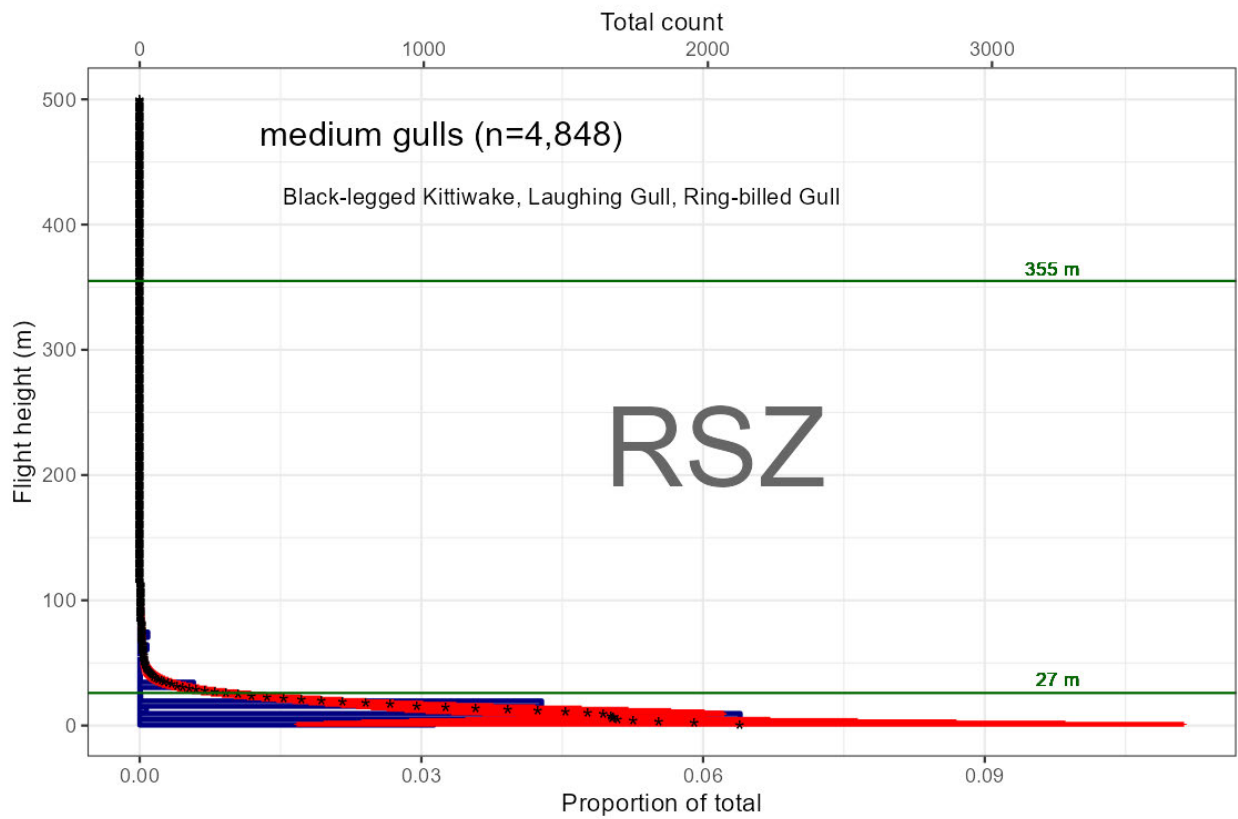


Figure 4-30: Monthly relative densities of gulls, jaegers, and skuas in the Lease Area from digital aerial surveys.



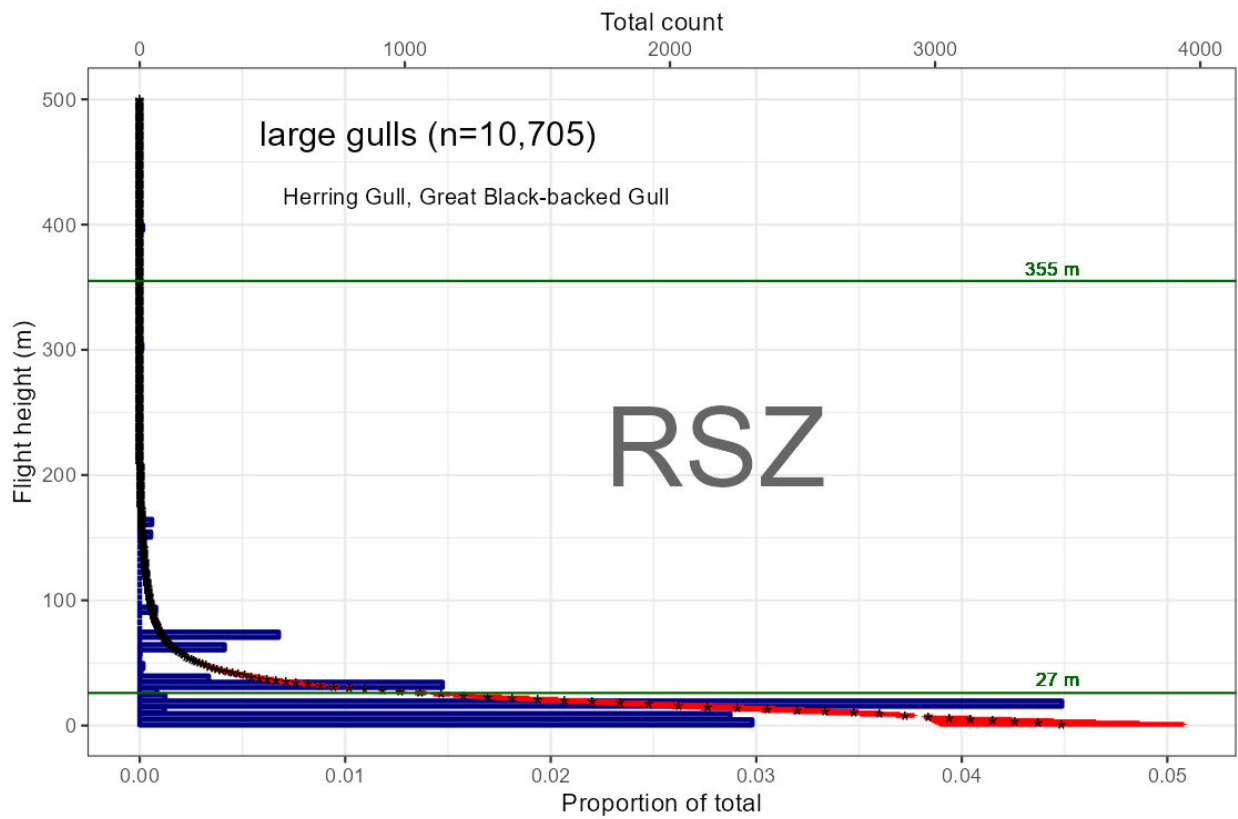
NOTE: Figure shows the actual number of birds in 5 m (16 ft) intervals (blue bars), the modeled average flight height in 1 m (3 ft) intervals (black asterisks), and the standard deviation (red lines), in relation to the upper and lower limits of a minimum and maximum RSZ scenario (27–355 m; green lines).

Figure 4-31: Flight heights of small gulls ($n=499$) derived from the Northwest Atlantic Seabird Catalog.



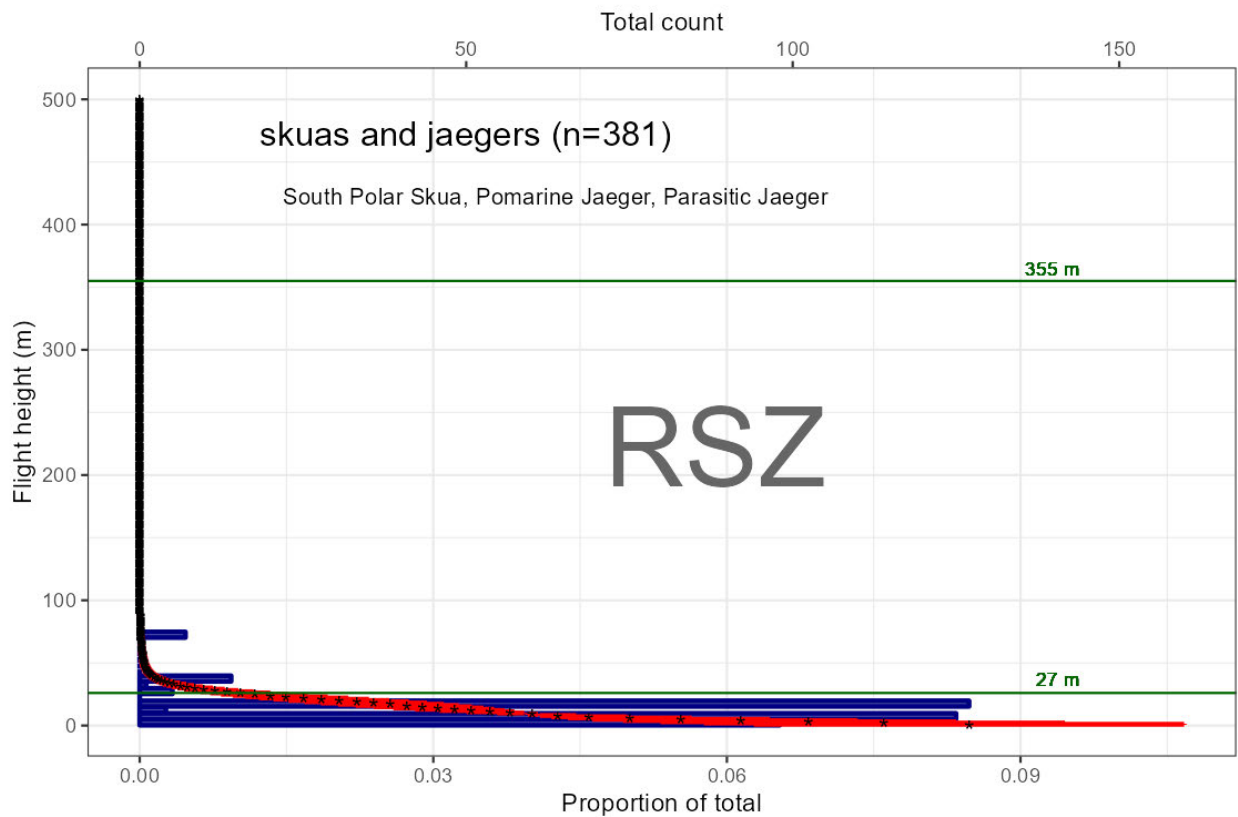
NOTE: Figure shows the actual number of birds in 5 m (16 ft) intervals (blue bars), the modeled average flight height in 1 m (3 ft) intervals (black asterisks), and the standard deviation (red lines), in relation to the upper and lower limits of a minimum and maximum RSZ scenario (27–355 m; green lines).

Figure 4-32: Flight heights of medium gulls (n=4,848) derived from the Northwest Atlantic Seabird Catalog.



NOTE: Figure shows the actual number of birds in 5 m (16 ft) intervals (blue bars), the modeled average flight height in 1 m (3 ft) intervals (black asterisks), and the standard deviation (red lines), in relation to the upper and lower limits of a minimum and maximum RSZ scenario (27–355 m; green lines).

Figure 4-33: Flight heights of large gulls ($n=10,705$) derived from the Northwest Atlantic Seabird Catalog.



NOTE: Figure shows the actual number of birds in 5 m (16 ft) intervals (blue bars), the modeled average flight height in 1 m (3 ft) intervals (black asterisks), and the standard deviation (red lines), in relation to the upper and lower limits of a minimum and maximum RSZ scenario (27–355 m; green lines).

Figure 4-34: Flight heights of jaegers (*n*=381) derived from the Northwest Atlantic Seabird Catalog.

Table 4-13: Vulnerability assessment rankings by species for the gulls and jaegers group.

Species	Collision Vulnerability (CV)	Displacement Vulnerability (DV)	Population Vulnerability (PV)
Parasitic Jaeger	medium (0.6)	low (0.3)	low (0.4)
Pomarine Jaeger	medium (0.73)	low (0.3)	low (0.4)
South Polar Skua	medium (0.73)	low (0.3)	medium (0.53)
Bonaparte's Gull	low (0.43)	medium (0.5)	low (0.33)
Black-legged Kittiwake	medium (0.57)	medium (0.6)	low (0.33)
Laughing Gull	low (0.43)	medium (0.5)	low (0.4)
Ring-billed Gull	medium (0.6)	low (0.4)	low (0.33)
Great Black-backed Gull	medium (0.53)	medium (0.7)	minimal (0.2)
Herring Gull	medium (0.6)	medium (0.5)	medium (0.53)

4.3.5 Terns

Minor Taxa Groups: Charadriiformes: Laridae: subfamily Sterninae (terns)

Collision Risk Determination: **Minimal**

Displacement Risk Determination: **Minimal**

4.3.5.1 Overview

Distribution and Habitat Preferences: Terns are broadly distributed across the globe and are highly migratory; the Arctic Tern (*Sterna paradisea*) undertakes the longest known annual migration of any animal (Egevang et al. 2010). Terns are found near water, breeding on coastal islands, beaches, or inland on wetlands. They migrate along rivers, coastlines, and offshore in marine habitats.

Behavior and Ecology: Terns mainly feed on small fish at or near the surface of the water and may forage far from breeding colonies and return carrying single fish in their bills. Unlike closely related gulls, terns feed by hovering and shallow plunge-diving into the ocean (Winkler et al. 2020). Terns can forage flexibly in habitats where small fish or aquatic invertebrates congregate at or near the surface.

Reproduction: Terns are colonial breeders, generally laying 1–2 eggs in shallow scrapes near other pairs. Breeding sites are typically along coastlines on beaches or islands, although some terns may nest in vegetation adjacent to wetlands. Both sexes incubate eggs and then provide food to chicks by carrying small fish in their bills back to the colony and directly feeding their young. Several tern species breed and nest in the New York Bight region (e.g., the Common Tern, Least Tern, Forster’s Tern, Gull-billed Tern, and Roseate Tern), often co-existing with other tern, seabird, and shorebird species at the same breeding sites. Roseate Terns in the region are only known to nest at sites where Common Terns also nest (Gochfeld and Burger 2020).

Conservation Status: Terns are highly sensitive to the abundance and distribution of forage fish, which face various impacts from commercial fishing and climate change (Arnold et al. 2020). Roseate Terns are federally listed and are discussed in Section 4.4 below. In New York, Black Terns are listed as *Endangered*, and Common Terns and Least Terns are *Threatened*. In New Jersey, Least Terns are listed as *Endangered*, while Caspian Terns, Common Terns, and Gull-billed Terns are *Special Concern*.

4.3.5.2 Exposure Assessment

Group exposure determination: **Minimal**

Assessment Method: **Semi-quantitative**

Main Information Sources: MDAT, baseline, site-specific

Supplemental Information Sources: Literature, tracking

Exposure Uncertainty: **Minimal**

Based on BRI’s exposure assessment, the group exposure determination for terns was **minimal** (Table 4-14). As indicated above in the overview, terns are unlikely to be exposed during breeding in summer, but they can fly through the OCS during migration. Mapping and exposure scoring

were done for three sub-groups: small terns, medium terns, and all terns. The mapped outputs of the spatial density models for terns show that the Lease Area lies outside areas of higher predicted density, except for medium terns (Figure 4-35, Figure 4-36, and Figure 4-37). Local exposure scores for the tern group for all seasons with models available were 0 except for medium terns in spring which was 1, corresponding to the low exposure category. Regional scores for the tern group were 0 for all seasons for which MDAT models were available, corresponding to the minimal exposure category. Exposure was minimal for all subgroups of terns in all seasons, except medium terns in spring with a total exposure score of 1, which corresponds to a low exposure category for that season. In the Lease Area, there were only observations of unidentified tern species (as shown by density values of 0.039 and 0.009 counts/km² in Table 4-28). Within the Lease Area, seasonal densities of terns were greatest in the spring and summer (Figure 4-38). Radio telemetry tracking data for Common Terns (*Sterna hirundo*) (Loring et al. 2019) indicates that this species is unlikely to use offshore areas in the vicinity of the Lease Area during spring and fall migration periods (Figure 4-39). It should be noted that tracking data is based on Motus VHF tags with land-based tracking stations, and, therefore, tracking information between stations is modeled as a straight line. Uncertainty is **minimal** for the exposure assessment due to the availability of baseline and site-specific digital aerial surveys, MDAT models, and tracking studies.

4.3.5.3 Behavioral Vulnerability Assessment

Collision Vulnerability Determination: **Low to Medium**

Assessment Method: **Semi-quantitative**

Collision Uncertainty: **Medium**

Based on BRI's vulnerability assessment, the collision vulnerability determination for terns was **low to medium** (Table 4-15). Three tern species—the Arctic Tern, Bridled Tern (*Onychoprion anaethetus*), and Sooty Tern (*Onychoprion fuscatus*)—were not assessed for collision due to a lack of available flight activity information. The two small tern species—Least Tern (*Sternula antillarum*) and Black Tern (*Chlidonias niger*)—were entirely excluded from the vulnerability assessment because of a general lack of available information. None of these excluded species are likely to be exposed, however, owing to a lack of frequent detections. The available flight height data from the Northwest Atlantic Seabird Catalog indicate that medium-sized terns fly in the RSZ approximately 4% of the time, and below the RSZ the remaining 96% of the time (Figure 4-40).

A movement study using NanoTags estimated that Common Terns primarily flew below the RSZ (<25 m [<82 ft]) and that the frequency of Common Terns flying offshore between 25–250 m (82–820 ft) ranged from 0.9–9.8% (Loring et al. 2019). While the NanoTag flight height estimated birds flying below 50 m (164 ft), radar and observational studies provide evidence that terns in some instances can undertake migration at higher altitudes of 1,000–3,000 m (3,000–10,000 ft)

(Loring et al. 2019). For Common Terns and Arctic Terns, the probability of fatality is predicted to decline as the distance from the colony increases. Based on one year of NanoTag data collected at Petit Manan Island, Maine, tests of a decision support model for offshore wind farm siting suggested that fatality rates during the breeding season at a turbine project would drop to near zero beyond 15 km (9.3 mi) from a tern colony (Cranmer et al. 2017). This finding is corroborated by fatality monitoring of small to medium WTGs (200 and 600 kilowatts [kW]) in Europe, where fatality rates of terns rapidly declined with distance from the breeding colony (Everaert and Stienen 2007). Most observed tern mortalities in Europe have occurred at WTGs within 30 m (98 ft) of breeding sites (Burger et al. 2011).

Uncertainty about this determination is **medium**; robust flight height and activity information is available, but avoidance behavior in terns is still poorly understood.

Displacement Vulnerability Determination: **Low to High** (lower range added)

Assessment Method: **Semi-quantitative** (with adjustment based on weight of evidence)

Displacement Uncertainty: **Medium**

Based on BRI's vulnerability assessment, the displacement vulnerability determination for terns was **low to high** (Table 4-15). Terns have been shown to have a 76% lower abundance inside offshore wind farms compared to adjacent waters and were estimated to start avoidance behaviors at 0.93 mi (1.5 km; Welcker and Nehls 2016). Common Terns and Roseate Terns have been demonstrated to avoid the airspace around a single 660 kW WTG (rotor-tip height: 73 m [240 ft]) in Buzzard's Bay, MA, when the WTG was rotating, and usually avoided the RSZ (Vlietstra 2007). Common Terns fall into the high category for macro-avoidance because of a 69.5% avoidance rate determined at Horns Rev (Cook et al. 2012), which had 2 MW WTGs (Petersen et al. 2006), and because Willmott et al. (2013) categorized tern avoidance as greater than 40%. Here, a lower range was added to the displacement score (Table 4-15) because: (1) terns received a "low" disturbance score according to Wade et al. (2016); (2) terns were determined to have a 30% macro-avoidance of WTGs at Egmond aan Zee, the Netherlands (Cook et al. 2012); (3) some tern species have high uncertainty scores (Wade et al. 2016); and (4) displacement in terns has not been well studied. Uncertainty about this determination is **medium** due to the lack of information about avoidance behavior.

Population vulnerability determination: **Low to Medium** (**High** for Roseate Terns)

Assessment Method: **Semi-quantitative**

Based on BRI's vulnerability assessment, the population vulnerability determination for terns was **low to medium** for all species except Roseate Terns, which have a **high** population vulnerability (Table 4-15). Terns have a relatively high adult survival, and for most species the conservation

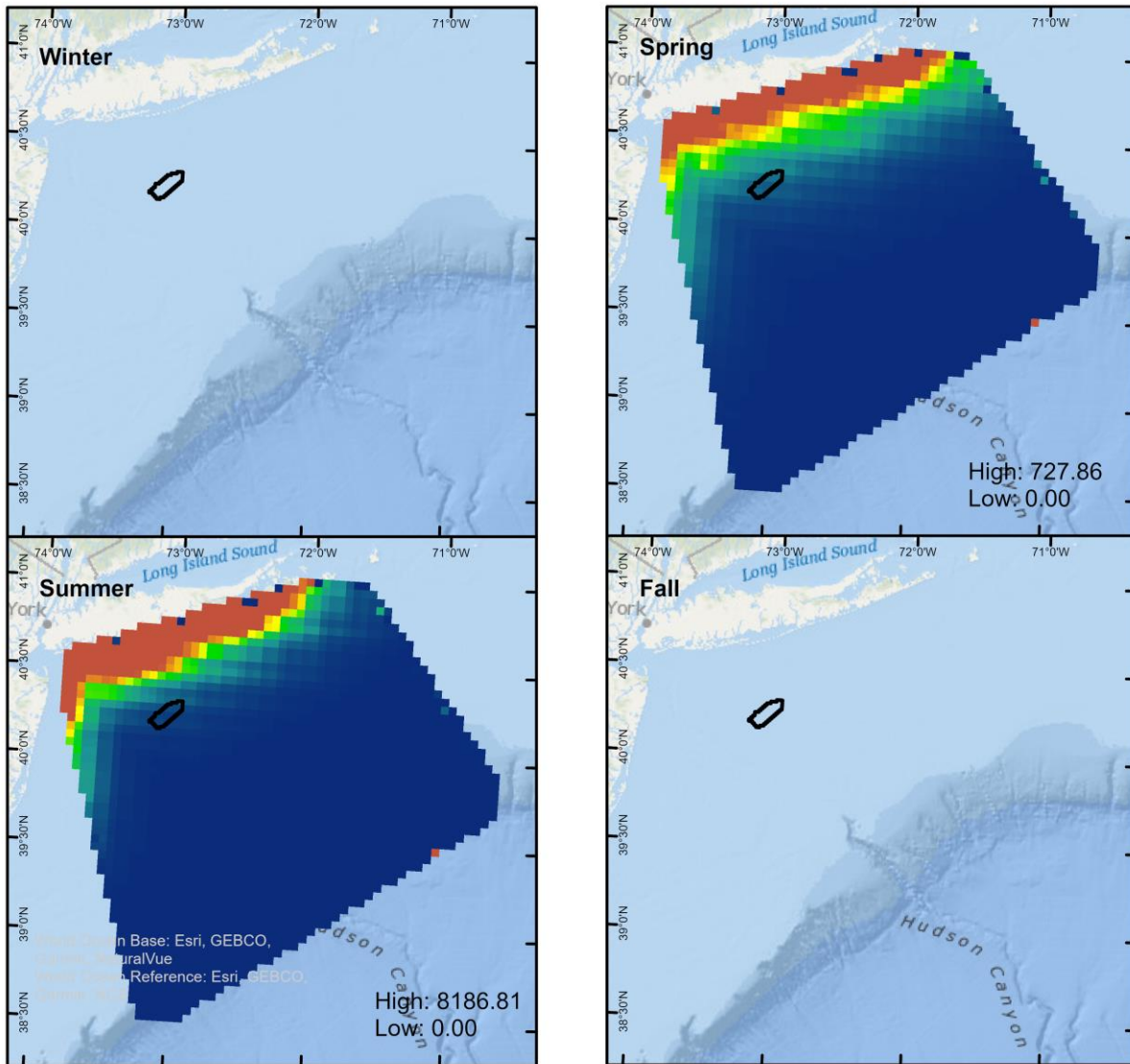
status is not high priority, with Roseate Terns and Least Terns (New York State listed) as notable exceptions.

4.3.5.4 Risk Determination

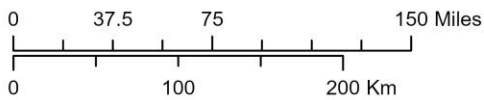
Terns received an exposure determination of minimal, a relative collision vulnerability determination of low to medium, a relative displacement vulnerability determination of low to high (adjusted), and a population vulnerability determination of low to medium (with Roseate Terns high, discussed separately). Based on BRI's risk assessment matrix (Table 2-1), final collision and displacement risk were both assessed as **minimal**. The risk determination for Roseate Terns is reported separately in Section 4.4.1.

4.3.5.5 Tables and Figures

Common Tern tracking data are shown in Figure 4-40. See Section 4.4.1 for observation data on Roseate Terns. Additional seasonal maps for species in the tern group are presented in Attachment A.



Modeled APDEM digital aerial surveys for small terns in Lease Area OCS-A 0544



CS: NAD 1983 UTM Zone 19N

Produced by: J. Stepanuk | VW544_apem_inla_cormorants | Version date: 6/26/2024

□ Lease Area OCS-A 0544

Total Density

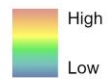
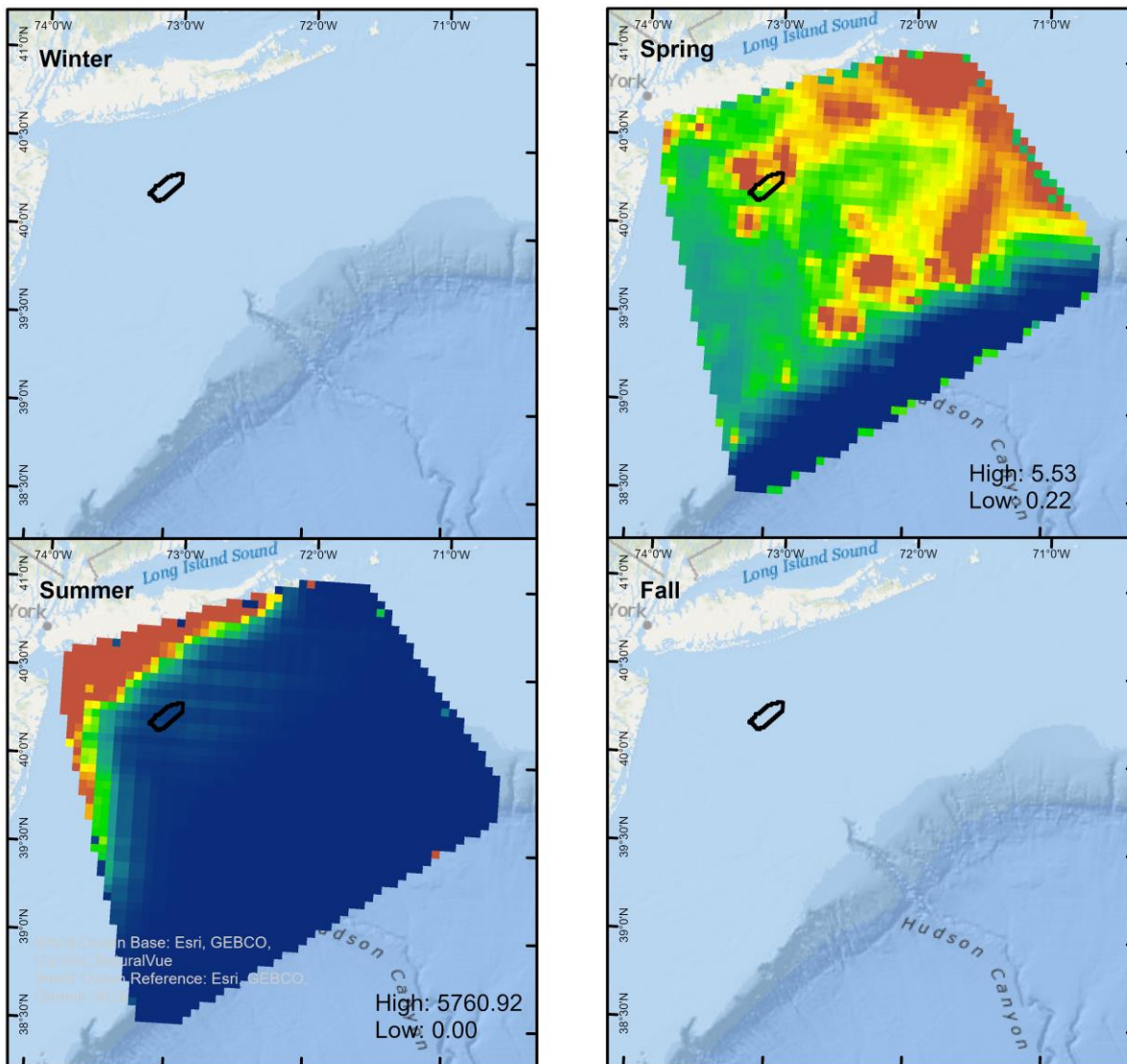
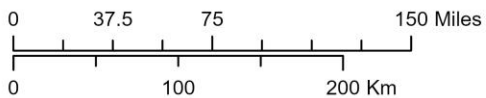


Figure 4-35: Modeled APDEM digital aerial surveys for small terns in the NY Bight survey area and Lease Area OCS-A 0544.



Modeled APEM digital aerial surveys for medium terns in Lease Area OCS-A 0544



CS: NAD 1983 UTM Zone 19N

Produced by: J. Stepanuk | VW544_apem_inla_cormorants | Version date: 6/26/2024



□ Lease Area OCS-A 0544

Total Density

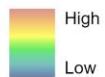
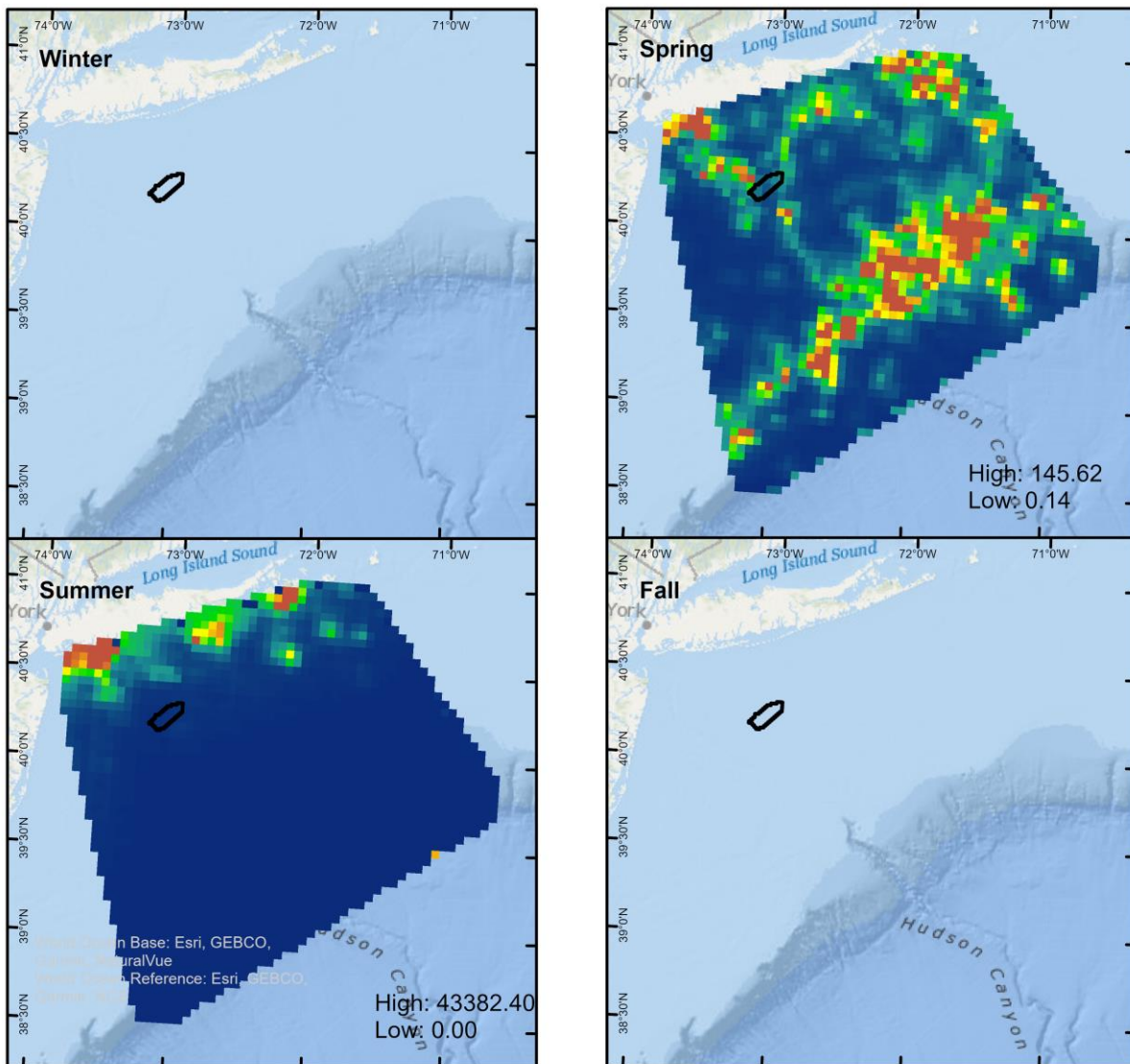
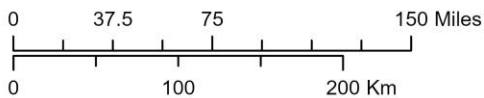


Figure 4-36: Modeled APEM digital aerial surveys for medium terns in the NY Bight survey area and Lease Area OCS-A 0544.



Modeled APTEM digital aerial surveys for all terns in Lease Area OCS-A 0544



CS: NAD 1983 UTM Zone 19N

Produced by: J. Stepanuk | VW544_apem_inla_cormorants | Version date: 6/26/2024

Lease Area OCS-A 0544

Total Density

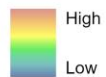


Figure 4-37: Modeled APTEM digital aerial surveys for all terns in the NY Bight survey area and Lease Area OCS-A 0544.

Table 4-14: Seasonal exposure rankings for the terns group.

Taxa Group	Season	Local Score	Regional Score	Total Score	Exposure Category
Small Terns	Winter	-	-	-	minimal
	Spring	0	0	0	minimal
	Summer	0	0	0	minimal
	Fall	-	-	-	minimal
Medium Terns	Winter	-	-	-	minimal
	Spring	1	0	1	low
	Summer	0	0	0	minimal
	Fall	-	0	-	minimal
All Terns	Winter	-	-	-	minimal
	Spring	0	0	0	minimal
	Summer	0	0	0	minimal
	Fall	-	0	-	minimal

Least Tern



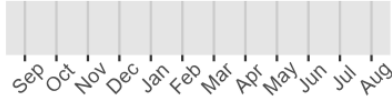
Black Tern



Sooty Tern



Bridled Tern



Roseate Tern



Common Tern



Arctic Tern



Forster's Tern



Royal Tern



Unidentified Tern

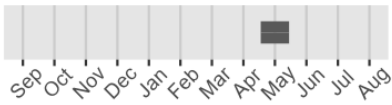


Figure 4-38: Monthly relative densities of terns in the Lease Area from digital aerial surveys.

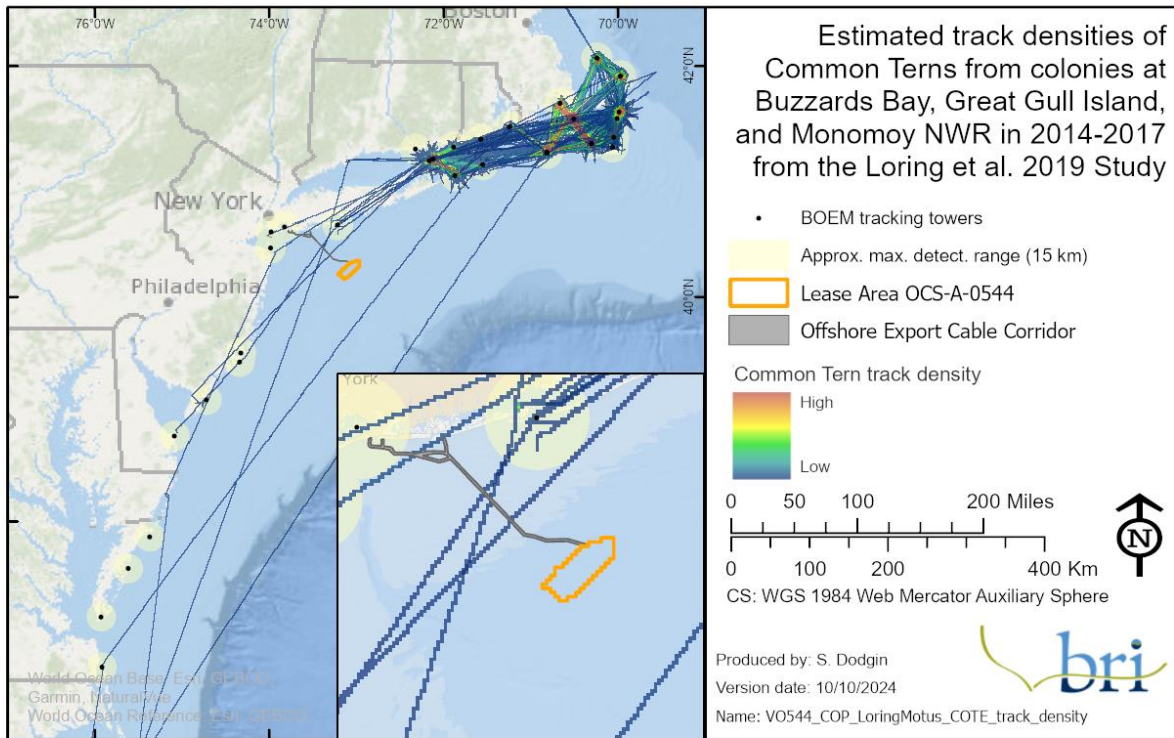
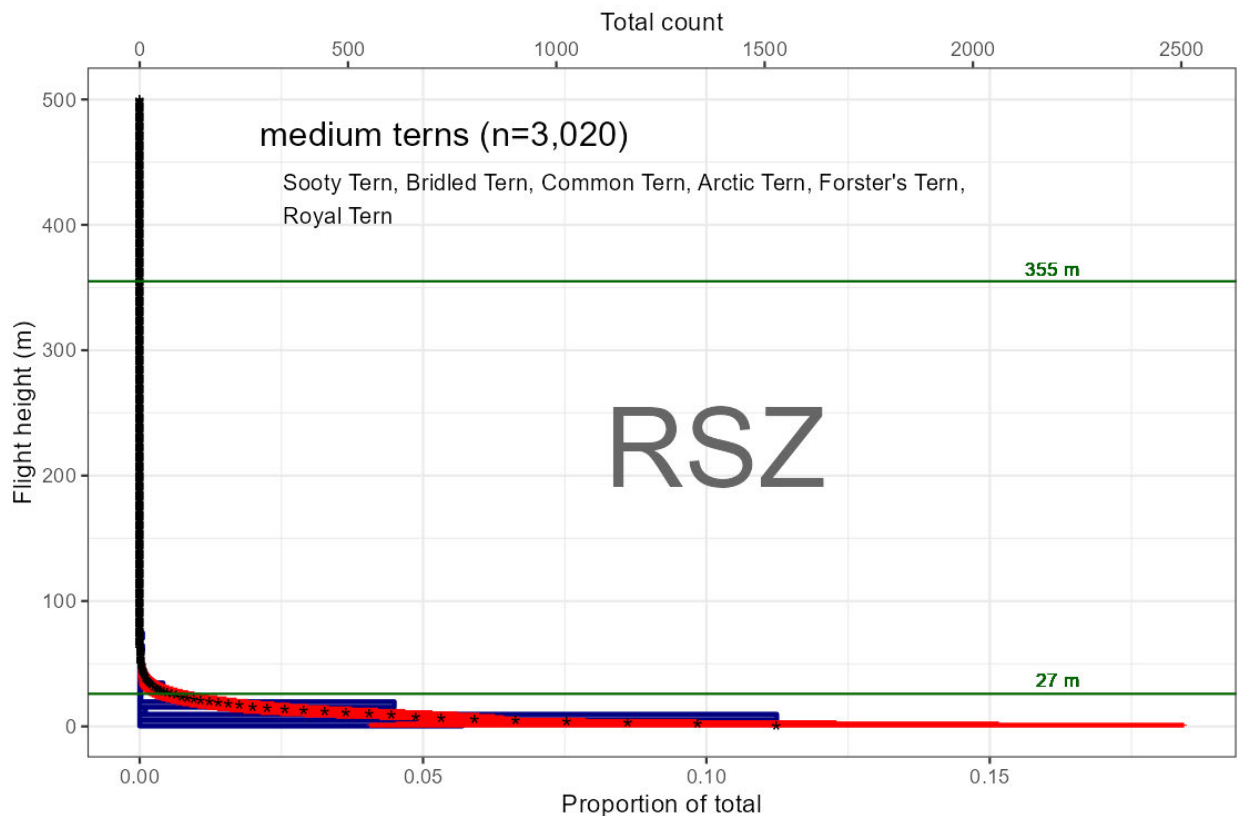


Figure 4-39: Common Tern ($n=30$) track locations and density from the Loring et al. (2019) radio telemetry study.



NOTE: Figure shows the actual number of birds in 5 m (16-ft) intervals (blue bars), the modeled average flight height in 1 m (3-ft) intervals (black asterisks), and the standard deviation (red lines), in relation to the upper and lower limits of a minimum and maximum RSZ scenario (27–355 m; green lines).

Figure 4-40: Flight heights of medium terns ($n=3,020$) derived from the Northwest Atlantic Seabird Catalog.

Table 4-15: Vulnerability assessment rankings by species for the terns group.

NOTE: A lower range limit is added to the Displacement Vulnerability score in green font because terns receive a low disturbance score in Wade et al. (2016); terns were determined to have a 30 % macro avoidance of WTGs at Egmond aan Zee (Cook et al. 2012); and displacement in terns has not been well studied.

Species	Collision Vulnerability (CV)	Displacement Vulnerability (DV)	Population Vulnerability (PV)
Arctic Tern	· (·)	medium-high (0.8)	medium (0.6)
Bridled Tern	· (·)	medium-high (0.8)	medium (0.53)
Common Tern	low (0.33)	medium-high (0.8)	medium (0.67)
Forster's Tern	medium (0.53)	low-medium (0.5)	low (0.4)
Roseate Tern	low (0.33)	medium-high (0.8)	high (0.87)
Royal Tern	medium (0.57)	low-medium (0.5)	medium (0.53)
Sooty Tern	· (·)	low-medium (0.7)	low (0.47)

4.3.6 Loons

Minor Taxa Groups: Gaviiformes: Gaviidae (loons)

Collision Risk Determination: **Minimal to Low**

Displacement Risk Determination: **Low**

4.3.6.1 Overview

Distribution and Habitat Preferences: Loons breed in freshwater habitats and overwinter in marine waters, feeding primarily on fish and supplementing with macroinvertebrates. Of the two species present in the New York Bight region, Common Loons breed in freshwater lakes in New York and New England (Paruk et al. 2021), while Red-throated Loons breed in northern boreal forest and tundra of Subarctic and Arctic regions of Canada (Rizzolo et al. 2020).

Behavior and Ecology: Loons can dive deeply (more than 60 m [197 ft]) to capture forage fish, although Red-throated Loons do not dive to as great a depth as Common Loons (Rizzolo et al. 2020). Loons are highly adept piscivores, although their diets may vary based on local food availability to include crabs, polychaetes, and other invertebrates. In marine foraging, both species tend to prefer more protected habitats close to shore, but they are also known to flock forage in less protected waters farther from shore (Paruk et al. 2021).

Reproduction: Loons choose freshwater breeding sites, preferring lakes >24 ha in size, on which the pair builds a nest slightly higher than the water's surface. Females lay 1–2 eggs, which the pair incubate for 26–28 days. Adults remain with chicks until fledging at roughly 12 weeks of age, after which fledglings flock for fall migration to the coast (Paruk et al. 2021; Rizzolo et al. 2020).

Conservation Status: Neither loon species present in the New York Bight is federally listed. However, Common Loons are listed as *Special Concern* in New York. Loons are highly sensitive to anthropogenic activity during the breeding season and are susceptible to contaminants including mercury and lead. At sea, Red-throated Loons are also highly sensitive to anthropogenic activities, such as vessel traffic (Burger et al. 2019).

4.3.6.2 Exposure Assessment

Group exposure determination: **Low**

Main Information Sources: MDAT, baseline, site-specific

Supplemental data sources: Literature, tracking

Exposure Uncertainty: **Minimal**

Based on BRI's exposure assessment, the group exposure determination for loons was **low** (Table 4-16). As discussed above in the overview, exposure should not be expected in summer when breeding loons are not in the New York Bight. The mapped outputs of the spatial density models for loons show the Lease Area further offshore than the highest density areas closest to shore (Figure 4-41). Local exposure scores for the loon group for spring were 1 and all remaining seasons were 0. Regional exposure for loons scored 1 in spring and fall. Total exposure scores ranged from 0–2, corresponding to a minimal to low exposure category. In the Lease Area, there were

observations of Red-throated Loons, Common Loons, and unidentified loon (as shown by density counts/km² in Table 4-28). Within the Lease Area, seasonal densities of the loons were greatest in the spring and fall (Figure 4-42). Tracking data for Red-throated Loons (Gray et al. 2017) indicates that this species is likely to use areas within the Lease Area during spring migration periods (Figure 4-43). Uncertainty is **minimal** for the exposure assessment due to the availability of regional and site-specific digital aerial surveys, MDAT models, and tracking studies.

4.3.6.3 Behavioral Vulnerability Assessment

Collision Vulnerability Determination: **Minimal to Low**

Assessment Method: **Semi-quantitative** (with adjustment based on weight of evidence)

Collision Uncertainty: **Low**

Based on BRI's vulnerability assessment, the collision vulnerability determination for loons was **low**, and a lower range is added based on the weight of the evidence in the literature that their strong avoidance response precludes their vulnerability to collision with WTGs (Table 4-17). In Europe, Red-throated Loons have consistently been documented to strongly avoid offshore wind projects and are widely considered to have low vulnerability to collision (Furness et al. 2013). Pre- and post-construction monitoring at offshore developments demonstrates that Red-throated Loons consistently avoid wind farms and do not habituate to the development (Percival 2010; Lindeboom et al. 2011). Less is known about how Common Loons respond to offshore wind. The available flight height data from the Northwest Atlantic Seabird Catalog indicate that loons fly in the RSZ 14% of the time (Figure 4-44). Uncertainty about this determination is **low** based on the high-quality information available.

Displacement Vulnerability Determination: **High**

Assessment Method: **Semi-quantitative**

Displacement Uncertainty: **Low**

Based on BRI's vulnerability assessment, the displacement vulnerability determination for loons was **high** (Table 4-17). In addition to the evidence of avoidance cited in the collision vulnerability assessment above, loons have long been considered the marine birds most vulnerable to displacement (Garthe and Hüppop 2004; Furness et al. 2013, Mendel et al. 2019). The clearest evidence yet of the displacement effect of offshore wind on loons came in a recent study in the North Sea conducted before and after the construction of offshore wind farms (Garthe et al. 2023). The study showed that Red-throated Loon distribution and abundance shifted dramatically after construction, with fewer birds in the study area, and those that remained aggregating far from the five offshore wind farms. Uncertainty about this determination is **low** based on the high-quality information available.

Population vulnerability determination: **Low to Medium**

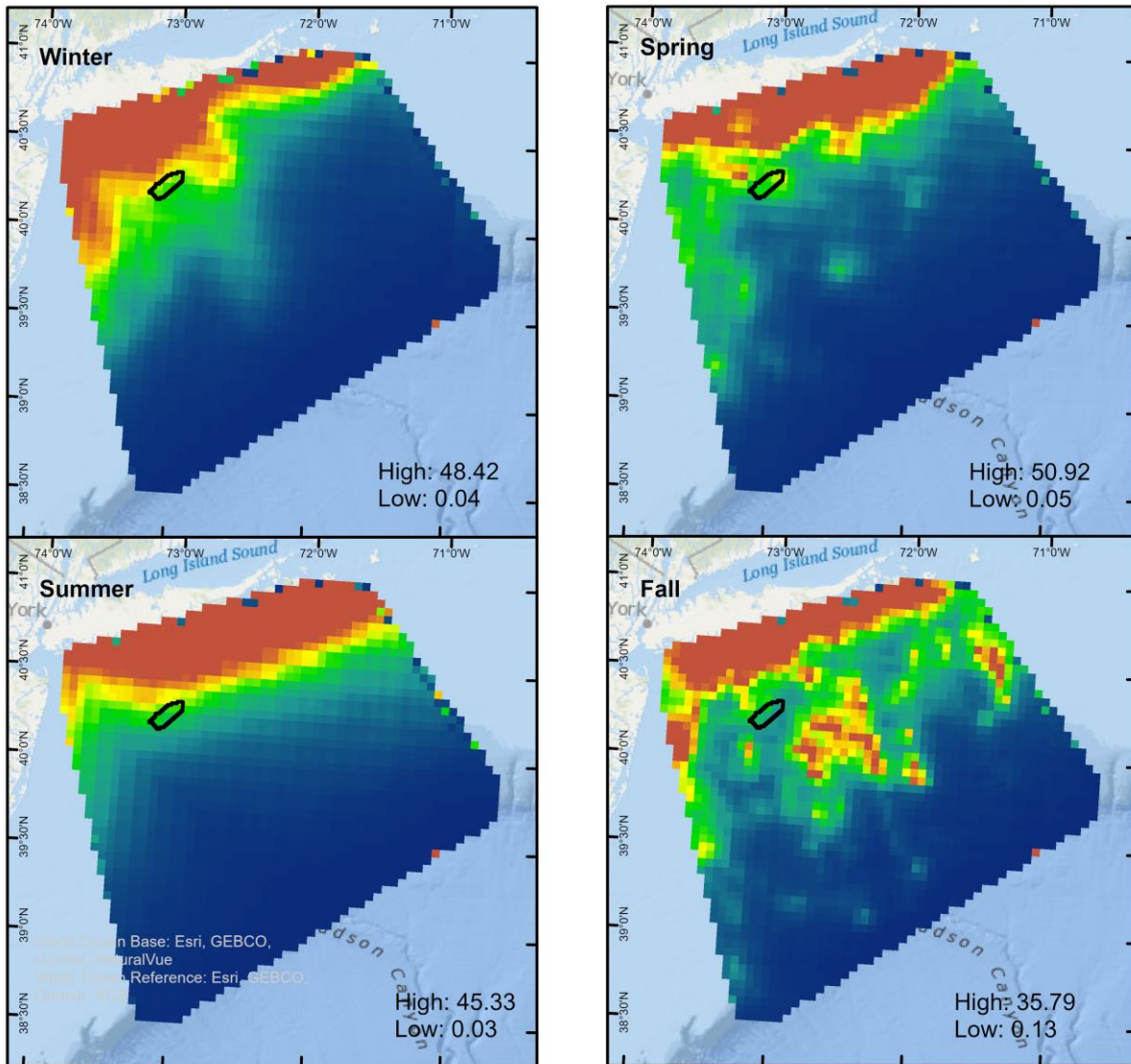
Assessment Method: **Semi-quantitative**

Based on BRI's vulnerability assessment, the population vulnerability determination for loons was **low** for (Red-throated Loons) to **medium** (for Common Loons; Table 4-17). Conservation status is not high priority for either species, but Common Loons have greater adult survival than Red-throated Loons.

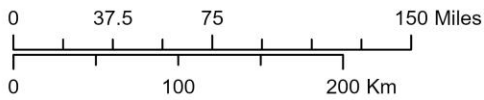
4.3.6.4 Risk Determination

Loons received an exposure determination of low, a relative collision vulnerability determination of minimal to low (adjusted), a relative displacement vulnerability determination of high, and a population vulnerability determination of low to medium. Based on BRI's risk assessment matrix (Table 2-1), final collision risk was **minimal to low** and displacement risk was **low**.

4.3.6.5 Tables and Figures



Modeled APEM digital aerial surveys for loons in Lease Area OCS-A 0544



CS: NAD 1983 UTM Zone 19N

Produced by: J. Stepanuk | VW544_apem_inla_cormorants | Version date: 6/26/2024

Lease Area OCS-A 0544

Total Density



Figure 4-41: Modeled APEM digital aerial surveys for loons in the NY Bight survey area and Lease Area OCS-A 0544.

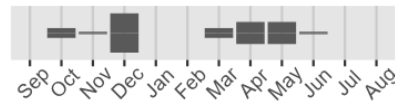
Table 4-16: Seasonal exposure rankings for the loons group.

Taxa Group	Season	Local Score	Regional Score	Total Score	Exposure Category
Loons	Winter	0	0	0	minimal
	Spring	1	1	2	low
	Summer	0	0	0	minimal
	Fall	0	1	1	low

Red-throated Loon



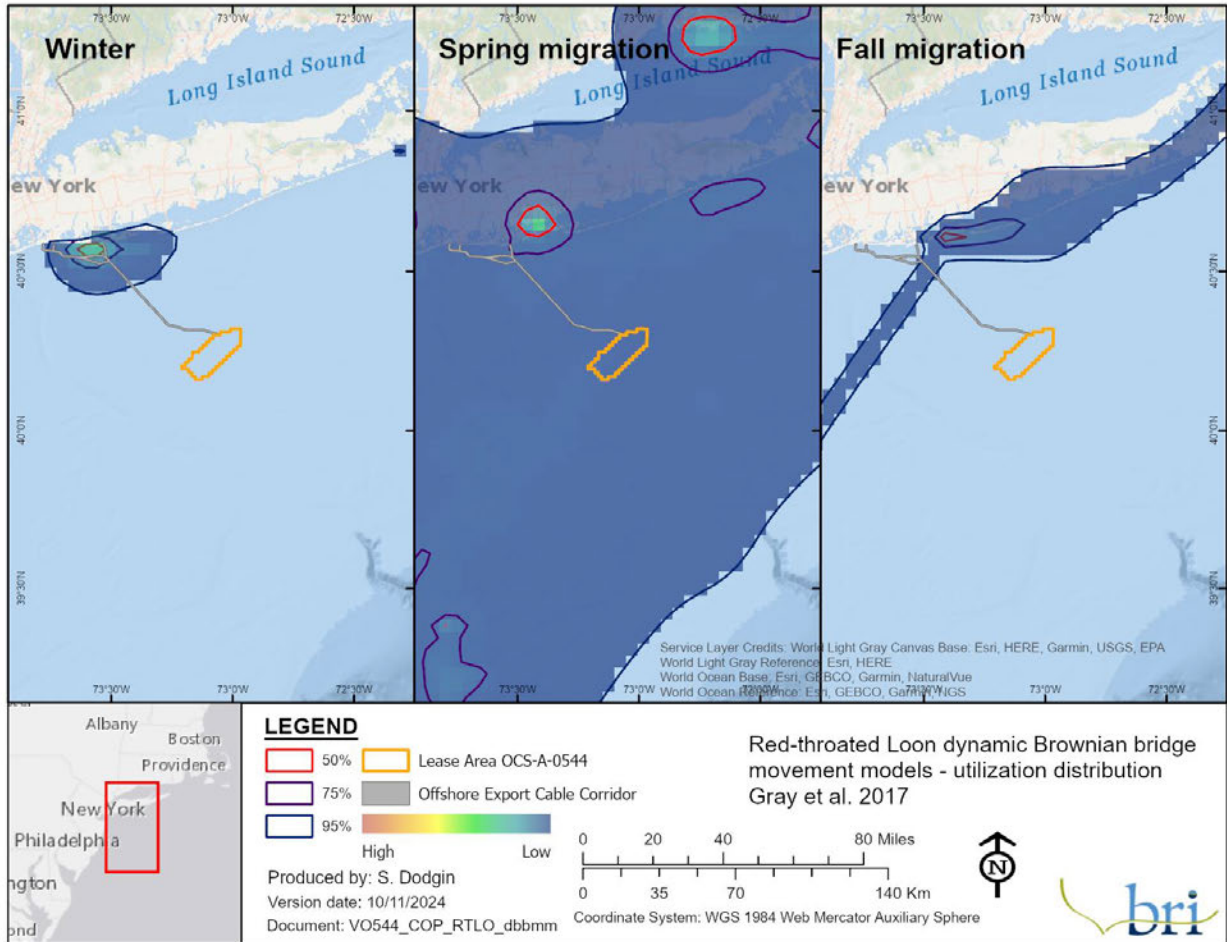
Common Loon



Unidentified Loon

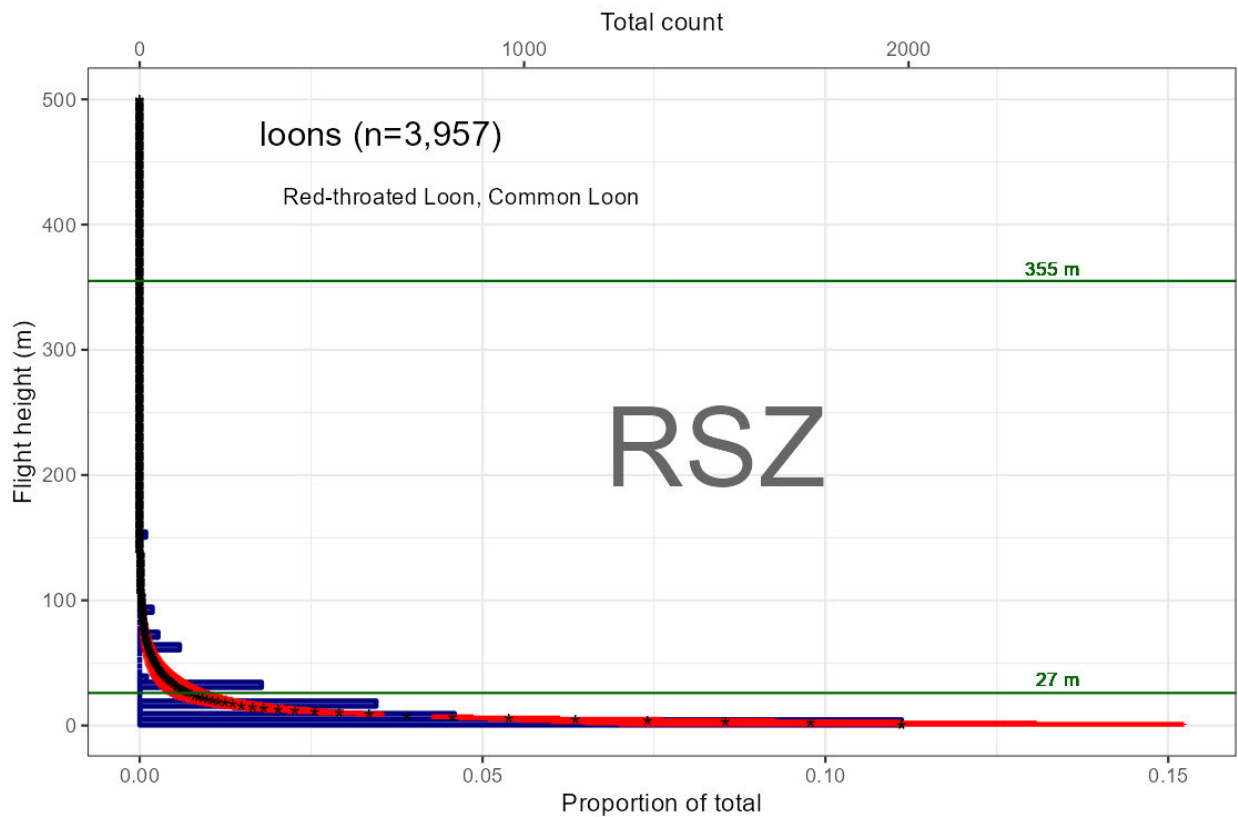


Figure 4-42: Monthly relative densities of loons in the Lease Area from digital aerial surveys



NOTE: Contours represent various levels of use, from 50% (core use) to 95% (home range).

Figure 4-43: Dynamic Brownian bridge movement models for Red-throated Loons ($n=46$ in winter, 46 in spring, and 31 in fall) that were tracked with satellite transmitters. The models indicate the birds stay close to shore in the winter and during fall migration, but may pass through the Lease Area during spring migration.



NOTE: Figure shows the actual number of birds in 5 m (16-ft) intervals (blue bars), the modeled average flight height in 1 m (3-ft) intervals (black asterisks), and the standard deviation (red lines), in relation to the upper and lower limits of a minimum and maximum RSZ scenario (27–355 m; green lines).

Figure 4-44: Flight heights of loons ($n=3,957$) derived from the Northwest Atlantic Seabird Catalog.

Table 4-17: Vulnerability assessment rankings by species for the loon group.

NOTE: A lower range limit of “minimal” is added to the Collision Vulnerability score in green font because there is little evidence in the literature that loons are vulnerable to collision, which is attributed to their very strong avoidance response.

Species	Collision Vulnerability (CV)	Displacement Vulnerability (DV)	Population Vulnerability (PV)
Common Loon	minimal-low (0.47)	high (0.8)	medium (0.6)
Red-throated Loon	minimal-low (0.37)	high (0.9)	low (0.47)

4.3.7 Shearwaters, Petrels, and Storm-Petrels

Minor Taxa Groups: Procellariiformes: Procellariidae (shearwaters and petrels), Hydrobatidae (storm-petrels). Note: ESA-listed Black-capped Petrel (*Pterodroma hasiata*) is discussed separately in Section 4.4.4 below.

Collision Risk Determination: **Minimal**

Displacement Risk Determination: **Minimal**

4.3.7.1 Overview

Distribution and Habitat Preferences: Shearwaters, petrels, and storm-petrels are all highly pelagic birds that spend the majority of their lives at sea, except for breeding (Winkler et al. 2020n). All are highly migratory, with Sooty Shearwaters having one of the longest annual migrations of any bird, although migration patterns may vary widely among species. Unlike many species of marine birds, not all breed in northern regions, with some species breeding in the Caribbean, or on remote islands of the South Atlantic and using the North Atlantic only during their non-breeding period (the austral winter/boreal summer).

Behavior and Ecology: Members of this group feed primarily on zooplankton and nekton, which they pluck individually from the surface of the water (Winkler et al. 2020n). During the non-breeding season, small flocks will follow prey availability in long-distance movements that may be north-south or even follow equatorial currents across the Atlantic Ocean.

Reproduction: Other than Northern Fulmars (*Fulmarus glacialis*), which generally nest on sheer cliffs, species of this group breed in burrows, cavities, or rock crevices, in which they lay a single egg (Winkler et al. 2020n). Incubation is much longer than in other birds, and semiprecocial chicks are brooded and fed oily regurgitate until fledge. Nesting sites are typically islands far from the mainland and lacking predators.

Conservation Status: Most birds in this group are highly susceptible to human disturbance at breeding sites, and especially to introduced predators. Many species breed at a select few locations, so impacts at such sites have magnified impacts on populations. The Black-capped Petrel is listed as *Endangered* under the ESA, and as such is discussed separately in Section 4.4.4. No species in this group is listed in New York or New Jersey.

4.3.7.2 Exposure Assessment

Group exposure determination: **Minimal**

Assessment Method: **Semi-quantitative**

Main Information Sources: MDAT, baseline, site-specific

Supplemental Information Sources: Literature

Exposure Uncertainty: **Low**

Based on BRI's exposure assessment, the group exposure determination for shearwaters, petrels, and storm-petrels was **minimal** (Table 4-18). Mapping and exposure scoring were done for two subgroups: (1) shearwaters and petrels; and (2) storm-petrels. The mapped outputs of the spatial density models show the Lease Area outside the areas of highest density within the NY Bight survey area; predicted densities are higher further offshore in winter, spring, and fall, and more evenly distributed in summer (Figure 4-45 and Figure 4-46). Local exposure scores were all 0 except for a

summer local score of 1 for storm-petrels. The regional exposure scores for shearwaters, petrels, and storm-petrels for all seasons were 0. Other than the low exposure in summer for storm-petrels, all total exposure scores were 0, corresponding to a minimal exposure category overall. In the Lease Area, based on aerial surveys, there were observations of Cory's Shearwater, Great Shearwater, Sooty Shearwater, unidentified shearwater, unidentified storm-petrel, and Wilson's Storm-Petrel (as shown by density values of greater than 0 counts/km² in Table 4-28). As indicated in the overview, some species in this group breed at different times in different locations, so seasonal exposure differs between species. Across the Lease Area, seasonal densities of the shearwaters, petrels, and storm-petrels taxa groups varied by species (Figure 4-47). In general, this group was most frequently observed in winter, spring, and summer, though some species were also frequently observed in fall: Audubon's Shearwater (*Puffinus lherminieri*), Black-capped Petrel, Wilson's Storm-Petrel (*Oceanites oceanicus*), Leach's Storm-Petrel (*Hydrobates leucorhous*), and unidentified small shearwaters. Uncertainty is **low** for the exposure assessment due to the availability of regional and site-specific digital aerial surveys, as well as MDAT models. No tracking studies are available for this group.

4.3.7.3 Behavioral Vulnerability Assessment

Collision Vulnerability Determination: **Low**

Assessment Method: **Semi-quantitative**

Collision Uncertainty: **Medium**

Based on BRI's vulnerability assessment, the collision vulnerability determination for shearwaters, petrels, and storm-petrels is **low** (Table 4-19). The available flight height data from the Northwest Atlantic Seabird Catalog indicate that birds in this group are nearly always observed flying low over the sea surface, with shearwaters and petrels only in the RSZ 0.1% of the time, and storm-petrels only 0.04% of the time (Figure 4-48 and Figure 4-49). There is some evidence that artificial lighting may attract this group, as some species forage at night on vertically migrating bioluminescent aquatic prey and are instinctively attracted to artificial light sources (Imber 1975; Montevecchi 2006). This may be particularly true during periods of poor visibility when collision risk is likely to be highest. However, there is little data on avian behavior in the marine environment during such periods, as surveys are limited to good weather during daylight hours. Several sources indicate that light-induced mass fatality events are primarily a land-based issue involving fledging birds leaving their colonies at night (Corre et al. 2002; Rodríguez et al. 2014; Rodríguez et al. 2015; Rodríguez et al. 2017). A recent report for the Scottish Government (Deakin et al. 2022) thoroughly reviewed the available literature on light attraction among members of this group; it is clear that powerful light can disorient these birds (especially fledglings in foggy conditions) and cause them to circle light sources, but the evidence on the existence and strength of light attraction is inconclusive. The distance of the Lease Area from shore and the nearest breeding colonies (Leach's Storm-Petrel colonies in the Gulf of

Maine) ensures that such an event would be exceedingly unlikely in the New York Bight. Uncertainty about this determination is **medium**, due to the lack of quality information to clarify the avoidance/attraction response of this group.

Displacement Vulnerability Determination: **Medium**

Assessment Method: **Semi-quantitative**

Displacement Uncertainty: **Medium**

Based on BRI's vulnerability assessment, the displacement vulnerability determination for shearwaters, petrels, and storm-petrels is **medium** (Table 4-19). Displacement has not been well studied for this taxonomic group, but Furness et al. (2013) ranked species in this group as having the lowest displacement rank. A study at Egmond aan Zee, the Netherlands, found that 50 percent (n=10) of "tube-nosed species" (this group) passed through the wind farm, which results in the birds receiving a displacement vulnerability score of 5 and, thus, "medium" vulnerability. Wade et al. (2016) identified that there was "very high" uncertainty on displacement vulnerability for these species. Uncertainty about this determination is **medium** based on the lack of quality information on avoidance.

Population vulnerability determination: **Low to Medium**

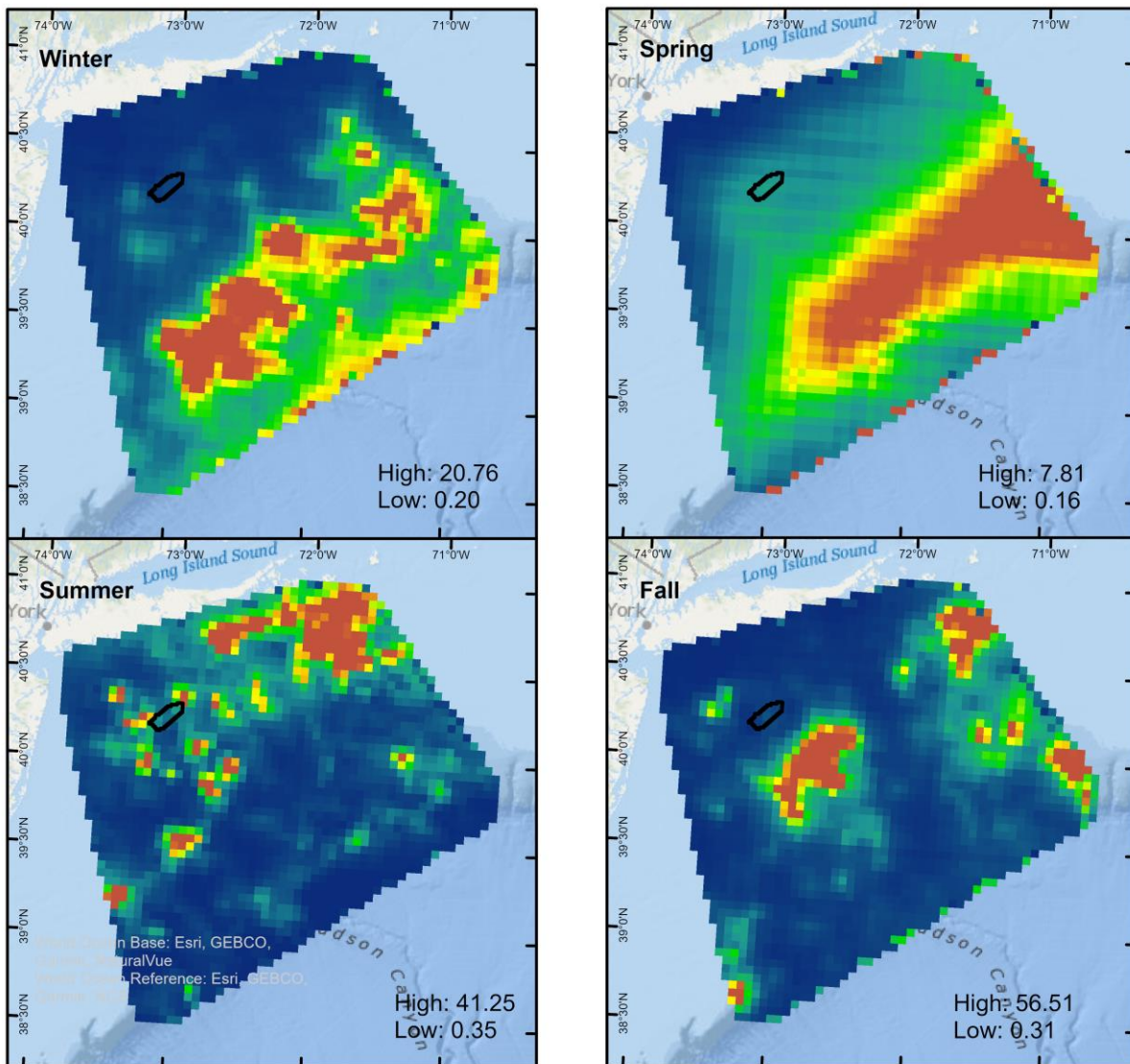
Assessment Method: **Semi-quantitative**

Based on BRI's vulnerability assessment, the population vulnerability determination for shearwaters, petrels, and storm-petrels is **low to medium** (Table 4-19). Adult survival is quite high for the members of this group, and Cory's Shearwater and Audubon's Shearwater have global conservation statuses of elevated priority.

4.3.7.4 Risk Determination

Shearwaters, petrels, and storm-petrels received an exposure determination of minimal, a relative collision vulnerability determination of low, a relative displacement vulnerability determination of medium, and a population vulnerability determination of low to medium. Based on BRI's risk assessment matrix (Table 2-1), final collision and displacement risk were both assessed as **minimal**.

4.3.7.5 Tables and Figures



Modeled APEM digital aerial surveys for shearwaters and petrels in Lease Area OCS-A 0544

0 37.5 75 150 Miles

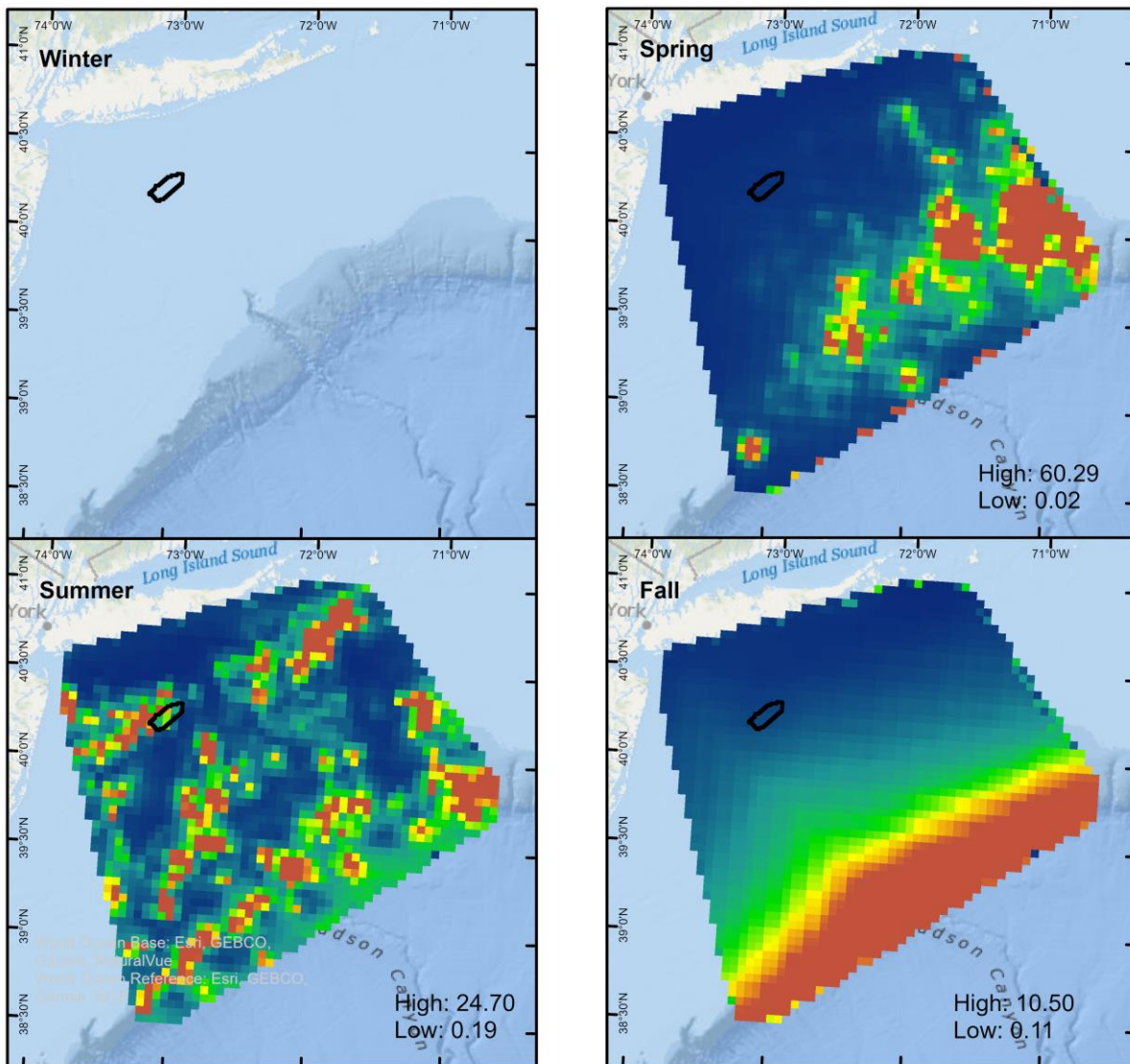
0 100 200 Km

CS: NAD 1983 UTM Zone 19N

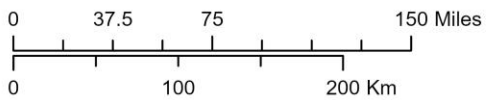
Produced by: J. Stepanuk | VW544_apem_inla_cormorants | Version date: 6/26/2024



Figure 4-45: Modeled APEM digital aerial surveys for petrels and shearwaters in the NY Bight survey area and Lease Area OCS-A 0544.



Modeled APTEM digital aerial surveys for storm-petrels in Lease Area OCS-A 0544



CS: NAD 1983 UTM Zone 19N

Produced by: J. Stepanuk | VW544_apem_inla_cormorants | Version date: 6/26/2024

□ Lease Area OCS-A 0544

Total Density

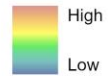


Figure 4-46: Modeled APTEM digital aerial surveys for storm-petrels in the NY Bight survey area and Lease Area OCS-A 0544.

Table 4-18: Seasonal exposure rankings for the shearwaters, petrels, and storm-petrels group.

Taxa Group	Season	Local Score	Regional Score	Total Score	Exposure Category
Shearwaters and Petrels	Winter	0	0	0	minimal
	Spring	0	0	0	minimal
	Summer	0	0	0	minimal
	Fall	0	0	0	minimal
Storm-Petrels	Winter	0	0	0	minimal
	Spring	0	0	0	minimal
	Summer	1	0	1	low
	Fall	0	0	0	minimal

Northern Fulmar



Trindade Petrel



Black-capped Petrel



Cory's Shearwater



Sooty Shearwater



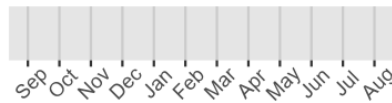
Great Shearwater



Manx Shearwater



Audubon's Shearwater



Unidentified Petrel



Unidentified Large Shearwater



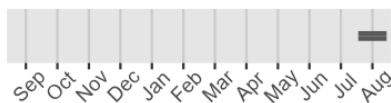
Unidentified Shearwater



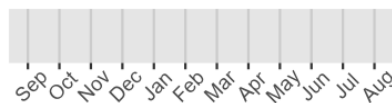
Unidentified Small Shearwater



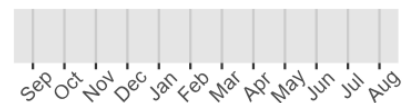
Wilson's Storm-Petrel



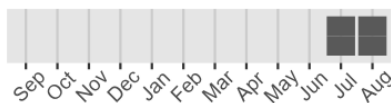
Leach's Storm-Petrel



Band-rumped Storm-petrel



Unidentified Storm-petrel



White-faced Storm-petrel

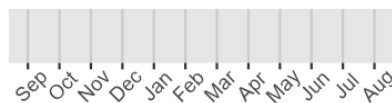
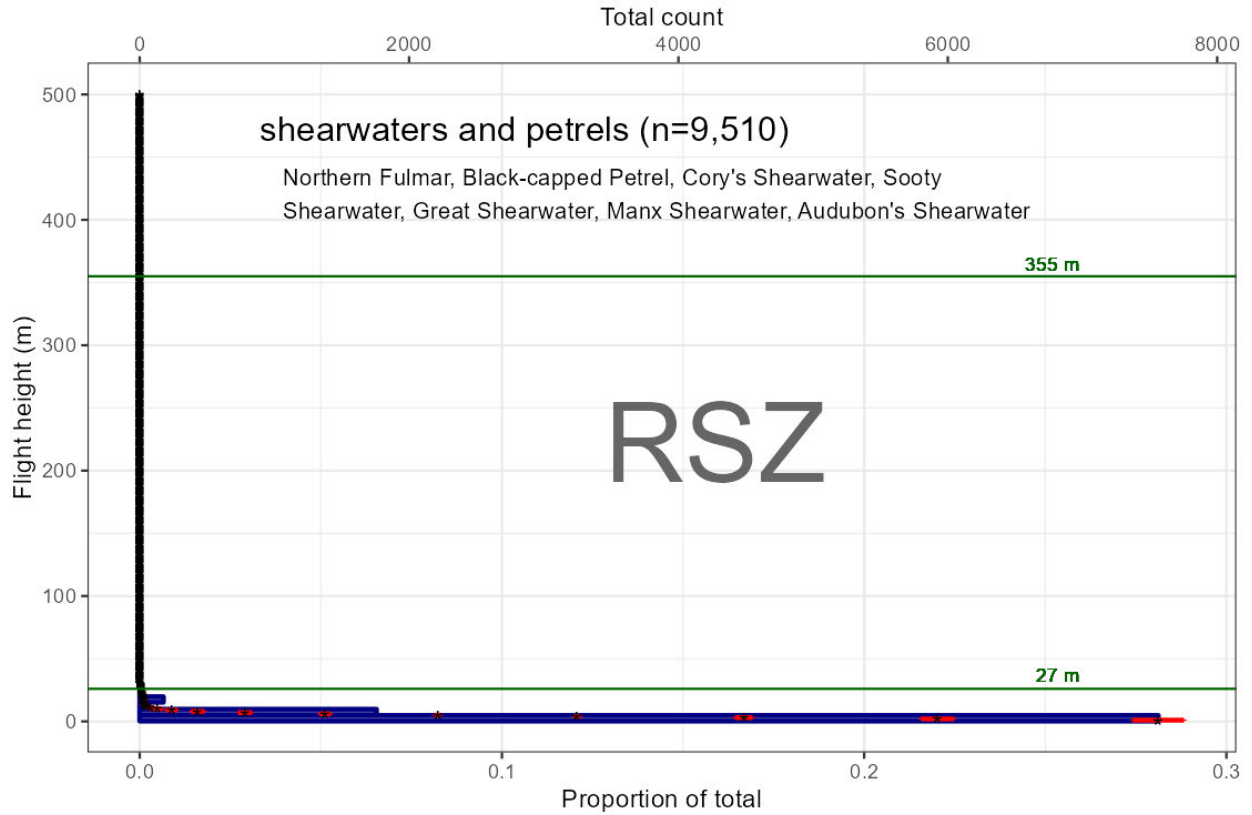
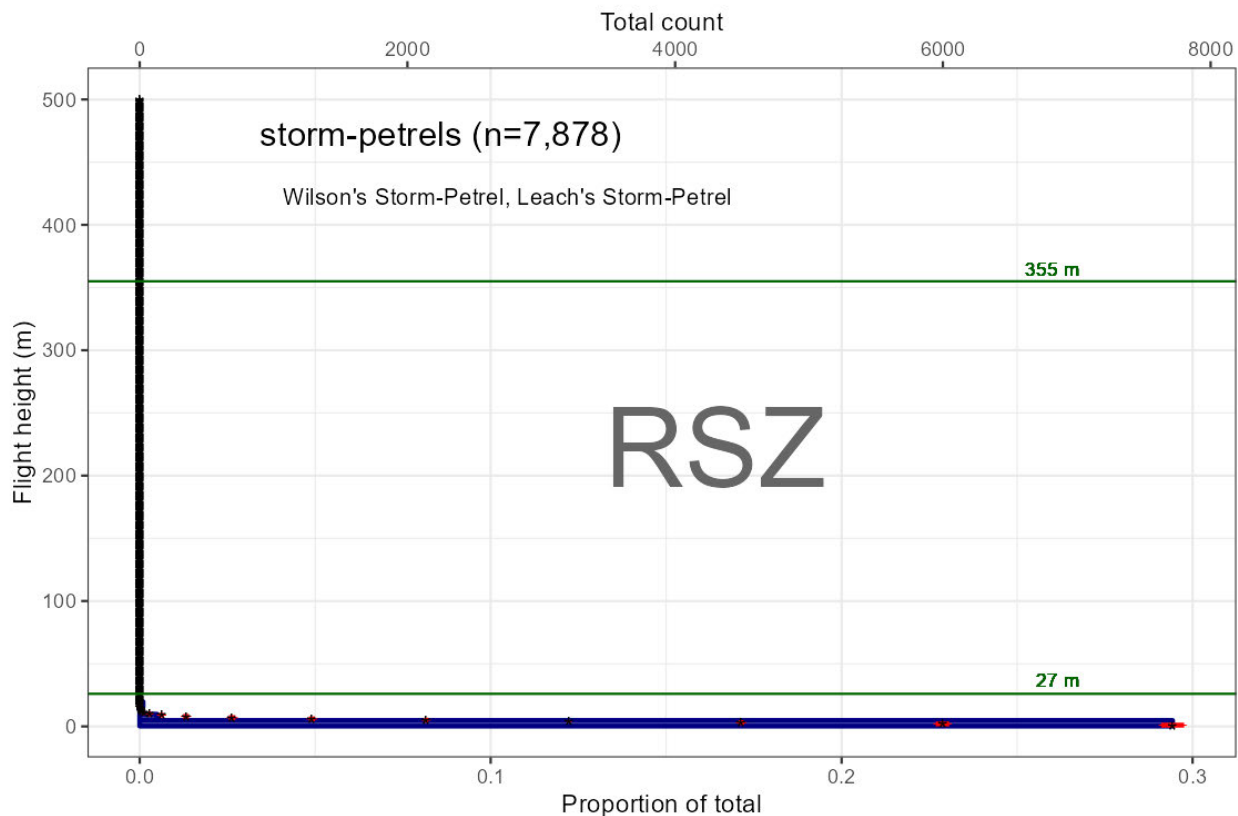


Figure 4-47: Monthly relative densities of shearwaters, petrels, and storm-petrels in the Lease Area from digital aerial surveys.



NOTE: Figure shows the actual number of birds in 5 m (16-ft) intervals (blue bars), the modeled average flight height in 1 m (3-ft) intervals (black asterisks), and the standard deviation (red lines), in relation to the upper and lower limits of a minimum and maximum RSZ scenario (27–355 m; green lines).

Figure 4-48: Flight heights of shearwaters and petrels (n=9,510) derived from the Northwest Atlantic Seabird Catalog.



NOTE: Figure shows the actual number of birds in 5 m (16-ft) intervals (blue bars), the modeled average flight height in 1 m (3-ft) intervals (black asterisks), and the standard deviation (red lines), in relation to the upper and lower limits of a minimum and maximum RSZ scenario (27–355 m; green lines).

Figure 4-49: Flight heights of storm-petrels ($n=7,878$) derived from the Northwest Atlantic Seabird Catalog.

Table 4-19: Vulnerability assessment rankings by species for the shearwaters, petrels, and storm-petrels group.

Species	Collision Vulnerability (CV)	Displacement Vulnerability (DV)	Population Vulnerability (PV)
Audubon's Shearwater	low (0.27)	medium (0.6)	medium (0.73)
Black-capped Petrel	low (0.43)	medium (0.6)	medium (0.67)
Cory's Shearwater	low (0.33)	medium (0.6)	medium (0.6)
Great Shearwater	low (0.33)	medium (0.6)	medium (0.67)
Manx Shearwater	low (0.27)	medium (0.6)	medium (0.53)
Northern Fulmar	low (0.4)	medium (0.6)	low (0.47)
Sooty Shearwater	low (0.3)	medium (0.6)	medium (0.53)
Leach's Storm-Petrel	low (0.43)	medium (0.6)	low (0.47)
Wilson's Storm-Petrel	low (0.4)	medium (0.6)	low (0.4)

4.3.8 Gannets

Minor Taxa Groups: Suliformes: Sulidae (Northern Gannets)

Collision Risk Determination: **Low**

Displacement Risk Determination: **Low**

4.3.8.1 Overview

Distribution and Habitat Preferences: Northern Gannets, the only member of this species to regularly range in the Northern Hemisphere, breed in six colonies in Atlantic Canada and overwinter in substantial numbers along the US Atlantic coast (Gulka et al. 2023), meaning that they are not usually present in the New York Bight in the summer months.

Behavior and Ecology: Gannets feed on fish and squid, which they reach by plunge-diving from 10–40 m above the sea surface (Mowbray 2020). In local areas near breeding colonies, gannets can have substantial impacts on forage fish populations. Breeding success is often associated with the ready availability of these prey species.

Reproduction: Gannets nest on rocky islands and cliffs, laying 1–2 eggs. They have altricial young which both adults feed and brood until fledge at roughly 12 weeks. Fledglings swim away from the breeding colony and begin migrating to southern overwintering areas (Mowbray 2020).

Conservation Status: Following long-term declines, Northern Gannet populations have stabilized, and are growing steadily at some colonies (Mowbray 2020). However, their populations worldwide, including Atlantic Canada, have been hit badly by highly pathogenic avian influenza (HPAI) in recent years (Lane et al. 2023).

4.3.8.2 Exposure Assessment

Group Exposure Determination: **Low**

Assessment Method: **Semi-quantitative**

Main Information Sources: MDAT, baseline, site-specific

Supplemental Information Sources: Literature, tracking

Exposure Uncertainty: **Minimal**

Based on BRI's exposure assessment, the exposure determination for Northern Gannets was **low** (Table 4-20). The mapped outputs of the spatial density models show the Lease Area outside the areas of highest density within the NY Bight survey area, which are mostly close to the coast during spring and fall and more dispersed in winter (Figure 4-50). Local exposure scores for the Northern Gannet for all seasons with models available were 0. Regional exposure scores for spring and fall were 1, which corresponds to a low exposure category. Total exposure scores ranged from 0-1, corresponding to minimal to low exposure categories. In the Lease Area, there were observations of Northern Gannet within all seasons except summer (as shown by density counts/km² in Table 4-28). Within the Lease Area, the Northern Gannet occurred throughout winter, spring, and fall (Figure 4-51), but not in summer as they are at breeding colonies in northern locales during summer, as described in the overview section above. Satellite tracking data for Northern Gannets

(Stenhouse et al. 2020) indicates that this species is likely to use areas within the Lease Area during winter as well as spring and fall migration periods (Figure 4-52). Uncertainty is **minimal** for the exposure assessment due to the availability of regional and site-specific digital aerial surveys, MDAT models, and tracking studies.

4.3.8.3 Behavioral Vulnerability Assessment

Collision Vulnerability Determination: **Low**

Assessment Method: **Semi-quantitative**

Collision Uncertainty: **Low**

Based on BRI's vulnerability assessment, the collision vulnerability determination for Northern Gannets is **low** (Table 4-21). The available flight height data from the Northwest Atlantic Seabird Catalog indicate that gannets fly in the RSZ 17% of the time (Figure 4-53). While Northern Gannets have been ranked more vulnerable to collision risk by some studies (Furness et al. 2013; Garthe et al. 2014; Cleasby et al. 2015), many studies indicate that they avoid wind developments (Hartman et al. 2012; Garthe et al. 2014; Vanermen et al. 2015). For example, avoidance rates have been estimated to be 64 to 84% (macro) and 99.1% (total; Cook et al. 2012; Krijgsveld et al. 2011; Vanermen et al. 2015; Skov et al. 2018). A recent study offshore of Aberdeen, Scotland (Tjørnløv et al. 2023), extensively studied flight behavior of Northern Gannets (as well as four gull species). Though Northern Gannets were documented flying through the wind farm, they showed strong avoidance behavior close to spinning turbine blades, and in 10,000 bird videos and over 3,000 combined video-radar tracks, there were no collisions or even near misses (Tjørnløv et al. 2023). Uncertainty about this determination is **low** due to the high quality of the available information on flight height, flight activity, and avoidance.

Displacement Vulnerability Determination: **Medium**

Assessment Method: **Semi-quantitative**

Displacement Uncertainty: **Low**

Based on BRI's vulnerability assessment, the displacement vulnerability determination for Northern Gannets is **medium** (Table 4-21). In Belgium, Northern Gannets have been shown to avoid wind development areas and have decreased in abundance by 85% after a project was constructed (Vanermen et al. 2015). Eighty-nine percent of tracked Northern Gannets breeding in Helgoland, Germany, predominantly avoided nearby operational offshore wind areas. If they did enter the area, they typically flew between 250 and 450 m (820 and 1,476 ft) from WTGs (not approaching closer than 79 m [259 ft]; Peschko et al. 2021), and there is some evidence that this displacement may be long-lasting. A study in the Belgian North Sea found that numbers of Northern Gannets dropped by 98% in the Thornton Bank offshore wind area (plus a 0.3 mi [0.5

km] buffer) after six years of post-construction monitoring; however, they were not displaced from the 0.3–1.9 mile (0.5–3 km) zone around the edge of the wind farm (Vanermen et al. 2019). Northern Gannets feed on highly mobile surface-fish and follow their prey throughout the OCS (Mowbray 2020), gaining some habitat flexibility. Uncertainty about this determination is **low** due to the high quality of information available.

Population vulnerability determination: **Low**

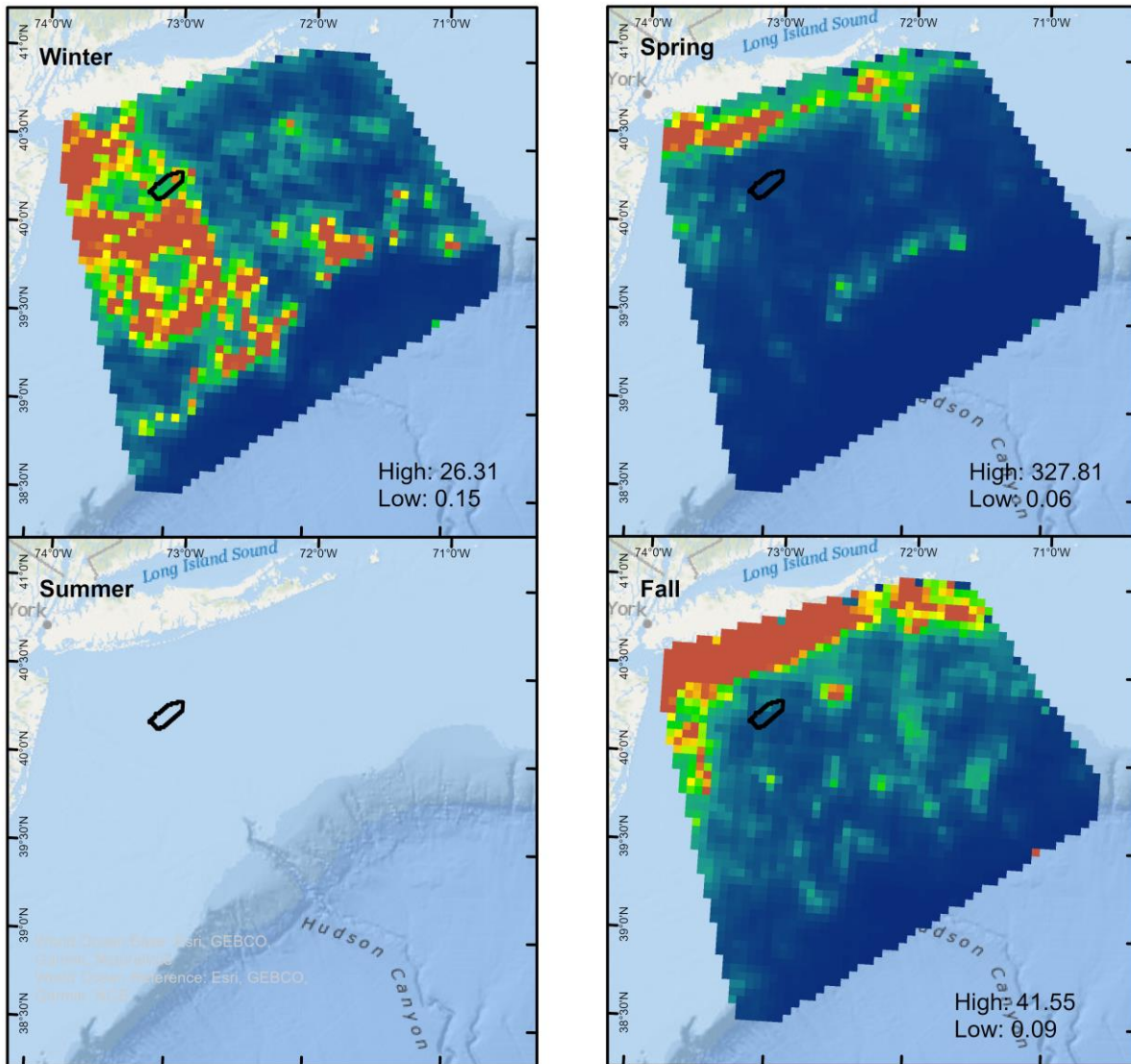
Assessment Method: **Semi-quantitative**

Based on BRI's vulnerability assessment, the population vulnerability determination for gannets is **low** (Table 4-21). Despite their high adult survival, their stable populations (at least in recent decades) lead to low priority conservation status.

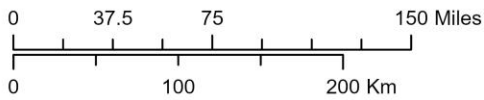
4.3.8.4 Risk Determination

Northern Gannets received an exposure determination of low, a relative collision vulnerability determination of low, a relative displacement vulnerability determination of medium, and a population vulnerability determination of low. Based on BRI's risk assessment matrix (Table 2-1), final collision and displacement risk were both assessed as **low**.

4.3.8.5 Tables and Figures



Modeled APem digital aerial surveys for gannets in Lease Area OCS-A 0544



Produced by: J. Stepanuk | VW544_apem_inla_cormorants | Version date: 6/26/2024

Lease Area OCS-A 0544

Total Density

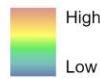


Figure 4-50: Modeled APem digital aerial surveys for gannets in the NY Bight survey area and Lease Area OCS-A 0544.

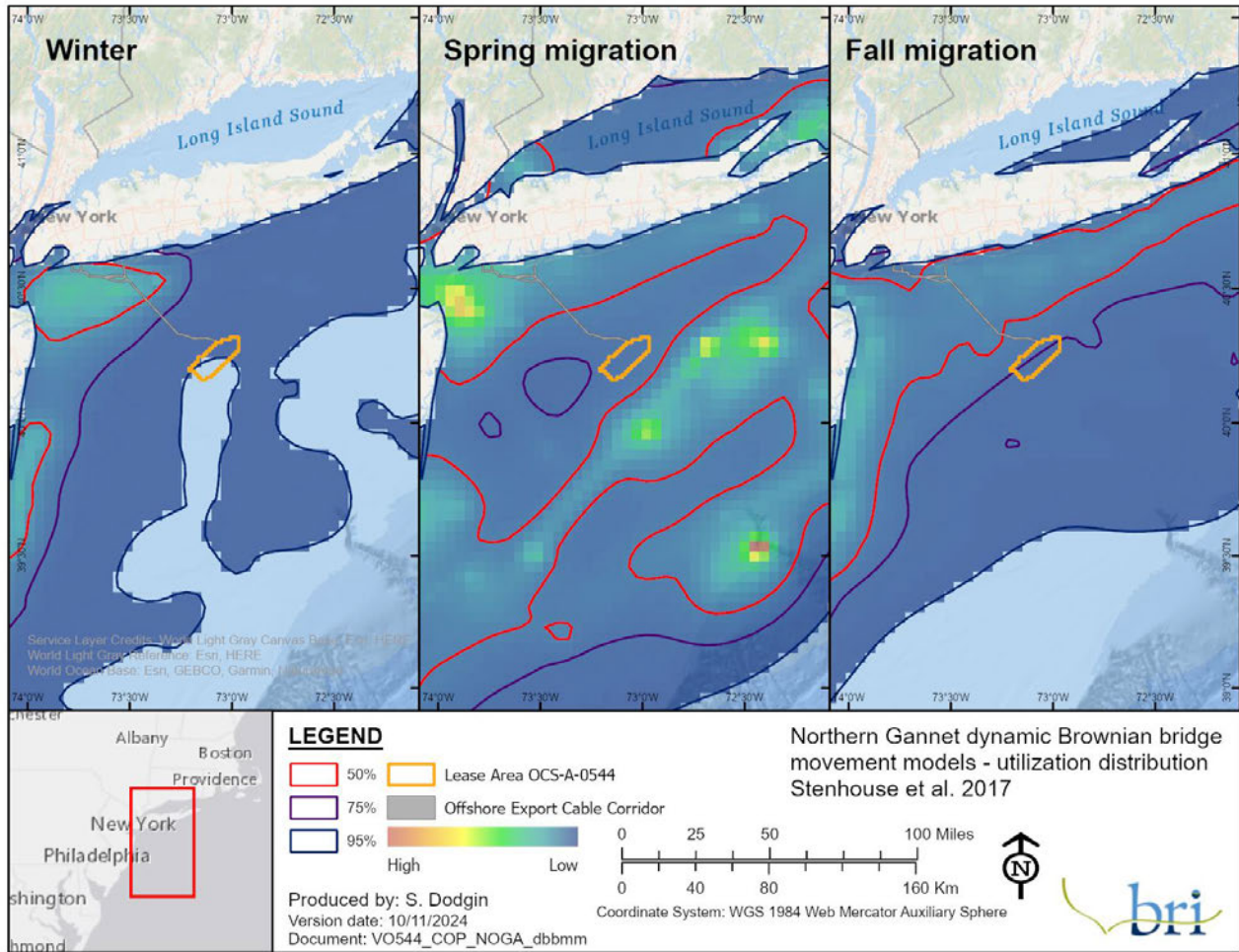
Table 4-20: Seasonal exposure scoring and categories for Northern Gannets.

Taxa Group	Season	Local Score	Regional Score	Total Score	Exposure Category
Gannets	Winter	0	0	0	minimal
	Spring	0	1	1	low
	Summer	-	0	-	minimal
	Fall	0	1	1	low

Northern Gannet

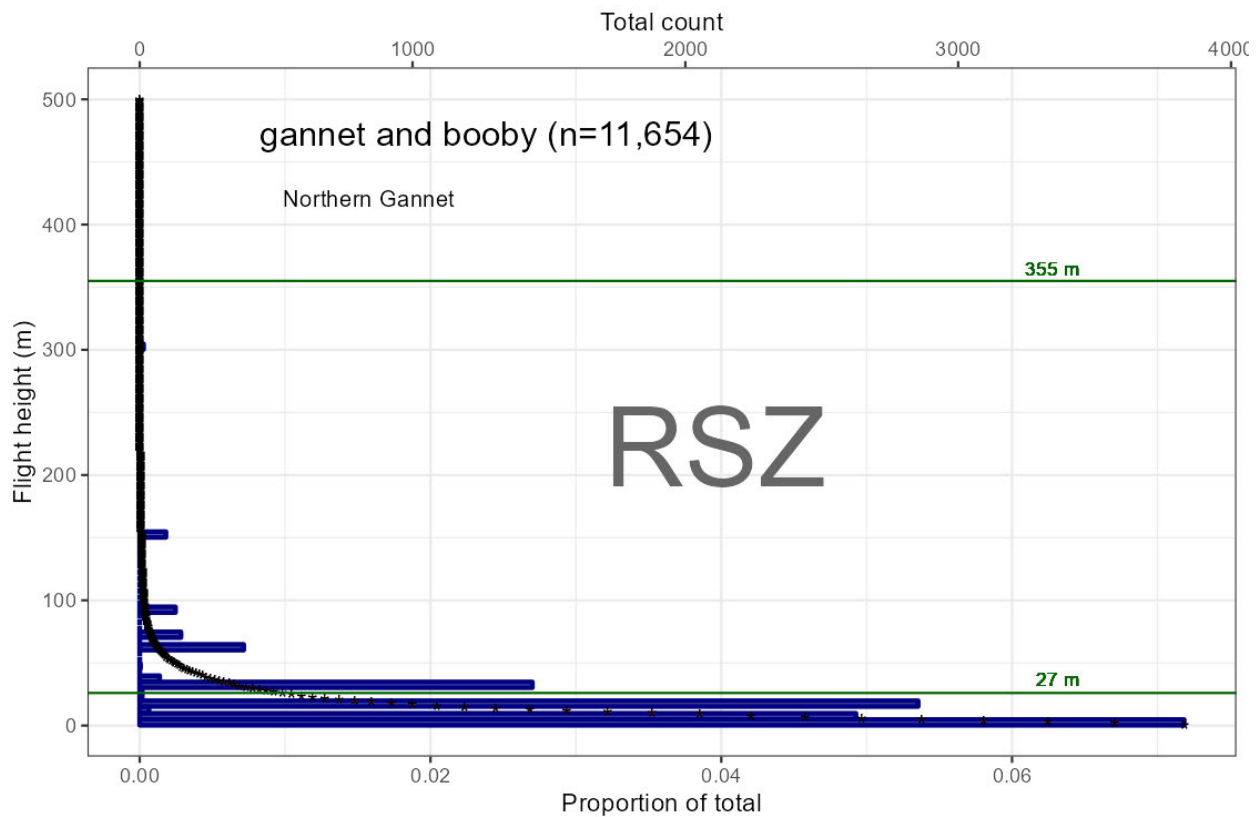


Figure 4-51: Monthly relative densities of Northern Gannets in the Lease Area from digital aerial surveys.



NOTE: Contours represent various levels of use, from 50% (core use) to 95% (home range).

Figure 4-52: Dynamic Brownian bridge movement models for Northern Gannets ($n=34$ in winter, 35 in spring, 36 in fall) that were tracked with satellite transmitters. The models indicate the Lease Area is used by Northern Gannets during the winter, spring, and fall.



NOTE: Figure shows the actual number of birds in 5 m (16-ft) intervals (blue bars), the modeled average flight height in 1 m (3-ft) intervals (black asterisks), and the standard deviation (red lines), in relation to the upper and lower limits of a minimum and maximum RSZ scenario (27–355 m; green lines).

Figure 4-53: Flight heights of Northern Gannets (n=11,654) derived from the Northwest Atlantic Seabird Catalog

Table 4-21: Vulnerability assessment rankings for Northern Gannets.

Species	Collision Vulnerability (CV)	Displacement Vulnerability (DV)	Population Vulnerability (PV)
Northern Gannet	low (0.4)	medium (0.6)	low (0.47)

4.3.9 Cormorants and Pelicans

Minor Taxa Groups: Phalacrocoracidae (cormorants); Pelecaniformes: Pelecanidae (Brown Pelicans)

Collision Risk Determination: **Minimal**

Displacement Risk Determination: **Minimal**

4.3.9.1 Overview

Distribution and Habitat Preferences: Cormorants are found in nearshore habitats along the entire US Atlantic coastline throughout the year, with Double-crested Cormorants (*Phalacrocorax auratus*) the most numerous and broadly distributed species (Dorr et al. 2021). Brown Pelicans breed along the southern Atlantic and Gulf coasts of the US and are permanent residents from Maryland south, while non-breeding individuals may migrate north along the Atlantic coast and occur in the New York Bight (Shields 2020).

Behavior and Ecology: Cormorants and pelicans feed primarily on fish. Cormorants begin their dives from the surface and actively pursue their prey underwater, and generally feed in shallower open water of less than 10 m (33 ft) depth (Dorr et al. 2021). Brown Pelicans (*Pelecanus occidentalis*), like Northern Gannets, are plunge divers who climb up to 20 m (66 ft) above the sea surface and plunge into the water in pursuit of prey (Shields 2020). They primarily forage in waters of less than 150 m (492 ft) depth, including continental shelf waters up to 20 km (12.4 mi) from shore.

Reproduction: Cormorants nest on islands and cliffs and lay 2–4 eggs, while Brown Pelicans nest in trees or on the ground and lay 2–3 eggs. All species have altricial young which both adults feed and brood until they fledge, by 10 weeks in cormorants to 11–12 weeks in pelicans.

Conservation Status: Cormorants are currently stable and broadly distributed. Brown Pelicans were formerly federally listed after nearly being extirpated from North America during the mid-20th century, largely due to organochlorine pesticides; populations recovered sufficiently to remove them from the list (Shields 2020). Acute anthropogenic threats (e.g., the Deepwater Horizon oil spill) can still have major impacts on pelican populations, however.

4.3.9.2 Exposure Assessment

Group Exposure Determination: **Minimal**

Assessment Method: **Semi-quantitative**

Main Information Sources: MDAT, baseline, site-specific

Supplemental Information Sources: Literature

Exposure Uncertainty: **Low**

Based on BRI's exposure assessment, the group exposure determination for cormorants and pelicans was minimal (Table 4-22). Mapping and exposure scoring were done for cormorants as one subgroup and pelicans as another. The mapped outputs of the spatial density models for cormorants show that the Lease area is further offshore than the higher density areas nearest to the shore (Figure 4-54), which should be expected from their shallow foraging habitats. Brown Pelicans had too few observations to produce spatial density models. Local exposure scores for the cormorants and Brown Pelican for all seasons with models available were 0. Regional exposure scores for cormorants for seasons with models available were 0; pelican regional

exposure scores were either 0 or not available. In the Lease Area, there were no observations of cormorants or Brown Pelicans (as shown by 0.0 density counts/km² in Table 4-28). Occurrence within the Lease Area for the group was most common in the spring and fall (Figure 4-55). Uncertainty is low for the exposure assessment due to the availability of regional and site-specific digital aerial surveys, and MDAT models. Tracking data are not available for any species in this group.

4.3.9.3 Behavioral Vulnerability Assessment

Collision Vulnerability Determination: **Medium**

Assessment Method: **Semi-quantitative**

Collision Uncertainty: **Low**

Based on BRI's vulnerability assessment, the collision vulnerability determination for cormorants and pelicans is **medium**, though a determination was not made for Brown Pelicans due to a lack of flight activity information (Table 4-23). The available flight height data from the Northwest Atlantic Seabird Catalog indicate that cormorants fly in the RSZ 36% of the time (Figure 4-56) and pelicans 8% of the time (Figure 4-57). Cormorants have been documented to be attracted to WTGs because of an increase in food resources and newly available loafing habitat (i.e., perching areas; Krijgsveld et al. 2011; Lindeboom et al. 2011). Brown Pelicans are noted for a very low avoidance response (Adams et al. 2016). Uncertainty about this determination is **low** due to the high quality of information available.

Displacement Vulnerability Determination: **Low to Medium**

Assessment Method: **Semi-quantitative**

Displacement Uncertainty: **Low**

Based on BRI's vulnerability assessment, the displacement vulnerability determination for cormorants and pelicans is **low to medium** (Table 4-23). The evidence of low avoidance among cormorants, and their documented attraction to WTGs, supports the low determination. The medium displacement vulnerability of Brown Pelicans is largely driven by their low habitat flexibility, though they are also noted for low avoidance behavior (Adams et al. 2016). Uncertainty about this determination is **low** due to the high quality of the available information.

Population vulnerability determination: **Minimal to Low**

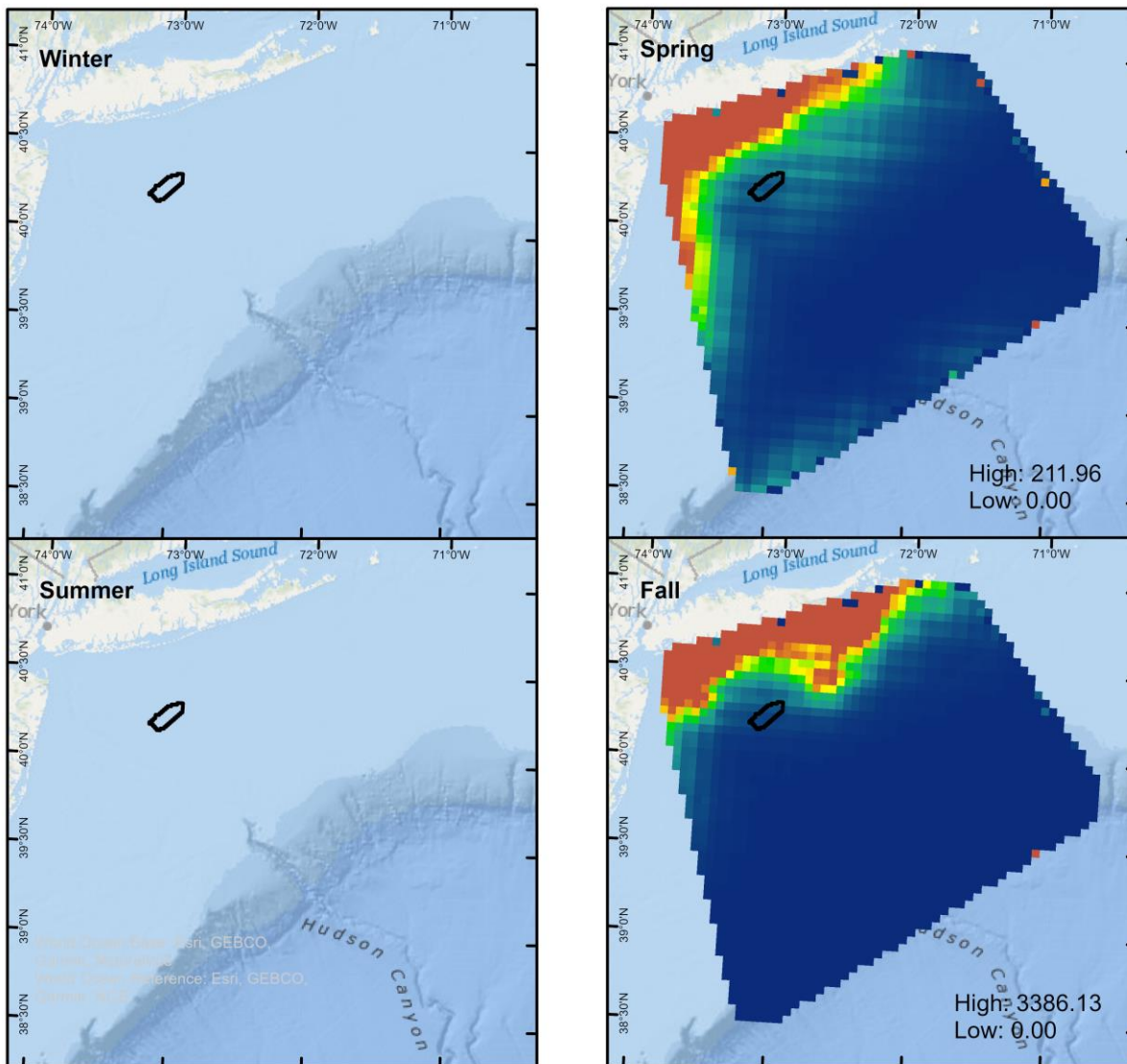
Assessment Method: **Semi-quantitative**

Based on BRI's vulnerability assessment, the population vulnerability determination for is **minimal to low** (Table 4-23). Conservation status is not a major factor in population vulnerability for either Double-crested Cormorants or Brown Pelicans.

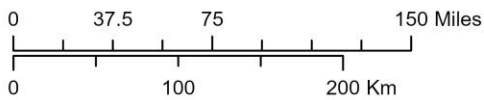
4.3.9.4 Risk Determination

Cormorants and pelicans received a group exposure determination of minimal, a relative collision vulnerability determination of medium, a relative displacement vulnerability determination of low to medium, and a population vulnerability determination of minimal to low. Based on BRI's risk assessment matrix (Table 2-1), final collision risk and vulnerability risk were both assessed as **minimal**.

4.3.9.5 Tables and Figures



Modeled APDEM digital aerial surveys for cormorants in Lease Area OCS-A 0544



CS: NAD 1983 UTM Zone 19N

Produced by: J. Stepanuk | VW544_apem_inla_cormorants | Version date: 6/26/2024



□ Lease Area OCS-A 0544

Total Density

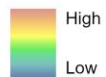


Figure 4-54: Modeled APDEM digital aerial surveys for cormorants in the NY Bight survey area and Lease Area OCS-A 0544.

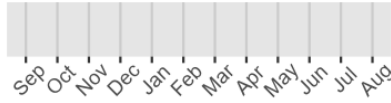
Table 4-22: Seasonal exposure rankings for cormorants and pelicans.

Taxa Groups	Season	Local Score	Regional Score	Total Score	Exposure Category
Cormorants	Winter	-	-	-	minimal
	Spring	0	0	0	minimal
	Summer	-	0	-	minimal
	Fall	0	0	0	minimal
Pelicans	Winter	-	-	-	minimal
	Spring	-	-	-	minimal
	Summer	-	-	-	minimal
	Fall	-	0	-	minimal

Double-crested Cormorant



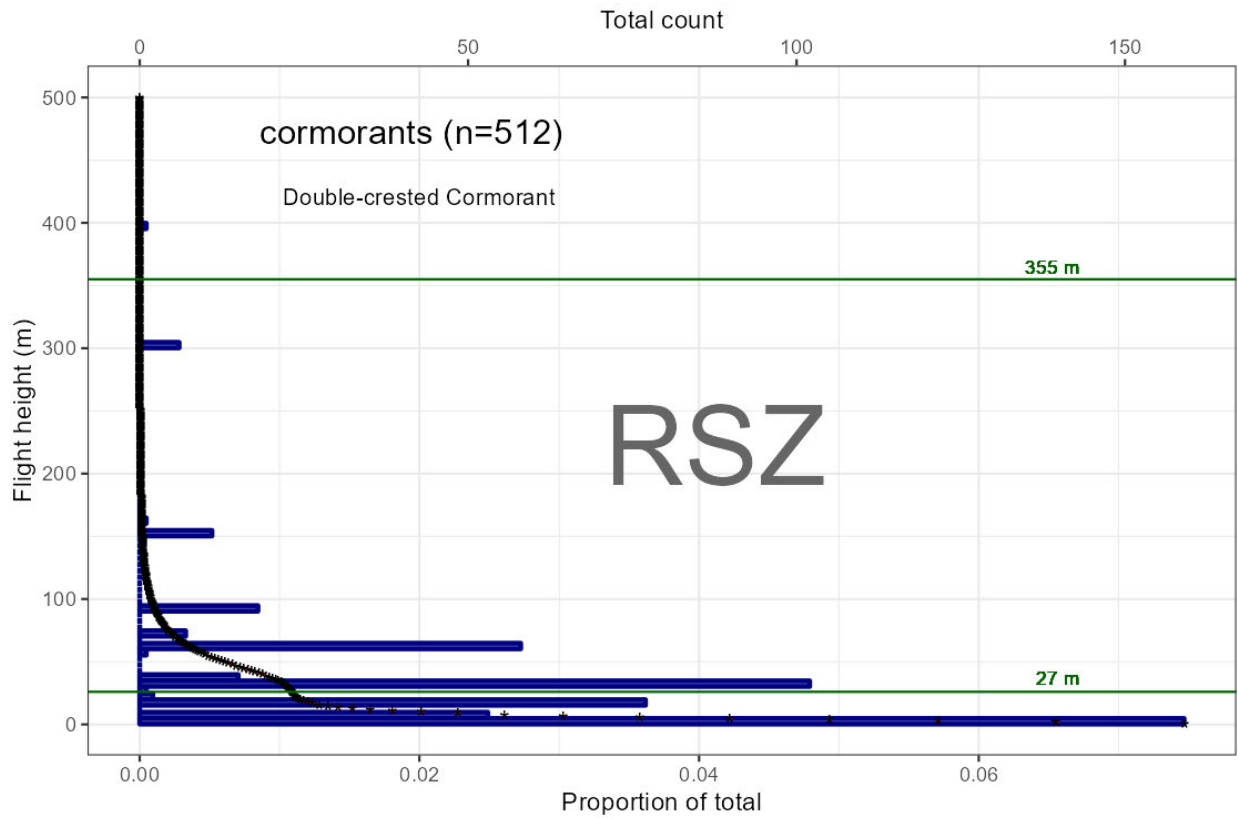
Unidentified Cormorant



Brown Pelican

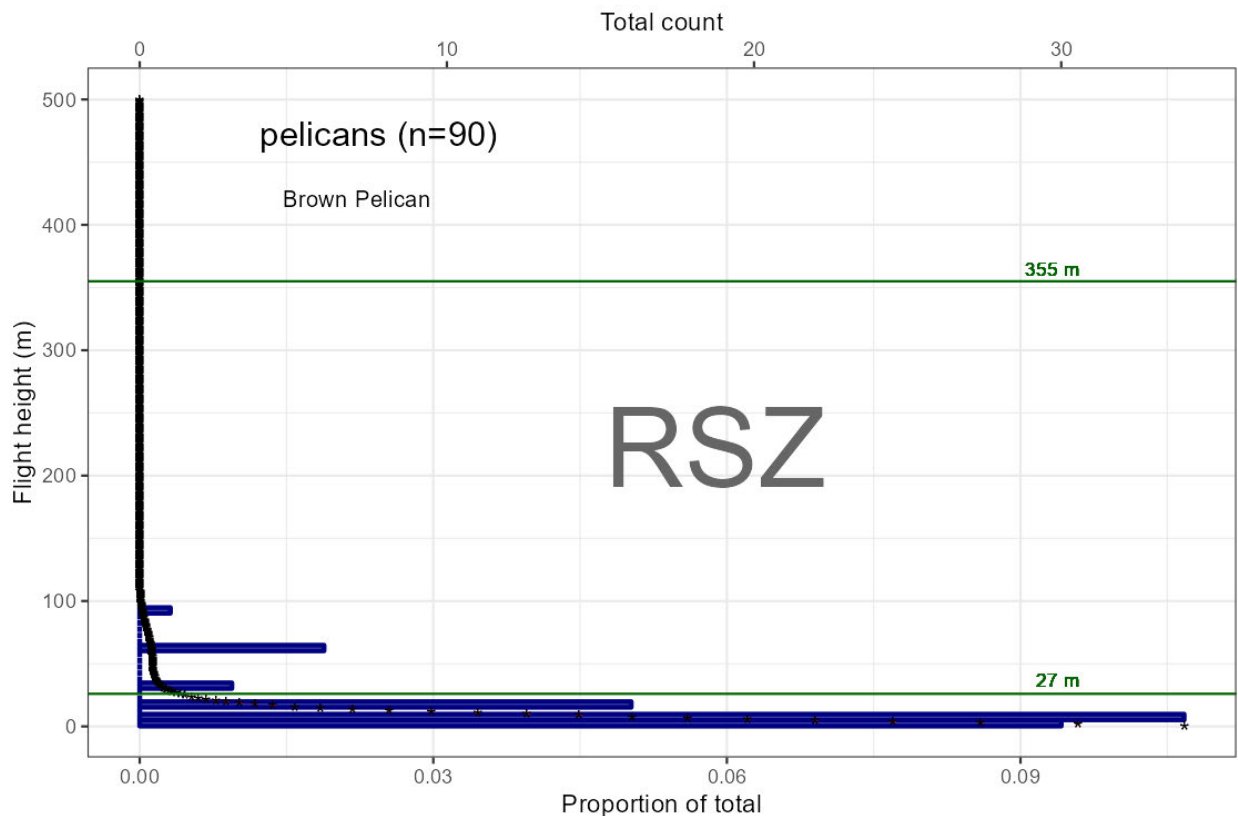


Figure 4-55: Monthly relative densities of cormorants and pelicans in the Lease Area from digital aerial surveys.



NOTE: Figure shows the actual number of birds in 5 m (16-ft) intervals (blue bars), the modeled average flight height in 1 m (3-ft) intervals (black asterisks), and the standard deviation (red lines), in relation to the upper and lower limits of a minimum and maximum RSZ scenario (27–355 m; green lines).

Figure 4-56: Flight heights of cormorants (n=512) derived from the Northwest Atlantic Seabird Catalog



NOTE: Figure shows the actual number of birds in 5 m (16-ft) intervals (blue bars), the modeled average flight height in 1 m (3-ft) intervals (black asterisks), and the standard deviation (red lines), in relation to the upper and lower limits of a minimum and maximum RSZ scenario (27–355 m; green lines).

Figure 4-57: Flight heights of pelicans (n=90) derived from the Northwest Atlantic Seabird Catalog.

Table 4-23: Vulnerability assessment rankings by species for cormorants and pelicans.

Species	Collision Vulnerability (CV)	Displacement Vulnerability (DV)	Population Vulnerability (PV)
Double-crested Cormorant	medium (0.73)	low (0.4)	minimal (0.13)
Brown Pelican	· (·)	medium (0.5)	low (0.4)

4.4 Protected Species and Species of Concern

Federally listed and candidate species under the ESA were also assessed, as were eagles, which are protected by the BGEPA. Each species is discussed individually below. Eastern Black Rails (listed) and Saltmarsh Sparrows (proposed for listing) are unlikely to be exposed to the Lease Area, as it is generally thought that neither species flies far offshore between winter and breeding habitats (BOEM 2022) and are not discussed further in this section. These species are, however, discussed in the onshore section of this report.

4.4.1 Roseate Tern, Northeastern Population (*Endangered*)

Collision Risk Determination: **Low**

Displacement Risk Determination: **Low**

4.4.1.1 *Overview*

Distribution and Habitat Preferences: The Roseate Tern is globally distributed in the marine environment, with breeding colonies on islands primarily throughout the tropics and subtropics. A few discrete breeding populations also exist in temperate regions. In North America, the Northeastern population of Roseate Terns breeds in northeastern United States and Atlantic Canada, and winters in South America, primarily in eastern Brazil (USFWS 2010; Mostello et al. 2014). Nearly all Roseate Terns in this population breed at three colony locations in Massachusetts (Bird Island, Ram Island, and Penikese Island in Buzzards Bay), and one colony location in New York (Great Gull Island; Mostello et al. 2014; Loring et al. 2017). Migration routes are poorly understood, but based on tracking studies, they appear to follow paths well offshore (Nisbet 1984; USFWS 2010; Burger et al. 2011; Mostello et al. 2014). Roseate Terns will only pass through the New York Bight during migration.

Behavior and Ecology: Roseate Terns forage by shallow plunge-diving or surface-dipping to catch small fish, such as sand lance (*Ammodytes spp.*; Goyert 2014; Mostello et al. 2014). During the breeding season, they generally feed in shallow water areas (USFWS 2010; Mostello et al. 2014) and stay within 6.2 mi (10 km) of the colony, but individuals may travel up to 31.1 mi (50 km) from the colony while provisioning chicks (USFWS 2010; Burger et al. 2011; Mostello et al. 2014; Loring et al. 2017). As such, Roseate Terns are unlikely to forage in the New York Bight area.

Reproduction: The Northeastern population of Roseate Terns nests colonially on islands. They generally arrive at their breeding colonies in late April to late May, with nesting occurring between roughly mid-May and late July. None of the Roseate Tern colonies occur within the New York Bight Wind Energy Area.

Conservation Status: USFWS listed the Northeast population of Roseate Terns as *Endangered* in 1987, with predation, limited food availability, and eroded nesting habitat posing the primary threats (USFWS 1998 SSA). During the non-breeding period along the coast of Brazil, Roseate Terns may also be exposed to and affected by industrial activities, such as power lines and offshore petroleum activities (Loring et al. 2023). The species is also listed as *Endangered* in New York and New Jersey. The Caribbean breeding population, federally listed as *Threatened*, is unlikely to occur in the New York Bight and not considered in this assessment.

4.4.1.2 Exposure Assessment

Species exposure determination: **Minimal to Low**

Assessment Method: **Qualitative**

Information Sources: MDAT, baseline, site-specific, tracking, literature

Exposure Uncertainty: **Low** (adjusted up due to the MDAT gap and lack of Motus coverage)

Based on BRI's exposure assessment, the species exposure determination for Roseate Terns was **minimal to low** (Table 4-24). Because the nearest breeding colony, Great Gull Island, is 120 km (75 mi) away from the Lease Area at the closest point, Roseate Terns would only potentially be exposed to the Lease during fall and spring migration periods. During fall and spring, the regional MDAT models indicate that Roseate Terns are generally concentrated closer to shore during spring migration and have low exposure in New Jersey and New York offshore waters during the summer and fall; however, there is a gap in the density surface across the Lease Area, making it difficult to accurately predict site-specific occurrence (Figure 4-58; Winship et al. 2023). Based on the digital aerial surveys and data from the Northwest Atlantic Seabird Catalog, no sightings of Roseate Terns have been documented in the Lease Area (Figure 4-59). An analysis of unknown tern observations in the Northwest Atlantic Seabird Catalog from within the NY Bight survey area indicates that 34 of the unknowns may be Roseate Terns but few, if any, occurred in the Lease Area.⁶

In addition, a Motus based Nanotag tracking study indicates that Roseate Terns ($n=145$) are unlikely to pass through the Lease Area, with only one estimated trackline passing near the northwest boundary, although the movement models are not representative of the entire breeding and post-breeding period for many tagged individuals, due to incomplete spatial coverage of the receiving stations and tag loss (Figure 4-60, Loring et al. 2019). Uncertainty is **low** (adjusted) for the exposure assessment due to the availability of regional digital aerial surveys, MDAT models, and tracking studies, although it is important to note that the receivers used in the Motus based tracking studies did not cover the Lease Area and there is a gap in the MDAT models.

⁶ To determine if unknown tern observations in the Northwest Atlantic Seabird Catalog were potentially Roseate Terns, the following analysis was conducted:
Step 1: All available tern data from the Northwest Atlantic Seabird Catalog database were cut down to the NYSERDA study area.
Step 2: The proportion of Roseate Terns to all identified terns was calculated (0.01).
Step 3: The proportions from step 2 were applied to the count of 3451 unidentified terns in the dataset, assuming the same proportions in unknown data apply.
Result: This returns an estimate of 34 additional Roseate Terns that could have occurred in the NYSERDA study area and 0.5 (~1) in the Lease Area.

4.4.1.3 Behavioral Vulnerability Assessment

Collision Vulnerability Determination: **Low**

Assessment Method: **Semi-quantitative**

Collision Uncertainty: **Medium**

Based on BRI's vulnerability assessment, the collision vulnerability determination for Roseate Terns was **low** (Table 4-24). This is supported by scientific literature and tracking studies. Previous vulnerability assessments also find that Roseate Terns rank low in collision risk (Furness et al. 2013). In addition, terns regularly exhibit micro-avoidance behaviors to avoid actively spinning WTG blades (Vlietstra 2007). In general, the species is unlikely to fly within the RSZ of Vineyard Mid-Atlantic (27–355 m), as flight heights of Roseate Terns during foraging are typically less than 40 ft (12 m) above the water's surface and most commonly less than 20 ft (6 m; Mostello et al. 2014). European studies of related tern species have suggested that up to 10% of birds may fly at a hypothetical rotor height (20–150 m [65.6–492.1 ft] above sea level) during local flights (Jongbloed 2016).

While data on Roseate Tern flight during migration is limited, a tracking study using NanoTags estimated that terns primarily flew below a hypothetical RSZ of 25–250 m (82–820 ft), and that Roseate Terns flying offshore only occasionally flew within the lower portion of the hypothetical RSZ (federal waters, 6.4%; WEAs, 0%; Loring et al. 2019). Data from other tern species suggest that flight height during migration varies with weather, as terns may fly at lower altitudes with headwinds and at higher altitudes in tailwinds (Jongbloed 2016). Uncertainty is **medium** in the collision determination due to the poor information data on avoidance rates.

Displacement Vulnerability Determination: **Medium to High**

Assessment Method: **Semi-quantitative**

Displacement Uncertainty: **Medium**

Based on BRI's vulnerability assessment, final displacement vulnerability determination for Roseate Terns was **medium to high** (Table 4-24). While displacement vulnerability was initially assessed as high, a lower range was added due to inconsistencies in the literature and the recognition that displacement in Roseate Terns has generally not been well studied.

Studies conducted at operational WTGs indicate that tern species typically exhibit avoidance behavior. Terns have been shown to have a 76% lower abundance inside offshore wind farms and were estimated to start avoidance behaviors at 0.93 mi (1.5 km; Welcker and Nehls 2016). Common Terns (generally similar in size and behavior) were estimated to have a 70% avoidance

rate of WTGs at Horns Rev, Denmark (Petersen and Maim 2006; Cook et al. 2012) and exhibited a 30% macro-avoidance of WTGs at Egmond aan Zee, the Netherlands (Cook et al. 2012).

However, terns in general are not considered vulnerable to disturbance (Furness et al. 2013). At the 660-kW terrestrial WTG in Buzzards Bay, Massachusetts, no tern mortalities were found during a multi-year study, even though Common Terns regularly flew within 50 m (164 ft) of the WTG (Vlietstra 2007). It is thought that terns may be able to detect WTG blades during operation, both visually and acoustically, and avoid flying between WTG rotors while they are in motion (Minerals Management Service 2007; Vlietstra 2007). Uncertainty about this determination is **medium** due to the lack of quality information about avoidance rates for Roseate Terns.

Population vulnerability determination: **High**

Assessment Method: **Semi-qualitative**

Based on BRI’s vulnerability assessment, final population vulnerability determination for Roseate Terns was **high** (Table 4-24). This is supported by species accounts, which reflect that while the US population is slowly recovering, the population in Canada has been declining since 2008, likely due to habitat degradation. Furthermore, the breeding population continues to concentrate on only a few islands in Massachusetts and New York, when recovery criteria require six large colonies with high productivity rates (USFWS 5 year review 2020).

4.4.1.4 Risk Determination

Roseate Terns received a final exposure determination of minimal to low, a relative collision vulnerability determination of low, and a relative displacement vulnerability determination of medium to high. Based on BRI’s risk assessment matrix (Table 2-1), both collision and displacement risk were initially assessed as minimal to low. However, due to the species’ high population vulnerability, the final risk determination was increased, leading to a risk determination of **low** for both collision and displacement.

4.4.1.5 Tables and Figures

Table 4-24: Vulnerability assessment rankings for the Roseate Tern. Based on the literature, displacement vulnerability was adjusted to include a lower range limit.

Species	Collision Vulnerability (CV)	Displacement Vulnerability (DV)	Population Vulnerability (PV)
Roseate Tern	low (0.33)	medium-high (0.8)	high (0.87)

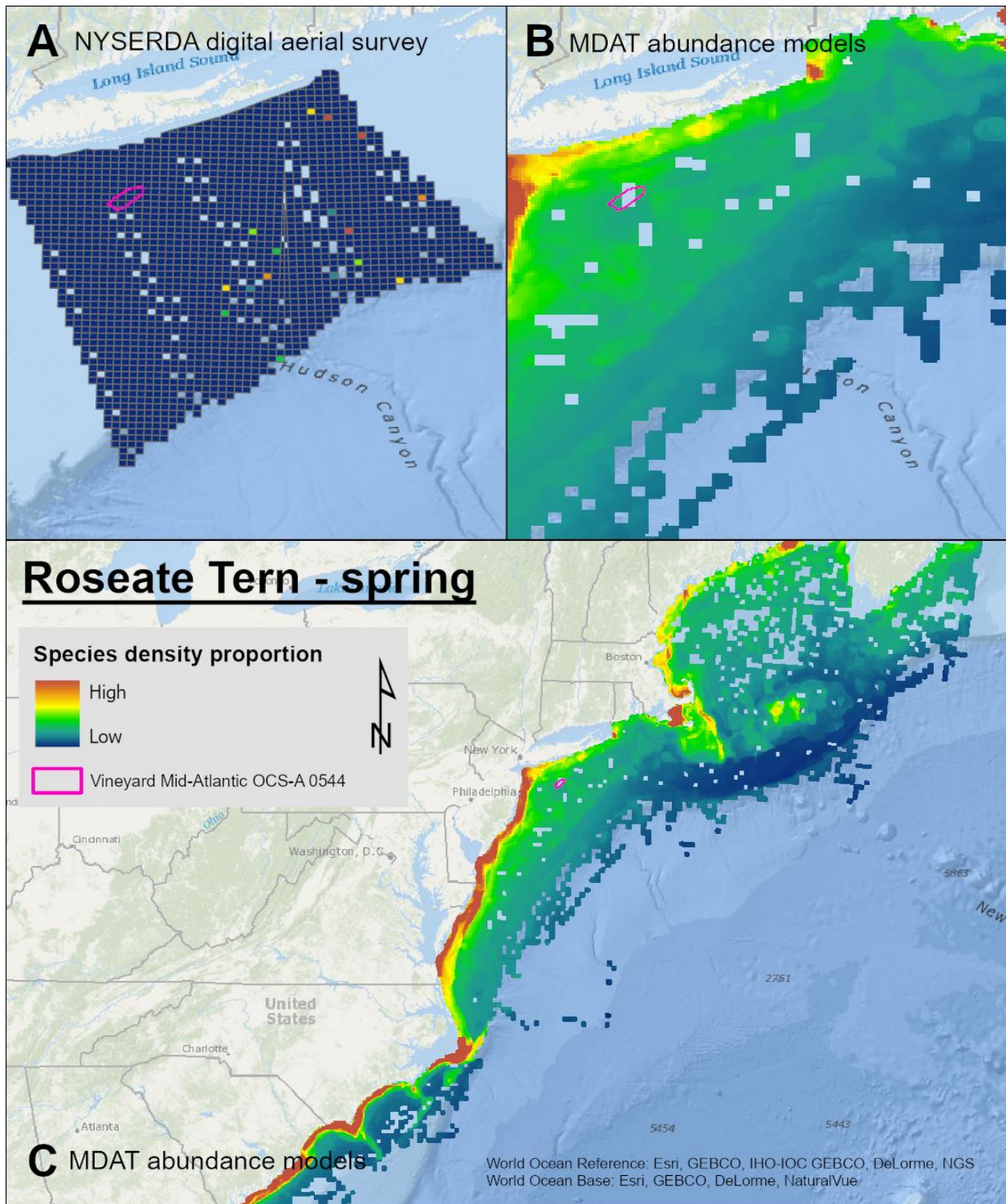


Figure 4-58: Spring Roseate Tern density proportions in the NY Bight survey data (A) and the MDAT model outputs at local (B) and regional scales (C). The scale for all maps is representative of relative spatial variation in the sites within the season for each data source.

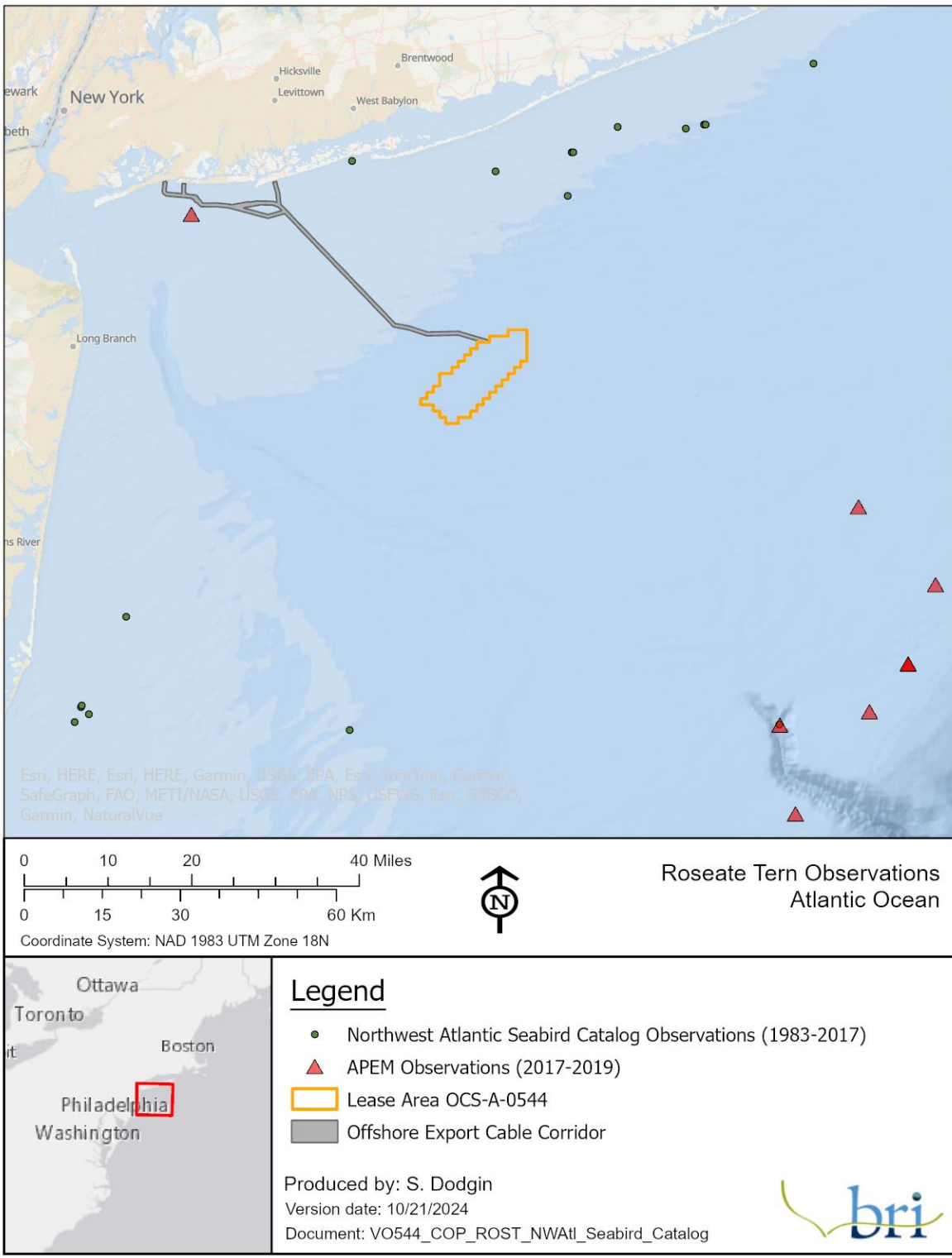


Figure 4-59: Roseate Tern observations from NY Bight surveys (“APEM Observations 2017-2019”); and from the Northwest Atlantic Seabird Catalog. Data provided by National Oceanic and Atmospheric Administration and used with permission.

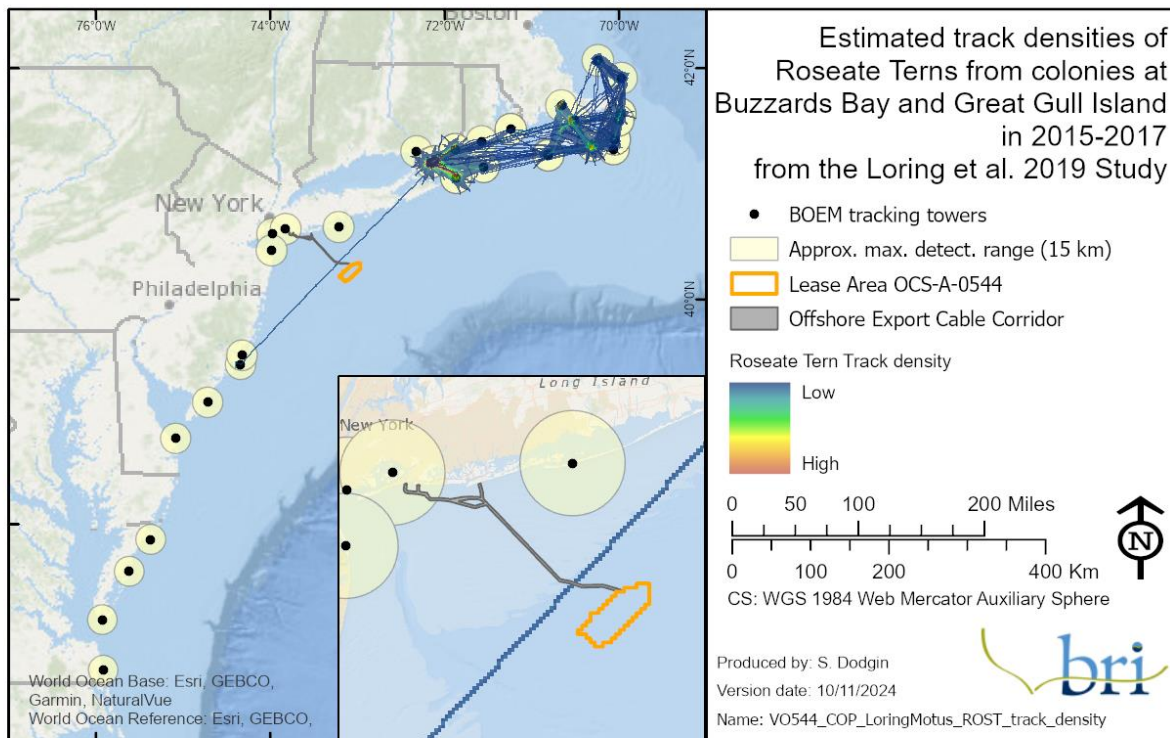


Figure 4-60: Roseate Tern ($n=149$) track locations and density from the Loring *et al.* (2019) radio telemetry study.

4.4.2 Piping Plover, Atlantic Coast Population (*Threatened*)

Collision Risk Determination: Low

Displacement Risk Determination: Minimal

4.4.2.1 *Overview*

Distribution and Habitat Preferences: The Piping Plover is a small shorebird with three distinct populations that breed: (1) along the Atlantic coast of North America, (2) in the Great Lakes, and (3) in the Midwestern plains (Elliott-Smith and Haig 2020). The Atlantic Coast population of Piping Plover (*Charadrius m. melodus*), which is the only population likely to occur in New Jersey and New York, winters along the southern Atlantic coast and the Gulf coast of Florida and breeds as individual pairs on sandy beaches from Newfoundland to North Carolina (Elliott-Smith and Haig 2020; USFWS 2009). Breeding generally occurs in May through early August, and post-breeding migratory movements can begin as early as June, with adult birds departing by late August (Elliott-Smith and Haig 2020; Loring et al. 2017). Piping Plovers were traditionally thought to migrate along the coast, but the infrequency of observations of migratory flocks along the

Atlantic coast suggests that, like other shorebirds, they make nonstop long-distance migratory flights (Normandeau Associates Inc. 2011, Loring et al. 2020). As such, Piping Plovers could occur in the New York Bight during migration.

Behavior and Ecology: Piping Plovers feed on terrestrial and aquatic invertebrates, particularly in the intertidal zone and along wrack lines, and spend most of their time on the ground rather than aloft (Elliott-Smith and Haig 2020). During the breeding period, nocturnal and daytime activities generally include foraging, incubating nests, and short local flights when birds are disturbed (Staine and Burger 1994). Activities during the breeding season are highly unlikely to overlap with the Lease Area but may be affected by onshore activities (see Section 3 for more information).

Reproduction: Piping Plovers nest on beaches, sand flats, and wetlands, with shallow nest cups often dug into the substrate. Females will raise only one brood but may lay several clutches if nests are destroyed (Elliott-Smith and Haig 2020). Nest sites will not be exposed to offshore activities.

Conservation Status: USFWS listed the Piping Plover species as *Endangered* in 1986, with habitat loss, predation, and human disturbance among the most critical listing factors (USFWS 1996). Recovery of the species is likely limited by threats occurring during migration or on the wintering grounds (Gratto-Trevor et al. 2013). The Atlantic Coast population is currently listed as *Threatened*, which is the only population likely to occur in the New York Bight during migration. The species is also listed as *Endangered* in New York and New Jersey.

4.4.2.2 Exposure Assessment

Species exposure determination: **Low**

Assessment Method: **Qualitative**

Information Sources: Tracking, literature

Exposure Uncertainty: **High**

Based on BRI's qualitative exposure assessment, the species exposure assessment for Piping Plovers was **low**. Exposure was assessed using only species accounts and the results of an individual tracking study, as no detections of Piping Plovers exist in the Northwest Atlantic Seabird Catalog in the New York Bight region or occurred during the NY Bight surveys.

Overall, there is no habitat for the species in the Lease Area, and Piping Plover exposure to Vineyard Mid-Atlantic will be limited to migration (Note: this exposure assessment covers only the offshore components of Vineyard Mid-Atlantic; Piping Plover exposure to onshore facilities is discussed in Section 3.3.2.1.2.). One NanoTag tracking study suggests that three tagged Piping

Plovers may have passed through the Lease Area based on estimated tracklines that cross the New York Bight, likely migratory flights (Loring et al. 2019; Figure 4-61). It is worth noting, though, that the NanoTag study receivers did not fully cover the offshore environment and there remains uncertainty on Piping Plover movements offshore. The exposure estimates are considered a minimum estimate because of lost tags and incomplete coverage of the offshore environment by land-based receivers. Uncertainty is **high** for the exposure assessment due to the availability of only tracking studies.

4.4.2.3 Behavioral Vulnerability Assessment

Collision Vulnerability Determination: **Low**

Assessment Method: **Qualitative**

Collision Uncertainty: **Medium**

Based on BRI's vulnerability assessment, the collision vulnerability determination for Piping Plovers was **low**. Collision vulnerability was assessed using tracking studies and literature on Piping Plovers and other shorebirds, and it should be noted that information on flight heights is limited. Only one tracking study has produced model-estimated flight heights for Piping Plovers, with a mean flight height of 317 m over WEAs in the Atlantic (Loring et al. 2019), which falls within the RSZ of Vineyard Mid-Atlantic. Shorebird flight heights are generally quite variable, as Loring et al. (2021) demonstrated that flight altitudes across a suite of shorebird species ranged from 28–2,940 m, with a mean of 918 m, which is far above the RSZ. Offshore radar studies have also recorded shorebirds flying at 1,000–2,000 m (3,000–6,500 ft) (Richardson 1976; Williams and Williams 1990 in Loring et al. 2019), while nearshore radar studies have recorded lower flight heights of 100 m (330 ft) (; Dirksen et al. 2000 in Loring et al. 2019). In addition, tracking data for Eurasian Curlews demonstrated that this shorebird species generally flew across the Baltic Sea at altitudes below 300 m (984 ft) and altitudes were significantly lower at sea than over land (Schwemmer et al. 2022). Flight heights of shorebirds can vary with weather, and during periods of poor visibility, Piping Plovers may fly lower (Loring et al. 2019, Loring et al. 2021, Dirksen et al. 2000 in Loring et al. 2019). Uncertainty is **medium** in the collision determination due to the lack of information about avoidance rates.

Displacement Vulnerability Determination: **Minimal**

Assessment Method: **Qualitative**

Displacement Uncertainty: **Medium**

Based on BRI's vulnerability assessment, the final displacement vulnerability determination for Piping Plovers was **minimal**. Displacement vulnerability was assessed using species accounts. Piping Plovers would not be displaced during breeding or migratory staging because the Lease

Area provides no habitat for the species during these life history stages. They could potentially be exposed to the Lease Area ephemerally during migration, but any avoidance behavior is not likely to displace them from key migratory habitat. Uncertainty about this determination is **medium** due to the lack of quality information about avoidance behavior for Piping Plovers.

Population vulnerability determination: **Medium**

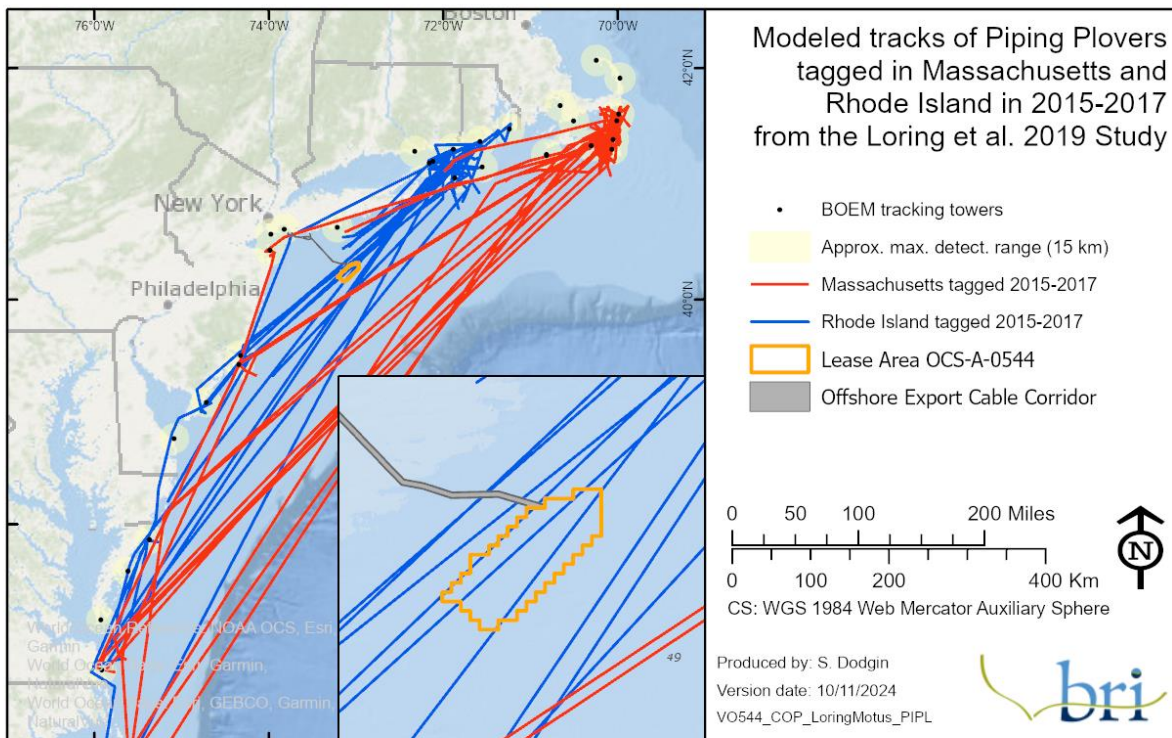
Assessment Method: **Semi-qualitative**

Based on BRI's vulnerability assessment, final population vulnerability determination for Piping Plovers was **medium**. This is supported by species accounts, which reflect that while the Atlantic Coast population has nearly tripled since the 1986 listing, growth has varied temporally and geographically across USFWS recovery units.

4.4.2.4 Risk Determination

Piping Plovers received a final exposure determination of low, a relative collision vulnerability determination of low, a relative displacement vulnerability determination of minimal, and a population vulnerability determination of medium. Based on BRI's risk assessment matrix (Table 2-1), final collision risk was assessed as **low** and displacement risk was assessed as **minimal**.

4.4.2.5 Tables and Figures



NOTE: All data are not actual flight paths but interpolated (model-generated) flight paths. Flight paths were modeled by detections of movements between land-based towers. Towers had a typical detection range <15 km (9.3 mi), so birds were only detected when flying within approximately 15 km (9.3 mi) of one of the towers. See Loring et al. (2019a and 2019b) for tower locations and detection probability. Data provided by USFWS and used with permission.

[Figure 4-61: Modeled flight paths of migratory Piping Plovers equipped with nanotags \(n=70\), based on data from Loring et al. \(2019\).](#)

4.4.3 Red Knot, rufa subspecies (*Threatened*)

Collision Risk Determination: **Minimal to Low**

Displacement Risk Determination: **Minimal**

4.4.3.1 *Overview*

Distribution and Habitat Preferences: The *rufa* subspecies of Red Knot is a medium-sized shorebird subspecies consisting of three seemingly distinct populations in the western Hemisphere, with individuals wintering in the southeastern US and Caribbean, northern Brazil, and Tierra del Fuego (Baker et al. 2020). All three populations breed in the High Arctic and share several key migration stopover areas along the Atlantic coast of the US, particularly in Delaware Bay and coastal islands of Virginia (Burger et al. 2011). Some individuals thus undertake flights of up to 8,000 km (4,970 mi), one of the longest nonstop shorebird migrations in the world (Baker et al. 2020). Migration routes appear to be highly diverse, with some individuals flying over the open ocean from the northeastern US directly to stopover and wintering sites in the Caribbean and South America, while others make the ocean “jump” from farther south or follow the US Atlantic coast for the duration of migration (Baker et al. 2020; BOEM 2014). Suitable habitat at stopover sites and wintering grounds generally consists of marine coastal and estuarine areas with large expanses of exposed sediment. Of the birds that winter on the southeast US coast and/or the Caribbean (considered short-distance migrants), a small proportion may migrate through the New York Bight region. Red Knots will only be present in the area during migration.

Behavior and Ecology: When not actively migrating, Red Knots feed exclusively in terrestrial locations. During the breeding season, Red Knots mainly eat insects, while during the non-breeding season, the species prefers mussels, clams, and other invertebrates in the intertidal zone (USFWS 2023). Consumption of horseshoe crab eggs at key stopover sites such as Delaware Bay allows Red Knots to rapidly gain weight, a critical energetic factor in its long-distance migration.

Reproduction: After arriving at breeding grounds in late May or early June, Red Knots establish nests in upland tundra habitat consisting of sparse vegetation, and typically lay four eggs (Baker et al. 2020, USFWS 2023). Chicks are precocial and begin foraging for themselves about 24 hours after hatching. Their growth is strongly linked with availability of insect prey but is generally much greater than that of other shorebirds.

Conservation Status: The *rufa* subspecies of the Red Knot was listed as *Threatened* under the ESA in 2015, primarily because the Atlantic flyway population decreased by approximately 70% from 1981 to 2012, to fewer than 30,000 individuals (Burger et al. 2011; USFWS 2015; Baker et al. 2020). Increasingly limited food resources in staging areas, as well as breeding conditions in the Arctic and habitat degradation on the wintering grounds, are thought to be contributing to the population's decline (Baker et al. 2020). Climate change impacts on habitats, food availability, and migration are also expected to negatively influence Red Knot populations. Population status is thought to be strongly influenced by adult survival and recruitment rates, conditions on the breeding grounds, and food availability on stopover sites (97–98 % of individuals are estimated to use the same small number of stopover locations in some areas; Baker et al. 2020). The subspecies is also listed as *Threatened* in New York and *Endangered* in New Jersey.

4.4.3.2 Exposure Assessment

Species qualitative exposure determination: **Minimal to Low**

Assessment Method: **Qualitative**

Information Sources: Tracking, literature

Exposure Uncertainty: **High**

Based on BRI's exposure assessment, the species exposure determination for Red Knots was **minimal to low**. Exposure was assessed using only species accounts, literature, and the results of tracking studies, as no detections of Red Knots exist in Northwest Atlantic Seabird Catalog in the vicinity of the New York Bight region or occurred during the NY Bight surveys.

Overall, there is no habitat for the species in the Lease Area, and Red Knot exposure to the Lease Area will be limited to migration. (Note: this exposure assessment covers only the offshore components of Vineyard Mid-Atlantic; Red Knot exposure to onshore facilities is discussed in Section 3.3.2.1.3). Migration flights are generally undertaken at night, but in favorable weather conditions, perhaps lessening any risk of collision (Loring et al. 2018). During their northbound migration, tagged birds have generally been tracked departing the US Atlantic coast and heading overland on a northwest trajectory to their breeding grounds (Pelton et al. 2022, Loring et al. 2021, Smith et al. 2023). As such, any exposure to Vineyard Mid-Atlantic will likely occur during southbound migrations. In a NanoTag tracking study, Loring et al. (2018) fitted 388 Red Knots with VHF transmitters at major stopover sites during their southbound migration, including New Jersey and Massachusetts. Over half of Red Knots tagged in Massachusetts and New Jersey passed through federal waters of the Atlantic OCS, and 11% were exposed to one or more BOEM wind energy areas, but only one bird is estimated to have crossed the Lease Area (Figure 4-62; Loring et al. 2018). It is worth noting, though, that the NanoTag study receivers did not fully

cover the offshore environment and there remains uncertainty on Red Knot movements. Uncertainty is **high** for the exposure assessment due to the availability of only tracking studies.

4.4.3.3 Behavioral Vulnerability Assessment

Collision Vulnerability Determination: **Low**

Assessment Method: **Qualitative**

Collision Uncertainty: **Medium**

Based on BRI's vulnerability assessment, the final collision vulnerability determination for Red Knots was **low**. Collision vulnerability was assessed using species accounts, literature, and tracking studies. Red Knots are traditionally thought to migrate at flight heights well above the RSZ (i.e., greater than 355 m [1,165 ft]). Long-distance migration flights are thought to normally be at 1,000–3,000 m (3,000–10,000 ft), except during takeoff and landing at terrestrial locations (Burger et al. 2011). Other aspects of Red Knot behavior minimize their vulnerability to collision, as birds likely adjust their altitudes based on local weather conditions (Biodiversity Research Institute 2021), including flying at lower altitudes in headwinds (Baker et al. 2020) or during periods of poor weather and high winds (Burger et al. 2011). Red Knots also have good visual acuity and maneuverability in the air (Burger et al. 2011), and migration flights are generally initiated at night in good weather conditions, lessening risk of collision (Loring et al. 2018).

However, studies show that Red Knot flight heights during migration can be variable. While tracking studies estimate that flight heights of some tagged Red Knots migrating over the proposed Atlantic OCS WEAs were higher than Vineyard Mid-Atlantic's RSZ, other birds were estimated to fly within a hypothetical RSZ of 20–200 m (65–656 ft), which is within the proposed RSZ of Vineyard Mid-Atlantic (Biodiversity Research Institute 2021, Loring et al. 2018). In addition, it is thought that the ability of Red Knots to avoid spinning WTGs may be reduced during periods of poor visibility, high winds, or inclement weather (Burger et al. 2011). Collision uncertainty is medium thanks to the availability of quality flight height and flight activity information, but little is known about shorebird avoidance of offshore wind. Uncertainty is **medium** in the collision determination due to the availability of information on time spent in the RSZ and flight activity.

Displacement Vulnerability Determination: **Minimal**

Displacement Uncertainty: **Medium**

Based on BRI's vulnerability assessment, the final displacement vulnerability determination for Red Knots was **minimal**. There is little evidence and research on shorebird avoidance at offshore wind developments, but Red Knots are not considered to be vulnerable to displacement because their feeding habitat is strictly coastal (Burger et al. 2011), and thus avoidance behavior is not

likely to lead to habitat loss offshore. Red Knots would not be displaced during breeding or migratory staging because the Lease Area provides no habitat for the species during these life history stages. Uncertainty about this determination is **medium** due to the lack of quality information about avoidance behavior for Red Knots.

Population vulnerability determination: **Medium**

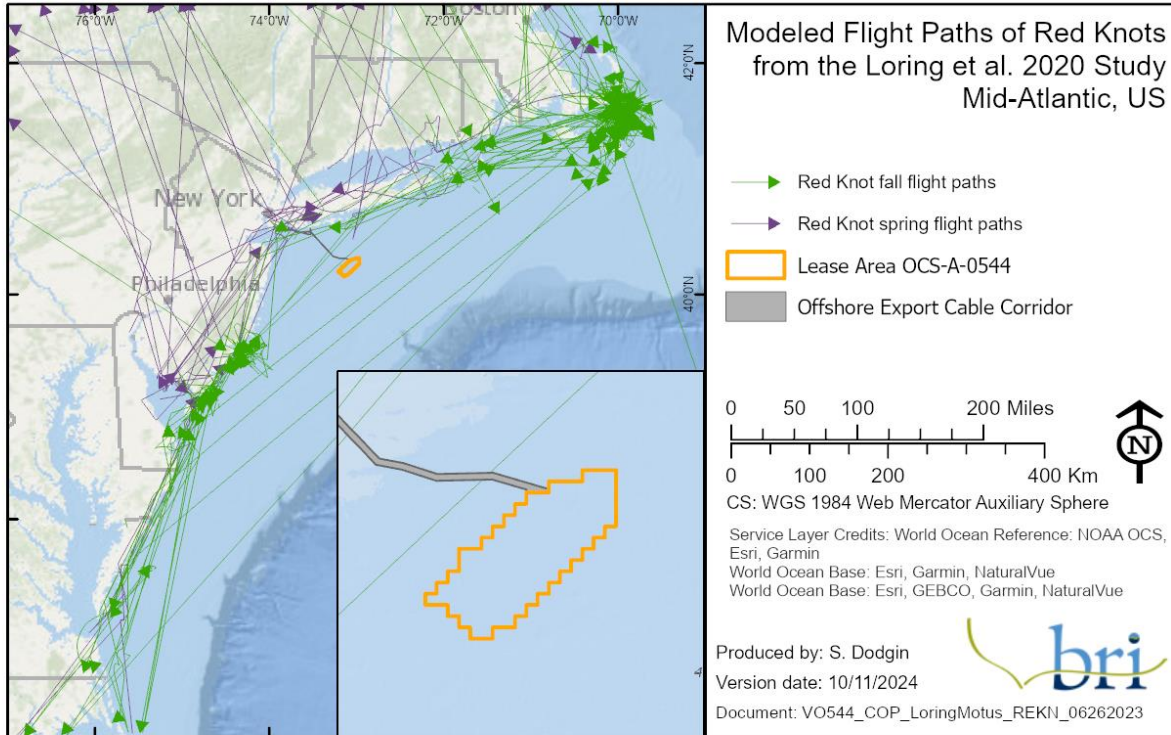
Assessment Method: **Semi-qualitative**

Based on BRI's vulnerability assessment, final population vulnerability determination for Red Knots was **medium**. This is supported by species accounts and literature. Over the last twenty years, the *rufa* subspecies of Red Knot has experienced a population decline of approximately 100,000 individuals to a current population estimate of 64,000 birds (Niles et al. 2018, USFWS 2020a). A particularly sharp decline in the southern population in the 2000s is likely largely responsible for the overall decline of the subspecies (USFWS 2020c, USFWS 2014). However, the USFWS currently considers *rufa* Red Knot abundance to be stable (USFWS 2023).

4.4.3.4 Risk Determination

Red Knots received a final exposure determination of minimal to low, a relative collision vulnerability determination of low, a relative displacement vulnerability determination of minimal, and a population vulnerability determination of medium. Based on BRI's risk assessment matrix (Table 2-1), final collision risk was assessed as **minimal to low** and displacement risk was assessed as **minimal**.

4.4.3.5 Tables and Figures



NOTE: All data are not actual flight paths but interpolated (model-generated) flight paths. Flight paths were modeled by detections of movements between land-based towers. Towers had a typical detection range <15 km (9.3 mi), so birds were only detected when flying within approximately 15 km (9.3 mi) of one of the towers. See Loring et al. (2018) for tower locations and detection probability. Data provided by USFWS and used with permission.

Figure 4-62: Modeled flight paths of migratory Red Knots equipped with nanotags based on data from Loring et al. (2020). Spring migration ($n=31$) and fall migration ($n=146$) in 2014-2017.

4.4.4 Black-capped Petrel (*Endangered*)

Collision Risk Determination: **Minimal**

Displacement Risk Determination: **Minimal**

4.4.4.1 Overview

Distribution and Habitat Preferences: The Black-capped Petrel (*Pterodroma hasitata*) is a pelagic seabird that breeds in small colonies on remote forested mountainsides of Caribbean islands, although breeding is now thought to be mostly restricted to the islands of Hispaniola (Haiti and the Dominican Republic) and possibly Cuba (Simons et al. 2013). Outside the breeding season, they regularly spend time in US waters along the shelf edge of the South Atlantic Bight, commonly as far north as Cape Hatteras and occasionally beyond (Jodice et al. 2015) but are

rarely seen in shelf waters off New York or New Jersey. MDAT models suggest a distribution limited to a narrow band of pelagic waters along the US Atlantic OCS, with seasonal hotspots off the South Atlantic Bight (spring, summer, and winter) and the Outer Banks of North Carolina (summer, fall, and winter; Winship et al. 2023).

Behavior and Ecology: During the breeding season (January–June), Black-capped Petrels travel long distances to forage for fish, squid, and crustaceans, over deeper waters (200–2,000 m [650–6,500 ft]) of the Gulf of Mexico, the Caribbean Basin, and out over the North America Basin of the North Atlantic (Simons et al. 2013; Satgé et al. 2023).

Reproduction: Black-capped Petrels breed in loose colonies in both broadleaf and pine forests on steep mountainous slopes primarily of dolomitic limestone. Members of a pair coordinate to dig a burrow, where the female lays a single egg, and share in incubation, brooding, and provisioning (Satgé et al. 2023).

Conservation Status: The small, declining global population of Black-capped Petrel, likely around 1,000 breeding pairs (Satgé et al. 2023), has been listed as *Endangered* on the International Union for Conservation of Nature’s Red List since 1994 (BirdLife International 2018). It was proposed for federal listing under the ESA as *Threatened* (USFWS 2018), due to its heavy use of the Gulf Stream within US waters (USFWS 2018), and then was listed as *Endangered* in January 2024. The species was pushed to the edge of extinction in the late 1800s due to hunting and harvest for food (Simons et al. 2013). Predation of adults and eggs by invasive mammals as well as breeding habitat loss and degradation remain major threats to their existence, while the effects of climate change on the biology of the species and its prey are largely unknown (Goetz et al. 2012). Nevertheless, an increase in the frequency and intensity of hurricanes due to climate change is expected to drastically increase fatality in breeding Black-capped Petrels (Hass et al. 2012). Given the small size of the breeding population, the species’ resiliency (i.e., the ability to withstand normal environmental variation and stochastic disturbances over time) is considered to be low (USFWS 2018).

4.4.4.2 Exposure Assessment

Species Exposure Determination: **Minimal**

Assessment Method: **Qualitative**

Information Sources: Baseline, site-specific, tracking, literature

Exposure Uncertainty: **Minimal**

Based on BRI’s exposure assessment, the species exposure determination for Black-capped Petrels was **minimal**. Exposure was assessed using species accounts, the results of individual tracking studies, and detections in the Northwest Atlantic Seabird Catalog within the NY Bight

survey area, which does not contain any observations within the Lease Area (Figure 4-63). A satellite telemetry study of tagged Black-capped Petrels (n=3) showed offshore tracks that went as far north as the Delmarva Peninsula (Figure 4-64; Jodice et al. 2015), providing supporting evidence to species accounts that the species typically does not range as far as the New York Bight. Overall, the highly pelagic nature of this species and its near absence from continental shelf waters of the southeastern US (Simons et al. 2013, Jodice et al. 2015), suggest that exposure will be rare. Uncertainty is **low** for the exposure assessment due to the availability of regional and site-specific digital aerial surveys, and tracking studies.

4.4.4.3 Behavioral Vulnerability Assessment

Collision Vulnerability Determination: **Low**

Assessment Method: **Qualitative**

Collision Uncertainty: **Medium**

Based on BRI’s vulnerability assessment, the collision vulnerability determination was **low**. Like most petrels, this species is attracted to lights, and is known to collide with lighted telecommunication towers on breeding islands (Goetz et al. 2012). This behavior could make Black-capped Petrels vulnerable to collision with lighted offshore vessels and structures (Jodice et al. 2021). Despite some concern about the potential effects of wind facilities on Black-capped Petrels at sea, the highly pelagic nature of this species and its near absence from continental shelf waters of the southeastern US, led Simons et al. (2013) to conclude it unlikely that wind facilities will be detrimental to this species. As noted above in Section 4.3.7 for shearwaters, petrels, and storm-petrels, a recent report for the Scottish Government (Deakin et al. 2022) thoroughly reviewed the available literature on lighting attraction among members of this group; it is clear that powerful light can disorient these birds (especially fledglings in foggy conditions) and cause them to circle light sources, but the evidence on the existence and strength of light attraction is inconclusive. Uncertainty for this determination is **medium** due to a lack of information on how this species will avoid offshore WTGs.

Displacement Vulnerability Determination: **Low to Medium**

Assessment Method: **Qualitative**

Displacement Uncertainty: **Medium**

Based on BRI’s vulnerability assessment, the displacement vulnerability determination for Black-capped Petrels is **low to medium**. While there is substantial uncertainty on how these birds will respond to large WTGs, they may exhibit some level of attraction, which would limit their vulnerability to displacement—see further discussion of the group in Section 4.3.7. Uncertainty

for this determination is **medium** due to a lack of information on how this species will avoid offshore wind turbines.

Population vulnerability determination: **Medium**

Assessment Method: **Semi-Quantitative**

Based on BRI's vulnerability assessment, the population vulnerability determination for Black-capped Petrels was **medium** due to being long-lived (i.e., high adult survival) and have declining populations and thus high priority conservation status.

4.4.4.4 Risk Determination

Black-capped Petrels received a final exposure determination of minimal, a relative collision vulnerability determination of low, a relative displacement vulnerability determination of low to medium, and a population vulnerability determination of medium. Based on BRI's risk assessment matrix (Table 2-1), final collision risk and displacement risk were both assessed as **minimal**.

4.4.4.5 Tables and Figures

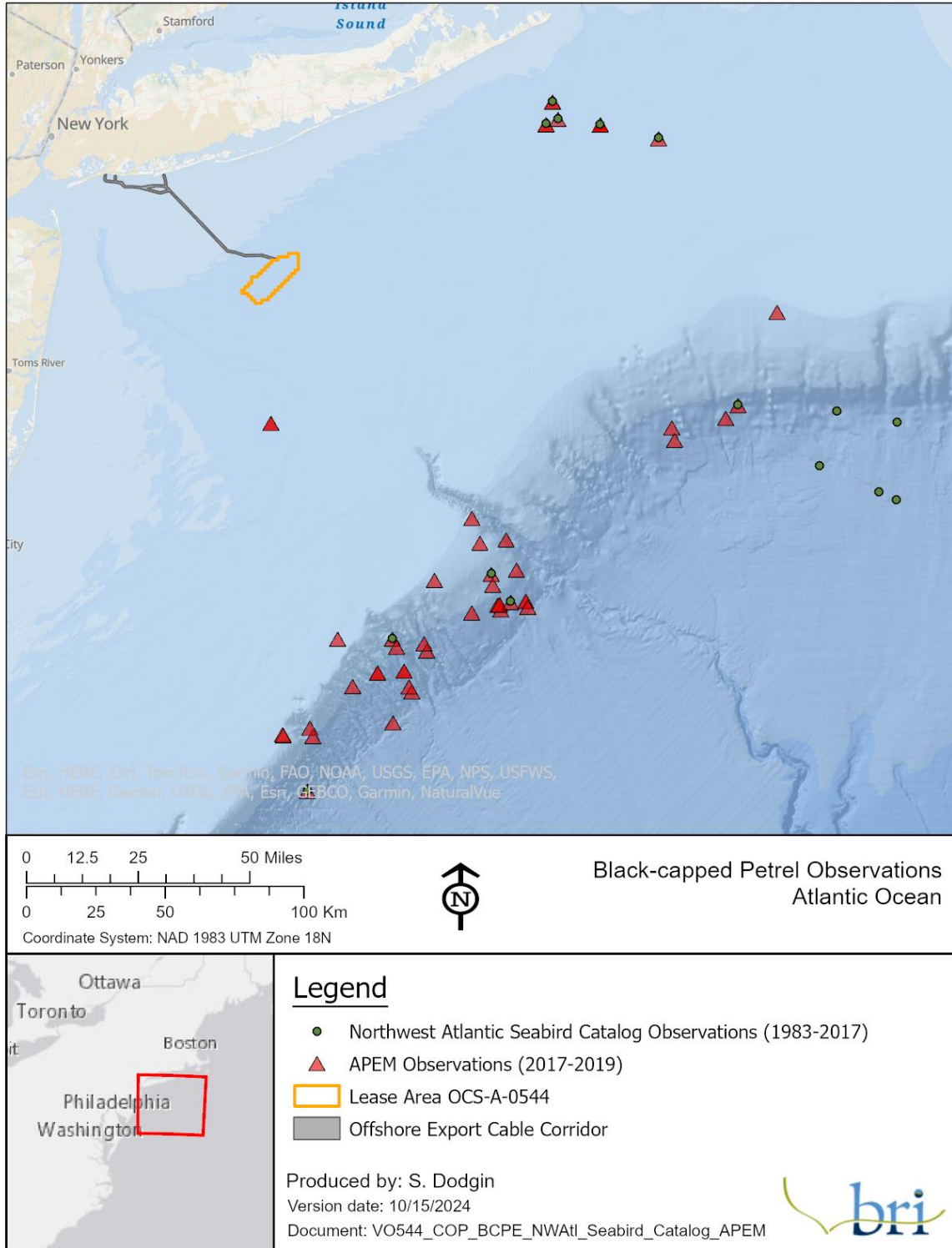


Figure 4-63: Black-capped Petrel observations from the Northwest Atlantic Seabird Catalog and APEM. Data provided by NOAA and used with permission.

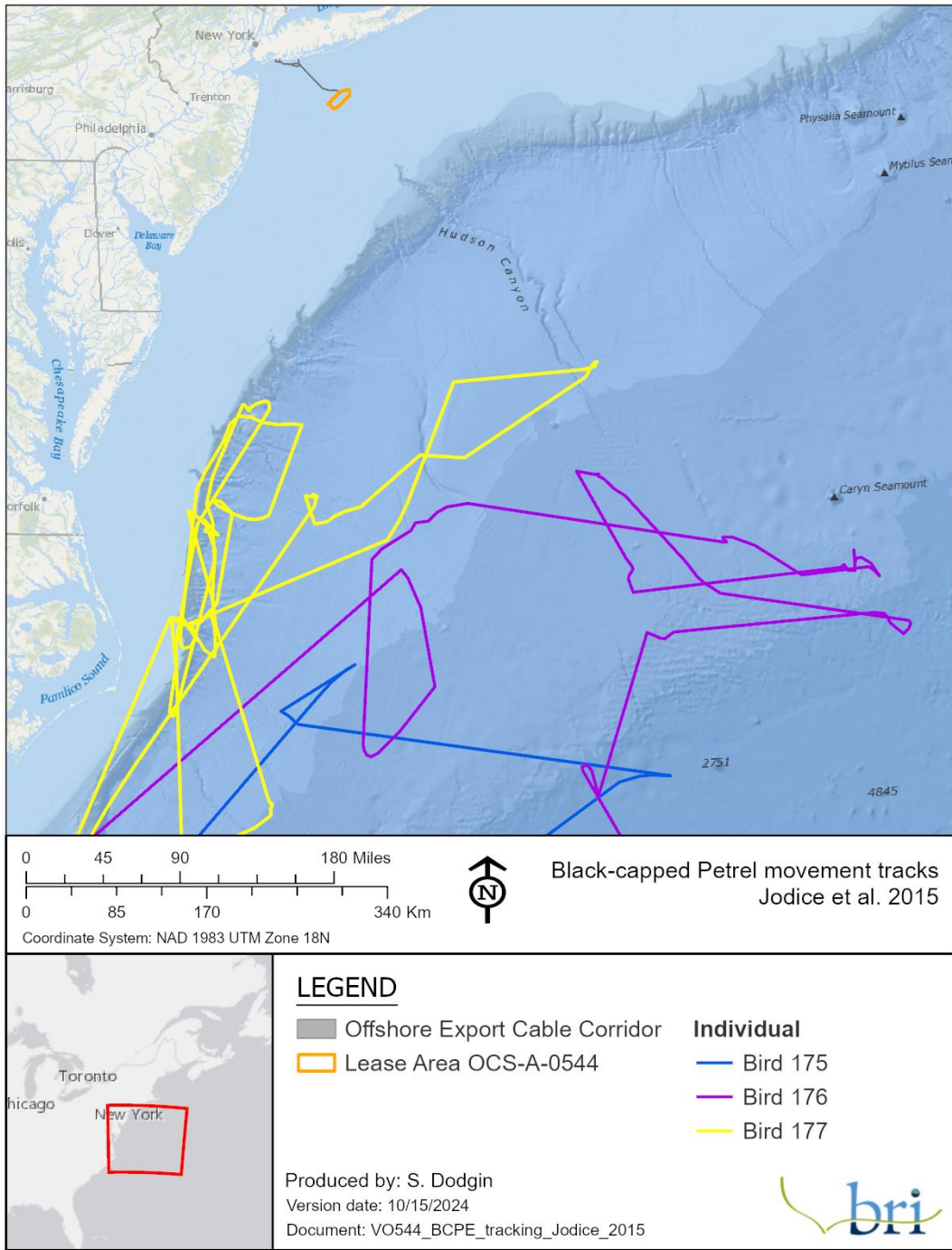


Figure 4-64: Export from Northeast Ocean Data Portal showing track lines of three Black-capped Petrels (purple, yellow, and blue lines each show a different individual) tagged with satellite transmitters.⁷ Offshore wind BOEM lease areas are also shown in colored polygons.

4.4.5 Bald Eagle (Protected by the Bald and Golden Eagle Protection Act)

Collision Risk Determination: **N/A**

Displacement Risk Determination: **N/A**

Note: As noted in the raptors section, Golden Eagles are not discussed in the offshore assessment, as breeding populations are extirpated in the eastern US and individuals are rarely observed, and the species generally uses inland migration routes rather than coastal migration flyways (Katzner et al. 2012, Kochert et al. 2002). Furthermore, BOEM's NOI checklist indicates that Golden Eagles do not use offshore waters (BOEM 2023).

4.4.5.1 *Overview*

Distribution and Habitat Preferences: The Bald Eagle is broadly distributed across North America and is present year-round in New Jersey and New York. The species generally nests and perches in association with water (lakes, rivers, bays) in both freshwater and marine-based habitats, often remaining within roughly 500 m (1,640 ft) of the shoreline (Buehler 2022). Bald Eagles will travel to coastal islands to nest, forage (i.e., at seabird colonies; Todd et al. 1982), and possibly to stopover during long-distance movements (Mojica et al. 2008). However, Bald Eagles are not thought to venture far offshore, and BOEM's NOI checklist indicates that Bald Eagles do not use offshore waters (BOEM 2023).

Behavior and Ecology: Bald Eagles are seasonally opportunistic foragers. In some regions, the diets of Bald Eagles nesting in coastal settings are dominated by birds (i.e., waterfowl, cormorants, and gulls), whereas the diets of inland nesters in New England consist largely of fish (Murie 1940; Todd et al. 1982). Bald Eagles also scavenge dead birds, fish, and mammals, particularly during the winter when live fish prey is often scarce and are known kleptoparasites (Buehler 2022).

Reproduction: Nesting in northern latitudes typically begins in early spring, and Bald Eagles will typically select the largest tree with accessible limbs capable of supporting a nest in a suitable area (Buehler 2022). Eagles have one brood per nesting season, and generally lay 2 eggs.

Conservation Status: The Bald Eagle was removed from the federal ESA list in 2007 but is currently listed as *Endangered* in New Jersey and *Threatened* in New York. Bald Eagles remain federally protected under the BGEPA.

⁷ <https://www.northeastoceandata.org/new-avian-movement-data-show-black-capped-petrel-offshore-foraging-activity/>

4.4.5.2 Exposure Assessment

Species qualitative exposure determination: **Minimal**

Assessment Method: **Qualitative**

Information Sources: Baseline, site-specific, literature

Exposure Uncertainty: **Medium**

Based on BRI's qualitative exposure assessment, the species exposure determination for Bald Eagles was **minimal**. This is based on species accounts, as the offshore area is not located along any likely or known Bald Eagle migration routes, individuals tend not to fly over large water bodies, and features that might potentially attract them offshore (i.e., islands) are absent nearby. In addition, the general morphology of Bald Eagles dissuades regular use of offshore habitats. This species generally relies on thermals, which are poorly developed over the ocean, during migration movements. Uncertainty is **medium** for the exposure assessment due to the availability of baseline and site-specific digital aerial survey data. Because there is no evidence that Bald Eagles will be exposed to the Lease Area, the species will not be addressed further.

4.4.5.3 Behavioral Vulnerability Assessment

Collision Vulnerability Determination: No vulnerability assessment was conducted for the Bald Eagle due to its infrequent occurrence in offshore waters.

Displacement Vulnerability Determination: No vulnerability assessment was conducted for the Bald Eagle due to its infrequent occurrence in offshore waters.

4.4.5.4 Risk Determination

No risk determination was conducted for the Bald Eagle due to its infrequent occurrence in offshore waters.

4.4.5.5 Tables and Figures

No observation, tracking, or modeling data are available for the Bald Eagle.

4.5 Conclusions

This offshore assessment considered the potential impacts on birds offshore during all phases of Vineyard Mid-Atlantic. The presence of structures and the potential risk of collision and/or displacement is the most significant potential impact to birds offshore, and so constitutes the central focus of the offshore risk assessment. Table 4-25 provides a concise summary of the

results of the assessment—exposure, vulnerability, and risk—for all avian groups and protected species (ESA-listed species and Bald Eagles protected under BGEPA) considered individually.

BRI's final risk determinations (which consider both exposure and vulnerability) for collision and displacement were minimal, minimal-low, or low for all avian groups and for the protected species considered individually. In general, the minimal and low risk determinations were mostly driven by a lack of exposure to the Lease Area.

In BRI's exposure assessment, final exposure determinations were minimal, minimal-low, or low for all avian groups and for all ESA-listed species and Bald Eagles. For certain groups among the marine birds, the exposure analysis highlights some seasonal variation in exposure, which is expected based on group-specific life histories. For example, medium terns had low exposure in spring when they are likely to be migrating, which dropped to minimal in the other seasons when they are either nesting in colonies or at their wintering grounds. Exposure of auks was minimal in summer and fall, when these colony-breeding birds are nesting farther north, and low in winter and spring when auks use the New York Bight as a winter foraging habitat.

Uncertainty in the exposure assessment is summarized in Table 4-26, using the scoring process described in Section 5.1. Marine bird groups and marine bird listed species had lower uncertainty than non-marine migratory birds, largely due to the availability of MDAT models for many more marine birds than non-marine birds. Exposure uncertainty was high for shorebirds and songbirds, and high for the two ESA-listed shorebirds, Red Knots and Piping Plovers. This high uncertainty is largely attributable to the small size of shorebirds and songbirds and their potential for nighttime migratory flights, both of which make digital aerial surveys poorly suited to characterize their presence in the offshore environment. The exposure assessment for Bald Eagles had medium uncertainty due to the lack of tracking data and MDAT models.

Behavioral vulnerability to collision ranged from minimal to medium across groups and protected species. The gulls, jaegers, and skuas group and the terns group had low to medium collision vulnerability owing to their proclivity to fly in the RSZ and their lack of avoidance behavior. The cormorants and pelicans group had medium collision vulnerability, owing to cormorants' frequent flights in the RSZ and their known attraction to WTGs. Behavioral vulnerability to displacement ranged from minimal to high, with loons representing the high end of the range and having the strongest known avoidance response to WTGs as shown in many studies of European offshore wind.

Uncertainty in BRI's vulnerability assessment is summarized in Table 4-27, using the scoring process described in Section 5.2. As with exposure uncertainty, vulnerability uncertainty was generally higher for non-marine migratory bird groups than for marine birds, with all non-marine groups having medium to high uncertainty for collision vulnerability and displacement vulnerability. Avoidance behavior in particular is not well studied for non-marine migratory birds

and represents a significant source of uncertainty for assessing the potential impacts of offshore wind on migration patterns and seasonal use of the outer continental shelf by these groups.

Table 4-28 reports seasonal and annual naive densities for each bird species detected in the larger NY Bight survey area, both within the larger survey area and the Lease Area. Where density is zero for a given species, this indicates that no observations were recorded in the Lease Area but some observations were recorded in the larger survey area.

Of the five protected bird species (either federally listed, candidates for federal listing, or afforded special protection under BGEPA) observed or expected to occur in the Offshore Development Area, exposure for all was minimal or minimal to low. It should be noted that the exposure determinations for Piping Plovers and Red Knots involve high uncertainty, and medium uncertainty for Bald Eagles. Risk determinations were of minimal to low risk of collision and/or displacement. As for other listed species (or species under consideration for listing), Eastern Black Rails and Saltmarsh Sparrows are unlikely to be exposed to the Lease Area, as it is generally thought that neither species flies far offshore between winter habitats and breeding sites (BOEM 2022). These two non-marine species are discussed in relation to Vineyard Mid-Atlantic's onshore facilities in Section 3.

Table 4-25: Overall summary of the assessment of potential effects on birds.

Group	Exposure	Relative Vulnerability			Collision Risk	Displacement Risk
		Collision	Displacement	Population		
Non-marine Migratory Birds						
Grebes and Waterfowl	min	•	•	•	min	min
Shorebirds	min–low	low	min–low	•	min–low	min
Wading Birds	min–low	low	min	•	min–low	min
Raptors ¹	min–low	low med	min–low	•	min–low	min–low
Songbirds (Passerines)	min–low	low–med	min–low	•	min–low	min–low
Marine Birds						
Sea Ducks	min	low	low–high	low–med	min	min
Phalaropes	min	low	med	low	min	min
Auks	low	min	med–high	low–med	min	low
Gulls, Jaegers, and Skuas	min–low	low–med	low–med	min–med	min–low	min–low
Terns	min	low–med	low–high	low–med	min	min
Loons	low	min–low	high	low–med	min–low	low
Shearwaters, Petrels, and Storm-petrels	min	low	med	low–med	min	min
Gannets (Northern Gannet)	low	low	med	low	low	low
Cormorants and Pelicans	min	med	low–med	min–low	min	min
Protected Species and Species of Concern						
Roseate Tern	min–low	low	med–high	high	low	low ²
Piping Plover	low	low–med	min	med	low	min
Red Knot	min–low	low	min	med	min–low	min
Black-capped Petrel	min	low	low–med	•	min	min
Bald Eagle	min	•	•	•	•	•
¹ Osprey were the only raptor species observed in the NY Bight surveys. ² Roseate Tern risk categories were adjusted (increased) due to high population vulnerability – shown in green text.						

Table 4-26: Information sources available, uncertainty scores, and uncertainty levels in exposure assessments.

Taxa	Literature	Information Sources				Score	Uncertainty
		MDAT	Baseline	Site specific	Tracking		
NON-MARINE BIRDS							
Grebes and waterfowl	•	1	1	1		3	low
Shorebirds	•				1	1	high
Wading birds	•		1	1	1	3	low
Raptors	•		1	1	1	3	low
Songbirds	•					0	high
MARINE BIRDS							
Sea ducks	•	1	1	1	1	4	minimal
Phalaropes	•	1	1	1		3	low
Auks	•	1	1	1		3	low
Gulls, Jaegers, Skuas	•	1	1	1		3	low
Terns	•	1	1	1	1	4	minimal
Loons	•	1	1	1	1	4	minimal
Shearwaters, Petrels, Storm-Petrels	•	1	1	1		3	low
Gannets	•	1	1	1	1	4	minimal
Cormorants and Pelicans	•	1	1	1		3	low
LISTED SPECIES							
Black-capped Petrel	•		1	1	1	3	low
Roseate Tern ²	•	0.5	1	1	0.5	3	low
Bald Eagle	•		1	1		2	medium
Piping Plover	•				1	1	high
Red Knot	•				1	1	high

Exposure uncertainty scores: 0-1 = High, 2 = Medium, 3 = Low, 4 = Minimal

¹For this assessment, the Empire Wind digital aerial surveys with their 4 km (2.5 mi) buffer are considered site-specific to Lease Area OCS-A 0544 (more details about level of coverage in Methods).

²Received a ½ score for MDAT because of a data gap and ½ for tracking because of a lack of Motus receiver coverage.

Table 4-27: Uncertainty scores for BRI's vulnerability assessment (for collision vulnerability and displacement vulnerability).

Taxa	CV component			CV uncertainty	DV component		DV uncertainty
	Time spent in RSZ	Avoidance	Flight activity		Avoidance	Habitat flexibility	
NON-MARINE MIGRATORY BIRDS							
Grebes and waterfowl	0	1	0	high	1	1	low
Shorebirds	1	0	1	medium	0	1	medium
Wading Birds	1	0	1	medium	0	1	medium
Raptors	1	1	1	low	1	1	low
Songbirds	0	0	0	high	0	1	medium
MARINE BIRDS							
Sea ducks	1	1	1	low	1	1	low
Phalaropes	1	0	0	high	0	1	medium
Auks	1	1	1	low	1	1	low
Gulls, Skuas, Jaegers	1	1	1	low	1	1	low
Terns	1	0	1	medium	0	1	medium
Loons	1	1	1	low	1	1	low
Petrels, Shearwaters, Storm-Petrels	1	0	1	medium	0	1	medium
Gannets	1	1	1	low	1	1	low
Cormorants and Pelicans	1	1	1	low	1	1	low
PROTECTED SPECIES AND SPECIES OF CONCERN							
Black-capped Petrel	1	0	1	medium	0	1	medium
Roseate Tern	1	0	1	medium	0	1	medium
Bald Eagle, Golden Eagle	0	1	1	medium	1	1	low
Piping Plover	1	0	1	medium	0	1	medium
Red Knot	1	0	1	medium	0	1	medium

CV Uncertainty Scores: 0-1 = High; 2 = Medium; and 3 = Low. DV Uncertainty Scores: 0 = High; 1 = Medium; and 2 = Low.

4.6 Supplemental Information: Seasonal Densities in the Lease Area

Table 4-28: Seasonal species naive densities (uncorrected count per square kilometer of survey transect) within Lease Area OCS-A 0544 and the NY Bight survey area.

Species	Mean naive density (uncorrected count/square km)										
	Lease Area OCS A 0544					NY Bight Study Area					Total count
	annual	winter	spring	summer	fall	annual	winter	spring	summer	fall	
Non marine Migratory Birds											
Grebes and Waterfowl											
American Black Duck	0	0	0	0	0	<0.001	0	0	0	0.001	29
Canada Goose	0	0	0	0	0	<0.001	<0.001	0	0	<0.001	3
Gadwall	0	0	0	0	0	<0.001	0	0	0	<0.001	3
Mallard	0	0	0	0	0	<0.001	<0.001	0	0	<0.001	7
Tundra Swan	0	0	0	0	0	<0.001	<0.001	0	0	0	12
Unidentified Duck	0.013	0.043	0.01	0	0	0.001	0.002	<0.001	0	0.001	48
Bufflehead	0	0	0	0	0	<0.001	<0.001	0	0	0	3
Common Goldeneye	0	0	0	0	0	<0.001	<0.001	0	0	0	1
Lesser Scaup	0	0	0	0	0	<0.001	<0.001	<0.001	0	0	8
Horned Grebe	0	0	0	0	0	<0.001	<0.001	<0.001	0	0	7
Unidentified Grebe	0	0	0	0	0	<0.001	0	<0.001	0	0	3
Shorebirds											
Black-bellied Plover	0	0	0	0	0	<0.001	0	0	<0.001	0	4
Semipalmated Plover	0	0	0	0	0	<0.001	0	0	<0.001	0	3
Unidentified shorebird	0	0	0	0	0	0.004	0.003	0.003	0.004	0.007	378
Wading Birds											
Great Blue Heron	0	0	0	0	0	<0.001	0	<0.001	0	<0.001	4
Raptors											
Osprey	0	0	0	0	0	<0.001	0	<0.001	0	0	1
Unidentified Raptor/Bird of Prey	0	0	0	0	0	0	0	0	0	<0.001	1

Species	Mean naive density (uncorrected count/square km)										
	Lease Area OCS A 0544					NY Bight Study Area					Total count
	annual	winter	spring	summer	fall	annual	winter	spring	summer	fall	
Nightjars and allies											
Common Nighthawk	0	0	0	0	0	<0.001	0	0	<0.001	0	1
Songbirds (Passerines)											
Unidentified Passerine (perching birds, songbirds)	0	0	0	0	0	<0.001	0	0	0	<0.001	4
Marine Birds											
Sea Ducks											
Black Scoter	0	0	0	0	0	0.042	0.104	0.002	0	0.063	1360
Common Eider	0	0	0	0	0	<0.001	<0.001	0	0	<0.001	7
Common Merganser	0	0	0	0	0	<0.001	0	0	0	<0.001	1
Long-tailed Duck	0	0	0	0	0	<0.001	0.002	<0.001	0	<0.001	32
Red-breasted Merganser	0	0	0	0	0	<0.001	<0.001	0.002	0	<0.001	24
Surf Scoter	0.002	0	0	0	0.008	0.011	0.03	0.008	0	0.009	439
Unidentified Scoter	0	0	0	0	0	0.136	0.075	0.475	0	0.009	5848
White-winged Scoter	0	0	0	0	0	0.055	0.188	0.031	0	0.005	2430
Phalaropes											
Red Phalarope	0.018	0.021	0	0	0.051	0.243	<0.001	0.31	0	0.678	12118
Red-necked Phalarope	0	0	0	0	0	0.017	0	0.064	<0.001	0.006	873
Unidentified Phalarope	0.006	0.003	0	0.005	0.016	0.198	0.025	0.365	0.009	0.41	6797
Auks											
Atlantic Puffin	0	0	0	0	0	0.096	0.309	0.081	0	0.002	4045
Black Guillemot	0	0	0	0	0	<0.001	<0.001	0	0	<0.001	10
Common Murre	0	0	0	0	0	<0.001	0	0	0	0.001	11
Dovekie	0	0	0	0	0	0.063	0.25	0.005	0	0.002	2893
Razorbill	0.061	0.24	0	0	0	0.07	0.226	0.053	0	0.004	2541
Unidentified Alcids	0.202	0.432	0.391	0	0	0.2	0.457	0.228	<0.001	0.129	10096

Species	Mean naive density (uncorrected count/square km)										
	Lease Area OCS A 0544					NY Bight Study Area					Total count
	annual	winter	spring	summer	fall	annual	winter	spring	summer	fall	
Unidentified Murre	0.013	0.051	0	0	0	0.003	0.001	0.013	0	0	192
Gulls, Jaegers, and Skuas											
Bonaparte's Gull	0.203	0.562	0.088	0	0.153	0.082	0.104	0.072	0	0.16	4488
Little Gull	0	0	0	0	0	<0.001	<0.001	<0.001	0	<0.001	13
Unidentified Small Gull	0.027	0.01	0.1	0	0.004	0.035	0.021	0.022	0.003	0.097	1847
Black-legged Kittiwake	0.045	0.039	0.003	0	0.136	0.073	0.015	0.001	0	0.279	3603
Laughing Gull	0.002	0.006	0.003	0	0	0.017	0.001	0.007	0.002	0.059	982
Ring-billed Gull	0	0	0	0	0	0.017	0.033	0.002	0.006	0.029	722
Glaucous Gull	0	0	0	0	0	<0.001	<0.001	<0.001	0	0	2
Great Black-backed Gull	0.02	0.019	0	0	0.057	0.118	0.314	0.069	0.02	0.077	5792
Herring Gull	0.044	0.077	0.025	0	0.072	0.433	0.826	0.403	0.009	0.526	19985
Iceland Gull	<0.001	0.003	0	0	0	<0.001	<0.001	<0.001	0	<0.001	13
Lesser Black-backed Gull	0.003	0	0.012	0	0	0.004	0.005	0.004	<0.001	0.004	146
Unidentified Large Gull	<0.001	0	0	0	0.003	0.007	0.011	0.005	0.002	0.012	391
Unidentified Gull	0	0	0	0	0	0.002	0.003	0.001	0.001	0.005	93
Great Skua	0	0	0	0	0	<0.001	<0.001	<0.001	0	0	7
Parasitic Jaeger	0	0	0	0	0	<0.001	0	0.001	<0.001	<0.001	16
Pomarine Jaeger	0	0	0	0	0	<0.001	0	<0.001	0	<0.001	2
South Polar Skua	0	0	0	0	0	<0.001	0	<0.001	0	0	2
Unidentified Skua	0	0	0	0	0	<0.001	<0.001	<0.001	0	0.001	8
Terns											
Black Tern	0	0	0	0	0	<0.001	0	<0.001	<0.001	0	4
Least Tern	0	0	0	0	0	0.002	<0.001	0.002	0.005	0	64
Arctic Tern	0	0	0	0	0	<0.001	0	0	0	0	1
Common Tern	0	0	0	0	0	0.018	<0.001	0.073	0	0	701
Forster's Tern	0	0	0	0	0	<0.001	0	0.001	<0.001	0	26

Species	Mean naive density (uncorrected count/square km)										
	Lease Area OCS A 0544					NY Bight Study Area					Total count
	annual	winter	spring	summer	fall	annual	winter	spring	summer	fall	
Royal Tern	0	0	0	0	0	<0.001	0	0	<0.001	<0.001	6
Unidentified Tern	0.009	0	0.039	0	0	0.062	0.001	0.233	0.017	0	2662
Loons											
Common Loon	0.051	0.109	0.066	0	0.03	0.056	0.068	0.116	0.001	0.044	2708
Red-throated Loon	0.031	0.047	0.049	0	0.029	0.03	0.036	0.023	0	0.064	1261
Unidentified Loon	0.003	0	0.012	0	0	0.001	0.001	0.001	<0.001	0.003	76
Shearwaters, Petrels, and Storm-petrels											
Audubon's Shearwater	0	0	0	0	0	<0.001	0	0	0.001	<0.001	12
Cory's Shearwater	0.006	0	0	0.025	0	0.032	0	0.001	0.101	0.019	1044
Great Shearwater	0.014	0	0	0.052	0.004	0.015	0	<0.001	0.048	0.009	651
Manx Shearwater	0	0	0	0	0	<0.001	<0.001	<0.001	<0.001	0.003	60
Northern Fulmar	0	0	0	0	0	0.022	0.063	0.013	0	0.014	1153
Sooty Shearwater	0.003	0	0.003	0.007	0	0.004	<0.001	0.016	0.001	0	136
Trindade Petrel	0	0	0	0	0	<0.001	0	<0.001	0	0	1
Unidentified Petrel	0	0	0	0	0	<0.001	<0.001	0	<0.001	0	9
Unidentified Shearwater	0.002	0	0	0.007	0	0.018	<0.001	0.004	0.043	0.023	864
Band-rumped Storm-Petrel (a.k.a. Madeiran SP, or Harcourt's SPI)	0	0	0	0	0	<0.001	0	<0.001	0	0	1
Leach's Storm-Petrel	0	0	0	0	0	<0.001	<0.001	<0.001	<0.001	<0.001	8
Unidentified Storm-Petrel	0.017	0.036	0	0.031	0	0.135	0.014	0.229	0.278	0.011	6782
White-faced Storm-Petrel	0	0	0	0	0	<0.001	0	0	<0.001	0	2
Wilson's Storm-Petrel	0.009	0	0	0.036	0	0.04	0	0.015	0.138	<0.001	1218
Gannets, Cormorants, and Pelicans											
Northern Gannet	0.161	0.557	0.062	0	0.019	0.322	0.69	0.18	<0.001	0.442	12149
Double-crested Cormorant	0	0	0	0	0	<0.001	0	<0.001	<0.001	0.003	54
Unidentified Cormorant	0	0	0	0	0	0.006	0	0.013	<0.001	0.011	429

Species	Mean naive density (uncorrected count/square km)										
	Lease Area OCS A 0544					NY Bight Study Area					Total count
	annual	winter	spring	summer	fall	annual	winter	spring	summer	fall	
Brown Pelican	0	0	0	0	0	<0.001	0	0	0	<0.001	1
Roseate Tern	0	0	0	0	0	0.001	0	0.004	<0.001	0	33
Piping Plover	No data	No data	No data	No data	No data	No data	No data	No data	No data	No data	No data
Red Knot	No data	No data	No data	No data	No data	No data	No data	No data	No data	No data	No data
Eastern Black Rail	No data	No data	No data	No data	No data	No data	No data	No data	No data	No data	No data
Black-capped Petrel	0.002	0	0	0.007	0	0.001	<0.001	0.002	0.002	<0.001	52
Saltmarsh Sparrow	No data	No data	No data	No data	No data	No data	No data	No data	No data	No data	No data
Bald Eagle and Golden Eagle	No data	No data	No data	No data	No data	No data	No data	No data	No data	No data	No data

5 Detailed Offshore Avian Assessment Methods

This section provides a detailed overview of the data sources and methods used in exposure and vulnerability assessments. As discussed in Section 2.3.2, exposure and vulnerability are combined into a final risk determination using the matrix in Table 2-1. Exposure was assessed for each species and taxonomic group, where “exposure” is defined as the proportion of the seasonal or annual population that overlaps the Lease Area for a given species. Vulnerability was assessed for marine birds using a scoring process focused on documented avoidance behaviors, estimated flight heights, and other factors.

5.1 Exposure Framework

Avian exposure has a horizontal component of two-dimensional overlap between bird occurrence and the Lease Area, as well as a vertical component of overlap between the birds’ flight height and the RSZ. In this exposure assessment, BRI focused exclusively on the horizontal exposure of birds. Vertical exposure (i.e., flight height) was considered within BRI’s assessment of vulnerability to collision. The exposure assessment was quantitative when local baseline survey data were available. For birds without data from the survey area, species accounts and scientific literature were used to conduct a qualitative assessment. For all marine birds, exposure was considered both in the context of the proportion of the population predicted to be exposed to the Lease Area, as well as absolute numbers of individuals. The following sections introduce the data sources used in the analysis, methods used to map species exposure, methods used to quantify exposure as a score, methods used to aggregate scores to year and taxonomic group, and conversion of exposure scores into exposure determinations.

5.1.1 Exposure Assessment Data Sources and Coverage

To assess the proportion of marine bird populations exposed to the Lease Area, two main data sources were used to evaluate local and regional marine bird use:

(1) Digital aerial surveys - the NYSERDA Digital Aerial Baseline Surveys of Marine Life (Normandeau Associates and APEM 2021b) and the Digital Aerial Wildlife Survey of BOEM Lease Area OCS-A 0512 (Normandeau Associates and APEM 2019, 2021c). The NYSERDA Digital Aerial Baseline Surveys of Marine Life (NYSERDA APEM surveys) provide local coverage of the Lease Area and surrounding waters (the study area). The Digital Aerial Wildlife Survey of BOEM Lease Area OCS-A 0512 (Lease Area OCS-A 0512 surveys) provides limited site-specific coverage of the Lease Area owing to the 4 km (2.5 mi) buffer around Lease Area OCS-A 0512 in that study and the resulting overlap with Lease Area OCS-A 0544. Throughout, when discussed in combination, the NYSERDA APEM surveys and Empire surveys are referred to collectively as the NY Bight surveys.

(2) Model outputs - Version 3 of the MDAT marine bird relative density and distribution models (Winship et al. 2023, Curtice et al. 2019). The MDAT-modeled abundance predictions provide a

large regional context for the Lease Area but are built from offshore survey data collected from 1999-2020. Of note, the MDAT models incorporate the digital aerial survey data described above.

Each of these data sources used for exposure assessment is described in more detail below, along with additional data sources such as tracking data that inform the avian impact assessment. Data collected during these surveys are in general agreement with BOEM guidelines and the goals detailed above and described below. All tracking data were used with written permission.

5.1.2 NYSERDA Digital Aerial Baseline Survey of Marine Wildlife

The NYSERDA Digital Aerial Baseline Survey of Marine Wildlife (Normandeau Associates and APEM 2021a, b) is the key existing dataset on bird species abundance and distribution offshore in the New York Bight, including the Lease Area. This dataset consists of 12 quarterly digital aerial surveys flown from 2016-2019 that cover the New York Offshore Planning Area (OPA), which is inclusive of the entirety of the Lease Area. NYSERDA's contractors, APEM and Normandeau Associates, conducted the digital aerial surveys from summer 2016 to spring 2019 using strip-transect-based non-overlapping imagery (Normandeau Associates and APEM 2021a, b). Twelve individual survey transects included coverage of the Lease Area, and each survey provided site coverage between 7 and 10 %, depending on the configuration of the transects and the camera used.

Two different camera systems were used for the surveys. The Shearwater II camera system was used during the summer 2016 survey, and the new Shearwater III camera system was used for all subsequent surveys. Both systems collected data at 1.5 cm (0.6 inch) ground sampling distance (GSD) and both surveys used a Piper Aztec twin engine aircraft. In addition, during the summer 2016 survey of the OPA, data were collected at 0.75 cm (0.3 inch) GSD on near shore sample lines, which were flown at the lower altitude of approximately 152 m (500 ft) to accommodate restrictions imposed in controlled airspace around the John F. Kennedy Airport. Flight altitude for the remaining survey lines of the summer survey was flown at 311 m (1,020 ft), and data were captured at 415 m (1,360 ft) for all the subsequent surveys. Daily survey time maximized crew hours and avoided midday when glare/glint was most prevalent. Surveys were conducted when sea state (Beaufort Scale) was less than 4 (Normandeau Associates and APEM 2021a).

5.1.3 Digital Aerial Wildlife Survey of BOEM Lease Area OCS-a 0512

Following the methods described for the NYSERDA digital aerial surveys, APEM also conducted 24 monthly surveys of BOEM Lease Area OCS-A 0512, plus a 4 km (2.5 mi) buffer, which overlaps with 45.1% of Lease Area OCS-A 0544, and the monthly imagery coverage ranges from 5.1 to 5.9% of Lease Area OCS-A 0544. The surveys were conducted from November 2017–October 2018 and February 2019–December 2019 following a grid-based sampling system. Images were captured in a grid pattern along 28 lines spaced ~0.8 km (0.5 mi) across-track and ~0.6 km (0.4

mi) along-track within the survey area (Figure 5-1 [see inset]; Normandeau Associates and APEM 2019, 2021c). Mean survey effort is shown in Figure 5-2.

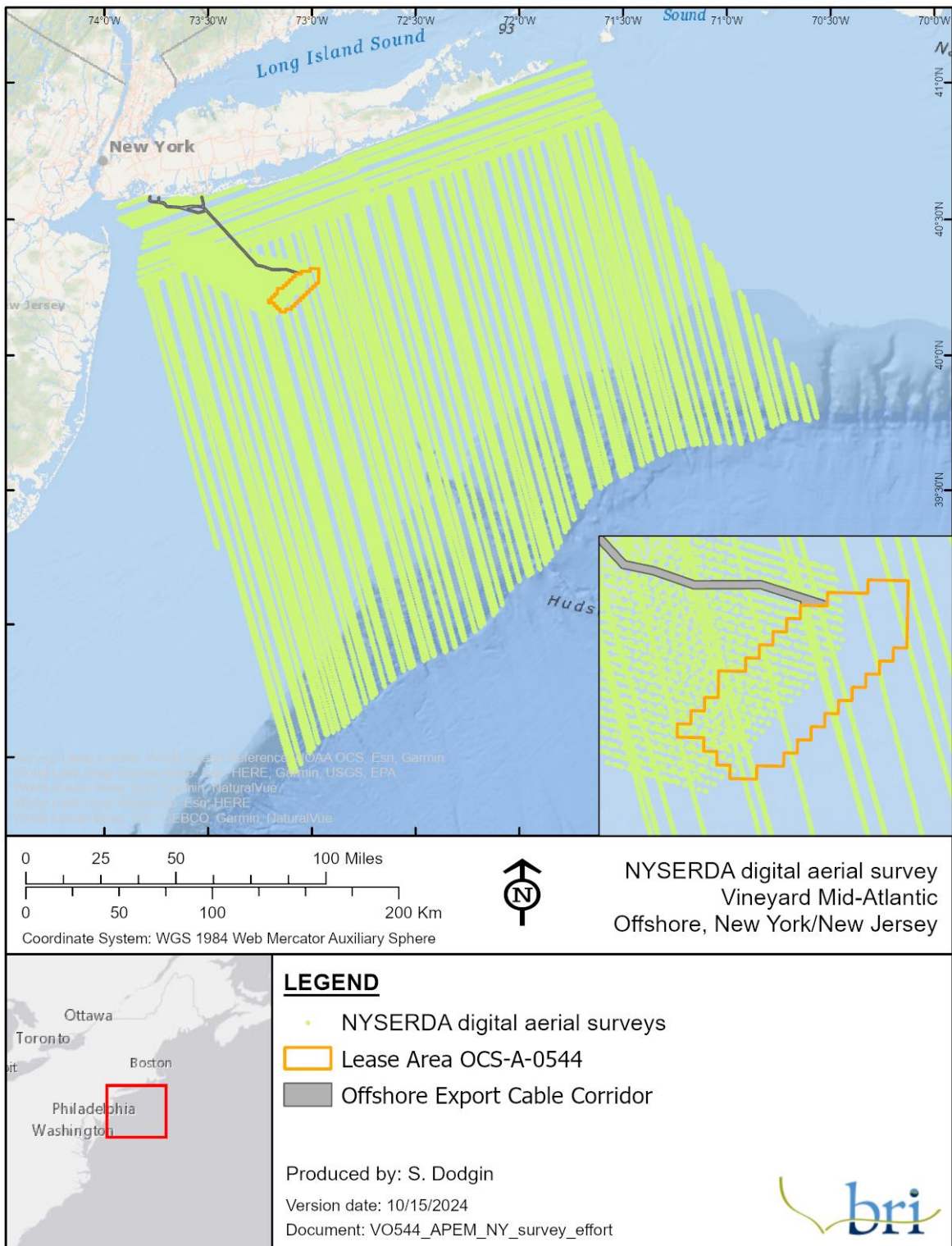


Figure 5-1: Location of digital aerial surveys conducted in the NYSERDA Digital Aerial Baseline Survey (Normandeau Associates and APEM 2021a, b) and the Digital Aerial Wildlife Survey of BOEM Lease Area OCS-A 0512 (Normandeau Associates and APEM 2019, 2021c) in relation to the Lease Area.

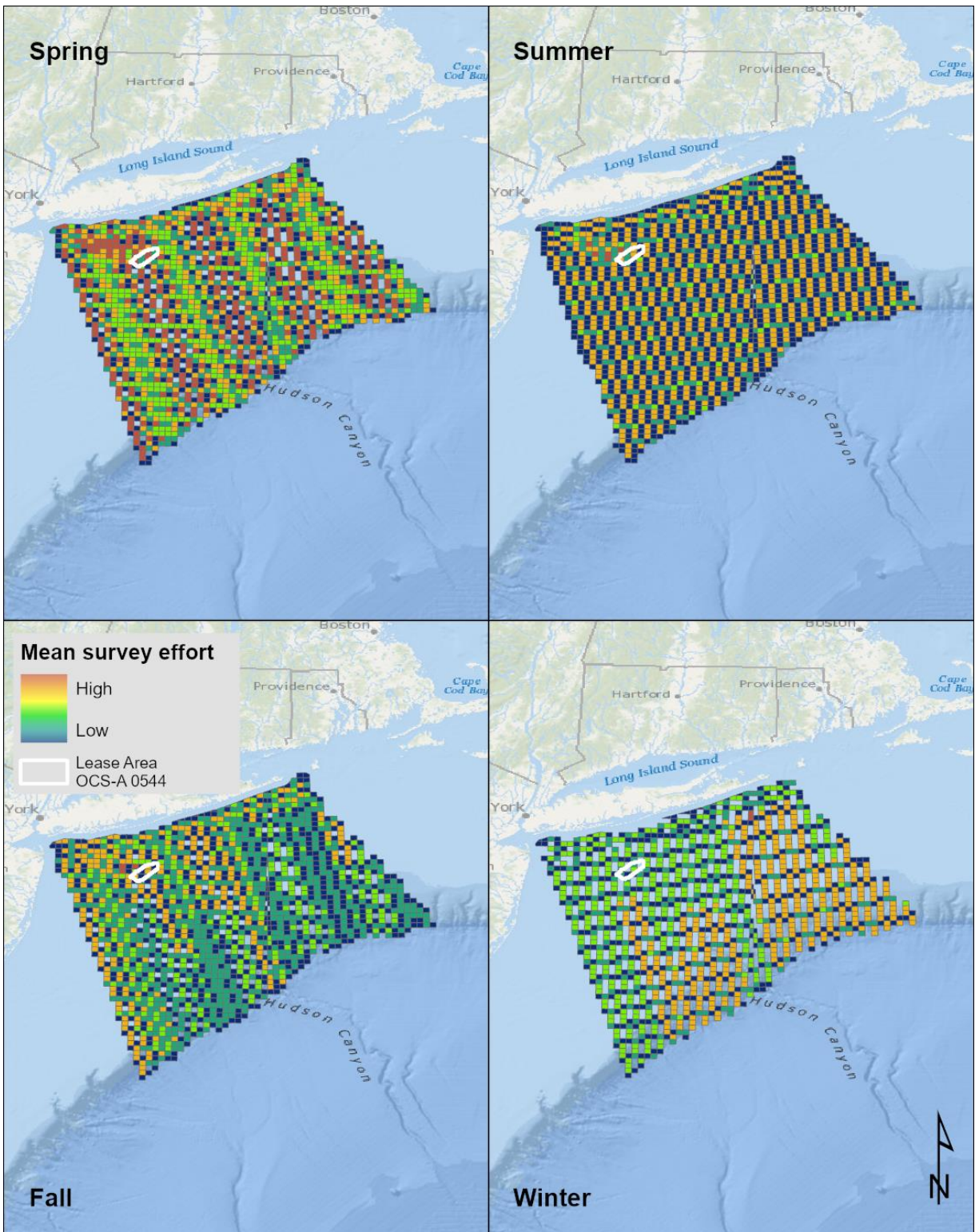


Figure 5-2: Overall survey effort by season. While effort varied by OCS lease block and season, the entire study area, including the Lease Area, was thoroughly surveyed each season.

5.1.4 MDAT Marine Bird Abundance and Occurrence Models

Seasonal predictions of density were developed to support Atlantic marine renewable energy planning. Distributed as MDAT bird models (Curtice et al. 2019; Winship et al. 2023), they describe regional-scale patterns of abundance. Updates to these models (Version 3) are available directly from Duke University’s Marine Geospatial Ecology Lab MDAT model web page.⁸ The MDAT analysis integrated survey data (1999–2020) from 28 vessel-based, visual aerial, or digital aerial surveys with a range of environmental variables to produce long-term average monthly models. These models were developed to support marine spatial planning in the northeast by the Northeast Regional Planning Body but are also available to support other planning efforts. Version 3 relative abundance and distribution models were produced for 49 avian species using US Atlantic waters from Florida to Maine, and thus provide excellent regional context for local relative densities calculated from the NYSERDA Digital Aerial Baseline Surveys and BOEM Lease Area OCS-A 0512 digital aerial surveys.

The MDAT and NY Bight survey formation sources each have strengths and weaknesses. The NYSERDA survey methods are robust, representative of local conditions, and the data are more recent than the data collected for MDAT, so they describe recent distribution patterns in the Lease Area and surrounding areas. However, these surveys covered a small area relative to the Northwest Atlantic distribution of most marine bird species, and the limited number of surveys conducted in each season means that individual observations (or lack of observations, for rare species) may, in some cases, carry substantial weight when determining seasonal exposure. A substantial number of sightings in the NY Bight surveys could not be identified at the species level and were instead categorized as “unidentified” observations (e.g., “unknown large gull” or “unknown small tern”), which lowers the sample size and weakens the evaluation of exposure at the species level.

The MDAT models, in contrast, are based on data collected at much larger geographic and temporal scales. These data were also collected over decades across the US Atlantic coast using a range of survey methods; relatively recent datasets collected near the New York Bight, such as the New Jersey Department of Environmental Protection Environmental Baseline Surveys, are included. The MDAT products are relative abundance predictions from the models that use relationships with environmental covariates and seasonal averages of those covariates—termed “Seasonal climatologies of dynamic spatial environmental predictors”—to project spatial changes over the study area. The larger, regional geographic scale is helpful for determining how marine birds use the Lease Area relative to other available locations in the northwest Atlantic and is thus essential for determining overall exposure. These models are based on survey data from the two most recent decades of surveys and use long-term relationships with climate and other environmental conditions to make predictions. As environmental conditions change, so too

⁸ <http://seamap.env.duke.edu/models/mdat>

might species' relationships with those drivers and these models might not be useful for predicting current or future areas of activity. Already, given changing climate conditions, these models may no longer accurately reflect current distribution patterns. Model outputs that incorporate environmental covariates to predict distributions across a broad spatial scale also vary in the accuracy of those predictions at a local scale.

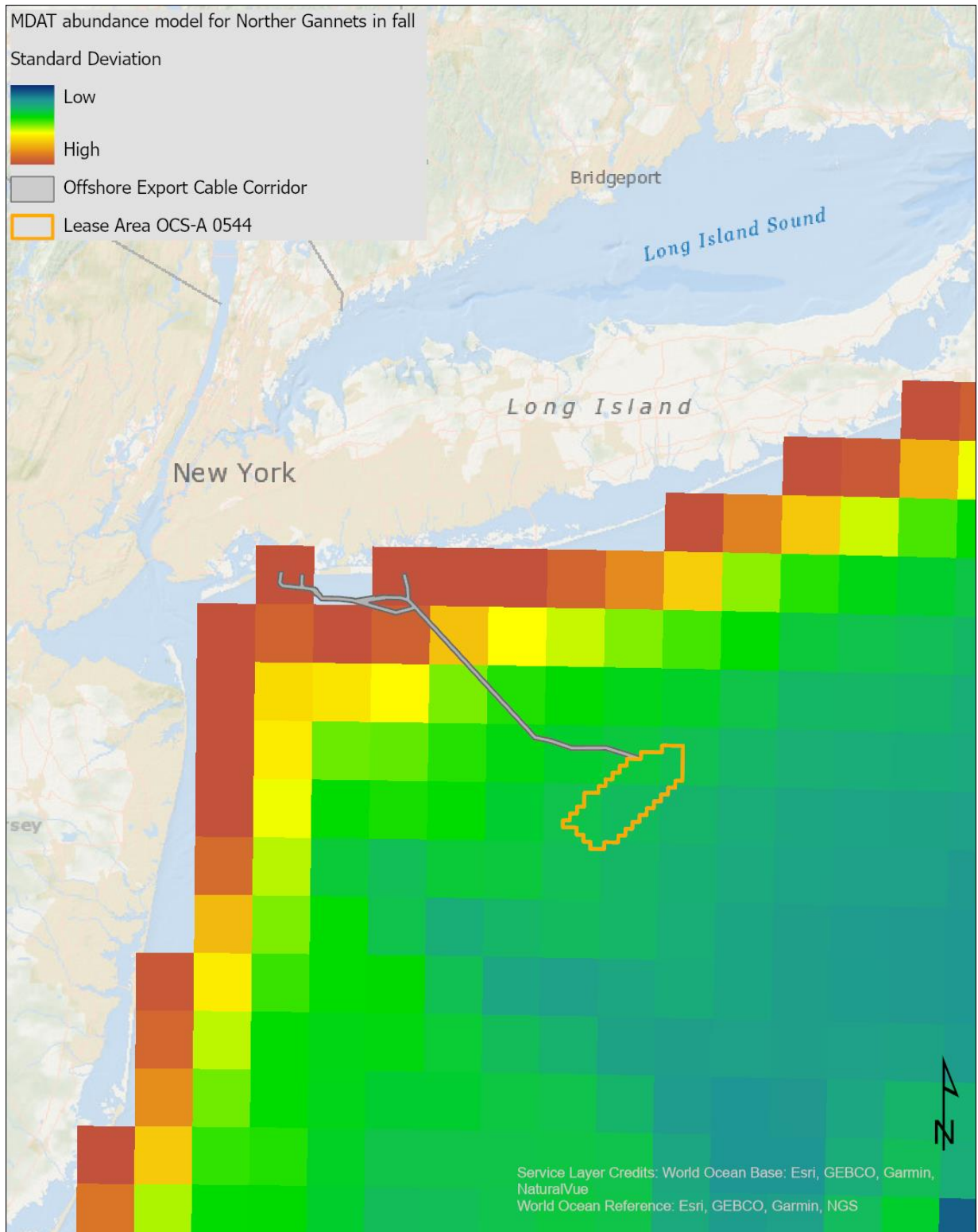


Figure 5-3: Example MDAT abundance model, in this case for the Northern Gannet in the fall.

5.1.5 Supplemental Data Sources

5.1.5.1 *Northwest Atlantic Seabird Catalog*

The Northwest Atlantic Seabird Catalog is the comprehensive database for most of the offshore and coastal seabird surveys conducted in US Atlantic waters from Maine to Florida. The database (version 4 May 2023) contains records from 1906–2020, having more than 300 datasets and approximately 1,120,000 observation records along with associated effort information (Arliiss Winship, personal communication, 4 May 2023). The database is currently being managed by NOAA’s National Centers for Coastal Ocean Science. With BOEM’s approval, NOAA provided the Catalog database to BRI to make queries for this assessment. All data received were mapped to determine the occurrence of rare species with the Lease Area and adjacent areas north and south of the Lease Area.

5.1.5.2 *Mid-Atlantic Diving Bird Tracking Study*

A satellite telemetry tracking study in the mid-Atlantic was developed and supported by BOEM and the USFWS with objectives aimed at determining fine scale use and movement patterns of three species of marine diving birds during migration and winter (Spiegel et al. 2017). These species—the Red-throated Loon, Surf Scoter, and Northern Gannet—exhibit various traits that make them vulnerable to offshore wind development. Nearly 400 individuals were tracked using satellite transmitters over the course of five years (2012–2016), including some tagged Surf Scoters as part of the Atlantic and Great Lakes Sea Duck Migration Study by SDJV partners.⁹ Results provide a better understanding of how these diving birds use offshore areas of the Mid-Atlantic OCS and beyond.

Utilization distributions (UDs) were determined for each species by calculating individual level dynamic Brownian-bridge movement model (dBBMM) surfaces (Kranstauber et al. 2012) using package Move for R (Kranstauber and Smolla 2016). Separate dBBMM surfaces were calculated for each of two winters with at least five days of data and combined into a weighted mean surface for each animal (as a percentage of the total number of days represented in the surface) with a minimum 30 total combined days of data. This method of combining multiple seasons was used for the migration periods as well, but with relaxed requirements for days of data, requiring only five days per year and seven total days per period since migration duration often occurred over a much shorter time period. Utilization contour levels of 50%, 75%, and 95% were calculated for the mean UD surface. The final UD was cropped to the 95% contour for mapping and further analyses (Spiegel et al. 2017).

⁹ <https://seaduckjv.org/science-resources/atlantic-and-great-lakes-sea-duck-migration-study>

5.1.5.3 Migrant Raptor Studies

Peregrine Falcon and Merlin

To facilitate research efforts on migrant raptors (i.e., migration routes, stopover sites, space use relative to Atlantic OCS wintering/summer range, origins, contaminant exposure), BRI has deployed satellite transmitters on fall migrating raptors at three different raptor migration research stations along the north Atlantic coast (DeSorbo et al. 2012). Research stations include the Block Island Raptor Research Station at Block Island, Rhode Island (Peregrine Falcons: 3 adult [ad.] females, 18 hatch year [HY] females, 17 HY males; Merlins: 3 ad. females and 13 HY females; DeSorbo et al. 2018); Monhegan Island, Maine (Peregrine Falcons: 2 HY females); and Cutler, Maine (Peregrine Falcons: 1 ad. female).

Satellite-tagged Peregrine Falcons and Merlins provided information on fall migration routes along the Atlantic flyway. Positional data was filtered to remove poor quality locations using the Douglas Argos Filtering tool (Douglas et al. 2012) available online on the Movebank data repository¹⁰ where these data are stored and processed.

Osprey

Between 2000 and 2019, 106 tracking devices were fitted to Ospreys captured at various locations between Chesapeake Bay and northern New Hampshire¹¹. This data set includes both adults and juveniles but emphasized tagging juveniles prior to their first migration. It represents the first dedicated study of dispersal, mortality, and migration in juvenile Ospreys. Satellite transmitters were used in early years, but beginning in 2012, higher-resolution cellular GPS transmitters were deployed on adult males to better document their foraging behavior around nests and to provide additional details about migration (e.g., thermal soaring over land and dynamic soaring over water; Horton et al. 2014).

Separately, satellite Argos platform transmitting terminal (PTT) tags were deployed on Ospreys in the US and Canada between 1995 and 2001 (Martell et al. 2001; Martell and Douglas 2019). This data has been used to delineate both fall and spring migratory routes used by Ospreys breeding in the US. Tagging locations included areas in Oregon, Washington, Minnesota, New York, and New Jersey. Birds tagged in eastern states generally migrated along the US Atlantic coast.

To characterize potential utilization of the offshore environment by Ospreys, UDs were generated for individual animals using a dBBMM (Kranstauber et al. 2012). Both Argos satellite data and GPS-derived positional data were used from the two different telemetry datasets from Movebank (as above). Both datasets were compiled together and a max speed filter by animal was applied, which excluded locations with instantaneous speeds greater than 100 km per hour

¹⁰ <https://www.movebank.org>

¹¹ www.ospreytrax.com

(62 miles per hour) and also filtered points outside of an extent including the eastern US and Atlantic Canada (including all offshore points for this region). Individual dBBMMs were generated for the last 365 consecutive days of available data per tag (or less if the tags provide less than 365 consecutive days), thus representing an annual cycle within the US. Models were composited into a weighted UD for the sampled population, weighting each animal's UD by the number of days data were available of the total number of days of all animals providing models.

5.1.5.4 Tracking Studies of Vulnerable Terns and Shorebirds in the Northwest Atlantic Using Nano Tags

Since 2013, BOEM and the USFWS have supported a study using NanoTags, a type of coded very high frequency (VHF) tags, and an array of automated VHF radio telemetry stations to track the movements of vulnerable species, such as terns and shorebirds. The study was designed to assess the degree to which these species use offshore federal waters during breeding, pre-migratory staging periods, and migrations. In a pilot study in 2013, researchers attached NanoTags to Common Terns and American Oystercatchers (*Haematopus palliatus*) and set up eight automated sentry stations (Loring et al. 2017). Having proved the methods successful, the study was expanded to 16 automated stations in 2014, and from 2015–2017, tagging efforts included Piping Plovers and Roseate Terns. This study provided new information on the offshore movements and flight altitudes for these species gathered from a network of 33 automated telemetry stations, including areas of Massachusetts, New York, New Jersey, Delaware, and Virginia (Loring et al. 2019).

5.1.5.5 Tracking Studies of rufa Red Knots in US Atlantic Outer Continental Shelf Waters

Building from a previous tracking study, *rufa* Red Knots were fitted with digital VHF transmitters during their 2016 southbound migration at stopover locations in both Canada and along the US Atlantic coast. Individuals were tracked via radio telemetry stations within the study area that extended from Cape Cod, Massachusetts, to Back Bay, Virginia. Modeling techniques were developed to describe the frequency and offshore movements over federal waters and specific WEAs within the study area. The primary study objectives were to: develop models related to offshore movements for *rufa* Red Knots; assess the exposure to each WEA during southbound migration; and examine WEA exposure and migratory departure movements in relation to various meteorological conditions (Loring et al. 2018).

5.1.5.6 Sea Duck Tracking Studies

The Atlantic and Great Lakes Sea Duck Migration Study, a multi-partner collaboration, was initiated by the SDJV in 2009 with the goals of: (1) fully describing full annual cycle migration patterns for four species of sea ducks (Surf Scoter, Black Scoter, White-winged Scoter, and Long-tailed Duck); (2) mapping local movements and estimating length-of-stay during winter for individual radio-marked ducks in areas proposed for placement of WTGs; (3) identifying nearshore and offshore habitats of high significance to sea ducks to help inform habitat

conservation efforts; and (4) estimating rates of annual site fidelity to wintering areas, breeding areas, and molting areas for all four focal species in the Atlantic flyway. To date, over 500 transmitters have been deployed in the US and Canada by various project partners, including BRI, Canadian Wildlife Service, US Geological Survey's Patuxent Wildlife Research Center, University of Rhode Island, Rhode Island Department of Environmental Management, USFWS, SDJV, and the University of Montreal. These collective studies have led to increased understanding of annual cycle dynamics of sea ducks, as well as potential interactions with and impacts from offshore wind energy development (Loring et al. 2014; SDJV 2015; Meattley et al. 2018; Meattley et al. 2019).

In addition, BOEM and USFWS partnered with SDJV during 2012–2016 to deploy transmitters in Surf Scoters as part of a satellite telemetry tracking study in the Mid-Atlantic, with the aim of determining fine scale use and movement patterns of three species of marine diving birds during migration and winter (Spiegel et al. 2017).

Sea duck UD's were determined for each species by calculating individual level dBBMM surfaces (Kranstauber et al. 2012) using package Move for R (Kranstauber and Smolla 2016). Separate dBBMM surfaces were calculated for each of two winters with at least five days of data and combined into a weighted mean surface for each bird (as a percentage of the total number of days represented in the surface) with a minimum 30 total combined days of data. This method of combining multiple seasons was used for the migration periods as well, but with relaxed requirements for days of data, requiring only five days per year and seven total days per period since migration duration often occurred over a much shorter time period. Utilization contour levels of 50%, 75%, and 95% were calculated for the mean UD surface. The final UD was cropped to the 95% contour for mapping and further analyses (Spiegel et al. 2017).

5.1.5.7 Great Blue Heron Tracking Study

Since 2016, the Maine Department of Inland Fisheries and Wildlife has been capturing Great Blue Herons each year in Maine and tracking their migrations with solar GPS satellite transmitters. Results to date indicate that Great Blue Herons breeding in Maine winter across the southeastern US and the Caribbean, as far south as Haiti. In general, herons travel coastally, but some have been tracked much farther offshore than previously anticipated, with one bird going as far east as Bermuda on one southbound migration, likely taking advantage of offshore prevailing winds at the time. The full dataset is available in the Movebank repository, Move Bank ID 17469219 (Brzorad 2023).

5.1.6 Digital Aerial Survey Density Modeling

Conservation decision-making relies on accurate descriptions of species density and occurrence to determine the potential costs and benefits of actions. However, it can be difficult to accurately understand density and characterize habitat use when survey coverage is low or sampling is not evenly distributed across the space of interest. Further, raw counts and

observations do not have measurements of uncertainty associated, which limits the ability to derive confidence from quantitative results. Spatial density modeling is one way to account for the limitations of using raw data, by interpolating between observations to (a) fill in gaps between sampling, and (b) assign a measure of confidence to resulting predictions of density. Sampling in the Lease Area included quarterly NYSERDA digital aerial surveys, and monthly surveys of Lease Area OCS-A 0512 with a 4 km (2.5 mi) buffer that overlapped Lease Area OCS-A 0544. Using a spatial density modeling approach, both surveys were integrated and modeled based on both the spatial relationships between points as well as relevant environmental covariates (e.g., distance from shore, SST) to characterize the density and confidence of estimates within and between surveyed areas across the NY Bight survey area.

5.1.6.1 Data Integration and Model Criteria

Data from the NYSERDA digital aerial surveys and the Empire lease area surveys were compiled for processing at the taxa and season level. The monthly Empire lease area sightings were aggregated to seasonal levels, and all species were assigned to taxa groups (Table 4-28). Monthly surveys were assigned to seasons as follows: December, January, and February were defined as “winter”; March, April, and May were defined as “spring”; June, July, and August were defined as “summer”; and September, October, and November were defined as “fall”. Survey effort was compiled to the season level as polygons indicating the ground spatial footprint of the camera system, which was merged so one spatial representation of survey effort was available for each season. Both observations and effort data were projected to a custom projection (Universal Transverse Mercator [UTM] Zone 18N with a length unit of “kilometers” in both latitudinal and longitudinal distance). For each season and taxon combination, models were developed if there were greater than 9 observations.

5.1.6.2 Spatial Modeling Framework

To model the observation density and account for the spatial dependence among observations, we fit spatially-explicit log Gaussian Cox Poisson (LGCP) process models to the year-round and seasonal survey data by species and taxa group using INLA—integrated nested Laplace approximation—for approximate Bayesian inference (Rue et al. 2009). The spatial dependence in the data is accounted for by incorporating a Gaussian Markov Random Field (GMRF) into the models as well as relationships to relevant environmental covariates. Briefly, LGCP models estimate the point density using a log link function, such that the log of the spatial inhomogeneous intensity function (λ) at any point is assumed to be Gaussian (Møller and Waagepetersen 2007). We implemented the stochastic partial differential equations (SPDE) approach (Lindgren et al. 2011) to incorporate the spatial random effect as a latent Gaussian Field (GF) with a Matérn covariance structure to account for the spatial dependence in the data. Put another way, bird densities are more likely to be similar in adjacent spatial units than in distant units; these models estimate these spatial correlations to evaluate changes in density over space.

The results of the SPDE approach can also be combined with relevant environmental covariates. In this instance, variance in the spatial LGCP can be attributed to the relationship with underlying environmental variables in addition to the SPDE model. The models built for the Lease Area were derived from a combination of the SPDE, distance to shore, and SST. Distance to shore was calculated by the Euclidean distance to the coastline (defined by the NOAA Global self-consistent, hierarchical, high-resolution geography database¹²), and SST (Canada Meteorological Center 2016) was calculated as a seasonal average across all years of survey (2016-2019). Both covariates were resampled to 15km² and were scaled by subtracting the covariate mean and dividing by the standard deviation.

To approximate the spatial relationships among observations, we constructed a constrained refined Delaunay triangulation spatial mesh covering the digital aerial survey area (Figure 5 2). An area of coarser density mesh (10% of the survey area diameter) was added beyond the survey area to remove boundary effects that cause increased variance at the borders (Lindgren et al. 2011). We built the mesh using all bird observations of a given taxa for each season as the initial triangulation nodes. To avoid an overly complex mesh, we also set cutoff values based on the clustering of observations for each taxa-season combination, such that a single vertex replaces points at a closer distance than this prior mesh creation (Table 5-1). We estimated smooth density surfaces by modeling the intensity (λ) at each spatial location (s) as a function of the spatial random effect (u).

$$\lambda(s) = \exp(\beta_0 + \mathbf{A}u(s) + sst(s) + dsh(s))$$

Where β_0 is an intercept term, u is the GF representing the spatial random effect, sst is the covariate for Sea Surface Temperature, and dsh is the covariate for distance from shore. The spatial effect u can be approximated at any point within the triangulated domain, using the projector matrix \mathbf{A} to link the spatial GF (defined by the mesh vertices or nodes) to the locations of the observed data, s (Krainski et al. 2018). The Matérn covariance matrix priors for the spatial effect were derived using a penalized complexity (PC) approach (Fuglstad et al. 2018), where the hyperparameters of range (r) and the marginalized standard deviation of the field (σ) define the spatial random effect so that $P(r > r_0) = p$ and $P(\sigma > \sigma_0) = p$. Using the PC priors, the prior probability and spatial variance was defined for each taxa-season combination based on the sample size and clustering of observations.

5.1.6.3 Model Prediction

Seasonal taxa density predictions were made at a 5 km (3.1 mi) resolution across the NY Bight survey area to approximately match the size of BOEM lease blocks. The full model, including the overall intercept, SST, distance to shore, and the spatial random effect, was used to calculate density for each 5 km grid cell. Model fit was assessed by visually assessing the predicted output,

¹² <https://www.ngdc.noaa.gov/mgg/shorelines/gshhs.html>

evaluating the posterior predictions for the spatial covariates as well as the spatial random effect parameters (range and the marginalized standard deviation), and by comparing the distribution of expected total density with the model predicted density across the NY Bight survey area. To develop an estimate of the expected total density (i.e., the “true” density across the NY Bight survey area), the density was integrated over the input mesh points, which were assigned weighted values, resulting in a Poisson probability density function centered around the expected integrated density value (*edv*). To develop an estimate of posterior density distribution across the NY Bight survey area, 2,000 samples of density were predicted across a range of possible density values indicated by

$$pdv = edv \pm (0.5 \times edv)$$

Where *pdv* is the possible density values and *edv* represents the expected density value across the NY Bight survey area. The result is a mean probability density function representing likelihood of density estimates across the range of *pdv* values. In summary, two density distributions are calculated across a range of *pdv*: one represents the model expected density, and the other represents the bootstrapped predicted values across the NY Bight survey area. The two resulting distributions were compared using a Wilcoxon ranked sign test, where statistically significant differences between distributions indicate a poor model fit (Table 5-1).

All models were fit in R (version 4.2.2), (R Core Team 2020), using the R-INLA (version 23.04.24, <https://www.r-inla.org>, (Lindgren and Rue 2015) and *inlabru* (version 2.8.0.9008, Bachl et al. 2019) packages.

Table 5-1: Summary of integrated density models.

Group	Season	Sample Size	Model Run	Mesh Cutoff Distance (km)	Prior Range Value (km) (probability of exceeding value)	Prior Standard Deviation (probability of exceeding value)	Wilcoxon Test	Estimated Median Density in Lease Area (Abundance/km ²)	Estimated Median Density in Study Area (Abundance/km ²)
All Gulls	Fall	19906	Y	2	15.0 (0.3)	0.01 (0.05)	0.03	<0.01	0.009
	Summer	727	Y	2	15.0 (0.3)	0.01 (0.05)	0.16	<0.01	0.090
	Winter	15035	Y	2	15.0 (0.3)	0.01 (0.05)	0.76	<0.01	0.005
	Spring	8042	Y	2	15.0 (0.3)	0.01 (0.05)	0.50	<0.01	0.005
All terns	Fall	6	N	2	NA	NA	NA	NA	NA
	Summer	546	Y	3	20 (0.3)	0.05 (0.05)	0.46	<0.01	0.174
	Winter	0	N	2	NA	NA	NA	NA	NA
	Spring	3443	Y	2	15.0 (0.3)	0.01 (0.05)	0.83	<0.01	0.004
Auks	Fall	1882	Y	2	15.0 (0.3)	0.01 (0.05)	0.83	<0.01	0.013
	Summer	5	N	2	NA	NA	NA	NA	NA
	Winter	13239	Y	2	15.0 (0.3)	0.01 (0.05)	0.83	<0.01	0.005
	Spring	5013	Y	2	15.0 (0.3)	0.01 (0.05)	0.92	<0.01	0.009
Cormorants	Fall	415	Y	3	30 (0.3)	0.01 (0.05)	0.44	<0.01	1.541
	Summer	10	N	2	NA	NA	NA	NA	NA
	Winter	4	N	2	NA	NA	NA	NA	NA
	Spring	235	Y	2	15.0 (0.3)	0.01 (0.05)	0.59	<0.01	0.065
Gannets	Fall	4973	Y	2	15.0 (0.3)	0.01 (0.05)	0.32	<0.01	0.009
	Summer	8	N	2	NA	NA	NA	NA	NA
	Winter	6470	Y	2	15.0 (0.3)	0.01 (0.05)	0.65	<0.01	0.005

Group	Season	Sample Size	Model Run	Mesh Cutoff Distance (km)	Prior Range Value (km) (probability of exceeding value)	Prior Standard Deviation (probability of exceeding value)	Wilcoxon Test	Estimated Median Density in Lease Area (Abundance/km ²)	Estimated Median Density in Study Area (Abundance/km ²)
	Spring	2927	Y	2	15.0 (0.3)	0.01 (0.05)	0.65	<0.01	0.008
Large Gulls	Fall	8518	Y	2	5.0 (0.3)	0.005 (0.05)	0.56	<0.01	0.008
	Summer	536	Y	2	15.0 (0.3)	0.01 (0.05)	0.24	<0.01	0.391
	Winter	13011	Y	2	15.0 (0.3)	0.01 (0.05)	0.90	<0.01	0.006
	Spring	6447	Y	2	15.0 (0.3)	0.01 (0.05)	0.33	<0.01	0.006
Loons	Fall	1518	Y	2	15.0 (0.3)	0.01 (0.05)	0.82	<0.01	0.005
	Summer	18	Y	6	20 (0.3)	0.08 (0.05)	0.19	<0.01	0.008
	Winter	1384	Y	2	15.0 (0.3)	0.01 (0.05)	0.93	<0.01	0.005
	Spring	1789	Y	2	15.0 (0.3)	0.01 (0.05)	0.72	<0.01	0.007
Medium Gulls	Fall	6579	Y	3	10 (0.3)	0.08 (0.05)	0.45	<0.01	0.11
	Summer	139	Y	3	10 (0.3)	0.08 (0.05)	0.69	0.010	344.750
	Winter	483	Y	3	10 (0.3)	0.08 (0.05)	0.61	<0.01	0.003
	Spring	164	Y	3	10 (0.3)	0.08 (0.05)	0.67	<0.01	0.004
Medium Terns	Fall	4	N	2	NA	NA	NA	NA	NA
	Summer	135	Y	3	2.0 (0.3)	0.02 (0.05)	0.19	<0.01	0.003
	Winter	0	N	2	NA	NA	NA	NA	NA
	Spring	748	Y	2	15.0 (0.3)	0.01 (0.05)	0.96	<0.01	0.002
Phalaropes	Fall	11398	Y	2	15.0 (0.3)	0.01 (0.05)	0.98	<0.01	0.012
	Summer	151	Y	2	15.0 (0.3)	0.01 (0.05)	0.68	<0.01	0.002
	Winter	258	Y	2	15.0 (0.3)	0.01 (0.05)	0.73	<0.01	0.006
	Spring	7981	Y	2	15.0 (0.3)	0.01 (0.05)	0.89	<0.01	0.012

Group	Season	Sample Size	Model Run	Mesh Cutoff Distance (km)	Prior Range Value (km) (probability of exceeding value)	Prior Standard Deviation (probability of exceeding value)	Wilcoxon Test	Estimated Median Density in Lease Area (Abundance/km ²)	Estimated Median Density in Study Area (Abundance/km ²)
Seaducks	Fall	3551	Y	2	3.0 (0.3)	0.0008 (0.05)	<0.01	<0.01	0.164
	Summer	0	N	3	NA	NA	NA	NA	NA
	Winter	8051	Y	3	5.0 (0.3)	0.08 (0.005)	0.94	<0.01	1.612
	Spring	6323	Y	3	5.0 (0.3)	0.08 (0.005)	0.94	<0.01	0.101
Shearwaters and Petrels	Fall	899	Y	2	15.0 (0.3)	0.01 (0.05)	0.74	<0.01	0.004
	Summer	2017	Y	2	15.0 (0.3)	0.01 (0.05)	0.84	<0.01	0.004
	Winter	827	Y	2	15.0 (0.3)	0.01 (0.05)	0.88	<0.01	0.004
	Spring	360	Y	2	15.0 (0.3)	0.01 (0.05)	0.85	<0.01	0.003
Skuas and Jaegers	Fall	11	Y	2	15.0 (0.3)	0.01 (0.05)	0.24	<0.01	0.053
	Summer	1	N	2	NA	NA	NA	NA	NA
	Winter	7	N	2	NA	NA	NA	NA	NA
	Spring	18	Y	2	15.0 (0.3)	0.01 (0.05)	0.59	<0.01	0.004
Small Gulls	Fall	4763	Y	2	15.0 (0.3)	0.01 (0.05)	0.22	<0.01	0.011
	Summer	48	Y	2	15.0 (0.3)	0.01 (0.05)	0.43	<0.01	0.004
	Winter	1511	Y	2	15.0 (0.3)	0.01 (0.05)	0.66	<0.01	0.004
	Spring	1415	Y	2	15.0 (0.3)	0.01 (0.05)	0.82	<0.01	0.006
Small Terns	Fall	0	N	2	NA	NA	NA	NA	NA
	Summer	92	Y	2	15.0 (0.3)	0.01 (0.05)	0.24	<0.01	0.508
	Winter	0	N	2	NA	NA	NA	NA	NA

Group	Season	Sample Size	Model Run	Mesh Cutoff Distance (km)	Prior Range Value (km) (probability of exceeding value)	Prior Standard Deviation (probability of exceeding value)	Wilcoxon Test	Estimated Median Density in Lease Area (Abundance/km ²)	Estimated Median Density in Study Area (Abundance/km ²)
	Spring	66	Y	6	2.0 (0.3)	0.08 (0.05)	0.44	<0.01	0.038
Storm-petrels	Fall	118	Y	2	15.0 (0.3)	0.01 (0.05)	0.68	<0.01	0.003
	Summer	5420	Y	2	15.0 (0.3)	0.01 (0.05)	0.96	<0.01	0.005
	Winter	71	Y	2	15.0 (0.3)	0.01 (0.05)	0.88	<0.01	8.684
	Spring	2407	Y	2	15.0 (0.3)	0.01 (0.05)	0.89	<0.01	0.011

5.1.7 Exposure Mapping

Maps were developed to visually display local and regional context for exposure assessments. A three-part map was created for each species-season combination that includes MDAT outputs and/or NY Bight survey data. Any species-season combination that did not have MDAT model outputs or NY Bight survey data (i.e., blank maps) was left out of the final map set. An example map for the Northern Gannet in the summer is provided in Figure 5-3. The complete set of species-season maps can be found in Attachment A.

To walk through the example figure, the first map panel (A) presents the NY Bight survey data as proportions of total effort-corrected counts. For each OCS lease block, the proportion of all effort-corrected counts (total counts per square kilometer) was calculated in the surveyed area that were located in that Lease Block (across all surveys in a given calendar season). By rescaling all density data as a quantile on a 0-1 scale, this method was useful for standardizing data visualizations between species. Exposure was ranked from low to high for each species based on weighted quantiles calculated for the OCS lease block proportion values. Quantiles were weighted by the densities in order for weighted quantiles to be comparable across species or groups. OCS lease blocks with zero counts were always the lowest, and blocks with more than one observation were divided into five weighted quantiles. Panel B similarly presents the NY Bight survey data, but as the output of the spatial density models built at the taxonomic level. The data are presented as the posterior median estimates of density (estimated abundance per 25 km² grid cell). The final map (Panel C) presents density outputs from MDAT models over the entire northwest Atlantic. Density data are scaled in a similar way to the NY Bight survey data, so that the low-high designation for density is similar for both datasets. However, there are no true zeroes in the model outputs, and thus no special category for them in the MDAT outputs. All MDAT models were masked to remove areas of zero effort within a season. These zero-effort areas do have density estimates, but generally are of low confidence, so they were excluded from mapping and analysis to reduce anomalies in predicted species densities and to strengthen the analysis. Additionally, while the color scale for the MDAT outputs is approximately matched to that used for the NY Bight survey data, the values that underlie the two model outputs are different (the MDAT outputs are symbolized using an ArcMap default color scale, which uses standard deviations from the mean to determine the color scale rather than quantiles). Similarly, the minimum and maximum densities calculated for both the digital aerial surveys and MDAT model outputs vary for each taxon and season combination. Therefore, maps should be viewed in a broadly relative way between local and regional assessments as well as even across taxa and season.

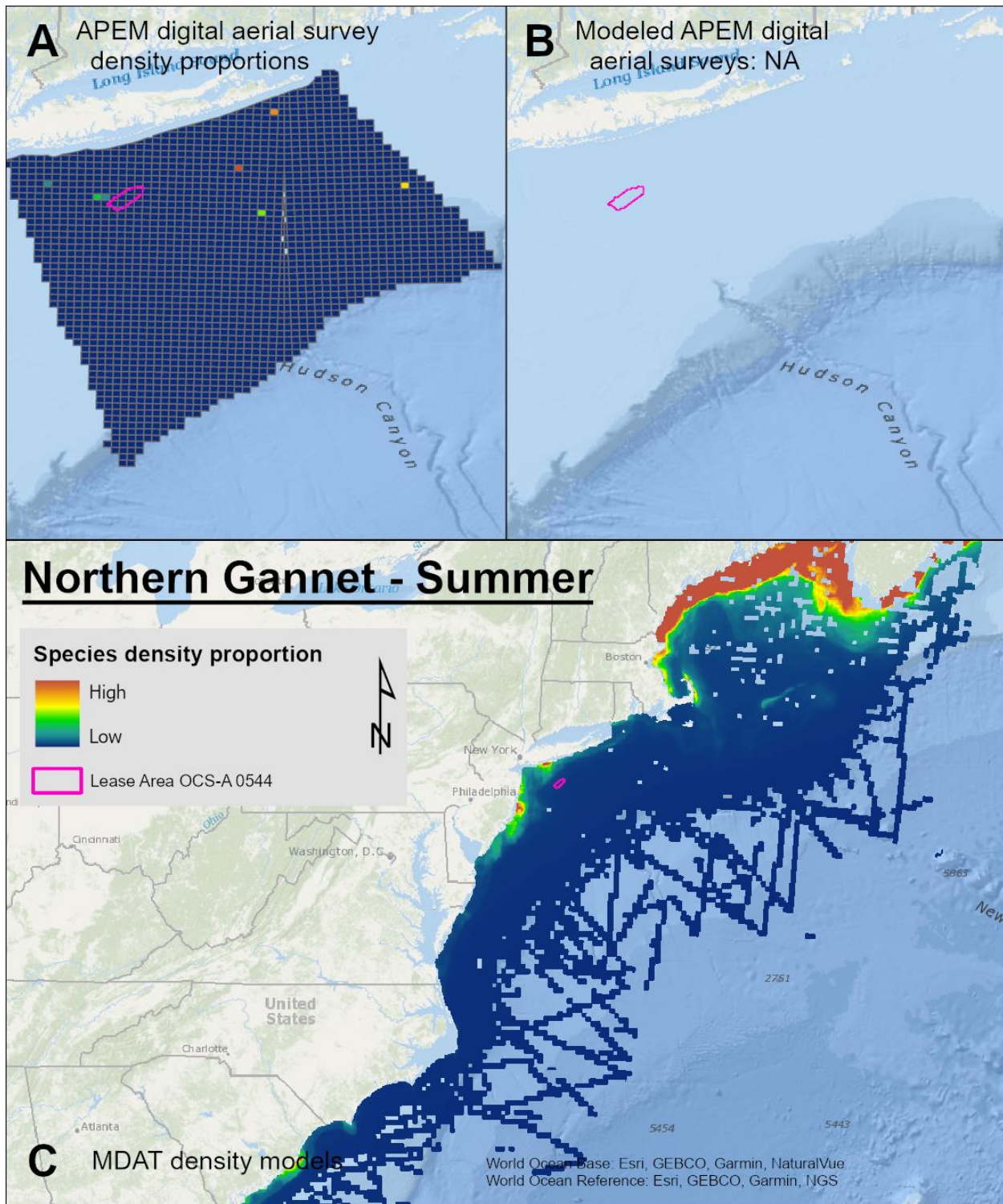


Figure 5-4: Example map of relative density proportions locally and regionally for Northern Gannet in the summer.

5.1.8 Exposure Assessment Metrics

BRI's exposure assessment was designed to assess bird exposure at both the local scale (the NY Bight survey area) and the regional scale (the MDAT scale of US Atlantic waters). At local and

regional scales, the Lease Area was compared to other similarly sized areas in each dataset for each season and taxa. For the local taxonomic density models, the seasonal predicted output of median density was analyzed by comparing the density of taxa within the 67 grid cells that comprise the Lease Area to other locations within the NYSEERDA region. To compare the Lease Area to other locations within the NY Bight survey area, the nearest 67 grid cells around each individual cell in the modeled output were identified and the relative density of each cell group was calculated. Thus, a dataset of relative densities for all possible Lease Area sized cell configurations was generated within the NY Bight survey area using the modeled density outputs. For the regional analysis, MDAT model outputs were masked to remove zero-effort predicted cells, and the predicted seasonal density surface for the species in a given taxonomic group was aggregated into a single density layer. The mean density estimate within the Lease Area was calculated by the spatially-weighted average of all regional density cells that overlapped the Lease Area. The cell size of the regional layer approximated the size of the Lease Area, so the resulting density estimate within the Lease Area was compared to the density predicted in all other cells. For both local and regional scoring, exposure was determined quantitatively at the taxonomic group level, rather than at the species level, because of the high prevalence of observations of unidentified members of a given group in the NY Bight survey datasets.

This process resulted in a dataset of true density estimates across the entire surveyed range of the taxa for areas the same size as the Lease Area across the NY Bight survey area, and a dataset of relative densities at the regional scale from the MDAT model outputs. The 25th, 50th, and 75th weighted quantiles of each dataset were calculated, as well as the quantile of the density estimate for the Lease Area for each species and season combination where taxa were sighted in the NY Bight survey area. Quantiles were weighted by using the proportion of the total density across the entire modeled area that each sample represented. Thus, quantile breaks represent proportions of the total bird density rather than proportions of the raw data. A score and category were assigned to the Lease Area for each season-taxa group combination: the score 0 (corresponding to the category Minimal) was assigned when the density estimate for the Lease Area was in the bottom 25%, 1 (Low) when it was between 25% and 50%, 2 (Medium) when it was between 50% and 75%, and 3 (High) when it was in the top quartile (>75%).

If a score for a given season-group combination was not available for the NY Bight survey area (local assessment), given that the avian surveys made all reasonable efforts to survey all species, excluding none, then the local assessment was scored a 0 (minimal) because no animals were sighted for that species season combination.

5.1.8.1 Exposure Scoring

To determine the relative exposure for a given group and season in the Lease Area compared to all other areas, the regional exposure score from the MDAT study region was added to the local exposure score from the NY Bight survey area to create a total season-group exposure score that

ranged from 0 to 6. The density information at both spatial scales was equally weighted, and thus accounted for both the local and regional importance of the Lease Area to a given group during a given season. However, if a season-group combination was not available for the MDAT regional assessment, then the score from the local assessment was accepted as the best available information for that season-group, and it was scaled to range from 0 to 6 (i.e., the available local or regional score was effectively doubled to arrive at the total score).

The total season-group exposure score was categorized as Minimal (a combined score of 0), Low (combined score of 1–2), Medium (combined score of 3–4), or High (combined score of 5–6; Table 5-2). In general terms, species-season combinations labeled as ‘Minimal’ had low densities at both the local and regional scales. ‘Low’ exposure was assessed for species with below-average densities at both spatial scales, or above-average density at one of the two scales and low density at the other scale. ‘Medium’ exposure describes several different combinations of densities; one or both scales must be at least above-average density, but this category can also include group-season combinations where density was high for one scale and low for another. ‘High’ exposure is when both scales are high density, or one is high, and the other is above average. Both local and regional exposure scores were viewed as equal in importance in the assessment of exposure.

Finally, because these scores are all relative to seasonal distribution, estimates of count density were provided within the Lease Area and over the entire survey area for each species from the NY Bight survey data (Table 4-28). Density estimates per square kilometer are presented to provide context for the exposure scores.

Table 5-2: Definitions of exposure levels developed for the avian assessment for each species and season.

NOTE: The listed scores represent the exposure scores from the local NY Bight surveys on the left and the regional MDAT on the right.

Exposure Level	Definition	Scores
Minimal	Densities at both local and regional scales are below the 25 th percentile.	0, 0
Low	Local and/or regional density is between the 25 th and 50 th percentiles. OR	0, 1 1, 0 1, 1
	Local density is between the 50 th and 75 th percentiles and regional density is below the 25 th percentile, or vice versa.	2, 0
Medium	Local or regional density is between the 50 th and 75 th percentiles. OR	2, 2
	Local density is between the 50 th and 75 th percentiles and regional density between the 25 th and 50 th percentiles, or vice versa. OR	2, 1
	Local density is greater than the 75 th percentile and regional density is below the 25 th percentile, or vice versa. OR	3, 0

Exposure Level	Definition	Scores
	Local density is greater than the 75 th percentile of all densities and regional density is between the 25 th and 50 th percentiles of all densities (or vice versa).	3, 1
High	Densities at both local and regional scales are above the 75 th percentile. OR	3, 3
	Local densities are greater than the 75 th percentile and regional densities are between the 50 th and 75 th percentiles, or vice versa.	3, 2

5.1.8.2 Interpreting Exposure Scores

The final exposure scores for each group and season should be interpreted as a measure of the relative importance of the Lease Area for a species/group, as compared to other surveyed areas in the region and in the northwest Atlantic. It does not indicate the absolute number of individuals likely to be exposed. Rather, the exposure score attempts to provide regional and population-level context for each taxon.

A High exposure score indicates that the observed and predicted densities of the taxon in the Lease Area were high relative to densities of that taxon in other surveyed areas. Conversely, a Low or Minimal exposure score means that the taxon was predicted to occur at much lower densities in the Lease Area than in other locations. A Minimal exposure score should not be interpreted to mean there are no individuals of that species in the Lease Area. In fact, common species may receive a Minimal exposure score even if there are still substantial numbers of individuals in the Lease Area, so long as their predicted densities *outside* are higher still. This quantitative annual exposure score was then considered with additional species-specific information, along with expert opinion, to place each species group within a final exposure category.

5.1.8.3 Exposure Categories

The quantitative assessment of exposure uses local and site-specific ecological baseline data (described above), model outputs (described above), tracking or other locally available data, existing literature, and species accounts to develop a final qualitative exposure determination. Final exposure level categories used in this assessment are described in Table 5-3.

Table 5-3: Assessment criteria used for assigning species to final (annual) exposure levels.

Final Exposure Level	Definition
Minimal	Minimal seasonal exposure scores in all seasons or minimal score in all but one season OR
	Based upon the literature—and, if available, other locally available tracking or survey data—little to no evidence of use (e.g., no record in Lease Area) of the offshore environment for breeding, wintering, or staging, and low predicted use during migration.

Final Exposure Level	Definition
Low	Low exposure scores in two or more seasons, or medium exposure score in one season OR Based upon the literature—and, if available, other locally available tracking or survey data—low evidence of use of the offshore environment during any season.
Medium	Medium exposure scores in two or more seasons, or High exposure score in one season OR Based upon the literature—and, if available, other locally available tracking or survey data—moderate evidence of use of the offshore environment during any season.
High	High exposure scores in two or more seasons OR Based upon the literature—and, if available, other locally available tracking or survey data—high evidence of use of the offshore environment, and the offshore environment is primary habitat during any season.

5.2 Vulnerability Framework

Researchers in Europe and the US have assessed the vulnerability of birds to offshore wind farms and general disturbance by combining ordinal scores across a range of key variables (Furness et al. 2013; Willmott et al. 2013; Wade et al. 2016; Kelsey et al. 2018; Fliessbach et al. 2019). The purpose of these indices was to prioritize species in environmental assessments (Desholm 2009) and provide a relative rank of vulnerability (Willmott et al. 2013). Importantly, past assessments and the one conducted here are intended to support decision-making by ranking the relative likelihood that a species will be sensitive to offshore wind farms, but should not be interpreted as an absolute determination that there will or will not be collision fatality or habitat loss. Therefore, the results should be interpreted as a guide to species that have a higher likelihood of vulnerability.

The existing vulnerability methods assess individual-level vulnerability to collision and displacement independently and then incorporate population-level vulnerability to develop a final species-specific vulnerability score. These past efforts provide useful rankings across a region but are not designed to assess the vulnerability of birds to a particular wind farm or certain WTG designs. Collision risk models (e.g., Band 2012) do estimate site-specific fatality, but are substantially influenced by assumptions about avoidance rates (Chamberlain et al. 2006). Furthermore, collision risk models do not explicitly assess vulnerability to displacement (i.e., macro-avoidance behaviors, leading to temporary or permanent displacement from a Lease Area, which can cause effective habitat loss). Thus, there is a need to develop a project-specific vulnerability score for each species that is inclusive of both collision and displacement and has fewer assumptions.

The scoring process in this assessment builds from the existing methods, incorporates the specifications of the WTGs being considered, utilizes local bird conservation status, and limits the

vulnerability score to the species observed in the local surveys. The results from this scoring method may differ for some species from the qualitative determinations made in other COP assessments because the input parameters use specific categorical definitions that in some cases are conservative (e.g., >40% macro-avoidance receives the highest score). The literature is also used to interpret scoring results, and, if empirical studies indicate a lower or higher vulnerability, a range is added to the final score (see uncertainty discussion below). For species or species groups for which inputs are lacking, the literature is used to qualitatively determine a vulnerability ranking using the criteria in Table 5-4. Below is a description of the scoring approach.

Table 5-4: Assessment criteria used for assigning species to each behavioral vulnerability level.

Behavioral Vulnerability	Definition
Minimal	0–0.25 ranking for collision or displacement risk in vulnerability scoring. OR No evidence of collisions or displacement in the literature. Unlikely to fly within the RSZ.
Low	0.26–0.50 ranking for collision or displacement risk in vulnerability scoring. OR Little evidence of collisions or displacement in the literature. Rarely flies within the RSZ.
Medium	0.51–0.75 ranking for collision or displacement risk in vulnerability scoring. OR Evidence of collisions or displacement in the literature. Occasionally flies within the RSZ.
High	0.76–1.0 ranking for collision or displacement risk in vulnerability scoring. OR Significant evidence of collisions or displacement in the literature. Regularly flies within the RSZ.

5.2.1 Population Vulnerability

Many factors contribute to how sensitive a population is to fatality or habitat loss related to the presence of a wind farm, including vital rates, existing population trends, and relative abundance of birds (Goodale and Stenhouse 2016). In this avian risk assessment, the relative abundance of birds is accounted for by the exposure analysis described above. The vulnerability assessment creates a population vulnerability score by using the Partners in Flight (PiF) “continental combined score” (CCSmax), a local “state status” (SSmax), and adult survival score (AS) (Equation 1). Survival is included as an independent variable that is not accounted for in the CCSmax. This approach is based upon methods used by Kelsey et al. (2018) and Fliessbach et al. (2019).

Each factor included in this assessment (CCSmax, SSmax, and AS) is weighted equally and receives a categorical score of 1–5 (Table 5-5). The final population level vulnerability scores are rescaled to a 0–1 scale, divided into quartiles, and are then translated into four final vulnerability

categories (Table 5-4). As using quartiles creates hard cut-off points and there is uncertainty present in all inputs (see discussion on uncertainty below), using scores alone can potentially misrepresent vulnerability (e.g., a 0.545 PV score leading to a minimal category). To account for this, the scores are considered along with information in existing literature. If there is evidence in the literature that conflicts with the vulnerability score, then the score will be appropriately adjusted (up or down) according to documented empirical evidence. For example, if a PV score was assessed as low, but a paper indicated an increasing population, the score would be adjusted to include a range of minimal–low.

$$PV = CCSmax + SSmax + AS \quad \text{Equation 1}$$

Specifics for each factor in PV are as follows:

- CCSmax is included in scoring because it integrates various factors PiF used to indicate global population health. It represents the maximum value for breeding and non-breeding birds developed by PiF, and combines the scores for population size, distribution, global threat status, and population trend (Panjabi et al. 2019). The CCSmax score from PiF was rescaled to a 1–5 scale to achieve consistent scoring among factors.
- SSmax is included in scoring to account for local conservation status, which is not included in the CCSmax. Local conservation status is generally determined independently by states and accounts for the local population size, population trends, and stressors on a species within a particular state. It was developed following methods by Adams et al. (2016) in which the state conservation status for the relevant adjacent states is placed within five categories (from 1 = no ranking to 5 = Endangered), and then, for each species, the maximum state ranking is selected.
- AS is included in the scoring because species with higher adult survival rates are more sensitive to increases in adult fatality because they tend to be species that are also long-lived and have low annual reproductive success (referred to by biologists as “K strategists”) (Desholm 2009; Adams et al. 2016). The five categories are based upon those used in several vulnerability assessments (Willmott et al. 2013; Kelsey et al. 2018; Fliessbach et al. 2019), and the species-specific values were used from Willmott et al. (2013).

Table 5-5: Data sources and scoring of factors used in the vulnerability assessment.

Vulnerability Component	Factor	Definition and Source	Scoring
Population Vulnerability (PV)	continental combined score (CCSmax)	CCSmax is Partners in Flight continental combined score: pif.birdconservancy.org/ACAD/Database.aspx	1 = Minor population sensitivity 2 = Low population sensitivity 3 = Medium population sensitivity 4 = High population sensitivity 5 = Very high population sensitivity

Vulnerability Component	Factor	Definition and Source	Scoring
	state status (<i>SSmax</i>)	SSmax from New York following Adams et al. (2016)	1 = No Ranking ¹ 2 = State/Federal Special Concern 3 = State/Federal Threatened 4 = State/Federal Endangered 5 = State & Federal Endangered and/or Threatened
	adult survival (<i>AS</i>)	AS score: scores and categories taken from Willmott et al. (2013)	1 = <0.75 2 = 0.75 to 0.80 3 = >0.80 to 0.85 4 = >0.85 to 0.90 5 = >0.90
Collision Vulnerability (<i>CV</i>)	rotor swept zone (<i>RSZt</i>)	WTG specific percentage of flight heights in RSZ. Flight heights modeled from Northwest Atlantic Seabird Catalog. Categories from Kelsey et al. (2018).	1 = <5% in RSZ 3 = 5–20% in RSZ 5 = >20% in RSZ
	macro-avoidance (<i>MAc</i>)	Avoidance rates and scoring categories from Willmott et al. (2013) and Kelsey et al. (2018).	1 = >40% avoidance 2 = 30 to 40% avoidance 3 = 18 to 29% avoidance 4 = 6 to 17% avoidance 5 = 0 to 5% avoidance
	Nocturnal Flight Activity (<i>NFA</i>) Diurnal Flight Activity (<i>DFA</i>)	NFA scores were taken from Willmott et al. (2013). DFA was calculated using NJDEP boat-based survey data that records behavior, including if birds are sitting or flying.	1 = 0 to 20% 2 = 21 to 40% 3 = 41 to 60% 4 = 61 to 80% 5 = 81 to 100%
Displacement Vulnerability (<i>DV</i>)	Macro-avoidance rate (<i>MAd</i>)	MAd rates that would decrease collision risk from Willmott et al. (2013) and Kelsey et al. (2018).	1 = 0 to 5% avoidance 2 = 6 to 17% avoidance 3 = 18 to 29% avoidance 4 = 30 to 40% avoidance 5 = >40% avoidance
	Habitat flexibility (<i>HF</i>)	The degree to which a species is considered a habitat generalist (i.e., can forage in a variety of habitats) or a specialist (i.e., requires specific habitat and prey type). HF score and categories taken from Willmott et al. (2013).	0 = species does not forage in the Atlantic Outer Continental Shelf 1 = species uses a wide range of habitats over a large area and usually has a wide range of prey available to it 2–4 = grades of behavior between Score 1 and Score 5 5 = species with habitat- and prey-specific requirements that do not have much flexibility in diving depth or choice of prey species

¹ Actual definitions for state conservation ranking may be adjusted to follow individual state language.

5.2.2 Collision Vulnerability

Collision vulnerability assessments can include a variety of factors including nocturnal flight activity, diurnal flight activity, avoidance, proportion of time within the RSZ, maneuverability in flight, and percentage of time flying (Furness et al. 2013; Willmott et al. 2013; Kelsey et al. 2018). The assessment process conducted here follows Kelsey et al. (2018) and includes proportion of time within the RSZ (RSZt), a measure of avoidance (MAc), and flight activity (NFA and DFA; see Equation 2, below). Each factor was weighted equally and given a categorical score of 1–5 (Table 5-5). The final collision vulnerability scores were rescaled to a 0–1 scale, divided into quartiles, and then translated into four final vulnerability categories (Table 5-4). As described in the PV section, the score is then considered along with information available in existing literature; if there is sufficient evidence to deviate from the quantitative score, a CV categorical range is assigned for each species.

$$CV = RSZt + MAc + (NFA + DFA)/2 \quad \text{Equation 2}$$

Specifics for each factor in CV are as follows:

- *RSZt* is included in the score to account for the probability that a bird may fly through the RSZ. Flight height data was selected from the Northwest Atlantic Seabird Catalog.

Many of the boat-based datasets provided flight heights as categorical ranges for which the mid-value of the range in meters were determined, as well as the lower and upper bounds of the category. Upper bounds that were given as greater than X m were capped at 500 m (1,640 ft) to estimate upper bounds. A few datasets provided exact flight height estimates which resulted in upper and lower ranges being the same as the mid-value. A total of 100 randomized datasets were generated per species using the uniform distribution to select possible flight height values between lower and upper flight height bounds. Similar to methods from Johnston et al. (2014), flight heights were modeled using a smooth spline of the square root of the binned counts in 10 meter (33 foot) bins. The integration of the smooth spline model count within each 1 meter (3 foot) increment was calculated and the mean and standard deviation of all 100 models were calculated across all 1 meter (3 foot) increments.

The proportion of animals within each RSZ was estimated by summing the 1 meter (3-foot) count integrations and dividing by the total estimate count of animals across all RSZ zones, then values were converted to a 1–5 scale based upon the categories used by Kelsey et al. (2018; Table 5-5). The RSZ was defined by the minimum air gap and the maximum rotor tip height, and should thus be considered the maximum design scenario (Table 5-6). The analysis was conducted in R Version 4.2.2.¹³ Of note, there are several

¹³ R Core Team (2021). R: A language and environment for statistical computing. R Foundation for Statistical Computing, Vienna, Austria. URL <https://www.R-project.org>

important uncertainties in flight height estimates: flight heights from boats can be skewed low; flight heights are generally recorded during daylight and in fair weather; and flight heights may change when WTGs are present.

Table 5-6: WTG specifications used in the vulnerability analysis. Mean sea level is the average hourly tidal height over 19 years.

WTG Parameter	Value
Blade tip lower height (clearance/air gap from mean sea level)	27 m (88.6 ft)
Blade tip upper height (from mean sea level)	355 m (1,164.7 ft)

- MAc* is included in the score to account for macro-avoidance rates that would decrease collision risk. Macro-avoidance is defined as a bird’s ability to change course to avoid the entire Lease Area (Kelsey et al. 2018), versus meso-avoidance (avoiding individual WTGs), and micro-avoidance (avoiding WTG blades; Skov et al. 2018). The scores used in the assessment were based on Willmott et al. (2013), who conducted a literature review to determine known macro-avoidance rates and then converted them to a 1–5 score based upon the categories in Table 5-5. The *MAc* indicates that this factor is used in the CV versus the *MA_d*, which was used in the displacement vulnerability score (described below). For the assessment conducted here, Willmott et al. (2013) avoidance rates were updated to reflect the most recent empirical studies (Krijgsveld et al. 2011; Cook et al. 2012; Vanermen et al. 2015; Cook et al. 2018), and indexes (Garthe and Hüppop 2004; Furness et al. 2013; Bradbury et al. 2014; Adams et al. 2016; Wade et al. 2016; Kelsey et al. 2018). For the empirical studies, the average avoidance was used when a range was provided in a paper. For the indices, the scores were converted to a continuous value using the median of a scores range; only one value was entered for related indices (e.g., Adams et al. 2016 and Kelsey et al. 2018). When multiple values were available for a species, the mean value was calculated. For some species, averaging the avoidance rates across both the empirical studies and indices led to some studies being counted multiple times. Indices were included to capture how the authors interpreted the avoidance studies and determined avoidance rates for species where data was not available. There are several important uncertainties in determining avoidance rates: the studies were all conducted in Europe; the studies were conducted at wind farms with WTGs smaller than are proposed for the Lease Area; the methods used to record avoidance rates varied and included surveys, radar, and observers; the analytical methods used to estimate avoidance rates also varied significantly between studies; and the avoidance rate for species where empirical data is not available were assumed to be similar to closely-related species.
- NFA* and *DFA* include scores of estimated percentages of time spent flying at night and during the day based upon the assumption that more time spent flying would increase

collision risk. The NFA scores were taken directly from the scores, based upon literature review, from Willmott et al. (2013). The DFA scores were calculated from the baseline survey data that categorized if a bird was sitting or flying for each bird observation. Per Kelsey et al. (2018), the NFA and DFA scores were equally weighted and averaged.

5.2.3 Displacement Vulnerability

Rankings of DV account for two factors: (1) disturbance from ship/helicopter traffic and the wind farm structures (MAd), and (2) habitat flexibility (HF; Furness et al. 2013; Kelsey et al. 2018). This assessment combines these two factors, weights them equally, and categorizes them from 1–5 (Equation 3 below; Table 5-5). It is worth noting that while Furness et al. (2013) down-weighted the DV score by dividing by 10 (they assumed displacement would have lower impacts on the population), the assessment conducted here maintains the two scores on the same scale.

Empirical studies indicate that for some species, particularly sea ducks, avoidance behavior may change through time and that several years after projects have been built some individuals may forage within the wind farm. The taxonomic specific text indicates whether there is evidence that displacement may be partially temporary. The final displacement vulnerability scores are rescaled to a 0–1 scale, divided into quartiles, and translated into four final vulnerability categories (Table 5-5). As described in the PV section, the score is then considered along with the literature; if there is sufficient evidence to deviate from the quantitative score, a DV categorical range is assigned for each species.

$$DV = MAd + HF \quad \text{Equation 3}$$

Specifics for each factor in DV are as follows:

- *MAd* is included to account for behavioral responses from birds that lead to macro-avoidance of wind farms, and that have the potential to cause effective habitat loss if the birds are permanently displaced (Fox et al. 2006). The MAd scores used in the assessment were based on Willmott et al. (2013) but updated to reflect the most recent empirical studies (Krijgsveld et al. 2011; Cook et al. 2012; Vanermen et al. 2015; Cook et al. 2018; Skov et al. 2018), and indexes (Garthe and Hüppop 2004; Furness et al. 2013; Bradbury et al. 2014; Adams et al. 2016; Wade et al. 2016; Kelsey et al. 2018). See MAC above for further details. The scores are the same as the MAC scores described above, but, following methods from Kelsey et al. (2018), are inverted so that a high avoidance rate (greater than 40 %) is scored as a 5. Since the greater than 40 % cutoff is a low threshold, many species can receive a high 5 score; there is a large range within this high category that includes species documented to have moderate avoidance rates (e.g., terns) and species with near complete avoidance (e.g., loons).

- *HF* accounts for the degree to which a species is considered a habitat generalist (i.e., can forage in a variety of habitats) or a specialist (i.e., requires specific habitat and prey type). The assumption is that generalists are less likely to be affected by displacement, whereas specialists are more likely to be affected (Kelsey et al. 2018). The values for HF used in this assessment were taken from Willmott et al. (2013). Note that Willmott et al. (2013) used a 1–5 scale plus a “0” to indicate that a species does not forage in the OCS.

5.3 Uncertainty

Uncertainty is recognized in this assessment for both exposure and vulnerability. Given the natural variability of ecosystems and recognized knowledge gaps, assessing how anthropogenic actions will affect the environment inherently involves a degree of uncertainty (Walker et al. 2003). Broadly defined, uncertainty is incomplete information about a subject (Masden et al. 2015) or a deviation from absolute determinism (Walker et al. 2003). In the risk assessment conducted here, uncertainty is broadly recognized as a factor in the process, and is accounted for by including, based on the best available data, a range for the exposure, vulnerability, and population scores when appropriate.

For offshore wind avian assessments, uncertainty primarily arises from two sources: predictions of bird use of a project area and region (i.e., exposure), and our understanding of how birds interact with WTGs (i.e., vulnerability). Uncertainty will always be present in any assessment of offshore wind, and acquiring data on bird movements during hours of darkness and in poor weather is difficult. Despite these challenges, overall knowledge on bird use of the marine environment has improved substantially in recent years through local survey efforts, revised regional modeling efforts, and individual tracking studies. For many species, multiple data sources may be available to make an exposure assessment, such as survey and individual tracking data. If the data sources show differing patterns in use of the Lease Area, then a range of exposure is provided (e.g., minimal–low) to account for all available data and to capture knowledge gaps and general uncertainty about bird movements. To quantify the uncertainty in BRI’s exposure assessments, we developed a simple process by which we score each taxonomic group or listed species for the number of significant data sources available, those used in the exposure assessment itself, and those that provide support for the result of the assessment. All species/group assessments start with information gleaned from available literature, including species accounts, published studies, incidental observations, and expert knowledge. Each species/group is then scored (1) for each additional data source (local baseline data, a regional database or distribution model, and spatial data from tracking studies), plus data sources that support the assessment (site-specific surveys), each of which is weighted equally. Scores are then tallied, and the more resources contributing to or supporting the assessment, the higher the score, the greater our confidence in the exposure assessment, and the lower the uncertainty – 0-1 = High, 2 = Medium, 3 = Low, 4 = Minimal (Table 5-7).

Table 5-7: Description of data sources and their contribution to uncertainty scores.

Data Source	Description	Added to score
Literature	Species accounts, published studies, incidental observations, expert opinion	•
MDAT	Modeled spatial distributions and predicted relative densities across time	1
Baseline	Regional ecological baseline data, either historical (>10 years) or recent	1
Site-specific	Local baseline data that specifically overlaps the development area (recent)	1
Tracking	Spatial data from tracking studies, including VHF (Motus), GPS, or satellite	1
Scores: 0-1 = High, 2 = Medium, 3 = Low, 4 = Minimal		

As with exposure, knowledge has been increasing on the vulnerability of birds to offshore wind facilities in Europe (e.g., Skov et al. 2018). Vulnerability assessments have either incorporated uncertainty into the scoring process to calculate a range of ranks (Willmott et al. 2013, Kelsey et al. 2018) or have developed separate standalone tables (Wade et al. 2016). In BRI’s vulnerability assessment, as with exposure, if there is evidence in the literature or from other data sources that conflicts with the initial vulnerability score, the resulting determination will be adjusted up or down, as appropriate, to include a range that extends into the next category. This approach accounts for knowledge gaps and general uncertainty about vulnerability. To quantify the uncertainty in our vulnerability assessment, we developed a similar approach to that described above for exposure; data sources are scored in quality for each of the parameters that are included in the vulnerability analysis. For collision vulnerability, the parameters are flight height, avoidance, and flight activity, and for displacement vulnerability the parameters are avoidance and habitat flexibility. The results of this vulnerability uncertainty scoring are presented in Table 4-27.

6 Literature Cited

- Adams J, Kelsey E C, Felis J, & Pereksta D M. 2016. Collision and displacement vulnerability among marine birds of the California Current System associated with offshore wind energy infrastructure (Issue July). <https://doi.org/10.3133/ofr20161154>
- Aiello-Lammens, M. E., M. L. Chu-Agor, M. Convertino, R. A. Fischer, I. Linkov, and H. Resit Akçakaya. 2011. "The impact of sea-level rise on Snowy Plovers in Florida: Integrating geomorphological, habitat, and metapopulation models." *Global Change Biology* 17 (12): 3644–54. doi:10.1111/j.1365-2486.2011.02497.x.
- Ainley, D. G., D. N. Nettleship, and A. E. Storey. 2021. Common Murre (*Uria aalge*), version 2.0. In *Birds of the World* (S. M. Billerman, P. G. Rodewald, and B. K. Keeney, Editors). Cornell Lab of Ornithology, Ithaca, NY, USA. <https://doi.org/10.2173/bow.commur.02>
- American Wind Wildlife Institute. 2016. "Wind Turbine Interactions with Wildlife and Their Habitats: A Summary of Research Results and Priority Questions. (Updated June 2016). Washington, DC. Available at [www.Awwi.Org](http://www.awwi.org)."
- Anderson, E. M., R. D. Dickson, E. K. Lok, E. C. Palm, J.-P. L. Savard, D. Bordage, and A. Reed 2020. Surf Scoter (*Melanitta perspicillata*), version 1.0. In *Birds of the World* (P. G. Rodewald, Editor). Cornell Lab of Ornithology, Ithaca, NY, USA. <https://doi.org/10.2173/bow.sursco.01>
- Arnold, J. M., S. A. Oswald, I. C. T. Nisbet, P. Pyle, and M. A. Patten (2020). Common Tern (*Sterna hirundo*), version 1.0. In *Birds of the World* (S. M. Billerman, Editor). Cornell Lab of Ornithology, Ithaca, NY, USA. <https://doi.org/10.2173/bow.comter.01>
- Atlantic Coast Joint Venture. 2022. "Saltmarsh Restoration Priorities for the Saltmarsh Sparrow New Jersey Goal Statement."
- American Wind Wildlife Institute (AWWI). 2020. AWWI Technical Report: 2nd Edition: Summary of Bird Fatality Monitoring Data Contained in AWWIC. Washington, DC. Available at www.awwi.org. © 2020 American Wind Wildlife Institute.
- Bachl FE, Lindgren F, Borchers DL, Illian JB. 2019. inlabru: an R package for Bayesian spatial modelling from ecological survey data. *Methods in Ecology and Evolution*. 10(6):760–766. doi:10.1111/2041-210X.13168.
- Baker, A., P. Gonzalez, R.I.G. Morrison, and B.A. Harrington. 2020. "Red Knot (*Calidris Canutus*), Version 1.0." In *Birds of the World*, edited by S.M. Billerman. Ithaca, NY, USA: Cornell Lab of Ornithology. <https://doi.org/10.2173/bna.563>.
- Baldassarre, G.A. 2014. *Ducks, Geese, and Swans of North America*. Johns Hopkins University Press. 1088 pp.

Ballerini, T., G. Tavecchia, F. Pezzo, S. Jenouvrier, and S. Olmastroni. 2015. "Predicting responses of the Adélie Penguin population of Edmonson Point to future sea ice changes in the Ross Sea." *Frontiers in Ecology and Evolution* 3 (FEB). Frontiers Media S. A. doi:10.3389/fevo.2015.00008.

Barbraud, C., P. Rivalan, P. Inchausti, M. Nevoux, V. Rolland, and H. Weimerskirch. 2011. "Contrasted demographic responses facing future climate change in Southern Ocean seabirds." *Journal of Animal Ecology* 80 (1): 89–100. doi:10.1111/j.1365-2656.2010.01752.x.

Bierregaard, R. O., A. F. Poole, M. S. Martell, P. Pyle, and M. A. Patten. 2020. Osprey (*Pandion haliaetus*), version 1.0. In *Birds of the World* (P. G. Rodewald, Editor). Cornell Lab of Ornithology, Ithaca, NY, USA. <https://doi.org/10.2173/bow.osprey.01>

Bonnot, T. W., F. R. Thompson, and J. J. Millspaugh. 2017. "Dynamic-landscape metapopulation models predict complex response of wildlife populations to climate and landscape change." *Ecosphere* 8 (7). Ecological Society of America. doi:10.1002/ecs2.1890.

Both, C., M. van Asch, R. G. Bijlsma, A. B. van den Burg, and M. E. Visser. 2009. "Climate change and unequal phenological changes across four trophic levels: constraints or adaptations?" *Journal of Animal Ecology* 78 (1): 73–83. doi:10.1111/j.1365-2656.2008.01458.x.

Bowman, T. D., Silverman, E. D., Gilliland, S. G., & Leirness, J. B. (2015). Status and trends of North American sea ducks: reinforcing the need for better monitoring. In J.-P. L. Savard, D. v. Derksen, D. Esler, & J. M. Eadie (Eds.), *Ecology and Conservation of North American Sea Ducks* (1st ed., pp. 1–28). CRC Press.

Brzorad, n. 2023. Data from: Egrets and Great Blue Heron. Movebank ID 17469219. https://www.movebank.org/cms/webapp?gwt_fragment=page=studies,path=study17469219

Buehler, D. A.. 2022. Bald Eagle (*Haliaeetus leucocephalus*), version 2.0. In *Birds of the World* (P. G. Rodewald and S. G. Mlodinow, Editors). Cornell Lab of Ornithology, Ithaca, NY, USA. <https://doi.org/10.2173/bow.baleag.02>

Bull, L S, S Fuller, and D Sim. 2013. "Post-Construction Avian Mortality Monitoring at Project West Wind." *New Zealand Journal of Zoology* 40 (1): 28–46. <https://doi.org/10.1080/03014223.2012.757242>.

Bureau of Ocean Energy Management. 2012. "Commercial Wind Lease Issuance and Site Characterization Activities on the Atlantic Outer Continental Shelf Offshore New Jersey, Delaware, Maryland, and Virginia Final Environmental Assessment." OCS Study BOEM 2012-003. US Department of the Interior, Bureau of Ocean Energy Management, Herndon, VA. 366 pp. <https://www.boem.gov/sites/default/files/documents/renewable-energy/state-activities/Mid-Atlantic-Final-EA-2012.pdf>.

Bureau of Ocean Energy Management. 2012. "Commercial Wind Lease Issuance and Site Characterization Activities on the Atlantic Outer Continental Shelf Offshore New Jersey, Delaware, Maryland, and Virginia Draft Environmental Assessment."

Bureau of Ocean Energy Management. 2012. "Developing Environmental Protocols and Modeling Tools to Support Ocean Renewable Energy and Stewardship. OCS 2012-082." Herndon, VA.

Bureau of Ocean Energy Management. 2014. "Commercial Wind Lease Issuance and Site Assessment Activities on the Atlantic Outer Continental Shelf Offshore Massachusetts: Revised Environmental Assessment." OCS EIS/EA BOEM 2014-603. US Department of the Interior, Bureau of Ocean Energy Management, Herndon, VA. 674 pp. <http://www.boem.gov/Revised-MA-EA-2014/>.

Bureau of Ocean Energy Management. 2018. "Vineyard Wind Offshore Wind Energy Project Draft Environmental Impact Statement. OCS EIS/EA BOEM 2018-060."

Bureau of Ocean Energy Management. 2018. "Vineyard Wind Offshore Wind Energy Project Draft Environmental Impact Statement. OCS EIS/EA BOEM 2018-060." US Department of the Interior, Bureau of Ocean Energy Management, Headquarters, Herndon, VA. 478 pp.

Bureau of Ocean Energy Management. 2019a. "National Environmental Policy Act Documentation for Impact-Producing Factors in the Offshore Wind Cumulative Impacts Scenario on the North Atlantic Continental Shelf. US Dept. of the Interior, Bureau of Ocean Energy Management, Office of Renewable Energy." <https://www.boem.gov/IPFs-in-the-Offshore-Wind-Cumulative-Impacts-Scenario-on-the-N-OCS/>.

Bureau of Ocean Energy Management. 2019b. "Vineyard Wind Offshore Wind Energy Project Biological Assessment: Final." Report by US Department of the Interior, Bureau of Ocean Energy Management for the US Fish and Wildlife Service. 51 pp.

Bureau of Ocean Energy Management. 2021. "Vineyard Wind 1 Offshore Wind Energy Project Final Environmental Impact Statement Volume II." OCS EIS/EA BOEM 2021-0012. p. 642. <https://www.boem.gov/vineyard-wind>.

Bureau of Ocean Energy Management. 2022. "Ocean Wind 1 Offshore Wind Farm Draft Environmental Impact Statement." OCS EIS/EA BOEM 2022-0021. US Department of the Interior, Bureau of Ocean Energy Management, Office of Renewable Energy Programs.

Bureau of Ocean Energy Management. 2023. Guidance on Information Needed for Issuance of a Notice of Intent (NOI) Under the National Environmental Policy Act (NEPA) for a Construction and Operations Plan. Published online August, 2023. <https://www.boem.gov/node/30996>

Burger, J., L.J. Niles, R.R. Porter, A.D. Dey, S. Kock, and C. Gordon. 2012. "Migration and Over-Wintering of Red Knots (*Calidris Canutus Rufa*) along the Atlantic Coast of the United States." *The Condor* 114 (2): 302–13. <https://doi.org/10.1525/cond.2012.110077>.

Burger, Joanna, Caleb Gordon, J. Lawrence, James Newman, Greg Forcey, and Lucy Vlietstra. 2011. "Risk Evaluation for Federally Listed (Roseate Tern, Piping Plover) or Candidate (Red Knot) Bird Species in Offshore Waters: A First Step for Managing the Potential Impacts of Wind Facility

Development on the Atlantic Outer Continental Shelf.” *Renewable Energy* 36 (1): 338–51.
<https://doi.org/10.1016/j.renene.2010.06.048>.

Burger, C., A. Schubert, S. Heinänen, M. Dorsch, B. Kleinschmidt, R. Žydelis, J. Morkūnas, P. Quillfeldt and G. Nehls. 2019. A novel approach for assessing effects of ship traffic on distributions and movements of seabirds. *Journal of Environmental Management* 251: 109511.

Canada Meteorological Center. 2016. GHRSSST Level 4 CMC 0.1 deg global sea surface temperature analysis. Ver. 3.0. PO.DAAC, CA, USA. Dataset accessed [2023-05-08] at <https://doi.org/10.5067/GHCMC-4FM03>

Choi, D.Y., T.W. Wittig, and B.M. Kluever. 2020. “An Evaluation of Bird and Bat Mortality at Wind Turbines in the Northeastern United States.” *PLoS ONE* 15 (8).

Cleasby, I.R., E.D. Wakefield, S. Bearhop, T.W. Bodey, S.C. Votier, and K.C. Hamer. 2015. “Three-Dimensional Tracking of a Wide-Ranging Marine Predator: Flight Heights and Vulnerability to Offshore Wind Farms.” *Journal of Applied Ecology* 52 (6): 1474–82.
<https://doi.org/10.1111/1365-2664.12529>.

Cochran, William W. 1985. “Ocean Migration of Peregrine Falcons: Is the Adult Male Pelagic?” In *Proceedings of Hawk Migration Conference IV*, edited by M. Harwood, 223–37. Rochester, NY: Hawk Migration Association of North America.

Cook, Aonghais S C P, Alison Johnston, Lucy J Wright, and Niall H K Burton. 2012. “A Review of Flight Heights and Avoidance Rates of Birds in Relation to Offshore Wind Farms.” BTO Research Report Number 618. British Trust for Ornithology, Thetford, UK. 61 pp.
http://www.bto.org/sites/default/files/u28/downloads/Projects/Final_Report_SOSS02_BTORevie w.pdf.

Cook, A. S. C. P., Humphreys, E. M., Bennet, F., Masden, E. A., & Burton, N. H. K. 2018. “Quantifying avian avoidance of offshore wind turbines: Current evidence and key knowledge gaps.” *Marine Environmental Research*, 140, 278–288.
<https://doi.org/https://doi.org/10.1016/j.marenvres.2018.06.017>

Cooke, Fred, Gregory J Robertson, Cyndi M Smith, R Ian Goudie, W Sean Boyd, and J Robertson. 2012. “SURVIVAL , EMIGRATION , AND WINTER POPULATION STRUCTURE OF HARLEQUIN DUCKS.” *The Condor* 102 (1): 137–44.

Corre, M le, A Ollivier, S Ribes, P Jouventin, and Anonymous. 2002. “Light-Induced Mortality of Petrels: A 4-Year Study from Réunion Island (Indian Ocean).” *Biological Conservation* 105 (1): 93–102. <http://www.scopus.com/scopus/inward/record.url?eid=2-s2.0-0036128791&partner=40&rel=R5.0.4>.

Cottam, C. 1939. “Food Habits of North American Diving Ducks.” US Department of Agriculture Technical Bulletin, 140.

Cranmer, Alexana, Jennifer R Smetzer, Linda Welch, and Erin Baker. 2017. "A Markov Model for Planning and Permitting Offshore Wind Energy: A Case Study of Radio-Tracked Terns in the Gulf of Maine, USA." *Journal of Environmental Management* 193: 400–409.

Curtice, C., J. Cleary, E. Scumchenia, and P.N. Halpin. 2019. "Marine-Life Data and Analysis Team (MDAT) Technical Report on the Methods and Development of Marine-Life Data to Support Regional Ocean Planning and Management. Prepared on Behalf of the Marine-Life Data and Analysis Team (MDAT)."

Deakin, Z., Cook, A., Daunt, F., McCluskie, A., Morley, N., Witcutt, E., Wright, L., & Bolton, M. (2022). A review to inform the assessment of the risk of collision and displacement in petrels and shearwaters from offshore wind developments in Scotland. Report Produced for the Scottish Government. <https://www.researchgate.net/publication/366139542>

DeLuca, William V, Kent P McFarland, Bradley K Woodworth, Christopher C Rimmer, Peter P Marra, et al. 2015. "Transoceanic Migration by a 12 g Songbird." *Biology Letters* 11: 20141045.

DeLuca, W., R. Holberton, P. D. Hunt, and B. C. Eliason (2020). Blackpoll Warbler (*Setophaga striata*), version 1.0. In *Birds of the World* (A. F. Poole, Editor). Cornell Lab of Ornithology, Ithaca, NY, USA. <https://doi.org/10.2173/bow.bkpwar.01>

Desholm, Mark, and Johnny Kahlert. 2005. "Avian Collision Risk at an Offshore Wind Farm." *Biology Letters* 1 (3): 296–98. <https://doi.org/10.1098/rsbl.2005.0336>.

DeSorbo, C. R., Christopher Persico, and Lauren Gilpatrick. 2018. "Studying Migrant Raptors Using the Atlantic Flyway. Block Island Raptor Research Station, Block Island, RI: 2017 Season." BRI Report # 2018-12 submitted to The Nature Conservancy, Block Island, Rhode Island, and The Bailey Wildlife Foundation, Cambridge, Massachusetts. Biodiversity Research Institute, Portland, Maine. 35 pp.

Desorbo, Christopher R., Christopher Persico, Rick B. Gray, and L. Gilpatrick. 2017. "Studying Migrant Raptors Using the Atlantic Flyway. Block Island Raptor Research Station, RI: 2016 Season." BRI Report #2017-08 submitted to The Nature Conservancy, Block Island, and The Bailey Wildlife Foundation, Cambridge, Massachusetts. Biodiversity Research Institute, Portland, Maine. 34 pp.

DeSorbo, Christopher R., Kenneth G. Wright, and Rick Gray. 2012. "Bird Migration Stopover Sites: Ecology of Nocturnal and Diurnal Raptors at Monhegan Island." Report BRI 2012-09 submitted to the Maine Outdoor Heritage Fund, Pittston, Maine, and the Davis Conservation Foundation, Yarmouth, Maine. Biodiversity Research Institute, Gorham, Maine. 43 pp. <http://www.briloon.org/raptors/monhegan>.

DeSorbo, C.R., R.B. Gray, J. Tash, C.E. Gray, K.A. Williams, and D. Riordan. 2015. "Offshore Migration of Peregrine Falcons (*Falco peregrinus*) Along the Atlantic Flyway. In *Wildlife Densities and Habitat Use Across Temporal and Spatial Scales on the Mid-Atlantic Outer Continental Shelf*:

Final Report to the Department of Energy EER.” Edited by Kathryn A. Williams, Emily E. Connelly, Sarah. M. Johnson, and Iain J. Stenhouse. Award Number: DE-EE0005362. Report BRI 2015-11, Biodiversity Research Institute, Portland, Maine. 28 pp.

Dias, M. P., R. Martin, E. J. Pearmain, I. J. Burfield, C. Small, R. A. Phillips, O. Yates, B. Lascelles, P. G. Borboroglu, and J. P. Croxall. 2019. “Threats to seabirds: a global assessment.” *Biological Conservation*. Elsevier Ltd. doi:10.1016/j.biocon.2019.06.033.

Dierschke, Volker, Robert W. Furness, and Stefan Garthe. 2016. “Seabirds and Offshore Wind Farms in European Waters: Avoidance and Attraction.” *Biological Conservation* 202: 59–68. <https://doi.org/10.1016/j.biocon.2016.08.016>.

DiGaudio, R., and G. R. Geupel. 2014. “Assessing Bird and Bat Mortality at the McEvoy Ranch Wind Turbine in Marin County, California, 2009-2012. Point Blue Conservation Science.”

Dirksen, S., A.L. Spaans, and J. van der Winden. 2000. “Studies on Nocturnal Flight Paths and Altitudes of Waterbirds in Relation to Wind Turbines: A Review of Current Research in the Netherlands. In Proceedings of the National Avian-Wind Power Planning Meeting III, San Diego, California, May 2000.”

Dolinski, Lauren. 2019. Landscape Factors Affecting Foraging Flight Altitudes of Great Blue Heron in Maine; Relevance to Wind Energy Development. Orono, ME: University of Maine.

Dorr, B.S., J.J. Hatch, and D.V. Weseloh. 2021. “Double-Crested Cormorant (*Phalacrocorax auritus*), Version 1.0.” In *Birds of the World*, edited by A.F. Poole. Ithaca, NY, USA: Cornell Lab of Ornithology. <https://doi.org/10.2173/bna.441>.

Dupigny-Giroux, L.-A., E. Mecray, M. Lemcke-Stampone, G. A. Hodgkins, E. E. Lentz, K. E. Mills, E. D. Lane, R. Miller, D. Hollinger, W. D. Solecki, G. A. Wellenius, P. E. Sheffield, A. B. MacDonald, and C. Caldwell. 2018. “Chapter 18 : Northeast. impacts, risks, and adaptation in the United States: The Fourth National Climate Assessment, Volume II.” Washington, DC. doi:10.7930/NCA4.2018.CH18.

Dürr, T. 2011. “Bird Loss of Wind Turbines in Germany: Data from the Central Register of the National Fund Ornithological Station State Office for Environment Office, Health and Consumer Protection, Brandenburg, Germany.” 2011.

Eadie, J. M., & Savard, J.-P. L. (2015). Breeding systems, spacing behavior, and reproductive behavior of sea ducks. In J.-P. L. Savard, D. v. Derksen, D. Esler, & J. M. Eadie (Eds.), *Ecology and Conservation of North American Sea Ducks* (1st ed., pp. 365–416). CRC Press. <https://doi.org/10.1201/b18406>

Egevang, C., I.J. Stenhouse, R.A. Phillips, A. Petersen, J.W. Fox & J.R.D. Silk. 2010. Tracking of Arctic Terns (*Sterna paradisaea*) reveals longest animal migration. *Proceedings of the National Academy of Sciences* 107: 2078-2081.

Elliott-Smith, Elise, and Susan M. Haig. 2020. "Piping Plover (*Charadrius Melodus*), Version 1.0." In *Birds of the World*, edited by A.F. Poole. Ithaca, NY, USA: Cornell Lab of Ornithology. <https://doi.org/DOI: 10.2173/bna.2>.

Epsilon Associates Inc. 2018. "Draft Construction and Operations Plan. Vineyard Wind Project. October 22, 2018. Accessed November 4, 2018. Retrieved from: <https://www.boem.gov/Vineyard-Wind/>."

Erickson, Wallace P., Melissa M. Wolfe, Kimberly J. Bay, Douglas H. Johnson, and Joelle L. Gehring. 2014. "A Comprehensive Analysis of Small-Passerine Fatalities from Collision with Turbines at Wind Energy Facilities." *PLoS ONE* 9 (9). <https://doi.org/10.1371/journal.pone.0107491>.

Erickson, W.P., J.D. Jeffrey, and V.K. Poulton. 2008. "Avian and Bat Monitoring: Year 1 Report. Puget Sound Energy Wild Horse Wind Project, Kittitas County, Washington." Western EcoSystems Technology, Inc. (WEST), Cheyenne, WY.

Everaert, Joris, and Eric W.M. Stienen. 2007. "Impact of Wind Turbines on Birds in Zeebrugge (Belgium): Significant Effect on Breeding Tern Colony Due to Collisions." *Biodiversity & Conservation* 16: 3345–59. <https://doi.org/10.1007/s10531-006-9082-1>.

Fox, A D, Mark Desholm, Johnny Kahlert, Thomas Kjaer Christensen, and I K Petersen. 2006. "Information Needs to Support Environmental Impact Assessment of the Effects of European Marine Offshore Wind Farms on Birds." *Ibis* 148 (01): 129–44. <https://doi.org/10.1111/j.1474-919X.2006.00510.x>.

Fox, A.D., and I.K. Petersen. 2019. "Offshore Wind Farms and Their Effects on Birds." *Dansk Orn. Foren. Tidsskr.* 113: 86–101.

Fuglstad GA, Simpson D, Lindgren F, Rue H. 2018. Constructing Priors that Penalize the Complexity of Gaussian Random Fields. <https://doi.org/10.1080/01621459.2017.1415907>. 114(525):445–452. doi:10.1080/01621459.2017.1415907.

Furness, R.W., H.M. Wade, and E.A. Masden. 2013. "Assessing Vulnerability of Marine Bird Populations to Offshore Wind Farms." *Journal of Environmental Management* 119: 56–66. <https://doi.org/10.1016/j.jenvman.2013.01.025>.

Galbraith, H., D. W. DesRochers, S. Brown, and J. M. Reed. 2002. "Global climate change and sea level rise: Potential losses of intertidal habitat for shorebirds." *Waterbirds* 25 (2). The Waterbird Society: 173–83. doi:10.1675/1524-4695(2002)025[0173:gccasl]2.0.co;2.

Galbraith, H., R. Jones, R. Park, J. Clough, S. Herrod-Julius, B. Harrington, and G. Page. 2014. "Predicting vulnerabilities of North American shorebirds to climate change." *PLoS ONE* 9 (9). Public Library of Science. doi:10.1371/journal.pone.0108899.

Garthe, S., N. Markones, and A.M. Corman. 2017. "Possible Impacts of Offshore Wind Farms on Seabirds: A Pilot Study in Northern Gannets in the Southern North Sea." *Journal of Ornithology* 158 (1): 345–49. <https://doi.org/10.1007/s10336-016-1402-y>.

Garthe, S., Guse, N., Montevecchi, W. A., Rail, J. F., & Grégoire, F. 2014. "The daily catch: Flight altitude and diving behavior of northern gannets feeding on Atlantic mackerel." *Journal of Sea Research*, 85: 456–462. <https://doi.org/10.1016/j.seares.2013.07.020>

Garthe, Stefan, and Ommo Hüppop. 2004. "Scaling Possible Adverse Effects of Marine Wind Farms on Seabirds: Developing and Applying a Vulnerability Index." *Journal of Applied Ecology* 41 (4): 724–34. <https://doi.org/10.1111/j.0021-8901.2004.00918.x>.

Garthe, S., Schwemmer, H., Peschko, V., Markones, N., Müller, S., Schwemmer, P., & Mercker, M. (2023). Large-scale effects of offshore wind farms on seabirds of high conservation concern. *Scientific Reports*, 13(1), 4779. <https://doi.org/10.1038/s41598-023-31601-z>

Gaston, A, and I.L. Jones. 1998. *The Auks*. Oxford, UK: Oxford University Press.

Gochfeld, M. and J. Burger (2020). Roseate Tern (*Sterna dougallii*), version 1.0. In *Birds of the World* (S. M. Billerman, Editor). Cornell Lab of Ornithology, Ithaca, NY, USA. <https://doi.org/10.2173/bow.roster.01>

Goodale, M W, and I J Stenhouse. 2016. "A Conceptual Model for Determining the Vulnerability of Wildlife Populations to Offshore Wind Energy Development." *Human-Wildlife Interactions* 10 (1): 53–61.

Goodale, M.W., and A. Milman. 2016. "Cumulative Adverse Effects of Offshore Wind Energy Development on Wildlife." *Journal of Environmental Planning and Management* 59 (1): 1–21. <https://doi.org/10.1080/09640568.2014.973483>.

Goudie, R. I., G. J. Robertson, and A. Reed (2020). Common Eider (*Somateria mollissima*), version 1.0. In *Birds of the World* (S. M. Billerman, Editor). Cornell Lab of Ornithology, Ithaca, NY, USA. <https://doi.org/10.2173/bow.comeid.01>

Goyert, Holly F. 2014. "Relationship among Prey Availability, Habitat, and the Foraging Behavior, Distribution, and Abundance of Common Terns *Sterna Hirundo* and Roseate Terns *S. Dougallii*." *Marine Ecology Progress Series* 506 (June): 291–302. <https://doi.org/10.3354/MEPS10834>.

Gratto-Trevor, C., Amirault-Langlais, D., Catlin, D., Cuthbert, F., Fraser, J., Maddock, S., Roche, E., & Shaffer, F. (2012). Connectivity in piping plovers: Do breeding populations have distinct winter distributions? *The Journal of Wildlife Management*, 76(2), 348–355.

Gray, Carrie E, Andrew T Gilbert, Iain J Stenhouse, and Alicia M Berlin. 2017. "Occurrence Patterns and Migratory Pathways of Red-Throated Loons Wintering in the Offshore Mid-Atlantic U. S., 2012-2016." In *Determining Fine-Scale Use and Movement Patterns of Diving Bird Species in Federal Waters of the Mid-Atlantic United States Using Satellite Telemetry*, edited by C.S.

Spiegel, A.M. Berlin, A.T. Gilbert, C.O. Gray, W.A. Montevecchi, I.J. Stenhouse, S.L. Ford, et al., 2012–16. Department of the Interior, Bureau of Ocean Energy Management. OCS Study BOEM 2017-069.

Green, R. M., Thaxter, C. B., Johnston, D. T., Boersch-Supan, P.H., Bouten, W., & Burton, N.H.K. 2023. Assessing movements of Lesser Black-backed Gulls using GPS tracking devices in relation to the Galloper Wind Farm. BTO Research Report 758. British Trust for Ornithology.

Gulka, J., Berlin, A., Friedland, K., Gilbert, A., Goetsch, C., Montevecchi, W., Perry, M., Stenhouse, I., Williams, K., & Adams, E. (2023). Assessing individual movement, habitat use, and behavior of non-breeding marine birds in relation to prey availability in the US Atlantic. *Marine Ecology Progress Series*, 711, 77–99. <https://doi.org/10.3354/meps14316>

Hakkinen, H., S. O. Petrovan, W. J. Sutherland, M. P. Dias, E. I. Ameca, S. Opper, I. Ramírez, B. Lawson, A. Lehtikoinen, K. M. Bowgen, N. G. Taylor, and N. Pettorelli. 2022. “Linking climate change vulnerability research and evidence on conservation action effectiveness to safeguard European seabird populations.” *Journal of Applied Ecology* 59 (5). John Wiley and Sons Inc: 1178–86. doi:10.1111/1365-2664.14133.

Haney, J. C. 1985. Wintering Phalaropes off the Southeastern United States: Application of Remote Sensing Imagery to Seabird Habitat Analysis at Oceanic Fronts. *Journal of Field Ornithology*, 56(4), 321–333.

Haney, J. C. 1986. Seabird patchiness in tropical oceanic waters: the influence of Sargassum "reefs." *Auk* 103:141-151.

Hartley, M J, and A J Weldon. 2020. “Saltmarsh Sparrow Conservation Plan. Atlantic Coast Joint Venture.” http://acjv.org/documents/SALS_plan_final.pdf.

Hartman, J.C., K.L. Krijgsveld, M.J.M. Poot, R.C. Fijn, M.F. Leopold, and S. Dirksen. 2012. “Effects on Birds of Offshore Wind Farm Egmond Aan Zee (OWEZ). An Overview and Integration of Insights Obtained.” Report 12-005. Bureau Waardenburg, Culemborg, Netherlands.

Hedenström, A., Z. Barta, B. Helm, A. I. Houston, J. M. McNamara, and N. Jonzén. 2007. “Migration speed and scheduling of annual events by migrating birds in relation to climate change.” *Climate Research* 35 (1–2): 79–91. doi:10.3354/cr00715.

Hijmans, R.J. 2020. “Raster: Geographic Data Analysis and Modeling. R Package Version 3.3-13. <https://CRAN.R-Project.Org/Package=raster>.” 2020.

Hill, Reinhold, Katrin Hill, Ralf Aumüller, Axel Schulz, Tobias Dittmann, Christoph Kulemeyer, and Timothy Coppack. 2014. “Of Birds, Blades, and Barriers: Detecting and Analysing Mass Migration Events at Alpha Ventus.” In *Ecological Research at the Offshore Windfarm Alpha Ventus*, edited by Federal Maritime and Hydrographic Agency and Federal Ministry of the Environment Nature Conservation and Nuclear Safety, 111–32. Berlin, Germany: Springer Spektrum. <https://doi.org/10.1007/978-3-658-02462-8>.

Holberton, R.L., P.D. Taylor, L.M. Tudor, K.M. O'Brien, G.H. Mittelhauser, and A. Breit. 2019. "Automated VHF Radiotelemetry Revealed Site-Specific Differences in Fall Migration Strategies of Semipalmated Sandpipers on Stopover in the Gulf of Maine." *Frontiers in Ecology and Evolution* 7: 1–14. <https://doi.org/10.3389/fevo.2019.00327>.

Hötker, Hermann, Kai-Michael Thomsen, and Heike Jeromin. 2006. "Impacts on Biodiversity of Exploitation of Renewable Energy Sources: The Example of Birds and Bats." - Facts, Gaps in Knowledge, Demands for Further Research, and Ornithological Guidelines for the Development of Renewable Energy Exploitation. Michael-Otto-Institut im NABU, Bergenhusen. 65 pp. <http://mhk.pnl.gov/publications/impacts-biodiversity-exploitation-renewable-energy-sources>.

Howell, J.E., A.E. McKellar, R.H.M. Espie, and C.A. Morrissey. 2019. "Predictable Shorebird Departure Patterns from a Staging Site Can Inform Collision Risks and Mitigation of Wind Energy Developments." *Ibis*, August. <https://doi.org/10.1111/ibi.12771>.

Hüppop, O., J. Dierschke, K-M. Exo, E. Fredrich, and R. Hill. 2006. "Bird Migration Studies and Potential Collision Risk with Offshore Wind Turbines." *Ibis* 148 (March): 90–109. <https://doi.org/10.1111/j.1474-919X.2006.00536.x>.

Imber, M.J. 1975. "Behaviour of Petrels in Relation to the Moon and Artificial Lights." *Journal of the Ornithological Society of New Zealand* 22: 302–6.

Jackson, B. J. and J. A. Jackson (2020). Killdeer (*Charadrius vociferus*), version 1.0. In *Birds of the World* (A. F. Poole and F. B. Gill, Editors). Cornell Lab of Ornithology, Ithaca, NY, USA. <https://doi.org/10.2173/bow.killde.01>

Jacobsen, Erik Mandrup, Flemming Pagh Jensen, and Jan Blew. 2019. "Avoidance Behaviour of Migrating Raptors Approaching an Offshore Wind Farm." In *Wind Energy and Wildlife Impacts : Balancing Energy Sustainability with Wildlife Conservation*, edited by Regina Bispo, Joana Bernardino, Helena Coelho, and José Lino Costa, 43–50. Cham: Springer International Publishing. https://doi.org/10.1007/978-3-030-05520-2_3.

Jodice, P.G.R., R.A. Ronconi, E. Rupp, G.E. Wallace, and Y. Satgé. 2015. "First Satellite Tracks of the Endangered Black-Capped Petrel." *Endangered Species Research* 29: 23–33. <https://doi.org/10.3354/esr00697>.

Jodice, P. G. R., Michael, P. E., Gleason, J. S., Haney, J. C., & Satgé, Y. G. (2021). Revising the marine range of the endangered black-capped petrel *Pterodroma hasitata*: occurrence in the northern Gulf of Mexico and exposure to conservation threats. *Endangered Species Research*, 46, 49–65. <https://doi.org/10.3354/ESR01143>

Johnson, J.A., J. Storrer, K. Fahy, and B. Reitherman. 2011. "Determining the Potential Effects of Artificial Lighting from Pacific Outer Continental Shelf (POCS) Region Oil and Gas Facilities on Migrating Birds." Prepared by Applied Marine Sciences, Inc. and Storrer Environmental Services

for the US Department of the Interior, Bureau of Ocean Energy Management, Regulations and Enforcement. Camarillo, CA. OCS Study BOEMRE 2011 - 047. 29 pp.

Johnston, A., A.S.C.P. Cook, L.J. Wright, E.M. Humphreys, and N.H.K. Burton. 2014. "Modelling Flight Heights of Marine Birds to More Accurately Assess Collision Risk with Offshore Wind Turbines." *Journal of Applied Ecology* 51 (1): 31–41. <https://doi.org/10.1111/1365-2664.12191>.

Jongbloed, Ruud H. 2016. "Flight Height of Seabirds. A Literature Study."

Kahlert, I., A. Fox, M. Desholm, I. Clausager, and J. Petersen. 2004. "Investigations of Birds During Construction and Operation of Nysted Offshore Wind Farm at Rødsand. Report by National Environmental Research Institute (NERI). Pp 88."

Kelsey, E. C., Felis, J. J., Czapanskiy, M., Pereksta, D. M., & Adams, J. 2018. "Collision and displacement vulnerability to offshore wind energy infrastructure among marine birds of the Pacific Outer Continental Shelf." *Journal of Environmental Management*, 227, 229–247. <https://doi.org/10.1016/j.jenvman.2018.08.051>

Kettel, Esther F, Louise K Gentle, and Richard W Yarnell. 2016. "Evidence of an Urban Peregrine Falcon (*Falco Peregrinus*) Feeding Young at Night." *Journal of Raptor Research* 50 (3): 321–23. <https://doi.org/10.3356/JRR-16-13.1>.

Klaassen, M., B. J. Hoyer, B. A. Nolet, and W. A. Buttemer. 2012. "Ecophysiology of avian migration in the face of current global hazards." *Philosophical Transactions of the Royal Society B: Biological Sciences*. Royal Society. doi:10.1098/rstb.2012.0008.

Koneff, M. D., Zimmerman, G. S., Dwyer, C. P., Fleming, K. K., Padding, I., Devers, P. K., Johnson, F. A., Runge, M. C., & Roberts, A. J. (2017). Evaluation of harvest and information needs for North American sea ducks. *PLoS ONE*, 1–29. <https://doi.org/https://doi.org/10.1371/journal.pone.0175411>

Krijgsveld, K.L., R.C. Fljn, M. Japink, P.W. van Horssen, C. Heunks, M.P. Collier, M.J.M. Poot, D. Beuker, and S. Birksen. 2011. "Effect Studies Offshore Wind Farm Egmond Aan Zee: Final Report on Fluxes, Flight Altitudes and Behaviour of Flying Birds." Bureau Waardenburg report no. 10-219. Institute for Marine Resources & Ecosystem Studies, Wageningen UR, Netherlands.

Lane, J.V., J.W.E. Jeglinski, S. Avery-Gomm, E. Ballstaedt, A.C. Banyard, T. Barychka, I.H. Brown, B. Brugger, T.V. Burt, N. Careen, J.H.F. Castenschiold, S. Christensen-Dalsgaard, S. Clifford, S.M. Collins, E. Cunningham, J. Danielsen, F. Daunt, K.J.N. d'Entremont, P. Doiron, S. Duffy, M.D. English, M. Falchieri, J. Giacinti, B. Gjerset, S. Granstad, D. Grémillet, M. Guillemette, G.T. Hallgrímsson, K.C. Hamer, S. Hammer, K. Harrison, J.D. Hart, C. Hatsell, R. Humpidge, J. James, A. Jenkinson, M. Jessopp, M.E.B. Jones, S. Lair, T. Lewis, A.A. Malinowska, A. McCluskie, G. McPhail, B. Moe, W.A. Montevecchi, G. Morgan, C. Nichol, C. Nisbet, B. Olsen, J. Provencher, P. Provost, A. Purdie, J.-F. Rail, G. Robertson, Y. Seyer, M. Sheddan, C. Soos, N. Stephens, H. Strøm, V. Svansson, T.D. Tierney, G. Tyler, T. Wade, S. Wanless, C.R.E. Ward, S. Wilhelm, S. Wischnewski,

- L.J. Wright, B. Zonfrillo, J. Matthiopoulos and S.C. Votier. 2023. High pathogenicity avian influenza (H5N1) in Northern Gannets: Global spread, clinical signs, and demographic consequences. bioRxiv Preprint. doi: <https://doi.org/10.1101/2023.05.01.538918>
- Langston, Rowena H.W. 2013. "Birds and Wind Projects across the Pond: A UK Perspective." *Wildlife Society Bulletin* 37 (1): 5–18.
- Larsen, Jesper K., and Magella Guillemette. 2007. "Effects of Wind Turbines on Flight Behaviour of Wintering Common Eiders: Implications for Habitat Use and Collision Risk." *Journal of Applied Ecology* 44 (3): 516–22. <https://doi.org/10.1111/J.1365-2664.2007.01303.X>.
- Lavers, J., J. M. Hipfner, and G. Chapdelaine. 2020. Razorbill (*Alca torda*), version 1.0. In *Birds of the World* (S. M. Billerman, Editor). Cornell Lab of Ornithology, Ithaca, NY, USA. <https://doi.org/10.2173/bow.razorb.01>
- Leonhard, Simon B, J Pedersen, P N Grøn, Henrik Skov, J Jansen, Christopher J Topping, and I K Petersen. 2013. "Wind Farms Affect Common Scoter and Red-Throated Diver Behaviour." *Danish Offshore Wind: Key Environmental Issues – A Follow-Up*. In *Danish Offshore Wind: Key Environmental Issues – A Follow-up*. The Environment Group: The Danish Energy Agency, The Danish Nature Agency, DONG Energy and Vattenfall, pp. 70–93 (Chapter 5).
- Lindeboom, H J, H J Kouwenhoven, M J N Bergman, S Bouma, S Brasseur, R Daan, R C Fijn, et al. 2011. "Short-Term Ecological Effects of an Offshore Wind Farm in the Dutch Coastal Zone; a Compilation." *Environmental Research Letters* 6 (3): 035101. <https://doi.org/10.1088/1748-9326/6/3/035101>.
- Lindgren F, Rue H, Lindstrom J. 2011. An explicit link between gaussian fields and gaussian Markov random fields: the stochastic partial differential equation approach (with discussion). *Journal of the Royal Statistical Society B*. 73(4):423–498. doi:10.1111/j.1467-9868.2011.00777.x.
- Lindgren F, Rue H. 2015. Bayesian Spatial Modelling with R - INLA . *Journal of Statistical Software*. 63(19). doi:10.18637/jss.v063.i19.
- Loring, P., H. Goyert, C. Griffin, P. Sievert, and P. Paton. 2017. "Tracking Movements of Common Terns, Endangered Roseate Terns, and Threatened Piping Plovers in the Northwest Atlantic." 2017 Annual Report to the Bureau of Ocean Energy Management. US Fish and Wildlife Service, Hadley, MA. 134 pp.
- Loring, PH, AK Lenske, JD McLaren, M Aikens, AM Anderson, Y Aubrey, E Dalton, et al. 2021. "Tracking Movements of Migratory Shorebirds in the US Atlantic Outer Continental Shelf Region. Sterling (VA): US Department of the Interior, Bureau of Ocean Energy Management. OCS Study BOEM 2021-008. 104 p."
- Loring, P.H., J.D. McLaren, H.F. Goyert, and P.W.C. Paton. 2020. "Supportive Wind Conditions Influence Offshore Movements of Atlantic Coast Piping Plovers during Fall Migration." *Condor* 122 (3): 1–16. <https://doi.org/10.1093/condor/duaa028>.

Loring, P.H., J.D. McLaren, P.A. Smith, L.J. Niles, S.L. Koch, H.F. Goyert, and H. Bai. 2018. "Tracking Movements of Threatened Migratory Rufa Red Knots in US Atlantic Outer Continental Shelf Waters." OCS Study BOEM 2018-046. US Department of the Interior, Bureau of Ocean Energy Management, Sterling, VA. 145 pp.

Loring, P.H., P.W.C. Paton, J.D. McLaren, H. Bai, R. Janaswamy, H.F. Goyert, C.R. Griffin, and P.R. Sievert. 2019. "Tracking Offshore Occurrence of Common Terns, Endangered Roseate Terns, and Threatened Piping Plovers with VHF Arrays. Sterling (VA): US Department of the Interior, Bureau of Ocean Energy Management. OCS Study BOEM 2019-017. 140 p."

Loring, P.H., P.W.C. Paton, J.E. Osenkowski, S.G. Gilliland, J-P.L. Savard, and S.R. McWilliams. 2014. "Habitat Use and Selection of Black Scoters in Southern New England and Siting of Offshore Wind Energy Facilities." *The Journal of Wildlife Management* 78 (4): 645–56. <https://doi.org/10.1002/jwmg.696>.

Lowther, P. E., A. W. Diamond, S. W. Kress, G. J. Robertson, K. Russell, D. N. Nettleship, G. M. Kirwan, D. A. Christie, C. J. Sharpe, E. F. J. Garcia, and P. F. D. Boesman. 2020. Atlantic Puffin (*Fratercula arctica*), version 1.0. In *Birds of the World* (S. M. Billerman, Editor). Cornell Lab of Ornithology, Ithaca, NY, USA. <https://doi.org/10.2173/bow.atlpuf.01>

Masden, E. A., McCluskie, A., Owen, E., & Langston, R. H. W. 2015. "Renewable energy developments in an uncertain world: The case of offshore wind and birds in the UK." *Marine Policy*, 51: 169–172. <https://doi.org/https://doi.org/10.1016/j.marpol.2014.08.006>

Masden, Elizabeth A., Daniel T. Haydon, Anthony D. Fox, Robert W. Furness, Rhys Bullman, and Mark Desholm. 2009. "Barriers to Movement: Impacts of Wind Farms on Migrating Birds." *ICES Journal of Marine Science* 66 (4): 746–53. <https://doi.org/10.1093/icesjms/fsp031>.

Mateos-Rodríguez, María, and Felix Liechti. 2012. "How Do Diurnal Long-Distance Migrants Select Flight Altitude in Relation to Wind?" *Behavioral Ecology* 23 (2): 403–9. <https://doi.org/10.1093/beheco/arr204>.

Meatley, D. E., McWilliams, S. R., Paton, P. W. C., Lepage, C., Gilliland, S. G., Savoy, L., Olsen, G. H., & Osenkowski, J. E. 2018. "Annual cycle of White-winged Scoters (*Melanitta fusca*) in eastern North America: migratory phenology, population delineation, and connectivity." *Canadian Journal of Zoology*, 96: 1353–1365.

Meatley, D. E., S. R. McWilliams, P. W. C. Paton, C. Lepage, S. G. Gilliland, L. Savoy, G. H. Olsen, and J. E. Osenkowski. 2019. "Resource Selection and Wintering Phenology of White-Winged Scoters in Southern New England: Implications for Offshore Wind Energy Development." *The Condor: Ornithological Applications* 121: 1–18. <https://doi.org/10.1093/condor/duy014>.

Meek, E. R., J. B. Ribbands, W. G. Christer, P. R. Davy, and I. Higginson. 1993. "The Effects of Aero-Generators on Moorland Bird Populations in the Orkney Islands, Scotland." *Bird Study* 40 (2): 140–43. <https://doi.org/10.1080/00063659309477139>.

Mendel, Bettina, Philipp Schwemmer, Verena Peschko, Sabine Müller, Henriette Schwemmer, Moritz Mercker, and Stefan Garthe. 2019. "Operational Offshore Wind Farms and Associated Ship Traffic Cause Profound Changes in Distribution Patterns of Loons (*Gavia Spp.*).” *Journal of Environmental Management* 231 (August 2018): 429–38. <https://doi.org/10.1016/j.jenvman.2018.10.053>.

Mitchell, I., F. Daunt, M. Frederiksen, and K. Wade. 2020. "Impacts of climate change on seabirds, relevant to the coastal and marine environment around the UK." *MCCIP Science Review*, 382–99. doi:10.14465/2020.arc17.sbi.

Mizrahi, D., R. Fogg, K. A. Peters, and P. A. Hodgetts. 2009. "Assessing Nocturnal Bird and Bat Migration Patterns on the Cape May Peninsula Using Marine Radar: Potential Effects of a Suspension Bridge Spanning Middle Thoroughfare, Cape May County, New Jersey." *New Jersey Audubon*, Cape May Court House, NJ, USA.

Mojica, E. K., Meyers, J. M., Millsap, B. a., & Haley, K. L. 2008. "Migration Of Florida Sub-Adult Bald Eagles." *The Wilson Journal of Ornithology*, 120(2): 304–310. <https://doi.org/10.1676/07-079.1>

Møller J, Waagepetersen RP. 2007. Modern Statistics for Spatial Point Processes*. *Scandinavian Journal of Statistics*. 34(4):643–684. doi:10.1111/J.1467-9469.2007.00569.X.

Montevecchi, W.A. 2006. "Influences of Artificial Light on Marine Birds." In *Ecological Consequences of Artificial Night Lighting*, edited by Catherine Rich and Travis Longcore, 94–113. Washington, D.C.: Island Press. <https://doi.org/10.1111/bph.13539>.

Mostello, C.S., I.C.T. Nisbet, S.A. Oswald, and J.W. Fox. 2014. "Non-Breeding Season Movements of Six North American Roseate Terns *Sterna Dougallii* Tracked with Geolocators." *Seabird* 27 (2014): 1–21.

Mowbray, T. B. 2020. Northern Gannet (*Morus bassanus*), version 1.0. In *Birds of the World* (S. M. Billerman, Editor). Cornell Lab of Ornithology, Ithaca, NY, USA. <https://doi.org/10.2173/bow.norgan.01>

Muller, M. J. and R. W. Storer (2020). Pied-billed Grebe (*Podilymbus podiceps*), version 1.0. In *Birds of the World* (A. F. Poole and F. B. Gill, Editors). Cornell Lab of Ornithology, Ithaca, NY, USA. <https://doi.org/10.2173/bow.pibgre.01>

Nisbet, Ian C. T., Richard R. Veit, Sasha A. Auer, and T.P. White. 2013. *Marine Birds of the Eastern United States and the Bay of Fundy: Distribution, Numbers, Trends, Threats, and Management*. No. 29. Cambridge, MA: Nuttall Ornithological Club.

Normandeau Associates Inc. 2011. "New Insights and New Tools Regarding Risk to Roseate Terns, Piping Plovers, and Red Knots from Wind Facility Operations on the Atlantic Outer Continental Shelf." Report No. BOEMRE 048-2011. US Department of the Interior, Bureau of Ocean Energy Management, Regulation and Enforcement, New Orleans, LA. 287 pp.

Normandeau Associates and APEM. 2019. Ornithological and Marine Fauna Aerial Survey Results of Lease Area OCS-A 0512: Annual Report: November 2017 to October 2018. Scientific Annual Report P00002032-01. Equinor, 06/10/2019, Final, 266pp.

Normandeau Associates and APEM. 2021a. Digital Aerial Baseline Survey of Marine Wildlife in Support of Offshore Wind Energy: Spatial and Temporal Marine Wildlife Distributions in the New York Offshore Planning Area, Summer 2016–Spring 2019. NYSERDA Report Number 21-07a. Prepared by Normandeau Associates, Inc., Gainesville, FL, and APEM, Ltd., Stockport, UK. nysesda.ny.gov/publications.

Normandeau Associates and APEM. 2021b. Digital Aerial Baseline Survey of Marine Wildlife in Support of Offshore Wind Energy: Spatial and Temporal Marine Wildlife Distributions in the New York Offshore Planning Area, Summer 2016–Spring 2019. Final Report Volume 2: Results (Birds). chrome-extension://efaidnbmninnibpcjpcglclefindmkaj/https://remote.normandeau.com/docs/21-07a_Digital_Aerial_Baseline_Survey_of_Marine_Wildlife_in_Support_of_Offshore_Wind_Energy.pdf

Normandeau Associates and APEM. 2021c. Year 2 Digital Aerial Wildlife Surveys of BOEM Lease Area OCSA 0512: February 2019 to December 2019. Scientific Annual Report P00004039-02. Equinor Wind US, 06/09/2021, Final, 386 pp.

Normandeau Associates. 2022. Postconstruction Bird and Bat Monitoring at the Coastal Virginia Offshore Wind Pilot Project: First Annual Report. 127 pp.

North American Bird Conservation Initiative. 2022. "State of the Birds Report." [StateoftheBirds.org](https://stateofthebirds.org).

[NYSDEC Black Rail] New York Department of Environmental Conservation. 2023. Black Rail. Accessed on Nov. 13 2023 at <https://www.dec.ny.gov/animals/61344.html>.

NYSERDA. 2015. "Master Plan: Shipping and Navigation Study." NYSERDA, no. 15.

NYSERDA. 2010. "Pre-development Assessment of Avian Species for the Proposed Long Island New York City Offshore Wind Project Area." NYSERDA Report No. 9998-03. New York State Energy Research and Development Authority

Olsen, J., and P. Olsen. 1980. "Alleviating the Impact of Human Disturbance on the Breeding Peregrine Falcon II: Public and Recreational Lands." *Corella* 4 (3): 54–57.

Ørsted. 2018. "Hornsea Three Offshore Wind Farm Environmental Statement: Volume 2, Chapter 5 – Offshore Ornithology. Report No. A6.2.5." London, UK.

Paruk, J. D., D. C. Evers, J. W. McIntyre, J. F. Barr, J. Mager, and W. H. Piper. 2021. Common Loon (*Gavia immer*), version 2.0. In *Birds of the World* (P. G. Rodewald and B. K. Keeney, Editors). Cornell Lab of Ornithology, Ithaca, NY, USA. <https://doi.org/10.2173/bow.comloo.02>

- Percival, S.M. 2010. "Kentish Flats Offshore Wind Farm: Diver Surveys 2009-10." Durham, UK.
- Peschko, Verena, Bettina Mendel, Moritz Mercker, Jochen Dierschke, and Stefan Garthe. 2021. "Northern Gannets (*Morus Bassanus*) Are Strongly Affected by Operating Offshore Wind Farms during the Breeding Season." *Journal of Environmental Management* 279 (February).
<https://doi.org/10.1016/j.jenvman.2020.111509>.
- Petersen, I.K., and A.D. Fox. 2007. "Changes in Bird Habitat Utilisation around the Horns Rev 1 Offshore Wind Farm, with Particular Emphasis on Common Scoter." <https://tethys.pnnl.gov/publications/changes-bird-habitat-utilisation-around-horns-rev-1-offshore-wind-farm-particular>.
- Petersen, Jens Kjerulf, and Torleif Maim. 2006. "Offshore Windmill Farms: Threats to or Possibilities for the Marine Environment." *Ambio* 35 (2): 75–80.
<http://www.ncbi.nlm.nih.gov/pubmed/16722252>.
- Pettersson, Jan. 2005. "The Impact of Offshore Wind Farms on Bird Life in Southern Kalmar Sound Sweden Final Report Based on Studies 1999-2003." Lunds universitet. Ekologiska, institutionen. Department Animal Ecology, Lund University.
- du Plessis, K. L., R. O. Martin, P. A. R. Hockey, S. J. Cunningham, and A. R. Ridley. 2012. "the costs of keeping cool in a warming world: Implications of high temperatures for foraging, thermoregulation and body condition of an arid-zone bird." *Global Change Biology* 18 (10): 3063–70. doi:10.1111/j.1365-2486.2012.02778.x.
- Pörtner, H.-O., D. C. Roberts, A. Alegría, M. Nicolai, A. Okem, J. Petzold, B. Rama, and N. M. Weyer. 2019. "IPCC special report on the ocean and cryosphere in a changing climate."
- R Core Team. 2021. "R: A Language and Environment for Statistical Computing." 2021.
- Reed, J. M., L. W. Oring, and E. M. Gray (2020). Spotted Sandpiper (*Actitis macularius*), version 1.0. In *Birds of the World* (A. F. Poole, Editor). Cornell Lab of Ornithology, Ithaca, NY, USA.
<https://doi.org/10.2173/bow.sposan.01>
- Richardson, W. John. 1976. "Autumn Migration over Puerto Rico and the Western Atlantic: A Radar Study." *Ibis* 118 (3): 309–32.
- Rizzolo, D. J., C. E. Gray, J. A. Schmutz, J. F. Barr, C. Eberl, and J. W. McIntyre (2020). Red-throated Loon (*Gavia stellata*), version 2.0. In *Birds of the World* (P. G. Rodewald and B. K. Keeney, Editors). Cornell Lab of Ornithology, Ithaca, NY, USA.
<https://doi.org/10.2173/bow.retloo.02>
- Rodríguez, Airam, Graeme Burgan, Peter Dann, Roz Jessop, Juan J. Negro, and Andre Chiaradia. 2014. "Fatal Attraction of Short-Tailed Shearwaters to Artificial Lights." *PLoS ONE* 9 (10): 1–10.
<https://doi.org/10.1371/journal.pone.0110114>.

Rodríguez, Airam, Peter Dann, and André Chiaradia. 2017. "Reducing Light-Induced Mortality of Seabirds: High Pressure Sodium Lights Decrease the Fatal Attraction of Shearwaters." *Journal for Nature Conservation* 39: 68–72. <https://doi.org/10.1016/j.jnc.2017.07.001>.

Rodríguez, Airam, Beneharo Rodríguez, and Juan J. Negro. 2015. "GPS Tracking for Mapping Seabird Mortality Induced by Light Pollution." *Scientific Reports* 5: 1–11. <https://doi.org/10.1038/srep10670>.

Rubega, Margaret A., Douglas Schamel, and Diane M. Tracy. 2020. "Red-Necked Phalarope (*Phalaropus lobatus*), Version 1.0." In *Birds of the World*, edited by S.M. Billerman. Ithaca, NY: Cornell Lab of Ornithology. <https://doi-org.uri.idm.oclc.org/10.2173/bow.renpha.01>.

Rue H, Martino S, Chopin N. 2009. Approximate Bayesian inference for latent Gaussian models using integrated nested Laplace approximations (with discussion). *Journal of the Royal Statistical Society B*. 71:319–392. doi:10.1111/j.1467-9868.2008.00700.x.

Saino, N., R. Ambrosini, D. Rubolini, J. von Hardenberg, A. Provenzale, K. Hüppop, O. Hüppop, A. Lehikoinen, E. Lehikoinen, K. Rainio, M. Romano, and L. Sokolov. 2011. "Climate warming, ecological mismatch at arrival and population decline in migratory birds." *Proceedings of the Royal Society B: Biological Sciences*, 278:835–42. Royal Society. doi:10.1098/rspb.2010.1778.

Schorger, A W. 1947. "The Deep Diving of the Loon and Old-Squaw and Its Mechanism." *The Wilson Bulletin* 59 (3): 151–59.

Schwemmer, P., Pederson, R., Haecker, K., Bocher, P., Fort, J., Mercker, M., Jiguet, F., Elts, J., Marja, R., Piha, M., Rousseau, P., & Garthe, S. 2023. Assessing potential conflicts between offshore wind farms and migration patterns of a threatened shorebird species. *Animal Conservation*, 26(3), 303–316. <https://doi.org/10.1111/acv.12817>

Sea Duck Joint Venture. (2022). Atlantic and Great Lakes Sea Duck Migration Study Atlantic and Great Lakes Sea Duck Migration Study: Final Report. Available at: <http://seaduckjv.org/science-resources/atlantic-and-great-lakes-sea-duck-migration-study/>. <http://seaduckjv.org/science-resources/atlantic->

Simons, T.R., D.S. Lee, and J.C. Hanley. 2013. "Diablotin (*Pterodroma hasitata*): A Biography of the Endangered Black-Capped Petrel." *Marine Ornithology* 41 (Special Issue): S3–43.

Skov, H., S. Heinanen, T. Norman, R.M. Ward, S. Mendez-Roldan, and I. Ellis. 2018. "ORJIP Bird Collision and Avoidance Study. Final Report - April 2018." Report by NIRAS and DHI to The Cabon Trust, U.K. 247 pp.

Skov, Henrik, Mark Desholm, Stefan Heinänen, Johnny A. Kahlert, Bjarke Laubek, Niels Einar Jensen, Ramūnas Žydelis, and Bo Præstegaard Jensen. 2016. "Patterns of Migrating Soaring Migrants Indicate Attraction to Marine Wind Farms." *Biology Letters* 12 (12): 20160804. <https://doi.org/10.1098/rsbl.2016.0804>.

Smallwood, K. Shawn. 2013. "Long-Term Trends in Fatality Rates of Birds and Bats in the Altamont Pass Wind Resource Area, California," no. July: 85 pp.

Smallwood, K. S., & Bell, D. A. (2020). Effects of Wind Turbine Curtailment on Bird and Bat Fatalities. *Journal of Wildlife Management*, 84(4), 685–696. <https://doi.org/10.1002/jwmg.21844>

Spiegel, C.S., A.M. Berlin, A.T. Gilbert, C.O. Gray, W.A. Montevecchi, I.J. Stenhouse, S.L. Ford, et al. 2017. "Determining Fine-Scale Use and Movement Patterns of Diving Bird Species in Federal Waters of the Mid-Atlantic United States Using Satellite Telemetry." Vol. 1.

Staine, Kevin J, and Joanna Burger. 1994. "Nocturnal Foraging Behavior of Breeding Piping Plovers (*Charadrius Melodus*) in New Jersey." *The Auk* 111 (3): 579–87.

Stedman, S. J. (2020). Horned Grebe (*Podiceps auritus*), version 1.0. In *Birds of the World* (S. M. Billerman, Editor). Cornell Lab of Ornithology, Ithaca, NY, USA. <https://doi.org/10.2173/bow.horgre.01>

Stenhouse, I.J., A.M. Berlin, A.T. Gilbert, M.W. Goodale, C.E. Gray, W.A. Montevecchi, L. Savoy, and C.S. Spiegel. 2020. "Assessing the Exposure of Three Diving Bird Species to Offshore Wind Areas on the US Atlantic Outer Continental Shelf Using Satellite Telemetry." *Diversity and Distributions* n/a (n/a). <https://doi.org/10.1111/ddi.13168>.

Stout, B.E., and G.L. Nuechterlein. 2020. "Red-Necked Grebe (*Podiceps Grisegena*), Version 1.0." In *Birds of the World*, edited by S.M. Billerman. Ithaca, NY: Cornell Lab of Ornithology. <https://doi-org.uri.idm.oclc.org/10.2173/bow.rengre.01>.

Sullivan, B.L., C.L. Wood, R.E. Iliff, R.E. Booney, D. Fink, and S. Kelling. 2009. "EBird: A Citizen-Based Bird Observation Network in the Biological Sciences." *Biological Conservation* 142: 2282–92.

Thaxter, C. B., V. H. Ross-Smith, and W. Bouten. 2015. "Seabird – Wind Farm Interactions during the Breeding Season Vary within and between Years: A Case Study of Lesser Black-Backed Gull *Larus Fuscus* in the UK." *Biological Conservation* 186: 347–58. <https://doi.org/10.1016/j.biocon.2015.03.027>.

Thorne, K. M., K. A. Spragens, K. J. Buffington, J. A. Rosencranz, and J. Takekawa. 2019. "Flooding regimes increase avian predation on wildlife prey in tidal marsh ecosystems." *Ecology and Evolution* 9 (3). John Wiley and Sons Ltd: 1083–94. doi:10.1002/ece3.4792.

Tjørnløv, R. S., Skov, H., Armitage, M., Barker, M., Jørgensen, J. B., Mortensen, L. O., Thomas, K., Uhrenholdt, T., & 11820296. (2023). Resolving Key Uncertainties of Seabird Flight and Avoidance Behaviours at Offshore Wind Farms: Final report for the study period 2020–2021 (Issue February).

https://group.vattenfall.com/uk/contentassets/1b23f720f2694bd1906c007effe2c85a/aowfl_abe_rdeen_seabird_study_final_report_20_february_2023.pdf

Tracy, D.M., D. Schamel, and J. Dale. 2020. "Red Phalarope (*Phalaropus Fulicarius*), Version 1.0." In *Birds of the World*, edited by S.M. Billerman. Ithaca, NY: Cornell Lab of Ornithology. <https://doi-org.uri.idm.oclc.org/10.2173/bow.redpha1.01>.

US Fish and Wildlife Service (USFWS). 2021. Piping Plover 5-Year Review: Summary and Evaluation. Hadley, Massachusetts and East Lansing, Michigan.

USFWS. 2014. "Rufa Red Knot Background Information and Threats Assessment." <https://rucore.libraries.rutgers.edu/rutgers-lib/46245/PDF/1/play/>.

USFWS. 2018. "Species Status Assessment Report for the Eastern Black Rail (*Laterallus jamaicensis jamaicensis*). Version 1.2." Accessed 6 October 2022. <https://ecos.fws.gov/ServCat/DownloadFile/154242>

USFWS. 2020a. "Piping Plover (*Charadrius Melodus*) 5-Year Review: Summary and Evaluation." https://ecos.fws.gov/docs/tess/species_nonpublish/3383.pdf.

USFWS. 2020b. "Roseate Tern North American Population 5-Year Review (*Sterna dougallii dougallii*): Summary and Evaluation." Concord, NH. <https://www.fws.gov/node/65860>.

USFWS. 2020c. "Species Status Assessment Report for the Rufa Red Knot (*Calidris canutus rufa*)."

<https://ecos.fws.gov/ServCat/DownloadFile/187781>.

van der Winden, J., M. J.M. Poot, and P. W. van Horssen. 2010. "Large Birds Can Migrate Fast: The Post-Breeding Flight of the Purple Heron *Ardea Purpurea* to the Sahel." *Ardea* 98 (3): 395–402. <https://doi.org/10.5253/078.098.0313>.

Vanermen, Nicolas, Wouter Courtens, Robin Daelemans, Luc Lens, Wendt Müller, Marc van de walle, Hilbran Verstraete, and Eric W M Stienen. 2019. "Attracted to the Outside: A Meso-Scale Response Pattern of Lesser Black-Backed Gulls at an Offshore Wind Farm Revealed by GPS Telemetry." *ICES Journal of Marine Science*. <https://doi.org/10.1093/icesjms/fsz199>.

Vanermen, Nicolas, Thierry Onkelinx, Wouter Courtens, Marc van de walle, Hilbran Verstraete, and Eric W. M. Stienen. 2015. "Seabird Avoidance and Attraction at an Offshore Wind Farm in the Belgian Part of the North Sea." *Hydrobiologia* 756 (1): 51–61. <https://doi.org/10.1007/s10750-014-2088-x>.

Vlietstra, L S. 2007. "Potential Impact of the Massachusetts Maritime Academy Wind Turbine on Common (*Sterna hirundo*) and Roseate (*S. dougallii*) Terns." Massachusetts Maritime Academy.

Voous, K. H. 1961. "Records of the Peregrine Falcon on the Atlantic Ocean." *Ardea* 49: 176–77.

Wade, H.M., E.A. Masden, A.C. Jackson, and R.W. Furness. 2016. "Incorporating Data Uncertainty When Estimating Potential Vulnerability of Scottish Seabirds to Marine Renewable Energy Developments." *Marine Policy* 70: 108–13. <https://doi.org/10.1016/j.marpol.2016.04.045>.

Walker, W. E., Harremoes, P., Rotmans, J., van der Sluijs, J. P., van Asselt, M. B. A., Janssen, P., & Kraye Von Krauss, M. P. 2003. "Defining Uncertainty". Integrated Assessment. <https://www.narcis.nl/publication/RecordID/oai:tudelft.nl:uuid:fdc0105c-e601-402a-8f16-ca97e9963592>

Weiskopf, S. R., Rubenstein, M. A., Crozier, L. G., Gaichas, S., Griffis, R., Halofsky, J. E., Hyde, K. J. W., Morelli, T. L., Morissette, J. T., Muñoz, R. C., Pershing, A. J., Peterson, D. L., Poudel, R., Staudinger, M. D., Sutton-Grier, A. E., Thompson, L., Vose, J., Weltzin, J. F., & Whyte, K. P. (2020). Climate change effects on biodiversity, ecosystems, ecosystem services, and natural resource management in the United States. *Science of the Total Environment* (Vol. 733). DOI: <https://doi.org/10.1016/j.scitotenv.2020.137782>

Welcker, Jorg, and Georg Nehls. 2016. "Displacement of Seabirds by an Offshore Wind Farm in the North Sea." *Marine Ecology Progress Series* 554: 173–82. <https://doi.org/10.3354/meps11812>.

White, C. M., N. J. Clum, T. J. Cade, and W. G. Hunt. 2020. Peregrine Falcon (*Falco peregrinus*), version 1.0. In *Birds of the World* (S. M. Billerman, Editor). Cornell Lab of Ornithology, Ithaca, NY, USA. <https://doi.org/10.2173/bow.perfal.01>

Williams, KA, EE Connelly, SM Johnson, and IJ Stenhouse, eds. 2015. "Baseline Wildlife Studies in Atlantic Waters Offshore of Maryland: Final Report to the Maryland Department of Natural Resources and the Maryland Energy Administration." Portland, ME: Report BRI 2015-17, Biodiversity Research Institute.

Williams, T.C., and J.M. Williams. 1990. "Open Ocean Bird Migration. IEEE Proceedings F - Radar and Signal Processing 137: 133-137."

Willmott, J. R., Forcey, G., & Kent, A. 2013. *The Relative Vulnerability of Migratory Bird Species to Offshore Wind Energy Projects on the Atlantic Outer Continental Shelf: An Assessment Method and Database*.

Winkler, D. W., S. M. Billerman, and I. J. Lovette (2020). Grebes (Podicipedidae), version 1.0. In *Birds of the World* (S. M. Billerman, B. K. Keeney, P. G. Rodewald, and T. S. Schulenberg, Editors). Cornell Lab of Ornithology, Ithaca, NY, USA. <https://doi.org/10.2173/bow.podici1.01>

Winkler, D. W., S. M. Billerman, and I. J. Lovette. 2020a. Plovers and Lapwings (*Charadriidae*), version 1.0. In *Birds of the World* (S. M. Billerman, B. K. Keeney, P. G. Rodewald, and T. S. Schulenberg, Editors). Cornell Lab of Ornithology, Ithaca, NY, USA. <https://doi.org/10.2173/bow.charad1.01>

Winkler, D. W., S. M. Billerman, and I. J. Lovette. 2020b. Stilts and Avocets (*Recurvirostridae*), version 1.0. In *Birds of the World* (S. M. Billerman, B. K. Keeney, P. G. Rodewald, and T. S. Schulenberg, Editors). Cornell Lab of Ornithology, Ithaca, NY,

USA. <https://doi.org/10.2173/bow.recurv1.01>Winkler, D.W., S. M. Billerman, and I. J. Lovette. 2020c.

Winkler, D. W., S. M. Billerman, and I. J. Lovette. 2020c. Oystercatchers (*Haematopodidae*), version 1.0. In Birds of the World (S. M. Billerman, B. K. Keeney, P. G. Rodewald, and T. S. Schulenberg, Editors). Cornell Lab of Ornithology, Ithaca, NY, USA. <https://doi.org/10.2173/bow.haemat1.01>

Winkler, D. W., S. M. Billerman, and I. J. Lovette 2020d. Sandpipers and Allies (*Scolopacidae*), version 1.0. In Birds of the World (S. M. Billerman, B. K. Keeney, P. G. Rodewald, and T. S. Schulenberg, Editors). Cornell Lab of Ornithology, Ithaca, NY, USA. <https://doi.org/10.2173/bow.scolop2.01>

Winkler, D. W., S. M. Billerman, and I. J. Lovette. 2020e. Herons, Egrets, and Bitterns (*Ardeidae*), version 1.0. In Birds of the World (S. M. Billerman, B. K. Keeney, P. G. Rodewald, and T. S. Schulenberg, Editors). Cornell Lab of Ornithology, Ithaca, NY, USA. <https://doi.org/10.2173/bow.ardeid1.01>

Winkler, D. W., S. M. Billerman, and I. J. Lovette. 2020f. Ibises and Spoonbills (*Threskiornithidae*), version 1.0. In Birds of the World (S. M. Billerman, B. K. Keeney, P. G. Rodewald, and T. S. Schulenberg, Editors). Cornell Lab of Ornithology, Ithaca, NY, USA. <https://doi.org/10.2173/bow.thresk1.01>

Winkler, D. W., S. M. Billerman, and I. J. Lovette. 2020g. Hawks, Eagles, and Kites (*Accipitridae*), version 1.0. In Birds of the World (S. M. Billerman, B. K. Keeney, P. G. Rodewald, and T. S. Schulenberg, Editors). Cornell Lab of Ornithology, Ithaca, NY, USA. <https://doi.org/10.2173/bow.accipi1.01>

Winkler, D. W., S. M. Billerman, and I. J. Lovette. 2020h. New World Vultures (*Cathartidae*), version 1.0. In Birds of the World (S. M. Billerman, B. K. Keeney, P. G. Rodewald, and T. S. Schulenberg, Editors). Cornell Lab of Ornithology, Ithaca, NY, USA. <https://doi.org/10.2173/bow.cathar2.01>

Winkler, D. W., S. M. Billerman, and I. J. Lovette. 2020i. Falcons and Caracaras (*Falconidae*), version 1.0. In Birds of the World (S. M. Billerman, B. K. Keeney, P. G. Rodewald, and T. S. Schulenberg, Editors). Cornell Lab of Ornithology, Ithaca, NY, USA. <https://doi.org/10.2173/bow.falcon1.01>

Winkler, D. W., S. M. Billerman, and I. J. Lovette. 2020j. Owls (Strigidae), version 1.0. In Birds of the World (S. M. Billerman, B. K. Keeney, P. G. Rodewald, and T. S. Schulenberg, Editors). Cornell Lab of Ornithology, Ithaca, NY, USA. <https://doi.org/10.2173/bow.strigi1.01>

Winkler, D. W., S. M. Billerman, and I. J. Lovette. 2020k. Auks, Murres, and Puffins (*Alcidae*), version 1.0. In Birds of the World (S. M. Billerman, B. K. Keeney, P. G. Rodewald, and T. S.

Schulenberg, Editors). Cornell Lab of Ornithology, Ithaca, NY, USA. <https://doi.org/10.2173/bow.alcida1.01>

Winkler, D. W., S. M. Billerman, and I. J. Lovette, 2020l. Gulls, Terns, and Skimmers (*Laridae*), version 1.0. In Birds of the World (S. M. Billerman, B. K. Keeney, P. G. Rodewald, and T. S. Schulenberg, Editors). Cornell Lab of Ornithology, Ithaca, NY, USA. <https://doi.org/10.2173/bow.larida1.01>

Winkler, D. W., S. M. Billerman, and I. J. Lovette. 2020m. Skuas and Jaegers (Stercorariidae), version 1.0. In Birds of the World (S. M. Billerman, B. K. Keeney, P. G. Rodewald, and T. S. Schulenberg, Editors). Cornell Lab of Ornithology, Ithaca, NY, USA. <https://doi.org/10.2173/bow.sterco1.01>

Winkler, D. W., S. M. Billerman, and I. J. Lovette. 2020n. Shearwaters and Petrels (Procellariidae), version 1.0. In Birds of the World (S. M. Billerman, B. K. Keeney, P. G. Rodewald, and T. S. Schulenberg, Editors). Cornell Lab of Ornithology, Ithaca, NY, USA. <https://doi.org/10.2173/bow.procel3.01>

Winship AJ, Leirness JB, Coyne M, Howell J, Saba VS, and Christensen J. 2023. Modeling the distributions of marine birds at sea to inform planning of energy development on the US Atlantic Outer Continental Shelf. Sterling (VA): U.S. Department of the Interior, Bureau of Ocean Energy Management. 413 p. Report No.: OCS Study BOEM 2023-060. Accessed at: https://espis.boem.gov/Final%20Reports/BOEM_2023-060.pdf

Attachment A: Maps of Exposure for Marine Birds

Table of Maps

Map 1. NYERDA APEM high resolution digital aerial seasonal survey effort. Mean survey effort in sq. km by full or partial lease block inside and outside the lease area.....	26
Map 2. Winter Common Eider density proportions in the NYERDA APEM and Empire Wind high resolution digital aerial survey data (A), the NYERDA APEM and Empire Wind high resolution digital aerial model outputs for seaducks in Winter (B) and, Winter Common Eider MDAT modeled abundance at the regional scale (C). The scale for all maps is representative of relative spatial variation in the sites within the season for each map input.	27
Map 3. Spring Common Eider density proportions in the NYERDA APEM and Empire Wind high resolution digital aerial survey data (A), the NYERDA APEM and Empire Wind high resolution digital aerial model outputs for seaducks in Spring (B) and, Spring Common Eider MDAT modeled abundance at the regional scale (C). The scale for all maps is representative of relative spatial variation in the sites within the season for each map input.	28
Map 4. Summer Common Eider density proportions in the NYERDA APEM and Empire Wind high resolution digital aerial survey data (A), the NYERDA APEM and Empire Wind high resolution digital aerial model outputs for seaducks in Summer (B) and, Summer Common Eider MDAT modeled abundance at the regional scale (C). The scale for all maps is representative of relative spatial variation in the sites within the season for each map input.....	29
Map 5. Fall Common Eider density proportions in the NYERDA APEM and Empire Wind high resolution digital aerial survey data (A), the NYERDA APEM and Empire Wind high resolution digital aerial model outputs for seaducks in Fall (B) and, Fall Common Eider MDAT modeled abundance at the regional scale (C). The scale for all maps is representative of relative spatial variation in the sites within the season for each map input.	30
Map 6. Winter Surf Scoter density proportions in the NYERDA APEM and Empire Wind high resolution digital aerial survey data (A), the NYERDA APEM and Empire Wind high resolution digital aerial model outputs for seaducks in Winter (B) and, Winter Surf Scoter MDAT modeled abundance at the regional scale (C). The scale for all maps is representative of relative spatial variation in the sites within the season for each map input.....	31
Map 7. Spring Surf Scoter density proportions in the NYERDA APEM and Empire Wind high resolution digital aerial survey data (A), the NYERDA APEM and Empire Wind high resolution digital aerial model outputs for seaducks in Spring (B) and, Spring Surf Scoter MDAT modeled abundance at the regional scale (C). The scale for all maps is representative of relative spatial variation in the sites within the season for each map input.....	32
Map 8. Summer Surf Scoter density proportions in the NYERDA APEM and Empire Wind high resolution digital aerial survey data (A), the NYERDA APEM and Empire Wind high resolution digital aerial model outputs for seaducks in Summer (B) and, Summer Surf Scoter MDAT modeled abundance at the regional scale (C). The scale for all maps is representative of relative spatial variation in the sites within the season for each map input.....	33
Map 9. Fall Surf Scoter density proportions in the NYERDA APEM and Empire Wind high resolution digital aerial survey data (A), the NYERDA APEM and Empire Wind high resolution digital aerial model outputs for seaducks in Fall (B) and, Fall Surf Scoter MDAT modeled abundance at the regional scale (C).	

The scale for all maps is representative of relative spatial variation in the sites within the season for each map input..... 34

Map 10. Winter White-winged Scoter density proportions in the NYSERDA APEM and Empire Wind high resolution digital aerial survey data (A), the NYSERDA APEM and Empire Wind high resolution digital aerial model outputs for seaducks in Winter (B) and, Winter White-winged Scoter MDAT modeled abundance at the regional scale (C). The scale for all maps is representative of relative spatial variation in the sites within the season for each map input..... 35

Map 11. Spring White-winged Scoter density proportions in the NYSERDA APEM and Empire Wind high resolution digital aerial survey data (A), the NYSERDA APEM and Empire Wind high resolution digital aerial model outputs for seaducks in Spring (B) and, Spring White-winged Scoter MDAT modeled abundance at the regional scale (C). The scale for all maps is representative of relative spatial variation in the sites within the season for each map input..... 36

Map 12. Summer White-winged Scoter density proportions in the NYSERDA APEM and Empire Wind high resolution digital aerial survey data (A), the NYSERDA APEM and Empire Wind high resolution digital aerial model outputs for seaducks in Summer (B) and, Summer White-winged Scoter MDAT modeled abundance at the regional scale (C). The scale for all maps is representative of relative spatial variation in the sites within the season for each map input..... 37

Map 13. Fall White-winged Scoter density proportions in the NYSERDA APEM and Empire Wind high resolution digital aerial survey data (A), the NYSERDA APEM and Empire Wind high resolution digital aerial model outputs for seaducks in Fall (B) and, Fall White-winged Scoter MDAT modeled abundance at the regional scale (C). The scale for all maps is representative of relative spatial variation in the sites within the season for each map input. 38

Map 14. Winter Black Scoter density proportions in the NYSERDA APEM and Empire Wind high resolution digital aerial survey data (A), the NYSERDA APEM and Empire Wind high resolution digital aerial model outputs for seaducks in Winter (B) and, Winter Black Scoter MDAT modeled abundance at the regional scale (C). The scale for all maps is representative of relative spatial variation in the sites within the season for each map input. 39

Map 15. Spring Black Scoter density proportions in the NYSERDA APEM and Empire Wind high resolution digital aerial survey data (A), the NYSERDA APEM and Empire Wind high resolution digital aerial model outputs for seaducks in Spring (B) and, Spring Black Scoter MDAT modeled abundance at the regional scale (C). The scale for all maps is representative of relative spatial variation in the sites within the season for each map input..... 40

Map 16. Summer Black Scoter density proportions in the NYSERDA APEM and Empire Wind high resolution digital aerial survey data (A), the NYSERDA APEM and Empire Wind high resolution digital aerial model outputs for seaducks in Summer (B) and, Summer Black Scoter MDAT modeled abundance at the regional scale (C). The scale for all maps is representative of relative spatial variation in the sites within the season for each map input. 41

Map 17. Fall Black Scoter density proportions in the NYSERDA APEM and Empire Wind high resolution digital aerial survey data (A), the NYSERDA APEM and Empire Wind high resolution digital aerial model outputs for seaducks in Fall (B) and, Fall Black Scoter MDAT modeled abundance at the regional scale (C). The scale for all maps is representative of relative spatial variation in the sites within the season for each map input. 42

Map 18. Winter Long-tailed Duck density proportions in the NYSERDA APEM and Empire Wind high resolution digital aerial survey data (A), the NYSERDA APEM and Empire Wind high resolution digital aerial model outputs for seaducks in Winter (B) and, Winter Long-tailed Duck MDAT modeled abundance at the regional scale (C). The scale for all maps is representative of relative spatial variation in the sites within the season for each map input..... 43

Map 19. Spring Long-tailed Duck density proportions in the NYSERDA APEM and Empire Wind high resolution digital aerial survey data (A), the NYSERDA APEM and Empire Wind high resolution digital aerial model outputs for seaducks in Spring (B) and, Spring Long-tailed Duck MDAT modeled abundance at the regional scale (C). The scale for all maps is representative of relative spatial variation in the sites within the season for each map input. 44

Map 20. Summer Long-tailed Duck density proportions in the NYSERDA APEM and Empire Wind high resolution digital aerial survey data (A), the NYSERDA APEM and Empire Wind high resolution digital aerial model outputs for seaducks in Summer (B) and, Summer Long-tailed Duck MDAT modeled abundance at the regional scale (C). The scale for all maps is representative of relative spatial variation in the sites within the season for each map input..... 45

Map 21. Fall Long-tailed Duck density proportions in the NYSERDA APEM and Empire Wind high resolution digital aerial survey data (A), the NYSERDA APEM and Empire Wind high resolution digital aerial model outputs for seaducks in Fall (B) and, Fall Long-tailed Duck MDAT modeled abundance at the regional scale (C). The scale for all maps is representative of relative spatial variation in the sites within the season for each map input. 46

Map 22. Fall Common Merganser density proportions in the NYSERDA APEM and Empire Wind high resolution digital aerial survey data (A), the NYSERDA APEM and Empire Wind high resolution digital aerial model outputs for seaducks in Fall (B) and, Fall Common Merganser MDAT modeled abundance at the regional scale (C). The scale for all maps is representative of relative spatial variation in the sites within the season for each map input. 47

Map 23. Winter Red-breasted Merganser density proportions in the NYSERDA APEM and Empire Wind high resolution digital aerial survey data (A), the NYSERDA APEM and Empire Wind high resolution digital aerial model outputs for seaducks in Winter (B) and, Winter Red-breasted Merganser MDAT modeled abundance at the regional scale (C). The scale for all maps is representative of relative spatial variation in the sites within the season for each map input. 48

Map 24. Spring Red-breasted Merganser density proportions in the NYSERDA APEM and Empire Wind high resolution digital aerial survey data (A), the NYSERDA APEM and Empire Wind high resolution digital aerial model outputs for seaducks in Spring (B) and, Spring Red-breasted Merganser MDAT modeled abundance at the regional scale (C). The scale for all maps is representative of relative spatial variation in the sites within the season for each map input. 49

Map 25. Summer Red-breasted Merganser density proportions in the NYSERDA APEM and Empire Wind high resolution digital aerial survey data (A), the NYSERDA APEM and Empire Wind high resolution digital aerial model outputs for seaducks in Summer (B) and, Summer Red-breasted Merganser MDAT modeled abundance at the regional scale (C). The scale for all maps is representative of relative spatial variation in the sites within the season for each map input. 50

Map 26. Fall Red-breasted Merganser density proportions in the NYSERDA APEM and Empire Wind high resolution digital aerial survey data (A), the NYSERDA APEM and Empire Wind high resolution digital

aerial model outputs for seaducks in Fall (B) and, Fall Red-breasted Merganser MDAT modeled abundance at the regional scale (C). The scale for all maps is representative of relative spatial variation in the sites within the season for each map input..... 51

Map 27. Winter Horned Grebe density proportions in the NYSERDA APEM and Empire Wind high resolution digital aerial survey data (A), the NYSERDA APEM and Empire Wind high resolution digital aerial model outputs for grebes in Winter (B) and, Winter Horned Grebe MDAT modeled abundance at the regional scale (C). The scale for all maps is representative of relative spatial variation in the sites within the season for each map input. 52

Map 28. Spring Horned Grebe density proportions in the NYSERDA APEM and Empire Wind high resolution digital aerial survey data (A), the NYSERDA APEM and Empire Wind high resolution digital aerial model outputs for grebes in Spring (B) and, Spring Horned Grebe MDAT modeled abundance at the regional scale (C). The scale for all maps is representative of relative spatial variation in the sites within the season for each map input. 53

Map 29. Summer Horned Grebe density proportions in the NYSERDA APEM and Empire Wind high resolution digital aerial survey data (A), the NYSERDA APEM and Empire Wind high resolution digital aerial model outputs for grebes in Summer (B) and, Summer Horned Grebe MDAT modeled abundance at the regional scale (C). The scale for all maps is representative of relative spatial variation in the sites within the season for each map input. 54

Map 30. Fall Horned Grebe density proportions in the NYSERDA APEM and Empire Wind high resolution digital aerial survey data (A), the NYSERDA APEM and Empire Wind high resolution digital aerial model outputs for grebes in Fall (B) and, Fall Horned Grebe MDAT modeled abundance at the regional scale (C). The scale for all maps is representative of relative spatial variation in the sites within the season for each map input..... 55

Map 31. Summer Black-bellied Plover density proportions in the NYSERDA APEM and Empire Wind high resolution digital aerial survey data (A), the NYSERDA APEM and Empire Wind high resolution digital aerial model outputs for shorebirds in Summer (B) and, Summer Black-bellied Plover MDAT modeled abundance at the regional scale (C). The scale for all maps is representative of relative spatial variation in the sites within the season for each map input..... 56

Map 32. Summer Semipalmated Plover density proportions in the NYSERDA APEM and Empire Wind high resolution digital aerial survey data (A), the NYSERDA APEM and Empire Wind high resolution digital aerial model outputs for shorebirds in Summer (B) and, Summer Semipalmated Plover MDAT modeled abundance at the regional scale (C). The scale for all maps is representative of relative spatial variation in the sites within the season for each map input. 57

Map 33. Winter Red-necked Phalarope density proportions in the NYSERDA APEM and Empire Wind high resolution digital aerial survey data (A), the NYSERDA APEM and Empire Wind high resolution digital aerial model outputs for phalaropes in Winter (B) and, Winter Red-necked Phalarope MDAT modeled abundance at the regional scale (C). The scale for all maps is representative of relative spatial variation in the sites within the season for each map input..... 58

Map 34. Spring Red-necked Phalarope density proportions in the NYSERDA APEM and Empire Wind high resolution digital aerial survey data (A), the NYSERDA APEM and Empire Wind high resolution digital aerial model outputs for phalaropes in Spring (B) and, Spring Red-necked Phalarope MDAT modeled

abundance at the regional scale (C). The scale for all maps is representative of relative spatial variation in the sites within the season for each map input..... 59

Map 35. Summer Red-necked Phalarope density proportions in the NYSERDA APEM and Empire Wind high resolution digital aerial survey data (A), the NYSERDA APEM and Empire Wind high resolution digital aerial model outputs for phalaropes in Summer (B) and, Summer Red-necked Phalarope MDAT modeled abundance at the regional scale (C). The scale for all maps is representative of relative spatial variation in the sites within the season for each map input. 60

Map 36. Fall Red-necked Phalarope density proportions in the NYSERDA APEM and Empire Wind high resolution digital aerial survey data (A), the NYSERDA APEM and Empire Wind high resolution digital aerial model outputs for phalaropes in Fall (B) and, Fall Red-necked Phalarope MDAT modeled abundance at the regional scale (C). The scale for all maps is representative of relative spatial variation in the sites within the season for each map input..... 61

Map 37. Winter Red Phalarope density proportions in the NYSERDA APEM and Empire Wind high resolution digital aerial survey data (A), the NYSERDA APEM and Empire Wind high resolution digital aerial model outputs for phalaropes in Winter (B) and, Winter Red Phalarope MDAT modeled abundance at the regional scale (C). The scale for all maps is representative of relative spatial variation in the sites within the season for each map input..... 62

Map 38. Spring Red Phalarope density proportions in the NYSERDA APEM and Empire Wind high resolution digital aerial survey data (A), the NYSERDA APEM and Empire Wind high resolution digital aerial model outputs for phalaropes in Spring (B) and, Spring Red Phalarope MDAT modeled abundance at the regional scale (C). The scale for all maps is representative of relative spatial variation in the sites within the season for each map input. 63

Map 39. Summer Red Phalarope density proportions in the NYSERDA APEM and Empire Wind high resolution digital aerial survey data (A), the NYSERDA APEM and Empire Wind high resolution digital aerial model outputs for phalaropes in Summer (B) and, Summer Red Phalarope MDAT modeled abundance at the regional scale (C). The scale for all maps is representative of relative spatial variation in the sites within the season for each map input..... 64

Map 40. Fall Red Phalarope density proportions in the NYSERDA APEM and Empire Wind high resolution digital aerial survey data (A), the NYSERDA APEM and Empire Wind high resolution digital aerial model outputs for phalaropes in Fall (B) and, Fall Red Phalarope MDAT modeled abundance at the regional scale (C). The scale for all maps is representative of relative spatial variation in the sites within the season for each map input..... 65

Map 41. Winter Great Skua density proportions in the NYSERDA APEM and Empire Wind high resolution digital aerial survey data (A), the NYSERDA APEM and Empire Wind high resolution digital aerial model outputs for skuas and jaegers in Winter (B) and, Winter Great Skua MDAT modeled abundance at the regional scale (C). The scale for all maps is representative of relative spatial variation in the sites within the season for each map input. 66

Map 42. Spring Great Skua density proportions in the NYSERDA APEM and Empire Wind high resolution digital aerial survey data (A), the NYSERDA APEM and Empire Wind high resolution digital aerial model outputs for skuas and jaegers in Spring (B) and, Spring Great Skua MDAT modeled abundance at the regional scale (C). The scale for all maps is representative of relative spatial variation in the sites within the season for each map input. 67

Map 43. Summer Great Skua density proportions in the NYSERDA APEM and Empire Wind high resolution digital aerial survey data (A), the NYSERDA APEM and Empire Wind high resolution digital aerial model outputs for skuas and jaegers in Summer (B) and, Summer Great Skua MDAT modeled abundance at the regional scale (C). The scale for all maps is representative of relative spatial variation in the sites within the season for each map input..... 68

Map 44. Fall Great Skua density proportions in the NYSERDA APEM and Empire Wind high resolution digital aerial survey data (A), the NYSERDA APEM and Empire Wind high resolution digital aerial model outputs for skuas and jaegers in Fall (B) and, Fall Great Skua MDAT modeled abundance at the regional scale (C). The scale for all maps is representative of relative spatial variation in the sites within the season for each map input..... 69

Map 45. Winter South Polar Skua density proportions in the NYSERDA APEM and Empire Wind high resolution digital aerial survey data (A), the NYSERDA APEM and Empire Wind high resolution digital aerial model outputs for skuas and jaegers in Winter (B) and, Winter South Polar Skua MDAT modeled abundance at the regional scale (C). The scale for all maps is representative of relative spatial variation in the sites within the season for each map input..... 70

Map 46. Spring South Polar Skua density proportions in the NYSERDA APEM and Empire Wind high resolution digital aerial survey data (A), the NYSERDA APEM and Empire Wind high resolution digital aerial model outputs for skuas and jaegers in Spring (B) and, Spring South Polar Skua MDAT modeled abundance at the regional scale (C). The scale for all maps is representative of relative spatial variation in the sites within the season for each map input..... 71

Map 47. Summer South Polar Skua density proportions in the NYSERDA APEM and Empire Wind high resolution digital aerial survey data (A), the NYSERDA APEM and Empire Wind high resolution digital aerial model outputs for skuas and jaegers in Summer (B) and, Summer South Polar Skua MDAT modeled abundance at the regional scale (C). The scale for all maps is representative of relative spatial variation in the sites within the season for each map input. 72

Map 48. Fall South Polar Skua density proportions in the NYSERDA APEM and Empire Wind high resolution digital aerial survey data (A), the NYSERDA APEM and Empire Wind high resolution digital aerial model outputs for skuas and jaegers in Fall (B) and, Fall South Polar Skua MDAT modeled abundance at the regional scale (C). The scale for all maps is representative of relative spatial variation in the sites within the season for each map input..... 73

Map 49. Winter Pomarine Jaeger density proportions in the NYSERDA APEM and Empire Wind high resolution digital aerial survey data (A), the NYSERDA APEM and Empire Wind high resolution digital aerial model outputs for skuas and jaegers in Winter (B) and, Winter Pomarine Jaeger MDAT modeled abundance at the regional scale (C). The scale for all maps is representative of relative spatial variation in the sites within the season for each map input..... 74

Map 50. Spring Pomarine Jaeger density proportions in the NYSERDA APEM and Empire Wind high resolution digital aerial survey data (A), the NYSERDA APEM and Empire Wind high resolution digital aerial model outputs for skuas and jaegers in Spring (B) and, Spring Pomarine Jaeger MDAT modeled abundance at the regional scale (C). The scale for all maps is representative of relative spatial variation in the sites within the season for each map input..... 75

Map 51. Summer Pomarine Jaeger density proportions in the NYSERDA APEM and Empire Wind high resolution digital aerial survey data (A), the NYSERDA APEM and Empire Wind high resolution digital

aerial model outputs for skuas and jaegers in Summer (B) and, Summer Pomarine Jaeger MDAT modeled abundance at the regional scale (C). The scale for all maps is representative of relative spatial variation in the sites within the season for each map input..... 76

Map 52. Fall Pomarine Jaeger density proportions in the NYSERDA APEM and Empire Wind high resolution digital aerial survey data (A), the NYSERDA APEM and Empire Wind high resolution digital aerial model outputs for skuas and jaegers in Fall (B) and, Fall Pomarine Jaeger MDAT modeled abundance at the regional scale (C). The scale for all maps is representative of relative spatial variation in the sites within the season for each map input..... 77

Map 53. Winter Parasitic Jaeger density proportions in the NYSERDA APEM and Empire Wind high resolution digital aerial survey data (A), the NYSERDA APEM and Empire Wind high resolution digital aerial model outputs for skuas and jaegers in Winter (B) and, Winter Parasitic Jaeger MDAT modeled abundance at the regional scale (C). The scale for all maps is representative of relative spatial variation in the sites within the season for each map input..... 78

Map 54. Spring Parasitic Jaeger density proportions in the NYSERDA APEM and Empire Wind high resolution digital aerial survey data (A), the NYSERDA APEM and Empire Wind high resolution digital aerial model outputs for skuas and jaegers in Spring (B) and, Spring Parasitic Jaeger MDAT modeled abundance at the regional scale (C). The scale for all maps is representative of relative spatial variation in the sites within the season for each map input..... 79

Map 55. Summer Parasitic Jaeger density proportions in the NYSERDA APEM and Empire Wind high resolution digital aerial survey data (A), the NYSERDA APEM and Empire Wind high resolution digital aerial model outputs for skuas and jaegers in Summer (B) and, Summer Parasitic Jaeger MDAT modeled abundance at the regional scale (C). The scale for all maps is representative of relative spatial variation in the sites within the season for each map input..... 80

Map 56. Fall Parasitic Jaeger density proportions in the NYSERDA APEM and Empire Wind high resolution digital aerial survey data (A), the NYSERDA APEM and Empire Wind high resolution digital aerial model outputs for skuas and jaegers in Fall (B) and, Fall Parasitic Jaeger MDAT modeled abundance at the regional scale (C). The scale for all maps is representative of relative spatial variation in the sites within the season for each map input..... 81

Map 57. Winter Dovekie density proportions in the NYSERDA APEM and Empire Wind high resolution digital aerial survey data (A), the NYSERDA APEM and Empire Wind high resolution digital aerial model outputs for auks in Winter (B) and, Winter Dovekie MDAT modeled abundance at the regional scale (C). The scale for all maps is representative of relative spatial variation in the sites within the season for each map input..... 82

Map 58. Spring Dovekie density proportions in the NYSERDA APEM and Empire Wind high resolution digital aerial survey data (A), the NYSERDA APEM and Empire Wind high resolution digital aerial model outputs for auks in Spring (B) and, Spring Dovekie MDAT modeled abundance at the regional scale (C). The scale for all maps is representative of relative spatial variation in the sites within the season for each map input..... 83

Map 59. Summer Dovekie density proportions in the NYSERDA APEM and Empire Wind high resolution digital aerial survey data (A), the NYSERDA APEM and Empire Wind high resolution digital aerial model outputs for auks in Summer (B) and, Summer Dovekie MDAT modeled abundance at the regional scale

(C). The scale for all maps is representative of relative spatial variation in the sites within the season for each map input. 84

Map 60. Fall Dovekie density proportions in the NYSERDA APEM and Empire Wind high resolution digital aerial survey data (A), the NYSERDA APEM and Empire Wind high resolution digital aerial model outputs for auks in Fall (B) and, Fall Dovekie MDAT modeled abundance at the regional scale (C). The scale for all maps is representative of relative spatial variation in the sites within the season for each map input.... 85

Map 61. Winter Common Murre density proportions in the NYSERDA APEM and Empire Wind high resolution digital aerial survey data (A), the NYSERDA APEM and Empire Wind high resolution digital aerial model outputs for auks in Winter (B) and, Winter Common Murre MDAT modeled abundance at the regional scale (C). The scale for all maps is representative of relative spatial variation in the sites within the season for each map input. 86

Map 62. Spring Common Murre density proportions in the NYSERDA APEM and Empire Wind high resolution digital aerial survey data (A), the NYSERDA APEM and Empire Wind high resolution digital aerial model outputs for auks in Spring (B) and, Spring Common Murre MDAT modeled abundance at the regional scale (C). The scale for all maps is representative of relative spatial variation in the sites within the season for each map input. 87

Map 63. Summer Common Murre density proportions in the NYSERDA APEM and Empire Wind high resolution digital aerial survey data (A), the NYSERDA APEM and Empire Wind high resolution digital aerial model outputs for auks in Summer (B) and, Summer Common Murre MDAT modeled abundance at the regional scale (C). The scale for all maps is representative of relative spatial variation in the sites within the season for each map input. 88

Map 64. Fall Common Murre density proportions in the NYSERDA APEM and Empire Wind high resolution digital aerial survey data (A), the NYSERDA APEM and Empire Wind high resolution digital aerial model outputs for auks in Fall (B) and, Fall Common Murre MDAT modeled abundance at the regional scale (C). The scale for all maps is representative of relative spatial variation in the sites within the season for each map input. 89

Map 65. Winter Thick-billed Murre density proportions in the NYSERDA APEM and Empire Wind high resolution digital aerial survey data (A), the NYSERDA APEM and Empire Wind high resolution digital aerial model outputs for auks in Winter (B) and, Winter Thick-billed Murre MDAT modeled abundance at the regional scale (C). The scale for all maps is representative of relative spatial variation in the sites within the season for each map input. 90

Map 66. Spring Thick-billed Murre density proportions in the NYSERDA APEM and Empire Wind high resolution digital aerial survey data (A), the NYSERDA APEM and Empire Wind high resolution digital aerial model outputs for auks in Spring (B) and, Spring Thick-billed Murre MDAT modeled abundance at the regional scale (C). The scale for all maps is representative of relative spatial variation in the sites within the season for each map input. 91

Map 67. Summer Thick-billed Murre density proportions in the NYSERDA APEM and Empire Wind high resolution digital aerial survey data (A), the NYSERDA APEM and Empire Wind high resolution digital aerial model outputs for auks in Summer (B) and, Summer Thick-billed Murre MDAT modeled abundance at the regional scale (C). The scale for all maps is representative of relative spatial variation in the sites within the season for each map input..... 92

Map 68. Fall Thick-billed Murre density proportions in the NYSERDA APEM and Empire Wind high resolution digital aerial survey data (A), the NYSERDA APEM and Empire Wind high resolution digital aerial model outputs for auks in Fall (B) and, Fall Thick-billed Murre MDAT modeled abundance at the regional scale (C). The scale for all maps is representative of relative spatial variation in the sites within the season for each map input. 93

Map 69. Winter Razorbill density proportions in the NYSERDA APEM and Empire Wind high resolution digital aerial survey data (A), the NYSERDA APEM and Empire Wind high resolution digital aerial model outputs for auks in Winter (B) and, Winter Razorbill MDAT modeled abundance at the regional scale (C). The scale for all maps is representative of relative spatial variation in the sites within the season for each map input..... 94

Map 70. Spring Razorbill density proportions in the NYSERDA APEM and Empire Wind high resolution digital aerial survey data (A), the NYSERDA APEM and Empire Wind high resolution digital aerial model outputs for auks in Spring (B) and, Spring Razorbill MDAT modeled abundance at the regional scale (C). The scale for all maps is representative of relative spatial variation in the sites within the season for each map input..... 95

Map 71. Summer Razorbill density proportions in the NYSERDA APEM and Empire Wind high resolution digital aerial survey data (A), the NYSERDA APEM and Empire Wind high resolution digital aerial model outputs for auks in Summer (B) and, Summer Razorbill MDAT modeled abundance at the regional scale (C). The scale for all maps is representative of relative spatial variation in the sites within the season for each map input. 96

Map 72. Fall Razorbill density proportions in the NYSERDA APEM and Empire Wind high resolution digital aerial survey data (A), the NYSERDA APEM and Empire Wind high resolution digital aerial model outputs for auks in Fall (B) and, Fall Razorbill MDAT modeled abundance at the regional scale (C). The scale for all maps is representative of relative spatial variation in the sites within the season for each map input.... 97

Map 73. Winter Black Guillemot density proportions in the NYSERDA APEM and Empire Wind high resolution digital aerial survey data (A), the NYSERDA APEM and Empire Wind high resolution digital aerial model outputs for auks in Winter (B) and, Winter Black Guillemot MDAT modeled abundance at the regional scale (C). The scale for all maps is representative of relative spatial variation in the sites within the season for each map input. 98

Map 74. Spring Black Guillemot density proportions in the NYSERDA APEM and Empire Wind high resolution digital aerial survey data (A), the NYSERDA APEM and Empire Wind high resolution digital aerial model outputs for auks in Spring (B) and, Spring Black Guillemot MDAT modeled abundance at the regional scale (C). The scale for all maps is representative of relative spatial variation in the sites within the season for each map input. 99

Map 75. Summer Black Guillemot density proportions in the NYSERDA APEM and Empire Wind high resolution digital aerial survey data (A), the NYSERDA APEM and Empire Wind high resolution digital aerial model outputs for auks in Summer (B) and, Summer Black Guillemot MDAT modeled abundance at the regional scale (C). The scale for all maps is representative of relative spatial variation in the sites within the season for each map input. 100

Map 76. Fall Black Guillemot density proportions in the NYSERDA APEM and Empire Wind high resolution digital aerial survey data (A), the NYSERDA APEM and Empire Wind high resolution digital aerial model outputs for auks in Fall (B) and, Fall Black Guillemot MDAT modeled abundance at the

regional scale (C). The scale for all maps is representative of relative spatial variation in the sites within the season for each map input. 101

Map 77. Winter Atlantic Puffin density proportions in the NYSERDA APEM and Empire Wind high resolution digital aerial survey data (A), the NYSERDA APEM and Empire Wind high resolution digital aerial model outputs for auks in Winter (B) and, Winter Atlantic Puffin MDAT modeled abundance at the regional scale (C). The scale for all maps is representative of relative spatial variation in the sites within the season for each map input. 102

Map 78. Spring Atlantic Puffin density proportions in the NYSERDA APEM and Empire Wind high resolution digital aerial survey data (A), the NYSERDA APEM and Empire Wind high resolution digital aerial model outputs for auks in Spring (B) and, Spring Atlantic Puffin MDAT modeled abundance at the regional scale (C). The scale for all maps is representative of relative spatial variation in the sites within the season for each map input. 103

Map 79. Summer Atlantic Puffin density proportions in the NYSERDA APEM and Empire Wind high resolution digital aerial survey data (A), the NYSERDA APEM and Empire Wind high resolution digital aerial model outputs for auks in Summer (B) and, Summer Atlantic Puffin MDAT modeled abundance at the regional scale (C). The scale for all maps is representative of relative spatial variation in the sites within the season for each map input. 104

Map 80. Fall Atlantic Puffin density proportions in the NYSERDA APEM and Empire Wind high resolution digital aerial survey data (A), the NYSERDA APEM and Empire Wind high resolution digital aerial model outputs for auks in Fall (B) and, Fall Atlantic Puffin MDAT modeled abundance at the regional scale (C). The scale for all maps is representative of relative spatial variation in the sites within the season for each map input. 105

Map 81. Winter Bonaparte's Gull density proportions in the NYSERDA APEM and Empire Wind high resolution digital aerial survey data (A), the NYSERDA APEM and Empire Wind high resolution digital aerial model outputs for small gulls in Winter (B) and, Winter Bonaparte's Gull MDAT modeled abundance at the regional scale (C). The scale for all maps is representative of relative spatial variation in the sites within the season for each map input. 106

Map 82. Spring Bonaparte's Gull density proportions in the NYSERDA APEM and Empire Wind high resolution digital aerial survey data (A), the NYSERDA APEM and Empire Wind high resolution digital aerial model outputs for small gulls in Spring (B) and, Spring Bonaparte's Gull MDAT modeled abundance at the regional scale (C). The scale for all maps is representative of relative spatial variation in the sites within the season for each map input. 107

Map 83. Summer Bonaparte's Gull density proportions in the NYSERDA APEM and Empire Wind high resolution digital aerial survey data (A), the NYSERDA APEM and Empire Wind high resolution digital aerial model outputs for small gulls in Summer (B) and, Summer Bonaparte's Gull MDAT modeled abundance at the regional scale (C). The scale for all maps is representative of relative spatial variation in the sites within the season for each map input. 108

Map 84. Fall Bonaparte's Gull density proportions in the NYSERDA APEM and Empire Wind high resolution digital aerial survey data (A), the NYSERDA APEM and Empire Wind high resolution digital aerial model outputs for small gulls in Fall (B) and, Fall Bonaparte's Gull MDAT modeled abundance at the regional scale (C). The scale for all maps is representative of relative spatial variation in the sites within the season for each map input. 109

Map 85. Winter Little Gull density proportions in the NYSERDA APEM and Empire Wind high resolution digital aerial survey data (A), the NYSERDA APEM and Empire Wind high resolution digital aerial model outputs for small gulls in Winter (B) and, Winter Little Gull MDAT modeled abundance at the regional scale (C). The scale for all maps is representative of relative spatial variation in the sites within the season for each map input..... 110

Map 86. Spring Little Gull density proportions in the NYSERDA APEM and Empire Wind high resolution digital aerial survey data (A), the NYSERDA APEM and Empire Wind high resolution digital aerial model outputs for small gulls in Spring (B) and, Spring Little Gull MDAT modeled abundance at the regional scale (C). The scale for all maps is representative of relative spatial variation in the sites within the season for each map input..... 111

Map 87. Fall Little Gull density proportions in the NYSERDA APEM and Empire Wind high resolution digital aerial survey data (A), the NYSERDA APEM and Empire Wind high resolution digital aerial model outputs for small gulls in Fall (B) and, Fall Little Gull MDAT modeled abundance at the regional scale (C). The scale for all maps is representative of relative spatial variation in the sites within the season for each map input..... 112

Map 88. Winter Black-legged Kittiwake density proportions in the NYSERDA APEM and Empire Wind high resolution digital aerial survey data (A), the NYSERDA APEM and Empire Wind high resolution digital aerial model outputs for medium gulls in Winter (B) and, Winter Black-legged Kittiwake MDAT modeled abundance at the regional scale (C). The scale for all maps is representative of relative spatial variation in the sites within the season for each map input..... 113

Map 89. Spring Black-legged Kittiwake density proportions in the NYSERDA APEM and Empire Wind high resolution digital aerial survey data (A), the NYSERDA APEM and Empire Wind high resolution digital aerial model outputs for medium gulls in Spring (B) and, Spring Black-legged Kittiwake MDAT modeled abundance at the regional scale (C). The scale for all maps is representative of relative spatial variation in the sites within the season for each map input..... 114

Map 90. Summer Black-legged Kittiwake density proportions in the NYSERDA APEM and Empire Wind high resolution digital aerial survey data (A), the NYSERDA APEM and Empire Wind high resolution digital aerial model outputs for medium gulls in Summer (B) and, Summer Black-legged Kittiwake MDAT modeled abundance at the regional scale (C). The scale for all maps is representative of relative spatial variation in the sites within the season for each map input. 115

Map 91. Fall Black-legged Kittiwake density proportions in the NYSERDA APEM and Empire Wind high resolution digital aerial survey data (A), the NYSERDA APEM and Empire Wind high resolution digital aerial model outputs for medium gulls in Fall (B) and, Fall Black-legged Kittiwake MDAT modeled abundance at the regional scale (C). The scale for all maps is representative of relative spatial variation in the sites within the season for each map input..... 116

Map 92. Winter Laughing Gull density proportions in the NYSERDA APEM and Empire Wind high resolution digital aerial survey data (A), the NYSERDA APEM and Empire Wind high resolution digital aerial model outputs for medium gulls in Winter (B) and, Winter Laughing Gull MDAT modeled abundance at the regional scale (C). The scale for all maps is representative of relative spatial variation in the sites within the season for each map input..... 117

Map 93. Spring Laughing Gull density proportions in the NYSERDA APEM and Empire Wind high resolution digital aerial survey data (A), the NYSERDA APEM and Empire Wind high resolution digital

aerial model outputs for medium gulls in Spring (B) and, Spring Laughing Gull MDAT modeled abundance at the regional scale (C). The scale for all maps is representative of relative spatial variation in the sites within the season for each map input. 118

Map 94. Summer Laughing Gull density proportions in the NYSERDA APEM and Empire Wind high resolution digital aerial survey data (A), the NYSERDA APEM and Empire Wind high resolution digital aerial model outputs for medium gulls in Summer (B) and, Summer Laughing Gull MDAT modeled abundance at the regional scale (C). The scale for all maps is representative of relative spatial variation in the sites within the season for each map input..... 119

Map 95. Fall Laughing Gull density proportions in the NYSERDA APEM and Empire Wind high resolution digital aerial survey data (A), the NYSERDA APEM and Empire Wind high resolution digital aerial model outputs for medium gulls in Fall (B) and, Fall Laughing Gull MDAT modeled abundance at the regional scale (C). The scale for all maps is representative of relative spatial variation in the sites within the season for each map input..... 120

Map 96. Winter Ring-billed Gull density proportions in the NYSERDA APEM and Empire Wind high resolution digital aerial survey data (A), the NYSERDA APEM and Empire Wind high resolution digital aerial model outputs for medium gulls in Winter (B) and, Winter Ring-billed Gull MDAT modeled abundance at the regional scale (C). The scale for all maps is representative of relative spatial variation in the sites within the season for each map input..... 121

Map 97. Spring Ring-billed Gull density proportions in the NYSERDA APEM and Empire Wind high resolution digital aerial survey data (A), the NYSERDA APEM and Empire Wind high resolution digital aerial model outputs for medium gulls in Spring (B) and, Spring Ring-billed Gull MDAT modeled abundance at the regional scale (C). The scale for all maps is representative of relative spatial variation in the sites within the season for each map input..... 122

Map 98. Summer Ring-billed Gull density proportions in the NYSERDA APEM and Empire Wind high resolution digital aerial survey data (A), the NYSERDA APEM and Empire Wind high resolution digital aerial model outputs for medium gulls in Summer (B) and, Summer Ring-billed Gull MDAT modeled abundance at the regional scale (C). The scale for all maps is representative of relative spatial variation in the sites within the season for each map input..... 123

Map 99. Fall Ring-billed Gull density proportions in the NYSERDA APEM and Empire Wind high resolution digital aerial survey data (A), the NYSERDA APEM and Empire Wind high resolution digital aerial model outputs for medium gulls in Fall (B) and, Fall Ring-billed Gull MDAT modeled abundance at the regional scale (C). The scale for all maps is representative of relative spatial variation in the sites within the season for each map input..... 124

Map 100. Winter Herring Gull density proportions in the NYSERDA APEM and Empire Wind high resolution digital aerial survey data (A), the NYSERDA APEM and Empire Wind high resolution digital aerial model outputs for large gulls in Winter (B) and, Winter Herring Gull MDAT modeled abundance at the regional scale (C). The scale for all maps is representative of relative spatial variation in the sites within the season for each map input. 125

Map 101. Spring Herring Gull density proportions in the NYSERDA APEM and Empire Wind high resolution digital aerial survey data (A), the NYSERDA APEM and Empire Wind high resolution digital aerial model outputs for large gulls in Spring (B) and, Spring Herring Gull MDAT modeled abundance at

the regional scale (C). The scale for all maps is representative of relative spatial variation in the sites within the season for each map input. 126

Map 102. Summer Herring Gull density proportions in the NYSERDA APEM and Empire Wind high resolution digital aerial survey data (A), the NYSERDA APEM and Empire Wind high resolution digital aerial model outputs for large gulls in Summer (B) and, Summer Herring Gull MDAT modeled abundance at the regional scale (C). The scale for all maps is representative of relative spatial variation in the sites within the season for each map input. 127

Map 103. Fall Herring Gull density proportions in the NYSERDA APEM and Empire Wind high resolution digital aerial survey data (A), the NYSERDA APEM and Empire Wind high resolution digital aerial model outputs for large gulls in Fall (B) and, Fall Herring Gull MDAT modeled abundance at the regional scale (C). The scale for all maps is representative of relative spatial variation in the sites within the season for each map input. 128

Map 104. Winter Iceland Gull density proportions in the NYSERDA APEM and Empire Wind high resolution digital aerial survey data (A), the NYSERDA APEM and Empire Wind high resolution digital aerial model outputs for large gulls in Winter (B) and, Winter Iceland Gull MDAT modeled abundance at the regional scale (C). The scale for all maps is representative of relative spatial variation in the sites within the season for each map input. 129

Map 105. Spring Iceland Gull density proportions in the NYSERDA APEM and Empire Wind high resolution digital aerial survey data (A), the NYSERDA APEM and Empire Wind high resolution digital aerial model outputs for large gulls in Spring (B) and, Spring Iceland Gull MDAT modeled abundance at the regional scale (C). The scale for all maps is representative of relative spatial variation in the sites within the season for each map input. 130

Map 106. Fall Iceland Gull density proportions in the NYSERDA APEM and Empire Wind high resolution digital aerial survey data (A), the NYSERDA APEM and Empire Wind high resolution digital aerial model outputs for large gulls in Fall (B) and, Fall Iceland Gull MDAT modeled abundance at the regional scale (C). The scale for all maps is representative of relative spatial variation in the sites within the season for each map input. 131

Map 107. Winter Lesser Black-backed Gull density proportions in the NYSERDA APEM and Empire Wind high resolution digital aerial survey data (A), the NYSERDA APEM and Empire Wind high resolution digital aerial model outputs for large gulls in Winter (B) and, Winter Lesser Black-backed Gull MDAT modeled abundance at the regional scale (C). The scale for all maps is representative of relative spatial variation in the sites within the season for each map input. 132

Map 108. Spring Lesser Black-backed Gull density proportions in the NYSERDA APEM and Empire Wind high resolution digital aerial survey data (A), the NYSERDA APEM and Empire Wind high resolution digital aerial model outputs for large gulls in Spring (B) and, Spring Lesser Black-backed Gull MDAT modeled abundance at the regional scale (C). The scale for all maps is representative of relative spatial variation in the sites within the season for each map input. 133

Map 109. Summer Lesser Black-backed Gull density proportions in the NYSERDA APEM and Empire Wind high resolution digital aerial survey data (A), the NYSERDA APEM and Empire Wind high resolution digital aerial model outputs for large gulls in Summer (B) and, Summer Lesser Black-backed Gull MDAT modeled abundance at the regional scale (C). The scale for all maps is representative of relative spatial variation in the sites within the season for each map input. 134

Map 110. Fall Lesser Black-backed Gull density proportions in the NYSERDA APEM and Empire Wind high resolution digital aerial survey data (A), the NYSERDA APEM and Empire Wind high resolution digital aerial model outputs for large gulls in Fall (B) and, Fall Lesser Black-backed Gull MDAT modeled abundance at the regional scale (C). The scale for all maps is representative of relative spatial variation in the sites within the season for each map input..... 135

Map 111. Winter Glaucous Gull density proportions in the NYSERDA APEM and Empire Wind high resolution digital aerial survey data (A), the NYSERDA APEM and Empire Wind high resolution digital aerial model outputs for large gulls in Winter (B) and, Winter Glaucous Gull MDAT modeled abundance at the regional scale (C). The scale for all maps is representative of relative spatial variation in the sites within the season for each map input. 136

Map 112. Spring Glaucous Gull density proportions in the NYSERDA APEM and Empire Wind high resolution digital aerial survey data (A), the NYSERDA APEM and Empire Wind high resolution digital aerial model outputs for large gulls in Spring (B) and, Spring Glaucous Gull MDAT modeled abundance at the regional scale (C). The scale for all maps is representative of relative spatial variation in the sites within the season for each map input. 137

Map 113. Winter Great Black-backed Gull density proportions in the NYSERDA APEM and Empire Wind high resolution digital aerial survey data (A), the NYSERDA APEM and Empire Wind high resolution digital aerial model outputs for large gulls in Winter (B) and, Winter Great Black-backed Gull MDAT modeled abundance at the regional scale (C). The scale for all maps is representative of relative spatial variation in the sites within the season for each map input. 138

Map 114. Spring Great Black-backed Gull density proportions in the NYSERDA APEM and Empire Wind high resolution digital aerial survey data (A), the NYSERDA APEM and Empire Wind high resolution digital aerial model outputs for large gulls in Spring (B) and, Spring Great Black-backed Gull MDAT modeled abundance at the regional scale (C). The scale for all maps is representative of relative spatial variation in the sites within the season for each map input. 139

Map 115. Summer Great Black-backed Gull density proportions in the NYSERDA APEM and Empire Wind high resolution digital aerial survey data (A), the NYSERDA APEM and Empire Wind high resolution digital aerial model outputs for large gulls in Summer (B) and, Summer Great Black-backed Gull MDAT modeled abundance at the regional scale (C). The scale for all maps is representative of relative spatial variation in the sites within the season for each map input. 140

Map 116. Fall Great Black-backed Gull density proportions in the NYSERDA APEM and Empire Wind high resolution digital aerial survey data (A), the NYSERDA APEM and Empire Wind high resolution digital aerial model outputs for large gulls in Fall (B) and, Fall Great Black-backed Gull MDAT modeled abundance at the regional scale (C). The scale for all maps is representative of relative spatial variation in the sites within the season for each map input..... 141

Map 117. Winter Least Tern density proportions in the NYSERDA APEM and Empire Wind high resolution digital aerial survey data (A), the NYSERDA APEM and Empire Wind high resolution digital aerial model outputs for small terns in Winter (B) and, Winter Least Tern MDAT modeled abundance at the regional scale (C). The scale for all maps is representative of relative spatial variation in the sites within the season for each map input..... 142

Map 118. Spring Least Tern density proportions in the NYSERDA APEM and Empire Wind high resolution digital aerial survey data (A), the NYSERDA APEM and Empire Wind high resolution digital aerial model

outputs for small terns in Spring (B) and, Spring Least Tern MDAT modeled abundance at the regional scale (C). The scale for all maps is representative of relative spatial variation in the sites within the season for each map input..... 143

Map 119. Summer Least Tern density proportions in the NYSERDA APEM and Empire Wind high resolution digital aerial survey data (A), the NYSERDA APEM and Empire Wind high resolution digital aerial model outputs for small terns in Summer (B) and, Summer Least Tern MDAT modeled abundance at the regional scale (C). The scale for all maps is representative of relative spatial variation in the sites within the season for each map input. 144

Map 120. Fall Least Tern density proportions in the NYSERDA APEM and Empire Wind high resolution digital aerial survey data (A), the NYSERDA APEM and Empire Wind high resolution digital aerial model outputs for small terns in Fall (B) and, Fall Least Tern MDAT modeled abundance at the regional scale (C). The scale for all maps is representative of relative spatial variation in the sites within the season for each map input. 145

Map 121. Spring Black Tern density proportions in the NYSERDA APEM and Empire Wind high resolution digital aerial survey data (A), the NYSERDA APEM and Empire Wind high resolution digital aerial model outputs for small terns in Spring (B) and, Spring Black Tern MDAT modeled abundance at the regional scale (C). The scale for all maps is representative of relative spatial variation in the sites within the season for each map input..... 146

Map 122. Summer Black Tern density proportions in the NYSERDA APEM and Empire Wind high resolution digital aerial survey data (A), the NYSERDA APEM and Empire Wind high resolution digital aerial model outputs for small terns in Summer (B) and, Summer Black Tern MDAT modeled abundance at the regional scale (C). The scale for all maps is representative of relative spatial variation in the sites within the season for each map input. 147

Map 123. Winter Sooty Tern density proportions in the NYSERDA APEM and Empire Wind high resolution digital aerial survey data (A), the NYSERDA APEM and Empire Wind high resolution digital aerial model outputs for medium terns in Winter (B) and, Winter Sooty Tern MDAT modeled abundance at the regional scale (C). The scale for all maps is representative of relative spatial variation in the sites within the season for each map input. 148

Map 124. Spring Sooty Tern density proportions in the NYSERDA APEM and Empire Wind high resolution digital aerial survey data (A), the NYSERDA APEM and Empire Wind high resolution digital aerial model outputs for medium terns in Spring (B) and, Spring Sooty Tern MDAT modeled abundance at the regional scale (C). The scale for all maps is representative of relative spatial variation in the sites within the season for each map input..... 149

Map 125. Summer Sooty Tern density proportions in the NYSERDA APEM and Empire Wind high resolution digital aerial survey data (A), the NYSERDA APEM and Empire Wind high resolution digital aerial model outputs for medium terns in Summer (B) and, Summer Sooty Tern MDAT modeled abundance at the regional scale (C). The scale for all maps is representative of relative spatial variation in the sites within the season for each map input..... 150

Map 126. Fall Sooty Tern density proportions in the NYSERDA APEM and Empire Wind high resolution digital aerial survey data (A), the NYSERDA APEM and Empire Wind high resolution digital aerial model outputs for medium terns in Fall (B) and, Fall Sooty Tern MDAT modeled abundance at the regional scale

(C). The scale for all maps is representative of relative spatial variation in the sites within the season for each map input. 151

Map 127. Winter Roseate Tern density proportions in the NYSERDA APEM and Empire Wind high resolution digital aerial survey data (A), the NYSERDA APEM and Empire Wind high resolution digital aerial model outputs for medium terns in Winter (B) and, Winter Roseate Tern MDAT modeled abundance at the regional scale (C). The scale for all maps is representative of relative spatial variation in the sites within the season for each map input..... 152

Map 128. Spring Roseate Tern density proportions in the NYSERDA APEM and Empire Wind high resolution digital aerial survey data (A), the NYSERDA APEM and Empire Wind high resolution digital aerial model outputs for medium terns in Spring (B) and, Spring Roseate Tern MDAT modeled abundance at the regional scale (C). The scale for all maps is representative of relative spatial variation in the sites within the season for each map input..... 153

Map 129. Summer Roseate Tern density proportions in the NYSERDA APEM and Empire Wind high resolution digital aerial survey data (A), the NYSERDA APEM and Empire Wind high resolution digital aerial model outputs for medium terns in Summer (B) and, Summer Roseate Tern MDAT modeled abundance at the regional scale (C). The scale for all maps is representative of relative spatial variation in the sites within the season for each map input..... 154

Map 130. Fall Roseate Tern density proportions in the NYSERDA APEM and Empire Wind high resolution digital aerial survey data (A), the NYSERDA APEM and Empire Wind high resolution digital aerial model outputs for medium terns in Fall (B) and, Fall Roseate Tern MDAT modeled abundance at the regional scale (C). The scale for all maps is representative of relative spatial variation in the sites within the season for each map input..... 155

Map 131. Winter Common Tern density proportions in the NYSERDA APEM and Empire Wind high resolution digital aerial survey data (A), the NYSERDA APEM and Empire Wind high resolution digital aerial model outputs for medium terns in Winter (B) and, Winter Common Tern MDAT modeled abundance at the regional scale (C). The scale for all maps is representative of relative spatial variation in the sites within the season for each map input..... 156

Map 132. Spring Common Tern density proportions in the NYSERDA APEM and Empire Wind high resolution digital aerial survey data (A), the NYSERDA APEM and Empire Wind high resolution digital aerial model outputs for medium terns in Spring (B) and, Spring Common Tern MDAT modeled abundance at the regional scale (C). The scale for all maps is representative of relative spatial variation in the sites within the season for each map input..... 157

Map 133. Summer Common Tern density proportions in the NYSERDA APEM and Empire Wind high resolution digital aerial survey data (A), the NYSERDA APEM and Empire Wind high resolution digital aerial model outputs for medium terns in Summer (B) and, Summer Common Tern MDAT modeled abundance at the regional scale (C). The scale for all maps is representative of relative spatial variation in the sites within the season for each map input..... 158

Map 134. Fall Common Tern density proportions in the NYSERDA APEM and Empire Wind high resolution digital aerial survey data (A), the NYSERDA APEM and Empire Wind high resolution digital aerial model outputs for medium terns in Fall (B) and, Fall Common Tern MDAT modeled abundance at the regional scale (C). The scale for all maps is representative of relative spatial variation in the sites within the season for each map input. 159

Map 135. Winter Arctic Tern density proportions in the NYSERDA APEM and Empire Wind high resolution digital aerial survey data (A), the NYSERDA APEM and Empire Wind high resolution digital aerial model outputs for medium terns in Winter (B) and, Winter Arctic Tern MDAT modeled abundance at the regional scale (C). The scale for all maps is representative of relative spatial variation in the sites within the season for each map input. 160

Map 136. Spring Arctic Tern density proportions in the NYSERDA APEM and Empire Wind high resolution digital aerial survey data (A), the NYSERDA APEM and Empire Wind high resolution digital aerial model outputs for medium terns in Spring (B) and, Spring Arctic Tern MDAT modeled abundance at the regional scale (C). The scale for all maps is representative of relative spatial variation in the sites within the season for each map input. 161

Map 137. Summer Arctic Tern density proportions in the NYSERDA APEM and Empire Wind high resolution digital aerial survey data (A), the NYSERDA APEM and Empire Wind high resolution digital aerial model outputs for medium terns in Summer (B) and, Summer Arctic Tern MDAT modeled abundance at the regional scale (C). The scale for all maps is representative of relative spatial variation in the sites within the season for each map input..... 162

Map 138. Fall Arctic Tern density proportions in the NYSERDA APEM and Empire Wind high resolution digital aerial survey data (A), the NYSERDA APEM and Empire Wind high resolution digital aerial model outputs for medium terns in Fall (B) and, Fall Arctic Tern MDAT modeled abundance at the regional scale (C). The scale for all maps is representative of relative spatial variation in the sites within the season for each map input. 163

Map 139. Spring Forster's Tern density proportions in the NYSERDA APEM and Empire Wind high resolution digital aerial survey data (A), the NYSERDA APEM and Empire Wind high resolution digital aerial model outputs for medium terns in Spring (B) and, Spring Forster's Tern MDAT modeled abundance at the regional scale (C). The scale for all maps is representative of relative spatial variation in the sites within the season for each map input..... 164

Map 140. Summer Forster's Tern density proportions in the NYSERDA APEM and Empire Wind high resolution digital aerial survey data (A), the NYSERDA APEM and Empire Wind high resolution digital aerial model outputs for medium terns in Summer (B) and, Summer Forster's Tern MDAT modeled abundance at the regional scale (C). The scale for all maps is representative of relative spatial variation in the sites within the season for each map input..... 165

Map 141. Winter Royal Tern density proportions in the NYSERDA APEM and Empire Wind high resolution digital aerial survey data (A), the NYSERDA APEM and Empire Wind high resolution digital aerial model outputs for medium terns in Winter (B) and, Winter Royal Tern MDAT modeled abundance at the regional scale (C). The scale for all maps is representative of relative spatial variation in the sites within the season for each map input. 166

Map 142. Spring Royal Tern density proportions in the NYSERDA APEM and Empire Wind high resolution digital aerial survey data (A), the NYSERDA APEM and Empire Wind high resolution digital aerial model outputs for medium terns in Spring (B) and, Spring Royal Tern MDAT modeled abundance at the regional scale (C). The scale for all maps is representative of relative spatial variation in the sites within the season for each map input..... 167

Map 143. Summer Royal Tern density proportions in the NYSERDA APEM and Empire Wind high resolution digital aerial survey data (A), the NYSERDA APEM and Empire Wind high resolution digital

aerial model outputs for medium terns in Summer (B) and, Summer Royal Tern MDAT modeled abundance at the regional scale (C). The scale for all maps is representative of relative spatial variation in the sites within the season for each map input..... 168

Map 144. Fall Royal Tern density proportions in the NYSERDA APEM and Empire Wind high resolution digital aerial survey data (A), the NYSERDA APEM and Empire Wind high resolution digital aerial model outputs for medium terns in Fall (B) and, Fall Royal Tern MDAT modeled abundance at the regional scale (C). The scale for all maps is representative of relative spatial variation in the sites within the season for each map input. 169

Map 145. Winter Red-throated Loon density proportions in the NYSERDA APEM and Empire Wind high resolution digital aerial survey data (A), the NYSERDA APEM and Empire Wind high resolution digital aerial model outputs for loons in Winter (B) and, Winter Red-throated Loon MDAT modeled abundance at the regional scale (C). The scale for all maps is representative of relative spatial variation in the sites within the season for each map input. 170

Map 146. Spring Red-throated Loon density proportions in the NYSERDA APEM and Empire Wind high resolution digital aerial survey data (A), the NYSERDA APEM and Empire Wind high resolution digital aerial model outputs for loons in Spring (B) and, Spring Red-throated Loon MDAT modeled abundance at the regional scale (C). The scale for all maps is representative of relative spatial variation in the sites within the season for each map input. 171

Map 147. Summer Red-throated Loon density proportions in the NYSERDA APEM and Empire Wind high resolution digital aerial survey data (A), the NYSERDA APEM and Empire Wind high resolution digital aerial model outputs for loons in Summer (B) and, Summer Red-throated Loon MDAT modeled abundance at the regional scale (C). The scale for all maps is representative of relative spatial variation in the sites within the season for each map input..... 172

Map 148. Fall Red-throated Loon density proportions in the NYSERDA APEM and Empire Wind high resolution digital aerial survey data (A), the NYSERDA APEM and Empire Wind high resolution digital aerial model outputs for loons in Fall (B) and, Fall Red-throated Loon MDAT modeled abundance at the regional scale (C). The scale for all maps is representative of relative spatial variation in the sites within the season for each map input. 173

Map 149. Winter Common Loon density proportions in the NYSERDA APEM and Empire Wind high resolution digital aerial survey data (A), the NYSERDA APEM and Empire Wind high resolution digital aerial model outputs for loons in Winter (B) and, Winter Common Loon MDAT modeled abundance at the regional scale (C). The scale for all maps is representative of relative spatial variation in the sites within the season for each map input. 174

Map 150. Spring Common Loon density proportions in the NYSERDA APEM and Empire Wind high resolution digital aerial survey data (A), the NYSERDA APEM and Empire Wind high resolution digital aerial model outputs for loons in Spring (B) and, Spring Common Loon MDAT modeled abundance at the regional scale (C). The scale for all maps is representative of relative spatial variation in the sites within the season for each map input. 175

Map 151. Summer Common Loon density proportions in the NYSERDA APEM and Empire Wind high resolution digital aerial survey data (A), the NYSERDA APEM and Empire Wind high resolution digital aerial model outputs for loons in Summer (B) and, Summer Common Loon MDAT modeled abundance at

the regional scale (C). The scale for all maps is representative of relative spatial variation in the sites within the season for each map input. 176

Map 152. Fall Common Loon density proportions in the NYSERDA APEM and Empire Wind high resolution digital aerial survey data (A), the NYSERDA APEM and Empire Wind high resolution digital aerial model outputs for loons in Fall (B) and, Fall Common Loon MDAT modeled abundance at the regional scale (C). The scale for all maps is representative of relative spatial variation in the sites within the season for each map input. 177

Map 153. Winter Wilson's Storm-Petrel density proportions in the NYSERDA APEM and Empire Wind high resolution digital aerial survey data (A), the NYSERDA APEM and Empire Wind high resolution digital aerial model outputs for storm-petrels in Winter (B) and, Winter Wilson's Storm-Petrel MDAT modeled abundance at the regional scale (C). The scale for all maps is representative of relative spatial variation in the sites within the season for each map input. 178

Map 154. Spring Wilson's Storm-Petrel density proportions in the NYSERDA APEM and Empire Wind high resolution digital aerial survey data (A), the NYSERDA APEM and Empire Wind high resolution digital aerial model outputs for storm-petrels in Spring (B) and, Spring Wilson's Storm-Petrel MDAT modeled abundance at the regional scale (C). The scale for all maps is representative of relative spatial variation in the sites within the season for each map input..... 179

Map 155. Summer Wilson's Storm-Petrel density proportions in the NYSERDA APEM and Empire Wind high resolution digital aerial survey data (A), the NYSERDA APEM and Empire Wind high resolution digital aerial model outputs for storm-petrels in Summer (B) and, Summer Wilson's Storm-Petrel MDAT modeled abundance at the regional scale (C). The scale for all maps is representative of relative spatial variation in the sites within the season for each map input. 180

Map 156. Fall Wilson's Storm-Petrel density proportions in the NYSERDA APEM and Empire Wind high resolution digital aerial survey data (A), the NYSERDA APEM and Empire Wind high resolution digital aerial model outputs for storm-petrels in Fall (B) and, Fall Wilson's Storm-Petrel MDAT modeled abundance at the regional scale (C). The scale for all maps is representative of relative spatial variation in the sites within the season for each map input..... 181

Map 157. Winter Leach's Storm-Petrel density proportions in the NYSERDA APEM and Empire Wind high resolution digital aerial survey data (A), the NYSERDA APEM and Empire Wind high resolution digital aerial model outputs for storm-petrels in Winter (B) and, Winter Leach's Storm-Petrel MDAT modeled abundance at the regional scale (C). The scale for all maps is representative of relative spatial variation in the sites within the season for each map input..... 182

Map 158. Spring Leach's Storm-Petrel density proportions in the NYSERDA APEM and Empire Wind high resolution digital aerial survey data (A), the NYSERDA APEM and Empire Wind high resolution digital aerial model outputs for storm-petrels in Spring (B) and, Spring Leach's Storm-Petrel MDAT modeled abundance at the regional scale (C). The scale for all maps is representative of relative spatial variation in the sites within the season for each map input..... 183

Map 159. Summer Leach's Storm-Petrel density proportions in the NYSERDA APEM and Empire Wind high resolution digital aerial survey data (A), the NYSERDA APEM and Empire Wind high resolution digital aerial model outputs for storm-petrels in Summer (B) and, Summer Leach's Storm-Petrel MDAT modeled abundance at the regional scale (C). The scale for all maps is representative of relative spatial variation in the sites within the season for each map input. 184

Map 160. Fall Leach's Storm-Petrel density proportions in the NYSERDA APEM and Empire Wind high resolution digital aerial survey data (A), the NYSERDA APEM and Empire Wind high resolution digital aerial model outputs for storm-petrels in Fall (B) and, Fall Leach's Storm-Petrel MDAT modeled abundance at the regional scale (C). The scale for all maps is representative of relative spatial variation in the sites within the season for each map input..... 185

Map 161. Winter Northern Fulmar density proportions in the NYSERDA APEM and Empire Wind high resolution digital aerial survey data (A), the NYSERDA APEM and Empire Wind high resolution digital aerial model outputs for shearwaters and petrels in Winter (B) and, Winter Northern Fulmar MDAT modeled abundance at the regional scale (C). The scale for all maps is representative of relative spatial variation in the sites within the season for each map input. 186

Map 162. Spring Northern Fulmar density proportions in the NYSERDA APEM and Empire Wind high resolution digital aerial survey data (A), the NYSERDA APEM and Empire Wind high resolution digital aerial model outputs for shearwaters and petrels in Spring (B) and, Spring Northern Fulmar MDAT modeled abundance at the regional scale (C). The scale for all maps is representative of relative spatial variation in the sites within the season for each map input. 187

Map 163. Summer Northern Fulmar density proportions in the NYSERDA APEM and Empire Wind high resolution digital aerial survey data (A), the NYSERDA APEM and Empire Wind high resolution digital aerial model outputs for shearwaters and petrels in Summer (B) and, Summer Northern Fulmar MDAT modeled abundance at the regional scale (C). The scale for all maps is representative of relative spatial variation in the sites within the season for each map input. 188

Map 164. Fall Northern Fulmar density proportions in the NYSERDA APEM and Empire Wind high resolution digital aerial survey data (A), the NYSERDA APEM and Empire Wind high resolution digital aerial model outputs for shearwaters and petrels in Fall (B) and, Fall Northern Fulmar MDAT modeled abundance at the regional scale (C). The scale for all maps is representative of relative spatial variation in the sites within the season for each map input..... 189

Map 165. Spring Trindade Petrel density proportions in the NYSERDA APEM and Empire Wind high resolution digital aerial survey data (A), the NYSERDA APEM and Empire Wind high resolution digital aerial model outputs for shearwaters and petrels in Spring (B) and, Spring Trindade Petrel MDAT modeled abundance at the regional scale (C). The scale for all maps is representative of relative spatial variation in the sites within the season for each map input. 190

Map 166. Winter Black-capped Petrel density proportions in the NYSERDA APEM and Empire Wind high resolution digital aerial survey data (A), the NYSERDA APEM and Empire Wind high resolution digital aerial model outputs for shearwaters and petrels in Winter (B) and, Winter Black-capped Petrel MDAT modeled abundance at the regional scale (C). The scale for all maps is representative of relative spatial variation in the sites within the season for each map input. 191

Map 167. Spring Black-capped Petrel density proportions in the NYSERDA APEM and Empire Wind high resolution digital aerial survey data (A), the NYSERDA APEM and Empire Wind high resolution digital aerial model outputs for shearwaters and petrels in Spring (B) and, Spring Black-capped Petrel MDAT modeled abundance at the regional scale (C). The scale for all maps is representative of relative spatial variation in the sites within the season for each map input. 192

Map 168. Summer Black-capped Petrel density proportions in the NYSERDA APEM and Empire Wind high resolution digital aerial survey data (A), the NYSERDA APEM and Empire Wind high resolution digital

aerial model outputs for shearwaters and petrels in Summer (B) and, Summer Black-capped Petrel MDAT modeled abundance at the regional scale (C). The scale for all maps is representative of relative spatial variation in the sites within the season for each map input..... 193

Map 169. Fall Black-capped Petrel density proportions in the NYSERDA APEM and Empire Wind high resolution digital aerial survey data (A), the NYSERDA APEM and Empire Wind high resolution digital aerial model outputs for shearwaters and petrels in Fall (B) and, Fall Black-capped Petrel MDAT modeled abundance at the regional scale (C). The scale for all maps is representative of relative spatial variation in the sites within the season for each map input..... 194

Map 170. Winter Cory's Shearwater density proportions in the NYSERDA APEM and Empire Wind high resolution digital aerial survey data (A), the NYSERDA APEM and Empire Wind high resolution digital aerial model outputs for shearwaters and petrels in Winter (B) and, Winter Cory's Shearwater MDAT modeled abundance at the regional scale (C). The scale for all maps is representative of relative spatial variation in the sites within the season for each map input. 195

Map 171. Spring Cory's Shearwater density proportions in the NYSERDA APEM and Empire Wind high resolution digital aerial survey data (A), the NYSERDA APEM and Empire Wind high resolution digital aerial model outputs for shearwaters and petrels in Spring (B) and, Spring Cory's Shearwater MDAT modeled abundance at the regional scale (C). The scale for all maps is representative of relative spatial variation in the sites within the season for each map input. 196

Map 172. Summer Cory's Shearwater density proportions in the NYSERDA APEM and Empire Wind high resolution digital aerial survey data (A), the NYSERDA APEM and Empire Wind high resolution digital aerial model outputs for shearwaters and petrels in Summer (B) and, Summer Cory's Shearwater MDAT modeled abundance at the regional scale (C). The scale for all maps is representative of relative spatial variation in the sites within the season for each map input. 197

Map 173. Fall Cory's Shearwater density proportions in the NYSERDA APEM and Empire Wind high resolution digital aerial survey data (A), the NYSERDA APEM and Empire Wind high resolution digital aerial model outputs for shearwaters and petrels in Fall (B) and, Fall Cory's Shearwater MDAT modeled abundance at the regional scale (C). The scale for all maps is representative of relative spatial variation in the sites within the season for each map input..... 198

Map 174. Winter Sooty Shearwater density proportions in the NYSERDA APEM and Empire Wind high resolution digital aerial survey data (A), the NYSERDA APEM and Empire Wind high resolution digital aerial model outputs for shearwaters and petrels in Winter (B) and, Winter Sooty Shearwater MDAT modeled abundance at the regional scale (C). The scale for all maps is representative of relative spatial variation in the sites within the season for each map input. 199

Map 175. Spring Sooty Shearwater density proportions in the NYSERDA APEM and Empire Wind high resolution digital aerial survey data (A), the NYSERDA APEM and Empire Wind high resolution digital aerial model outputs for shearwaters and petrels in Spring (B) and, Spring Sooty Shearwater MDAT modeled abundance at the regional scale (C). The scale for all maps is representative of relative spatial variation in the sites within the season for each map input. 200

Map 176. Summer Sooty Shearwater density proportions in the NYSERDA APEM and Empire Wind high resolution digital aerial survey data (A), the NYSERDA APEM and Empire Wind high resolution digital aerial model outputs for shearwaters and petrels in Summer (B) and, Summer Sooty Shearwater MDAT

modeled abundance at the regional scale (C). The scale for all maps is representative of relative spatial variation in the sites within the season for each map input. 201

Map 177. Fall Sooty Shearwater density proportions in the NYSERDA APEM and Empire Wind high resolution digital aerial survey data (A), the NYSERDA APEM and Empire Wind high resolution digital aerial model outputs for shearwaters and petrels in Fall (B) and, Fall Sooty Shearwater MDAT modeled abundance at the regional scale (C). The scale for all maps is representative of relative spatial variation in the sites within the season for each map input..... 202

Map 178. Winter Great Shearwater density proportions in the NYSERDA APEM and Empire Wind high resolution digital aerial survey data (A), the NYSERDA APEM and Empire Wind high resolution digital aerial model outputs for shearwaters and petrels in Winter (B) and, Winter Great Shearwater MDAT modeled abundance at the regional scale (C). The scale for all maps is representative of relative spatial variation in the sites within the season for each map input. 203

Map 179. Spring Great Shearwater density proportions in the NYSERDA APEM and Empire Wind high resolution digital aerial survey data (A), the NYSERDA APEM and Empire Wind high resolution digital aerial model outputs for shearwaters and petrels in Spring (B) and, Spring Great Shearwater MDAT modeled abundance at the regional scale (C). The scale for all maps is representative of relative spatial variation in the sites within the season for each map input. 204

Map 180. Summer Great Shearwater density proportions in the NYSERDA APEM and Empire Wind high resolution digital aerial survey data (A), the NYSERDA APEM and Empire Wind high resolution digital aerial model outputs for shearwaters and petrels in Summer (B) and, Summer Great Shearwater MDAT modeled abundance at the regional scale (C). The scale for all maps is representative of relative spatial variation in the sites within the season for each map input. 205

Map 181. Fall Great Shearwater density proportions in the NYSERDA APEM and Empire Wind high resolution digital aerial survey data (A), the NYSERDA APEM and Empire Wind high resolution digital aerial model outputs for shearwaters and petrels in Fall (B) and, Fall Great Shearwater MDAT modeled abundance at the regional scale (C). The scale for all maps is representative of relative spatial variation in the sites within the season for each map input..... 206

Map 182. Winter Manx Shearwater density proportions in the NYSERDA APEM and Empire Wind high resolution digital aerial survey data (A), the NYSERDA APEM and Empire Wind high resolution digital aerial model outputs for shearwaters and petrels in Winter (B) and, Winter Manx Shearwater MDAT modeled abundance at the regional scale (C). The scale for all maps is representative of relative spatial variation in the sites within the season for each map input. 207

Map 183. Spring Manx Shearwater density proportions in the NYSERDA APEM and Empire Wind high resolution digital aerial survey data (A), the NYSERDA APEM and Empire Wind high resolution digital aerial model outputs for shearwaters and petrels in Spring (B) and, Spring Manx Shearwater MDAT modeled abundance at the regional scale (C). The scale for all maps is representative of relative spatial variation in the sites within the season for each map input. 208

Map 184. Summer Manx Shearwater density proportions in the NYSERDA APEM and Empire Wind high resolution digital aerial survey data (A), the NYSERDA APEM and Empire Wind high resolution digital aerial model outputs for shearwaters and petrels in Summer (B) and, Summer Manx Shearwater MDAT modeled abundance at the regional scale (C). The scale for all maps is representative of relative spatial variation in the sites within the season for each map input. 209

Map 185. Fall Manx Shearwater density proportions in the NYSERDA APEM and Empire Wind high resolution digital aerial survey data (A), the NYSERDA APEM and Empire Wind high resolution digital aerial model outputs for shearwaters and petrels in Fall (B) and, Fall Manx Shearwater MDAT modeled abundance at the regional scale (C). The scale for all maps is representative of relative spatial variation in the sites within the season for each map input..... 210

Map 186. Winter Audubon's Shearwater density proportions in the NYSERDA APEM and Empire Wind high resolution digital aerial survey data (A), the NYSERDA APEM and Empire Wind high resolution digital aerial model outputs for shearwaters and petrels in Winter (B) and, Winter Audubon's Shearwater MDAT modeled abundance at the regional scale (C). The scale for all maps is representative of relative spatial variation in the sites within the season for each map input. 211

Map 187. Spring Audubon's Shearwater density proportions in the NYSERDA APEM and Empire Wind high resolution digital aerial survey data (A), the NYSERDA APEM and Empire Wind high resolution digital aerial model outputs for shearwaters and petrels in Spring (B) and, Spring Audubon's Shearwater MDAT modeled abundance at the regional scale (C). The scale for all maps is representative of relative spatial variation in the sites within the season for each map input..... 212

Map 188. Summer Audubon's Shearwater density proportions in the NYSERDA APEM and Empire Wind high resolution digital aerial survey data (A), the NYSERDA APEM and Empire Wind high resolution digital aerial model outputs for shearwaters and petrels in Summer (B) and, Summer Audubon's Shearwater MDAT modeled abundance at the regional scale (C). The scale for all maps is representative of relative spatial variation in the sites within the season for each map input. 213

Map 189. Fall Audubon's Shearwater density proportions in the NYSERDA APEM and Empire Wind high resolution digital aerial survey data (A), the NYSERDA APEM and Empire Wind high resolution digital aerial model outputs for shearwaters and petrels in Fall (B) and, Fall Audubon's Shearwater MDAT modeled abundance at the regional scale (C). The scale for all maps is representative of relative spatial variation in the sites within the season for each map input. 214

Map 190. Winter Northern Gannet density proportions in the NYSERDA APEM and Empire Wind high resolution digital aerial survey data (A), the NYSERDA APEM and Empire Wind high resolution digital aerial model outputs for gannet and booby in Winter (B) and, Winter Northern Gannet MDAT modeled abundance at the regional scale (C). The scale for all maps is representative of relative spatial variation in the sites within the season for each map input..... 215

Map 191. Spring Northern Gannet density proportions in the NYSERDA APEM and Empire Wind high resolution digital aerial survey data (A), the NYSERDA APEM and Empire Wind high resolution digital aerial model outputs for gannet and booby in Spring (B) and, Spring Northern Gannet MDAT modeled abundance at the regional scale (C). The scale for all maps is representative of relative spatial variation in the sites within the season for each map input..... 216

Map 192. Summer Northern Gannet density proportions in the NYSERDA APEM and Empire Wind high resolution digital aerial survey data (A), the NYSERDA APEM and Empire Wind high resolution digital aerial model outputs for gannet and booby in Summer (B) and, Summer Northern Gannet MDAT modeled abundance at the regional scale (C). The scale for all maps is representative of relative spatial variation in the sites within the season for each map input. 217

Map 193. Fall Northern Gannet density proportions in the NYSERDA APEM and Empire Wind high resolution digital aerial survey data (A), the NYSERDA APEM and Empire Wind high resolution digital

aerial model outputs for gannet and booby in Fall (B) and, Fall Northern Gannet MDAT modeled abundance at the regional scale (C). The scale for all maps is representative of relative spatial variation in the sites within the season for each map input..... 218

Map 194. Winter Double-crested Cormorant density proportions in the NYSERDA APEM and Empire Wind high resolution digital aerial survey data (A), the NYSERDA APEM and Empire Wind high resolution digital aerial model outputs for cormorants in Winter (B) and, Winter Double-crested Cormorant MDAT modeled abundance at the regional scale (C). The scale for all maps is representative of relative spatial variation in the sites within the season for each map input. 219

Map 195. Spring Double-crested Cormorant density proportions in the NYSERDA APEM and Empire Wind high resolution digital aerial survey data (A), the NYSERDA APEM and Empire Wind high resolution digital aerial model outputs for cormorants in Spring (B) and, Spring Double-crested Cormorant MDAT modeled abundance at the regional scale (C). The scale for all maps is representative of relative spatial variation in the sites within the season for each map input. 220

Map 196. Summer Double-crested Cormorant density proportions in the NYSERDA APEM and Empire Wind high resolution digital aerial survey data (A), the NYSERDA APEM and Empire Wind high resolution digital aerial model outputs for cormorants in Summer (B) and, Summer Double-crested Cormorant MDAT modeled abundance at the regional scale (C). The scale for all maps is representative of relative spatial variation in the sites within the season for each map input..... 221

Map 197. Fall Double-crested Cormorant density proportions in the NYSERDA APEM and Empire Wind high resolution digital aerial survey data (A), the NYSERDA APEM and Empire Wind high resolution digital aerial model outputs for cormorants in Fall (B) and, Fall Double-crested Cormorant MDAT modeled abundance at the regional scale (C). The scale for all maps is representative of relative spatial variation in the sites within the season for each map input. 222

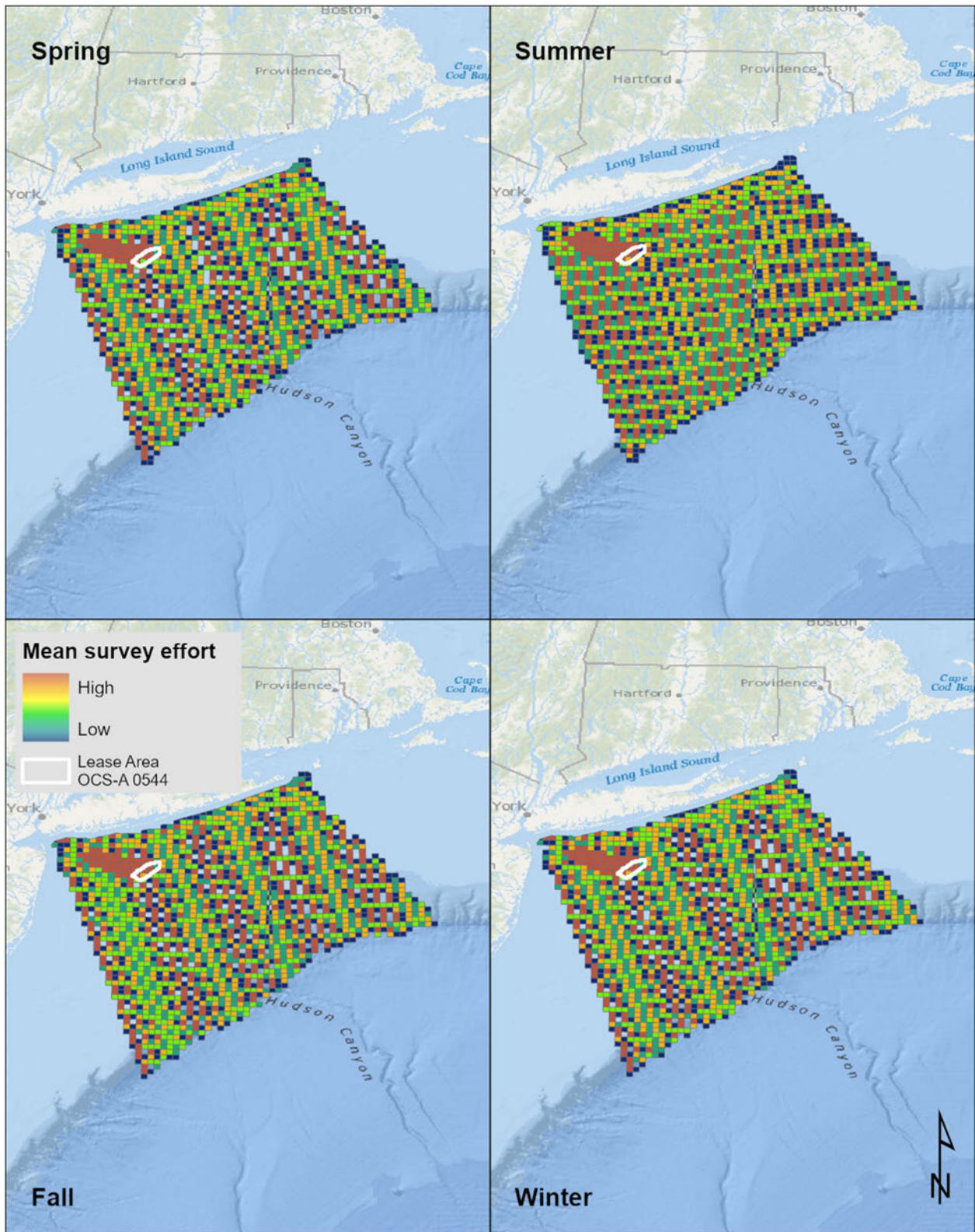
Map 198. Winter Brown Pelican density proportions in the NYSERDA APEM and Empire Wind high resolution digital aerial survey data (A), the NYSERDA APEM and Empire Wind high resolution digital aerial model outputs for pelicans in Winter (B) and, Winter Brown Pelican MDAT modeled abundance at the regional scale (C). The scale for all maps is representative of relative spatial variation in the sites within the season for each map input. 223

Map 199. Spring Brown Pelican density proportions in the NYSERDA APEM and Empire Wind high resolution digital aerial survey data (A), the NYSERDA APEM and Empire Wind high resolution digital aerial model outputs for pelicans in Spring (B) and, Spring Brown Pelican MDAT modeled abundance at the regional scale (C). The scale for all maps is representative of relative spatial variation in the sites within the season for each map input. 224

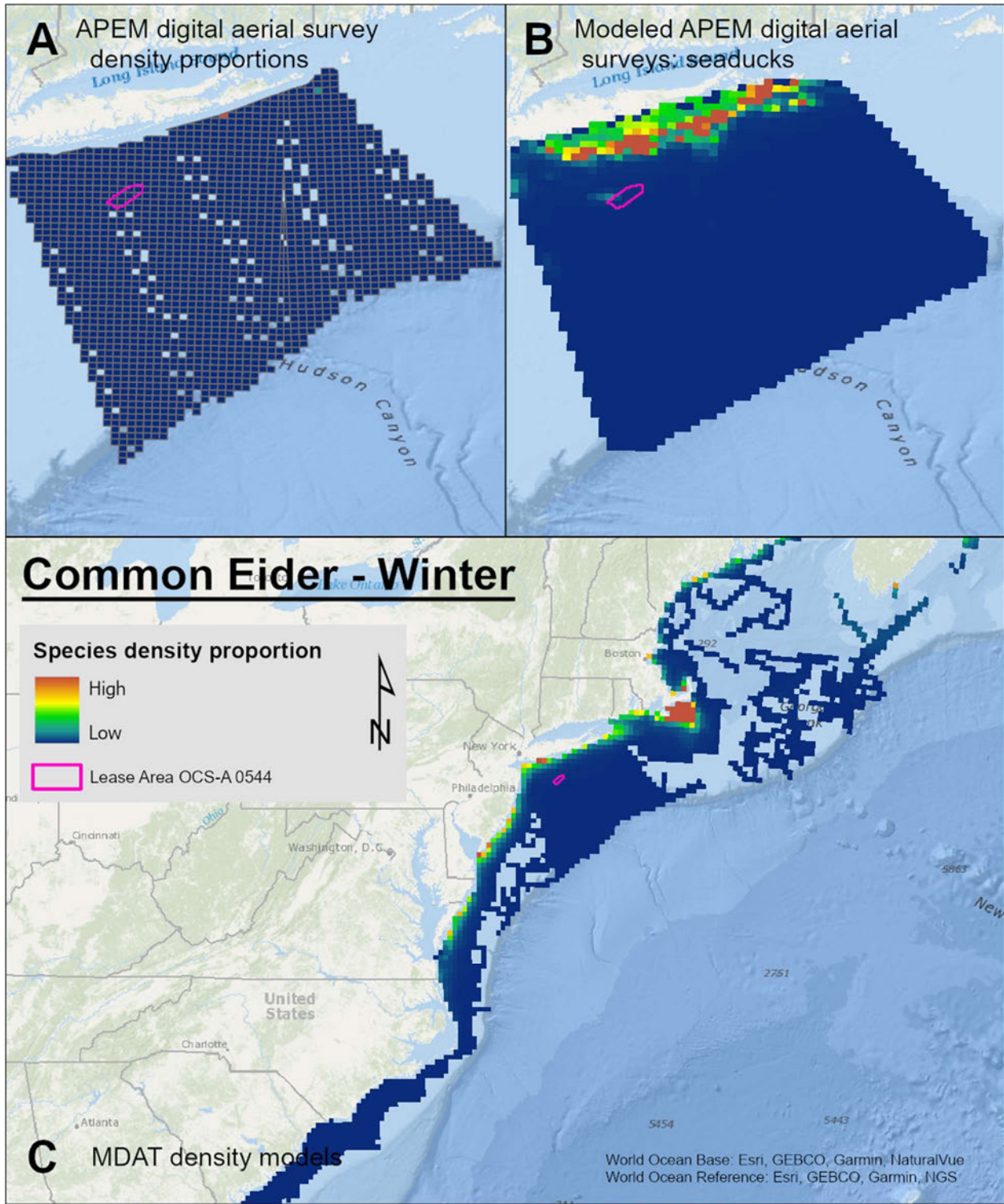
Map 200. Summer Brown Pelican density proportions in the NYSERDA APEM and Empire Wind high resolution digital aerial survey data (A), the NYSERDA APEM and Empire Wind high resolution digital aerial model outputs for pelicans in Summer (B) and, Summer Brown Pelican MDAT modeled abundance at the regional scale (C). The scale for all maps is representative of relative spatial variation in the sites within the season for each map input. 225

Map 201. Fall Brown Pelican density proportions in the NYSERDA APEM and Empire Wind high resolution digital aerial survey data (A), the NYSERDA APEM and Empire Wind high resolution digital aerial model outputs for pelicans in Fall (B) and, Fall Brown Pelican MDAT modeled abundance at the

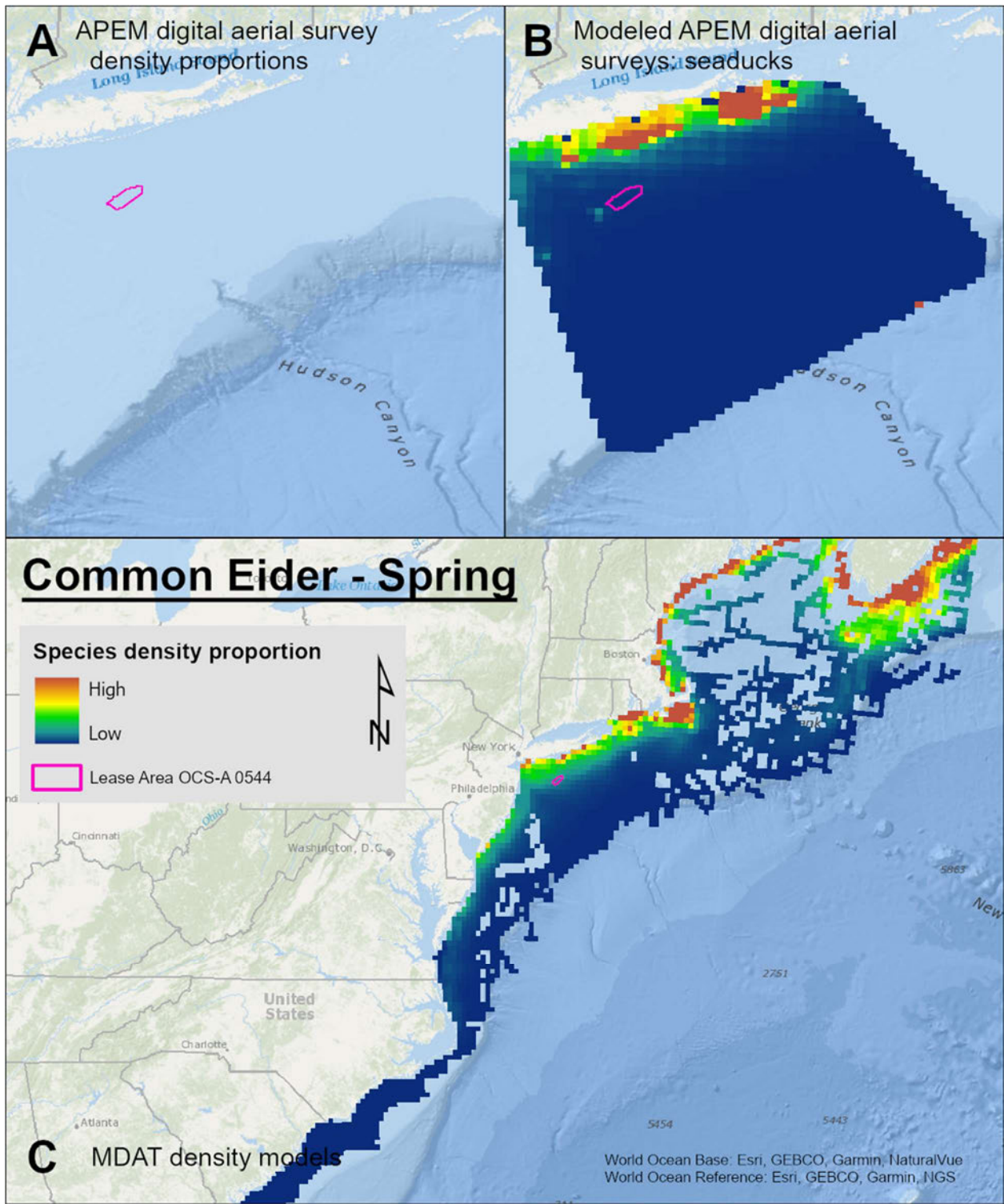
regional scale (C). The scale for all maps is representative of relative spatial variation in the sites within the season for each map input. 226



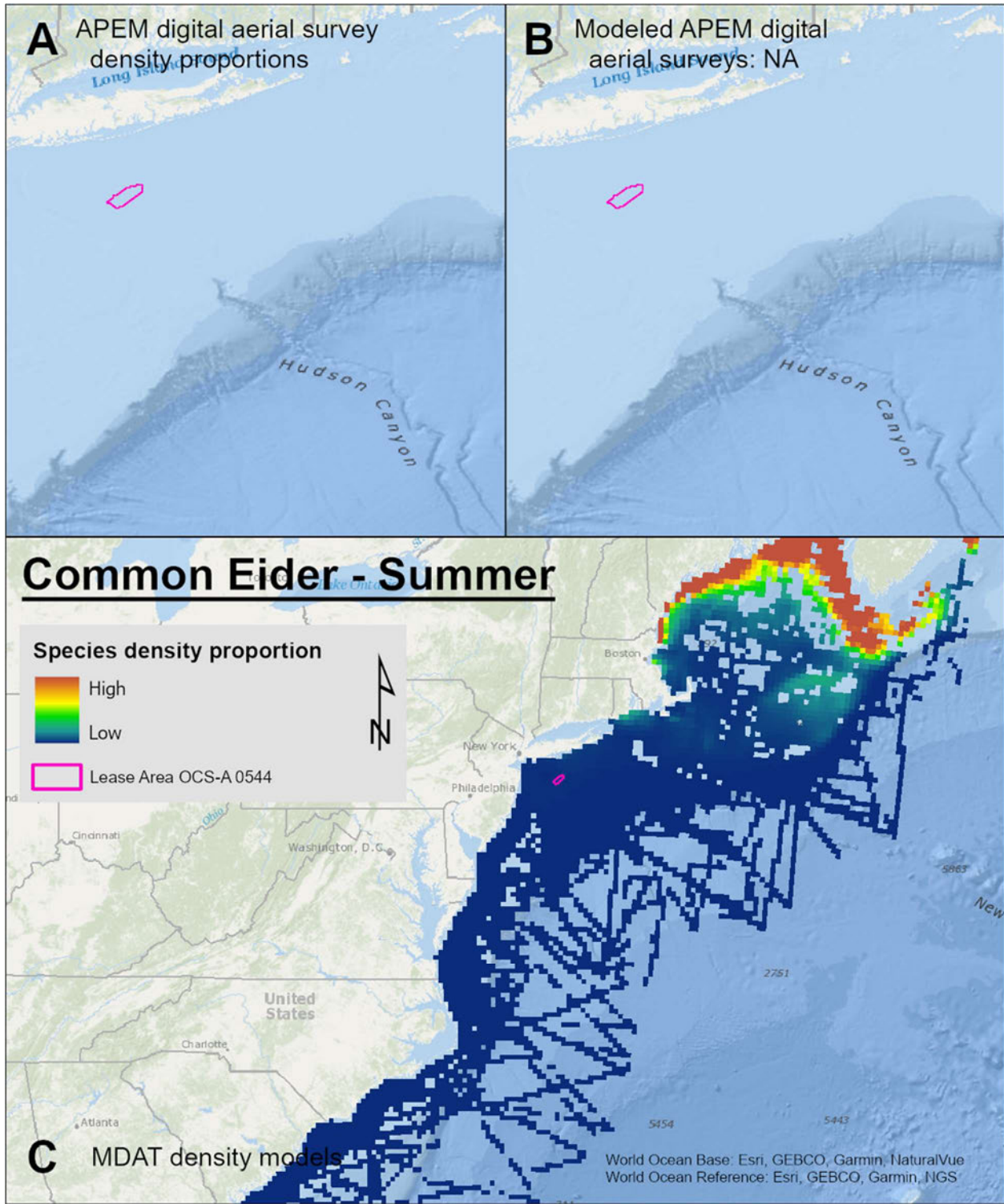
Map 1. NYERDA APEM high resolution digital aerial seasonal survey effort. Mean survey effort in sq. km by full or partial lease block inside and outside the lease area.



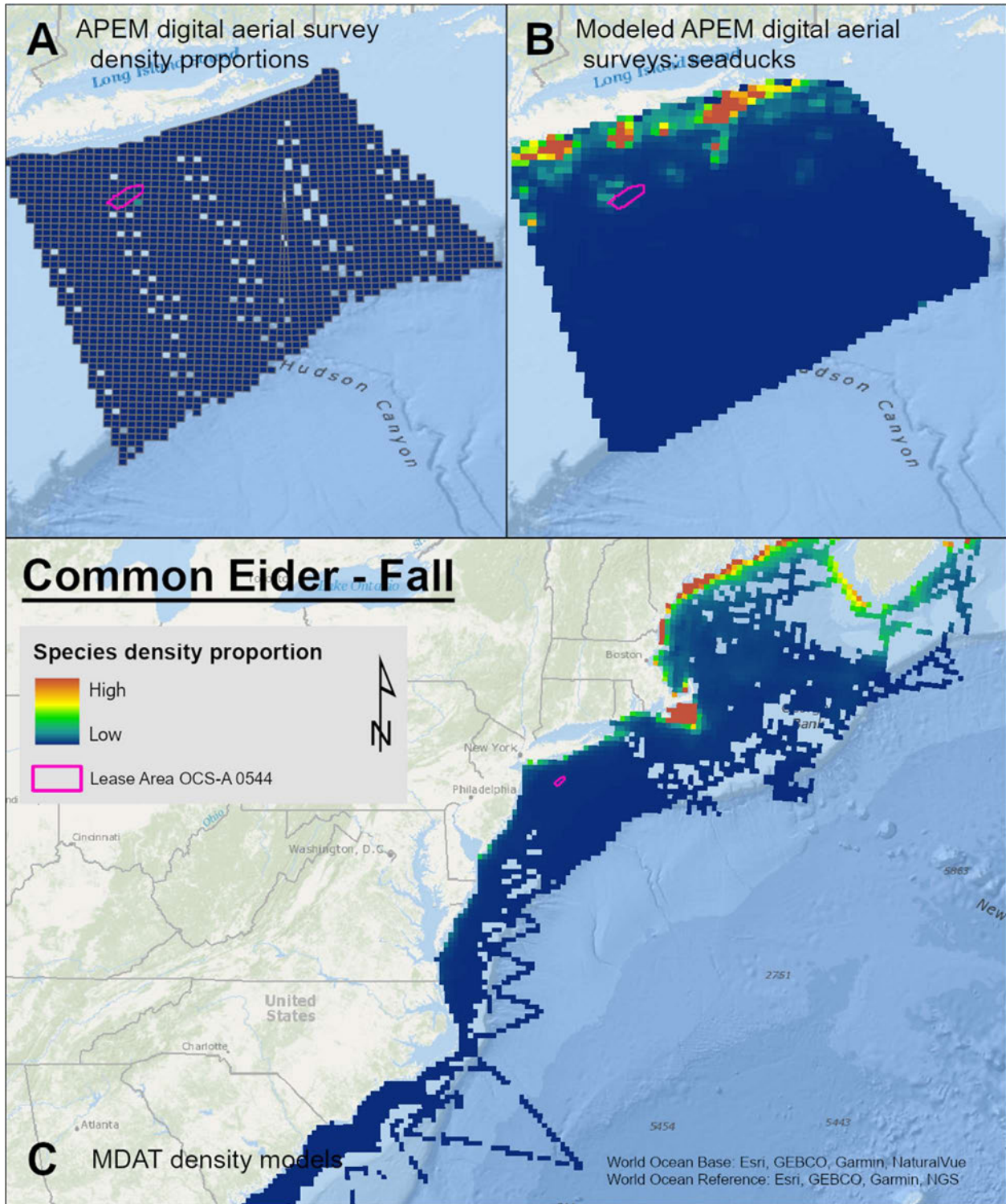
Map 2. Winter Common Eider density proportions in the NYSERDA APEM and Empire Wind high resolution digital aerial survey data (A), the NYSERDA APEM and Empire Wind high resolution digital aerial model outputs for seaducks in Winter (B) and, Winter Common Eider MDAT modeled abundance at the regional scale (C). The scale for all maps is representative of relative spatial variation in the sites within the season for each map input.



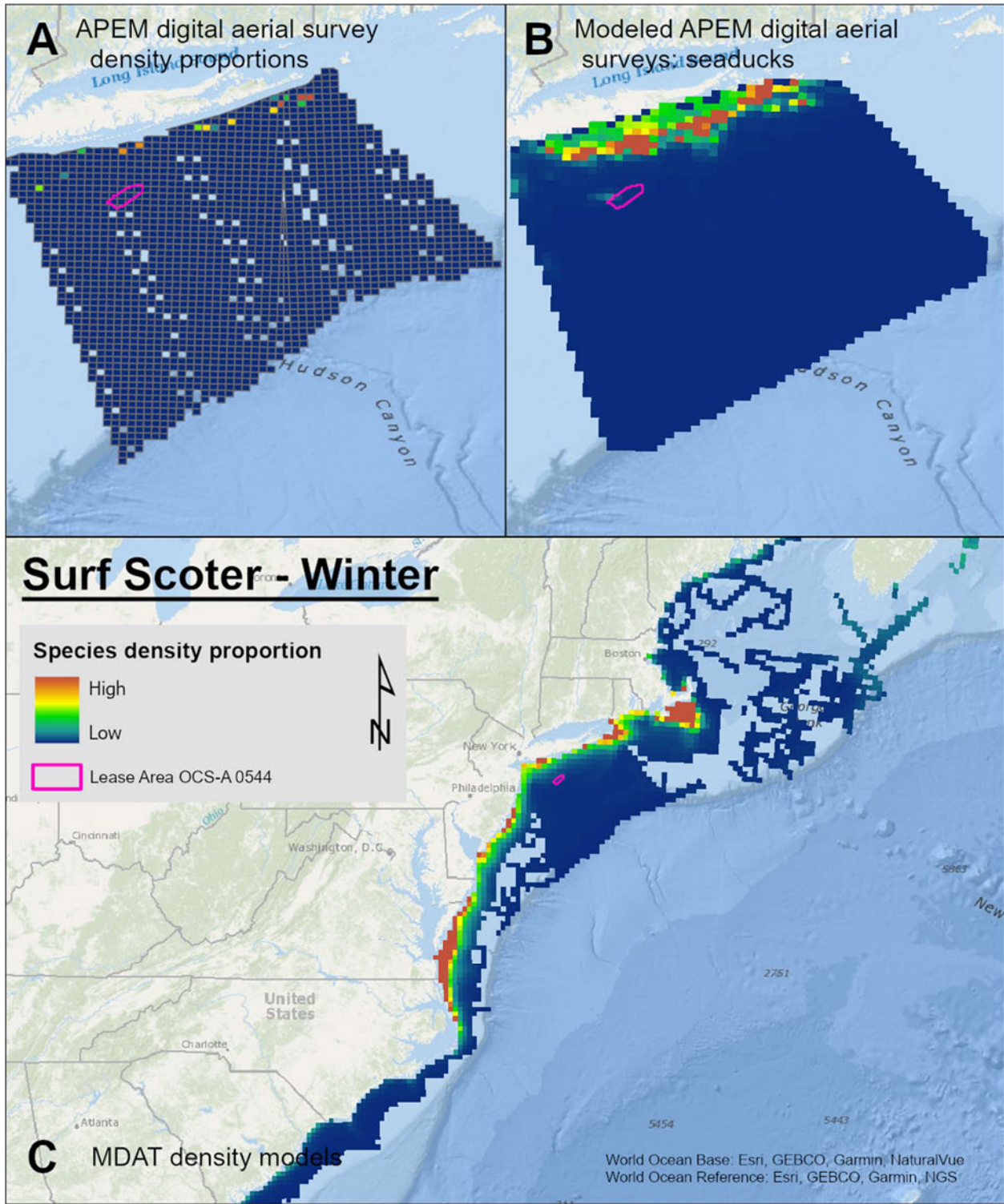
Map 3. Spring Common Eider density proportions in the NYSERDA APEM and Empire Wind high resolution digital aerial survey data (A), the NYSERDA APEM and Empire Wind high resolution digital aerial model outputs for seaducks in Spring (B) and, Spring Common Eider MDAT modeled abundance at the regional scale (C). The scale for all maps is representative of relative spatial variation in the sites within the season for each map input.



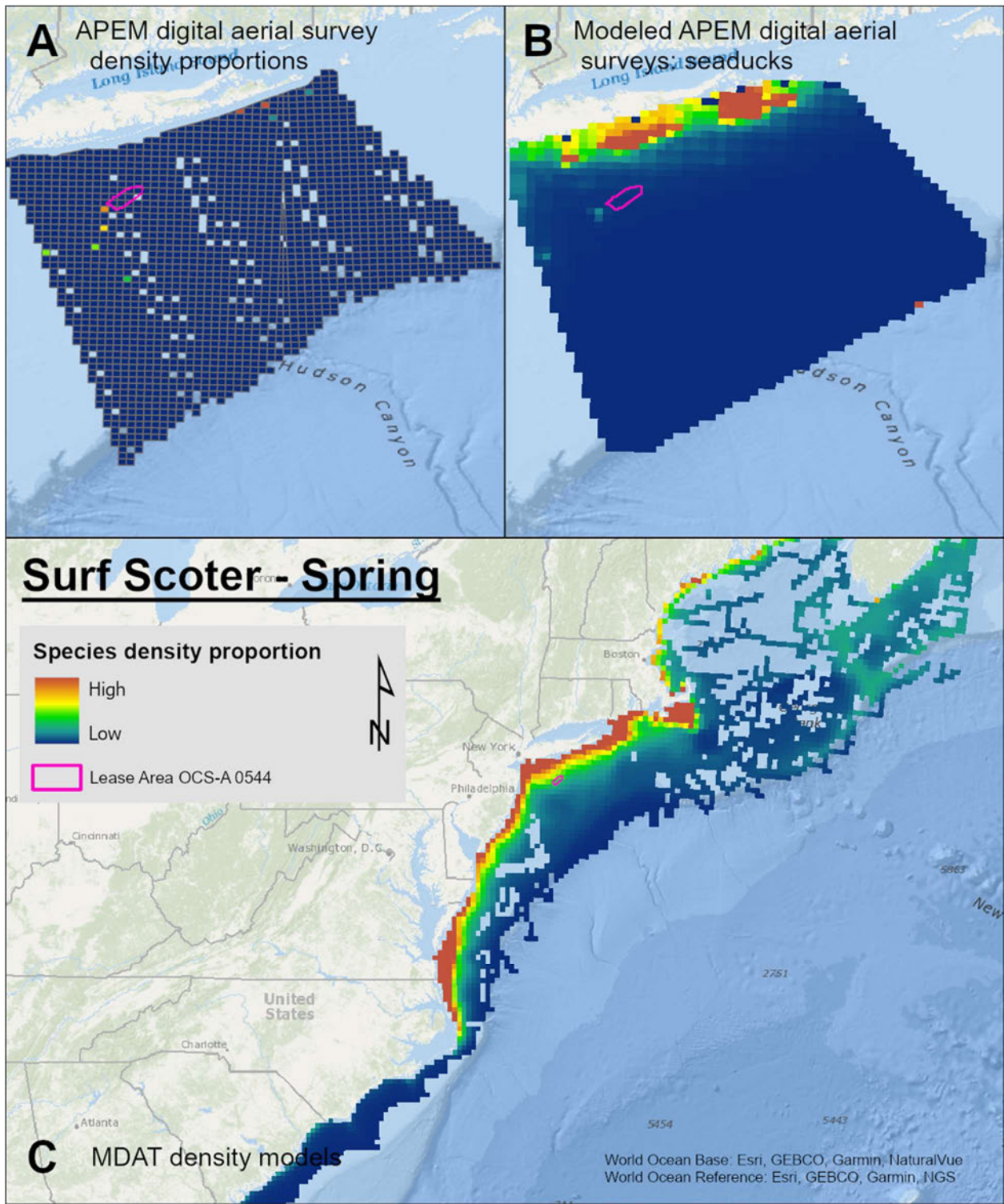
Map 4. Summer Common Eider density proportions in the NYSERDA APEM and Empire Wind high resolution digital aerial survey data (A), the NYSERDA APEM and Empire Wind high resolution digital aerial model outputs for seabirds in Summer (B) and, Summer Common Eider MDAT modeled abundance at the regional scale (C). The scale for all maps is representative of relative spatial variation in the sites within the season for each map input.



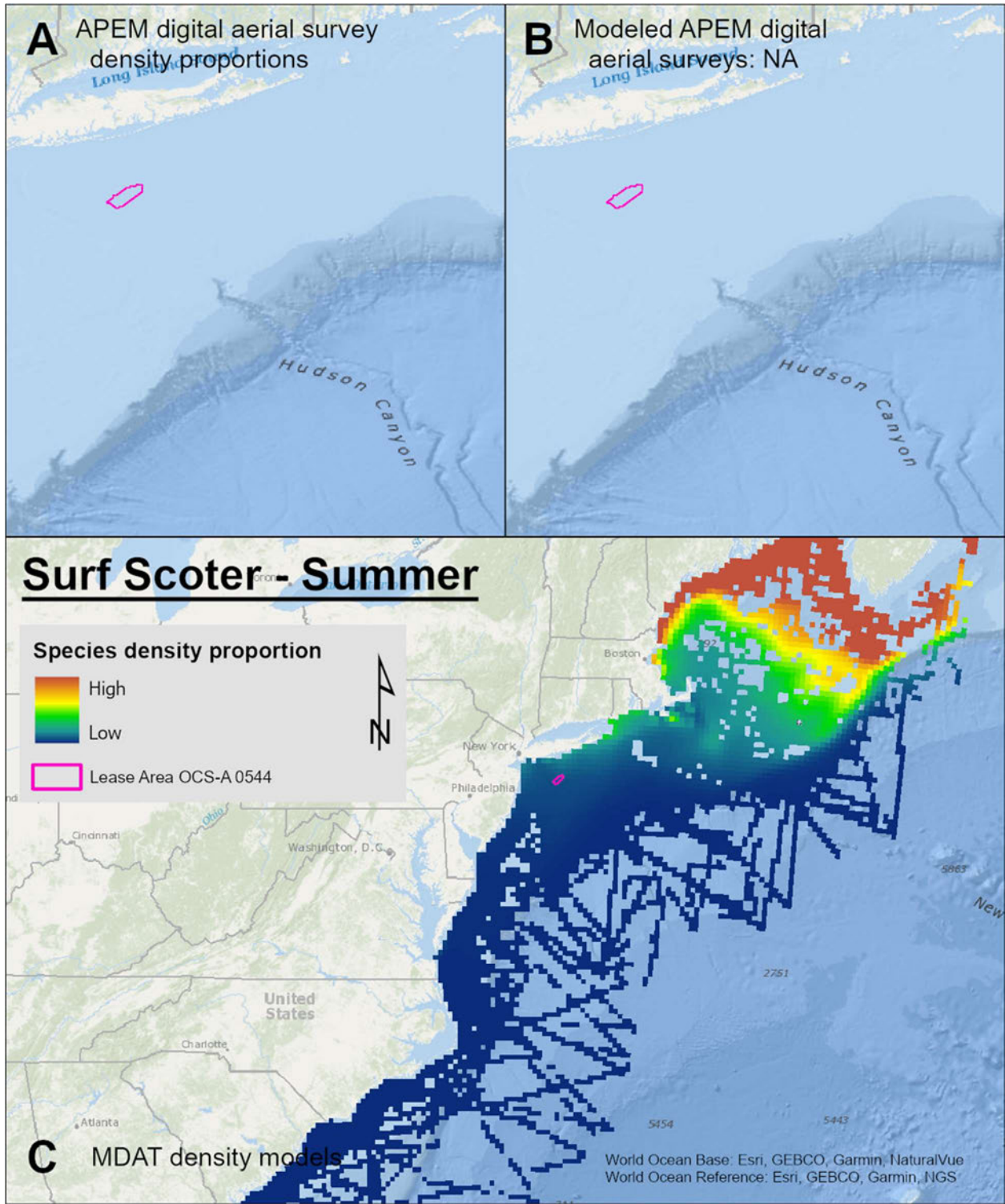
Map 5. Fall Common Eider density proportions in the NYSERDA APEM and Empire Wind high resolution digital aerial survey data (A), the NYSERDA APEM and Empire Wind high resolution digital aerial model outputs for seaducks in Fall (B) and, Fall Common Eider MDAT modeled abundance at the regional scale (C). The scale for all maps is representative of relative spatial variation in the sites within the season for each map input.



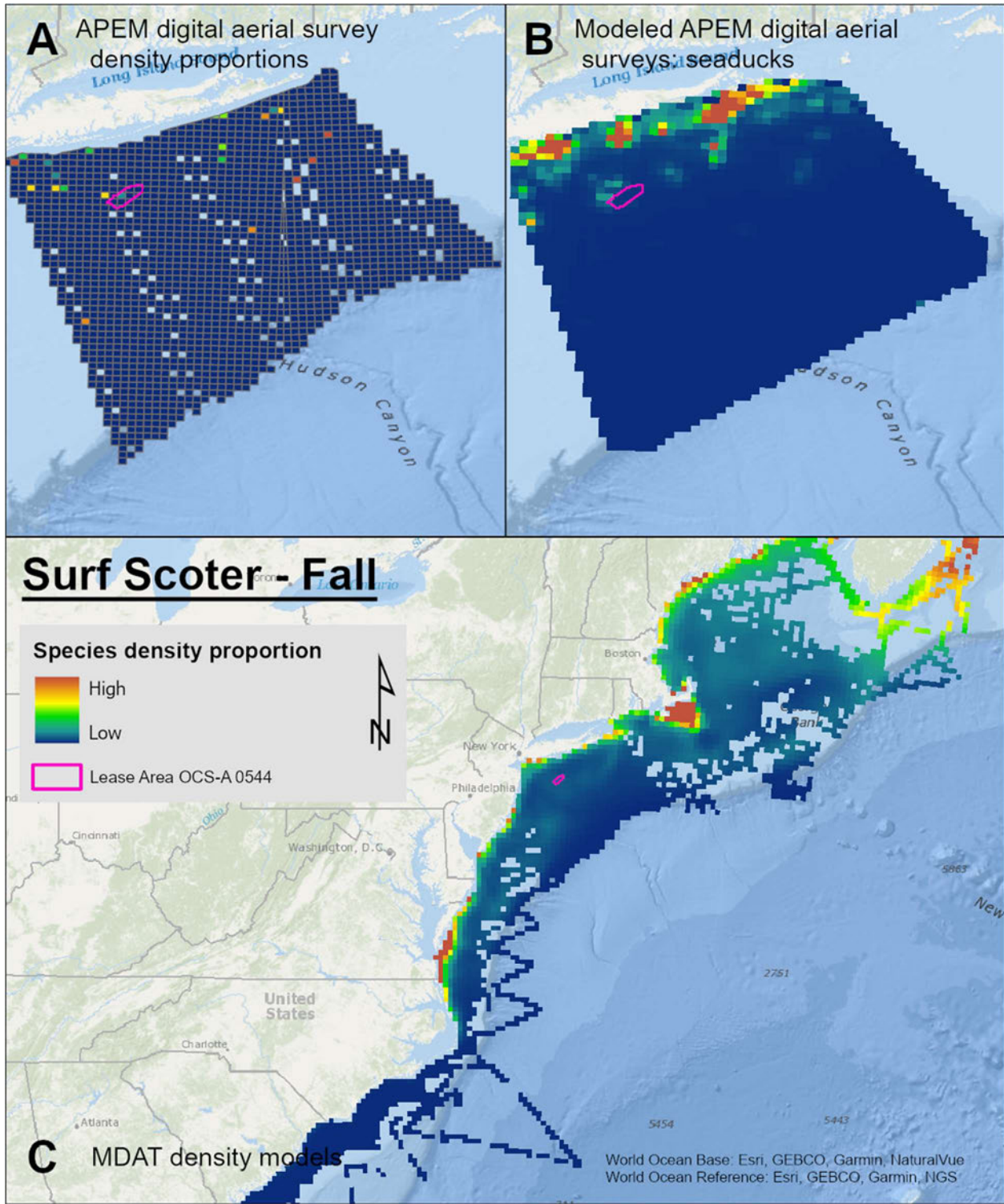
Map 6. Winter Surf Scoter density proportions in the NYSERDA APEM and Empire Wind high resolution digital aerial survey data (A), the NYSERDA APEM and Empire Wind high resolution digital aerial model outputs for seaducks in Winter (B) and, Winter Surf Scoter MDAT modeled abundance at the regional scale (C). The scale for all maps is representative of relative spatial variation in the sites within the season for each map input.



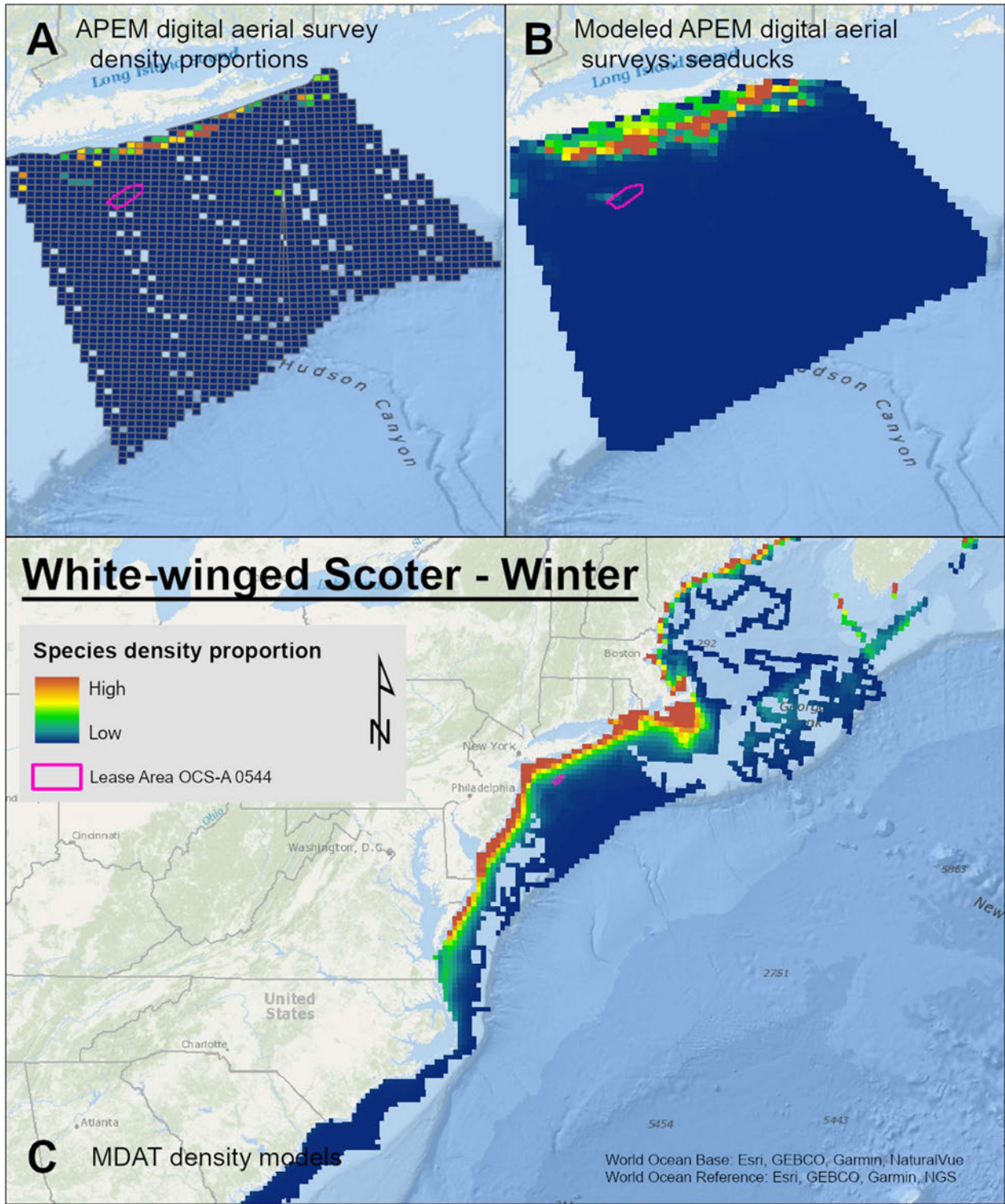
Map 7. Spring Surf Scoter density proportions in the NYSERDA APEM and Empire Wind high resolution digital aerial survey data (A), the NYSERDA APEM and Empire Wind high resolution digital aerial model outputs for seaducks in Spring (B) and, Spring Surf Scoter MDAT modeled abundance at the regional scale (C). The scale for all maps is representative of relative spatial variation in the sites within the season for each map input.



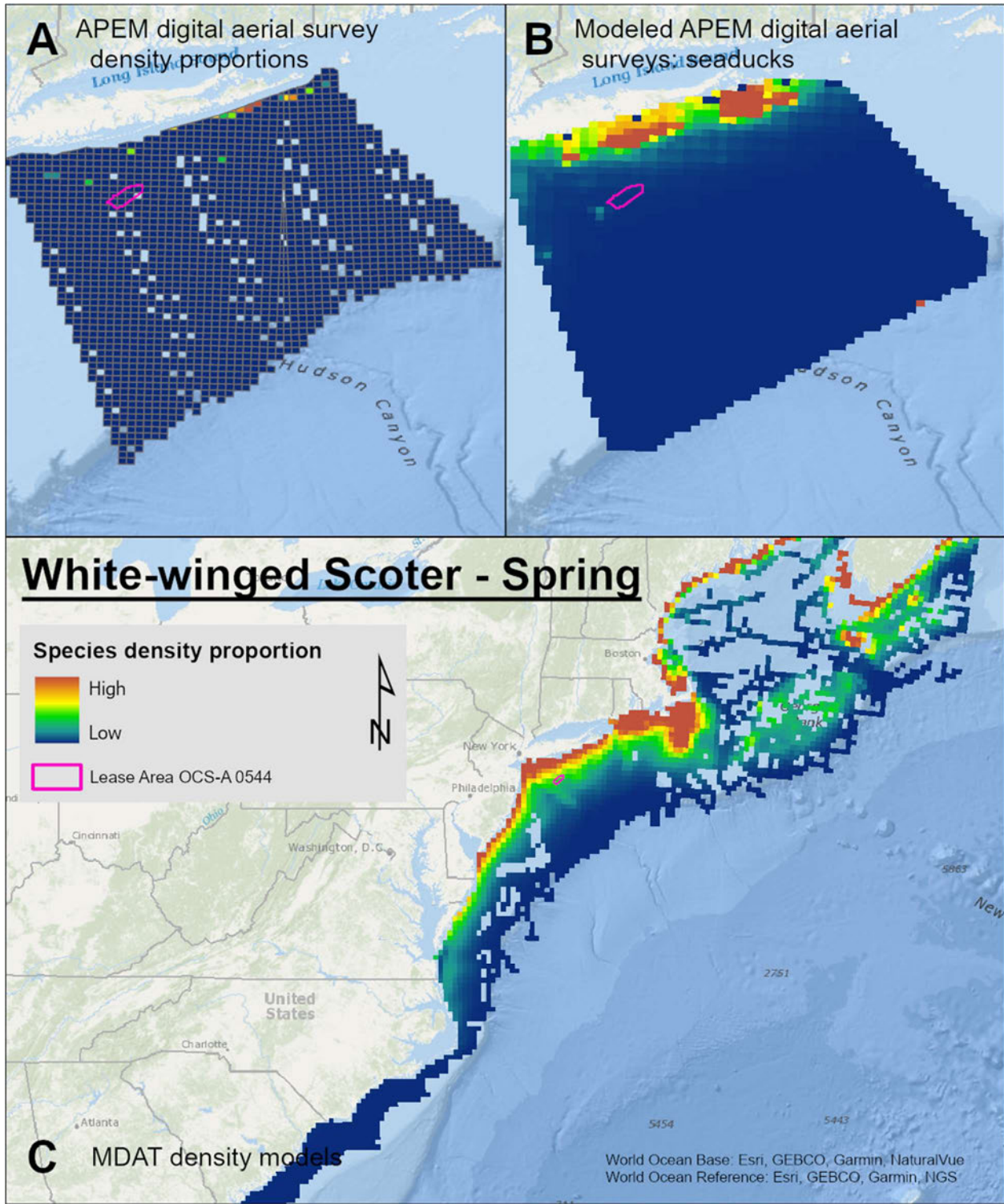
Map 8. Summer Surf Scoter density proportions in the NYSERDA APEM and Empire Wind high resolution digital aerial survey data (A), the NYSERDA APEM and Empire Wind high resolution digital aerial model outputs for seaducks in Summer (B) and, Summer Surf Scoter MDAT modeled abundance at the regional scale (C). The scale for all maps is representative of relative spatial variation in the sites within the season for each map input.



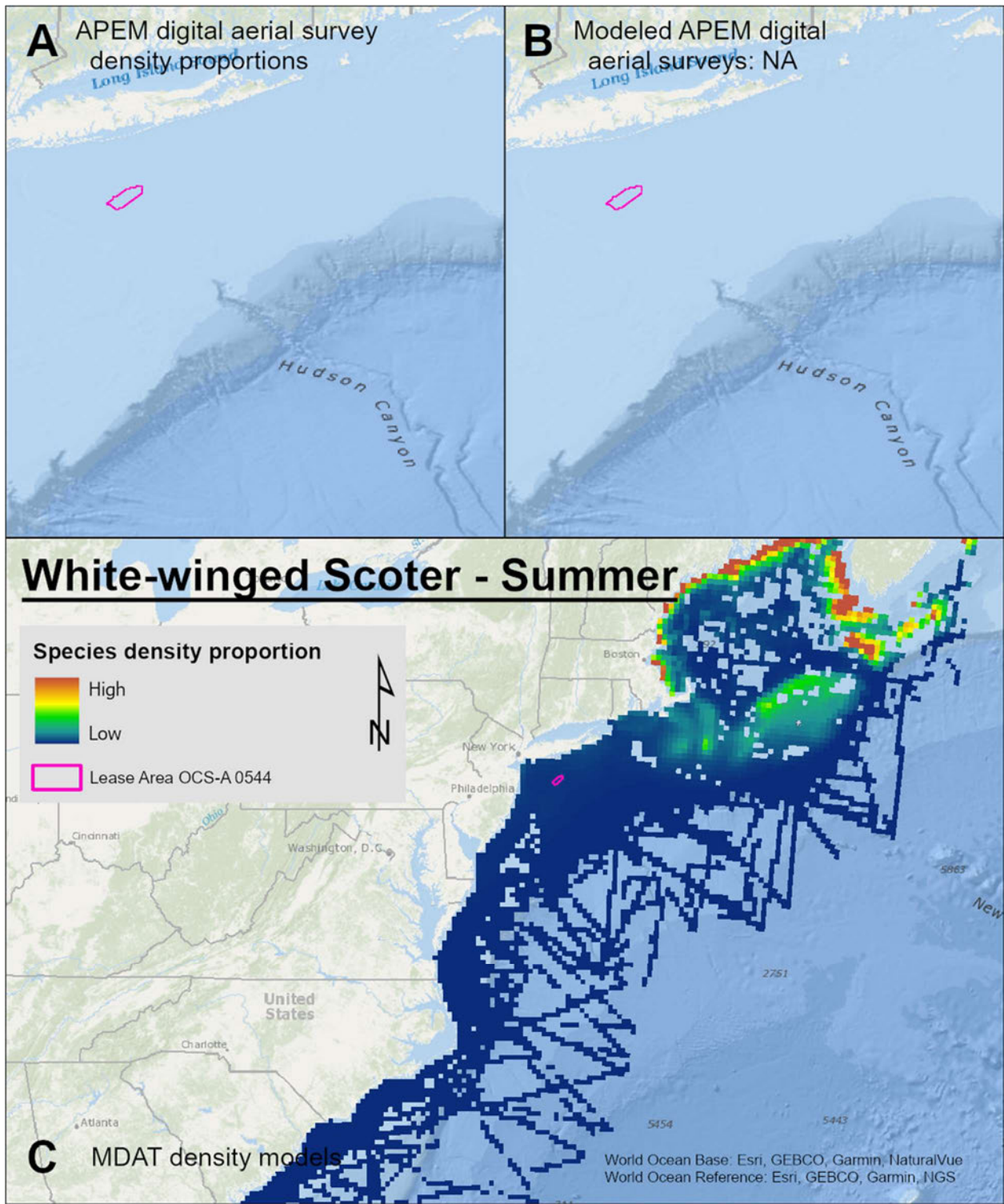
Map 9. Fall Surf Scoter density proportions in the NYSERDA APEM and Empire Wind high resolution digital aerial survey data (A), the NYSERDA APEM and Empire Wind high resolution digital aerial model outputs for seaducks in Fall (B) and, Fall Surf Scoter MDAT modeled abundance at the regional scale (C). The scale for all maps is representative of relative spatial variation in the sites within the season for each map input.



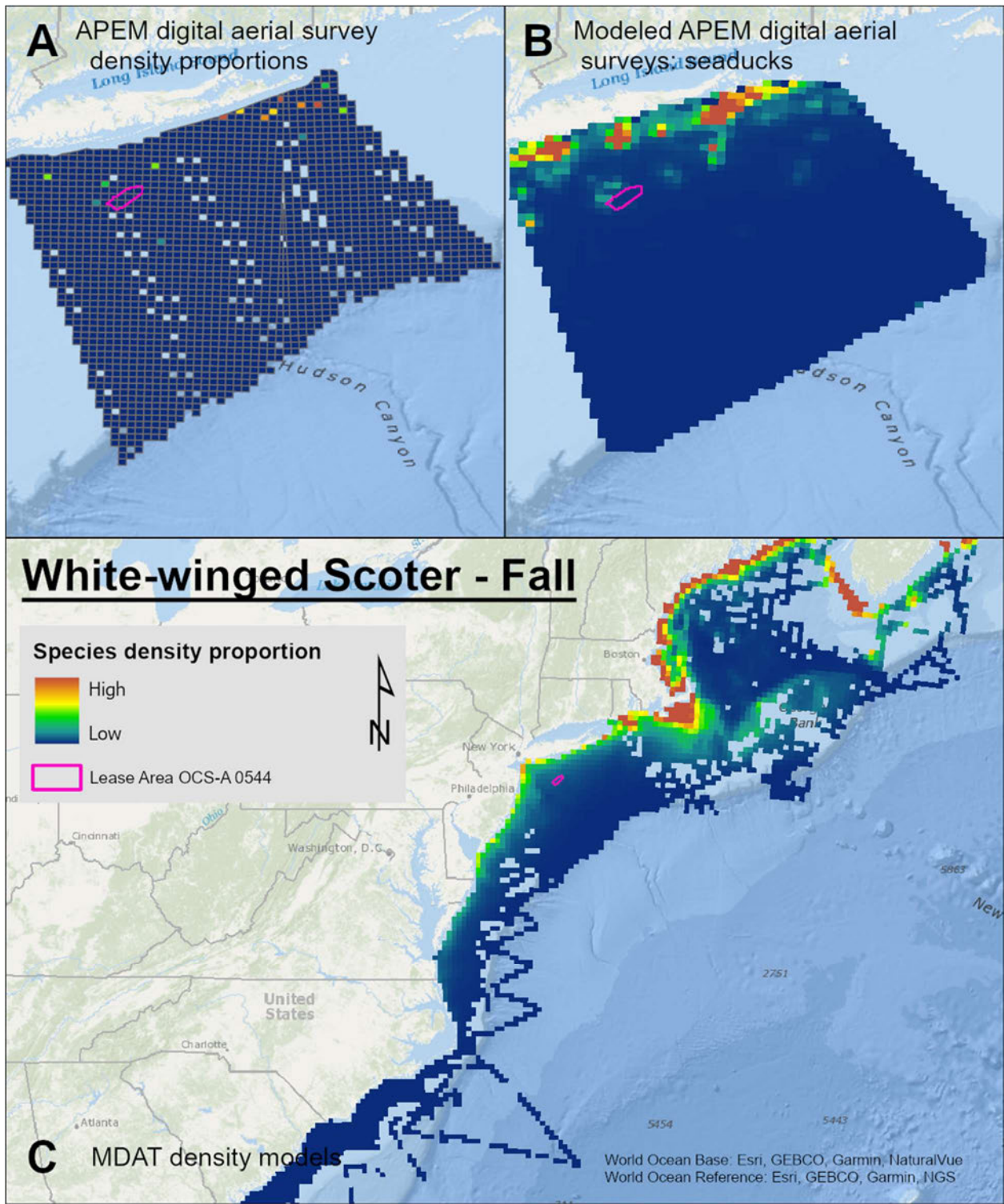
Map 10. Winter White-winged Scoter density proportions in the NYSERDA APEM and Empire Wind high resolution digital aerial survey data (A), the NYSERDA APEM and Empire Wind high resolution digital aerial model outputs for seaducks in Winter (B) and, Winter White-winged Scoter MDAT modeled abundance at the regional scale (C). The scale for all maps is representative of relative spatial variation in the sites within the season for each map input.



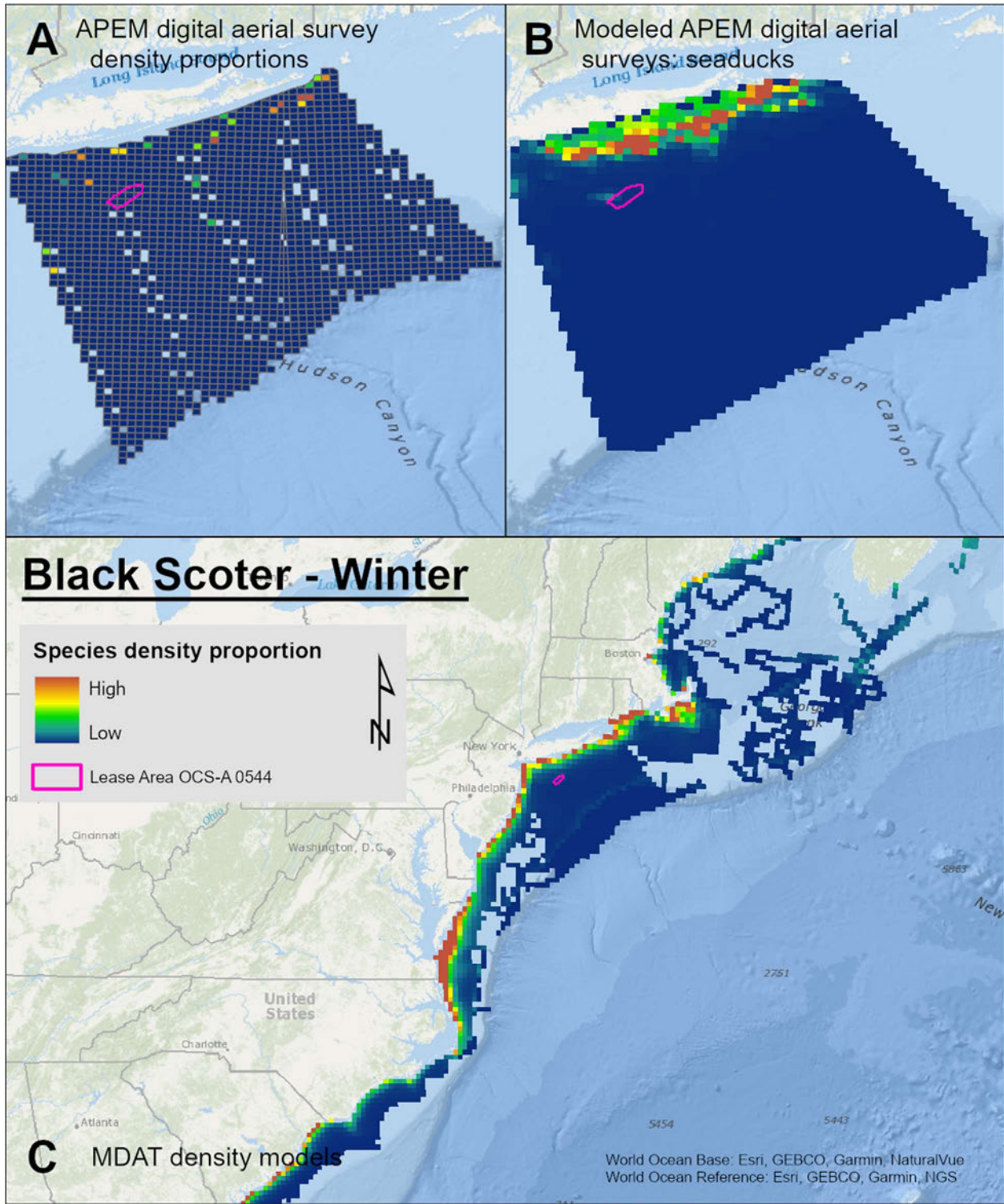
Map 11. Spring White-winged Scoter density proportions in the NYSERDA APEM and Empire Wind high resolution digital aerial survey data (A), the NYSERDA APEM and Empire Wind high resolution digital aerial model outputs for seaducks in Spring (B) and, Spring White-winged Scoter MDAT modeled abundance at the regional scale (C). The scale for all maps is representative of relative spatial variation in the sites within the season for each map input.



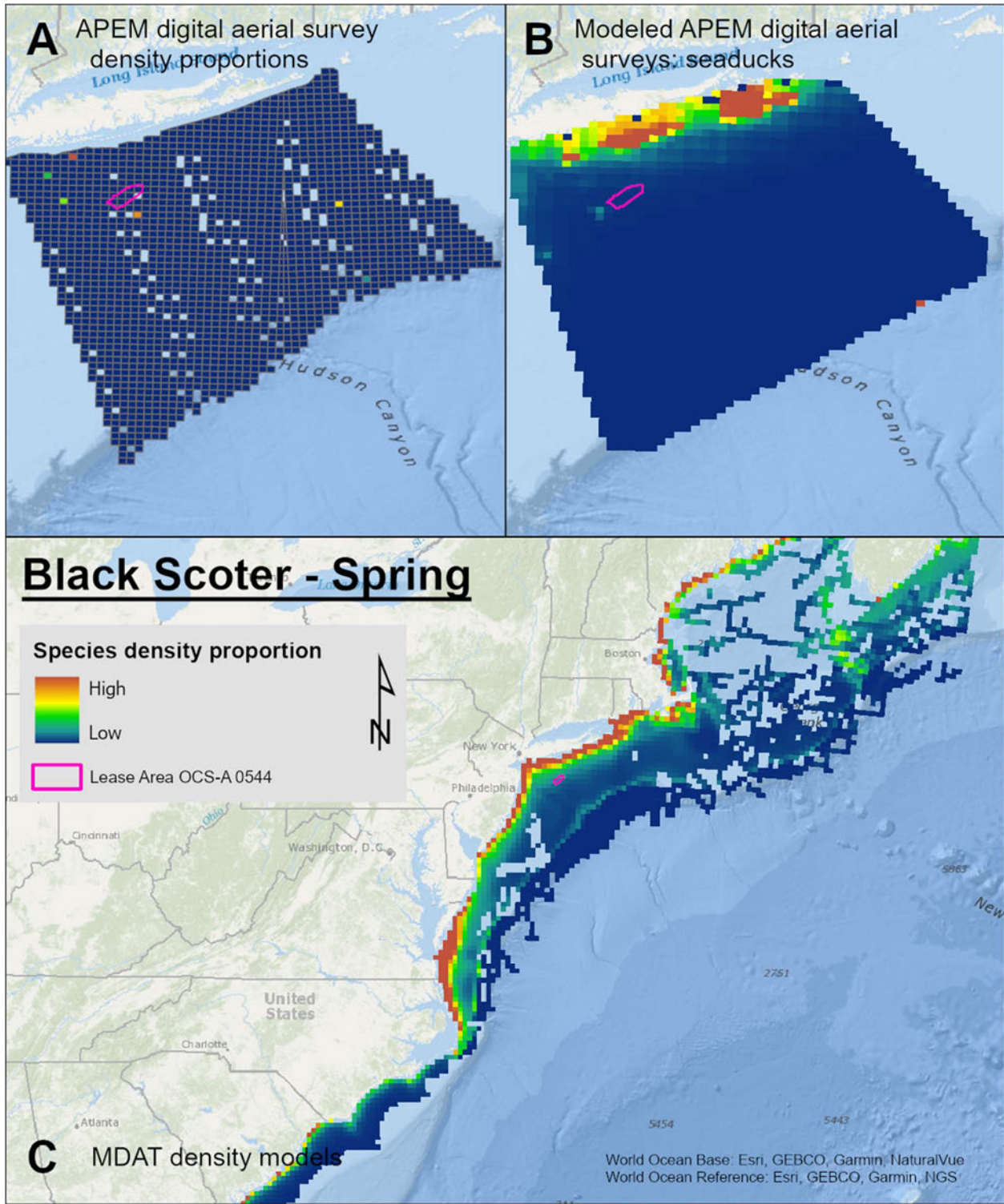
Map 12. Summer White-winged Scoter density proportions in the NYSERDA APEM and Empire Wind high resolution digital aerial survey data (A), the NYSERDA APEM and Empire Wind high resolution digital aerial model outputs for seaducks in Summer (B) and, Summer White-winged Scoter MDAT modeled abundance at the regional scale (C). The scale for all maps is representative of relative spatial variation in the sites within the season for each map input.



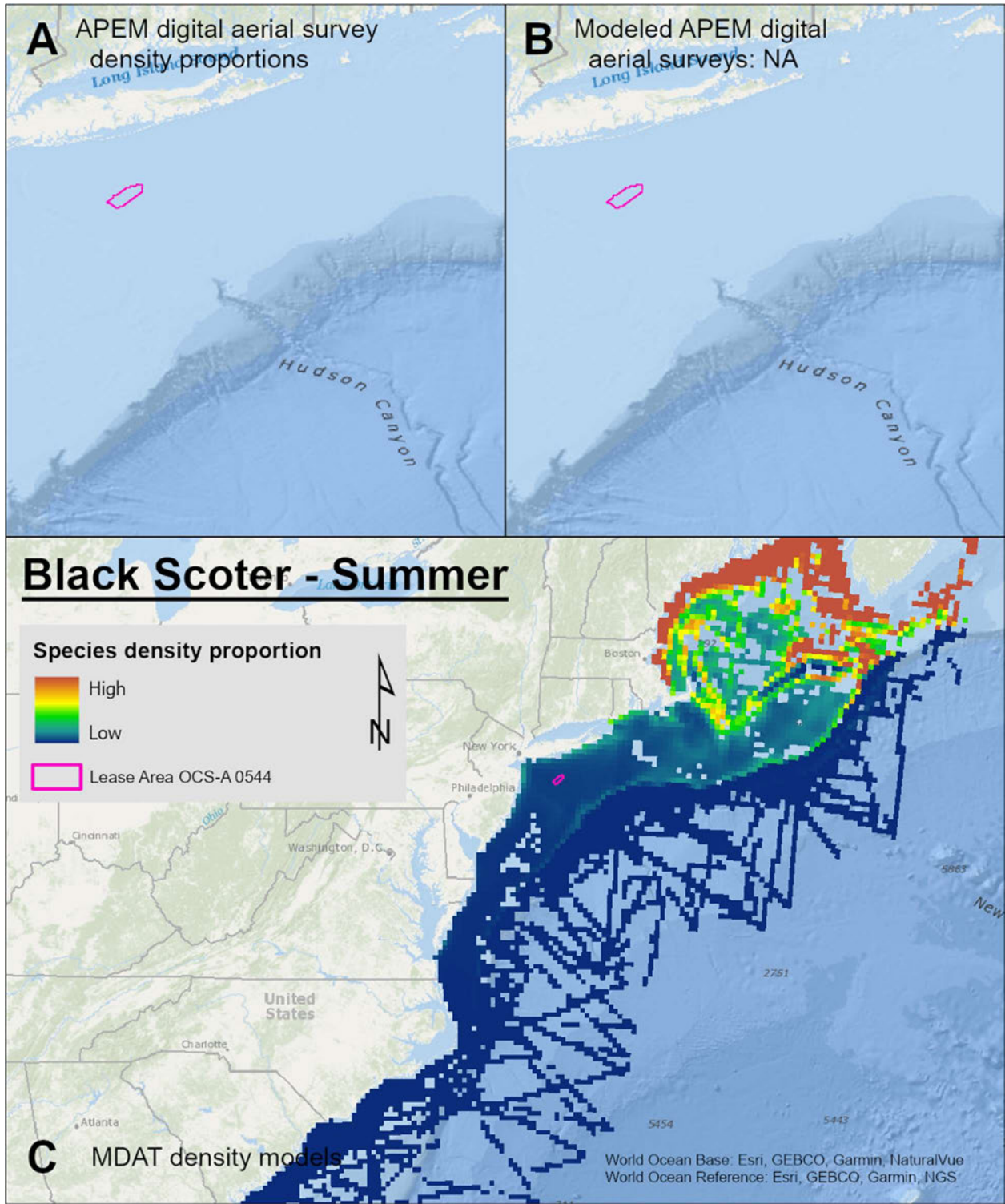
Map 13. Fall White-winged Scoter density proportions in the NYSERDA APEM and Empire Wind high resolution digital aerial survey data (A), the NYSERDA APEM and Empire Wind high resolution digital aerial model outputs for seaducks in Fall (B) and, Fall White-winged Scoter MDAT modeled abundance at the regional scale (C). The scale for all maps is representative of relative spatial variation in the sites within the season for each map input.



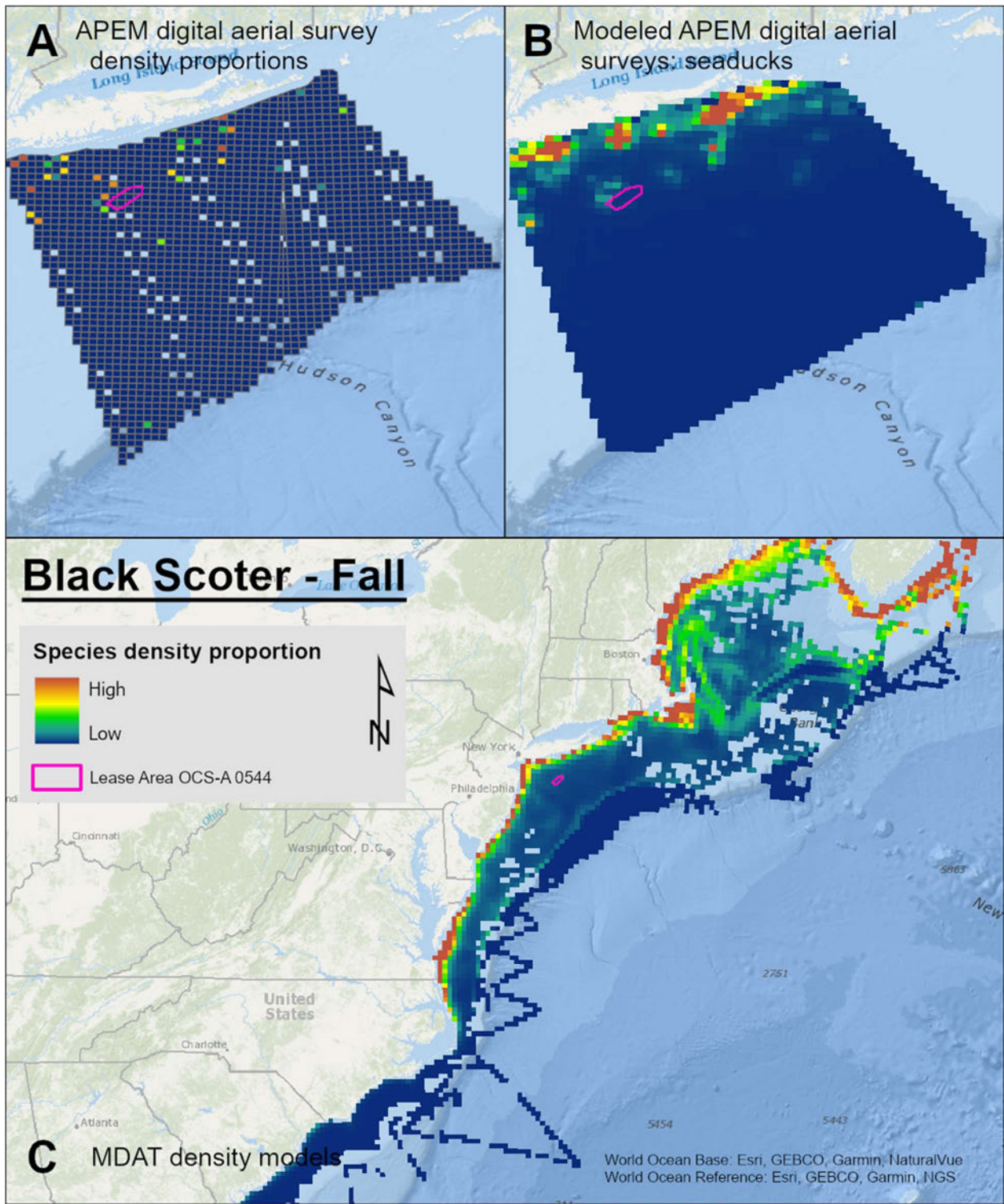
Map 14. Winter Black Scoter density proportions in the NYSERDA APEM and Empire Wind high resolution digital aerial survey data (A), the NYSERDA APEM and Empire Wind high resolution digital aerial model outputs for seaducks in Winter (B) and, Winter Black Scoter MDAT modeled abundance at the regional scale (C). The scale for all maps is representative of relative spatial variation in the sites within the season for each map input.



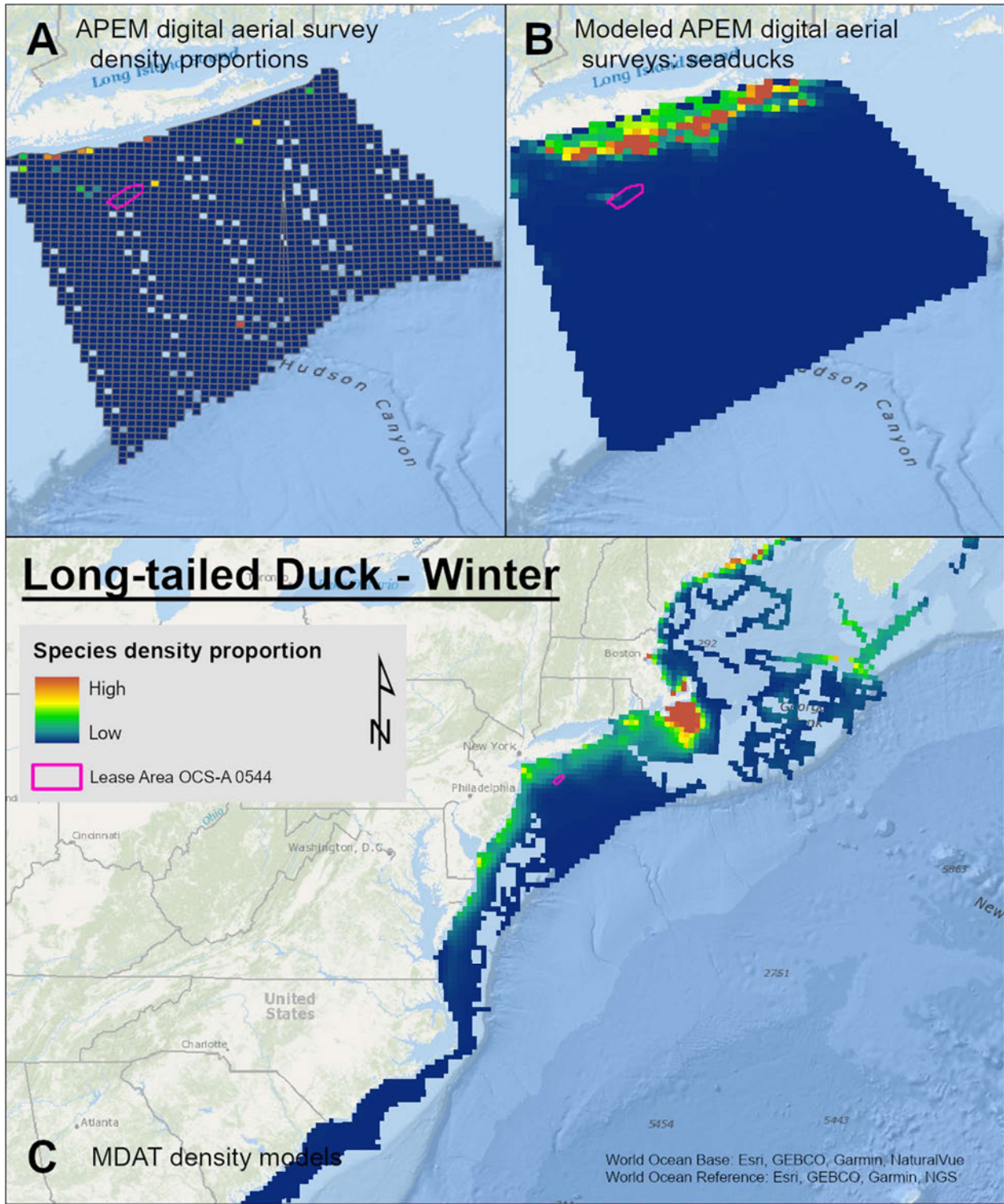
Map 15. Spring Black Scoter density proportions in the NYSERDA APEM and Empire Wind high resolution digital aerial survey data (A), the NYSERDA APEM and Empire Wind high resolution digital aerial model outputs for seaducks in Spring (B) and, Spring Black Scoter MDAT modeled abundance at the regional scale (C). The scale for all maps is representative of relative spatial variation in the sites within the season for each map input.



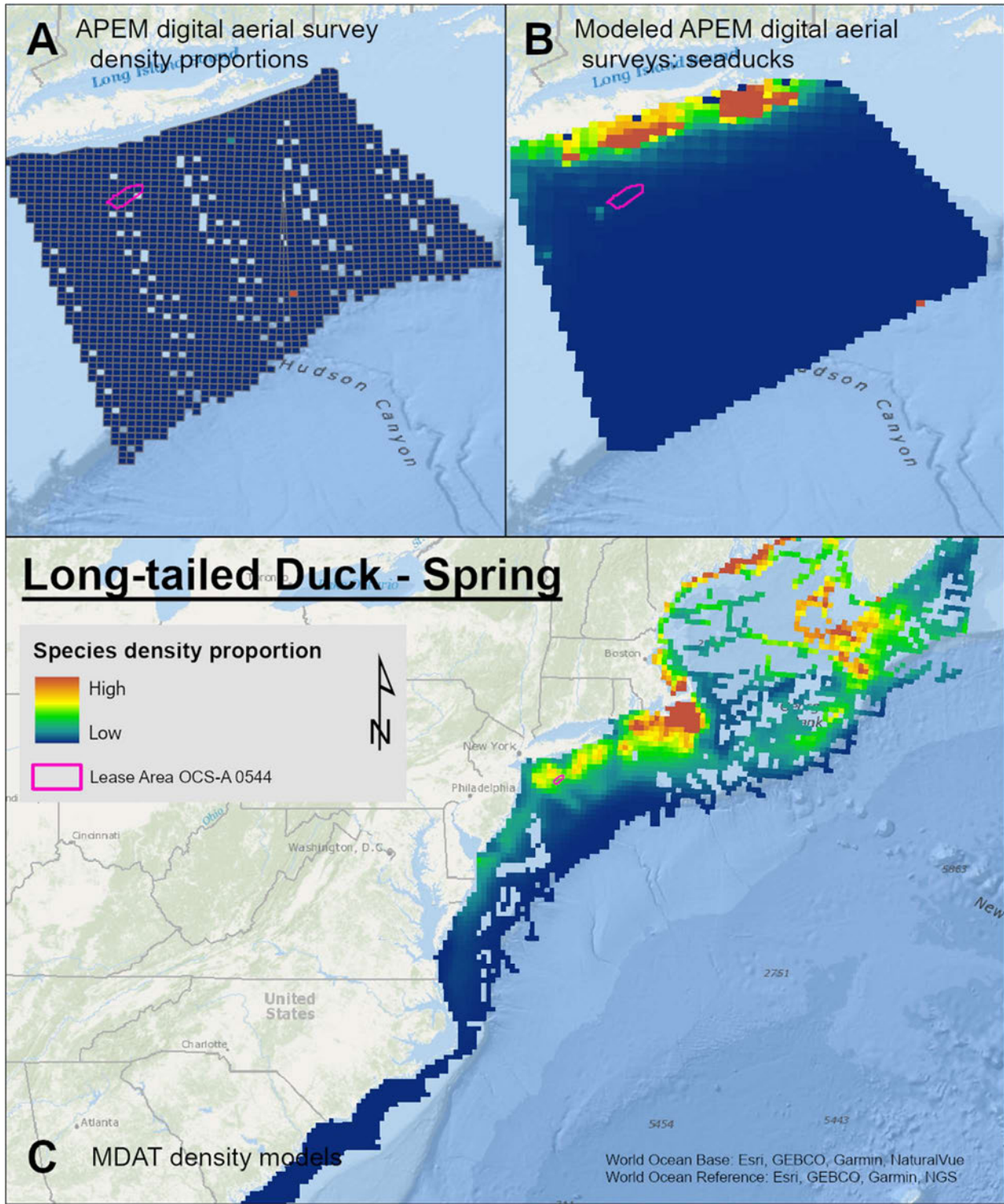
Map 16. Summer Black Scoter density proportions in the NYSERDA APEM and Empire Wind high resolution digital aerial survey data (A), the NYSERDA APEM and Empire Wind high resolution digital aerial model outputs for seabirds in Summer (B) and, Summer Black Scoter MDAT modeled abundance at the regional scale (C). The scale for all maps is representative of relative spatial variation in the sites within the season for each map input.



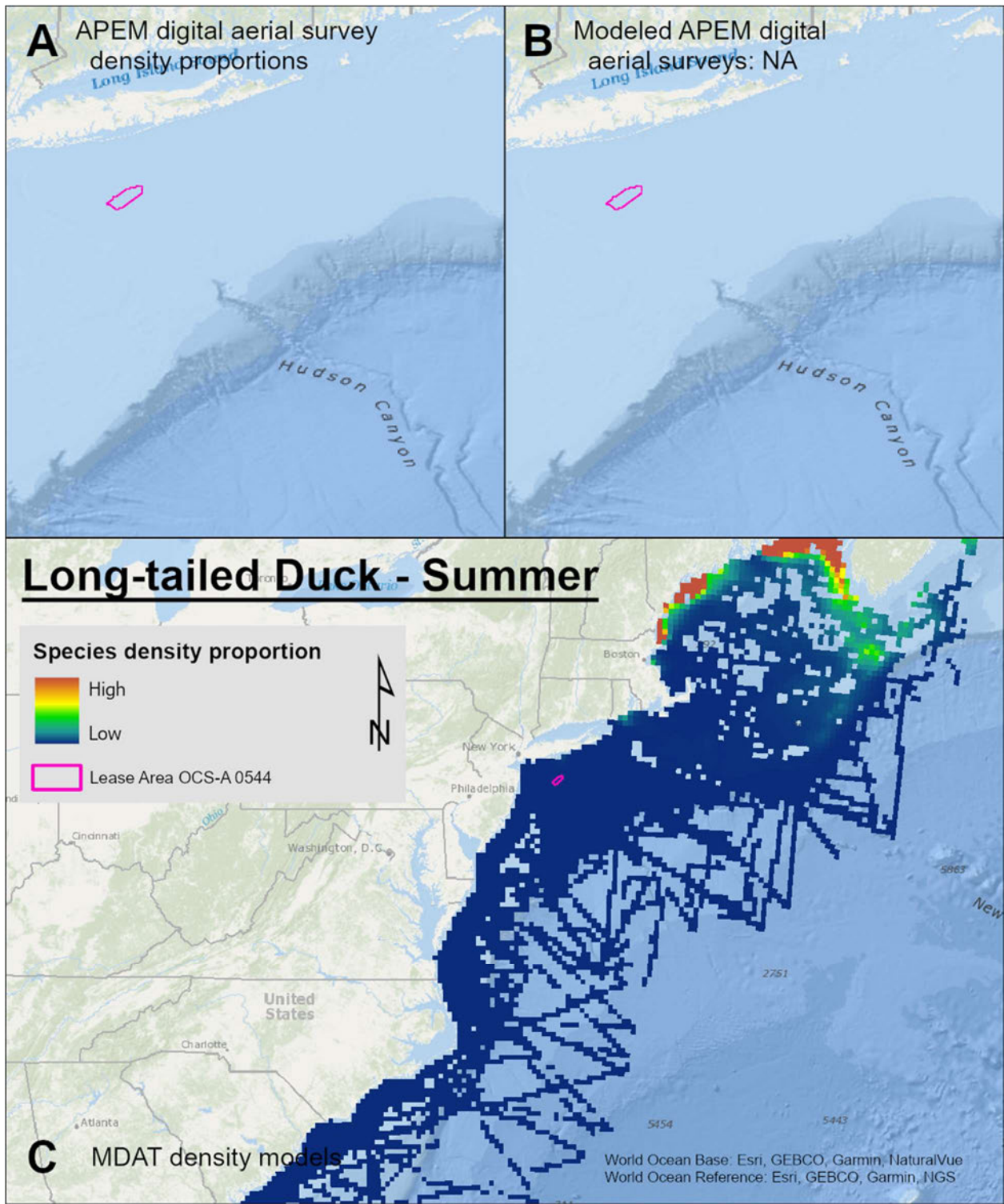
Map 17. Fall Black Scoter density proportions in the NYSERDA APEM and Empire Wind high resolution digital aerial survey data (A), the NYSERDA APEM and Empire Wind high resolution digital aerial model outputs for seaducks in Fall (B) and, Fall Black Scoter MDAT modeled abundance at the regional scale (C). The scale for all maps is representative of relative spatial variation in the sites within the season for each map input.



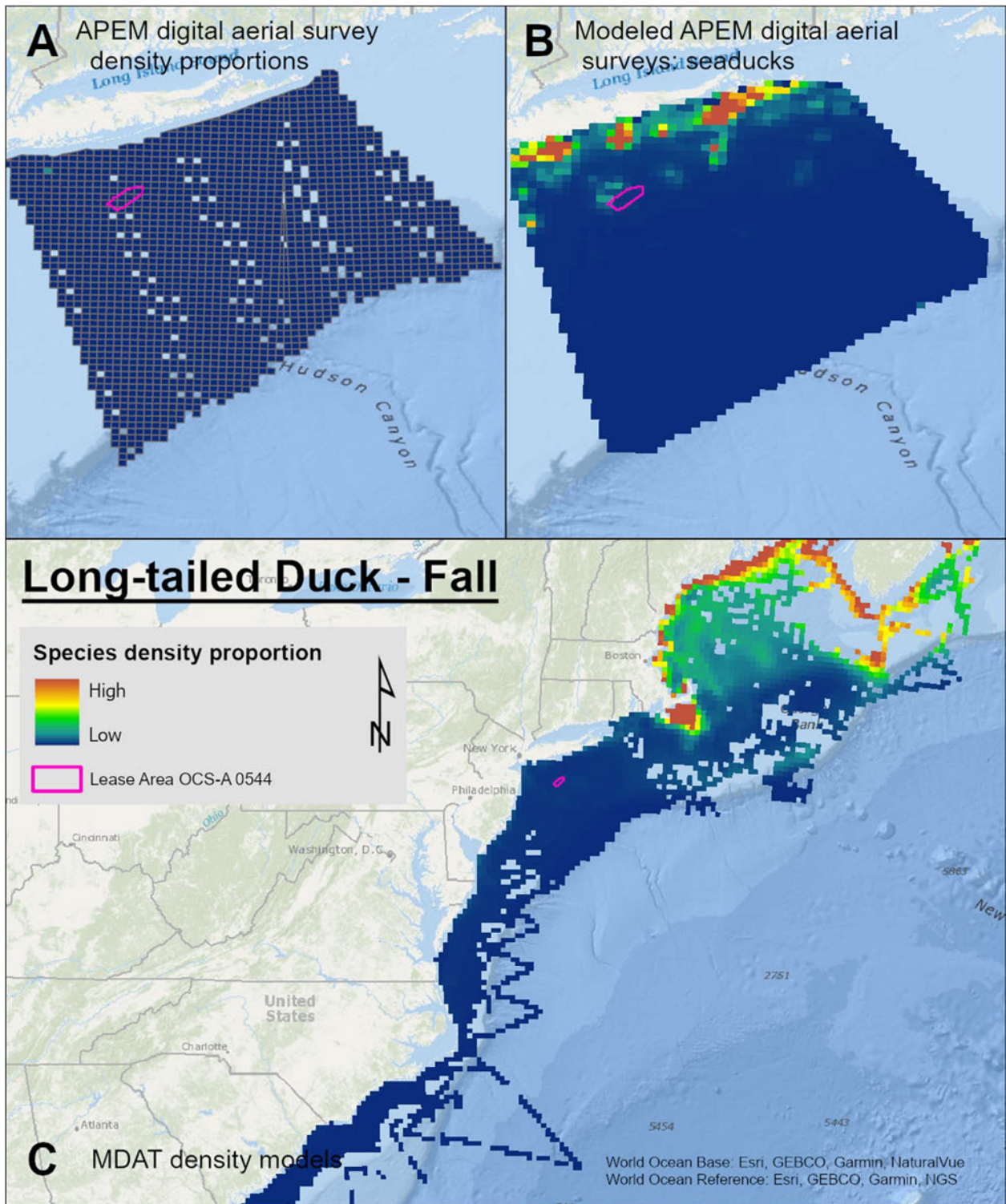
Map 18. Winter Long-tailed Duck density proportions in the NYSERDA APEM and Empire Wind high resolution digital aerial survey data (A), the NYSERDA APEM and Empire Wind high resolution digital aerial model outputs for seaducks in Winter (B) and, Winter Long-tailed Duck MDAT modeled abundance at the regional scale (C). The scale for all maps is representative of relative spatial variation in the sites within the season for each map input.



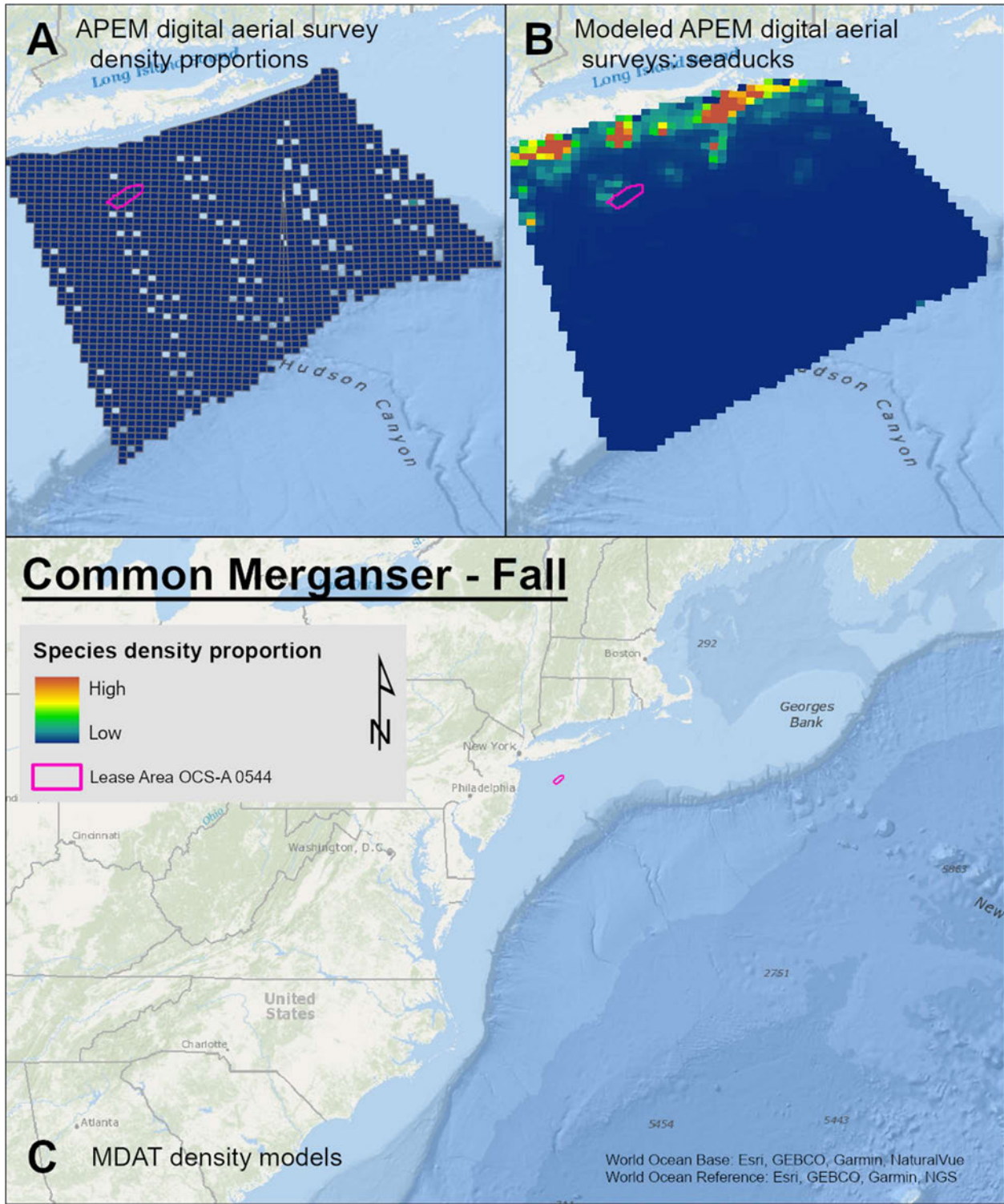
Map 19. Spring Long-tailed Duck density proportions in the NYSERDA APEM and Empire Wind high resolution digital aerial survey data (A), the NYSERDA APEM and Empire Wind high resolution digital aerial model outputs for seaducks in Spring (B) and, Spring Long-tailed Duck MDAT modeled abundance at the regional scale (C). The scale for all maps is representative of relative spatial variation in the sites within the season for each map input.



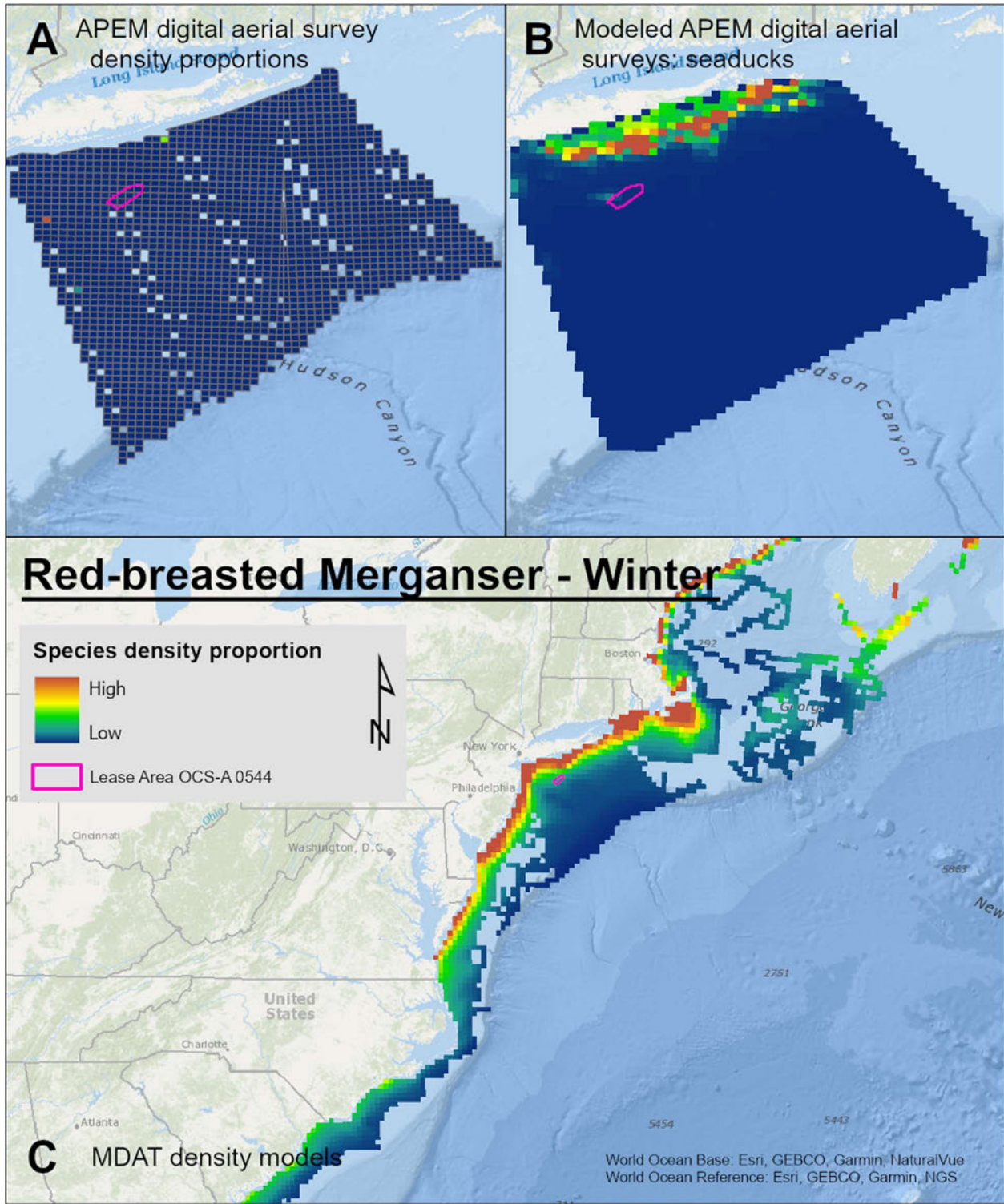
Map 20. Summer Long-tailed Duck density proportions in the NYSERDA APEM and Empire Wind high resolution digital aerial survey data (A), the NYSERDA APEM and Empire Wind high resolution digital aerial model outputs for seabirds in Summer (B) and, Summer Long-tailed Duck MDAT modeled abundance at the regional scale (C). The scale for all maps is representative of relative spatial variation in the sites within the season for each map input.



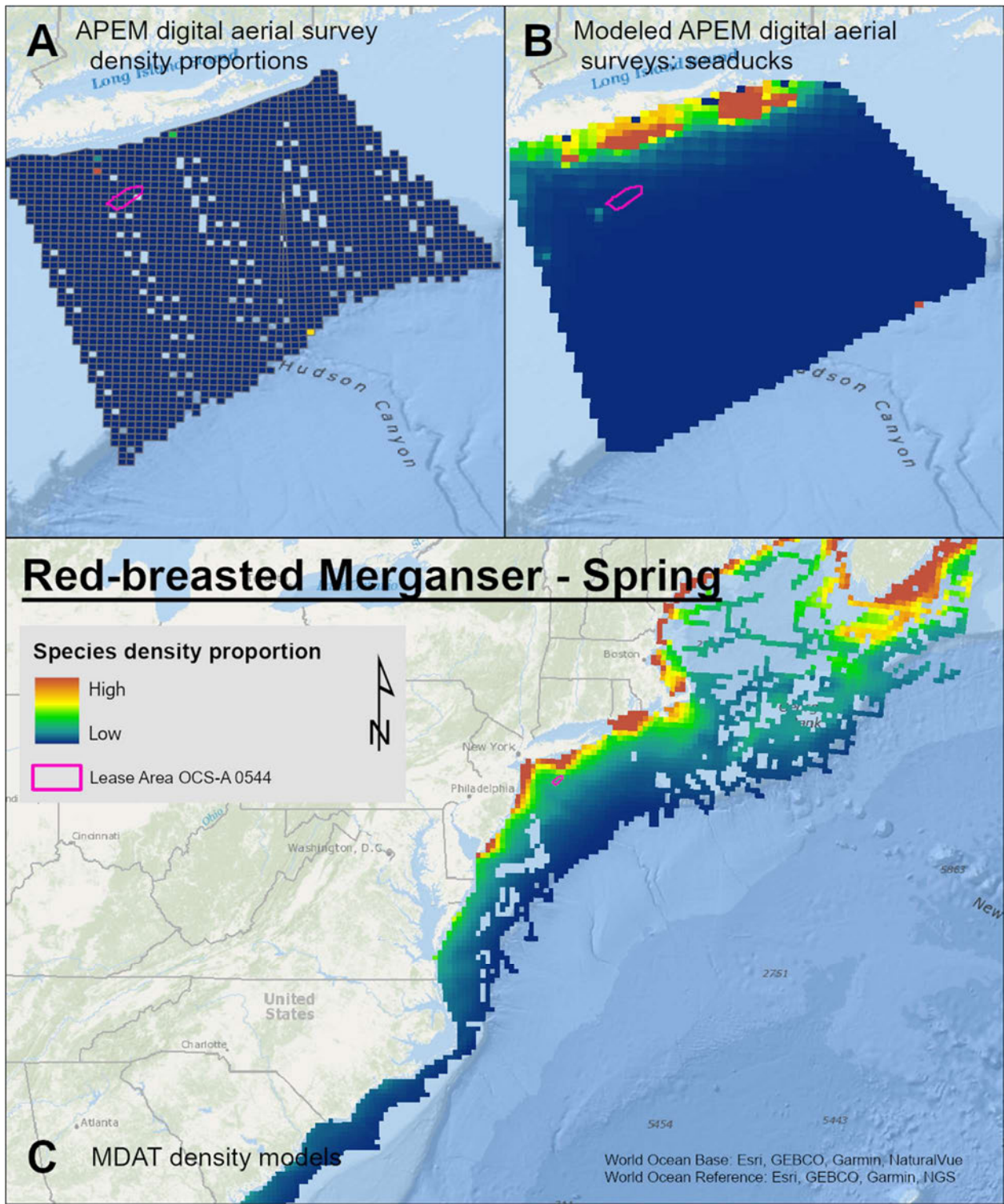
Map 21. Fall Long-tailed Duck density proportions in the NYSERDA APEM and Empire Wind high resolution digital aerial survey data (A), the NYSERDA APEM and Empire Wind high resolution digital aerial model outputs for seaducks in Fall (B) and, Fall Long-tailed Duck MDAT modeled abundance at the regional scale (C). The scale for all maps is representative of relative spatial variation in the sites within the season for each map input.



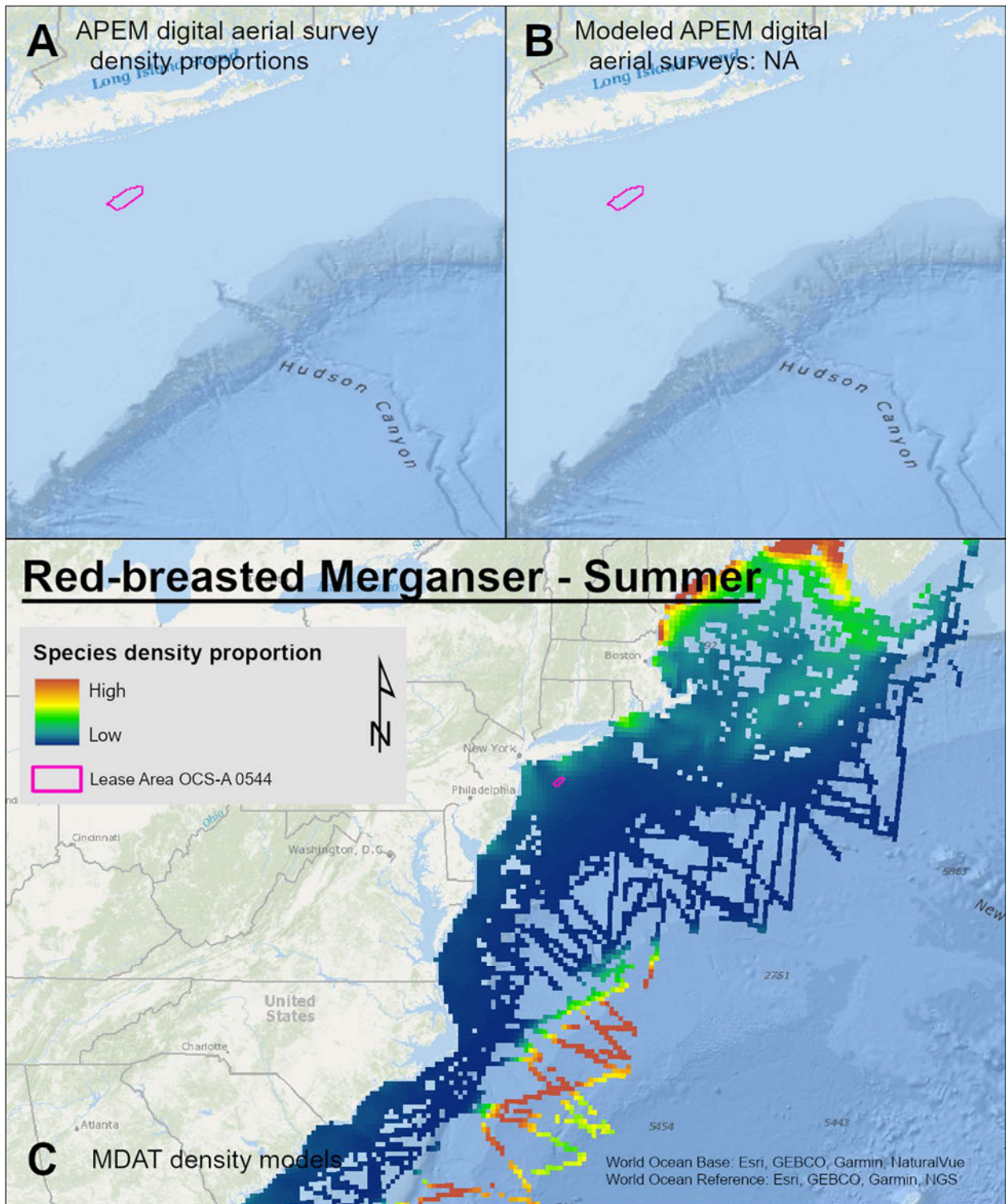
Map 22. Fall Common Merganser density proportions in the NYSERDA APEM and Empire Wind high resolution digital aerial survey data (A), the NYSERDA APEM and Empire Wind high resolution digital aerial model outputs for seaducks in Fall (B) and, Fall Common Merganser MDAT modeled abundance at the regional scale (C). The scale for all maps is representative of relative spatial variation in the sites within the season for each map input.



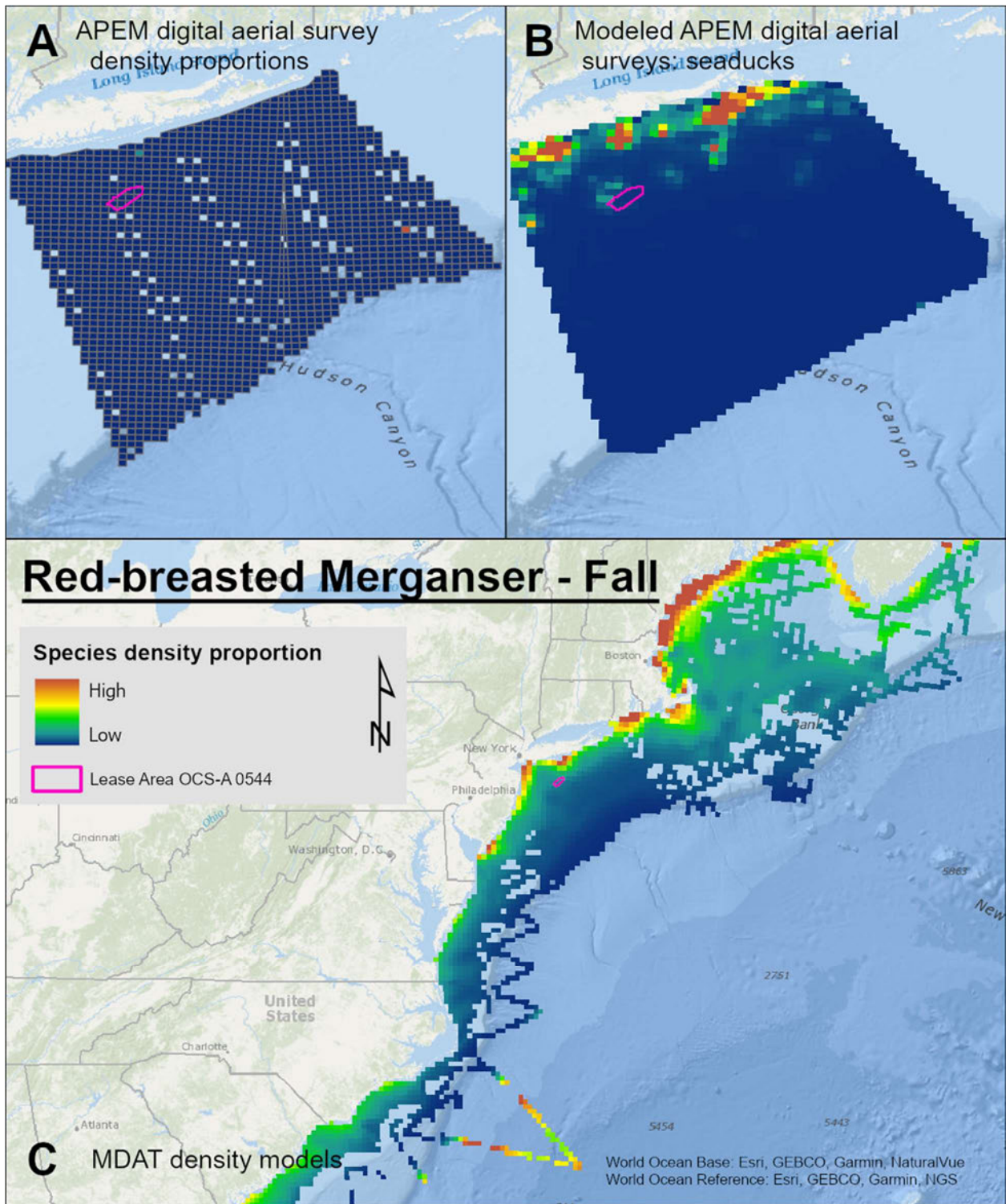
Map 23. Winter Red-breasted Merganser density proportions in the NYSERDA APEM and Empire Wind high resolution digital aerial survey data (A), the NYSERDA APEM and Empire Wind high resolution digital aerial model outputs for seaducks in Winter (B) and, Winter Red-breasted Merganser MDAT modeled abundance at the regional scale (C). The scale for all maps is representative of relative spatial variation in the sites within the season for each map input.



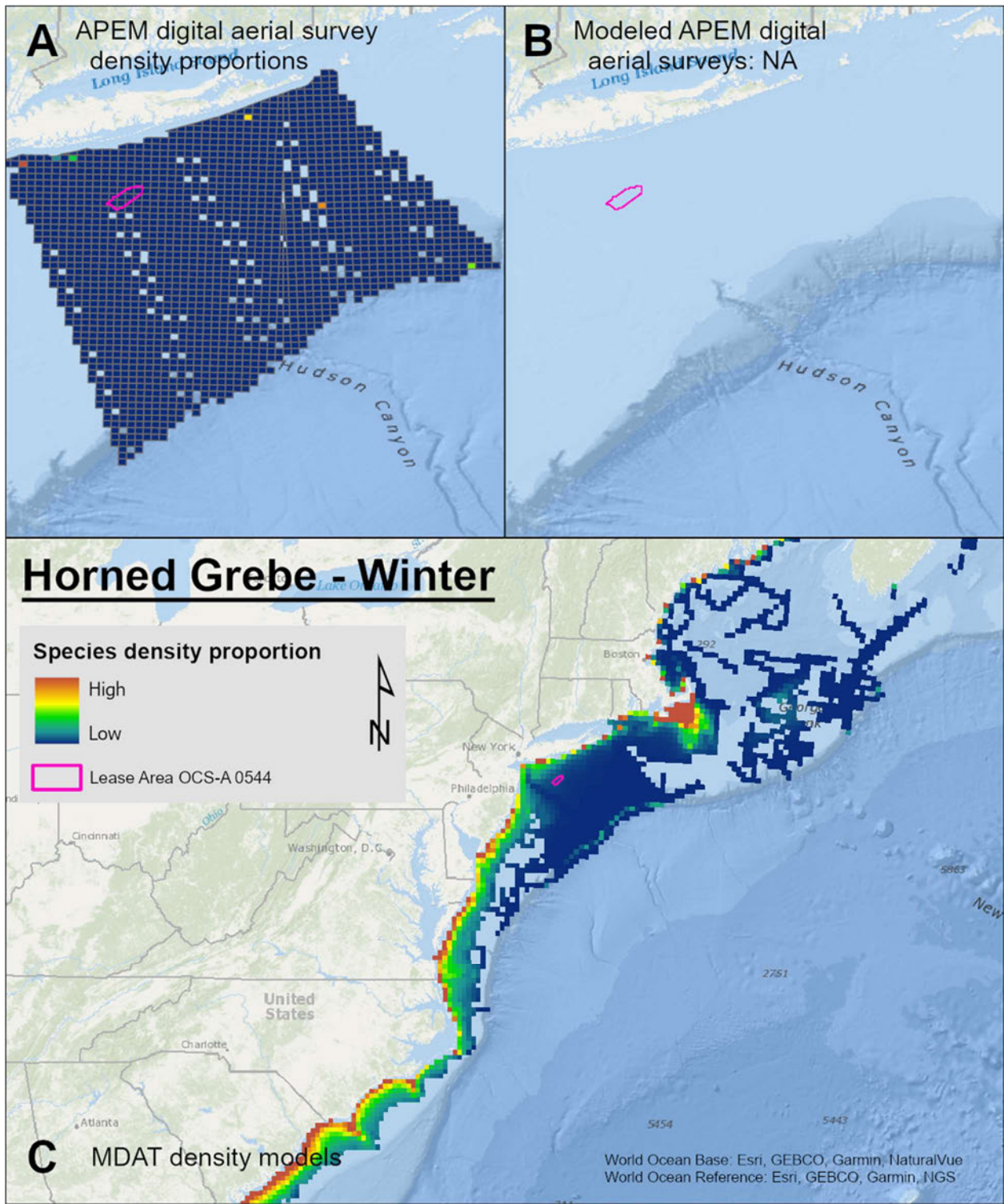
Map 24. Spring Red-breasted Merganser density proportions in the NYSEDA APEM and Empire Wind high resolution digital aerial survey data (A), the NYSEDA APEM and Empire Wind high resolution digital aerial model outputs for seaducks in Spring (B) and, Spring Red-breasted Merganser MDAT modeled abundance at the regional scale (C). The scale for all maps is representative of relative spatial variation in the sites within the season for each map input.



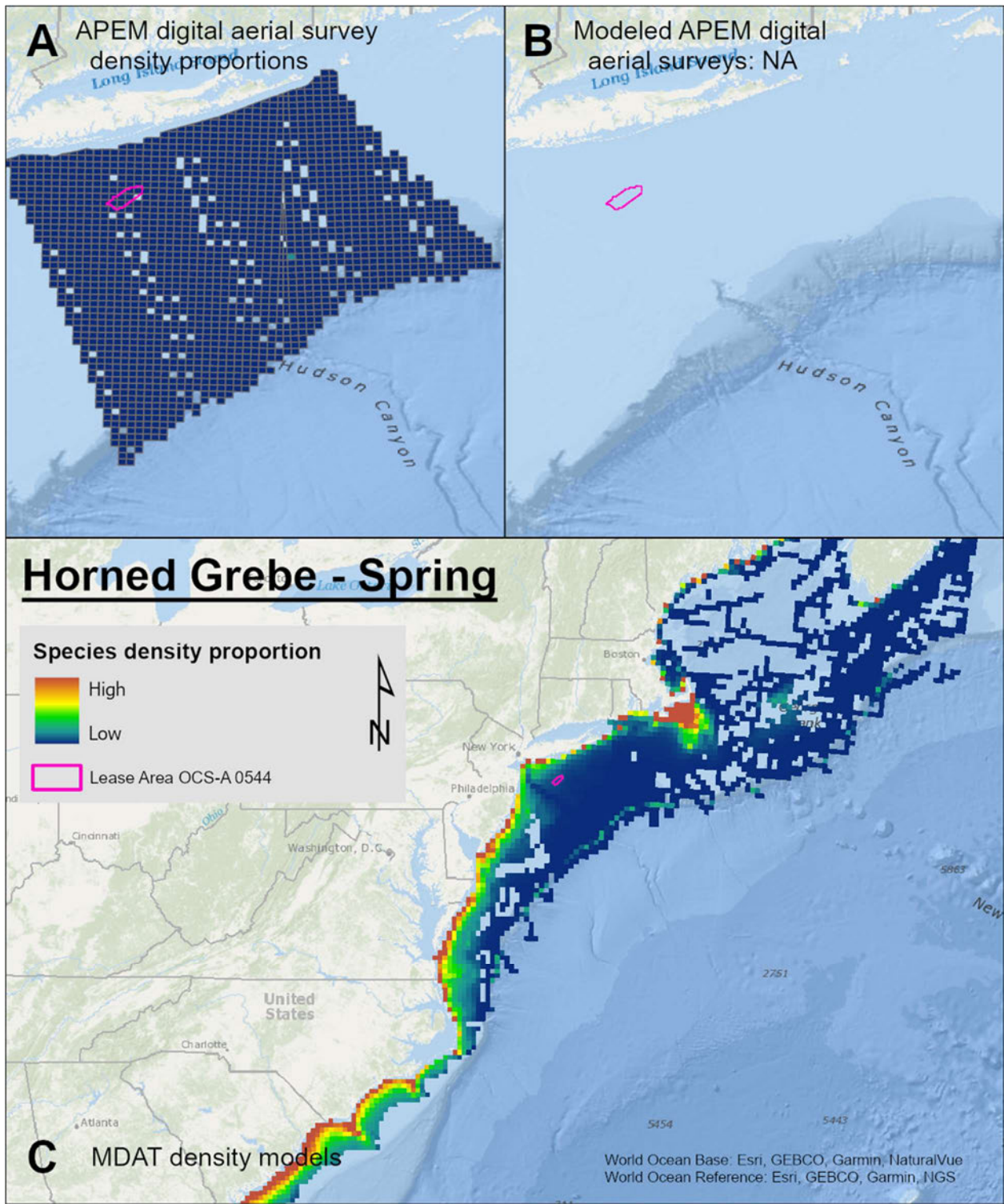
Map 25. Summer Red-breasted Merganser density proportions in the NYSERDA APEM and Empire Wind high resolution digital aerial survey data (A), the NYSERDA APEM and Empire Wind high resolution digital aerial model outputs for seaducks in Summer (B) and, Summer Red-breasted Merganser MDAT modeled abundance at the regional scale (C). The scale for all maps is representative of relative spatial variation in the sites within the season for each map input.



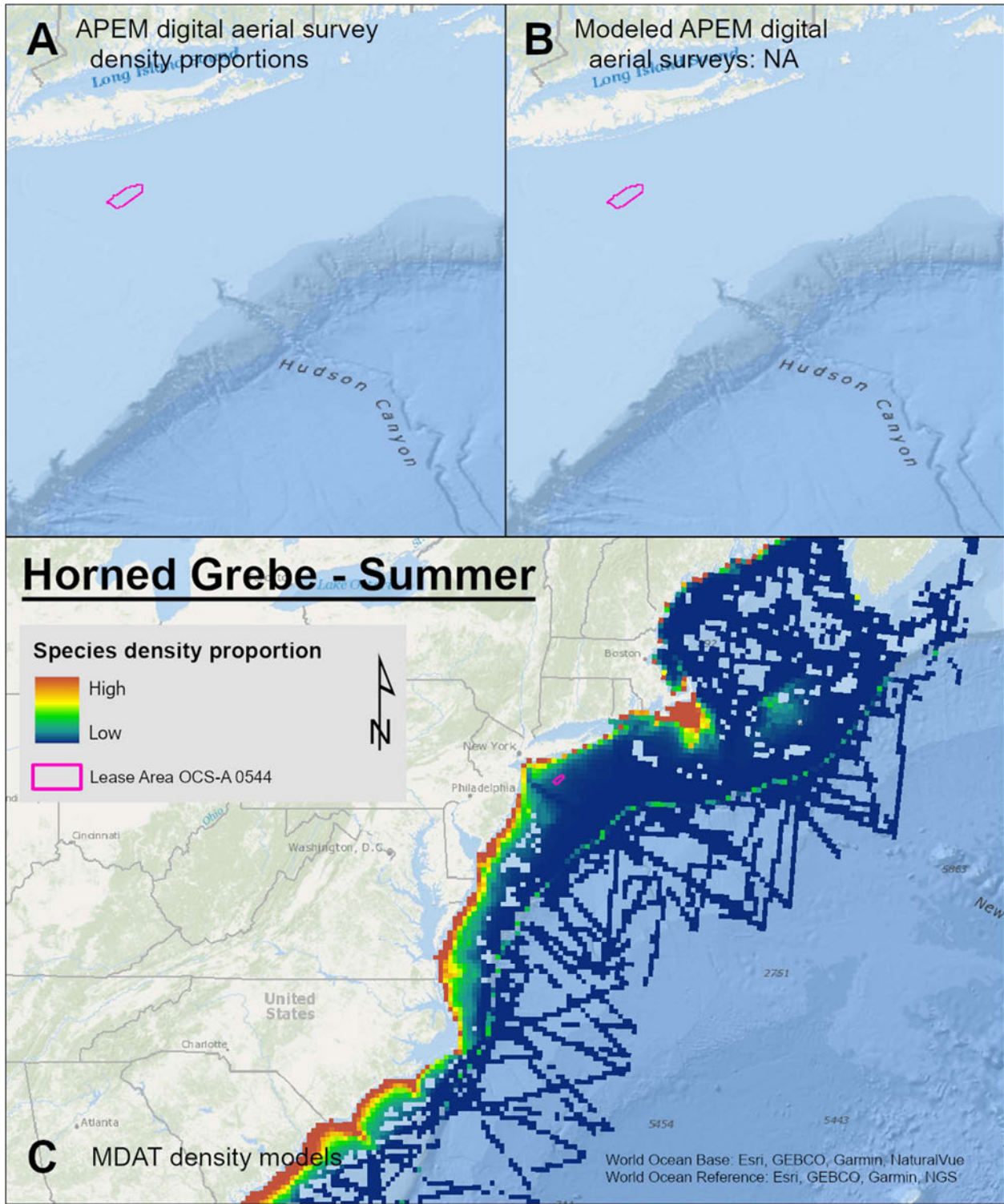
Map 26. Fall Red-breasted Merganser density proportions in the NYSERDA APEM and Empire Wind high resolution digital aerial survey data (A), the NYSERDA APEM and Empire Wind high resolution digital aerial model outputs for seaducks in Fall (B) and, Fall Red-breasted Merganser MDAT modeled abundance at the regional scale (C). The scale for all maps is representative of relative spatial variation in the sites within the season for each map input.



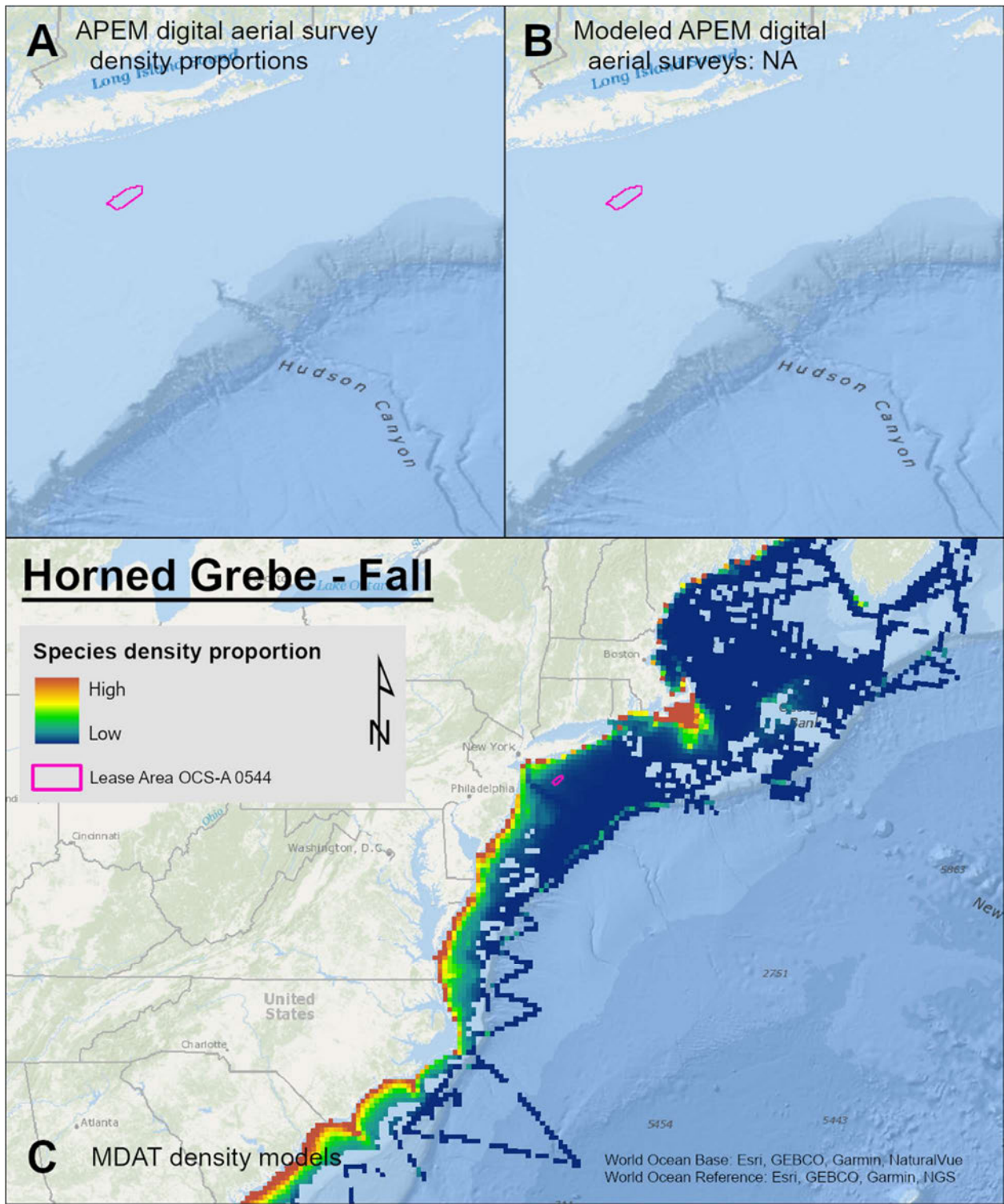
Map 27. Winter Horned Grebe density proportions in the NYSERDA APEM and Empire Wind high resolution digital aerial survey data (A), the NYSERDA APEM and Empire Wind high resolution digital aerial model outputs for grebes in Winter (B) and, Winter Horned Grebe MDAT modeled abundance at the regional scale (C). The scale for all maps is representative of relative spatial variation in the sites within the season for each map input.



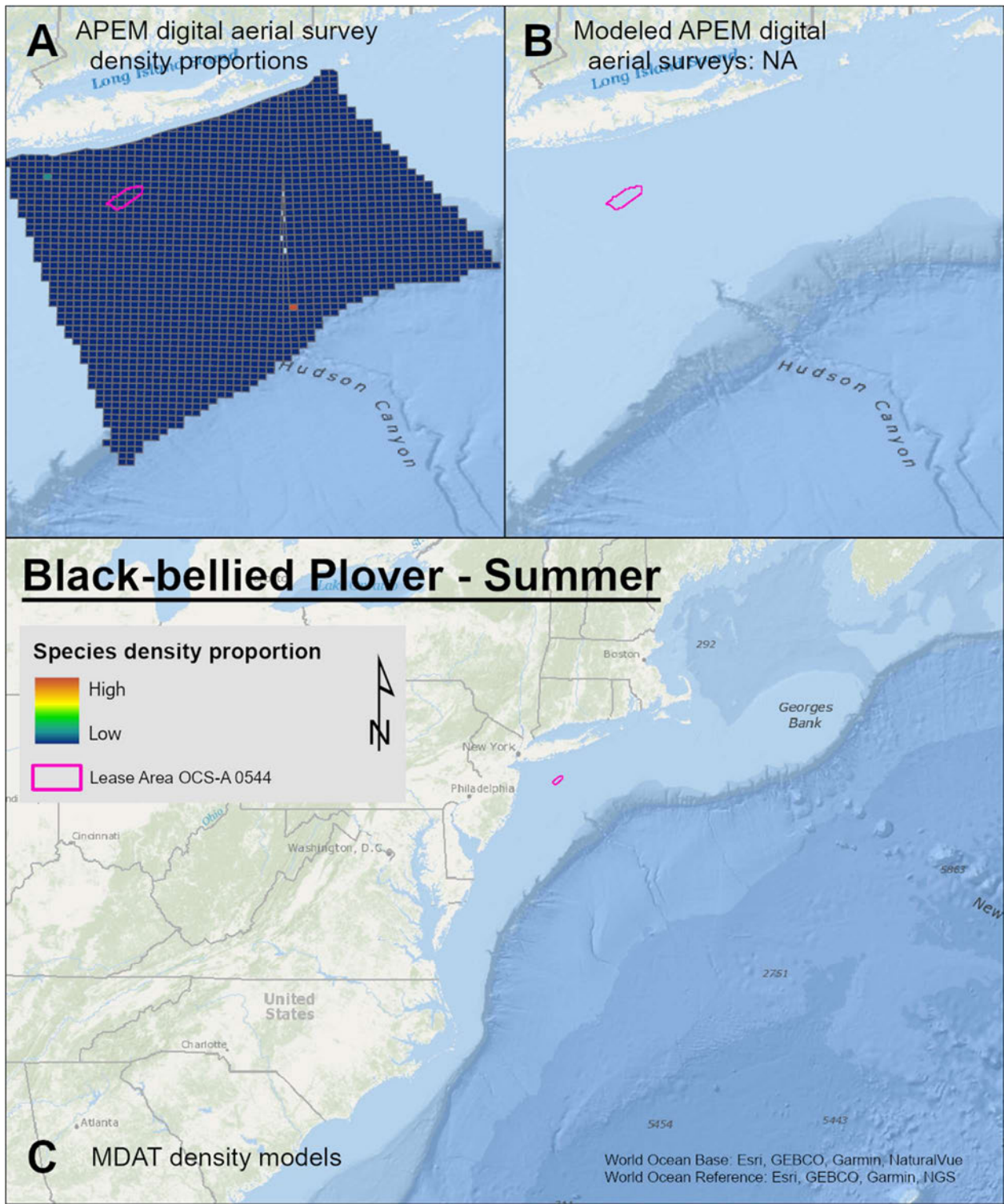
Map 28. Spring Horned Grebe density proportions in the NYSERDA APEM and Empire Wind high resolution digital aerial survey data (A), the NYSERDA APEM and Empire Wind high resolution digital aerial model outputs for grebes in Spring (B) and, Spring Horned Grebe MDAT modeled abundance at the regional scale (C). The scale for all maps is representative of relative spatial variation in the sites within the season for each map input.



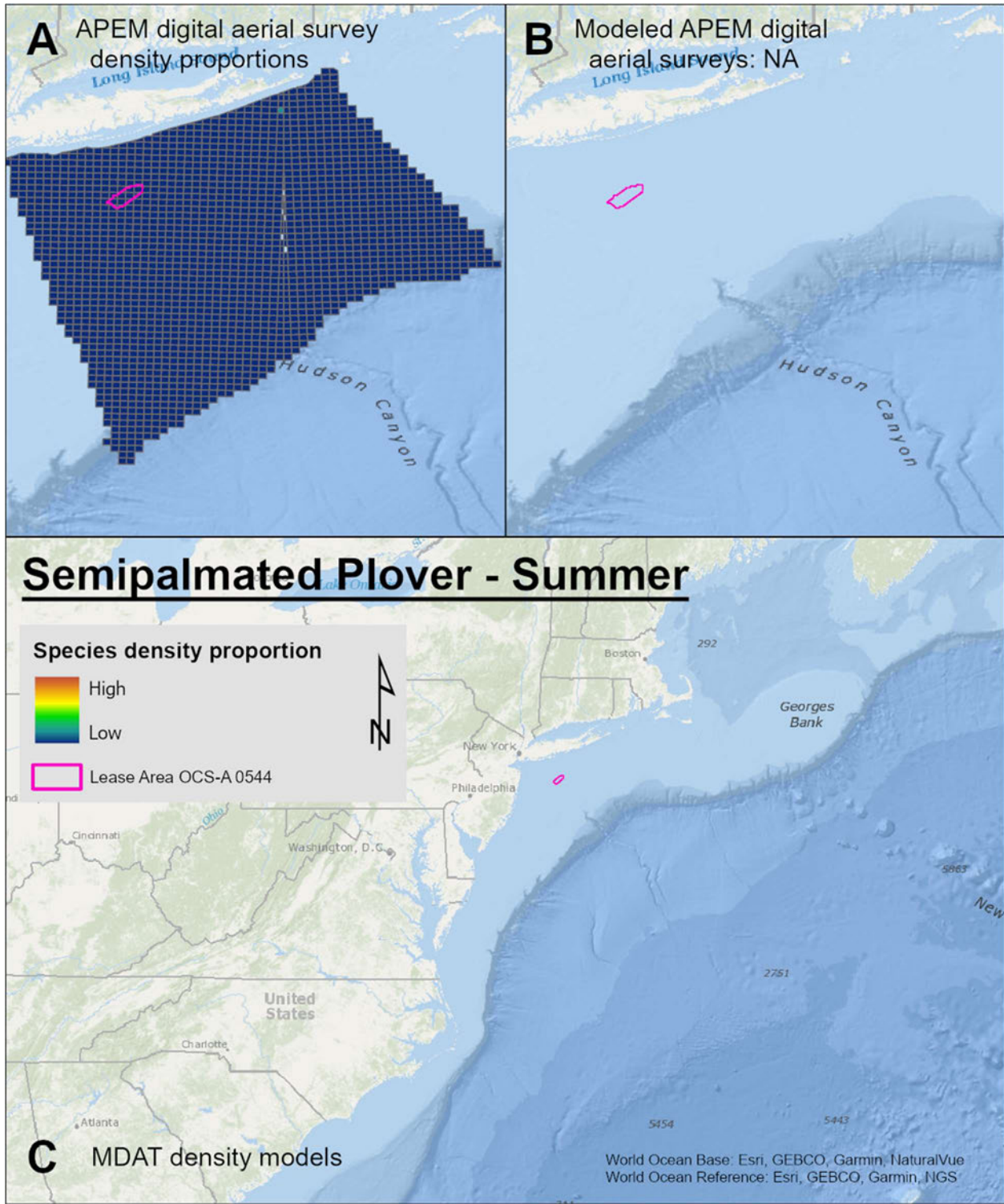
Map 29. Summer Horned Grebe density proportions in the NYSERDA APEM and Empire Wind high resolution digital aerial survey data (A), the NYSERDA APEM and Empire Wind high resolution digital aerial model outputs for grebes in Summer (B) and, Summer Horned Grebe MDAT modeled abundance at the regional scale (C). The scale for all maps is representative of relative spatial variation in the sites within the season for each map input.



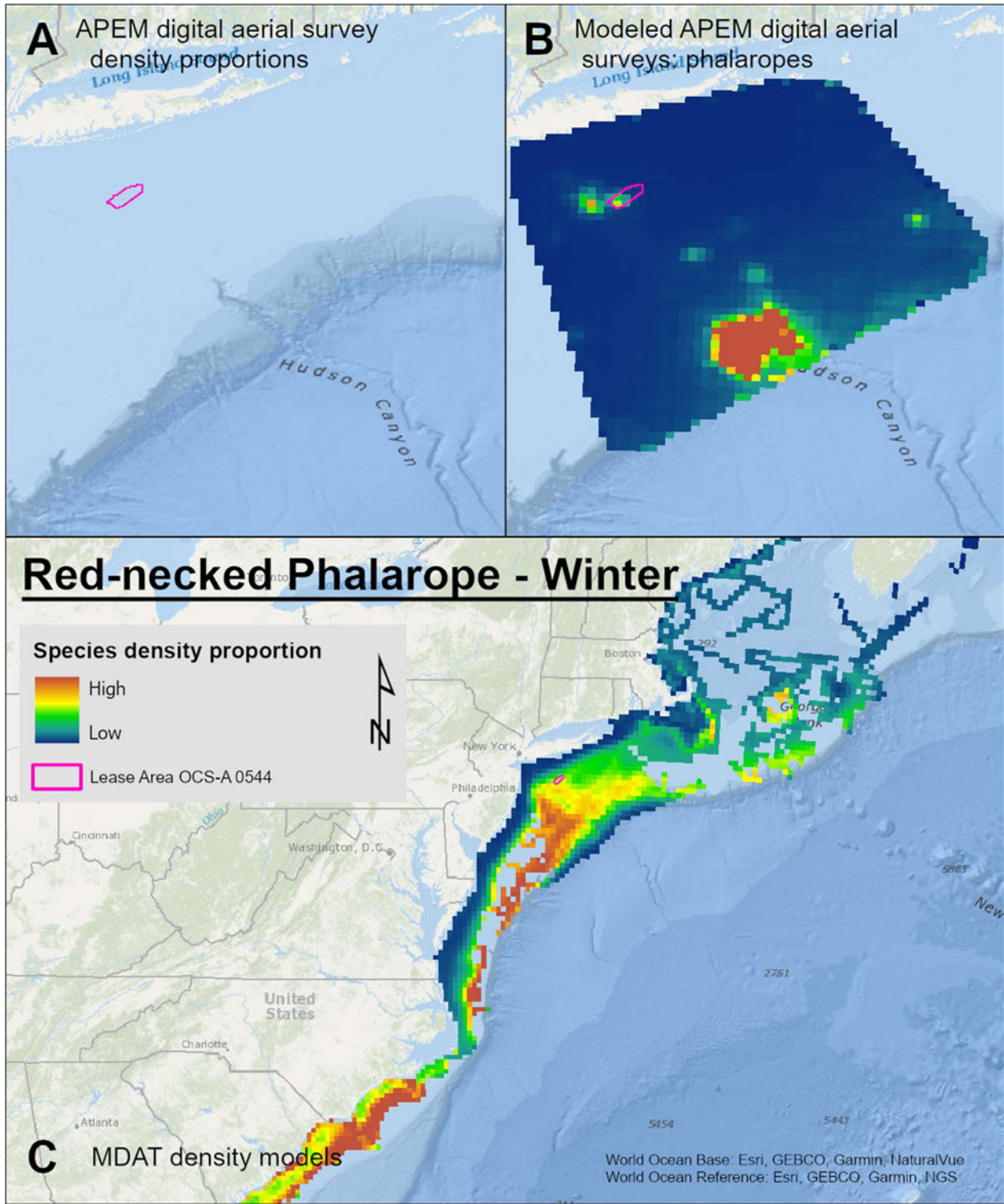
Map 30. Fall Horned Grebe density proportions in the NYSERDA APEM and Empire Wind high resolution digital aerial survey data (A), the NYSERDA APEM and Empire Wind high resolution digital aerial model outputs for grebes in Fall (B) and, Fall Horned Grebe MDAT modeled abundance at the regional scale (C). The scale for all maps is representative of relative spatial variation in the sites within the season for each map input.



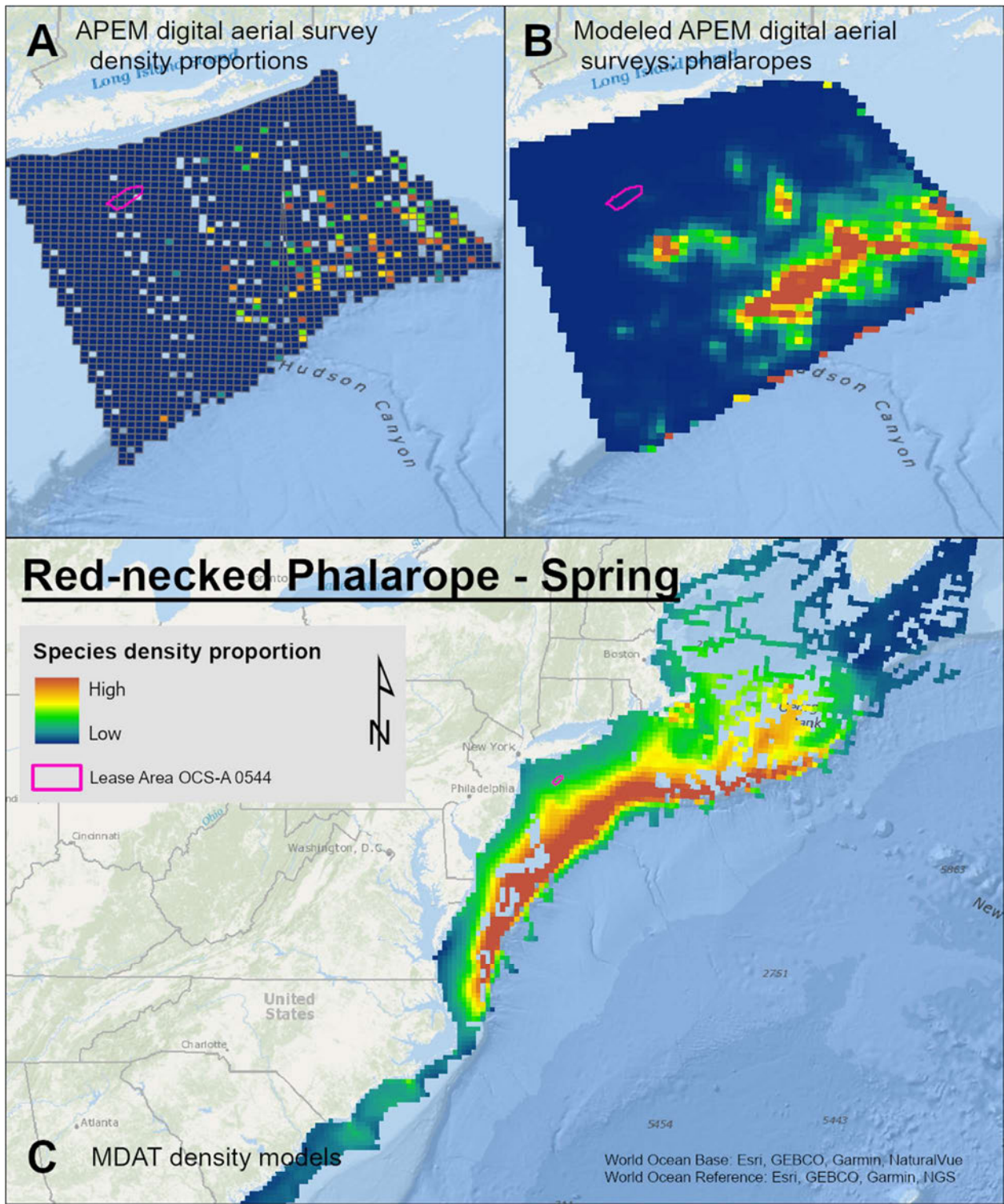
Map 31. Summer Black-bellied Plover density proportions in the NYSERDA APEM and Empire Wind high resolution digital aerial survey data (A), the NYSERDA APEM and Empire Wind high resolution digital aerial model outputs for shorebirds in Summer (B) and, Summer Black-bellied Plover MDAT modeled abundance at the regional scale (C). The scale for all maps is representative of relative spatial variation in the sites within the season for each map input.



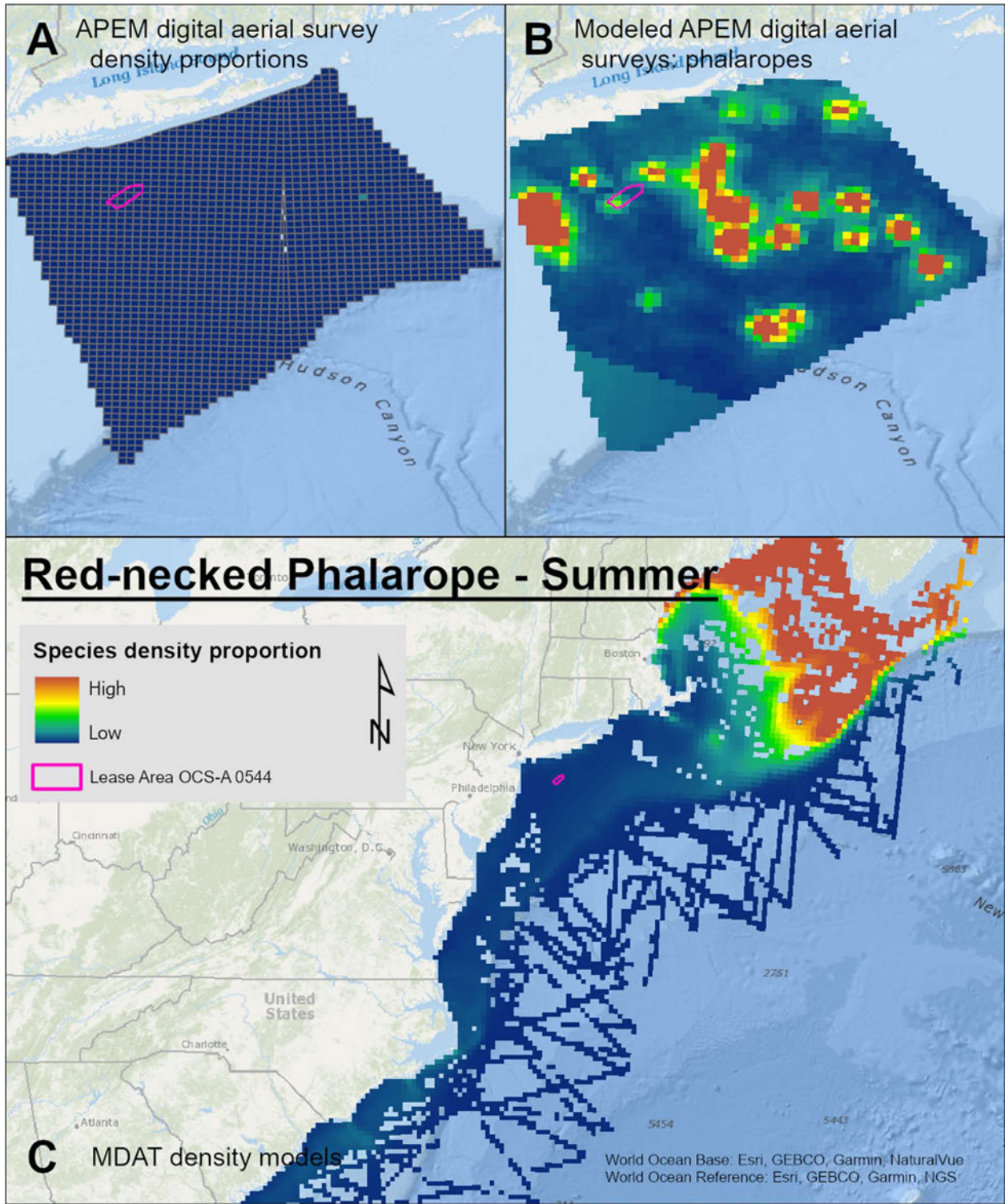
Map 32. Summer Semipalmated Plover density proportions in the NYSERDA APEM and Empire Wind high resolution digital aerial survey data (A), the NYSERDA APEM and Empire Wind high resolution digital aerial model outputs for shorebirds in Summer (B) and, Summer Semipalmated Plover MDAT modeled abundance at the regional scale (C). The scale for all maps is representative of relative spatial variation in the sites within the season for each map input.



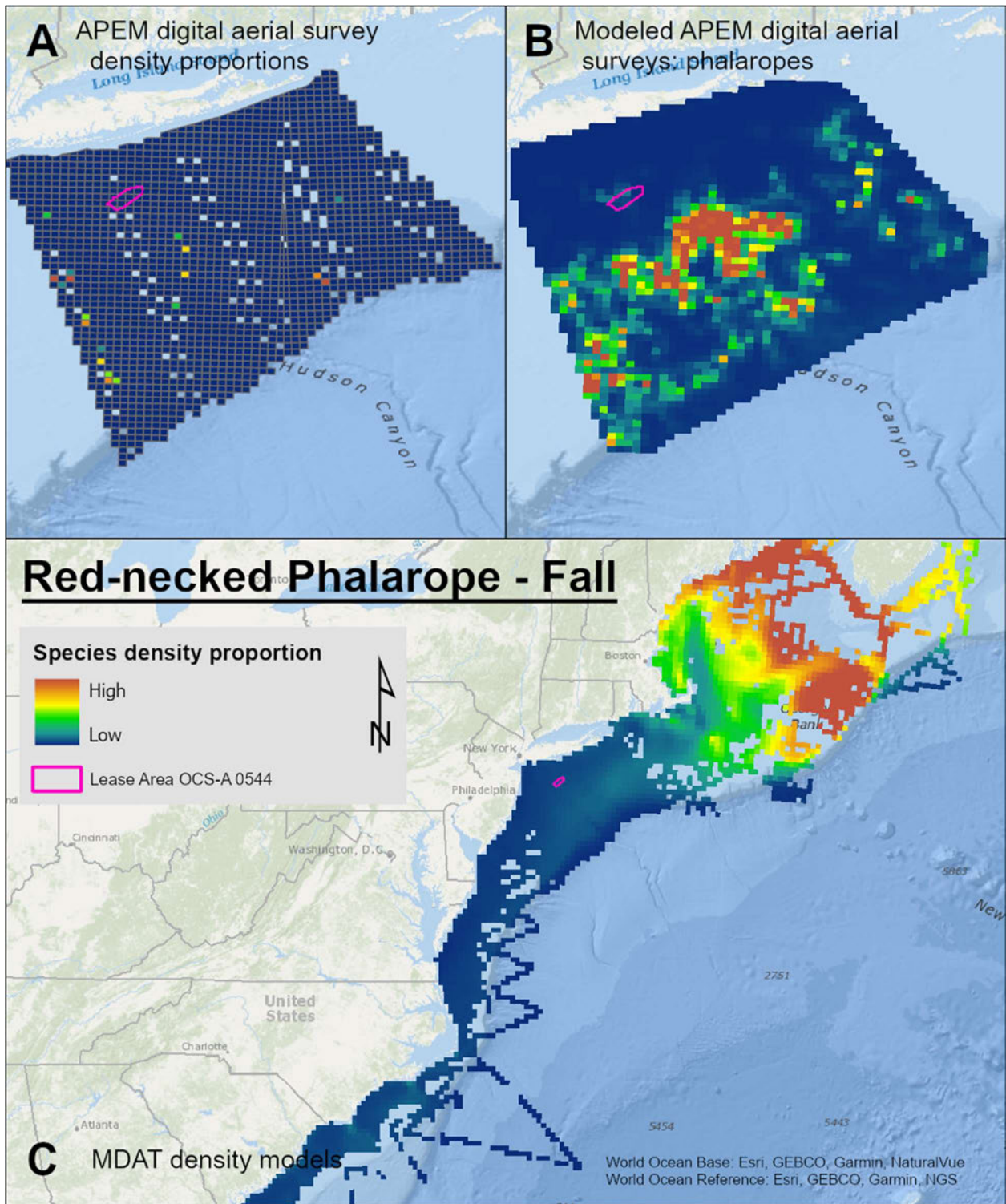
Map 33. Winter Red-necked Phalarope density proportions in the NYSERDA APEM and Empire Wind high resolution digital aerial survey data (A), the NYSERDA APEM and Empire Wind high resolution digital aerial model outputs for phalaropes in Winter (B) and, Winter Red-necked Phalarope MDAT modeled abundance at the regional scale (C). The scale for all maps is representative of relative spatial variation in the sites within the season for each map input.



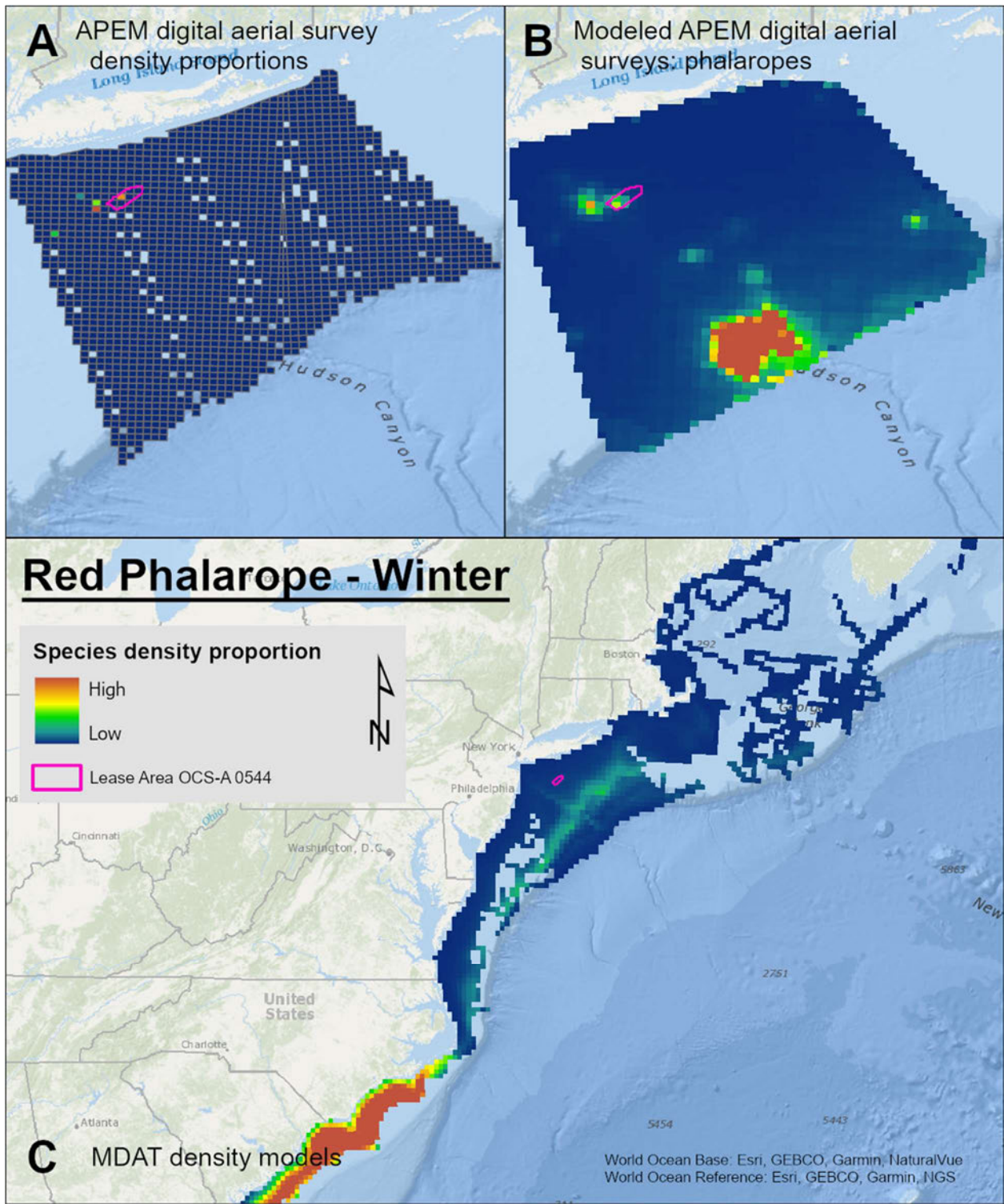
Map 34. Spring Red-necked Phalarope density proportions in the NYSERDA APEM and Empire Wind high resolution digital aerial survey data (A), the NYSERDA APEM and Empire Wind high resolution digital aerial model outputs for phalaropes in Spring (B) and, Spring Red-necked Phalarope MDAT modeled abundance at the regional scale (C). The scale for all maps is representative of relative spatial variation in the sites within the season for each map input.



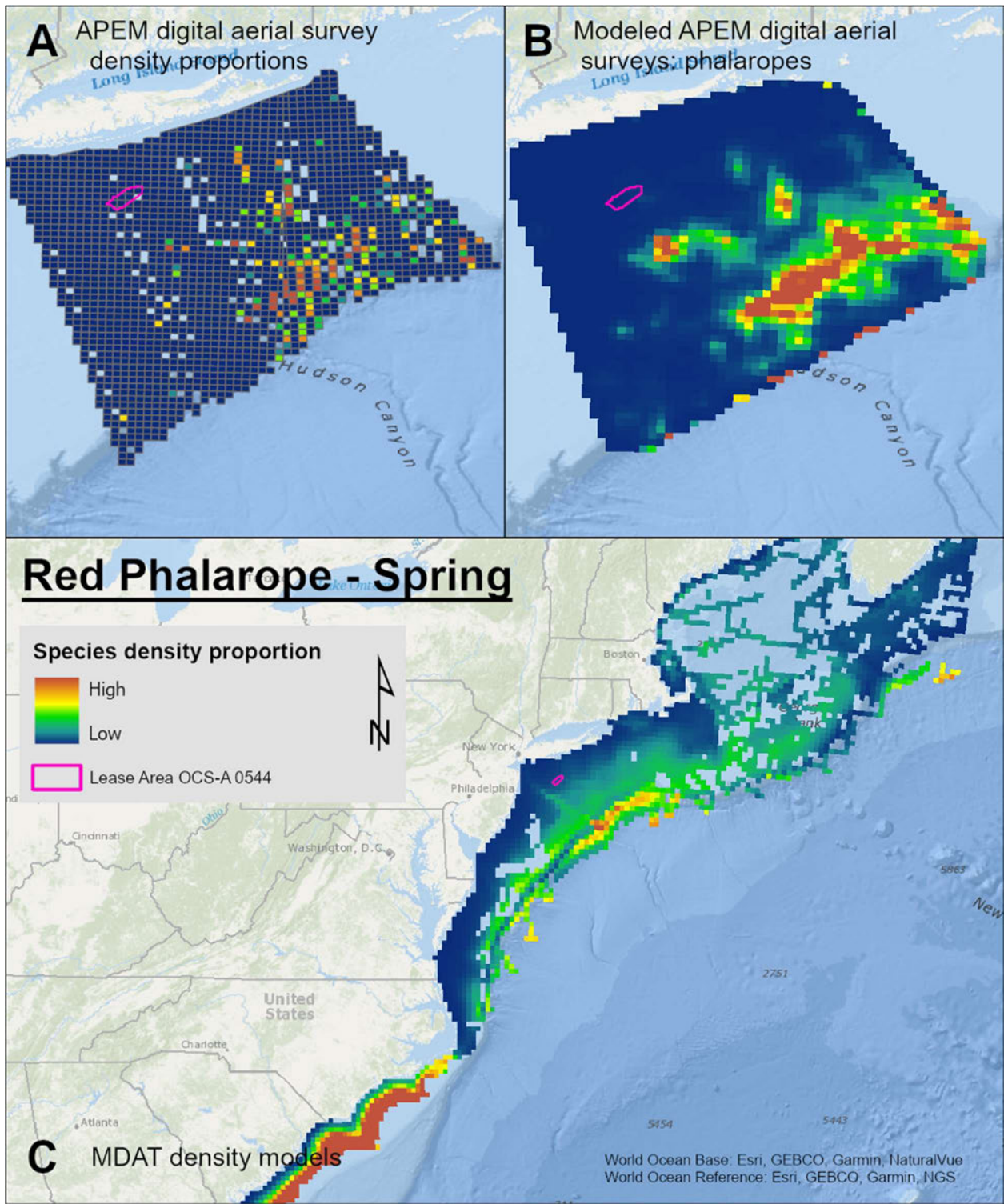
Map 35. Summer Red-necked Phalarope density proportions in the NYSERDA APEM and Empire Wind high resolution digital aerial survey data (A), the NYSERDA APEM and Empire Wind high resolution digital aerial model outputs for phalaropes in Summer (B) and, Summer Red-necked Phalarope MDAT modeled abundance at the regional scale (C). The scale for all maps is representative of relative spatial variation in the sites within the season for each map input.



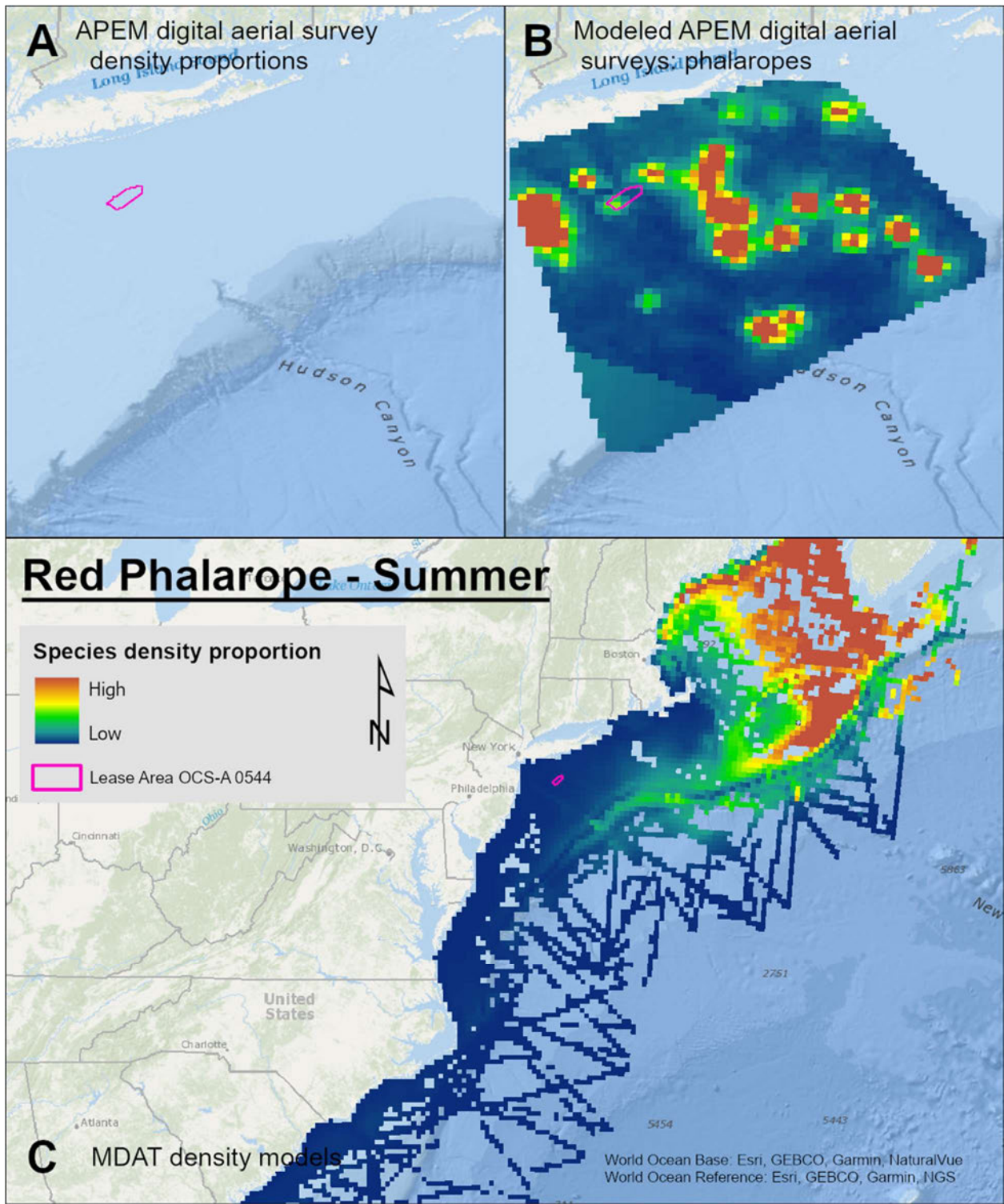
Map 36. Fall Red-necked Phalarope density proportions in the NYSERDA APEM and Empire Wind high resolution digital aerial survey data (A), the NYSERDA APEM and Empire Wind high resolution digital aerial model outputs for phalaropes in Fall (B) and, Fall Red-necked Phalarope MDAT modeled abundance at the regional scale (C). The scale for all maps is representative of relative spatial variation in the sites within the season for each map input.



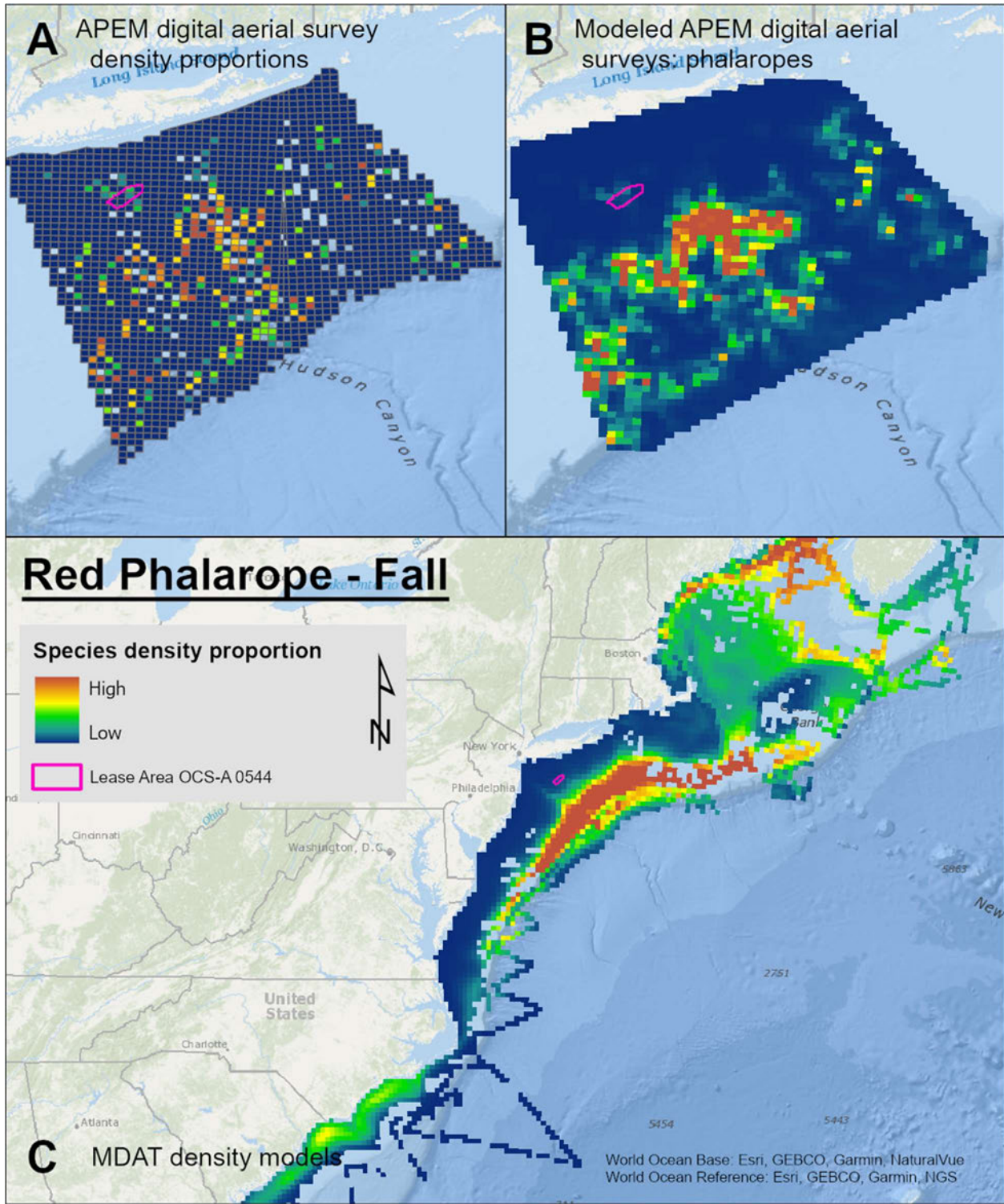
Map 37. Winter Red Phalarope density proportions in the NYSERDA APEM and Empire Wind high resolution digital aerial survey data (A), the NYSERDA APEM and Empire Wind high resolution digital aerial model outputs for phalaropes in Winter (B) and, Winter Red Phalarope MDAT modeled abundance at the regional scale (C). The scale for all maps is representative of relative spatial variation in the sites within the season for each map input.



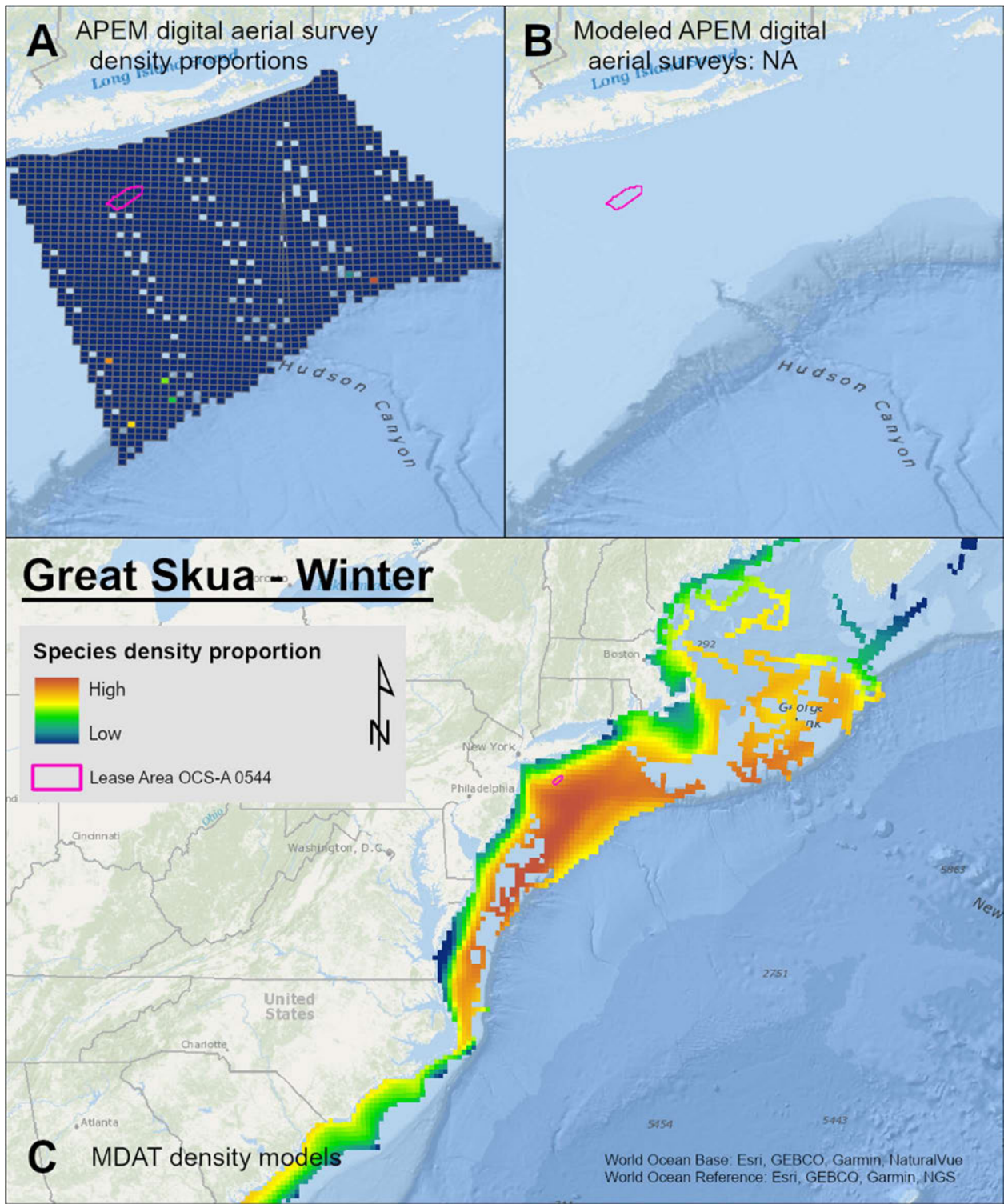
Map 38. Spring Red Phalarope density proportions in the NYSERDA APEM and Empire Wind high resolution digital aerial survey data (A), the NYSERDA APEM and Empire Wind high resolution digital aerial model outputs for phalaropes in Spring (B) and, Spring Red Phalarope MDAT modeled abundance at the regional scale (C). The scale for all maps is representative of relative spatial variation in the sites within the season for each map input.



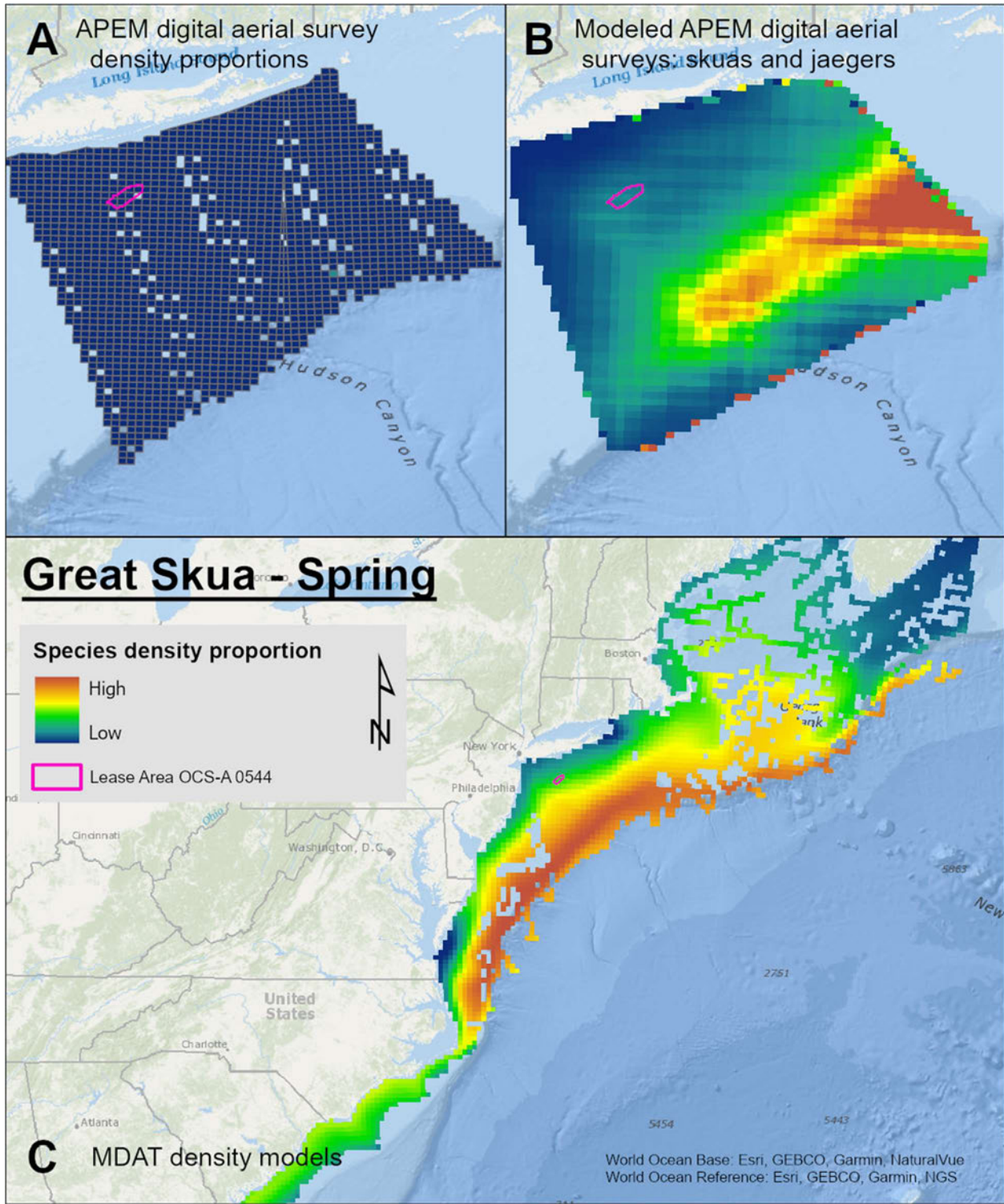
Map 39. Summer Red Phalarope density proportions in the NYSERDA APEM and Empire Wind high resolution digital aerial survey data (A), the NYSERDA APEM and Empire Wind high resolution digital aerial model outputs for phalaropes in Summer (B) and, Summer Red Phalarope MDAT modeled abundance at the regional scale (C). The scale for all maps is representative of relative spatial variation in the sites within the season for each map input.



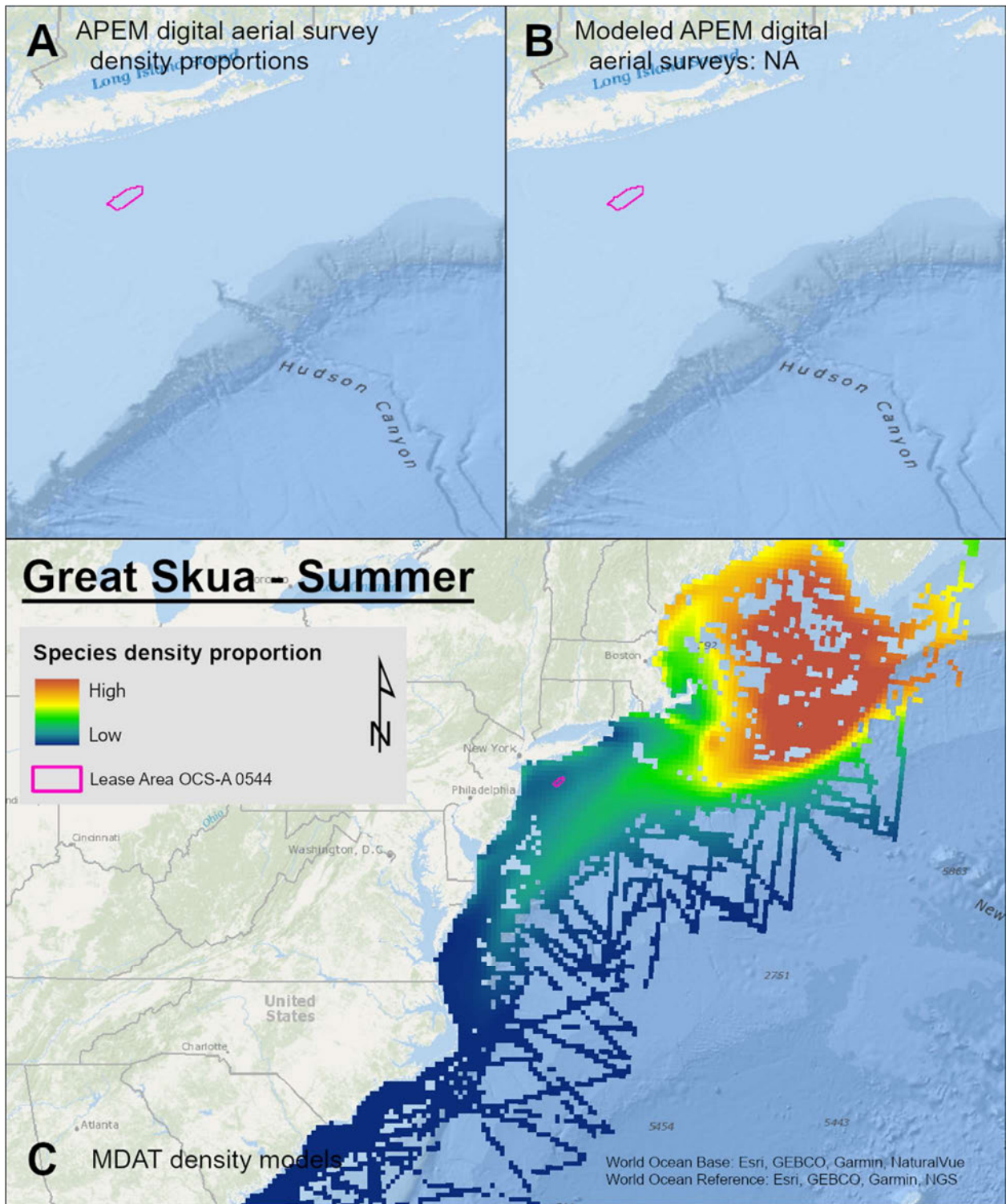
Map 40. Fall Red Phalarope density proportions in the NYSERDA APEM and Empire Wind high resolution digital aerial survey data (A), the NYSERDA APEM and Empire Wind high resolution digital aerial model outputs for phalaropes in Fall (B) and, Fall Red Phalarope MDAT modeled abundance at the regional scale (C). The scale for all maps is representative of relative spatial variation in the sites within the season for each map input.



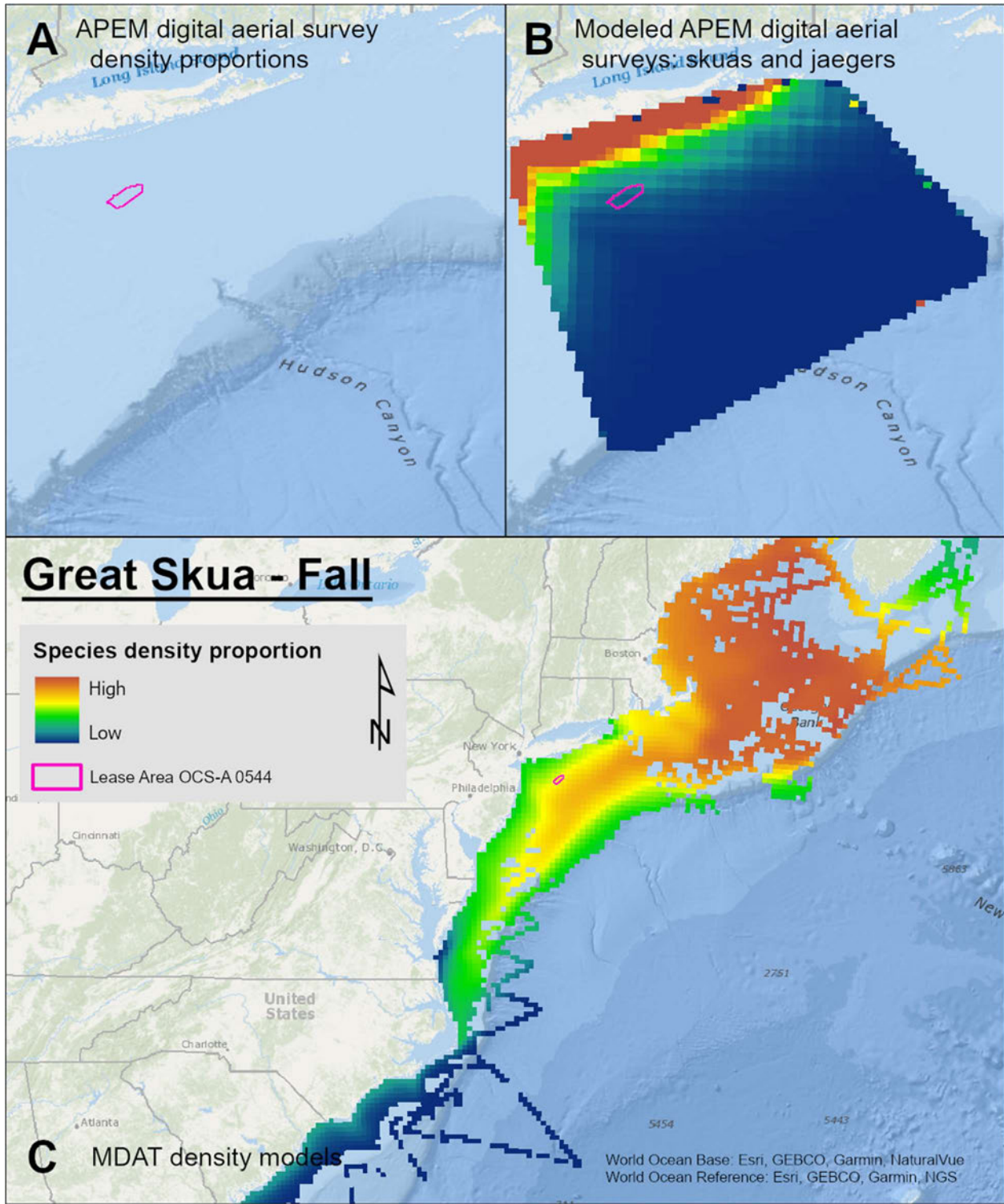
Map 41. Winter Great Skua density proportions in the NYSERDA APEM and Empire Wind high resolution digital aerial survey data (A), the NYSERDA APEM and Empire Wind high resolution digital aerial model outputs for skuas and jaegers in Winter (B) and, Winter Great Skua MDAT modeled abundance at the regional scale (C). The scale for all maps is representative of relative spatial variation in the sites within the season for each map input.



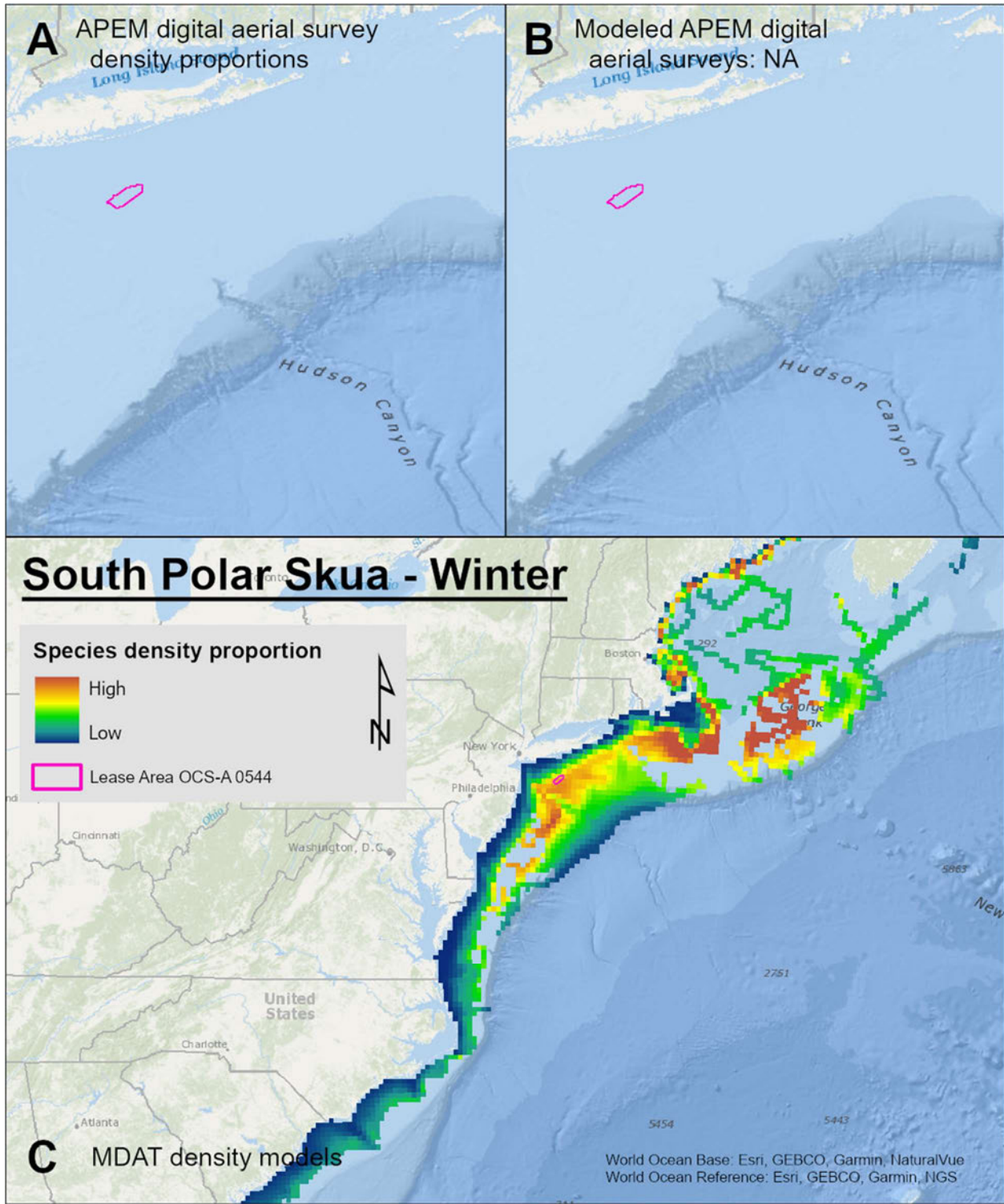
Map 42. Spring Great Skua density proportions in the NYSERDA APEM and Empire Wind high resolution digital aerial survey data (A), the NYSERDA APEM and Empire Wind high resolution digital aerial model outputs for skuas and jaegers in Spring (B) and, Spring Great Skua MDAT modeled abundance at the regional scale (C). The scale for all maps is representative of relative spatial variation in the sites within the season for each map input.



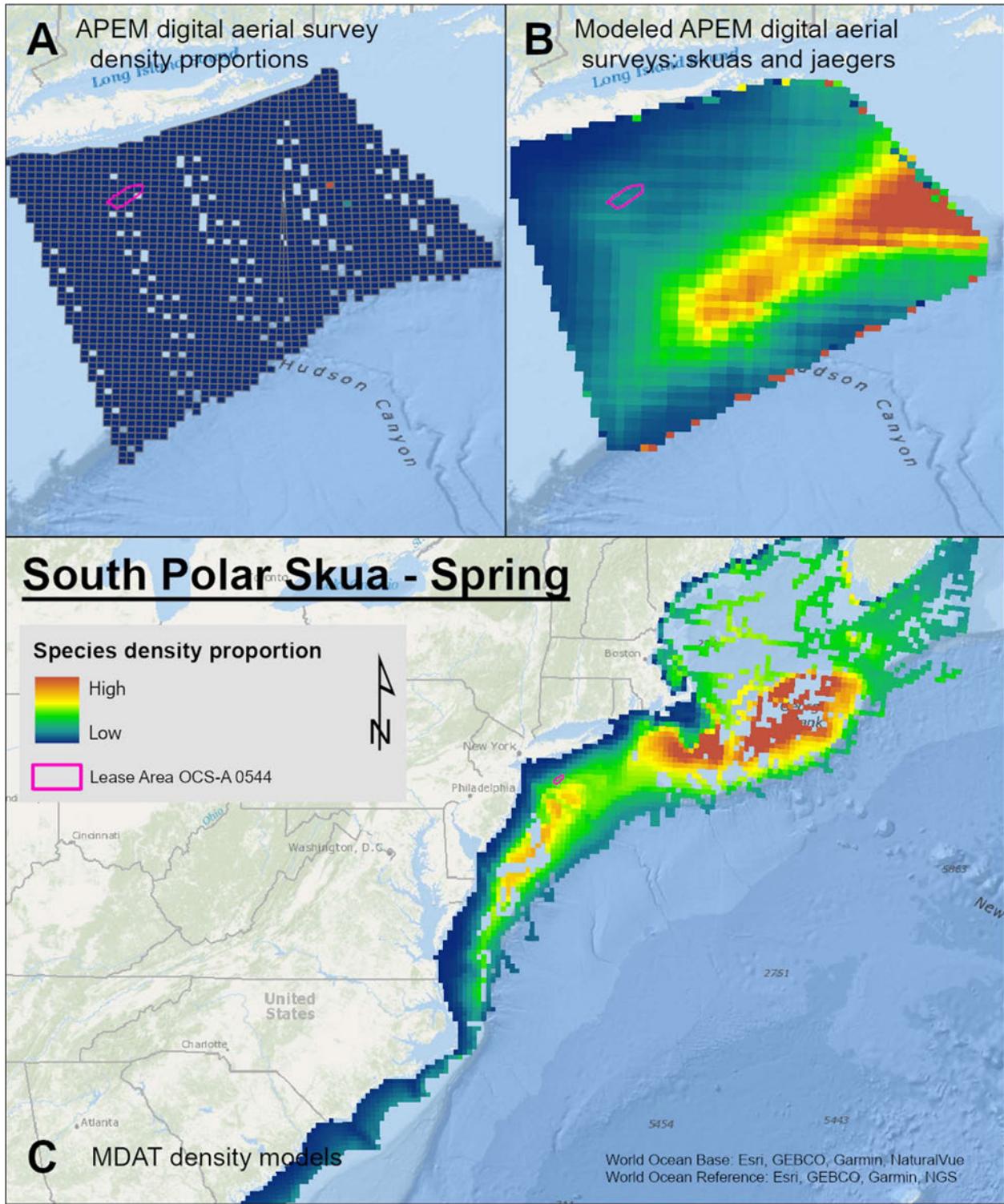
Map 43. Summer Great Skua density proportions in the NYSERDA APEM and Empire Wind high resolution digital aerial survey data (A), the NYSERDA APEM and Empire Wind high resolution digital aerial model outputs for skuas and jaegers in Summer (B) and, Summer Great Skua MDAT modeled abundance at the regional scale (C). The scale for all maps is representative of relative spatial variation in the sites within the season for each map input.



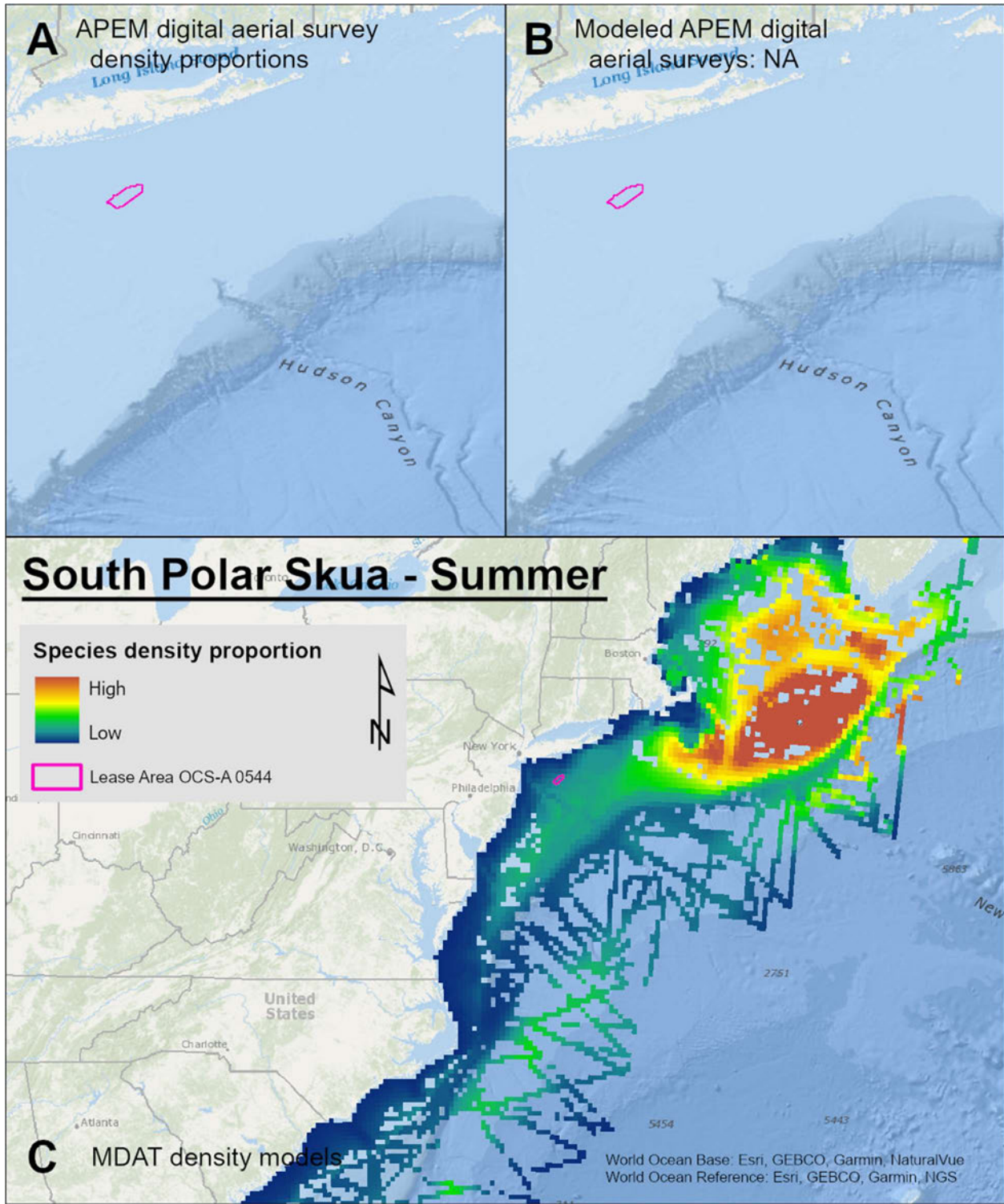
Map 44. Fall Great Skua density proportions in the NYSERDA APEM and Empire Wind high resolution digital aerial survey data (A), the NYSERDA APEM and Empire Wind high resolution digital aerial model outputs for skuas and jaegers in Fall (B) and, Fall Great Skua MDAT modeled abundance at the regional scale (C). The scale for all maps is representative of relative spatial variation in the sites within the season for each map input.



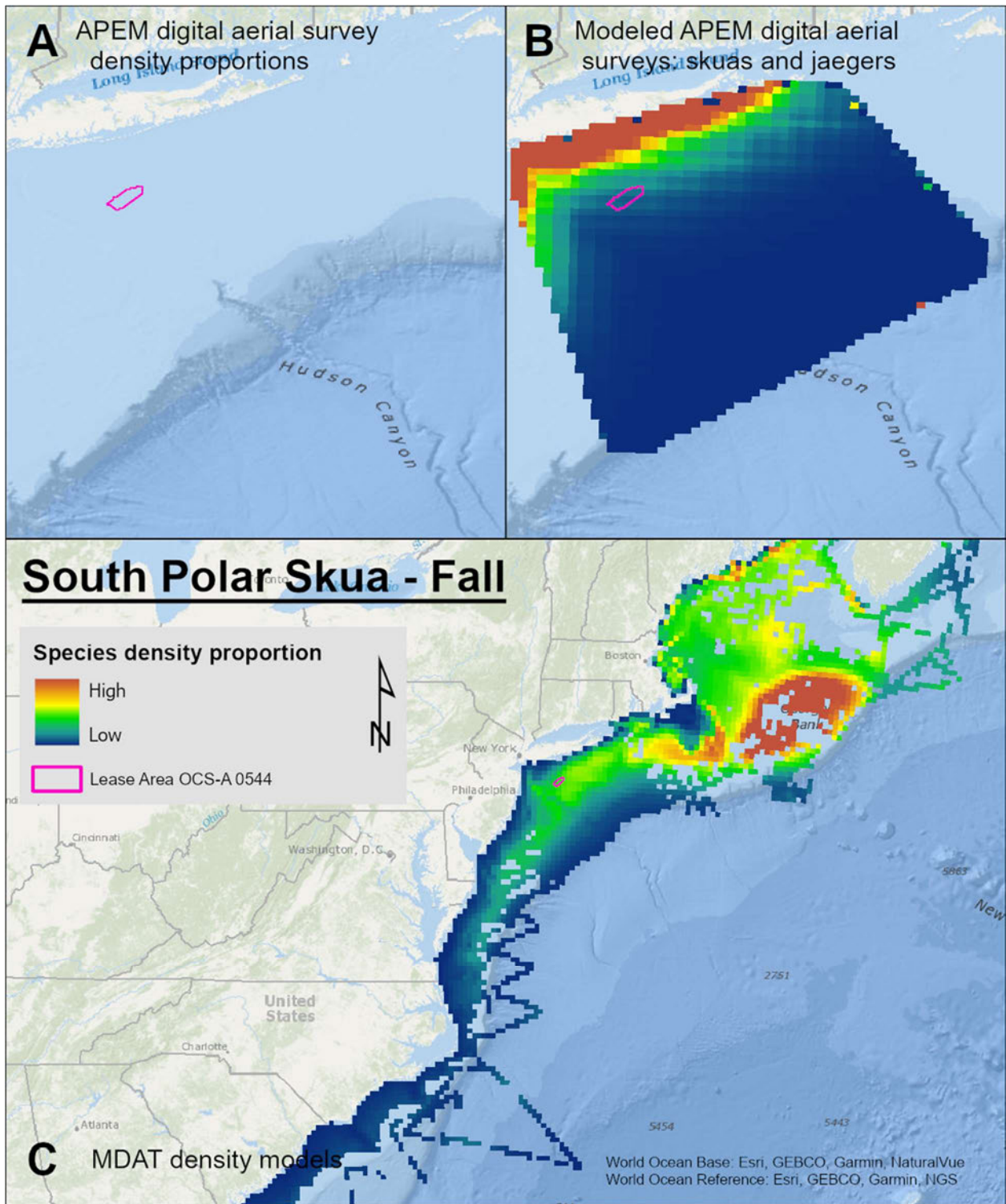
Map 45. Winter South Polar Skua density proportions in the NYSERDA APEM and Empire Wind high resolution digital aerial survey data (A), the NYSERDA APEM and Empire Wind high resolution digital aerial model outputs for skuas and jaegers in Winter (B) and, Winter South Polar Skua MDAT modeled abundance at the regional scale (C). The scale for all maps is representative of relative spatial variation in the sites within the season for each map input.



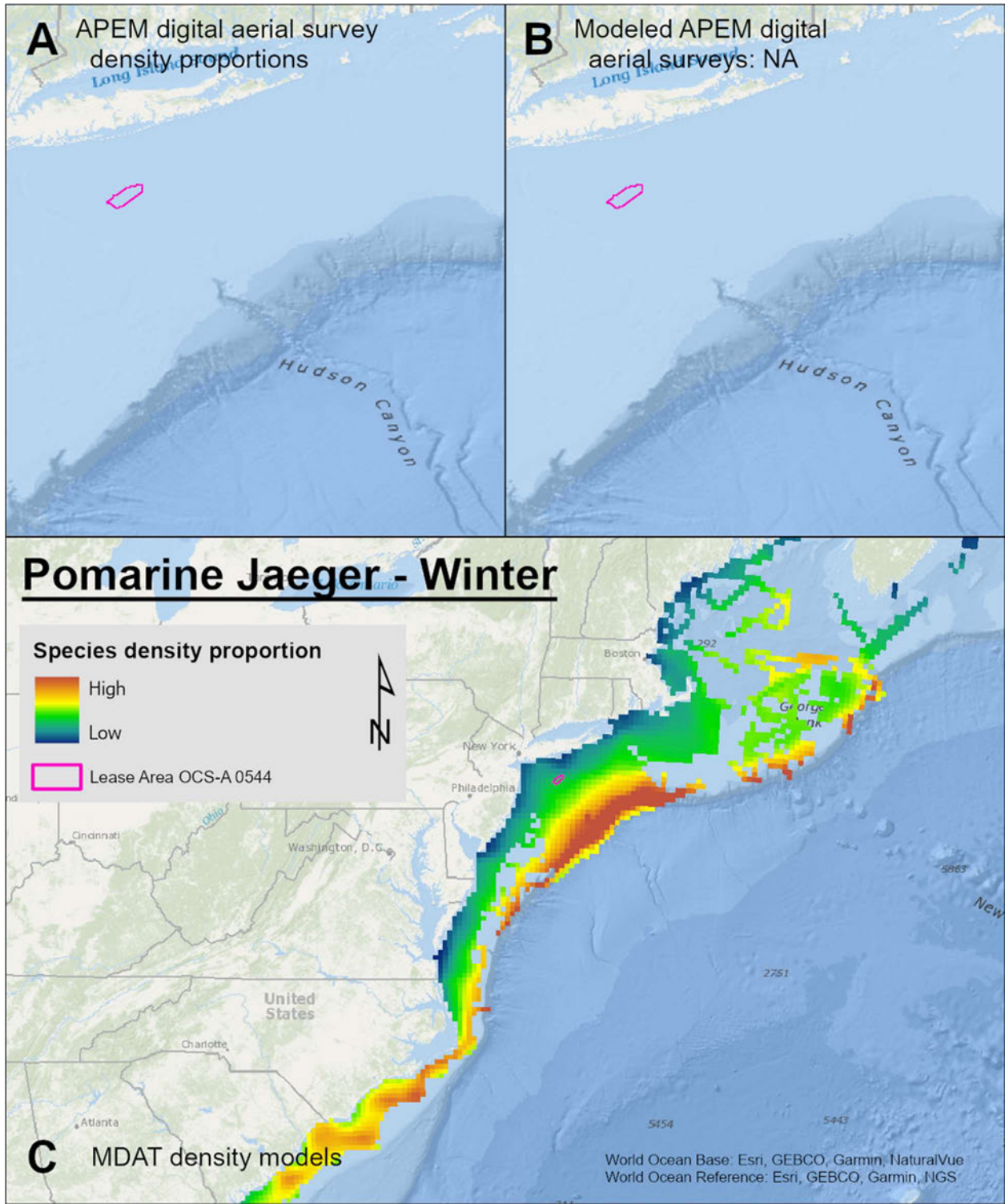
Map 46. Spring South Polar Skua density proportions in the NYSERDA APEM and Empire Wind high resolution digital aerial survey data (A), the NYSERDA APEM and Empire Wind high resolution digital aerial model outputs for skuas and jaegers in Spring (B) and, Spring South Polar Skua MDAT modeled abundance at the regional scale (C). The scale for all maps is representative of relative spatial variation in the sites within the season for each map input.



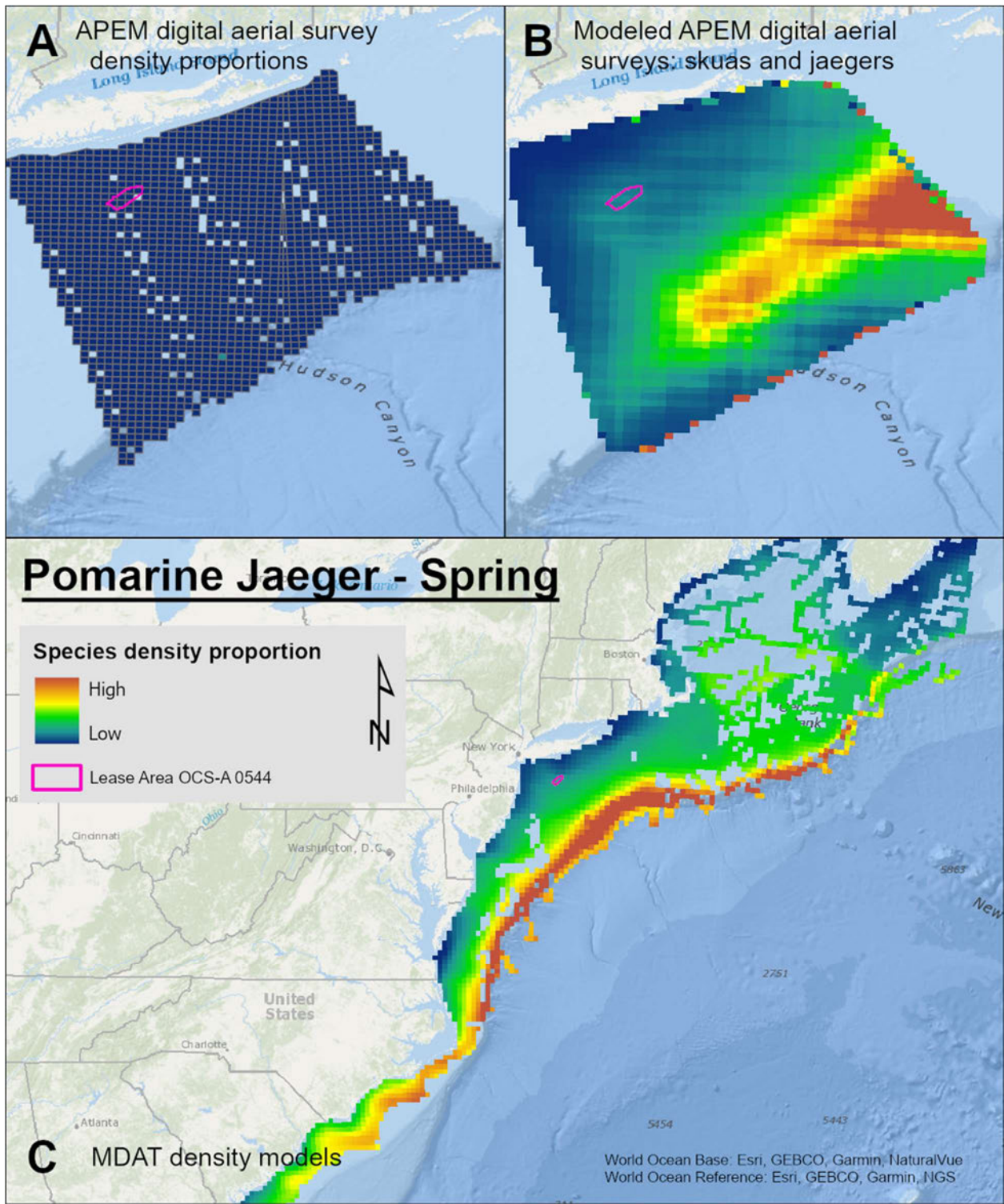
Map 47. Summer South Polar Skua density proportions in the NYSERDA APEM and Empire Wind high resolution digital aerial survey data (A), the NYSERDA APEM and Empire Wind high resolution digital aerial model outputs for skuas and jaegers in Summer (B) and, Summer South Polar Skua MDAT modeled abundance at the regional scale (C). The scale for all maps is representative of relative spatial variation in the sites within the season for each map input.



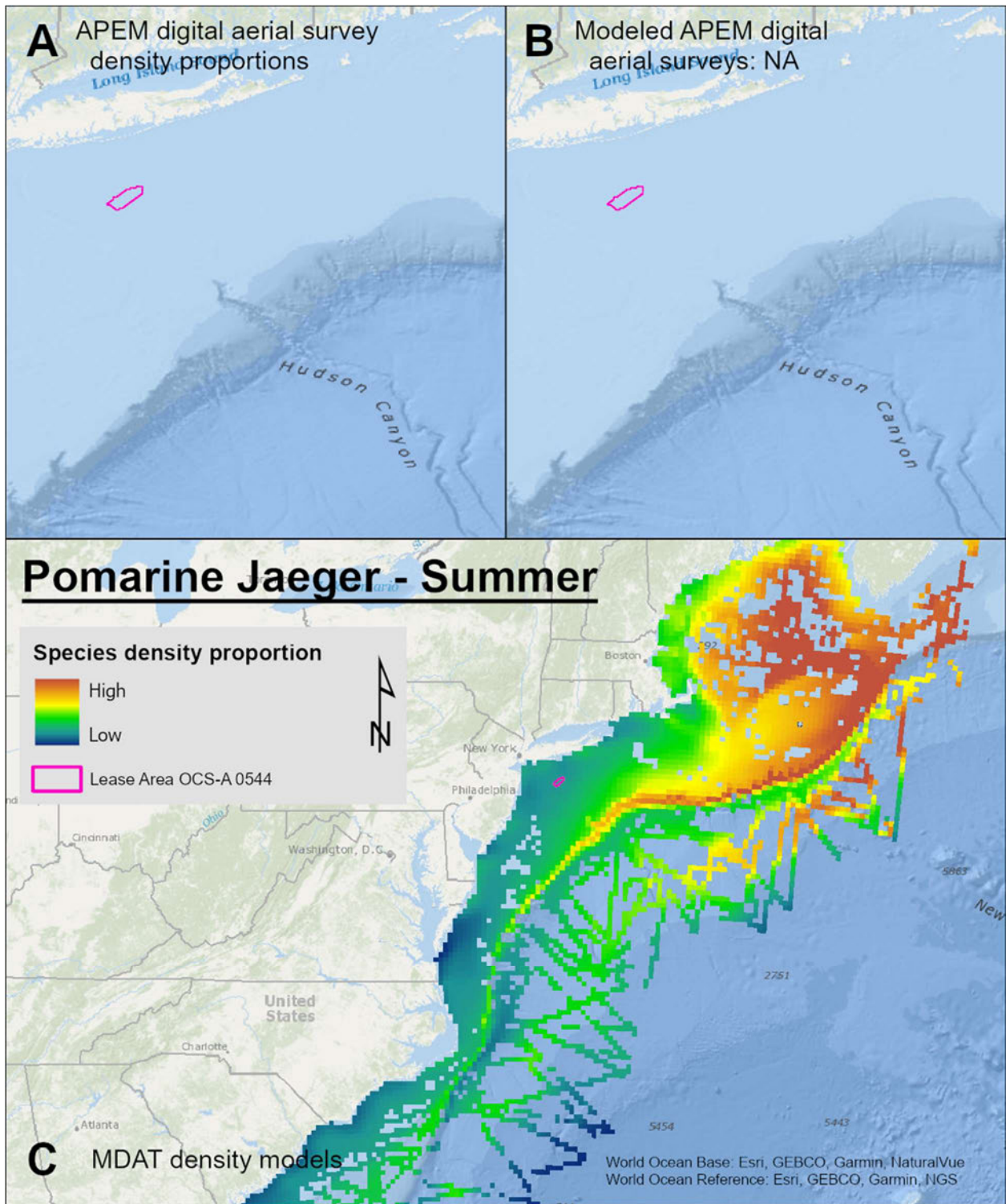
Map 48. Fall South Polar Skua density proportions in the NYSERDA APEM and Empire Wind high resolution digital aerial survey data (A), the NYSERDA APEM and Empire Wind high resolution digital aerial model outputs for skuas and jaegers in Fall (B) and, Fall South Polar Skua MDAT modeled abundance at the regional scale (C). The scale for all maps is representative of relative spatial variation in the sites within the season for each map input.



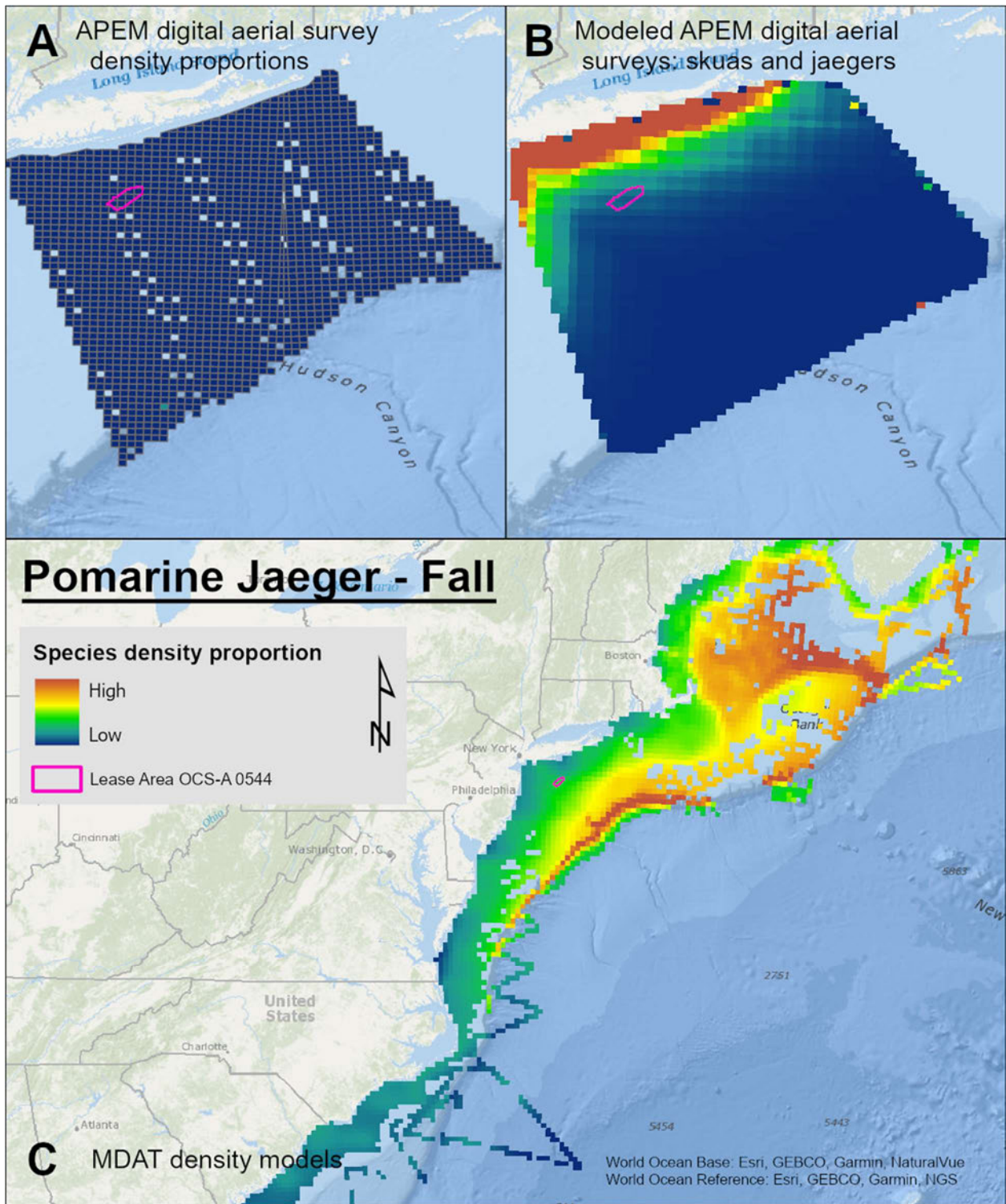
Map 49. Winter Pomarine Jaeger density proportions in the NYSERDA APEM and Empire Wind high resolution digital aerial survey data (A), the NYSERDA APEM and Empire Wind high resolution digital aerial model outputs for skuas and jaegers in Winter (B) and, Winter Pomarine Jaeger MDAT modeled abundance at the regional scale (C). The scale for all maps is representative of relative spatial variation in the sites within the season for each map input.



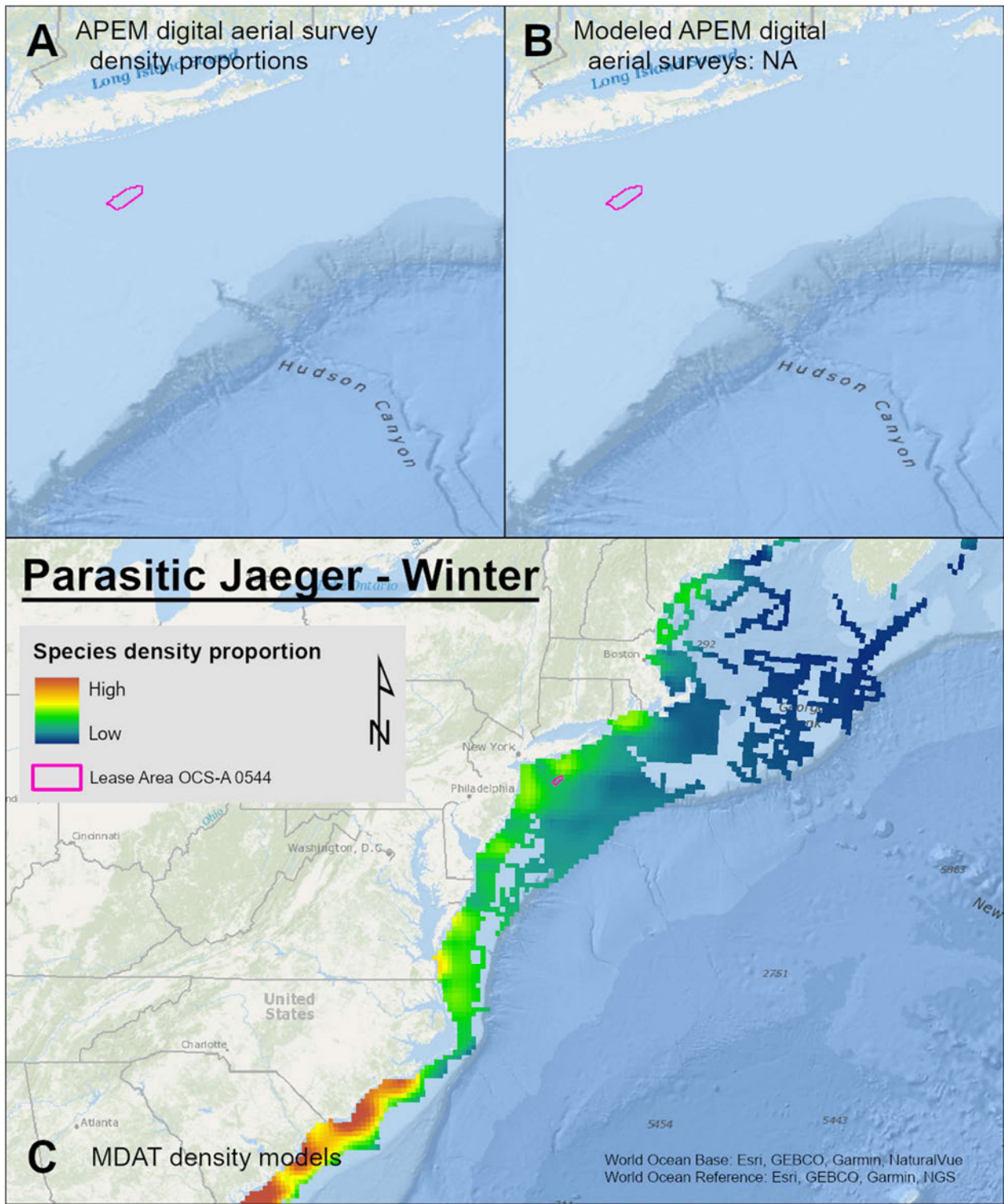
Map 50. Spring Pomarine Jaeger density proportions in the NYSERDA APEM and Empire Wind high resolution digital aerial survey data (A), the NYSERDA APEM and Empire Wind high resolution digital aerial model outputs for skuas and jaegers in Spring (B) and, Spring Pomarine Jaeger MDAT modeled abundance at the regional scale (C). The scale for all maps is representative of relative spatial variation in the sites within the season for each map input.



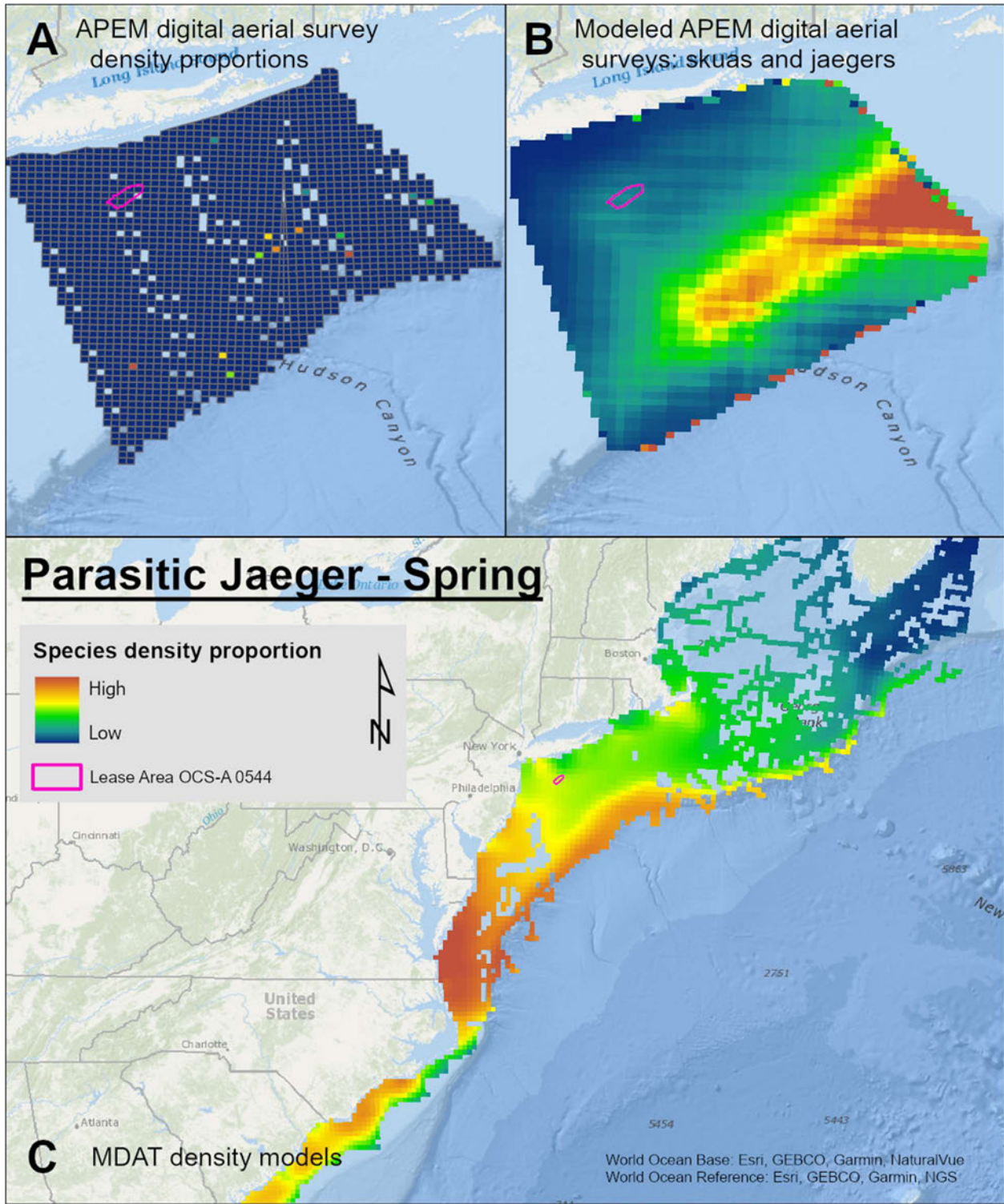
Map 51. Summer Pomarine Jaeger density proportions in the NYSERDA APEM and Empire Wind high resolution digital aerial survey data (A), the NYSERDA APEM and Empire Wind high resolution digital aerial model outputs for skuas and jaegers in Summer (B) and, Summer Pomarine Jaeger MDAT modeled abundance at the regional scale (C). The scale for all maps is representative of relative spatial variation in the sites within the season for each map input.



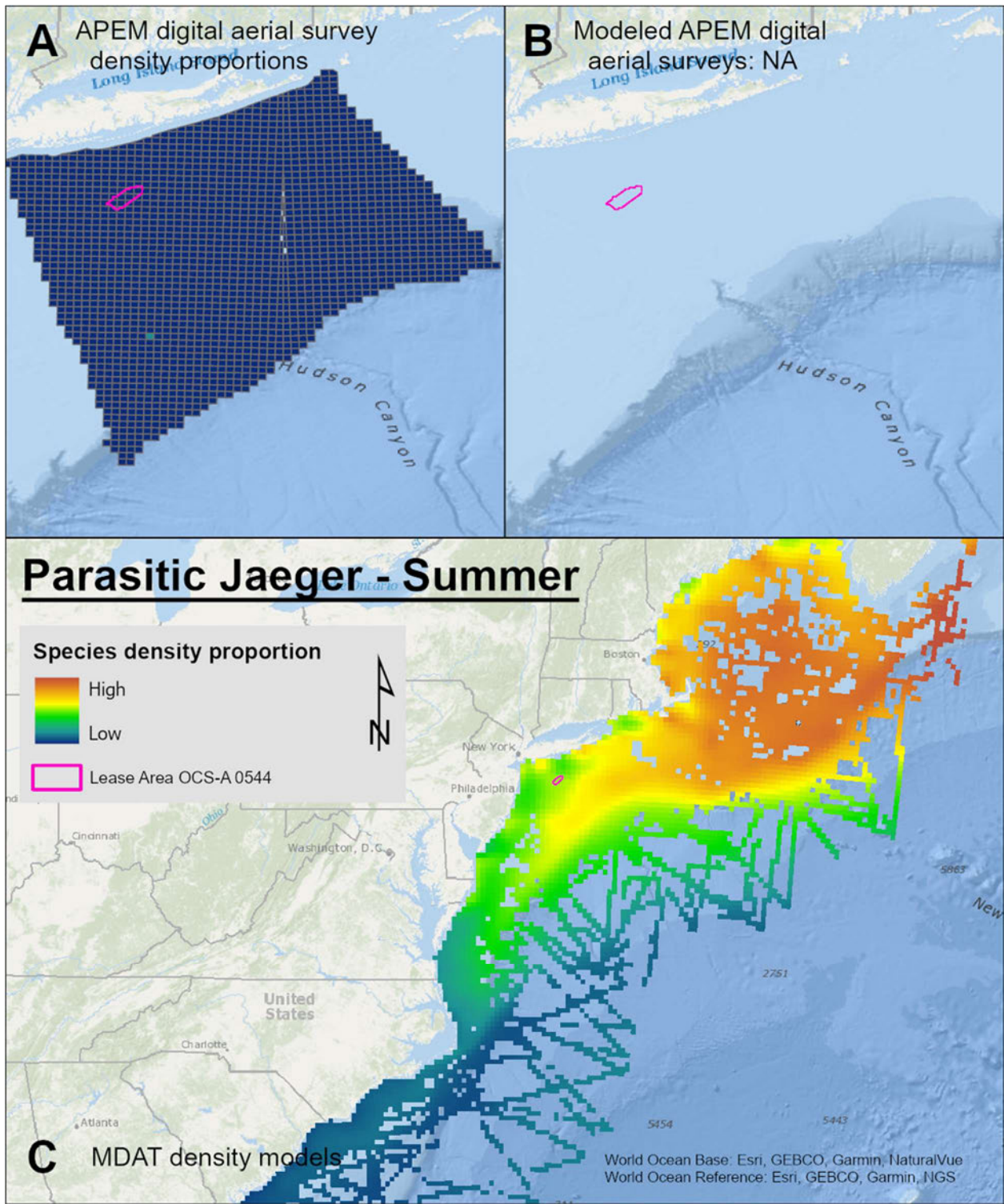
Map 52. Fall Pomarine Jaeger density proportions in the NYSERDA APEM and Empire Wind high resolution digital aerial survey data (A), the NYSERDA APEM and Empire Wind high resolution digital aerial model outputs for skuas and jaegers in Fall (B) and, Fall Pomarine Jaeger MDAT modeled abundance at the regional scale (C). The scale for all maps is representative of relative spatial variation in the sites within the season for each map input.



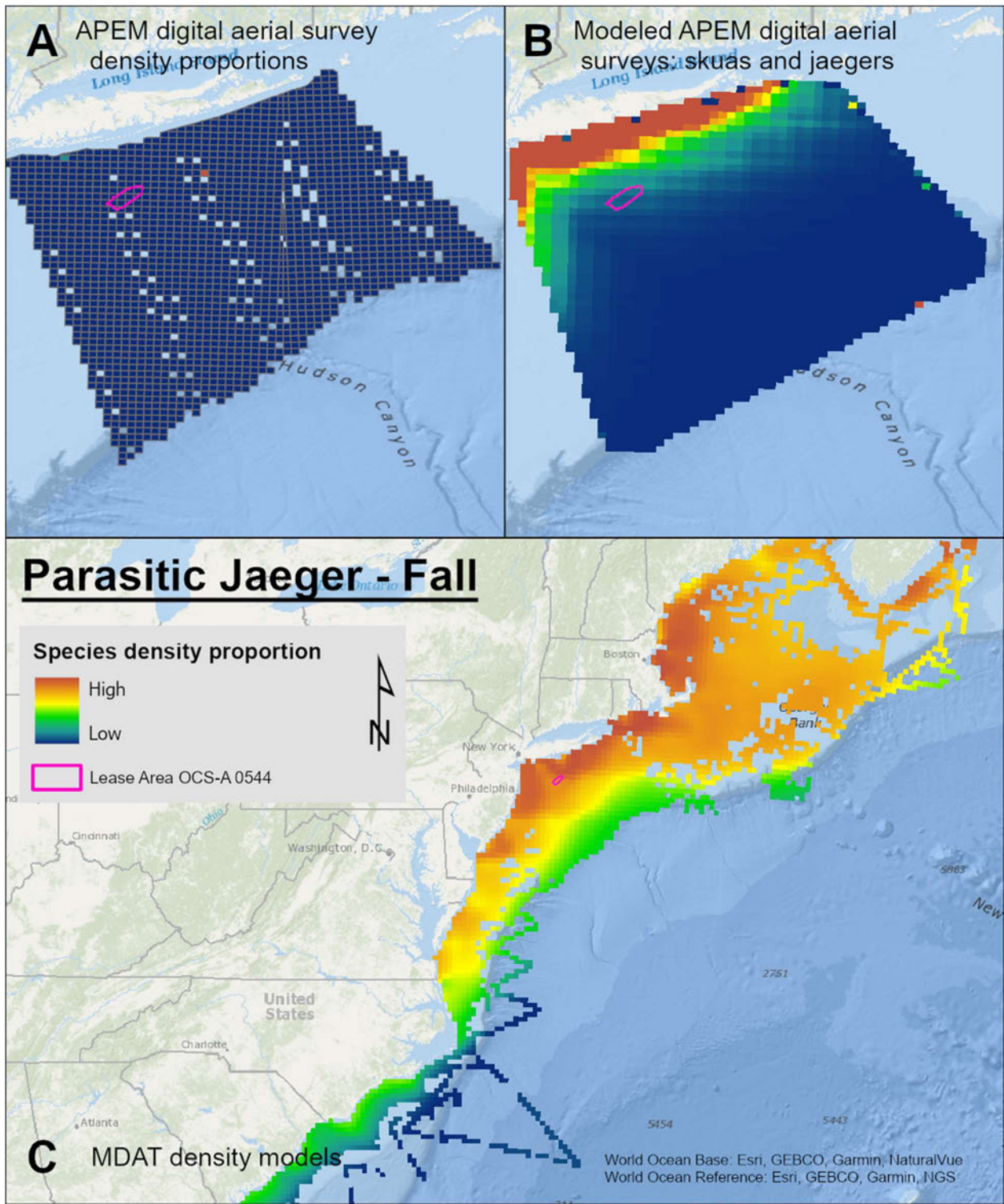
Map 53. Winter Parasitic Jaeger density proportions in the NYSERDA APEM and Empire Wind high resolution digital aerial survey data (A), the NYSERDA APEM and Empire Wind high resolution digital aerial model outputs for skuas and jaegers in Winter (B) and, Winter Parasitic Jaeger MDAT modeled abundance at the regional scale (C). The scale for all maps is representative of relative spatial variation in the sites within the season for each map input.



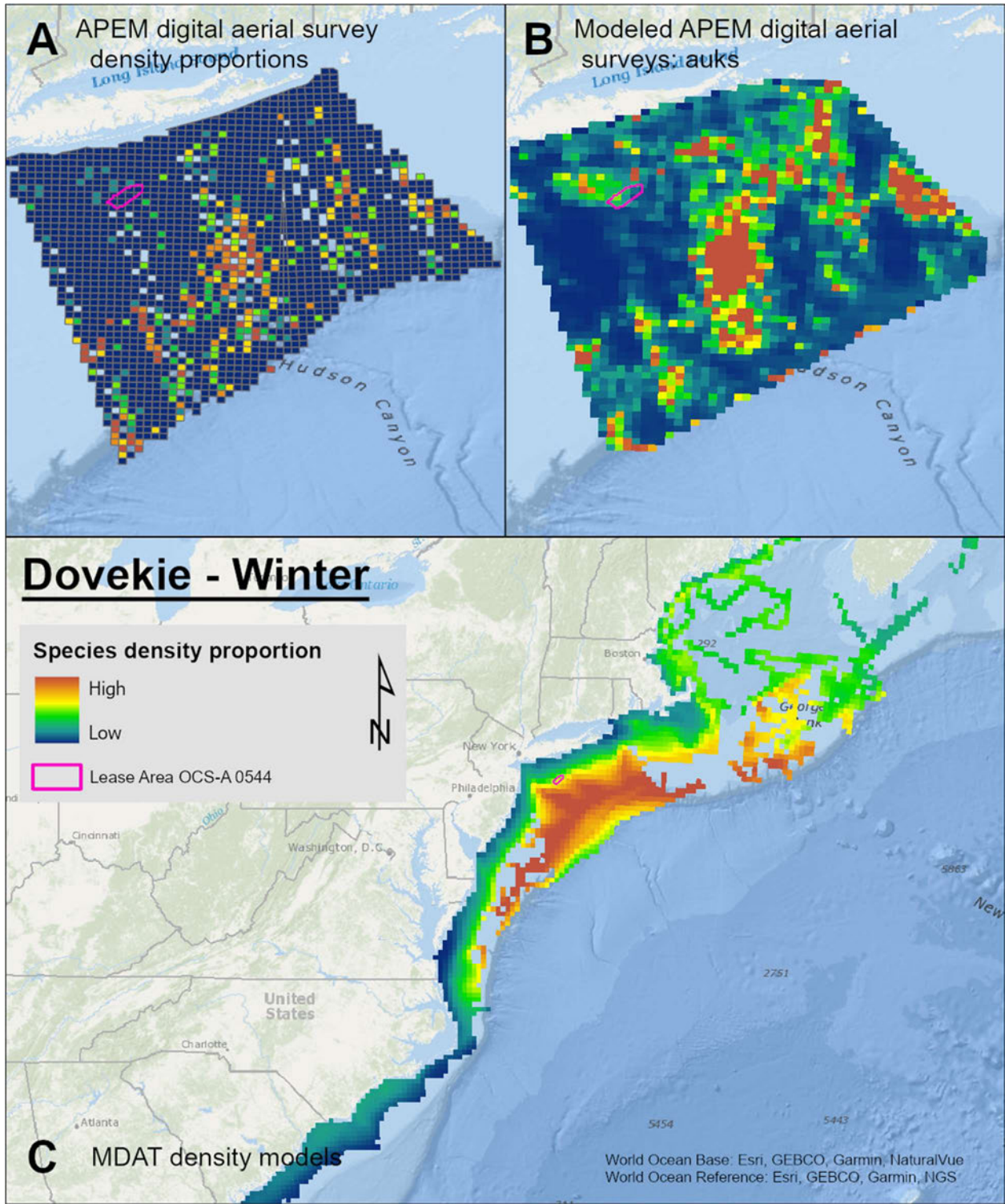
Map 54. Spring Parasitic Jaeger density proportions in the NYSERDA APEM and Empire Wind high resolution digital aerial survey data (A), the NYSERDA APEM and Empire Wind high resolution digital aerial model outputs for skuas and jaegers in Spring (B) and, Spring Parasitic Jaeger MDAT modeled abundance at the regional scale (C). The scale for all maps is representative of relative spatial variation in the sites within the season for each map input.



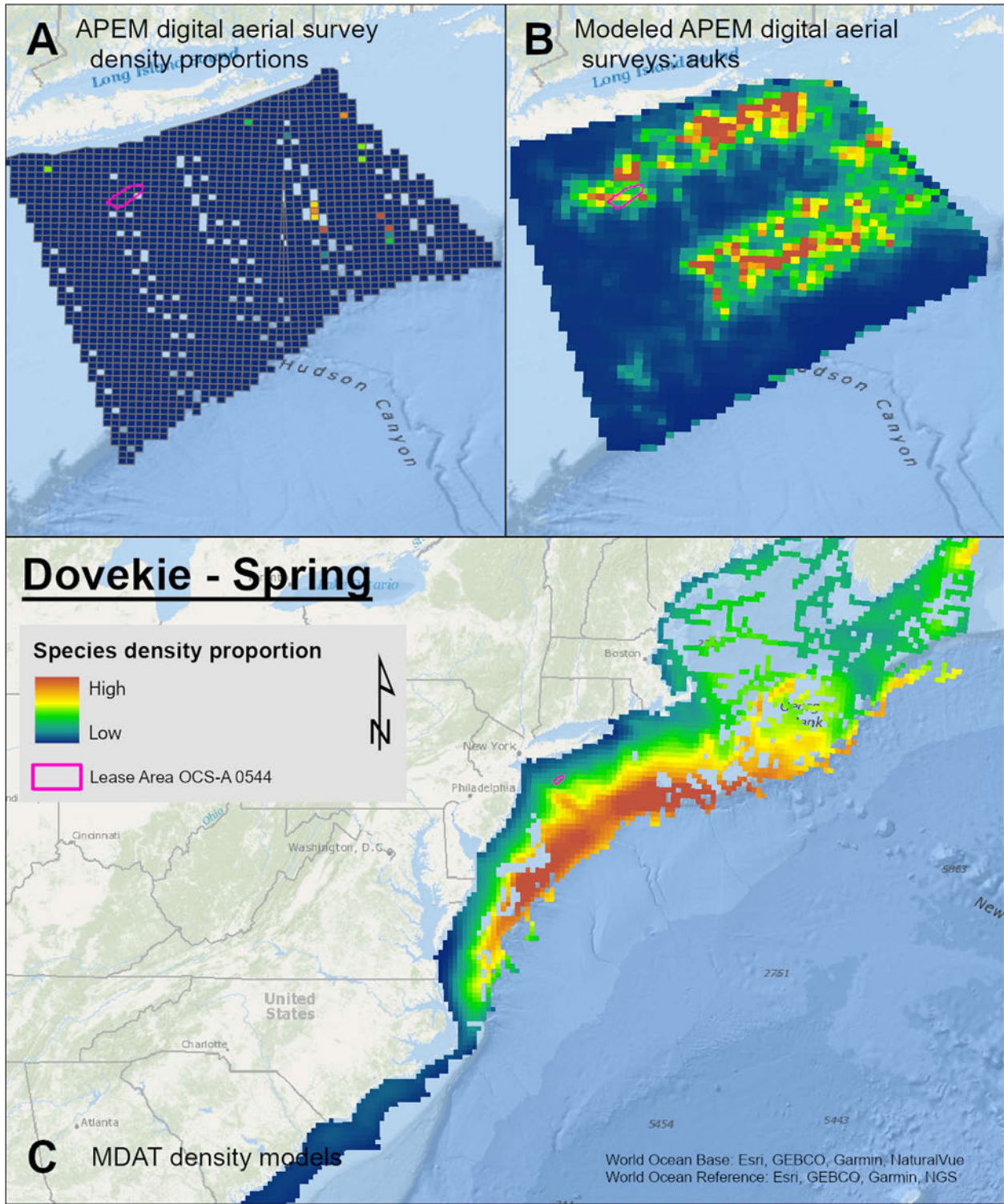
Map 55. Summer Parasitic Jaeger density proportions in the NYSERDA APEM and Empire Wind high resolution digital aerial survey data (A), the NYSERDA APEM and Empire Wind high resolution digital aerial model outputs for skuas and jaegers in Summer (B) and, Summer Parasitic Jaeger MDAT modeled abundance at the regional scale (C). The scale for all maps is representative of relative spatial variation in the sites within the season for each map input.



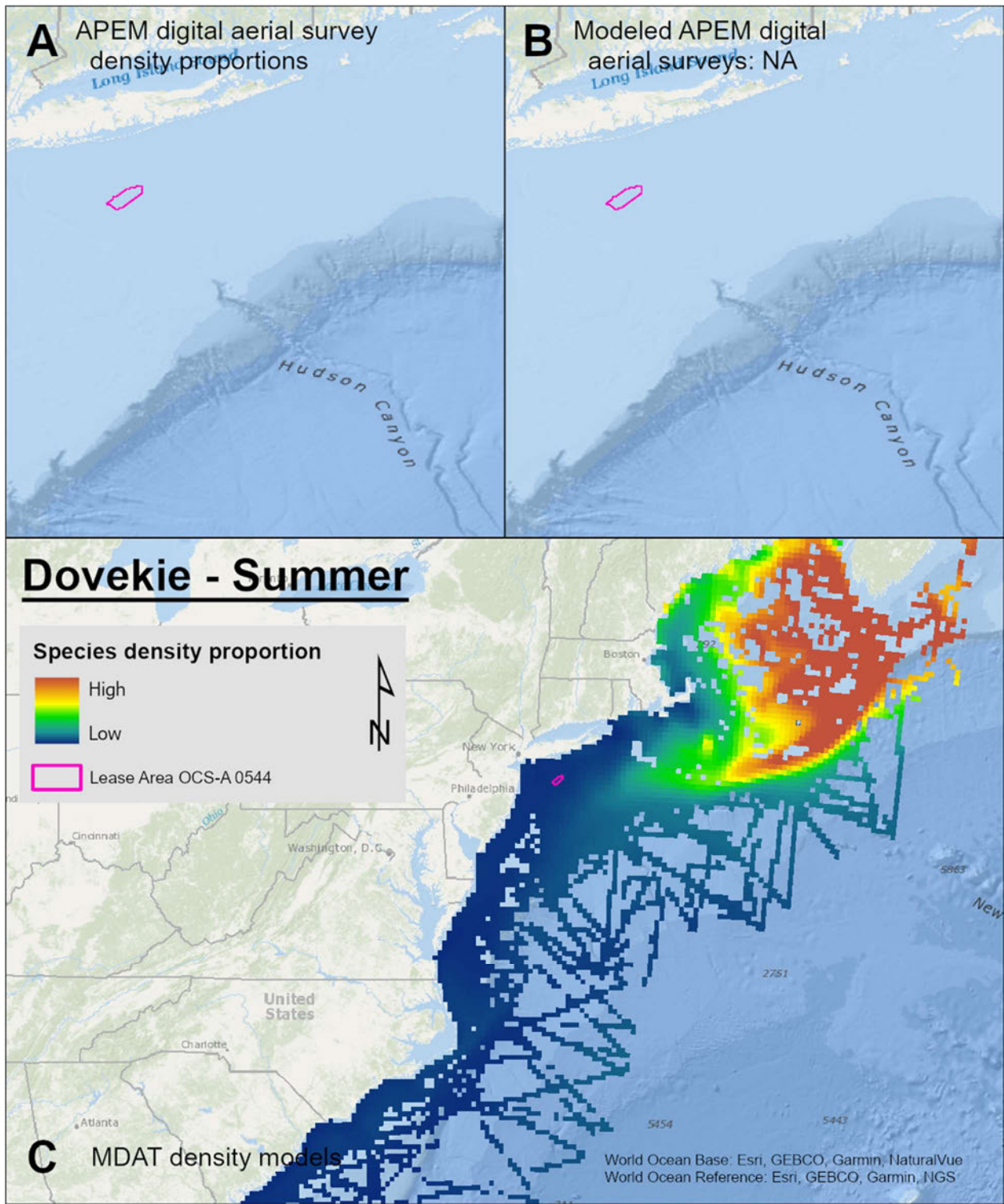
Map 56. Fall Parasitic Jaeger density proportions in the NYSERDA APEM and Empire Wind high resolution digital aerial survey data (A), the NYSERDA APEM and Empire Wind high resolution digital aerial model outputs for skuas and jaegers in Fall (B) and, Fall Parasitic Jaeger MDAT modeled abundance at the regional scale (C). The scale for all maps is representative of relative spatial variation in the sites within the season for each map input.



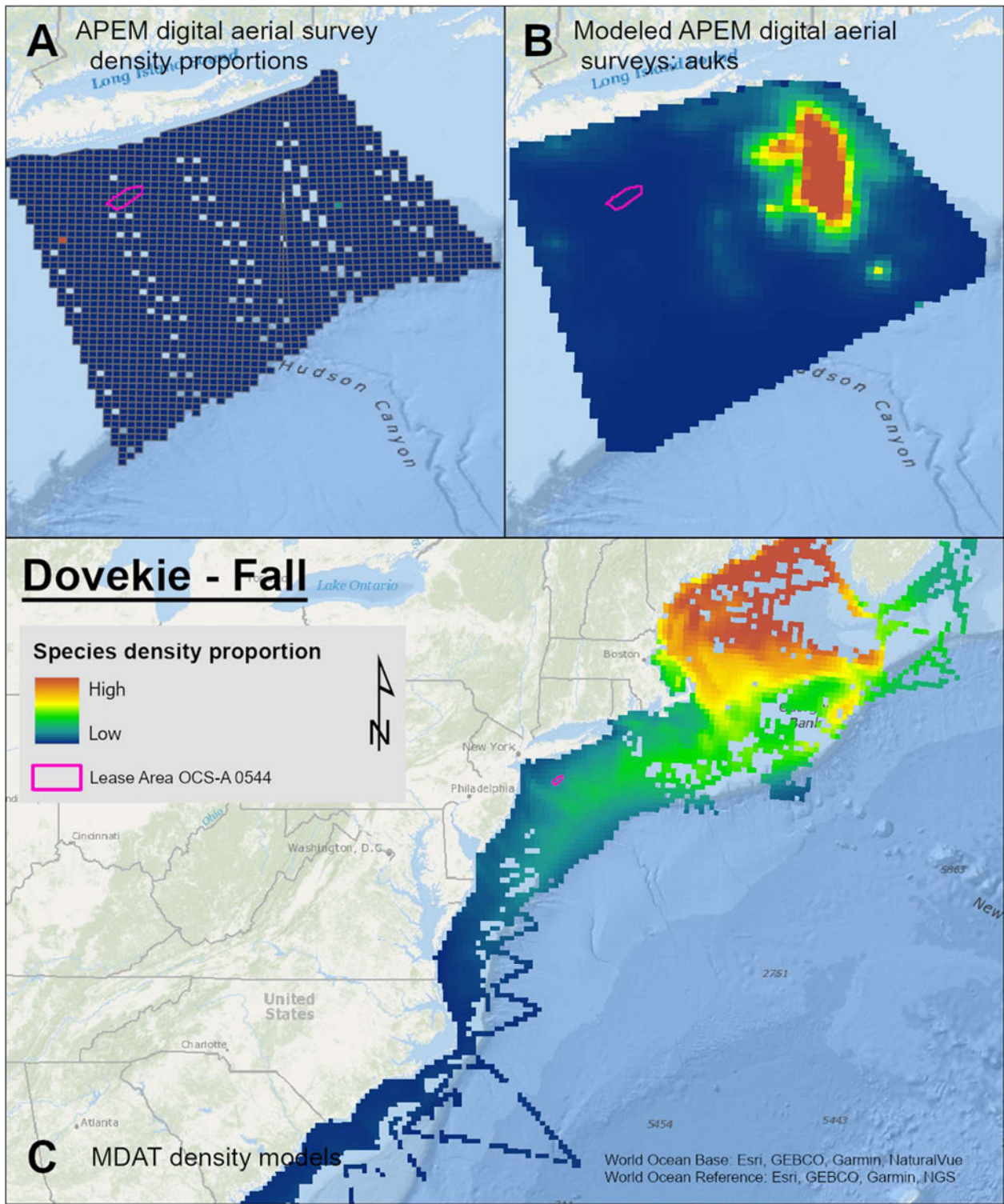
Map 57. Winter Dovekie density proportions in the NYSERDA APEM and Empire Wind high resolution digital aerial survey data (A), the NYSERDA APEM and Empire Wind high resolution digital aerial model outputs for auks in Winter (B) and, Winter Dovekie MDAT modeled abundance at the regional scale (C). The scale for all maps is representative of relative spatial variation in the sites within the season for each map input.



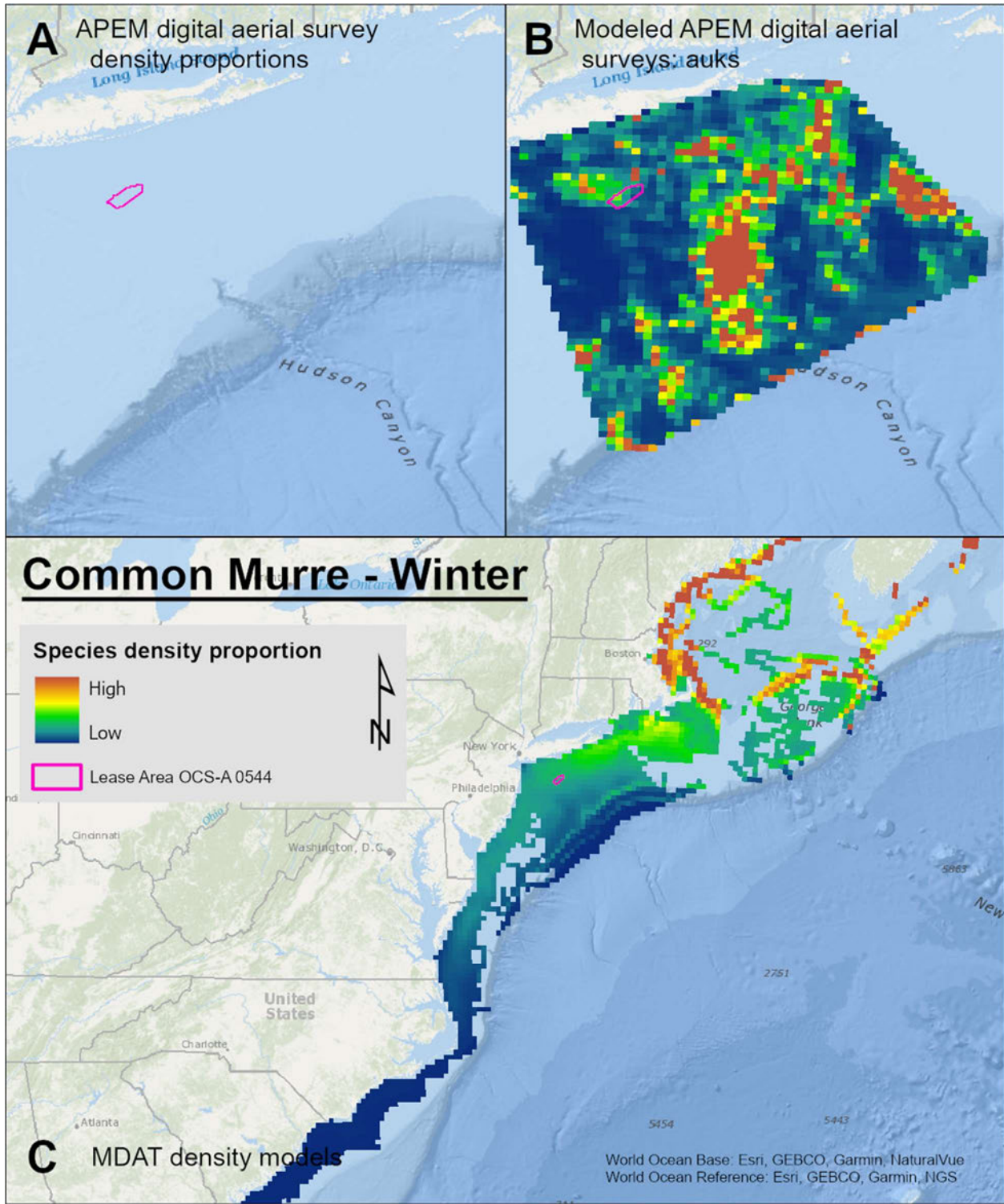
Map 58. Spring Dovekie density proportions in the NYSERDA APEM and Empire Wind high resolution digital aerial survey data (A), the NYSERDA APEM and Empire Wind high resolution digital aerial model outputs for auks in Spring (B) and, Spring Dovekie MDAT modeled abundance at the regional scale (C). The scale for all maps is representative of relative spatial variation in the sites within the season for each map input.



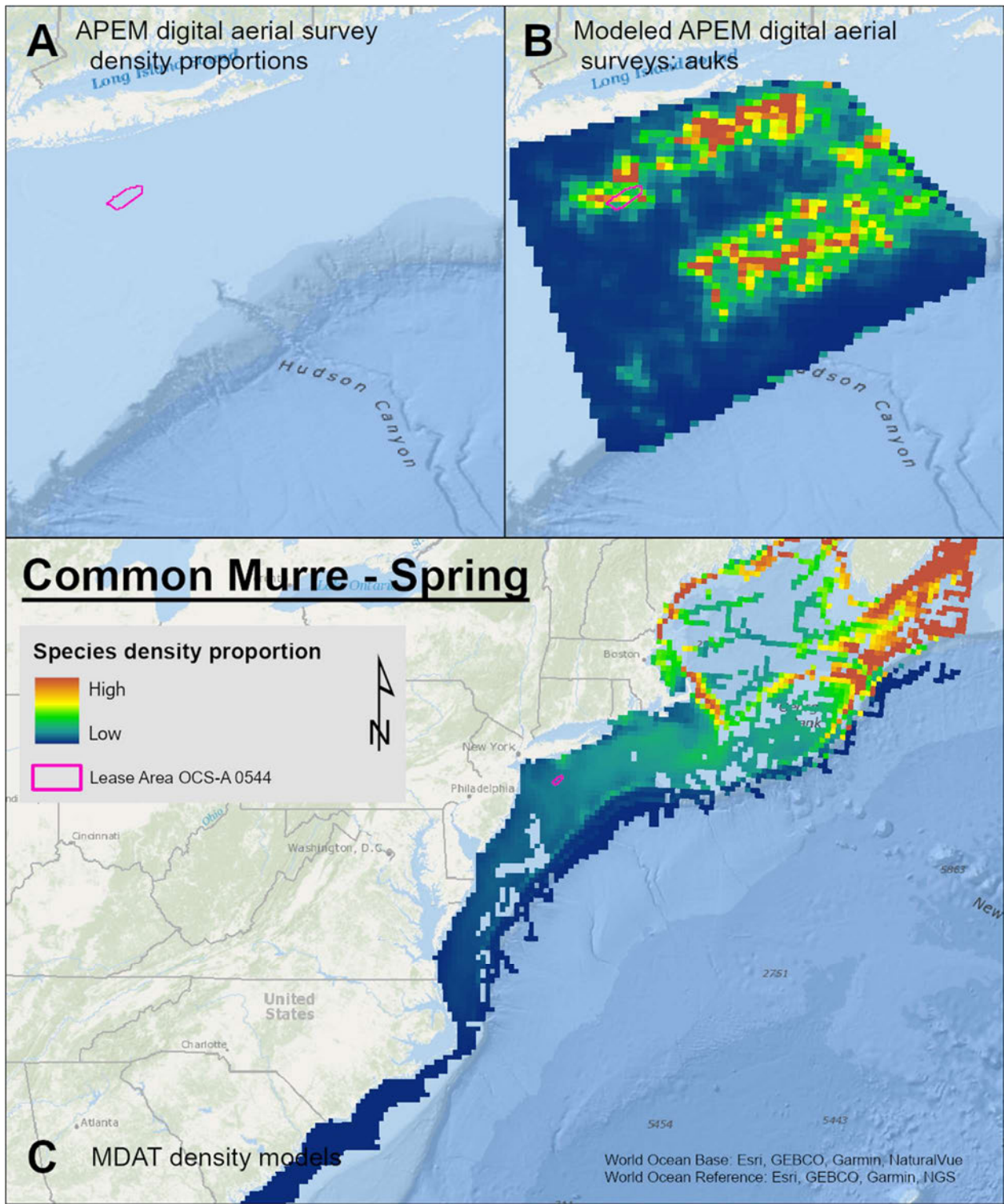
Map 59. Summer Dovekie density proportions in the NYSERDA APEM and Empire Wind high resolution digital aerial survey data (A), the NYSERDA APEM and Empire Wind high resolution digital aerial model outputs for auks in Summer (B) and, Summer Dovekie MDAT modeled abundance at the regional scale (C). The scale for all maps is representative of relative spatial variation in the sites within the season for each map input.



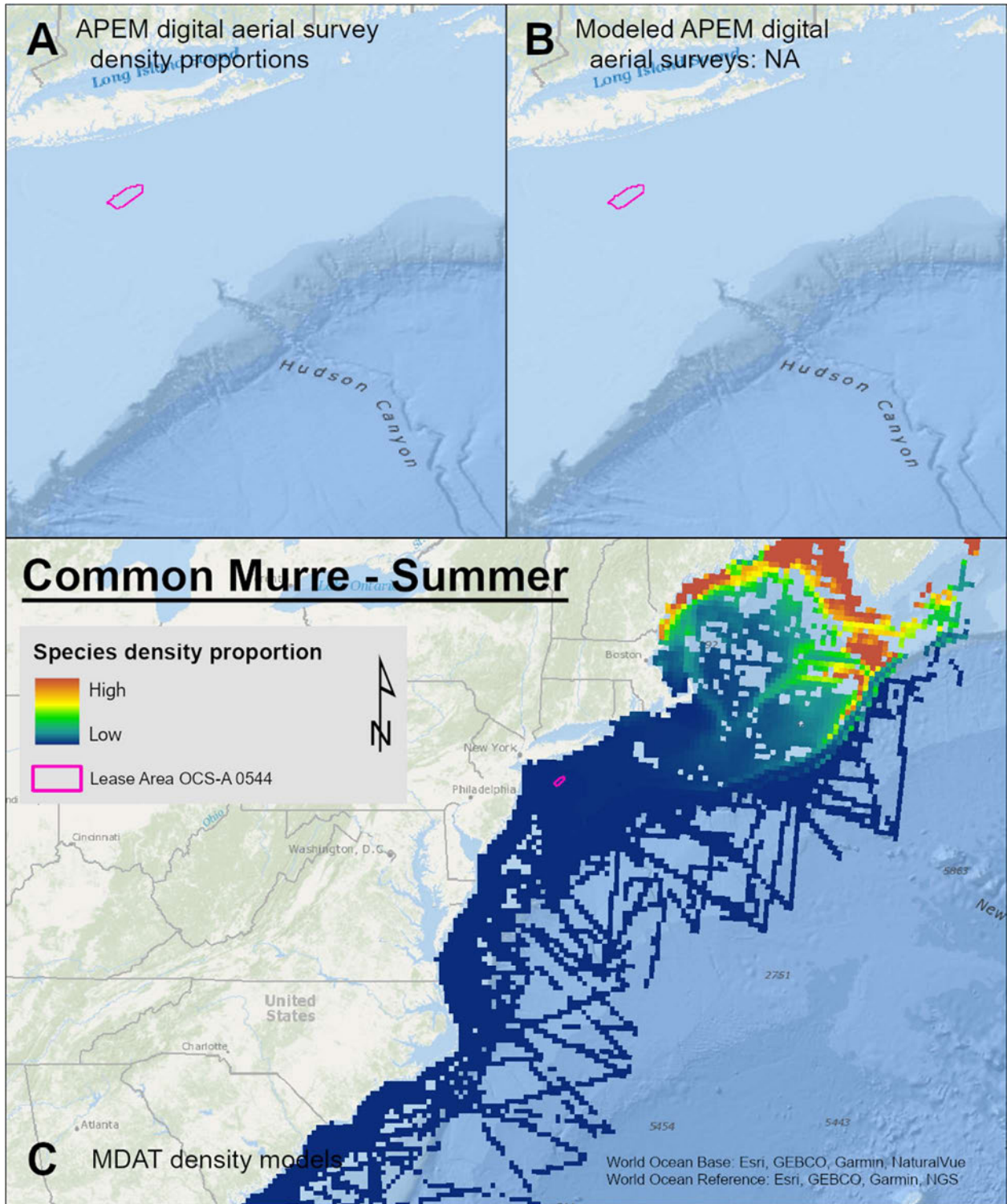
Map 60. Fall Dovekie density proportions in the NYSERDA APEM and Empire Wind high resolution digital aerial survey data (A), the NYSERDA APEM and Empire Wind high resolution digital aerial model outputs for auks in Fall (B) and, Fall Dovekie MDAT modeled abundance at the regional scale (C). The scale for all maps is representative of relative spatial variation in the sites within the season for each map input.



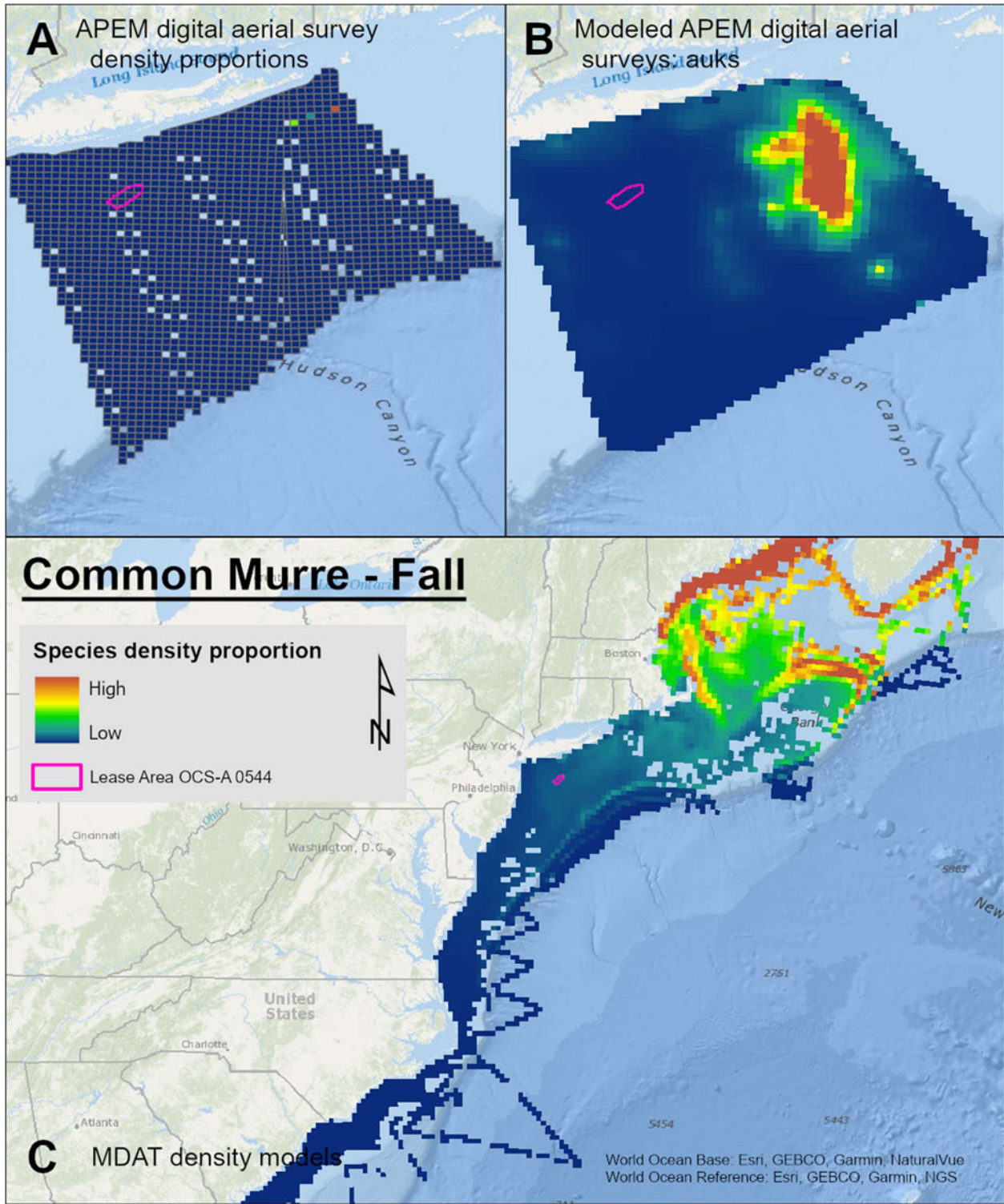
Map 61. Winter Common Murre density proportions in the NYSERDA APEM and Empire Wind high resolution digital aerial survey data (A), the NYSERDA APEM and Empire Wind high resolution digital aerial model outputs for auks in Winter (B) and, Winter Common Murre MDAT modeled abundance at the regional scale (C). The scale for all maps is representative of relative spatial variation in the sites within the season for each map input.



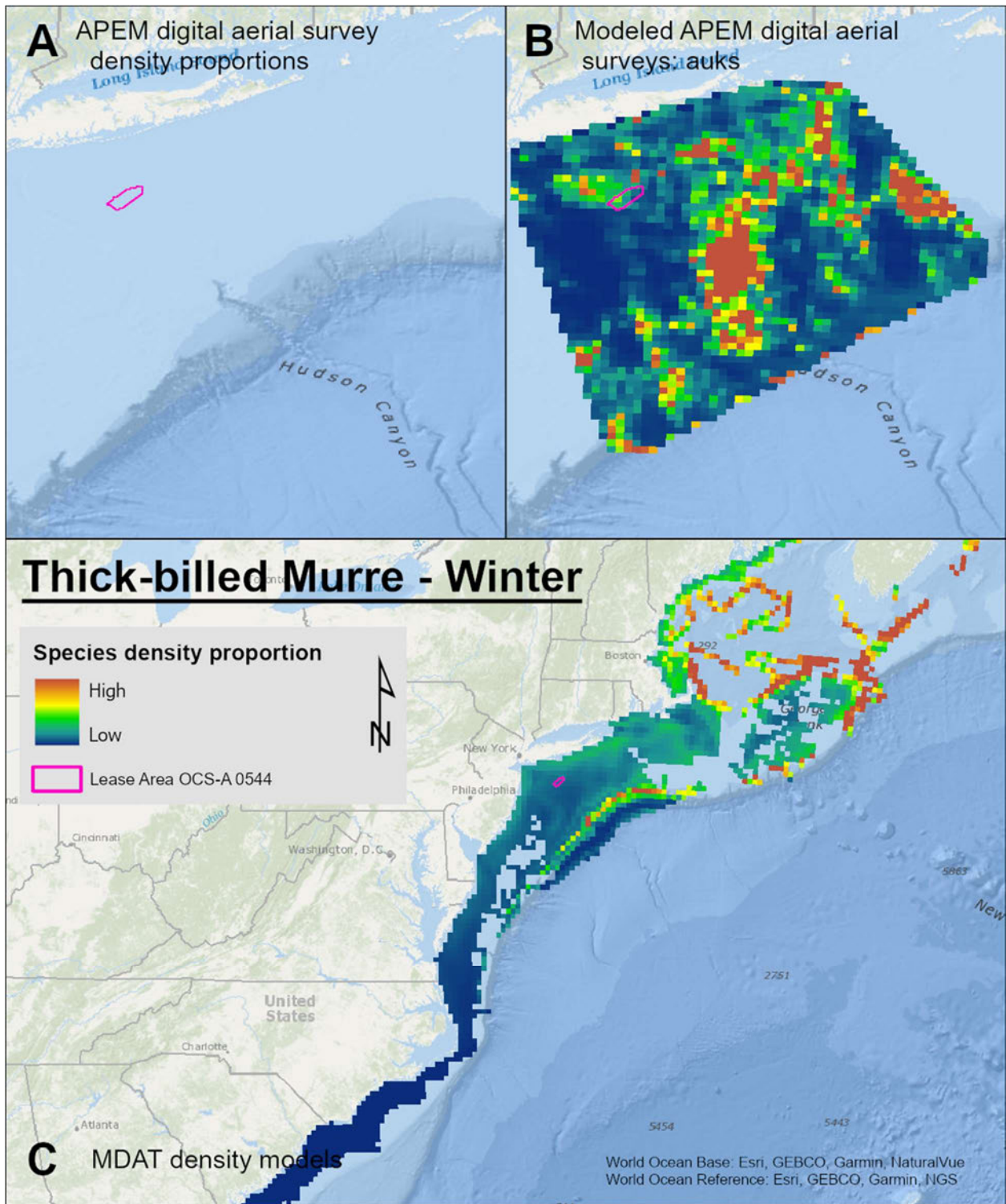
Map 62. Spring Common Murre density proportions in the NYSERDA APEM and Empire Wind high resolution digital aerial survey data (A), the NYSERDA APEM and Empire Wind high resolution digital aerial model outputs for auks in Spring (B) and, Spring Common Murre MDAT modeled abundance at the regional scale (C). The scale for all maps is representative of relative spatial variation in the sites within the season for each map input.



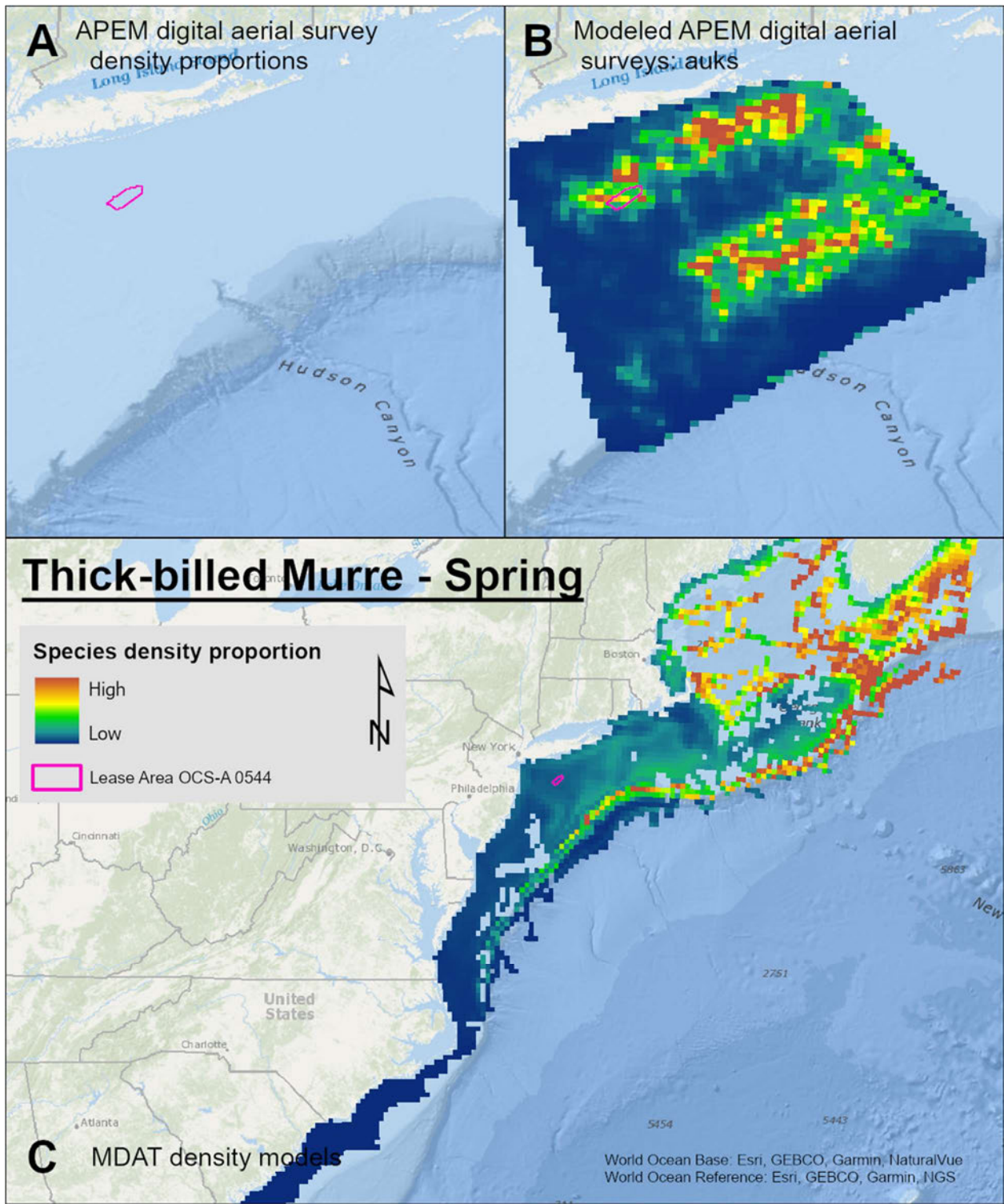
Map 63. Summer Common Murre density proportions in the NYSERDA APEM and Empire Wind high resolution digital aerial survey data (A), the NYSERDA APEM and Empire Wind high resolution digital aerial model outputs for auks in Summer (B) and, Summer Common Murre MDAT modeled abundance at the regional scale (C). The scale for all maps is representative of relative spatial variation in the sites within the season for each map input.



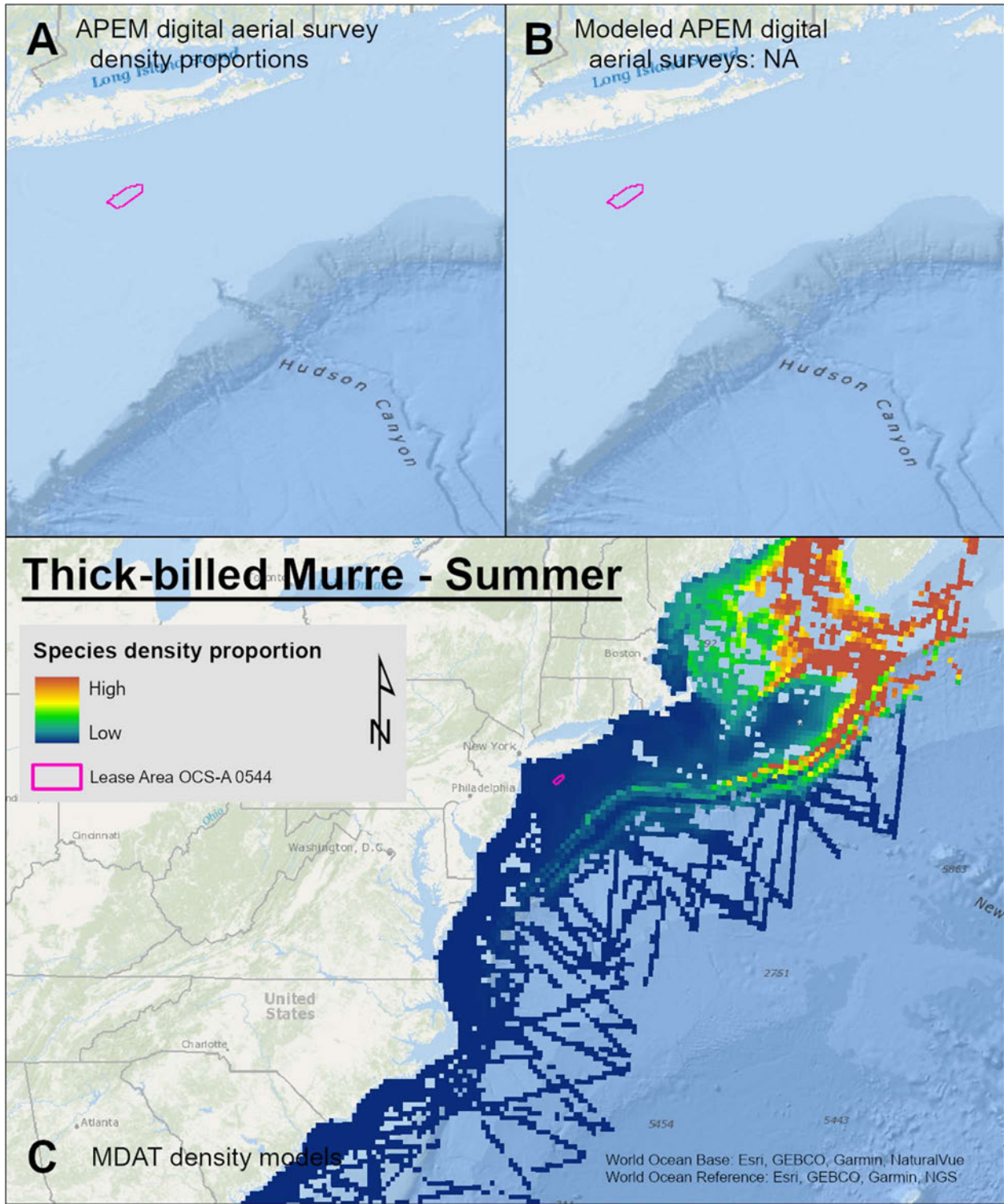
Map 64. Fall Common Murre density proportions in the NYSERDA APEM and Empire Wind high resolution digital aerial survey data (A), the NYSERDA APEM and Empire Wind high resolution digital aerial model outputs for auks in Fall (B) and, Fall Common Murre MDAT modeled abundance at the regional scale (C). The scale for all maps is representative of relative spatial variation in the sites within the season for each map input.



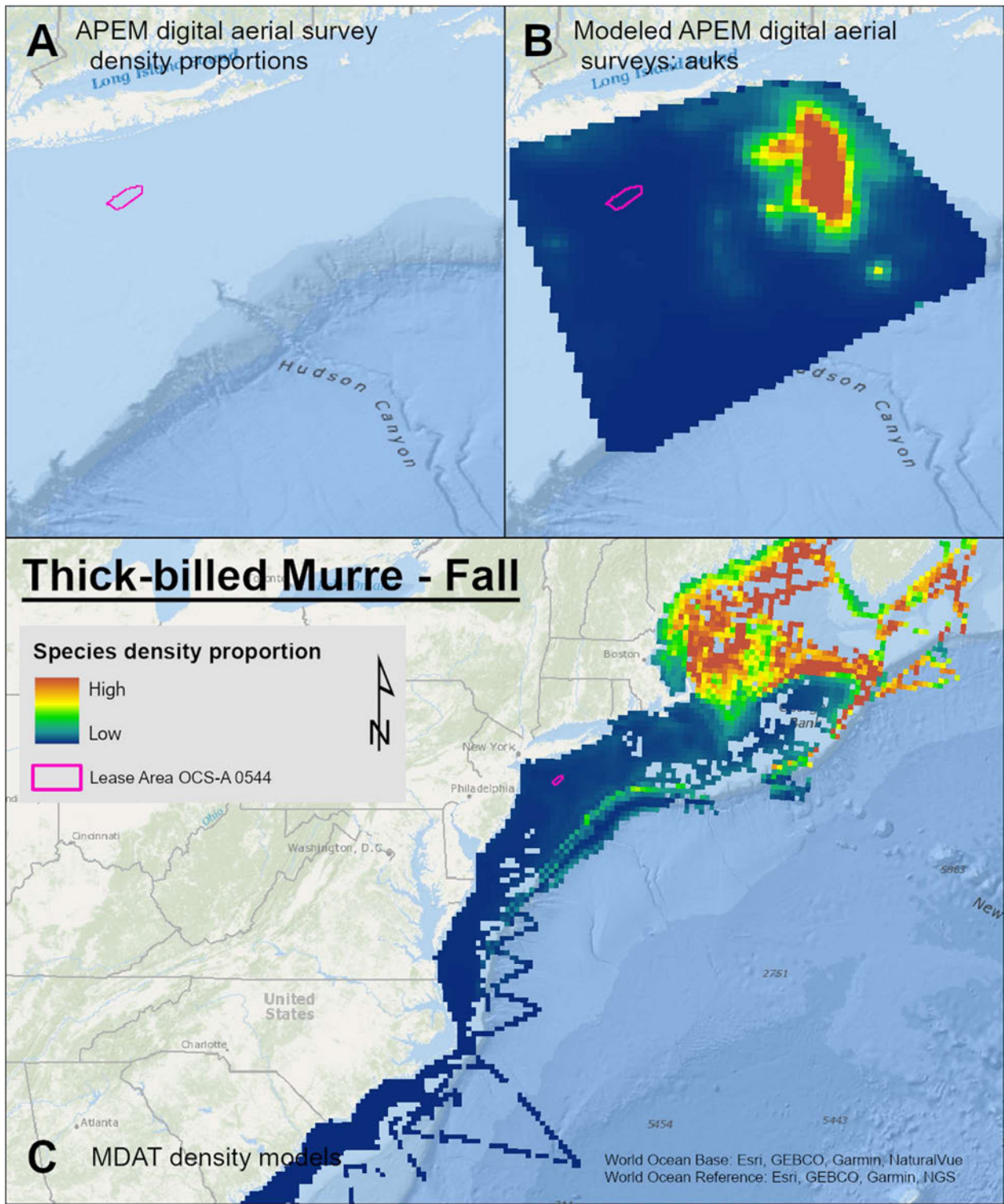
Map 65. Winter Thick-billed Murre density proportions in the NYSERDA APEM and Empire Wind high resolution digital aerial survey data (A), the NYSERDA APEM and Empire Wind high resolution digital aerial model outputs for auks in Winter (B) and, Winter Thick-billed Murre MDAT modeled abundance at the regional scale (C). The scale for all maps is representative of relative spatial variation in the sites within the season for each map input.



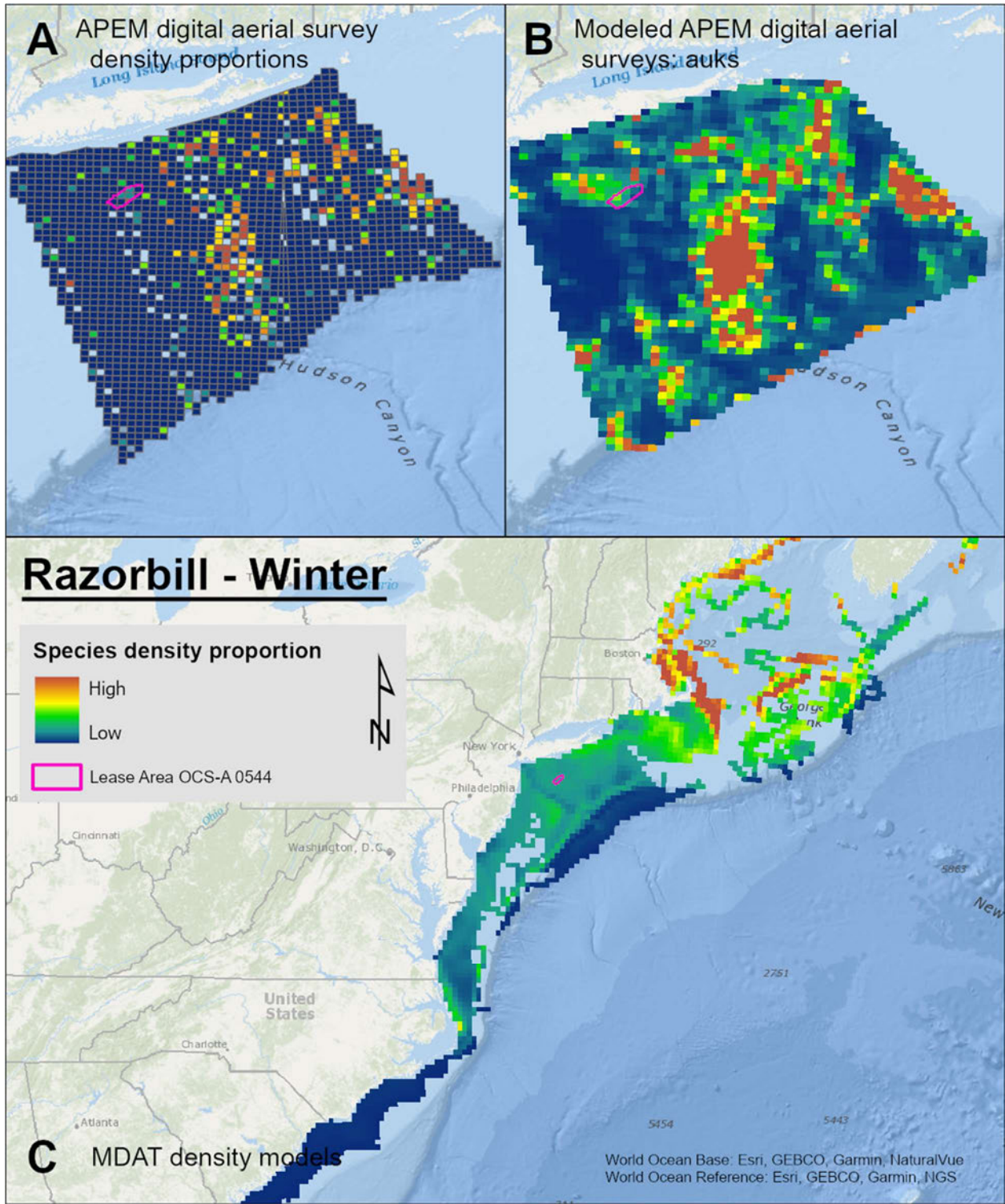
Map 66. Spring Thick-billed Murre density proportions in the NYSERDA APEM and Empire Wind high resolution digital aerial survey data (A), the NYSERDA APEM and Empire Wind high resolution digital aerial model outputs for auks in Spring (B) and, Spring Thick-billed Murre MDAT modeled abundance at the regional scale (C). The scale for all maps is representative of relative spatial variation in the sites within the season for each map input.



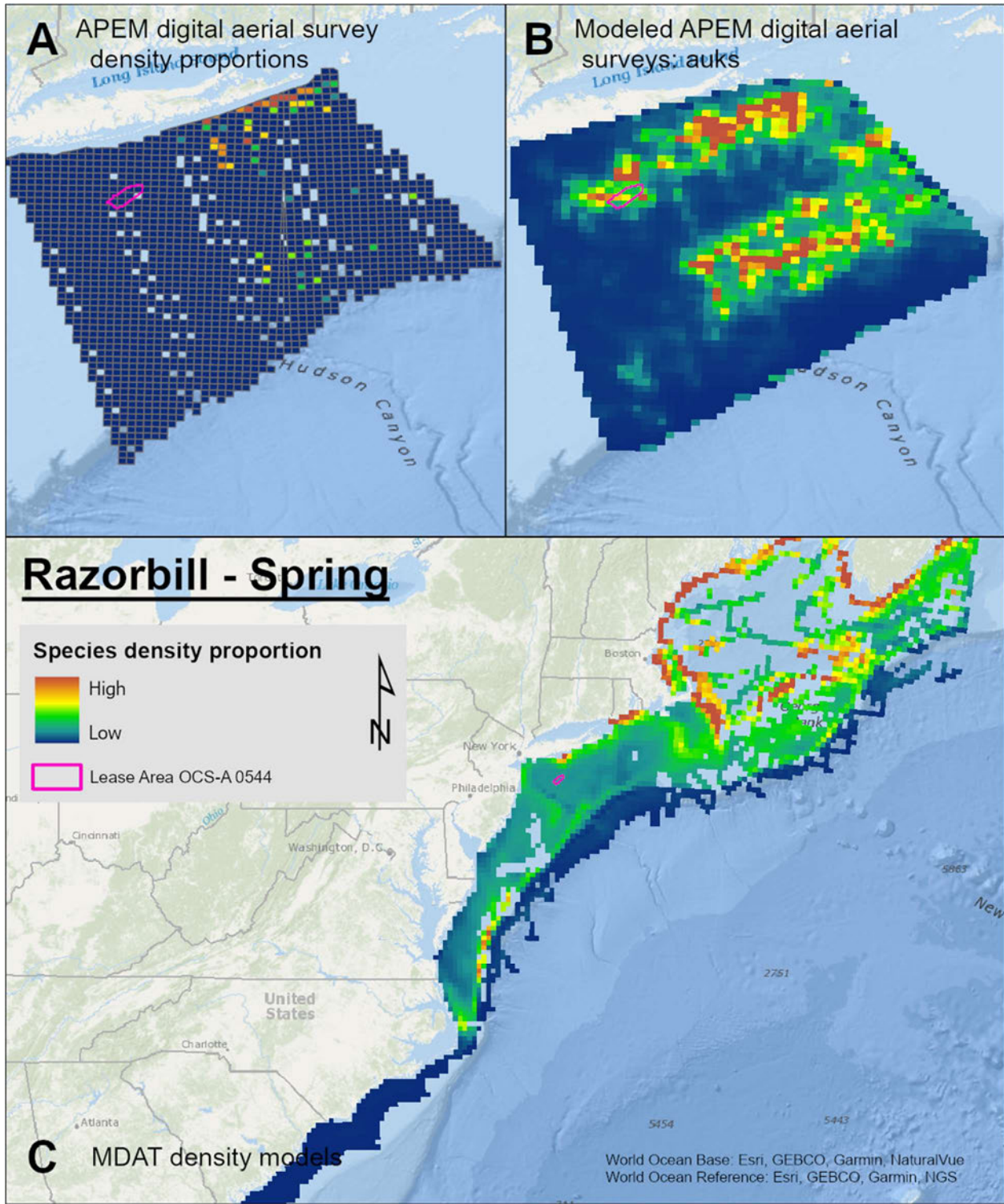
Map 67. Summer Thick-billed Murre density proportions in the NYSERDA APEM and Empire Wind high resolution digital aerial survey data (A), the NYSERDA APEM and Empire Wind high resolution digital aerial model outputs for auks in Summer (B) and, Summer Thick-billed Murre MDAT modeled abundance at the regional scale (C). The scale for all maps is representative of relative spatial variation in the sites within the season for each map input.



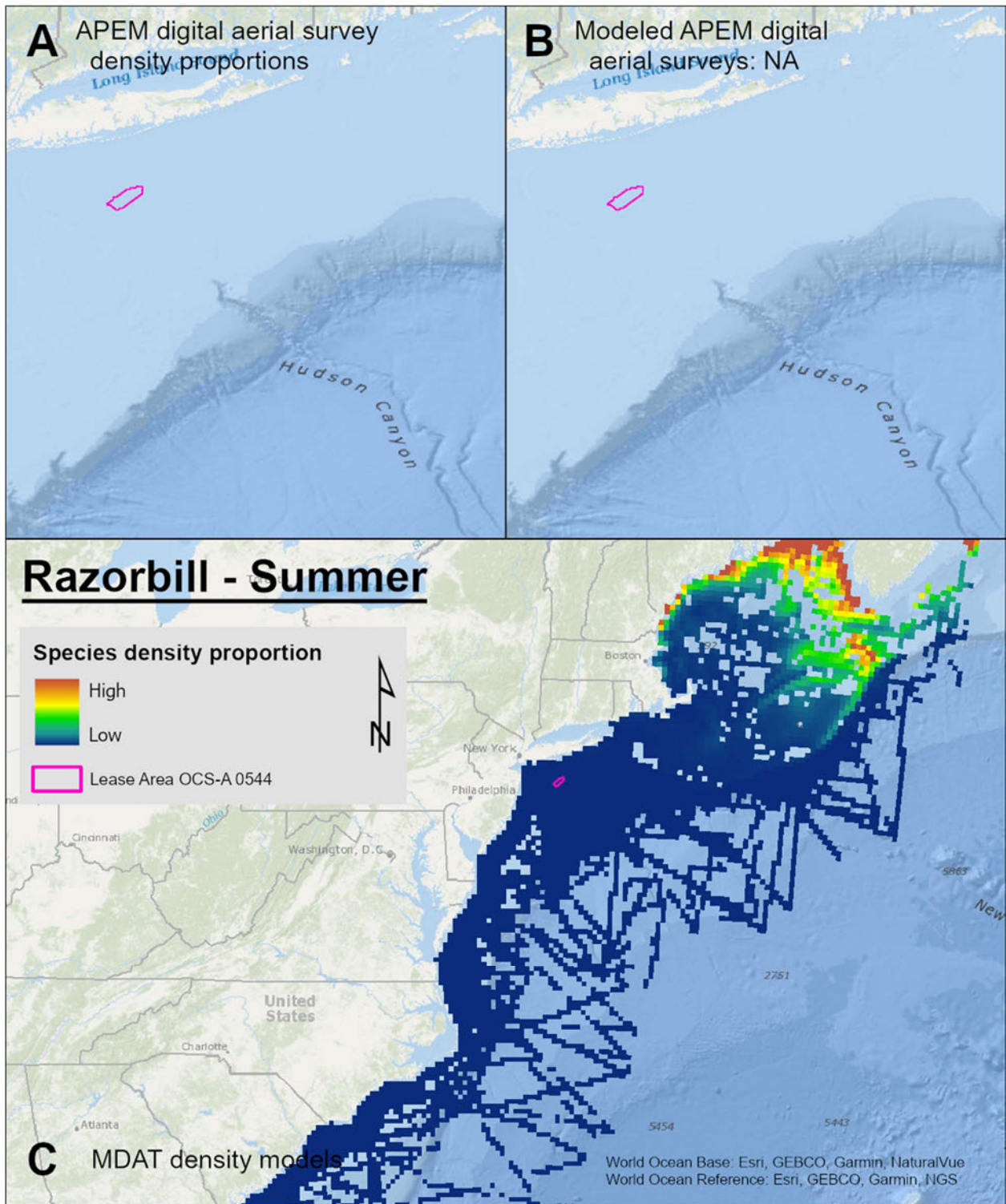
Map 68. Fall Thick-billed Murre density proportions in the NYSERDA APEM and Empire Wind high resolution digital aerial survey data (A), the NYSERDA APEM and Empire Wind high resolution digital aerial model outputs for auks in Fall (B) and, Fall Thick-billed Murre MDAT modeled abundance at the regional scale (C). The scale for all maps is representative of relative spatial variation in the sites within the season for each map input.



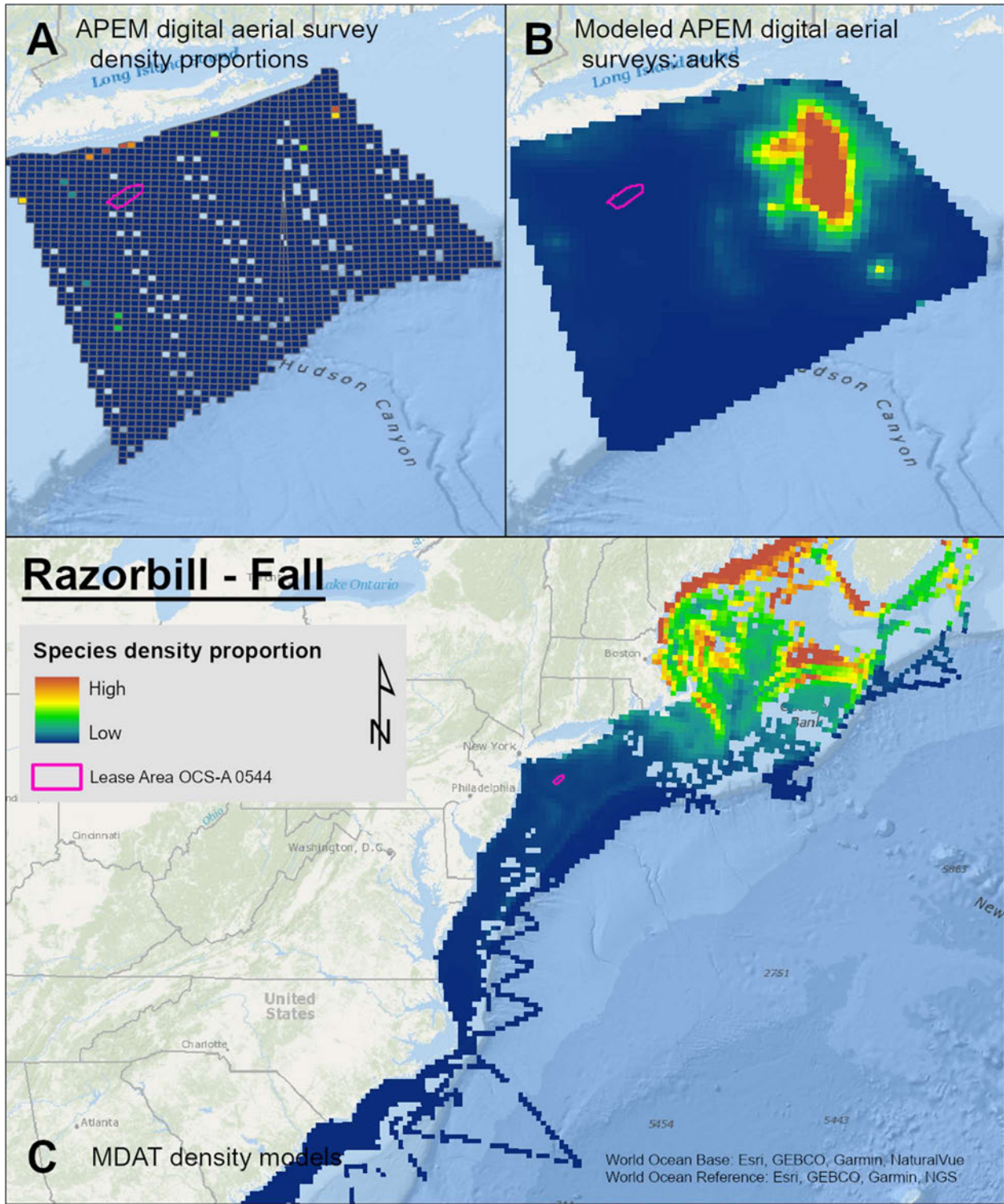
Map 69. Winter Razorbill density proportions in the NYSERDA APEM and Empire Wind high resolution digital aerial survey data (A), the NYSERDA APEM and Empire Wind high resolution digital aerial model outputs for auks in Winter (B) and, Winter Razorbill MDAT modeled abundance at the regional scale (C). The scale for all maps is representative of relative spatial variation in the sites within the season for each map input.



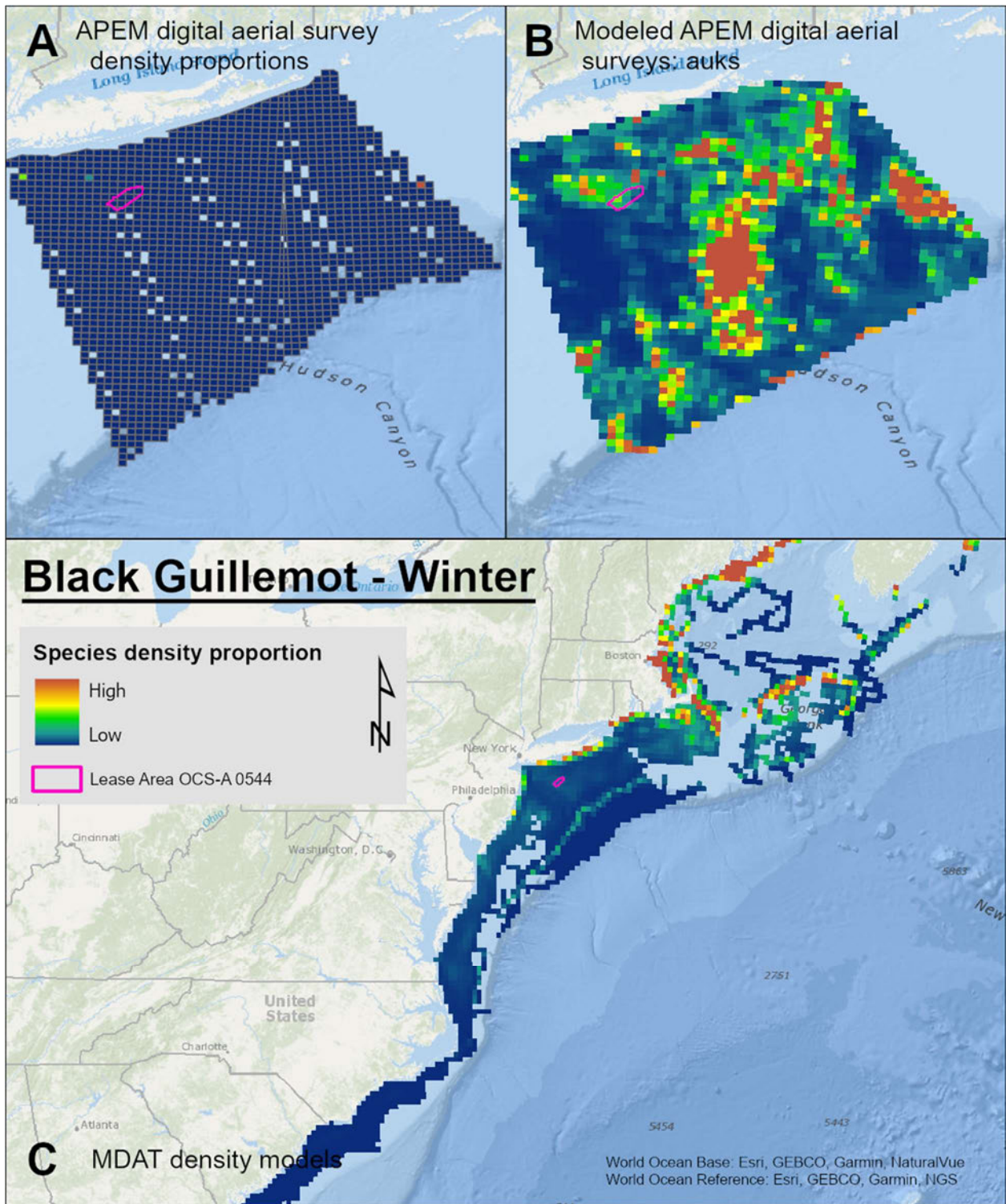
Map 70. Spring Razorbill density proportions in the NYSEDA APEM and Empire Wind high resolution digital aerial survey data (A), the NYSEDA APEM and Empire Wind high resolution digital aerial model outputs for auks in Spring (B) and, Spring Razorbill MDAT modeled abundance at the regional scale (C). The scale for all maps is representative of relative spatial variation in the sites within the season for each map input.



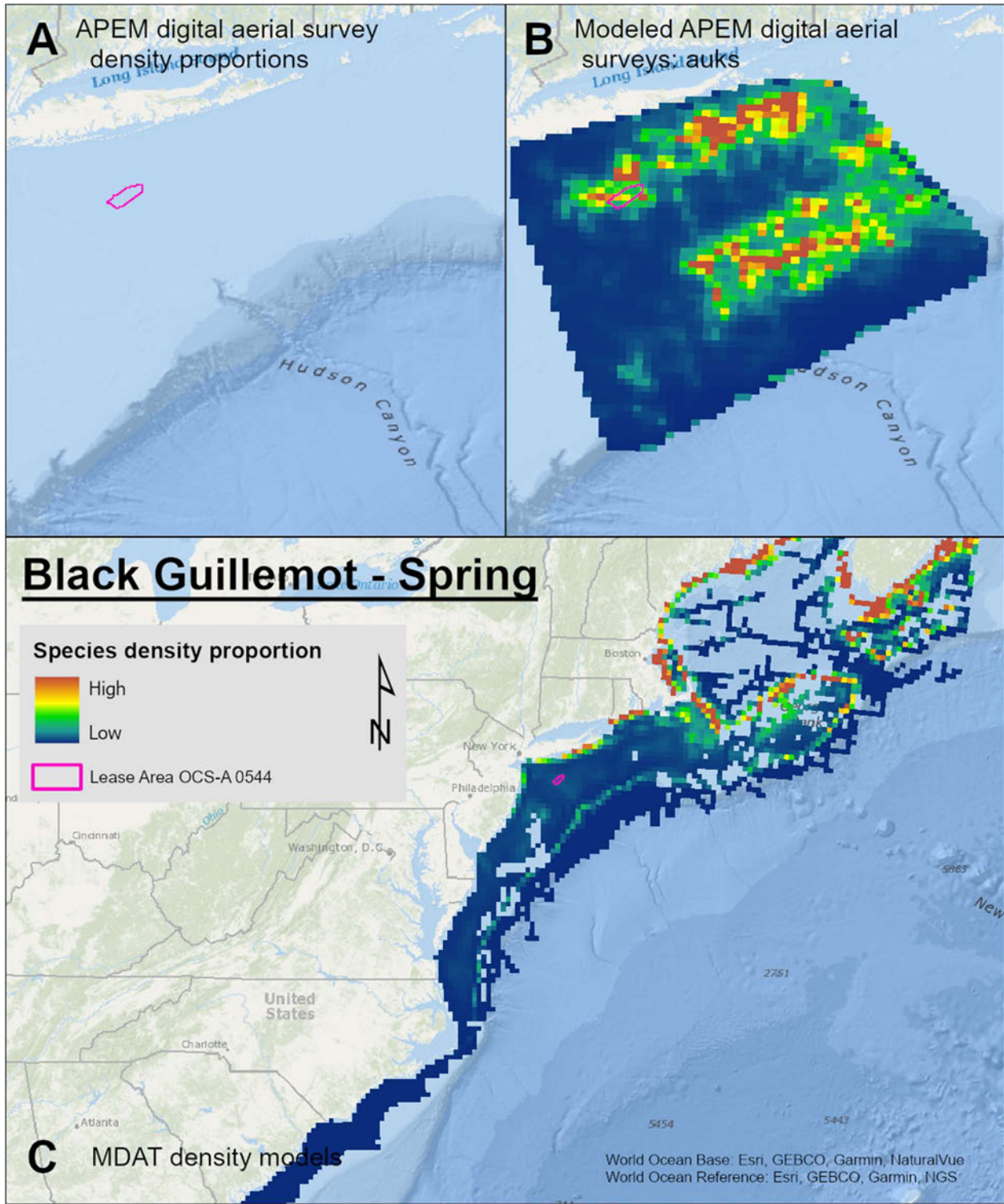
Map 71. Summer Razorbill density proportions in the NYSERDA APEM and Empire Wind high resolution digital aerial survey data (A), the NYSERDA APEM and Empire Wind high resolution digital aerial model outputs for auks in Summer (B) and, Summer Razorbill MDAT modeled abundance at the regional scale (C). The scale for all maps is representative of relative spatial variation in the sites within the season for each map input.



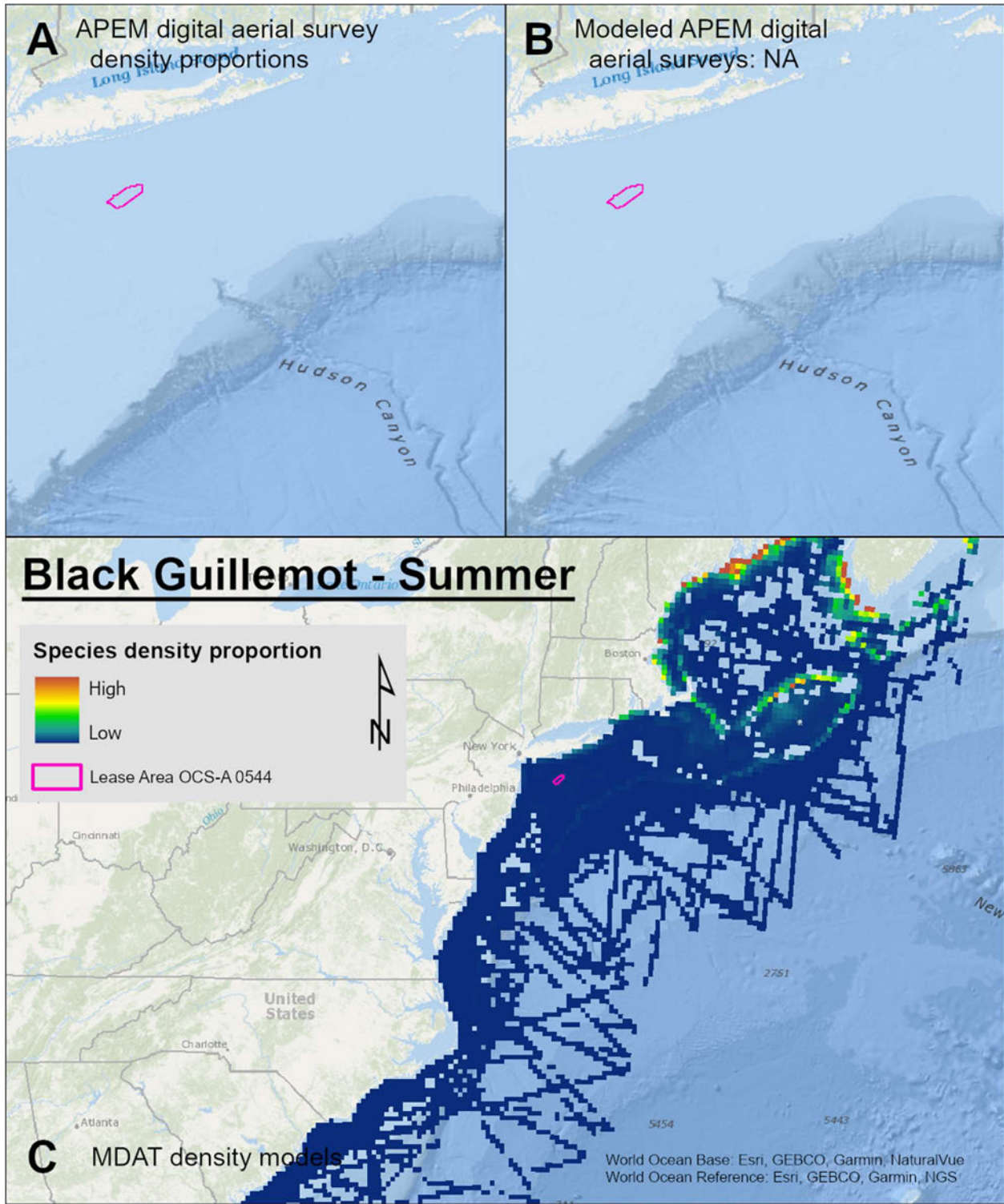
Map 72. Fall Razorbill density proportions in the NYSERDA APEM and Empire Wind high resolution digital aerial survey data (A), the NYSERDA APEM and Empire Wind high resolution digital aerial model outputs for auks in Fall (B) and, Fall Razorbill MDAT modeled abundance at the regional scale (C). The scale for all maps is representative of relative spatial variation in the sites within the season for each map input.



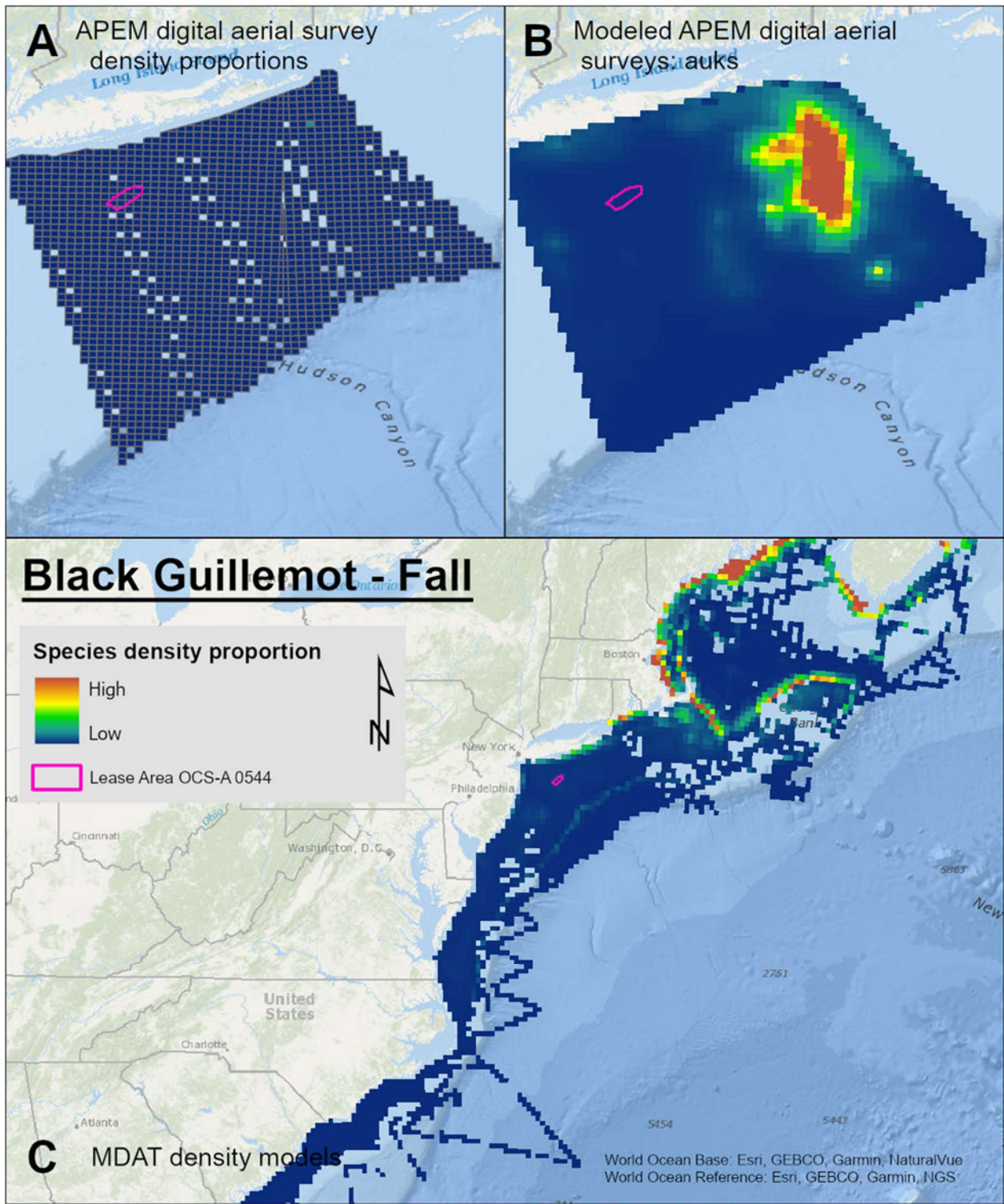
Map 73. Winter Black Guillemot density proportions in the NYSERDA APEM and Empire Wind high resolution digital aerial survey data (A), the NYSERDA APEM and Empire Wind high resolution digital aerial model outputs for auks in Winter (B) and, Winter Black Guillemot MDAT modeled abundance at the regional scale (C). The scale for all maps is representative of relative spatial variation in the sites within the season for each map input.



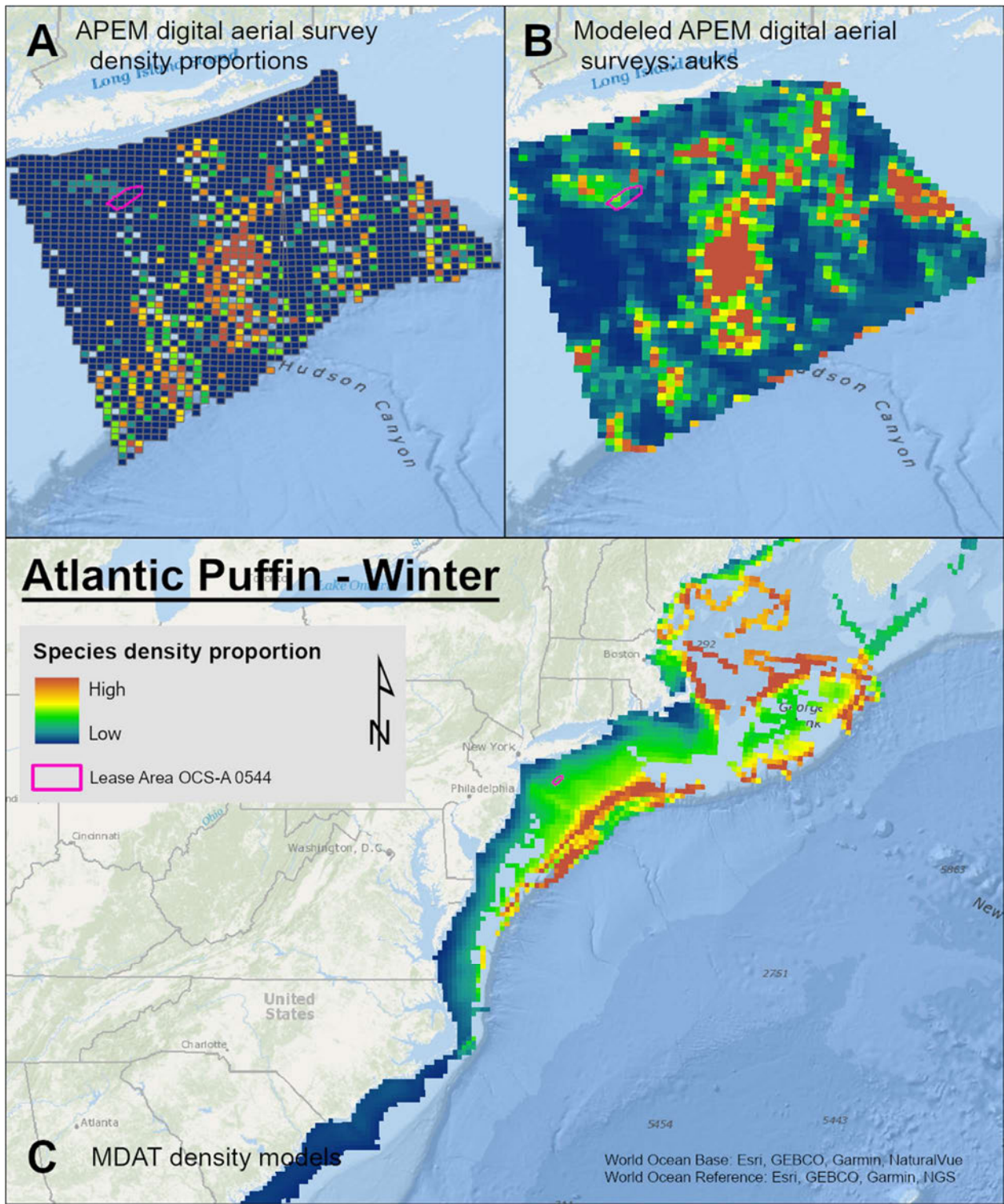
Map 74. Spring Black Guillemot density proportions in the NYSERDA APEM and Empire Wind high resolution digital aerial survey data (A), the NYSERDA APEM and Empire Wind high resolution digital aerial model outputs for auks in Spring (B) and, Spring Black Guillemot MDAT modeled abundance at the regional scale (C). The scale for all maps is representative of relative spatial variation in the sites within the season for each map input.



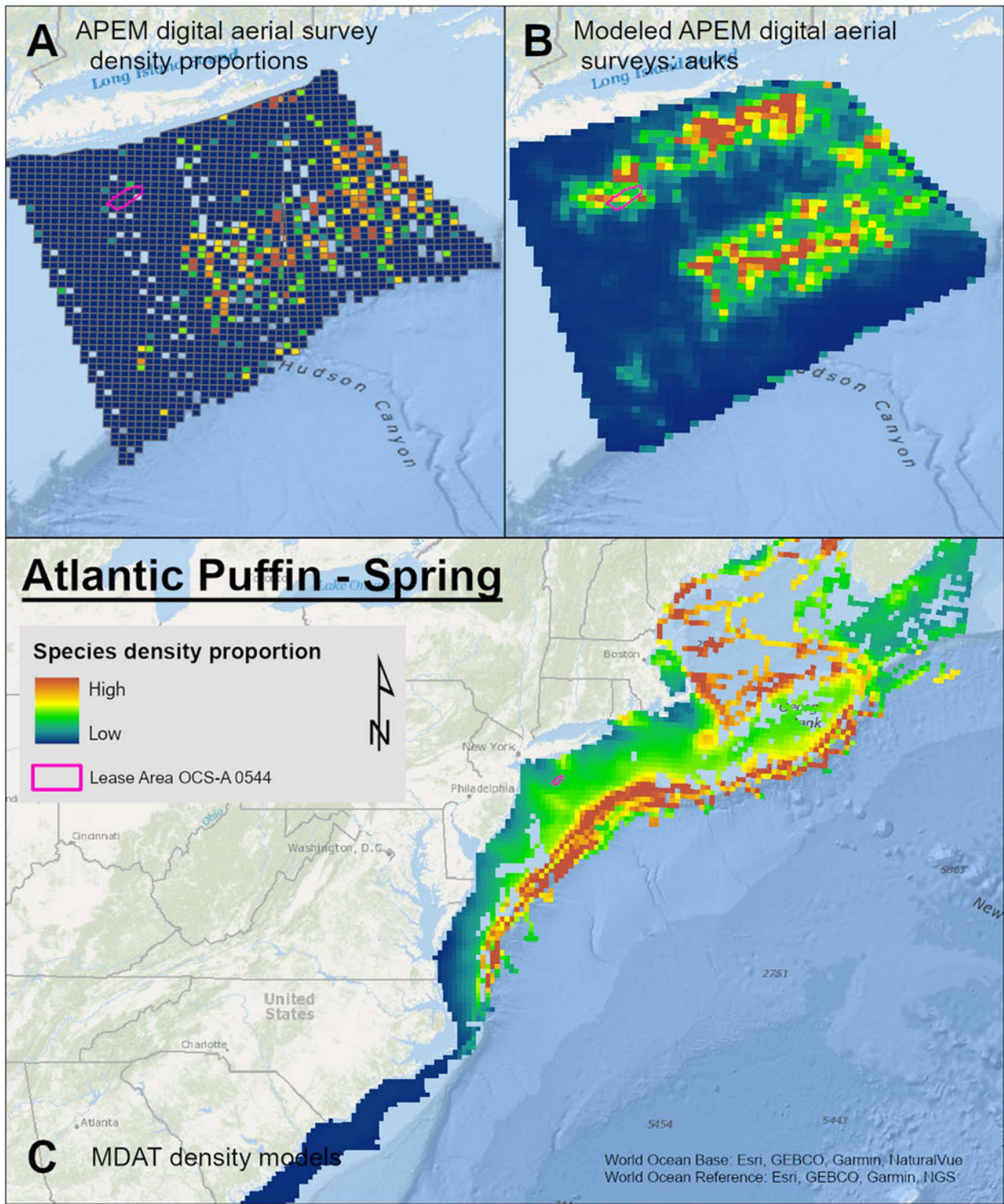
Map 75. Summer Black Guillemot density proportions in the NYSERDA APEM and Empire Wind high resolution digital aerial survey data (A), the NYSERDA APEM and Empire Wind high resolution digital aerial model outputs for auks in Summer (B) and, Summer Black Guillemot MDAT modeled abundance at the regional scale (C). The scale for all maps is representative of relative spatial variation in the sites within the season for each map input.



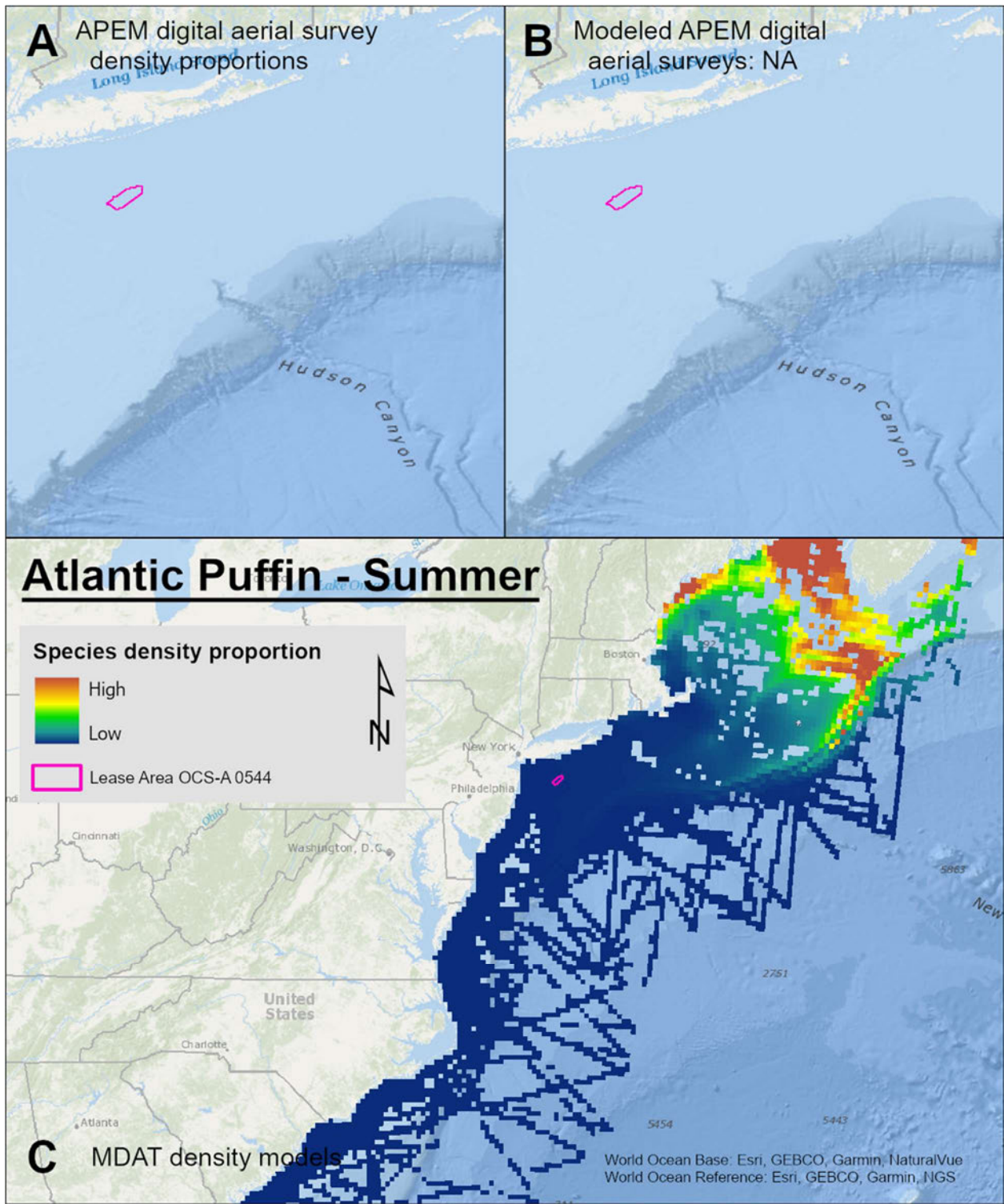
Map 76. Fall Black Guillemot density proportions in the NYSERDA APEM and Empire Wind high resolution digital aerial survey data (A), the NYSERDA APEM and Empire Wind high resolution digital aerial model outputs for auks in Fall (B) and, Fall Black Guillemot MDAT modeled abundance at the regional scale (C). The scale for all maps is representative of relative spatial variation in the sites within the season for each map input.



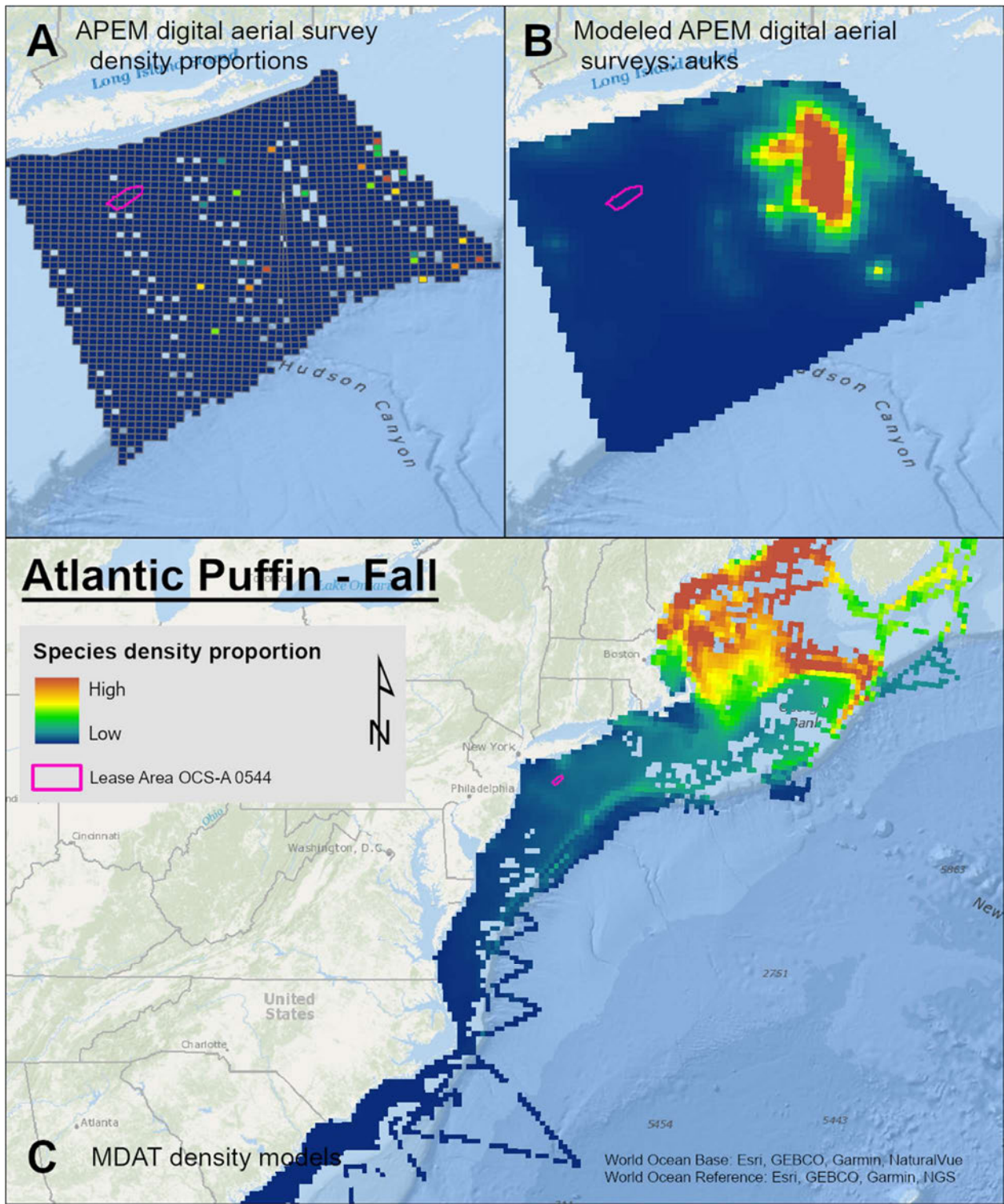
Map 77. Winter Atlantic Puffin density proportions in the NYSERDA APEM and Empire Wind high resolution digital aerial survey data (A), the NYSERDA APEM and Empire Wind high resolution digital aerial model outputs for auks in Winter (B) and, Winter Atlantic Puffin MDAT modeled abundance at the regional scale (C). The scale for all maps is representative of relative spatial variation in the sites within the season for each map input.



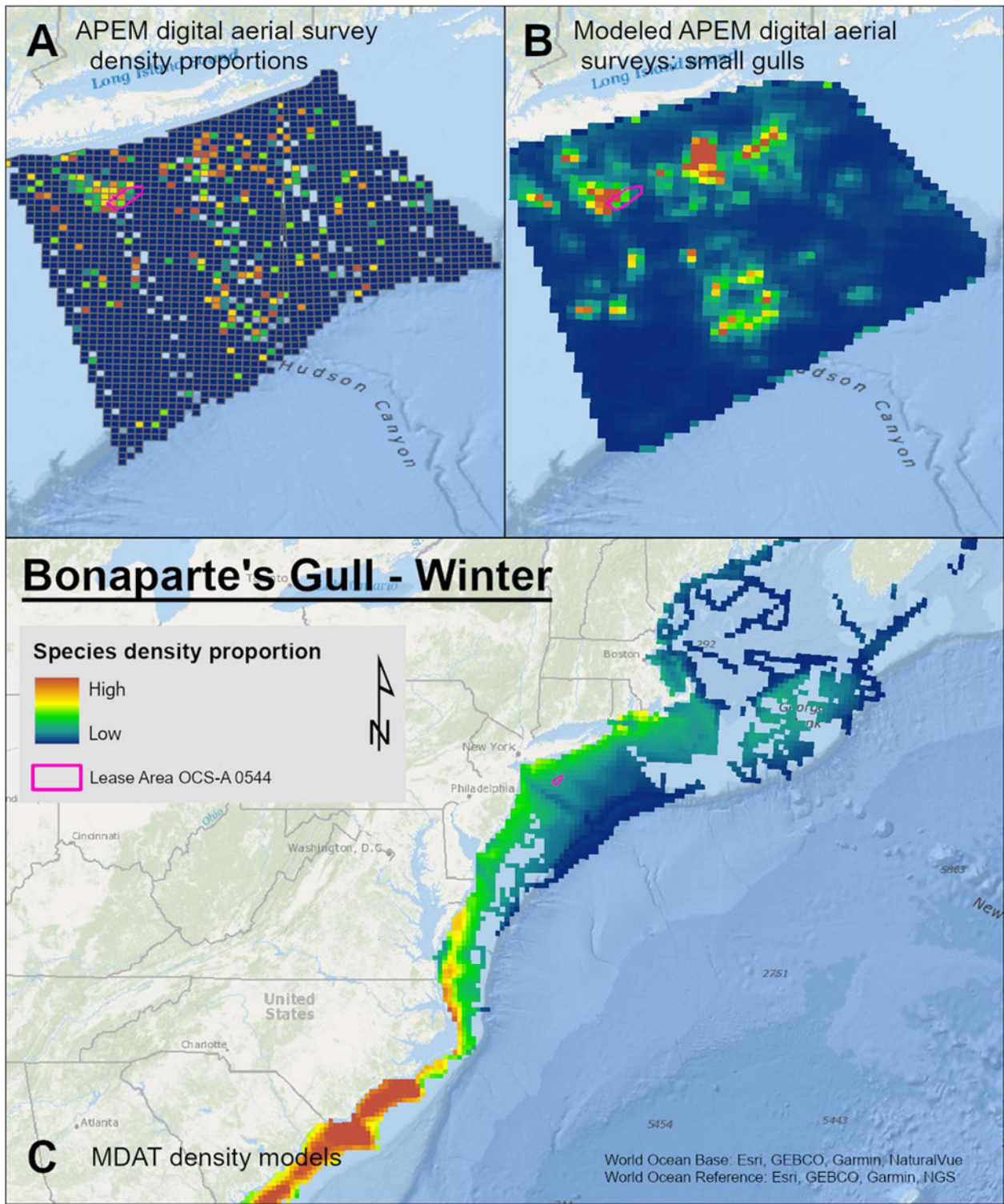
Map 78. Spring Atlantic Puffin density proportions in the NYSERDA APEM and Empire Wind high resolution digital aerial survey data (A), the NYSERDA APEM and Empire Wind high resolution digital aerial model outputs for auks in Spring (B) and, Spring Atlantic Puffin MDAT modeled abundance at the regional scale (C). The scale for all maps is representative of relative spatial variation in the sites within the season for each map input.



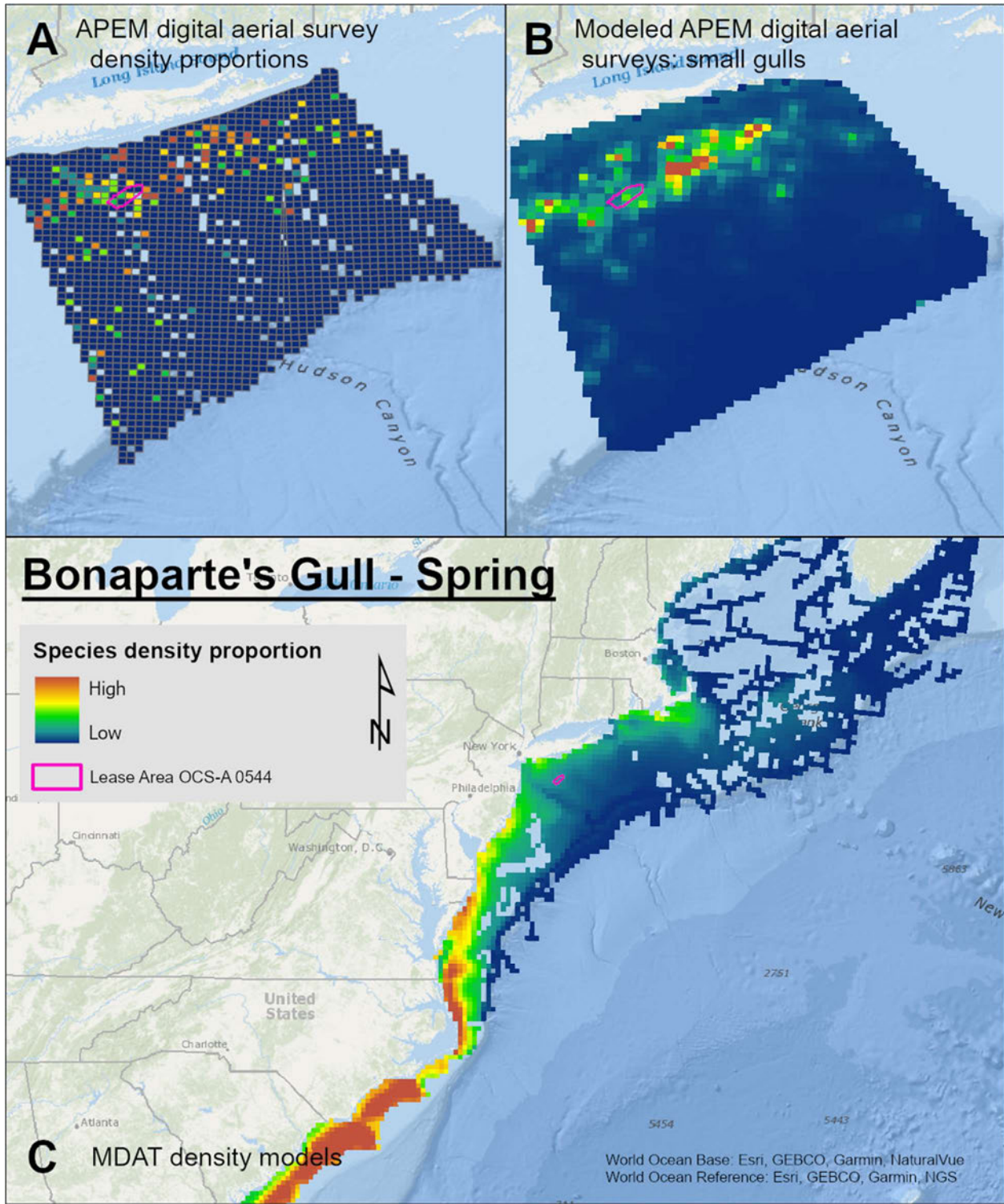
Map 79. Summer Atlantic Puffin density proportions in the NYSERDA APEM and Empire Wind high resolution digital aerial survey data (A), the NYSERDA APEM and Empire Wind high resolution digital aerial model outputs for auks in Summer (B) and, Summer Atlantic Puffin MDAT modeled abundance at the regional scale (C). The scale for all maps is representative of relative spatial variation in the sites within the season for each map input.



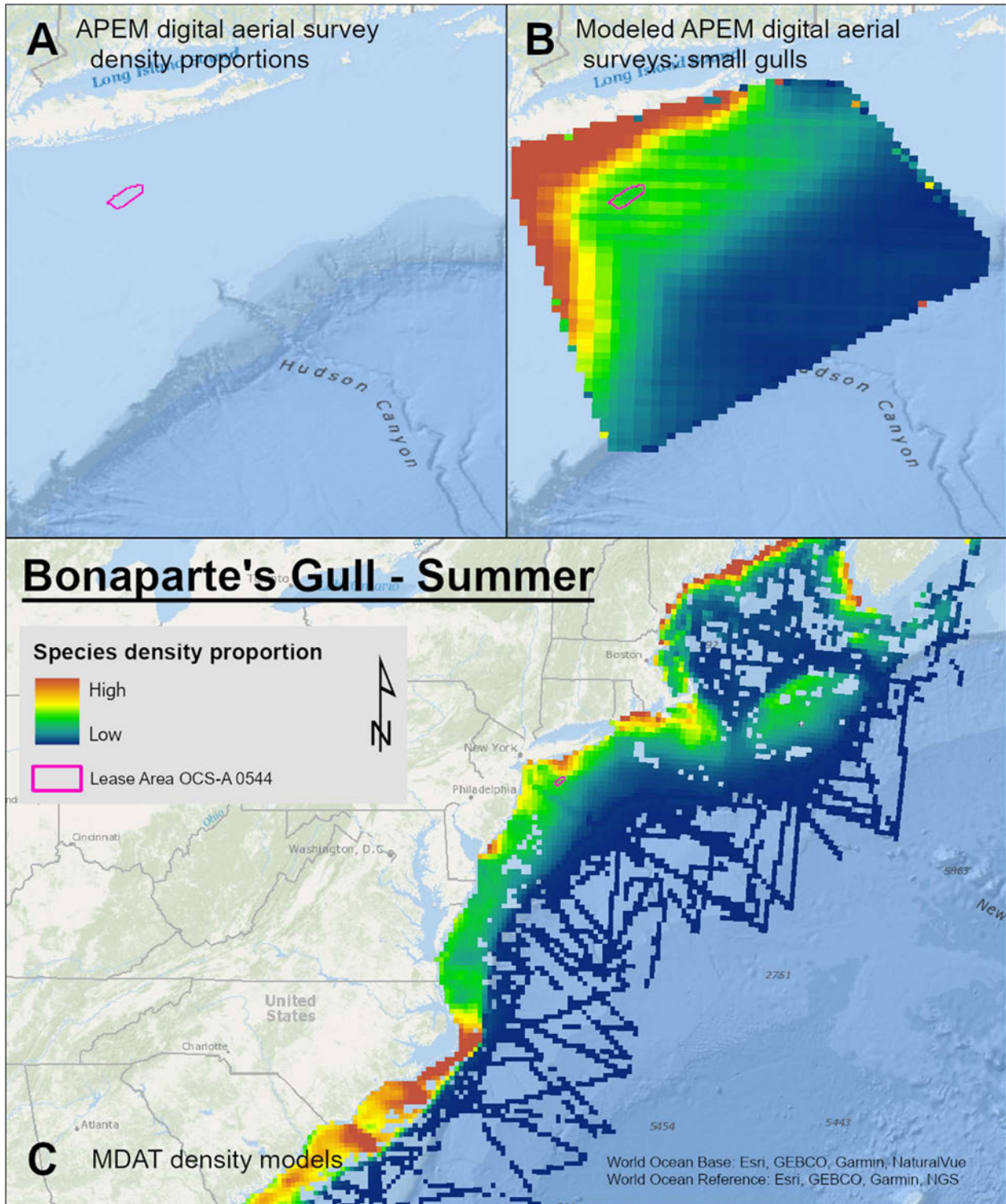
Map 80. Fall Atlantic Puffin density proportions in the NYSERDA APEM and Empire Wind high resolution digital aerial survey data (A), the NYSERDA APEM and Empire Wind high resolution digital aerial model outputs for auks in Fall (B) and, Fall Atlantic Puffin MDAT modeled abundance at the regional scale (C). The scale for all maps is representative of relative spatial variation in the sites within the season for each map input.



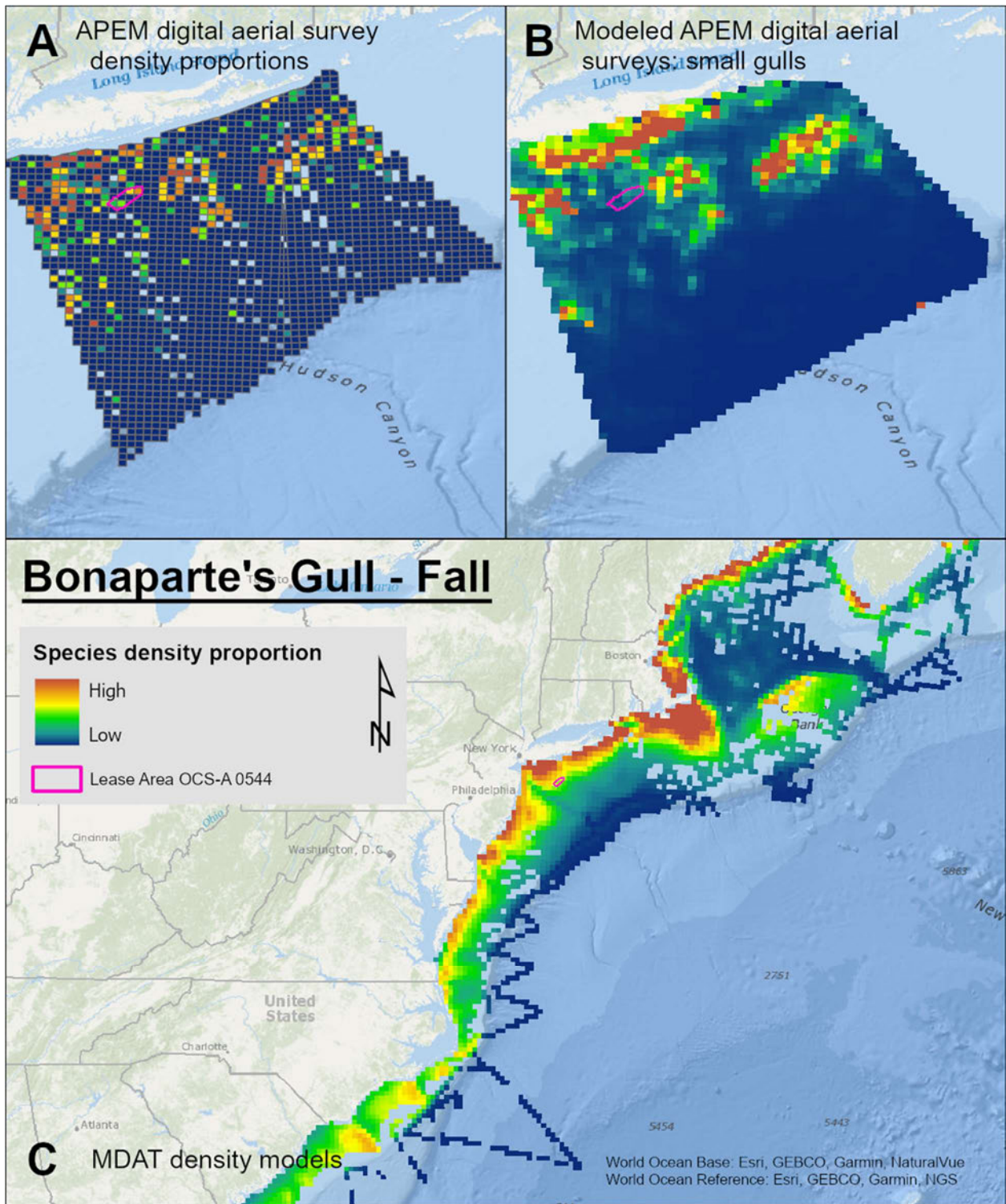
Map 81. Winter Bonaparte's Gull density proportions in the NYSERDA APEM and Empire Wind high resolution digital aerial survey data (A), the NYSERDA APEM and Empire Wind high resolution digital aerial model outputs for small gulls in Winter (B) and, Winter Bonaparte's Gull MDAT modeled abundance at the regional scale (C). The scale for all maps is representative of relative spatial variation in the sites within the season for each map input.



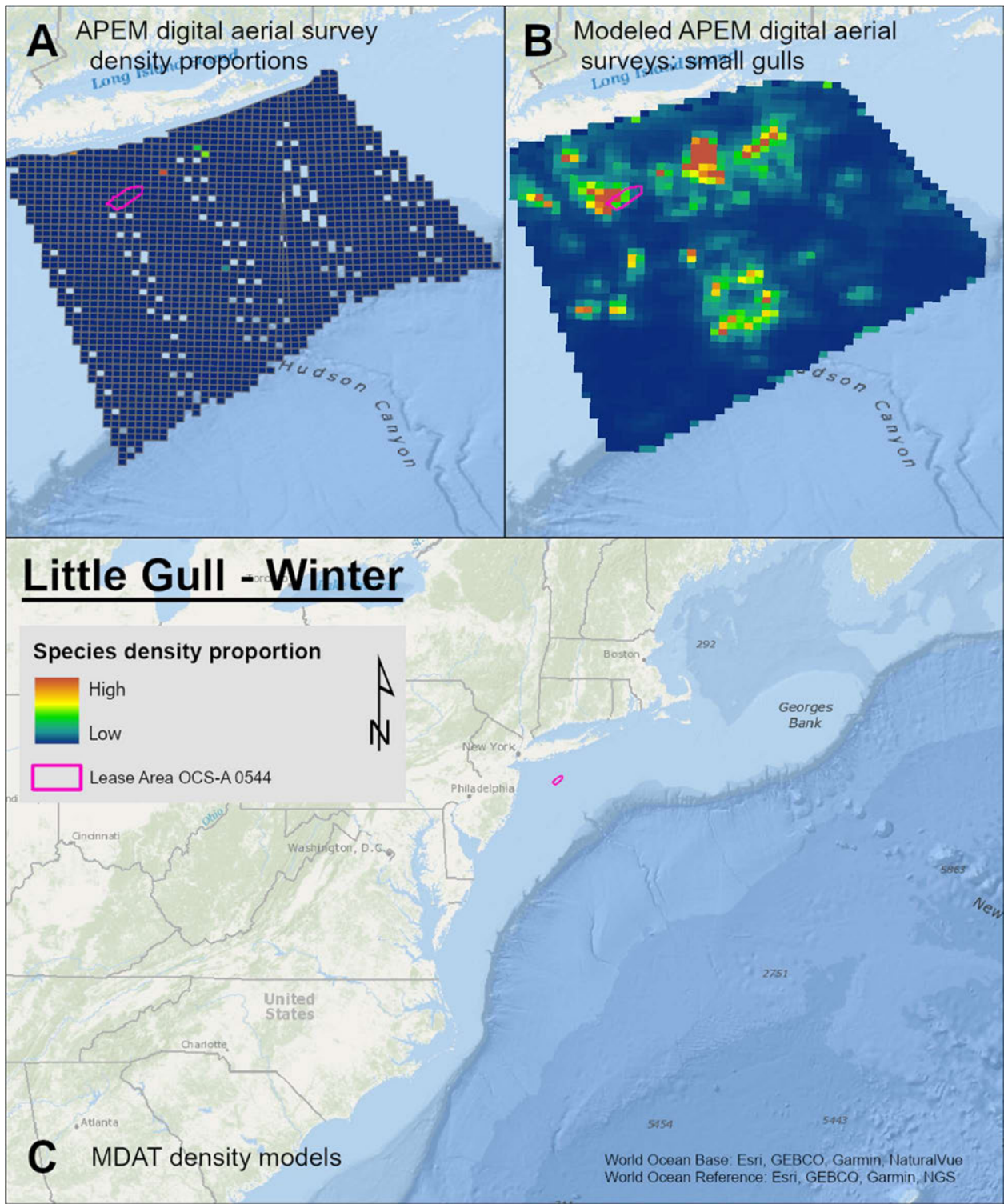
Map 82. Spring Bonaparte's Gull density proportions in the NYSERDA APEM and Empire Wind high resolution digital aerial survey data (A), the NYSERDA APEM and Empire Wind high resolution digital aerial model outputs for small gulls in Spring (B) and, Spring Bonaparte's Gull MDAT modeled abundance at the regional scale (C). The scale for all maps is representative of relative spatial variation in the sites within the season for each map input.



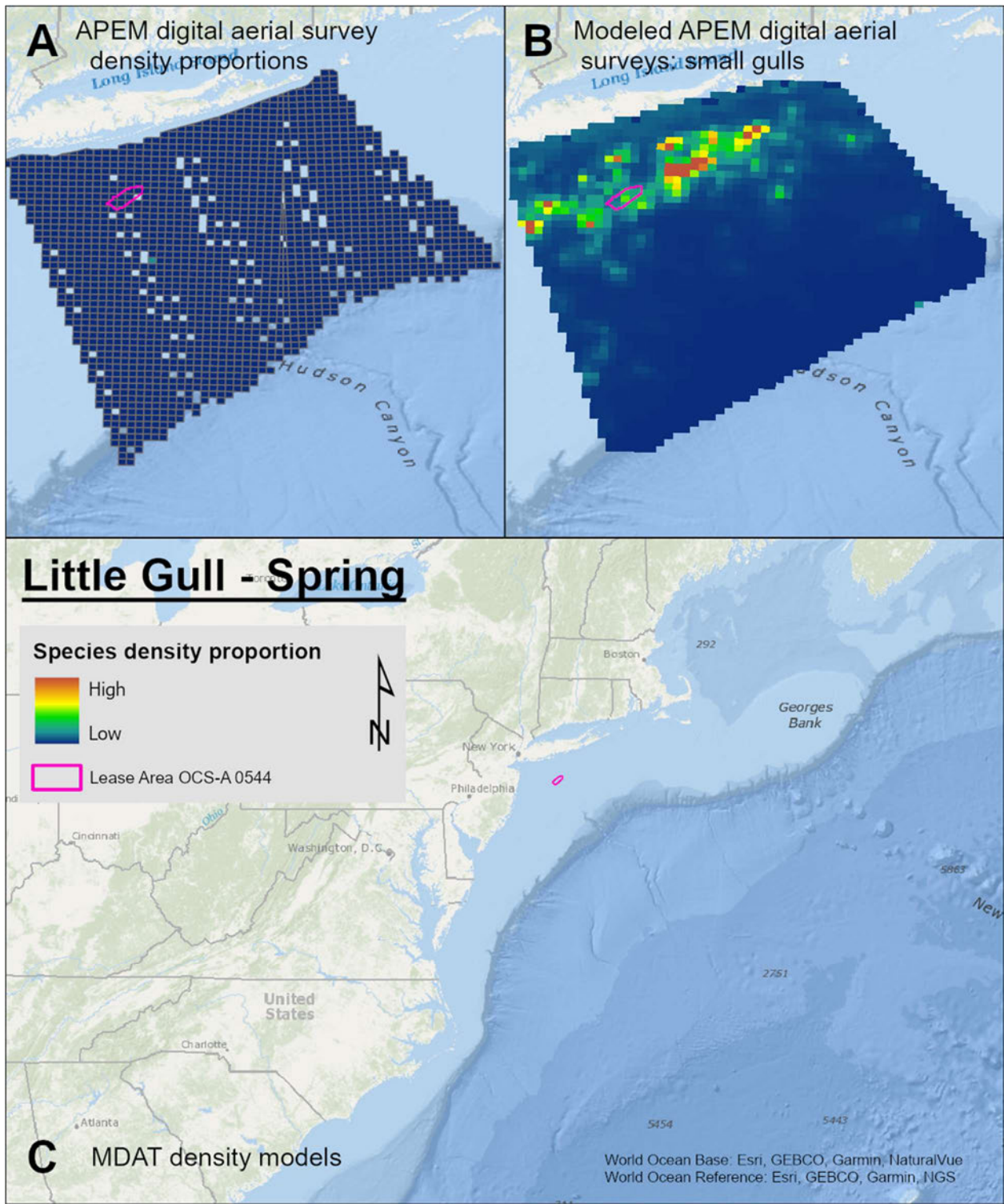
Map 83. Summer Bonaparte's Gull density proportions in the NYSERDA APEM and Empire Wind high resolution digital aerial survey data (A), the NYSERDA APEM and Empire Wind high resolution digital aerial model outputs for small gulls in Summer (B) and, Summer Bonaparte's Gull MDAT modeled abundance at the regional scale (C). The scale for all maps is representative of relative spatial variation in the sites within the season for each map input.



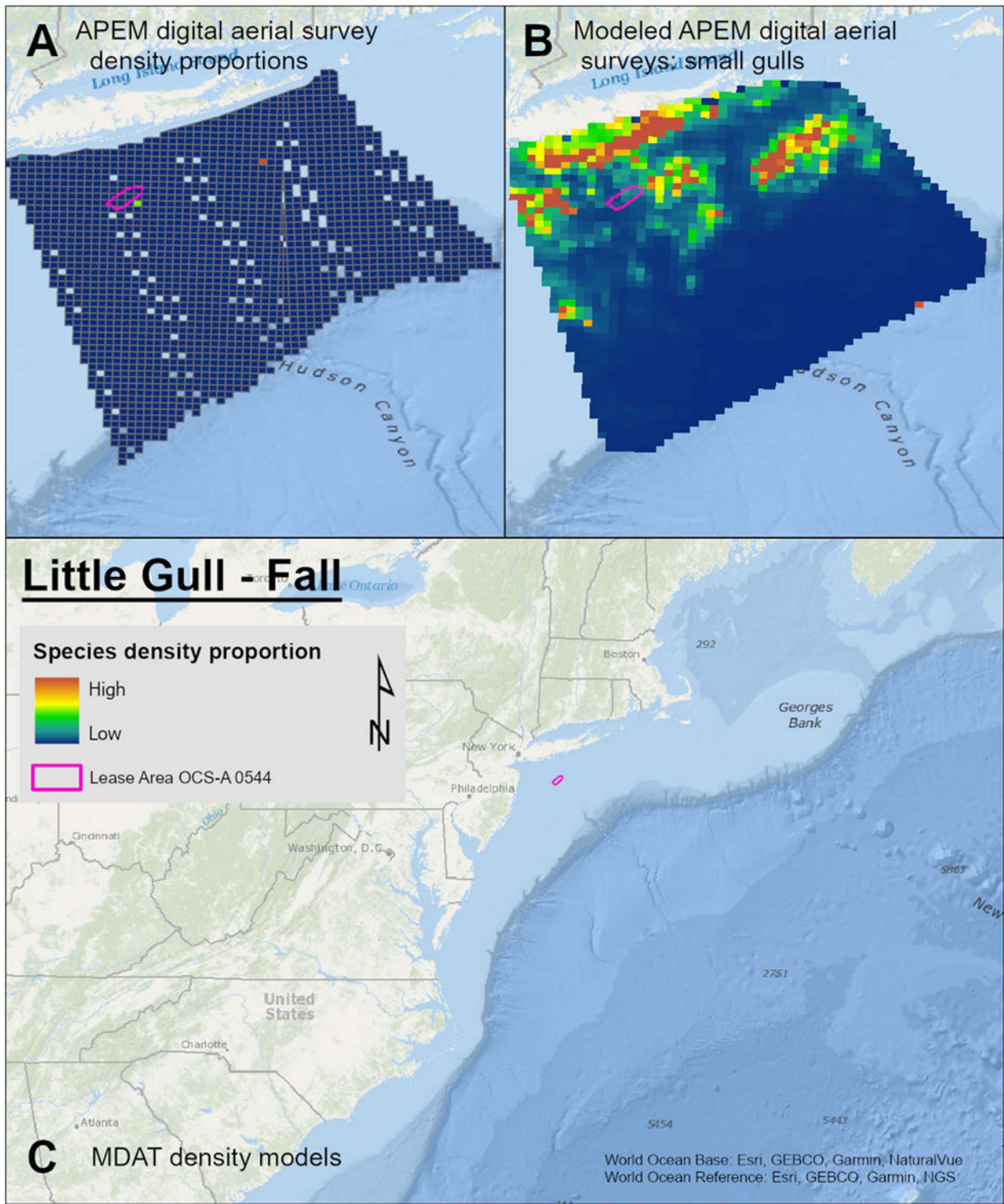
Map 84. Fall Bonaparte's Gull density proportions in the NYSERDA APEM and Empire Wind high resolution digital aerial survey data (A), the NYSERDA APEM and Empire Wind high resolution digital aerial model outputs for small gulls in Fall (B) and, Fall Bonaparte's Gull MDAT modeled abundance at the regional scale (C). The scale for all maps is representative of relative spatial variation in the sites within the season for each map input.



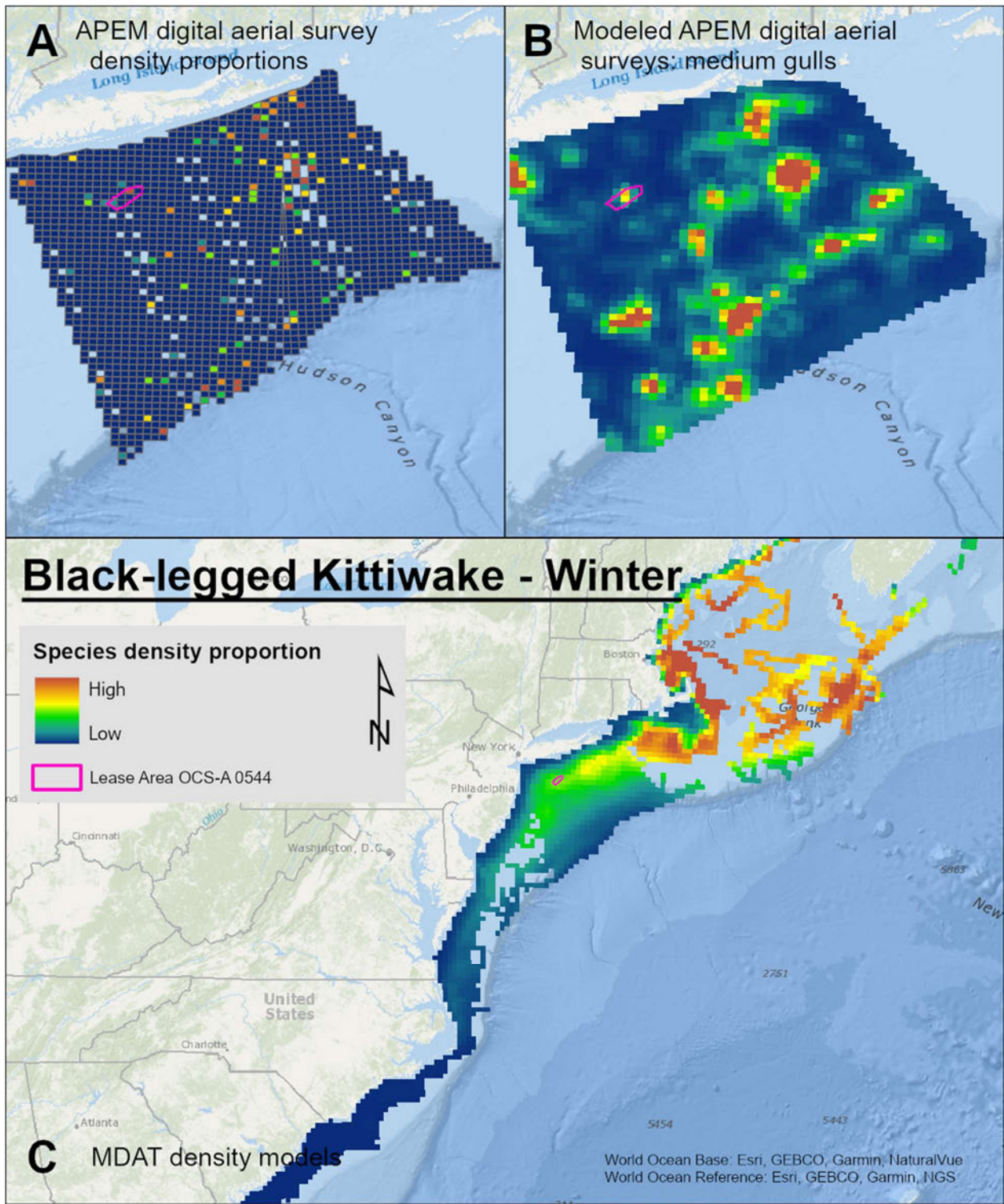
Map 85. Winter Little Gull density proportions in the NYSERDA APEM and Empire Wind high resolution digital aerial survey data (A), the NYSERDA APEM and Empire Wind high resolution digital aerial model outputs for small gulls in Winter (B) and, Winter Little Gull MDAT modeled abundance at the regional scale (C). The scale for all maps is representative of relative spatial variation in the sites within the season for each map input.



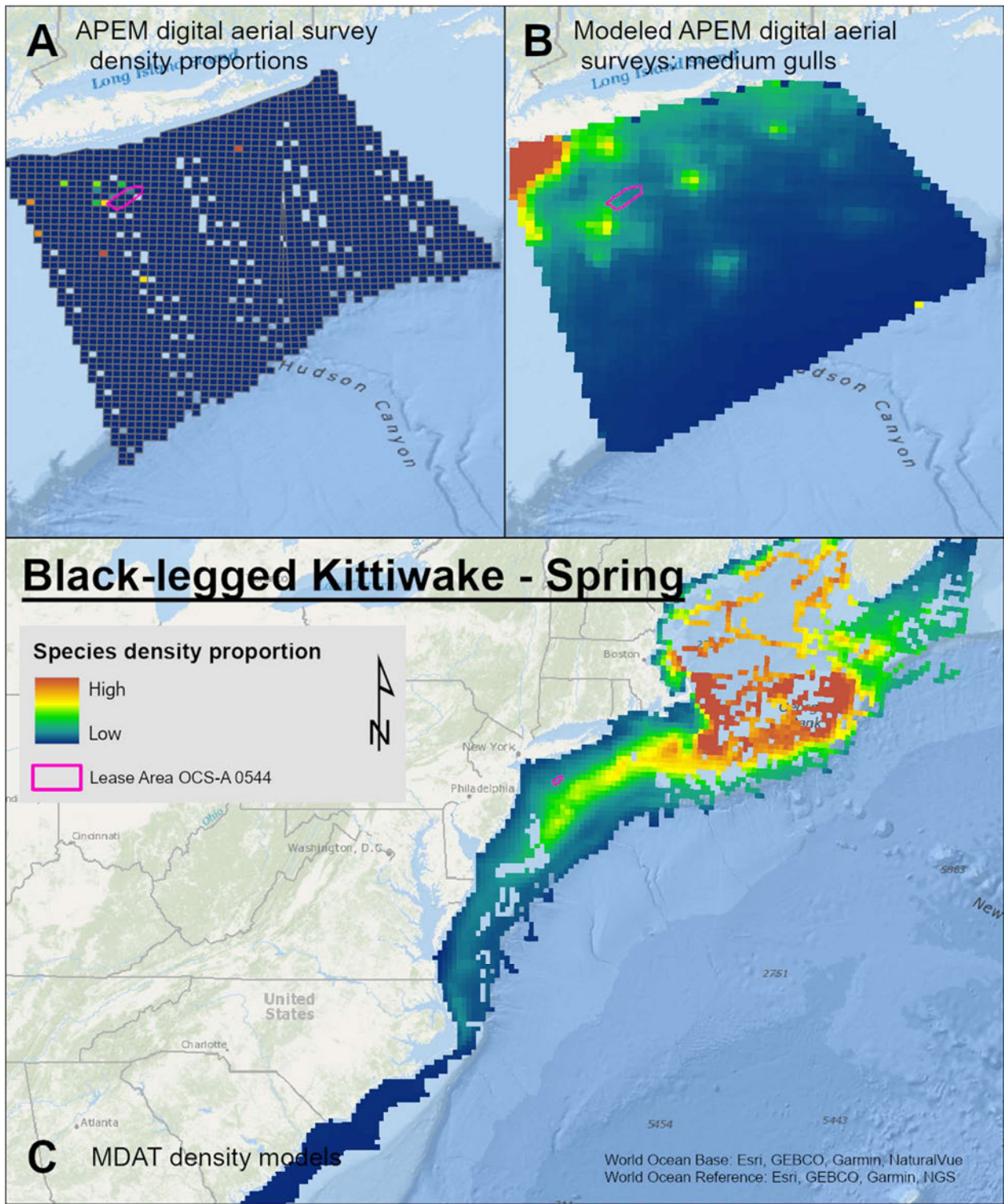
Map 86. Spring Little Gull density proportions in the NYSDERA APEM and Empire Wind high resolution digital aerial survey data (A), the NYSDERA APEM and Empire Wind high resolution digital aerial model outputs for small gulls in Spring (B) and, Spring Little Gull MDAT modeled abundance at the regional scale (C). The scale for all maps is representative of relative spatial variation in the sites within the season for each map input.



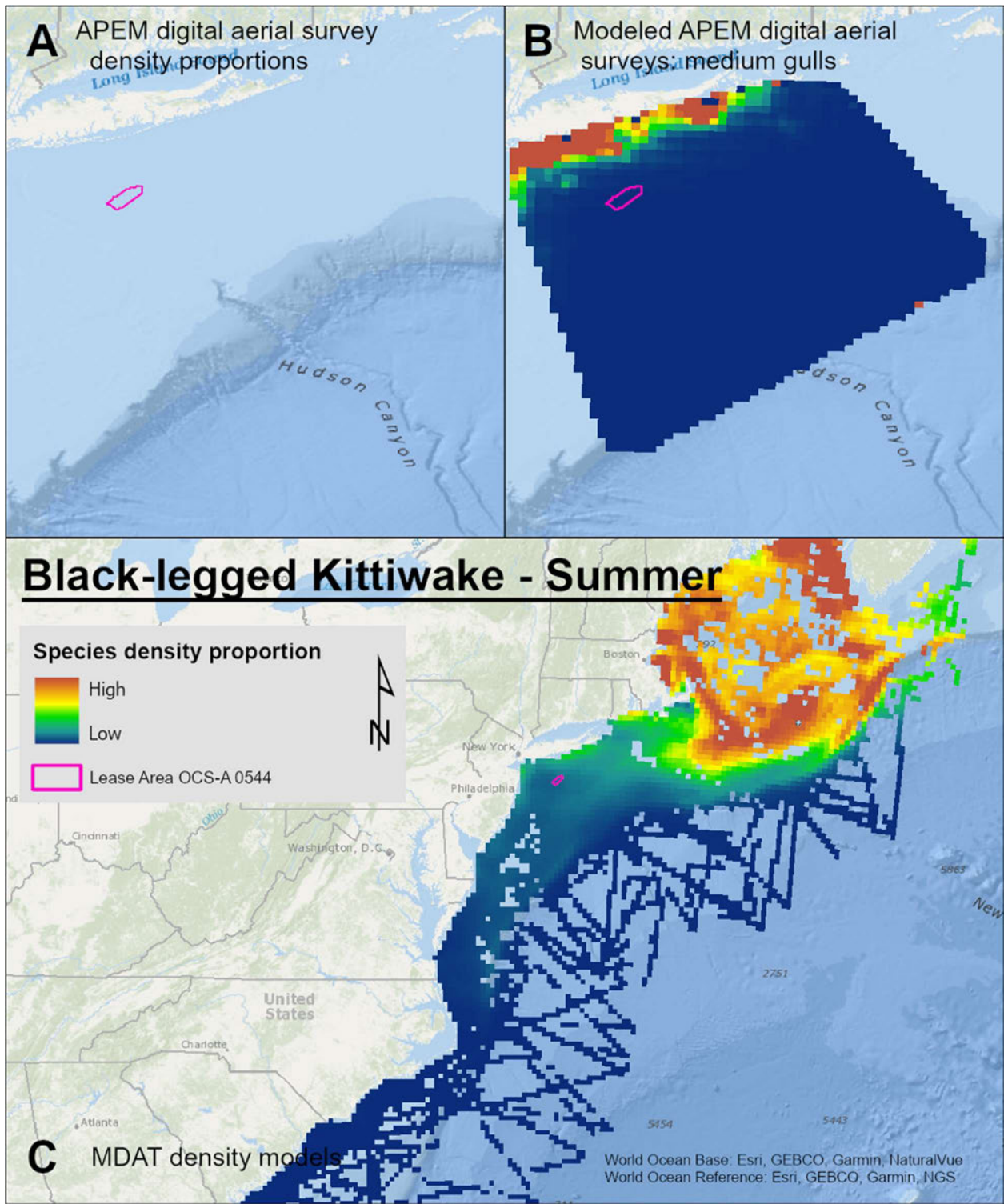
Map 87. Fall Little Gull density proportions in the NYSERDA APEM and Empire Wind high resolution digital aerial survey data (A), the NYSERDA APEM and Empire Wind high resolution digital aerial model outputs for small gulls in Fall (B) and, Fall Little Gull MDAT modeled abundance at the regional scale (C). The scale for all maps is representative of relative spatial variation in the sites within the season for each map input.



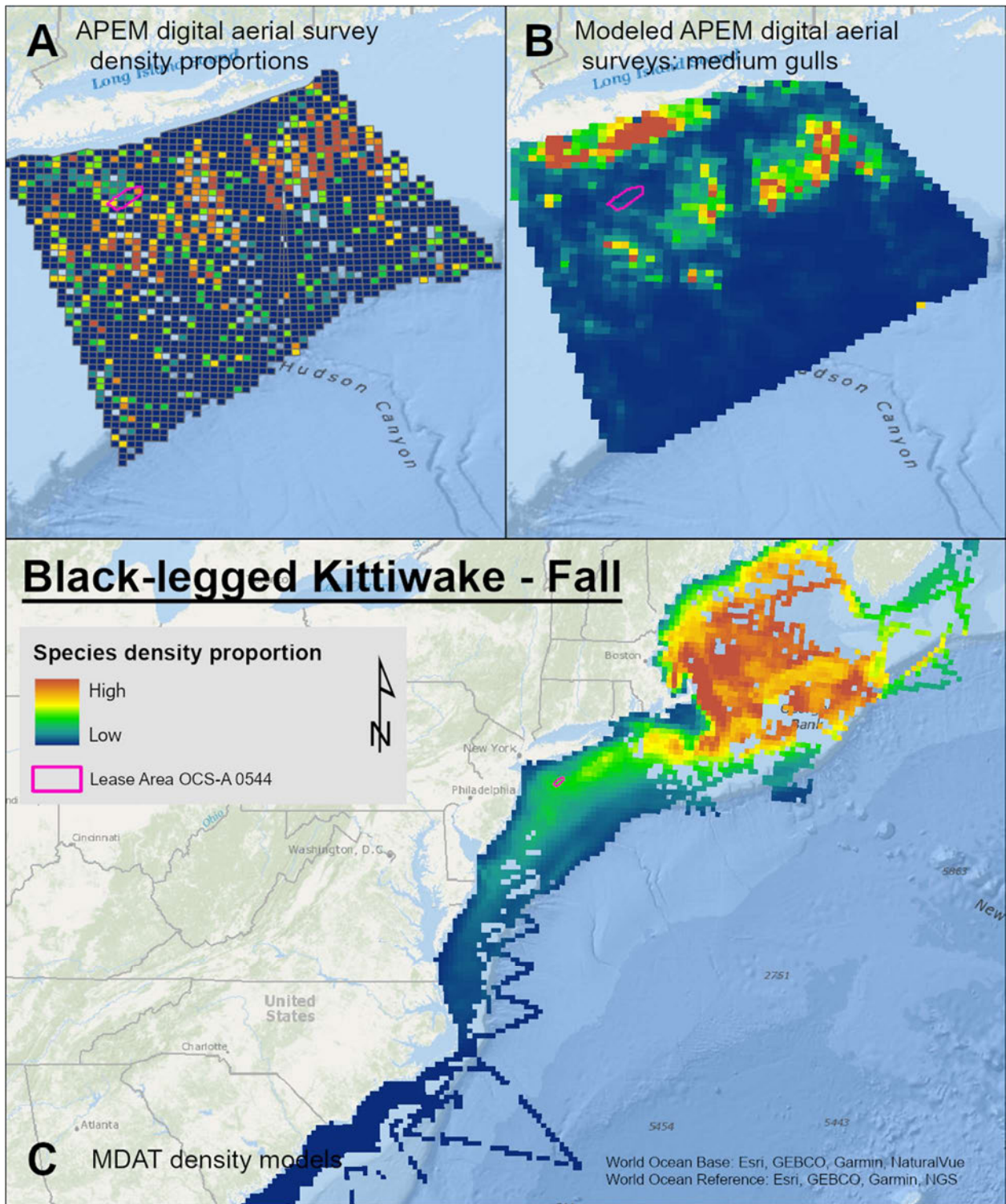
Map 88. Winter Black-legged Kittiwake density proportions in the NYSERDA APEM and Empire Wind high resolution digital aerial survey data (A), the NYSERDA APEM and Empire Wind high resolution digital aerial model outputs for medium gulls in Winter (B) and, Winter Black-legged Kittiwake MDAT modeled abundance at the regional scale (C). The scale for all maps is representative of relative spatial variation in the sites within the season for each map input.



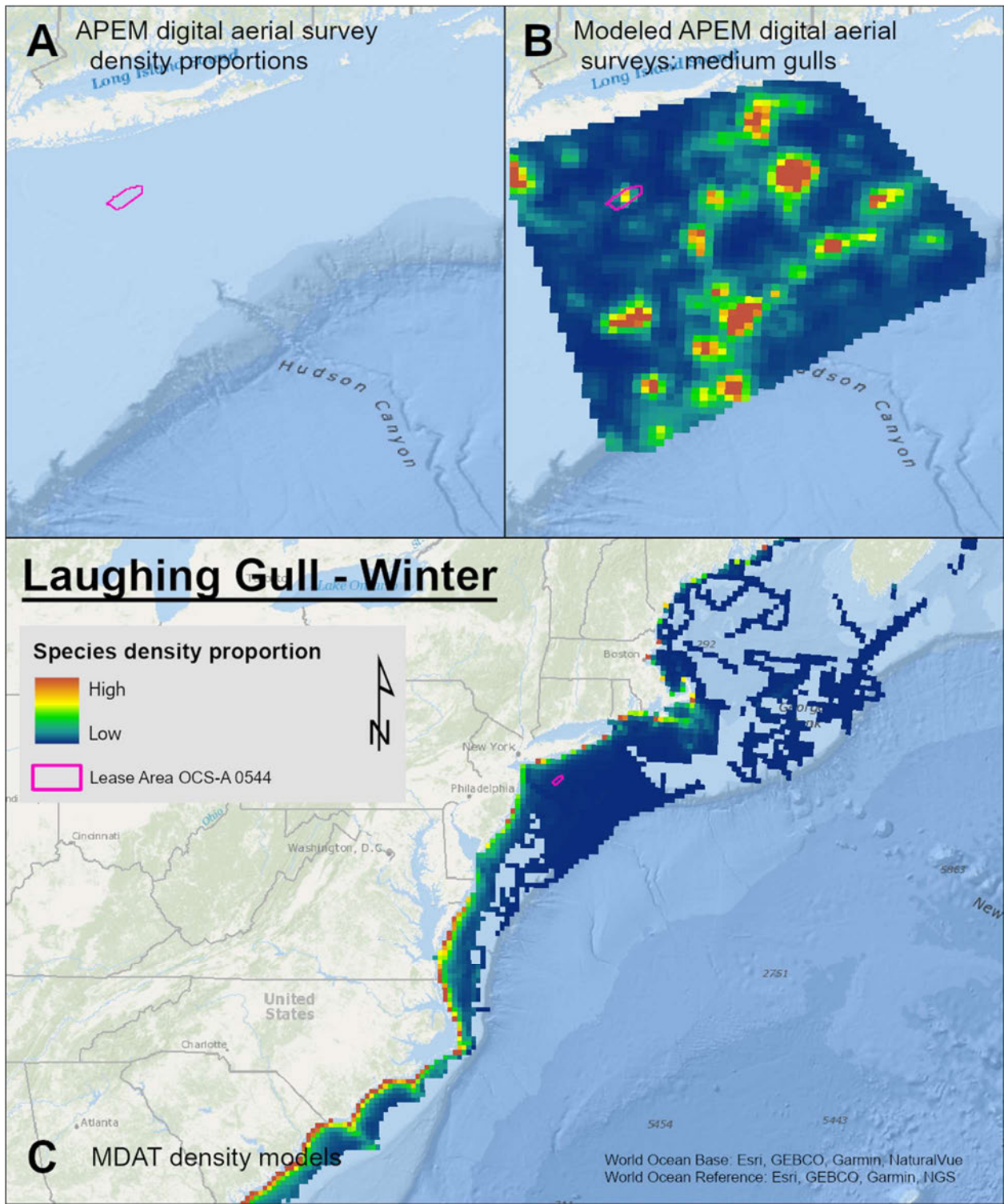
Map 89. Spring Black-legged Kittiwake density proportions in the NYSERDA APEM and Empire Wind high resolution digital aerial survey data (A), the NYSERDA APEM and Empire Wind high resolution digital aerial model outputs for medium gulls in Spring (B) and, Spring Black-legged Kittiwake MDAT modeled abundance at the regional scale (C). The scale for all maps is representative of relative spatial variation in the sites within the season for each map input.



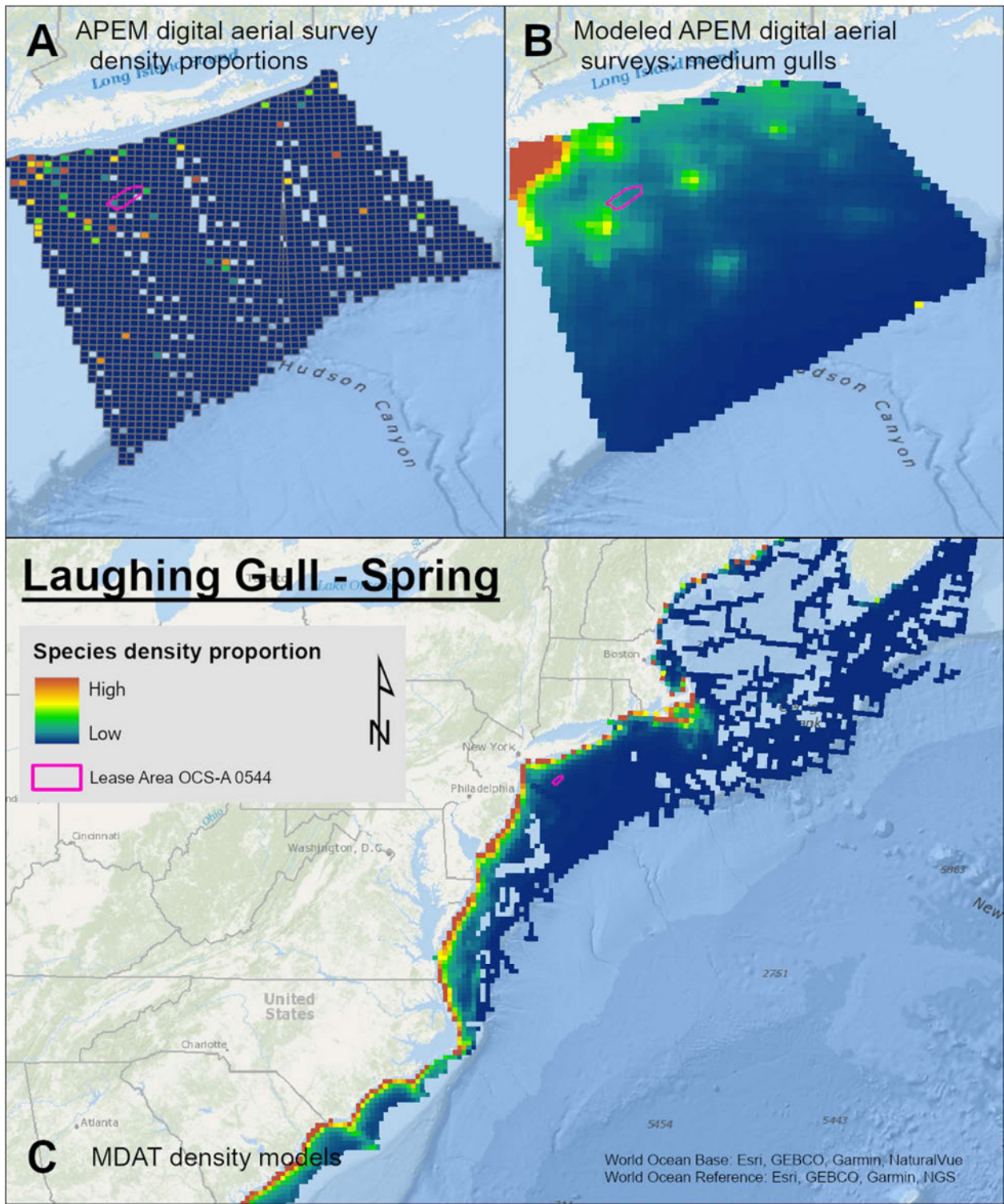
Map 90. Summer Black-legged Kittiwake density proportions in the NYSERDA APEM and Empire Wind high resolution digital aerial survey data (A), the NYSERDA APEM and Empire Wind high resolution digital aerial model outputs for medium gulls in Summer (B) and, Summer Black-legged Kittiwake MDAT modeled abundance at the regional scale (C). The scale for all maps is representative of relative spatial variation in the sites within the season for each map input.



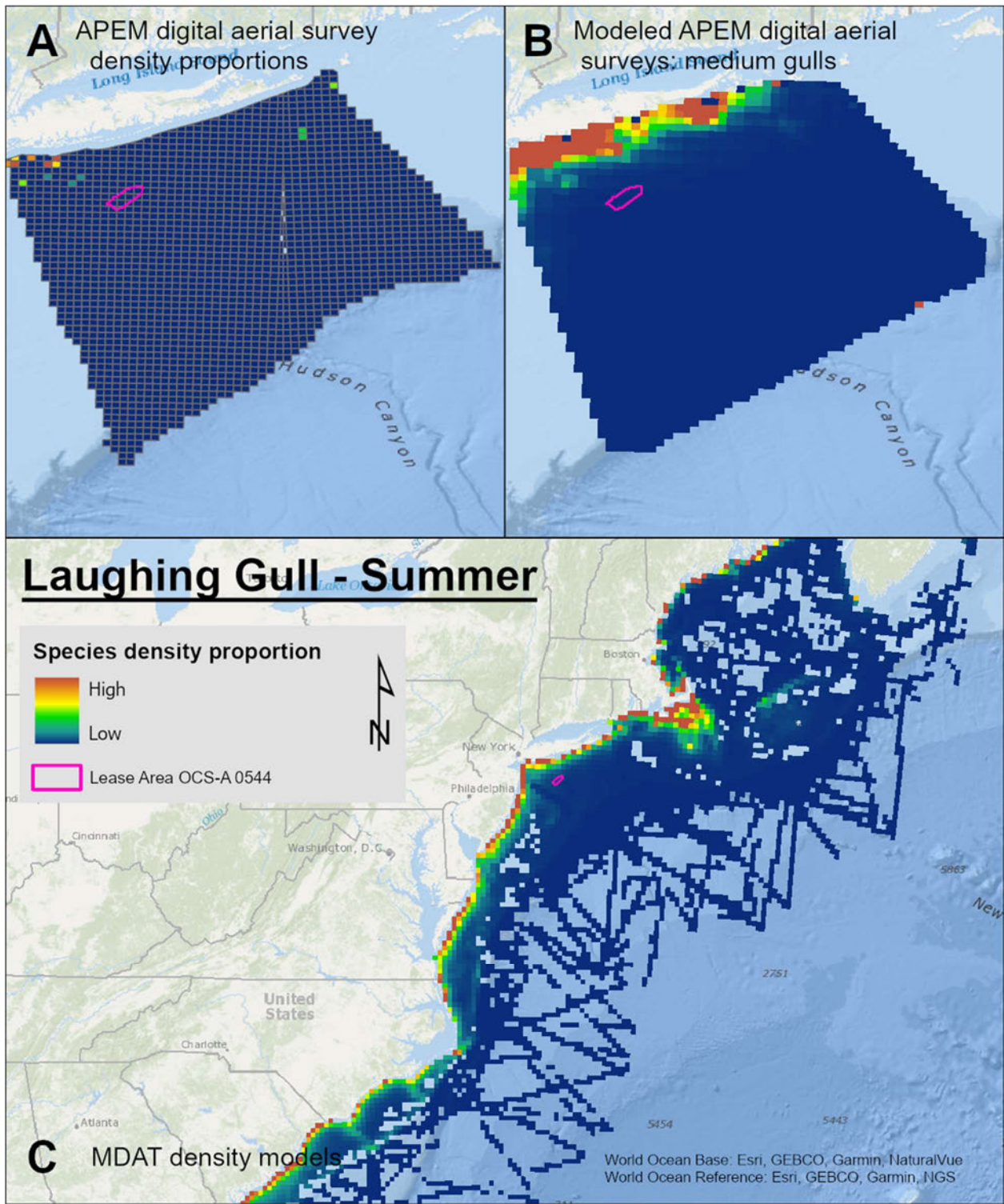
Map 91. Fall Black-legged Kittiwake density proportions in the NYSERDA APEM and Empire Wind high resolution digital aerial survey data (A), the NYSERDA APEM and Empire Wind high resolution digital aerial model outputs for medium gulls in Fall (B) and, Fall Black-legged Kittiwake MDAT modeled abundance at the regional scale (C). The scale for all maps is representative of relative spatial variation in the sites within the season for each map input.



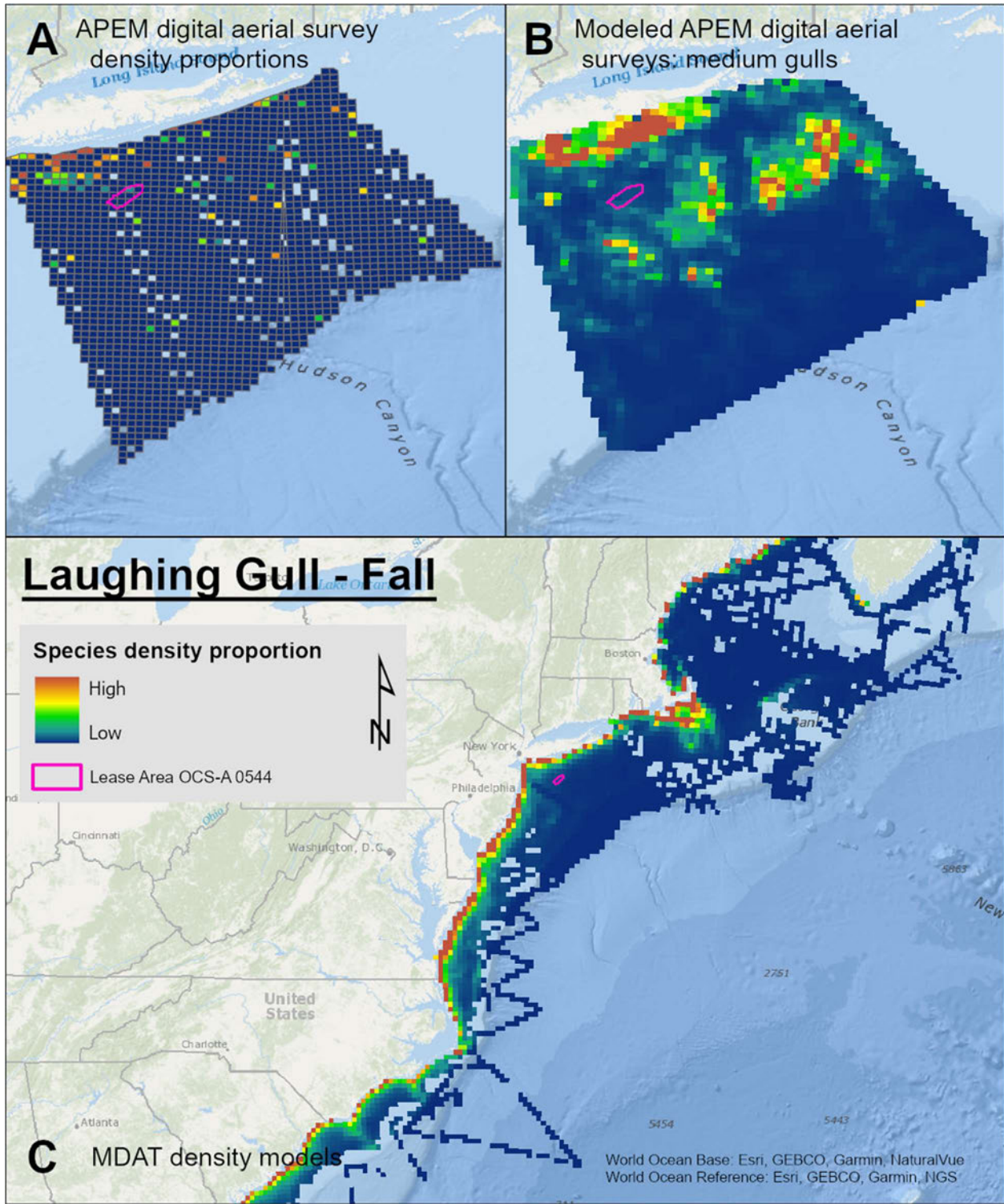
Map 92. Winter Laughing Gull density proportions in the NYSERDA APEM and Empire Wind high resolution digital aerial survey data (A), the NYSERDA APEM and Empire Wind high resolution digital aerial model outputs for medium gulls in Winter (B) and, Winter Laughing Gull MDAT modeled abundance at the regional scale (C). The scale for all maps is representative of relative spatial variation in the sites within the season for each map input.



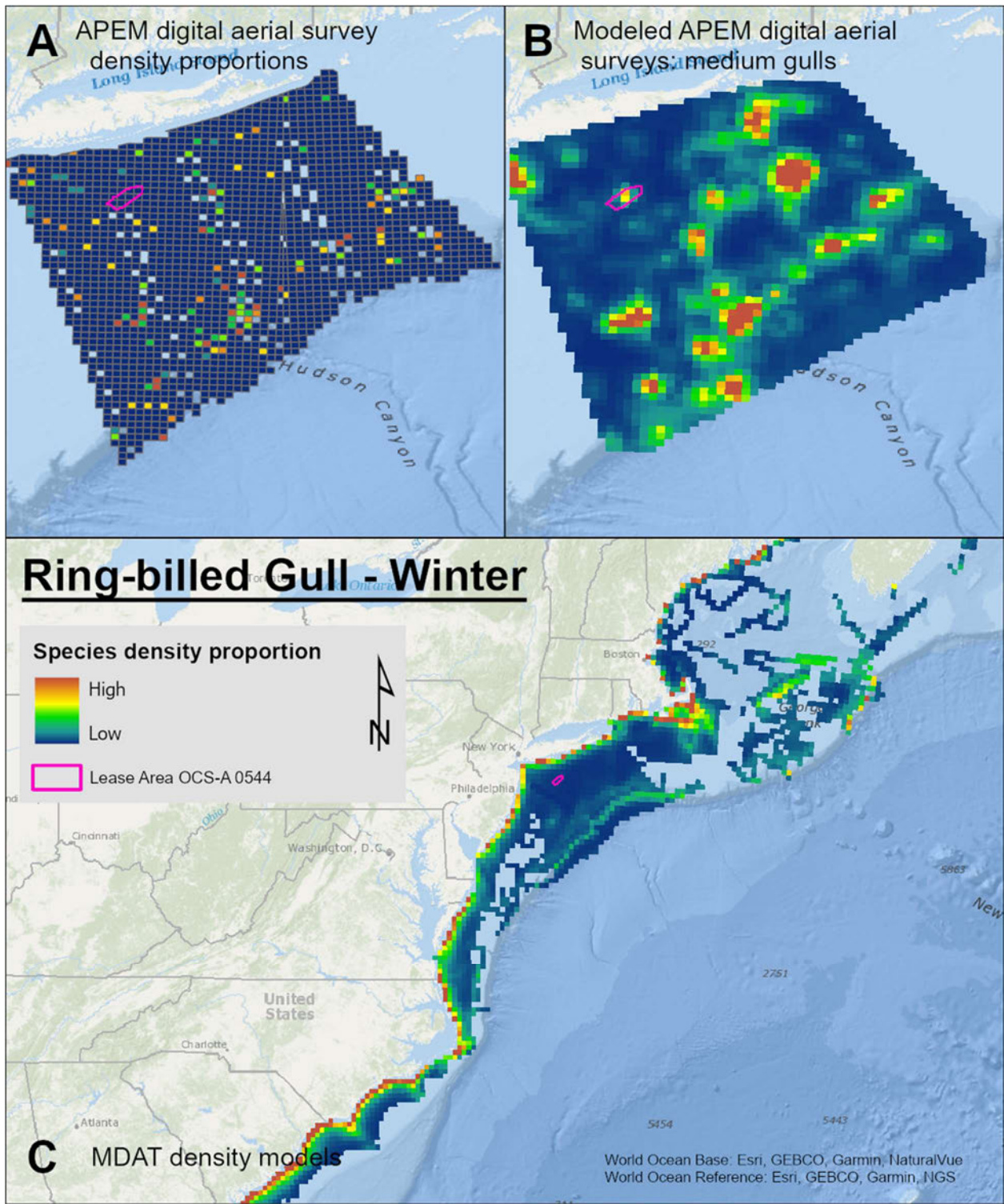
Map 93. Spring Laughing Gull density proportions in the NYSEERDA APEM and Empire Wind high resolution digital aerial survey data (A), the NYSEERDA APEM and Empire Wind high resolution digital aerial model outputs for medium gulls in Spring (B) and, Spring Laughing Gull MDAT modeled abundance at the regional scale (C). The scale for all maps is representative of relative spatial variation in the sites within the season for each map input.



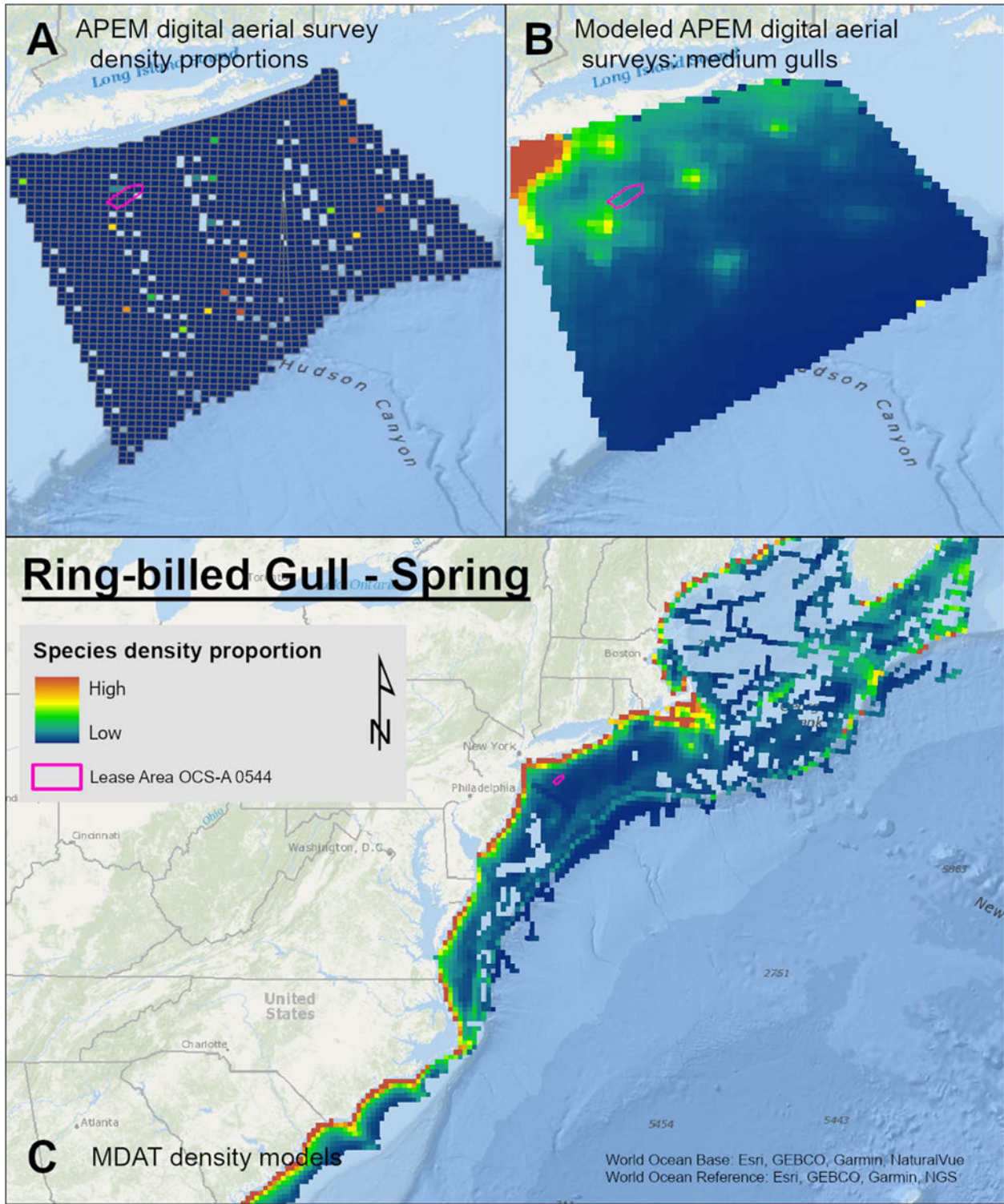
Map 94. Summer Laughing Gull density proportions in the NYSERDA APEM and Empire Wind high resolution digital aerial survey data (A), the NYSERDA APEM and Empire Wind high resolution digital aerial model outputs for medium gulls in Summer (B) and, Summer Laughing Gull MDAT modeled abundance at the regional scale (C). The scale for all maps is representative of relative spatial variation in the sites within the season for each map input.



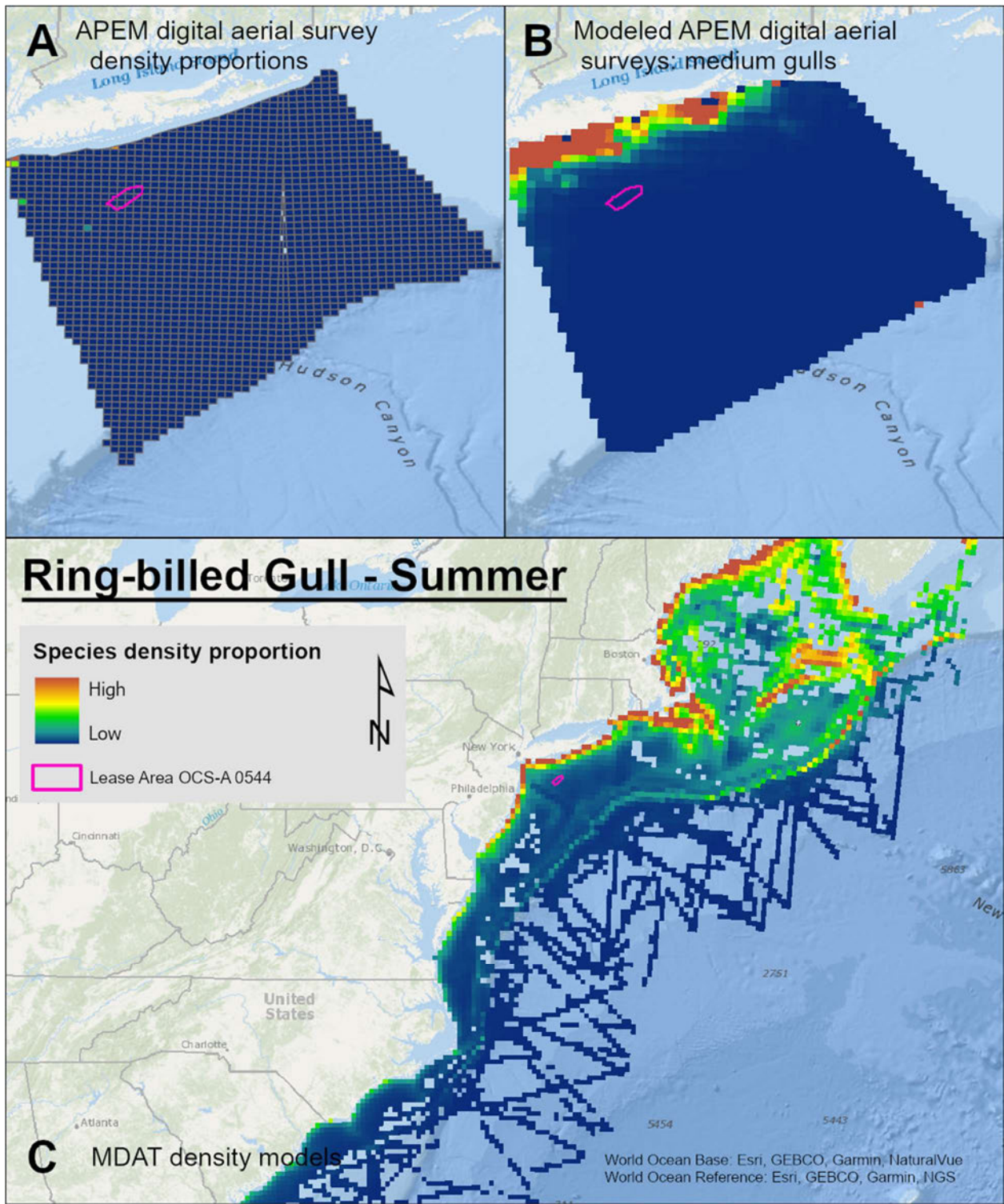
Map 95. Fall Laughing Gull density proportions in the NYSERDA APEM and Empire Wind high resolution digital aerial survey data (A), the NYSERDA APEM and Empire Wind high resolution digital aerial model outputs for medium gulls in Fall (B) and, Fall Laughing Gull MDAT modeled abundance at the regional scale (C). The scale for all maps is representative of relative spatial variation in the sites within the season for each map input.



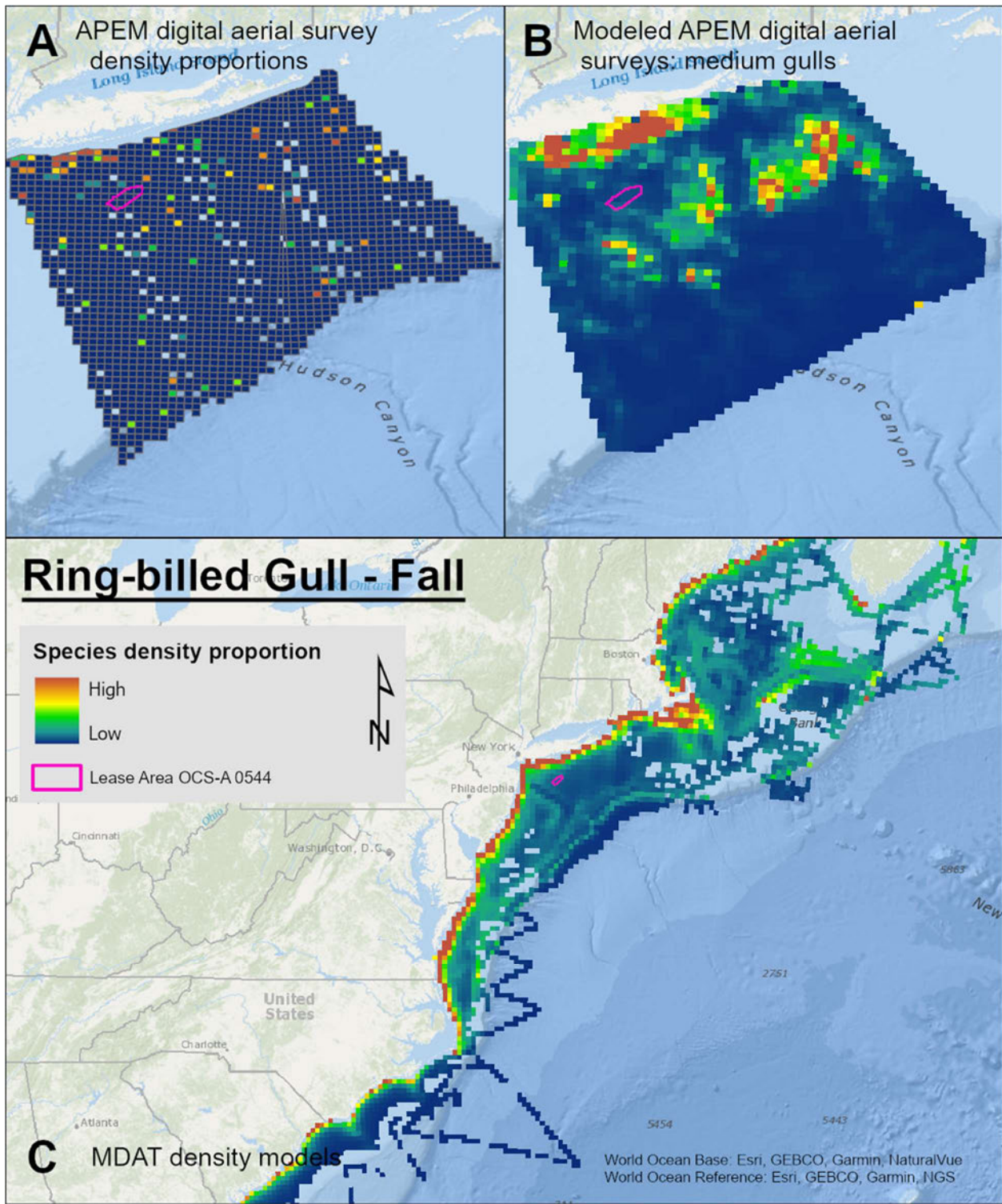
Map 96. Winter Ring-billed Gull density proportions in the NYSERDA APEM and Empire Wind high resolution digital aerial survey data (A), the NYSERDA APEM and Empire Wind high resolution digital aerial model outputs for medium gulls in Winter (B) and, Winter Ring-billed Gull MDAT modeled abundance at the regional scale (C). The scale for all maps is representative of relative spatial variation in the sites within the season for each map input.



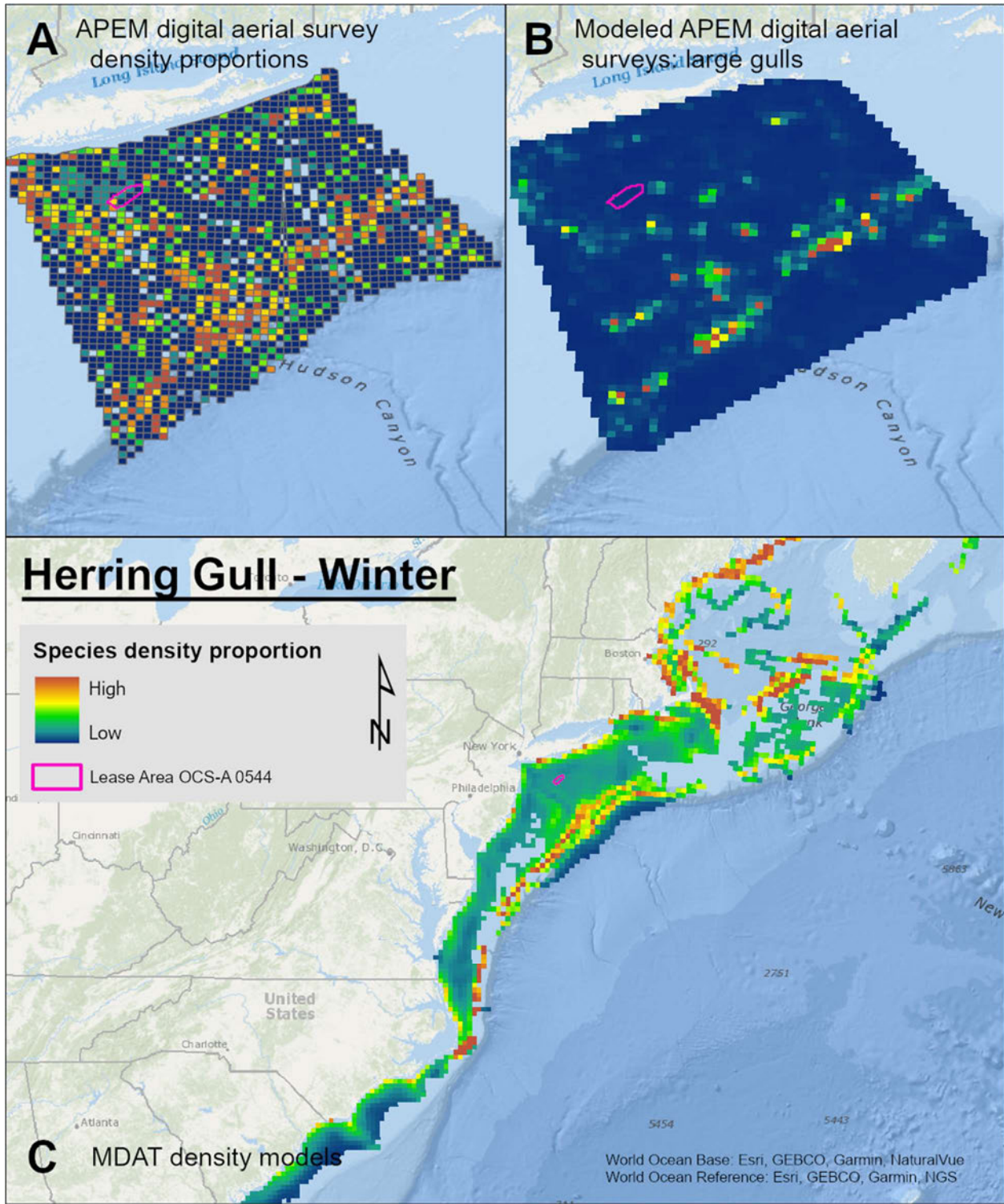
Map 97. Spring Ring-billed Gull density proportions in the NYSEDA APEM and Empire Wind high resolution digital aerial survey data (A), the NYSEDA APEM and Empire Wind high resolution digital aerial model outputs for medium gulls in Spring (B) and, Spring Ring-billed Gull MDAT modeled abundance at the regional scale (C). The scale for all maps is representative of relative spatial variation in the sites within the season for each map input.



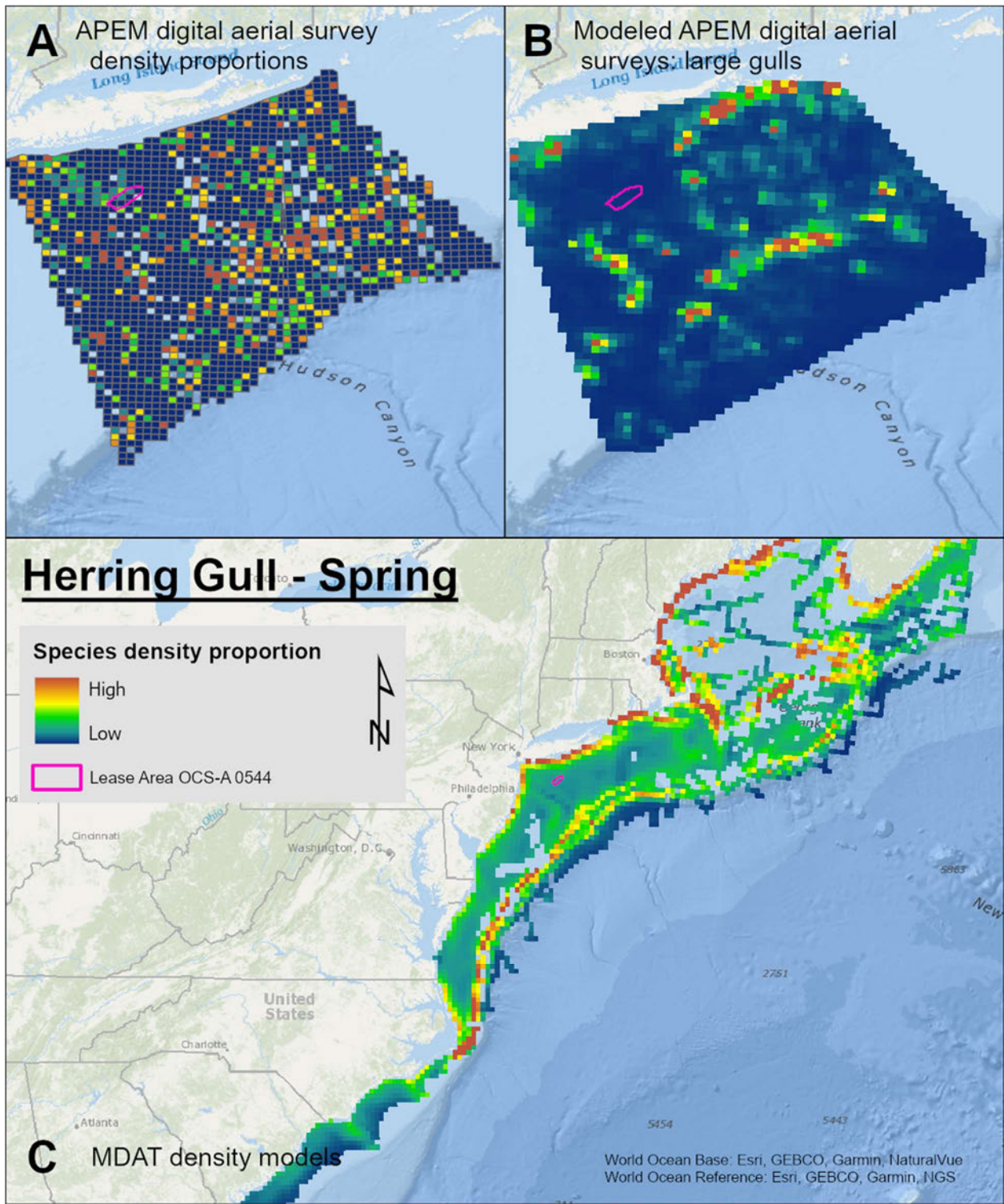
Map 98. Summer Ring-billed Gull density proportions in the NYSERDA APEM and Empire Wind high resolution digital aerial survey data (A), the NYSERDA APEM and Empire Wind high resolution digital aerial model outputs for medium gulls in Summer (B) and, Summer Ring-billed Gull MDAT modeled abundance at the regional scale (C). The scale for all maps is representative of relative spatial variation in the sites within the season for each map input.



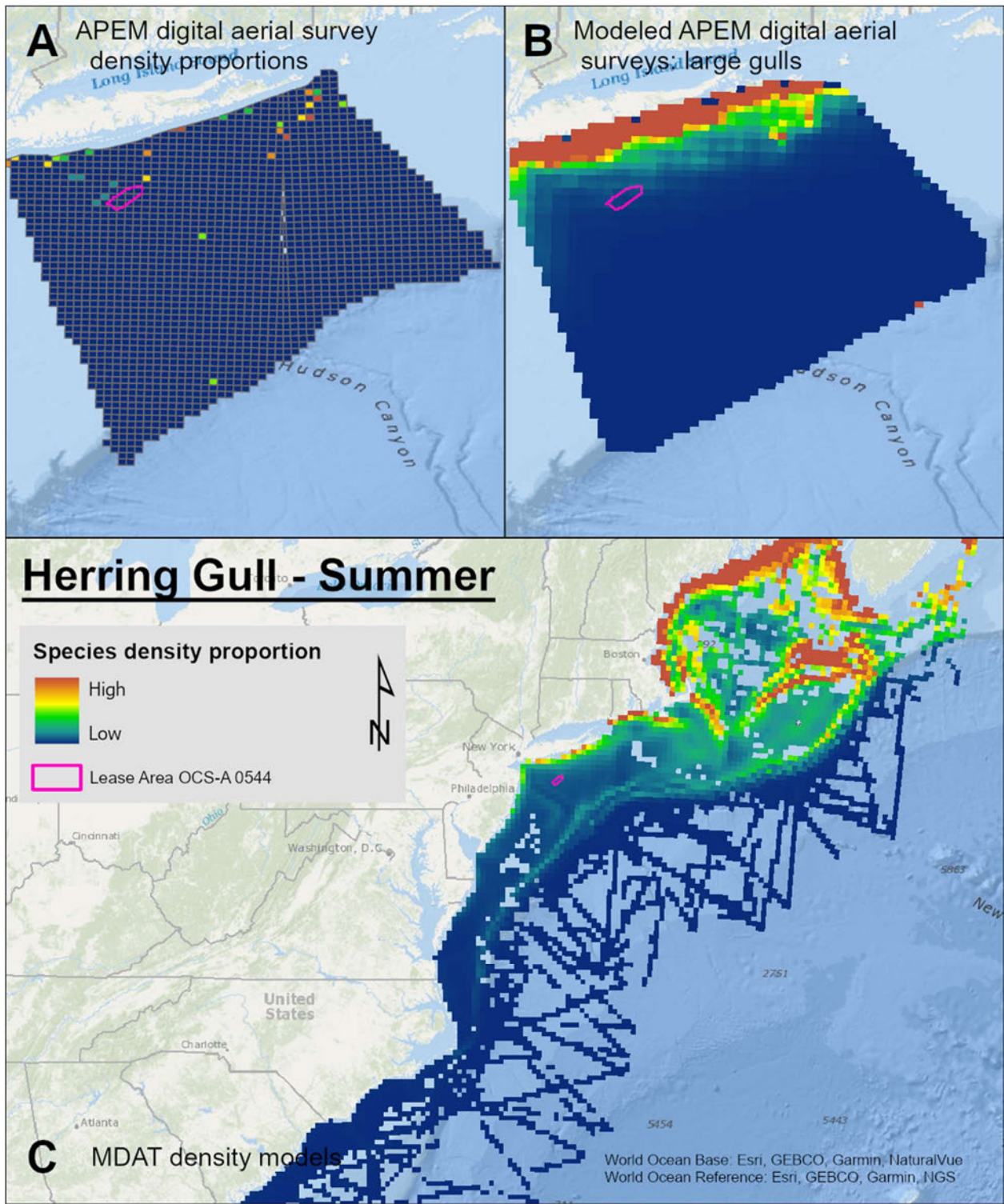
Map 99. Fall Ring-billed Gull density proportions in the NYSERDA APEM and Empire Wind high resolution digital aerial survey data (A), the NYSERDA APEM and Empire Wind high resolution digital aerial model outputs for medium gulls in Fall (B) and, Fall Ring-billed Gull MDAT modeled abundance at the regional scale (C). The scale for all maps is representative of relative spatial variation in the sites within the season for each map input.



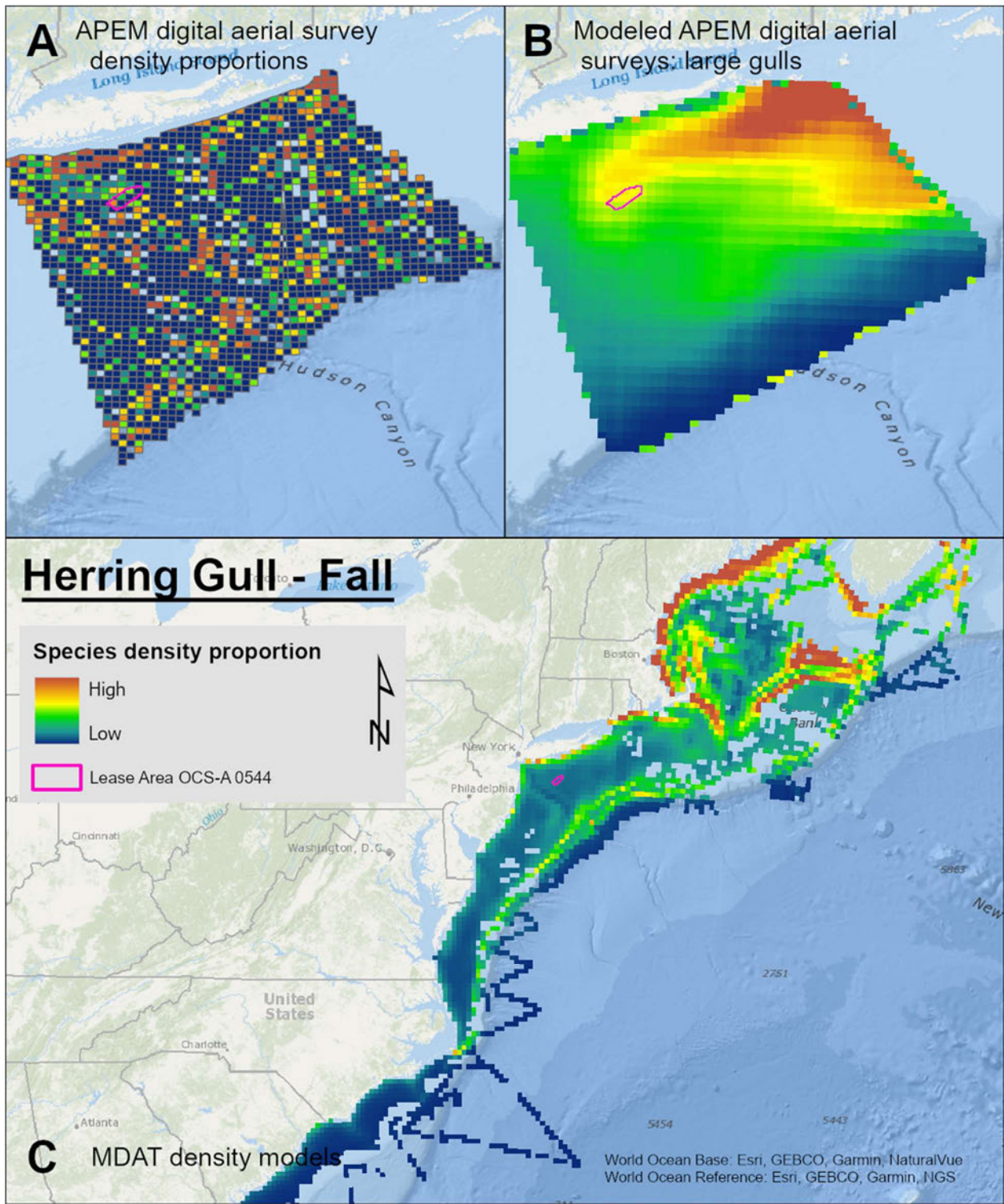
Map 100. Winter Herring Gull density proportions in the NYSERDA APEM and Empire Wind high resolution digital aerial survey data (A), the NYSERDA APEM and Empire Wind high resolution digital aerial model outputs for large gulls in Winter (B) and, Winter Herring Gull MDAT modeled abundance at the regional scale (C). The scale for all maps is representative of relative spatial variation in the sites within the season for each map input.



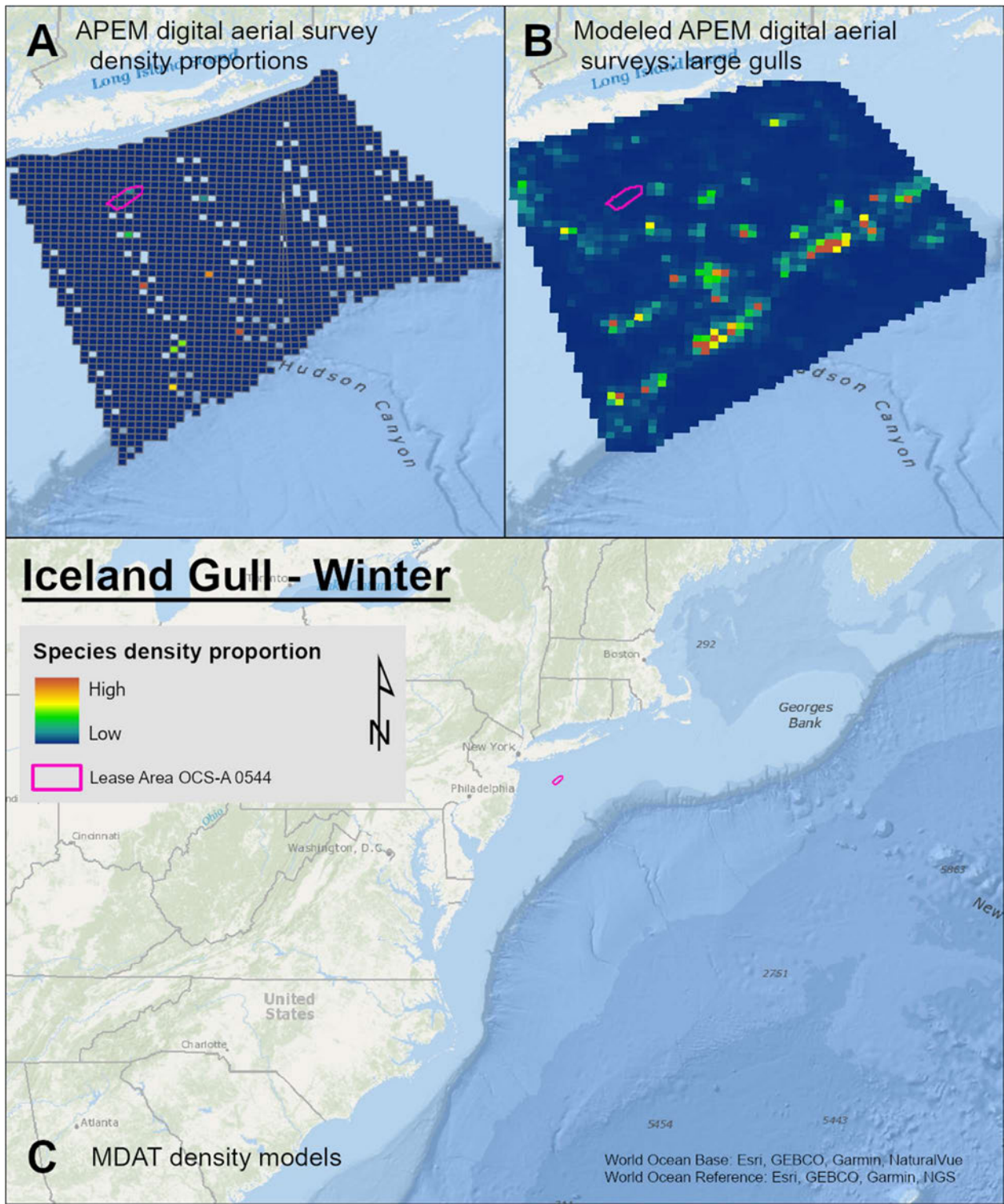
Map 101. Spring Herring Gull density proportions in the NYSERDA APEM and Empire Wind high resolution digital aerial survey data (A), the NYSERDA APEM and Empire Wind high resolution digital aerial model outputs for large gulls in Spring (B) and, Spring Herring Gull MDAT modeled abundance at the regional scale (C). The scale for all maps is representative of relative spatial variation in the sites within the season for each map input.



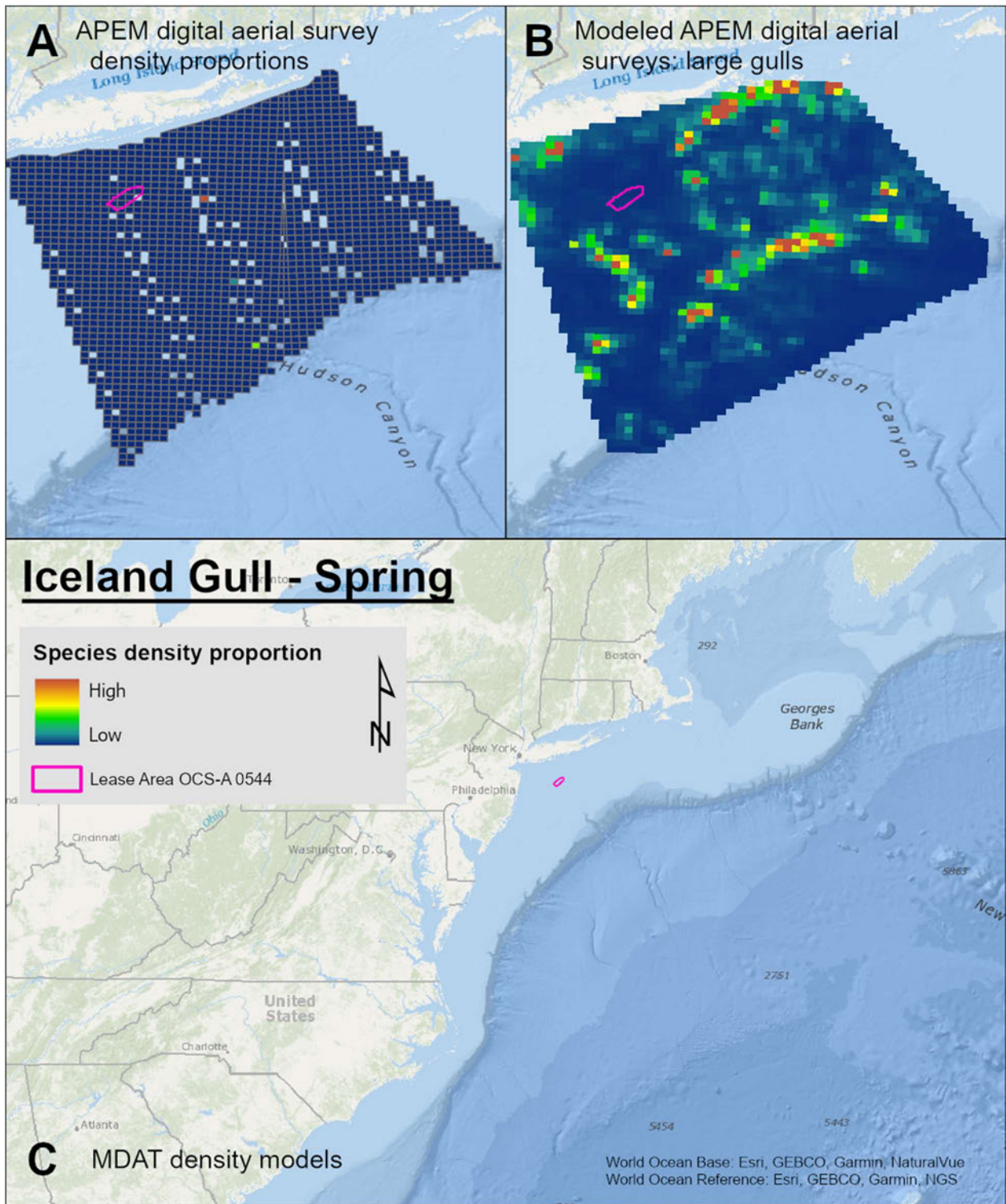
Map 102. Summer Herring Gull density proportions in the NYSEDA APEM and Empire Wind high resolution digital aerial survey data (A), the NYSEDA APEM and Empire Wind high resolution digital aerial model outputs for large gulls in Summer (B) and, Summer Herring Gull MDAT modeled abundance at the regional scale (C). The scale for all maps is representative of relative spatial variation in the sites within the season for each map input.



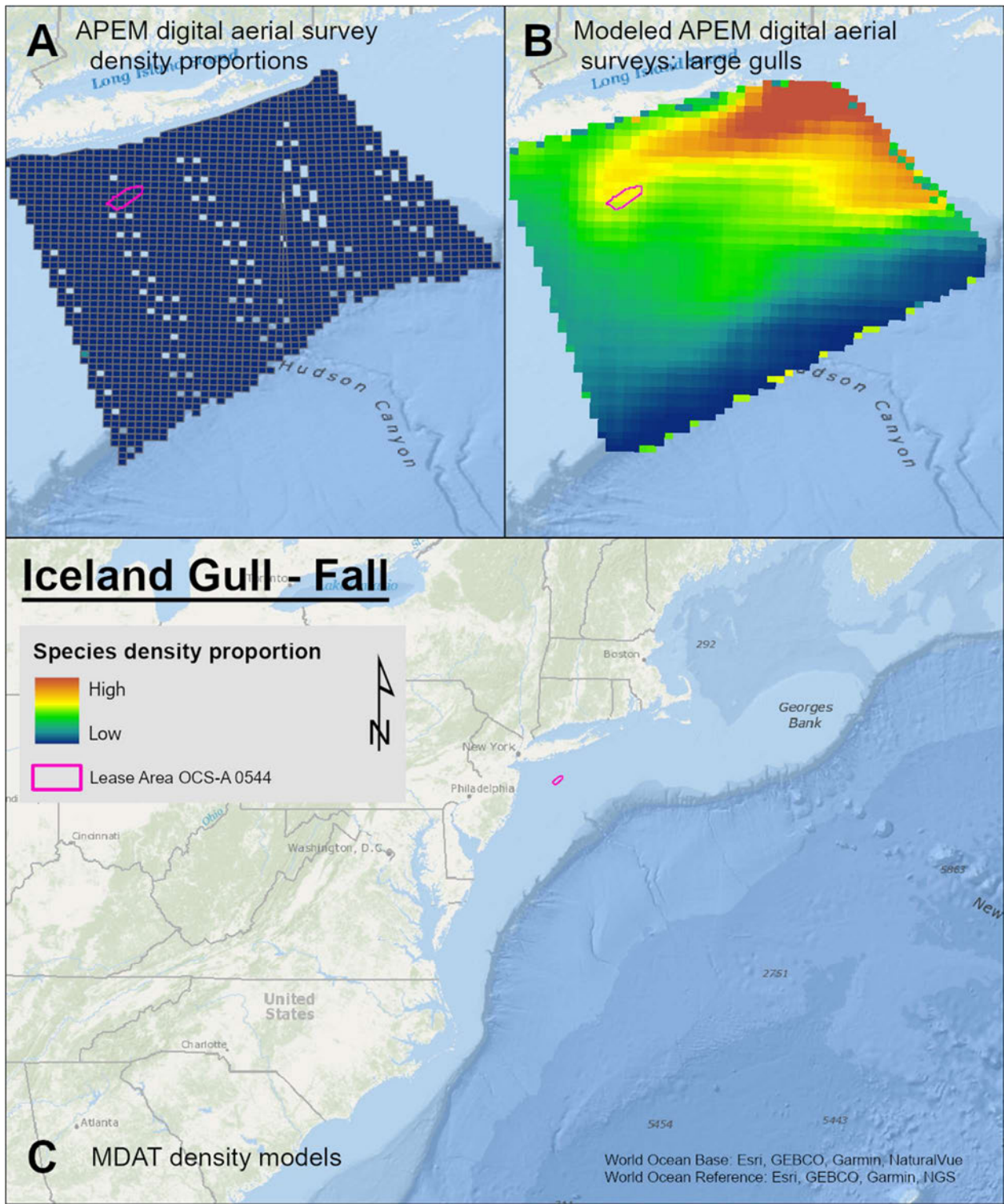
Map 103. Fall Herring Gull density proportions in the NYSEERDA APEM and Empire Wind high resolution digital aerial survey data (A), the NYSEERDA APEM and Empire Wind high resolution digital aerial model outputs for large gulls in Fall (B) and, Fall Herring Gull MDAT modeled abundance at the regional scale (C). The scale for all maps is representative of relative spatial variation in the sites within the season for each map input.



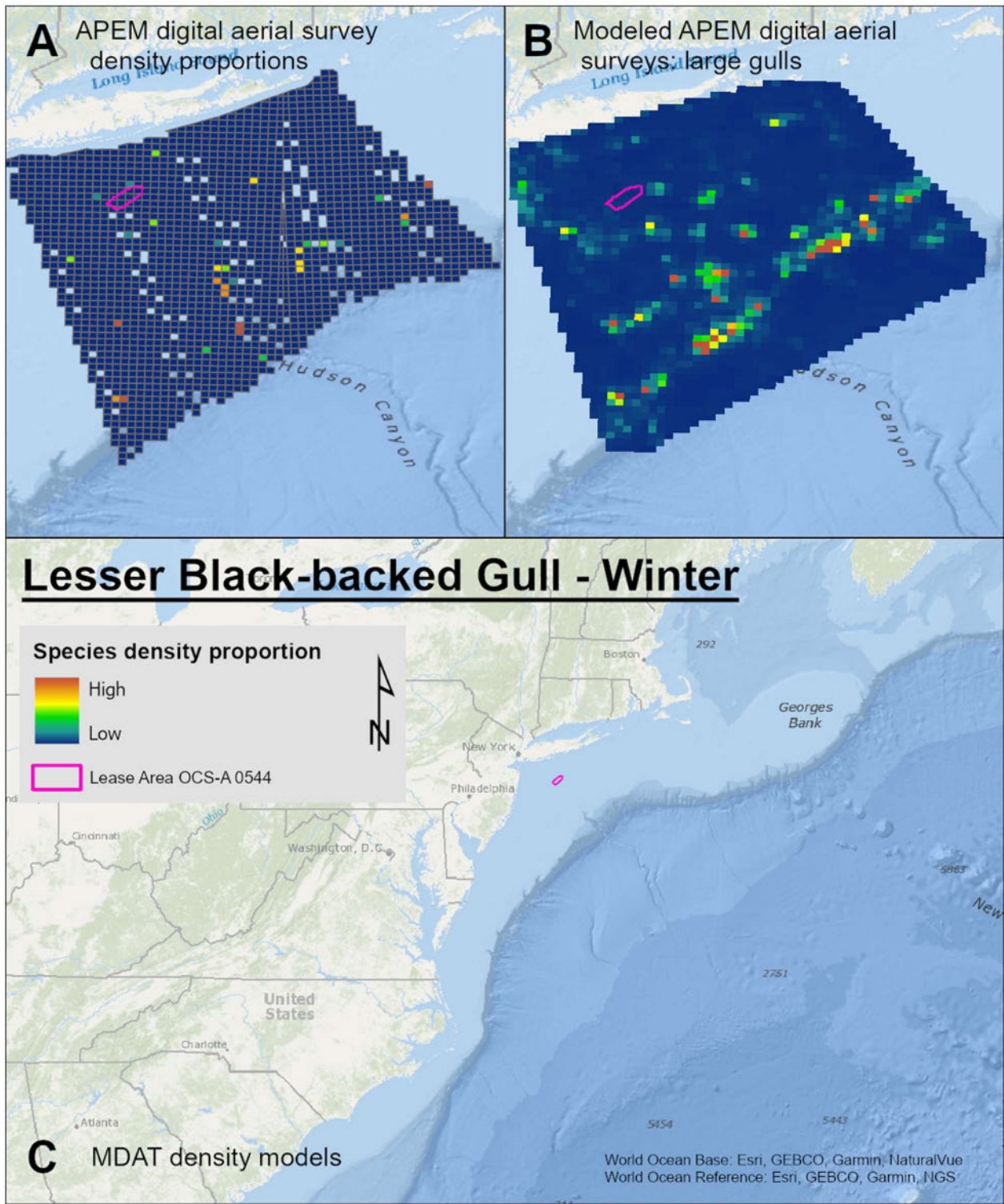
Map 104. Winter Iceland Gull density proportions in the NYSERDA APEM and Empire Wind high resolution digital aerial survey data (A), the NYSERDA APEM and Empire Wind high resolution digital aerial model outputs for large gulls in Winter (B) and, Winter Iceland Gull MDAT modeled abundance at the regional scale (C). The scale for all maps is representative of relative spatial variation in the sites within the season for each map input.



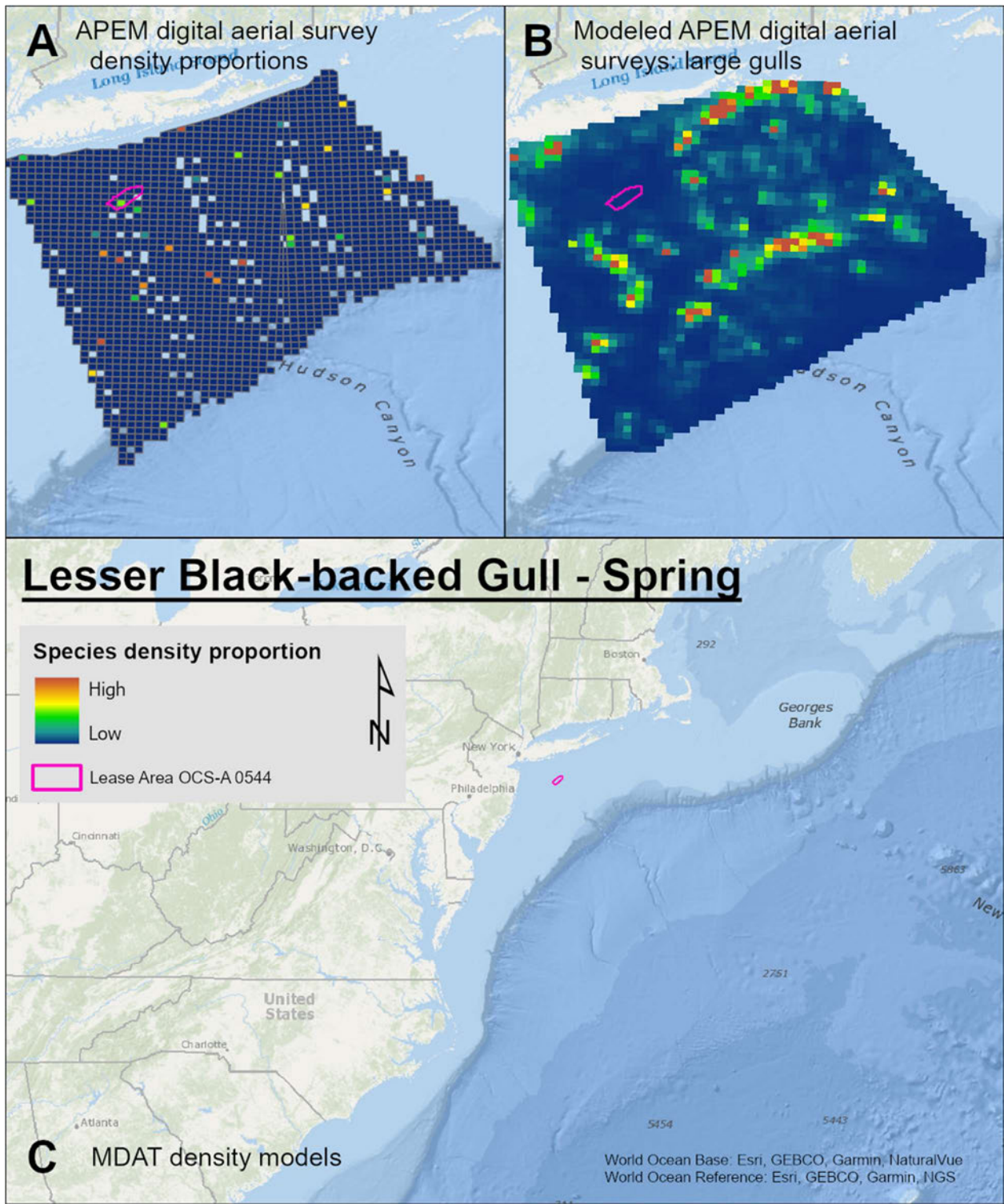
Map 105. Spring Iceland Gull density proportions in the NYSERDA APEM and Empire Wind high resolution digital aerial survey data (A), the NYSERDA APEM and Empire Wind high resolution digital aerial model outputs for large gulls in Spring (B) and, Spring Iceland Gull MDAT modeled abundance at the regional scale (C). The scale for all maps is representative of relative spatial variation in the sites within the season for each map input.



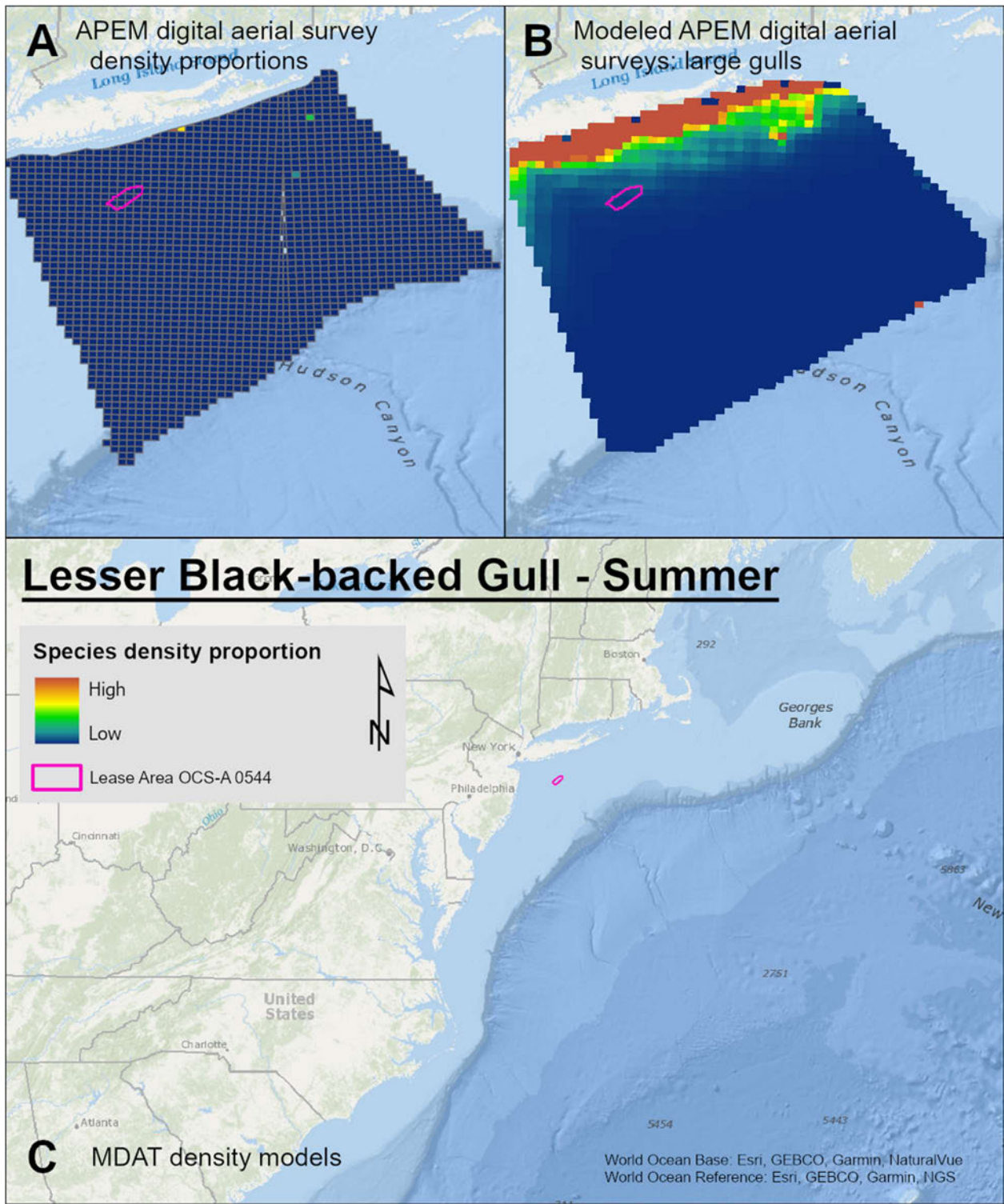
Map 106. Fall Iceland Gull density proportions in the NYSERDA APEM and Empire Wind high resolution digital aerial survey data (A), the NYSERDA APEM and Empire Wind high resolution digital aerial model outputs for large gulls in Fall (B) and, Fall Iceland Gull MDAT modeled abundance at the regional scale (C). The scale for all maps is representative of relative spatial variation in the sites within the season for each map input.



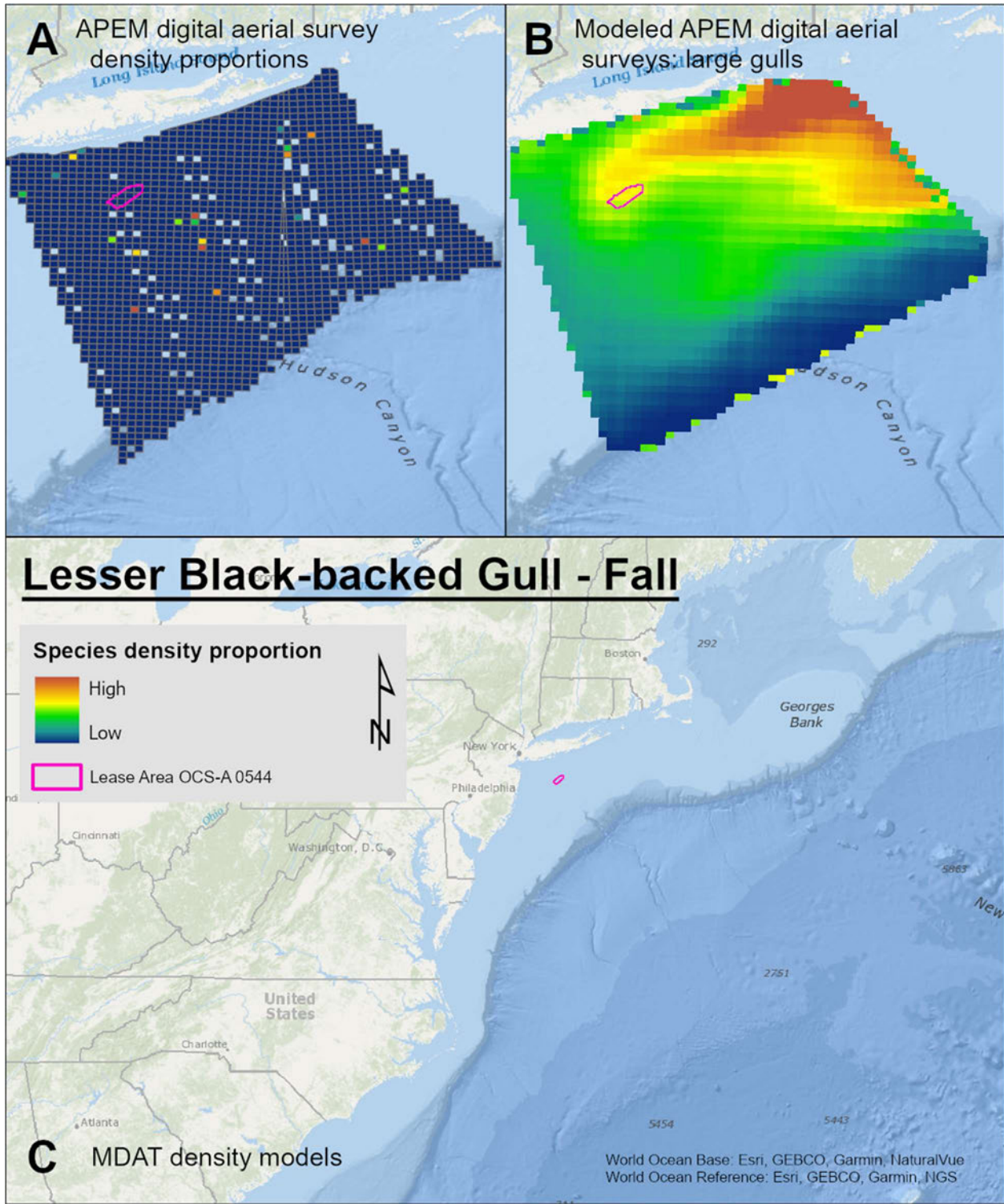
Map 107. Winter Lesser Black-backed Gull density proportions in the NYSERDA APEM and Empire Wind high resolution digital aerial survey data (A), the NYSERDA APEM and Empire Wind high resolution digital aerial model outputs for large gulls in Winter (B) and, Winter Lesser Black-backed Gull MDAT modeled abundance at the regional scale (C). The scale for all maps is representative of relative spatial variation in the sites within the season for each map input.



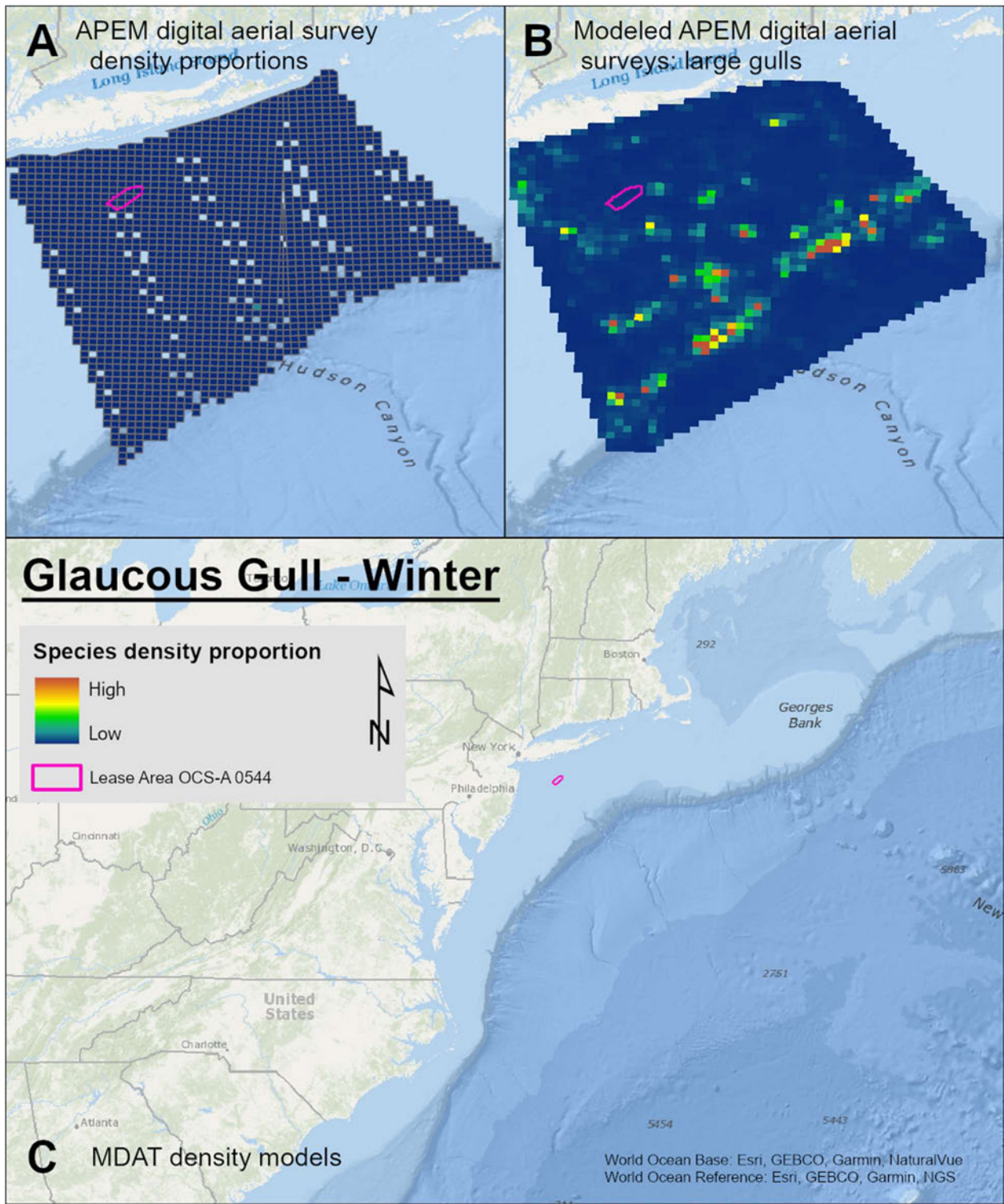
Map 108. Spring Lesser Black-backed Gull density proportions in the NYSERDA APEM and Empire Wind high resolution digital aerial survey data (A), the NYSERDA APEM and Empire Wind high resolution digital aerial model outputs for large gulls in Spring (B) and, Spring Lesser Black-backed Gull MDAT modeled abundance at the regional scale (C). The scale for all maps is representative of relative spatial variation in the sites within the season for each map input.



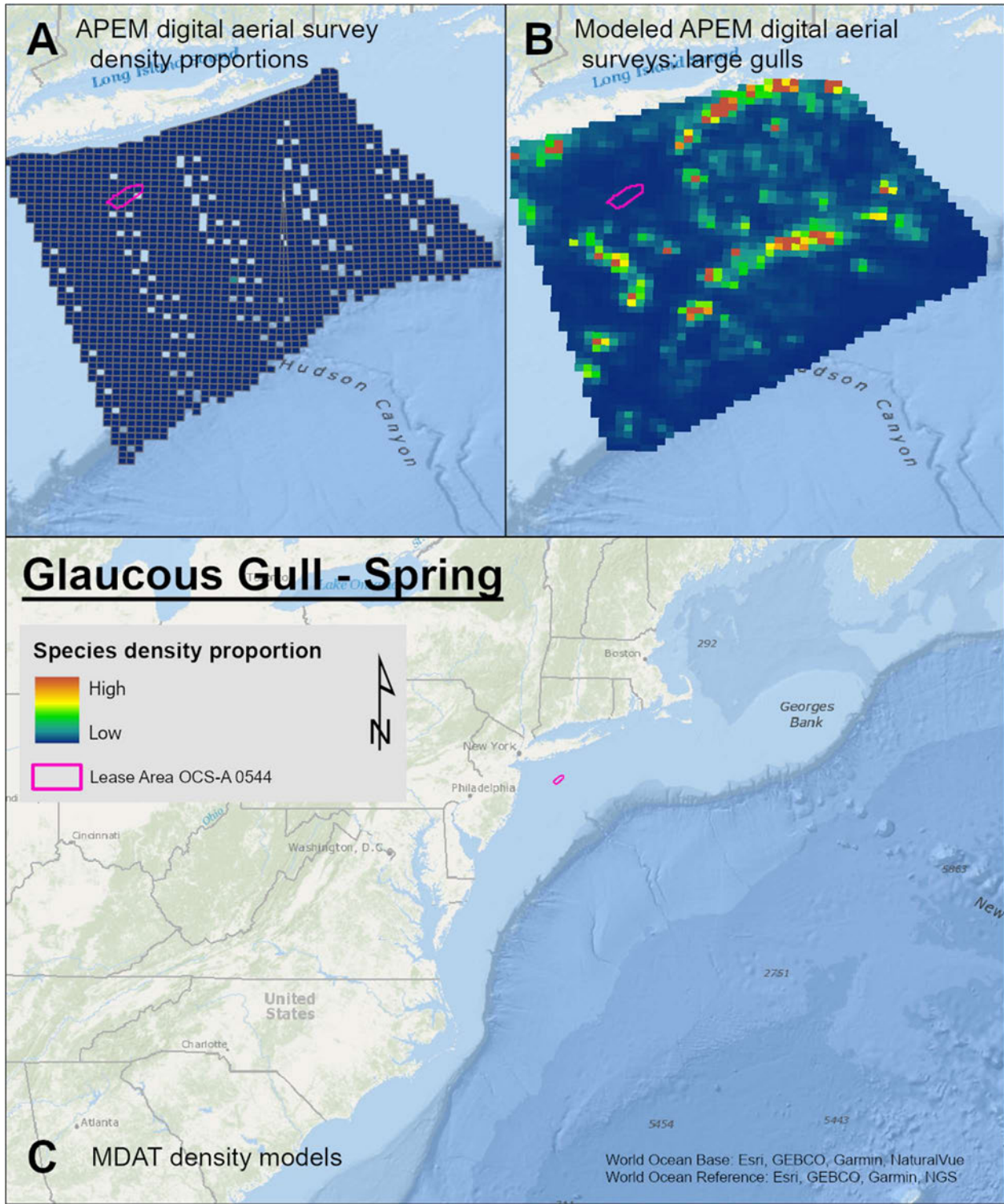
Map 109. Summer Lesser Black-backed Gull density proportions in the NYSERDA APEM and Empire Wind high resolution digital aerial survey data (A), the NYSERDA APEM and Empire Wind high resolution digital aerial model outputs for large gulls in Summer (B) and, Summer Lesser Black-backed Gull MDAT modeled abundance at the regional scale (C). The scale for all maps is representative of relative spatial variation in the sites within the season for each map input.



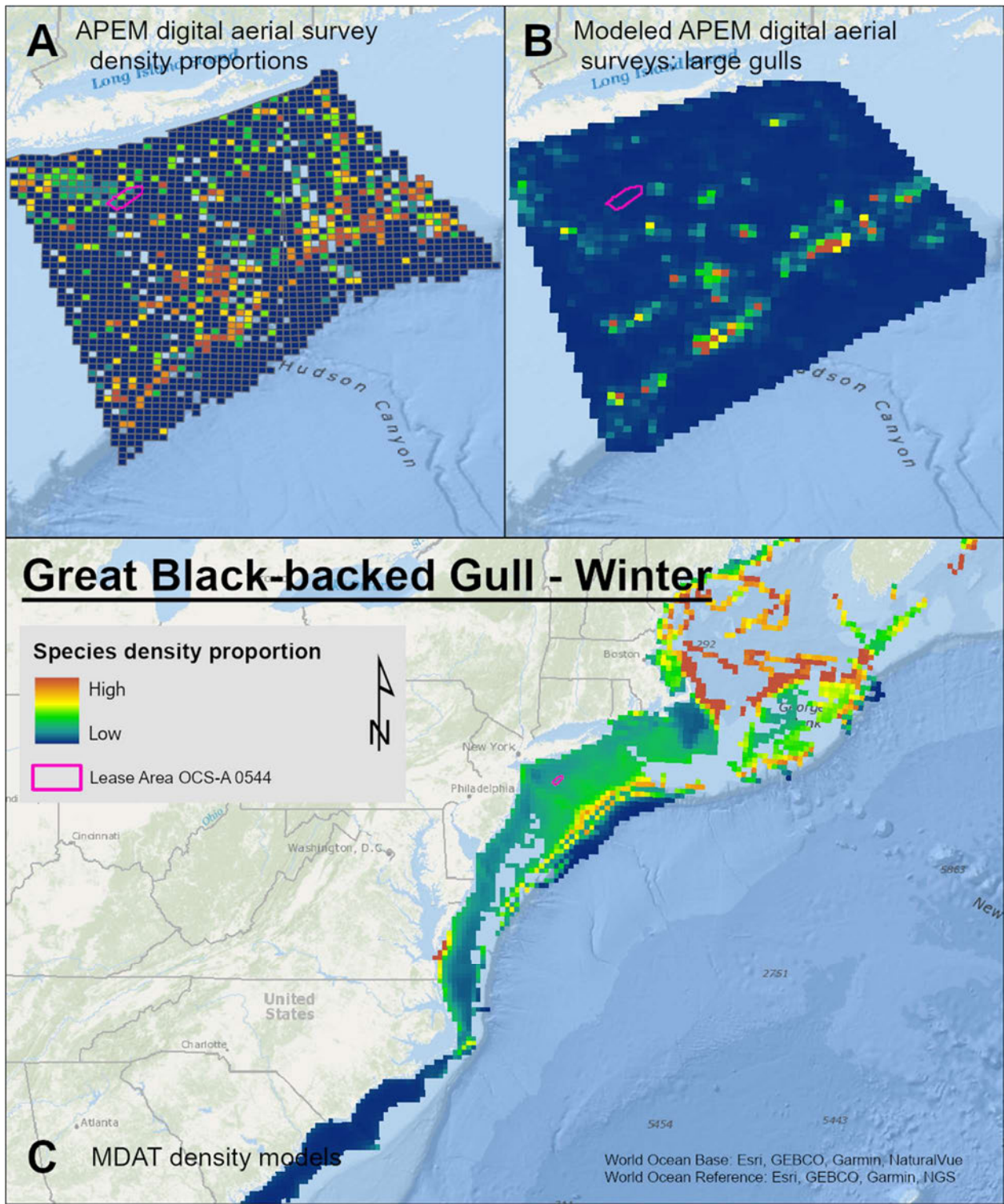
Map 110. Fall Lesser Black-backed Gull density proportions in the NYSERDA APEM and Empire Wind high resolution digital aerial survey data (A), the NYSERDA APEM and Empire Wind high resolution digital aerial model outputs for large gulls in Fall (B) and, Fall Lesser Black-backed Gull MDAT modeled abundance at the regional scale (C). The scale for all maps is representative of relative spatial variation in the sites within the season for each map input.



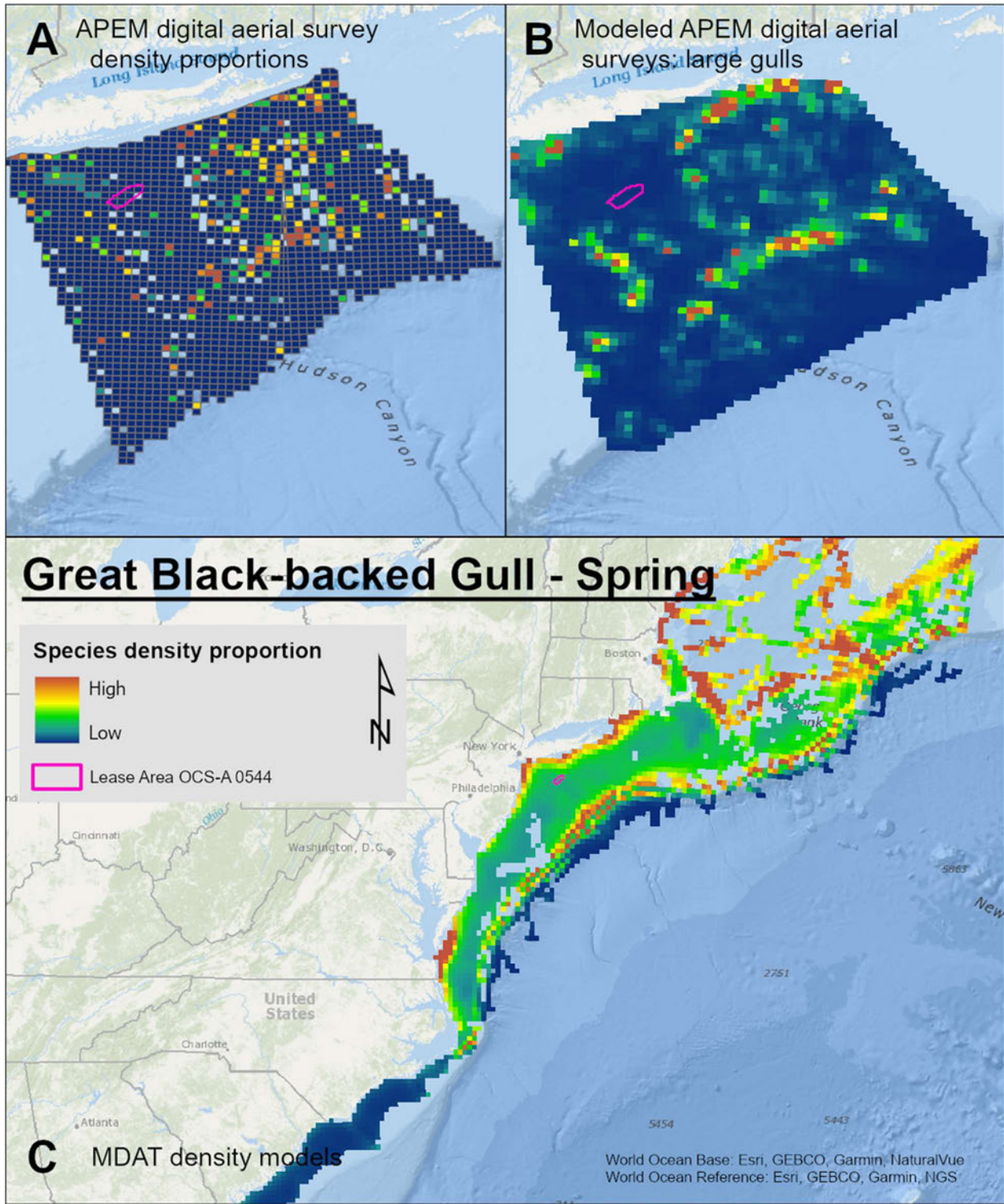
Map 111. Winter Glaucous Gull density proportions in the NYSERDA APEM and Empire Wind high resolution digital aerial survey data (A), the NYSERDA APEM and Empire Wind high resolution digital aerial model outputs for large gulls in Winter (B) and, Winter Glaucous Gull MDAT modeled abundance at the regional scale (C). The scale for all maps is representative of relative spatial variation in the sites within the season for each map input.



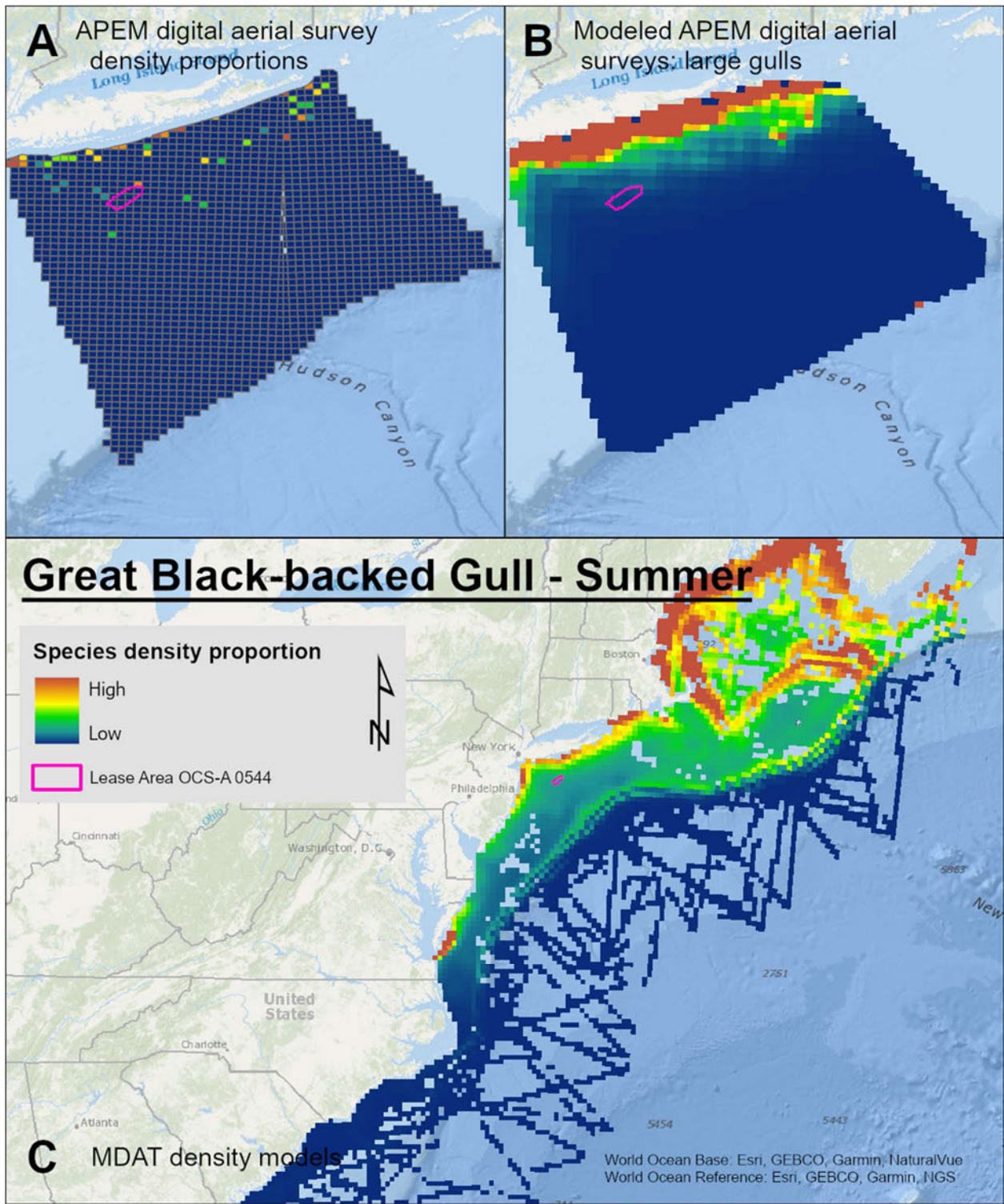
Map 112. Spring Glaucous Gull density proportions in the NYSERDA APEM and Empire Wind high resolution digital aerial survey data (A), the NYSERDA APEM and Empire Wind high resolution digital aerial model outputs for large gulls in Spring (B) and, Spring Glaucous Gull MDAT modeled abundance at the regional scale (C). The scale for all maps is representative of relative spatial variation in the sites within the season for each map input.



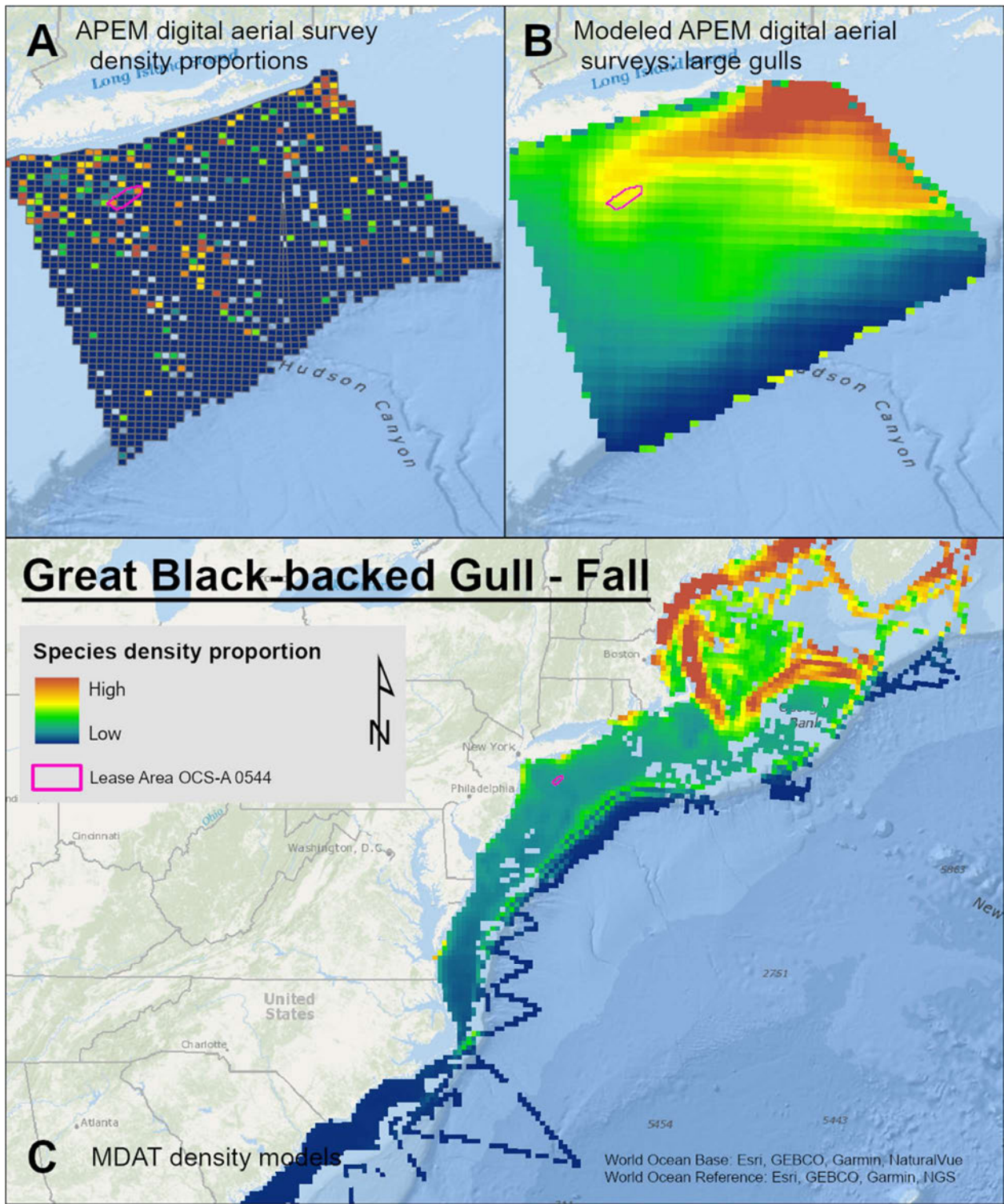
Map 113. Winter Great Black-backed Gull density proportions in the NYSERDA APEM and Empire Wind high resolution digital aerial survey data (A), the NYSERDA APEM and Empire Wind high resolution digital aerial model outputs for large gulls in Winter (B) and, Winter Great Black-backed Gull MDAT modeled abundance at the regional scale (C). The scale for all maps is representative of relative spatial variation in the sites within the season for each map input.



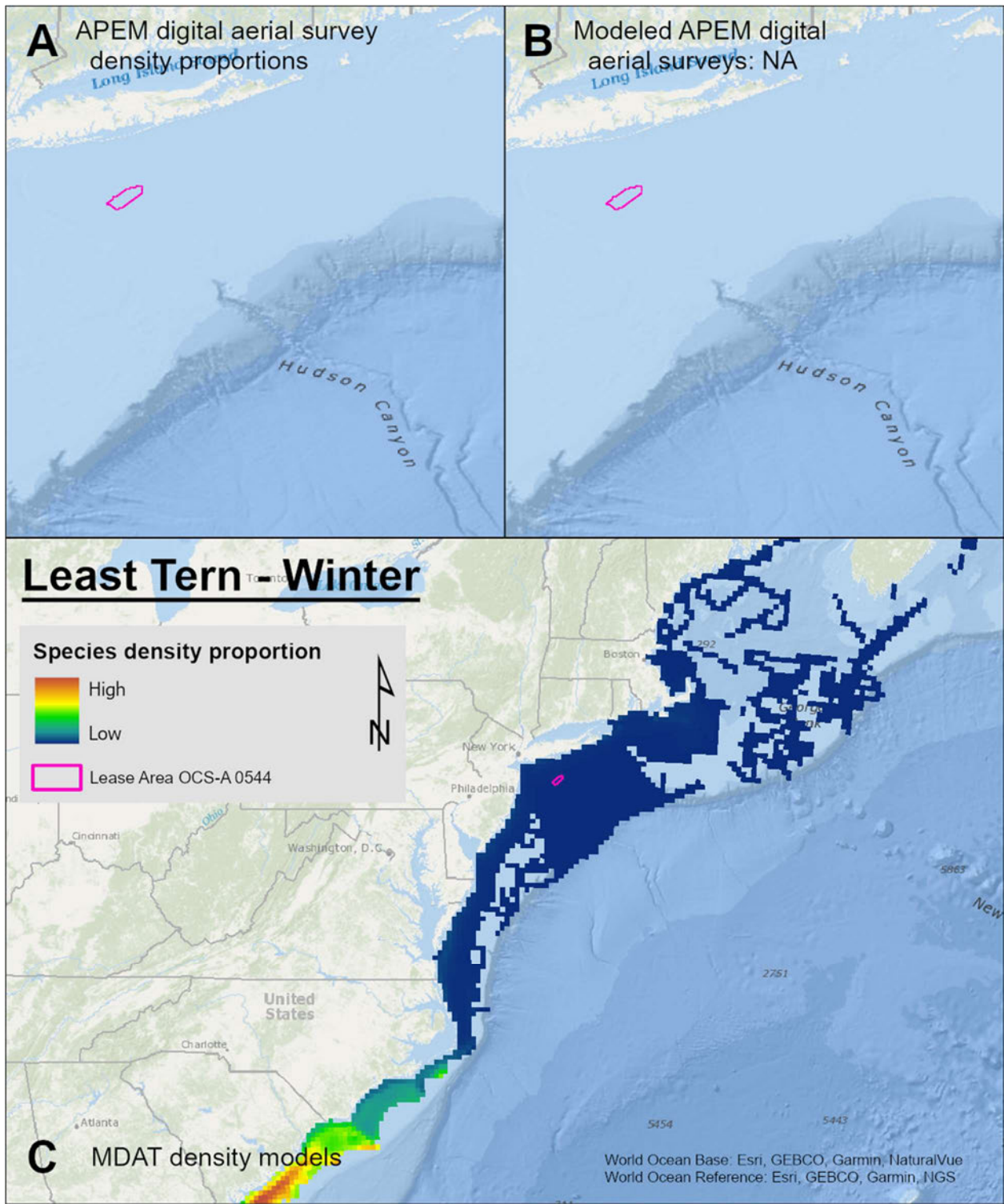
Map 114. Spring Great Black-backed Gull density proportions in the NYSERDA APEM and Empire Wind high resolution digital aerial survey data (A), the NYSERDA APEM and Empire Wind high resolution digital aerial model outputs for large gulls in Spring (B) and, Spring Great Black-backed Gull MDAT modeled abundance at the regional scale (C). The scale for all maps is representative of relative spatial variation in the sites within the season for each map input.



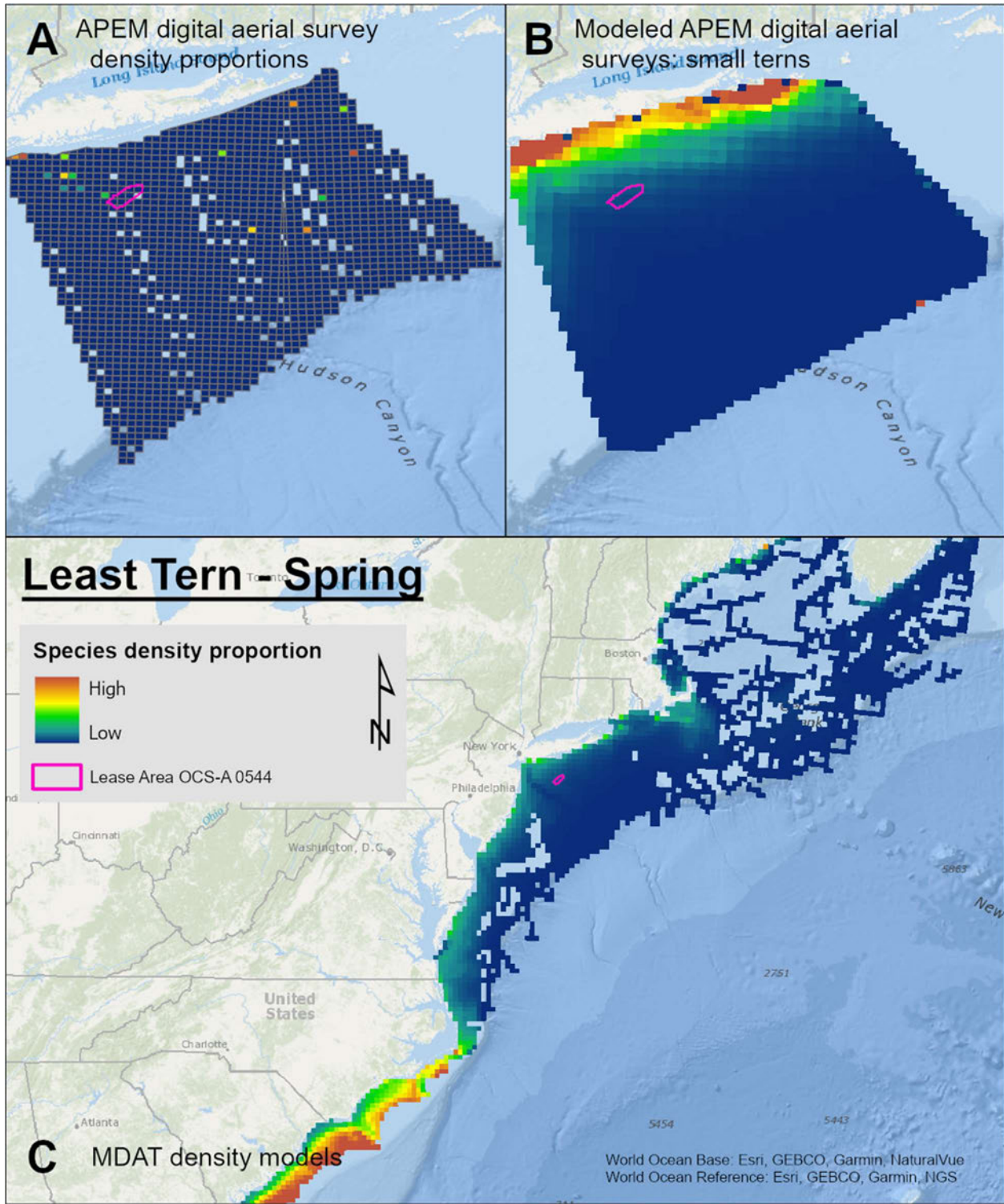
Map 115. Summer Great Black-backed Gull density proportions in the NYSERDA APEM and Empire Wind high resolution digital aerial survey data (A), the NYSERDA APEM and Empire Wind high resolution digital aerial model outputs for large gulls in Summer (B) and, Summer Great Black-backed Gull MDAT modeled abundance at the regional scale (C). The scale for all maps is representative of relative spatial variation in the sites within the season for each map input.



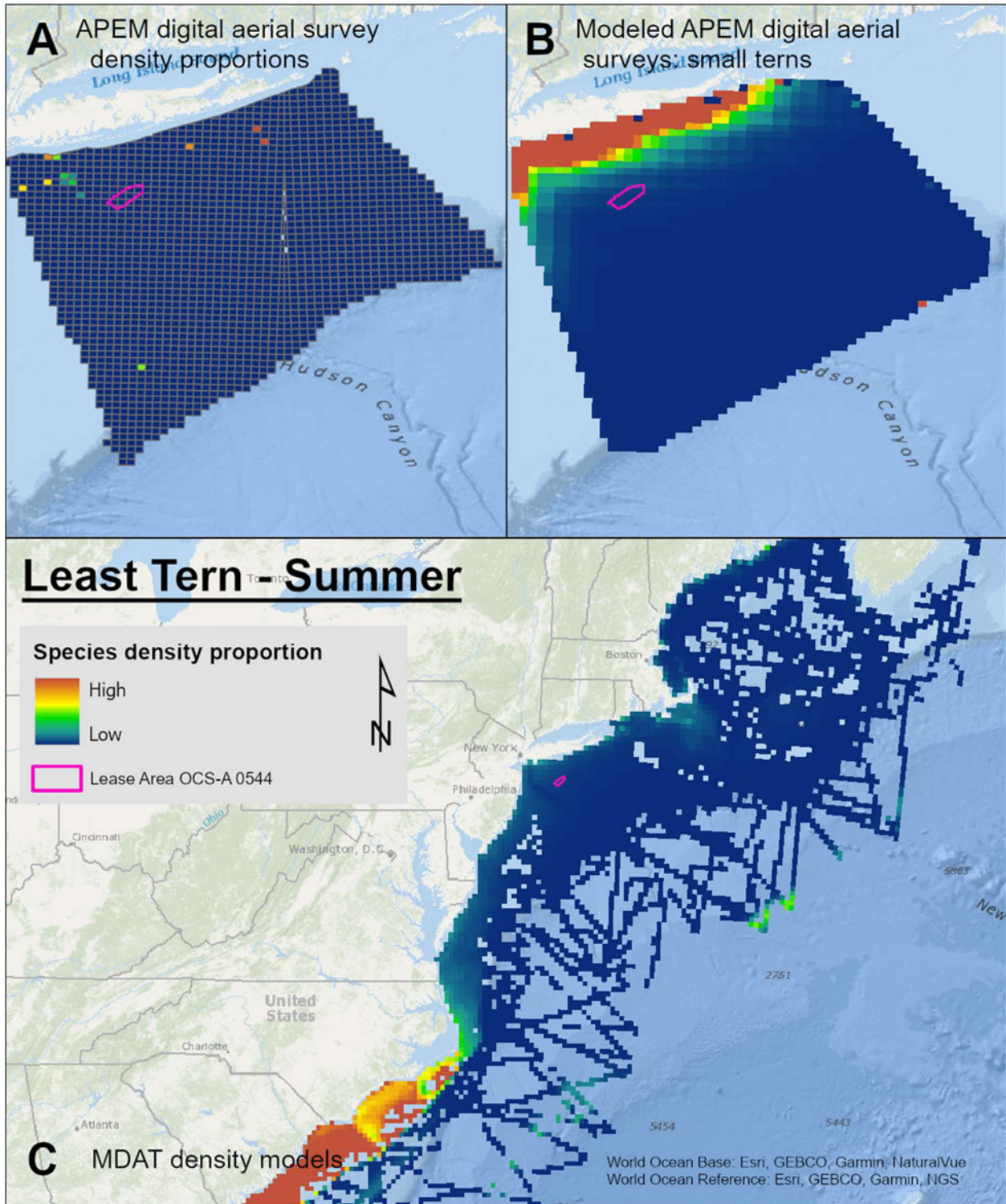
Map 116. Fall Great Black-backed Gull density proportions in the NYSERDA APEM and Empire Wind high resolution digital aerial survey data (A), the NYSERDA APEM and Empire Wind high resolution digital aerial model outputs for large gulls in Fall (B) and, Fall Great Black-backed Gull MDAT modeled abundance at the regional scale (C). The scale for all maps is representative of relative spatial variation in the sites within the season for each map input.



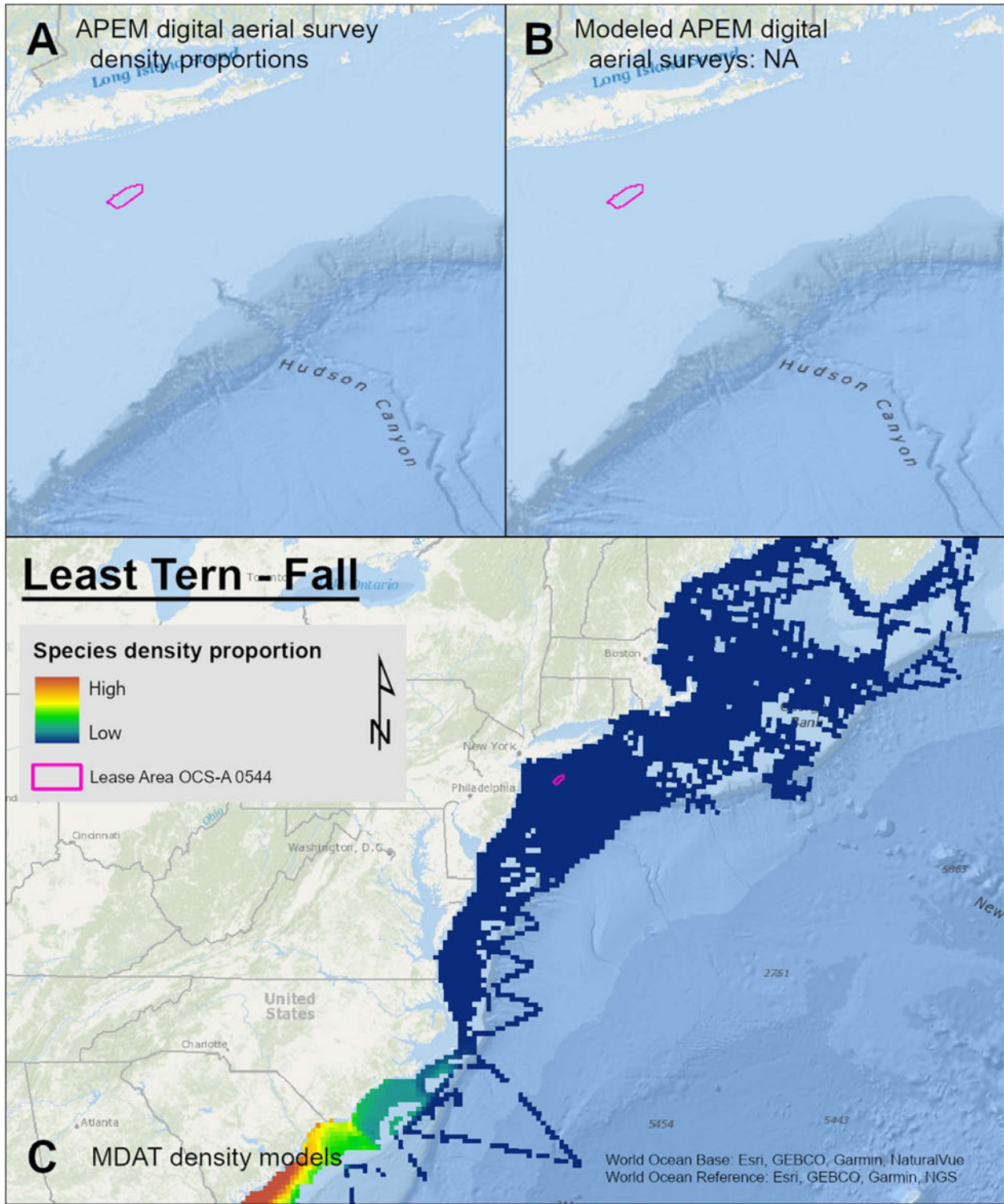
Map 117. Winter Least Tern density proportions in the NYSERDA APEM and Empire Wind high resolution digital aerial survey data (A), the NYSERDA APEM and Empire Wind high resolution digital aerial model outputs for small terns in Winter (B) and, Winter Least Tern MDAT modeled abundance at the regional scale (C). The scale for all maps is representative of relative spatial variation in the sites within the season for each map input.



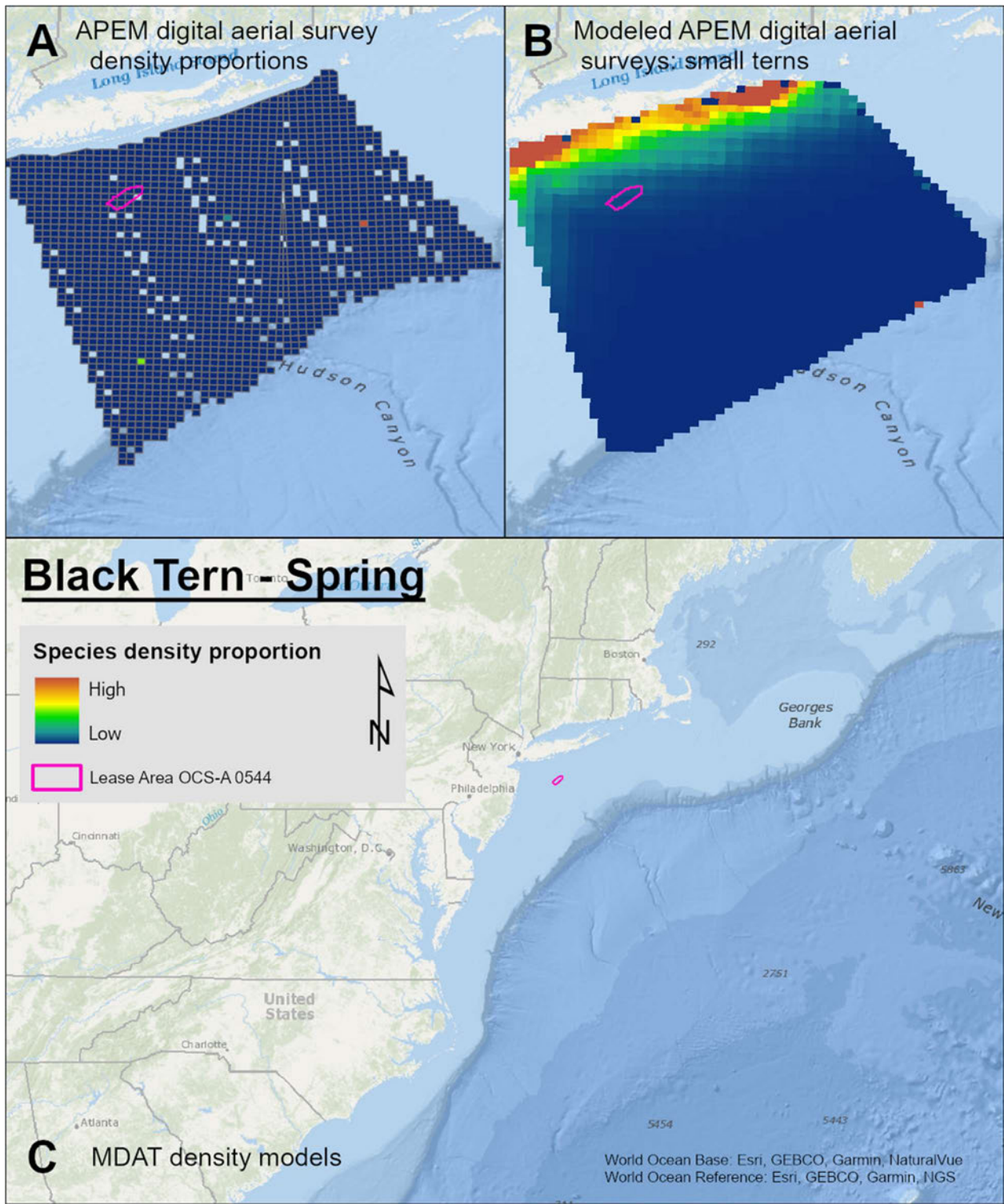
Map 118. Spring Least Tern density proportions in the NYSERDA APEM and Empire Wind high resolution digital aerial survey data (A), the NYSERDA APEM and Empire Wind high resolution digital aerial model outputs for small terns in Spring (B) and, Spring Least Tern MDAT modeled abundance at the regional scale (C). The scale for all maps is representative of relative spatial variation in the sites within the season for each map input.



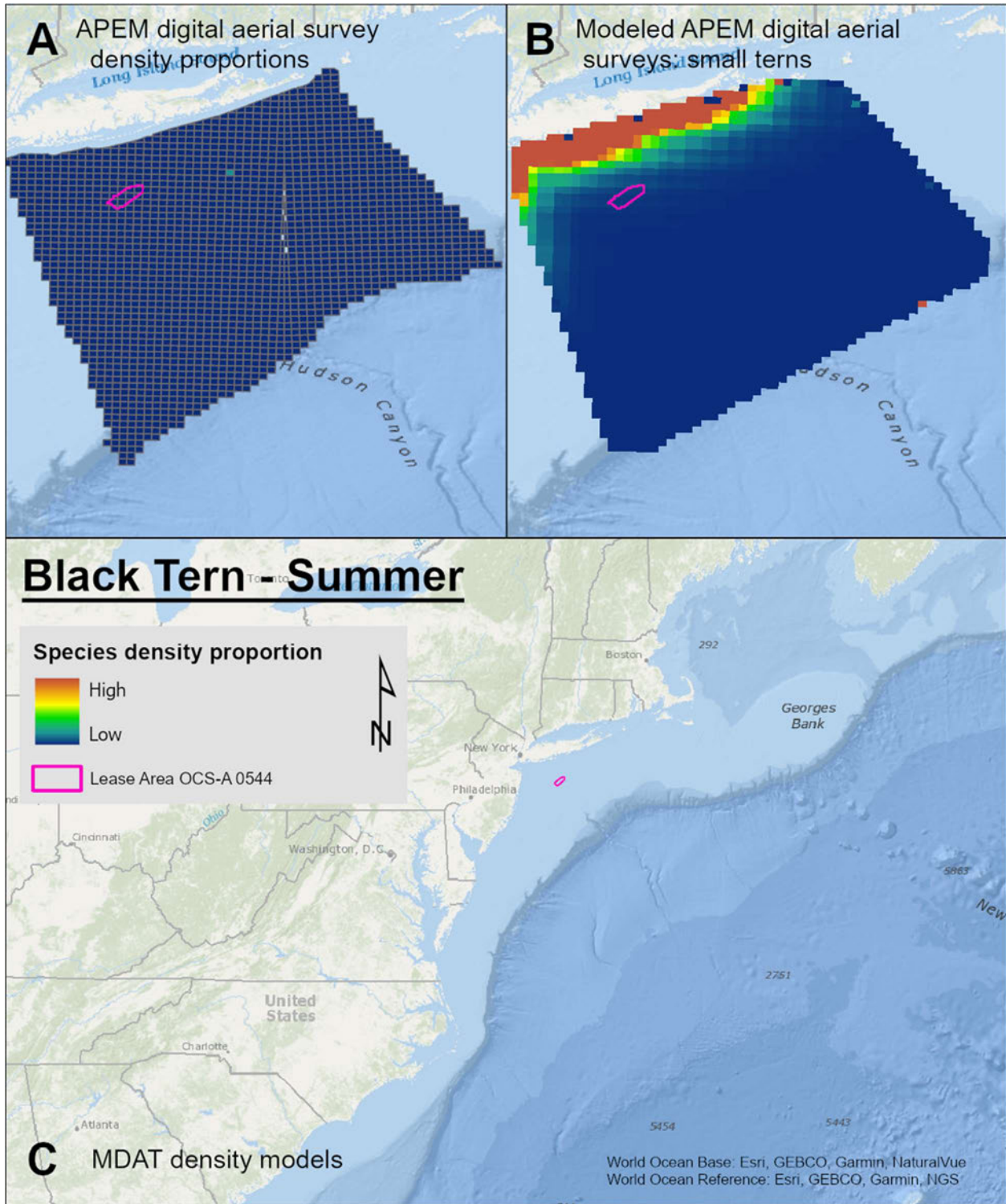
Map 119. Summer Least Tern density proportions in the NYSERDA APEM and Empire Wind high resolution digital aerial survey data (A), the NYSERDA APEM and Empire Wind high resolution digital aerial model outputs for small terns in Summer (B) and, Summer Least Tern MDAT modeled abundance at the regional scale (C). The scale for all maps is representative of relative spatial variation in the sites within the season for each map input.



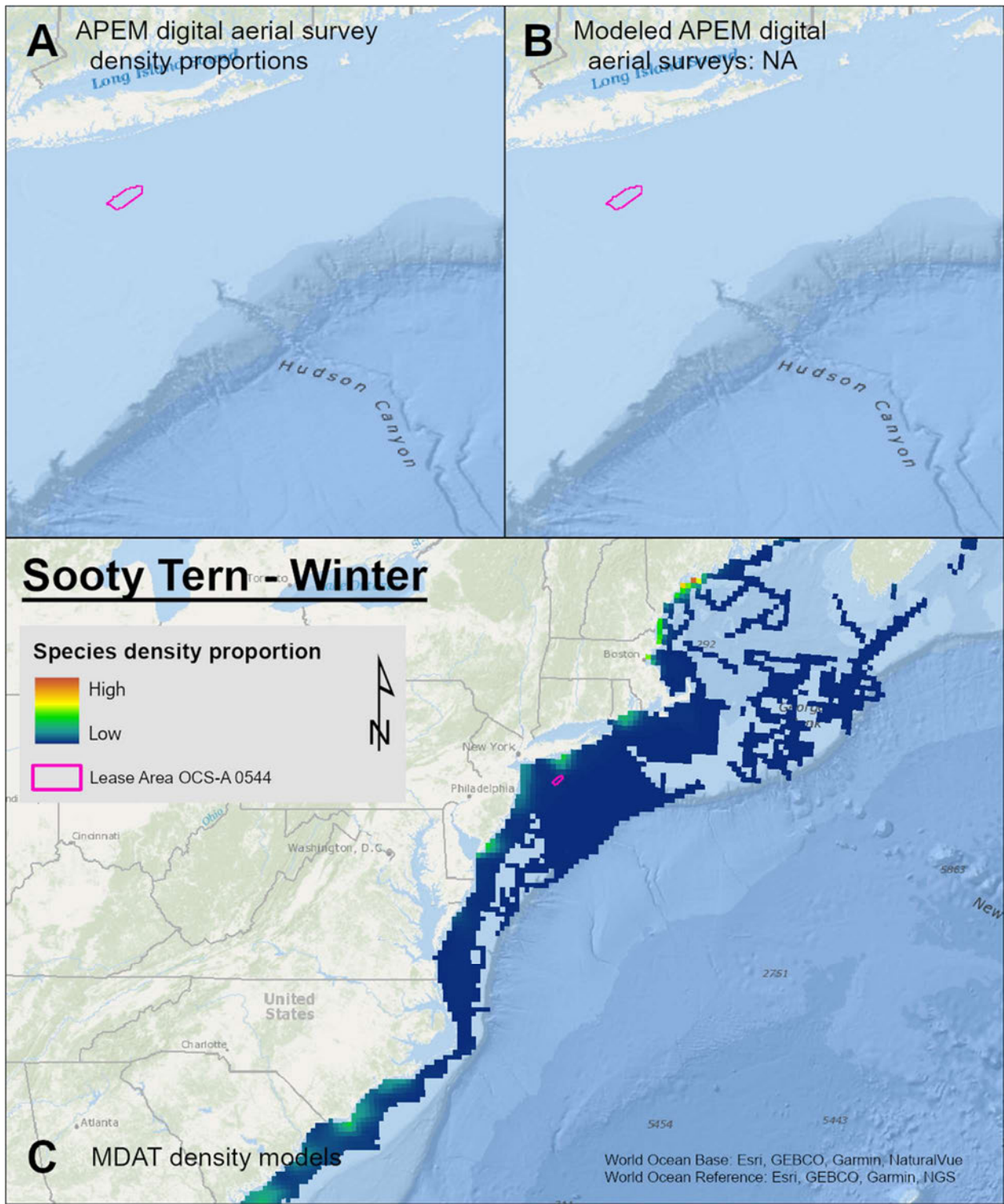
Map 120. Fall Least Tern density proportions in the NYSERDA APEM and Empire Wind high resolution digital aerial survey data (A), the NYSERDA APEM and Empire Wind high resolution digital aerial model outputs for small terns in Fall (B) and, Fall Least Tern MDAT modeled abundance at the regional scale (C). The scale for all maps is representative of relative spatial variation in the sites within the season for each map input.



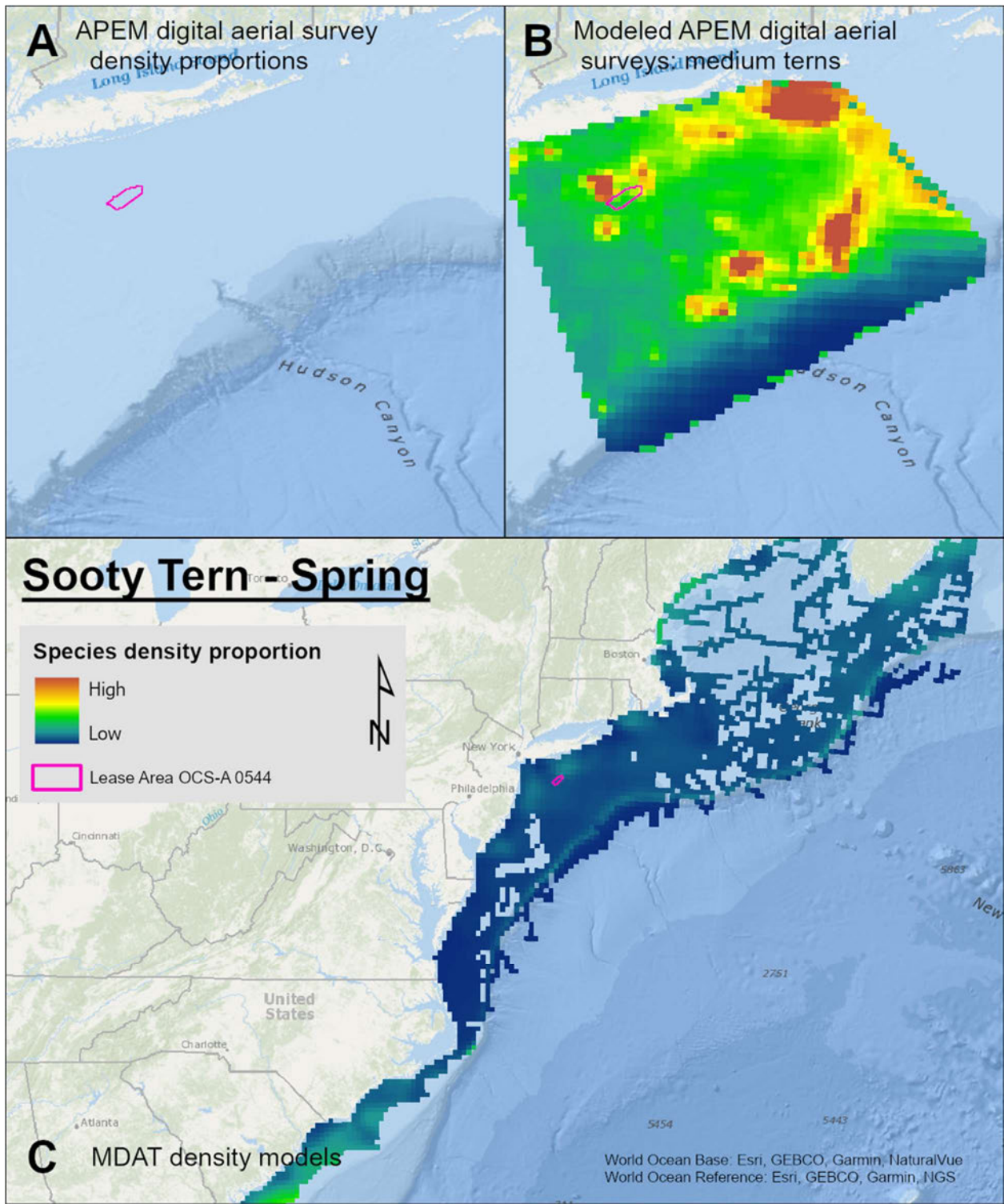
Map 121. Spring Black Tern density proportions in the NYSERDA APEM and Empire Wind high resolution digital aerial survey data (A), the NYSERDA APEM and Empire Wind high resolution digital aerial model outputs for small terns in Spring (B) and, Spring Black Tern MDAT modeled abundance at the regional scale (C). The scale for all maps is representative of relative spatial variation in the sites within the season for each map input.



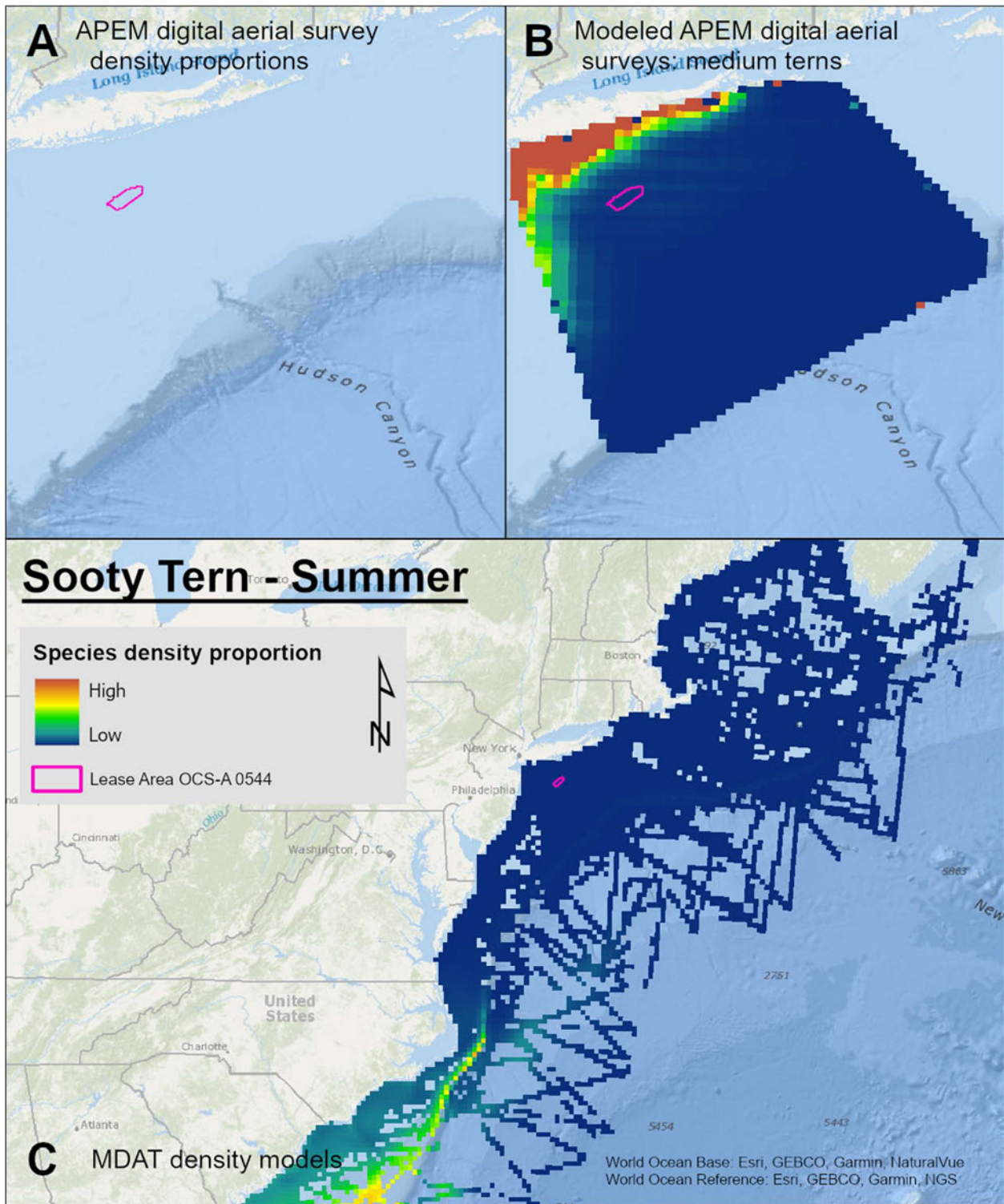
Map 122. Summer Black Tern density proportions in the NYSERDA APEM and Empire Wind high resolution digital aerial survey data (A), the NYSERDA APEM and Empire Wind high resolution digital aerial model outputs for small terns in Summer (B) and, Summer Black Tern MDAT modeled abundance at the regional scale (C). The scale for all maps is representative of relative spatial variation in the sites within the season for each map input.



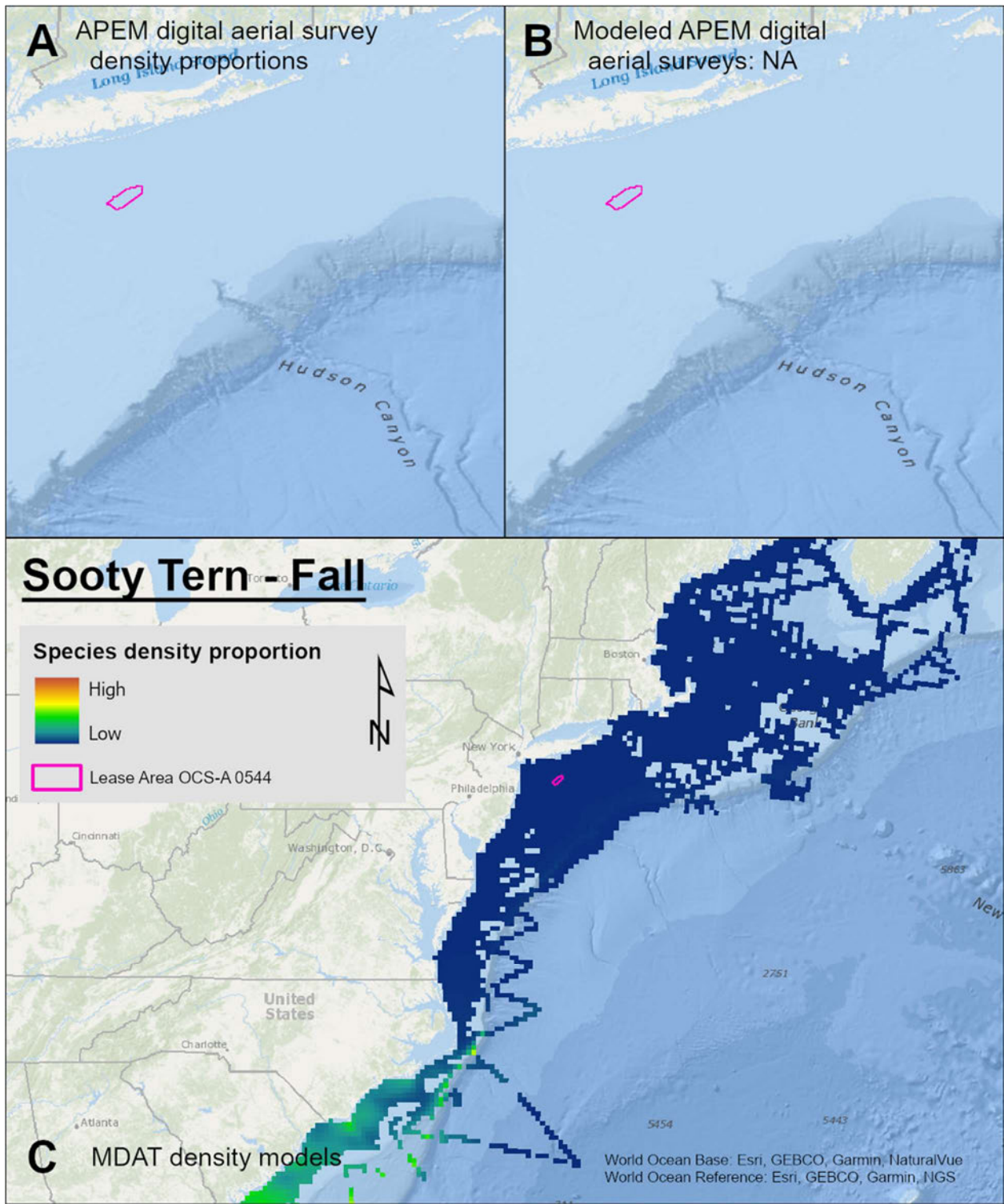
Map 123. Winter Sooty Tern density proportions in the NYSERDA APEM and Empire Wind high resolution digital aerial survey data (A), the NYSERDA APEM and Empire Wind high resolution digital aerial model outputs for medium terns in Winter (B) and, Winter Sooty Tern MDAT modeled abundance at the regional scale (C). The scale for all maps is representative of relative spatial variation in the sites within the season for each map input.



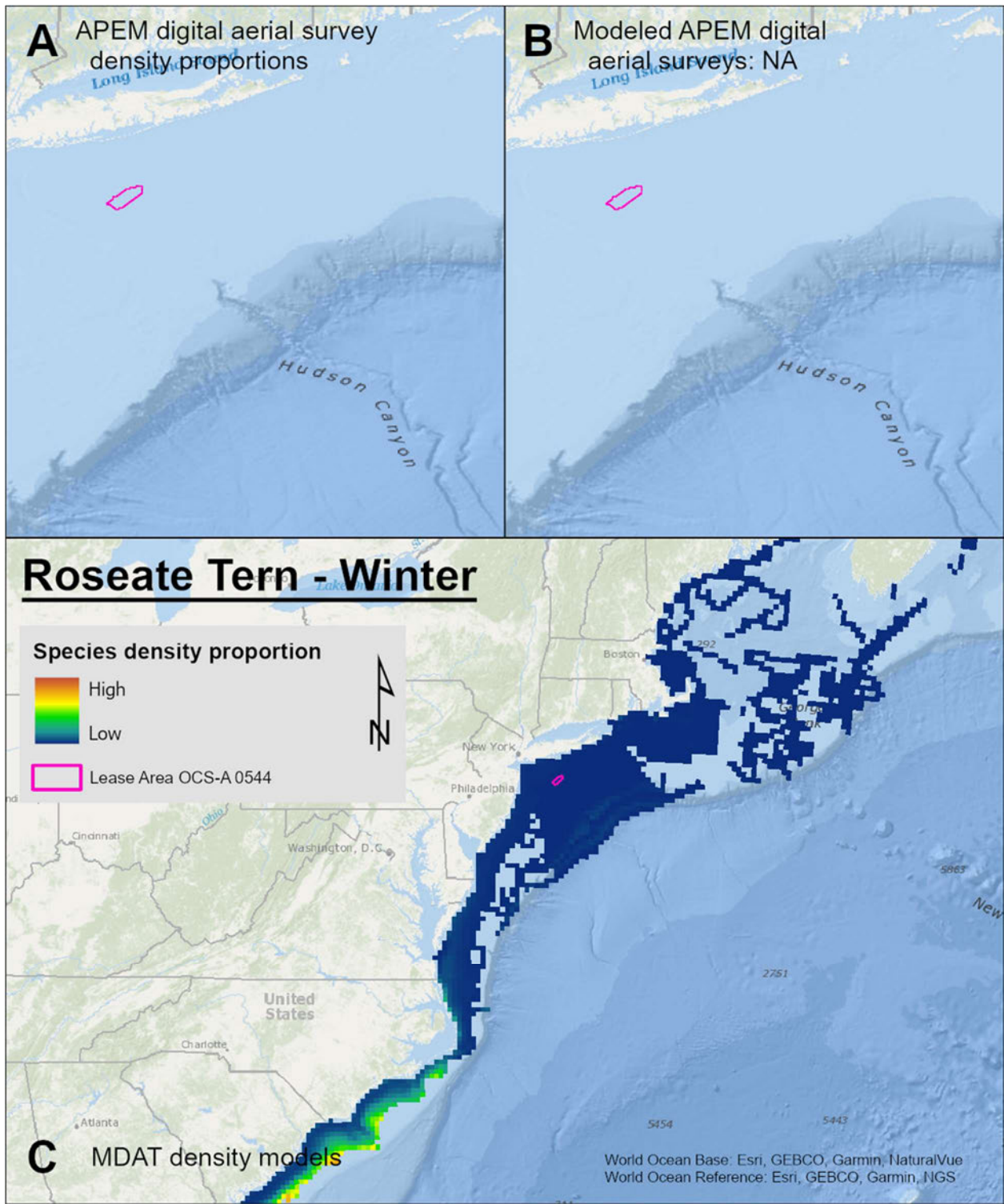
Map 124. Spring Sooty Tern density proportions in the NYSERDA APEM and Empire Wind high resolution digital aerial survey data (A), the NYSERDA APEM and Empire Wind high resolution digital aerial model outputs for medium terns in Spring (B) and, Spring Sooty Tern MDAT modeled abundance at the regional scale (C). The scale for all maps is representative of relative spatial variation in the sites within the season for each map input.



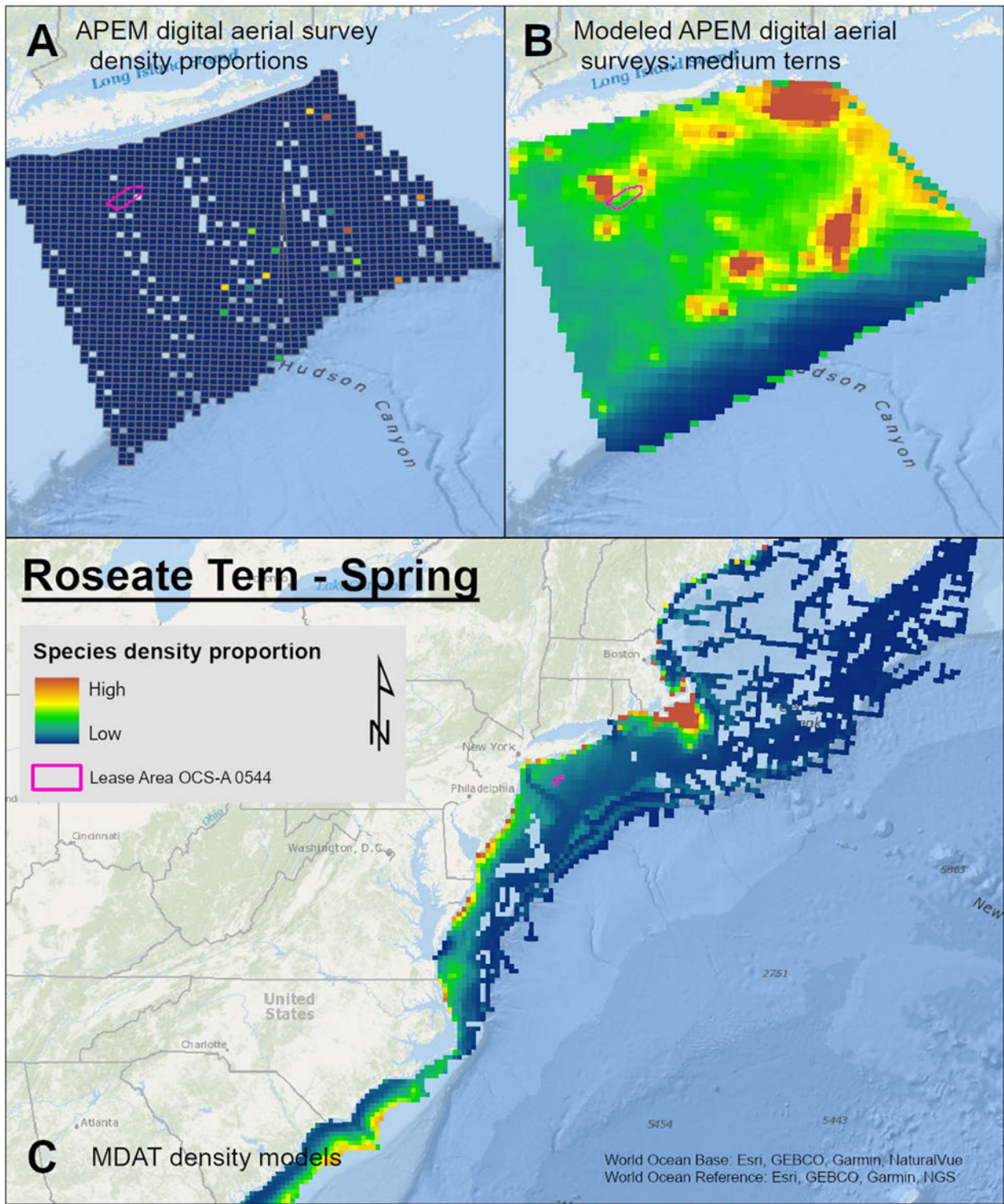
Map 125. Summer Sooty Tern density proportions in the NYSERDA APEM and Empire Wind high resolution digital aerial survey data (A), the NYSERDA APEM and Empire Wind high resolution digital aerial model outputs for medium terns in Summer (B) and, Summer Sooty Tern MDAT modeled abundance at the regional scale (C). The scale for all maps is representative of relative spatial variation in the sites within the season for each map input.



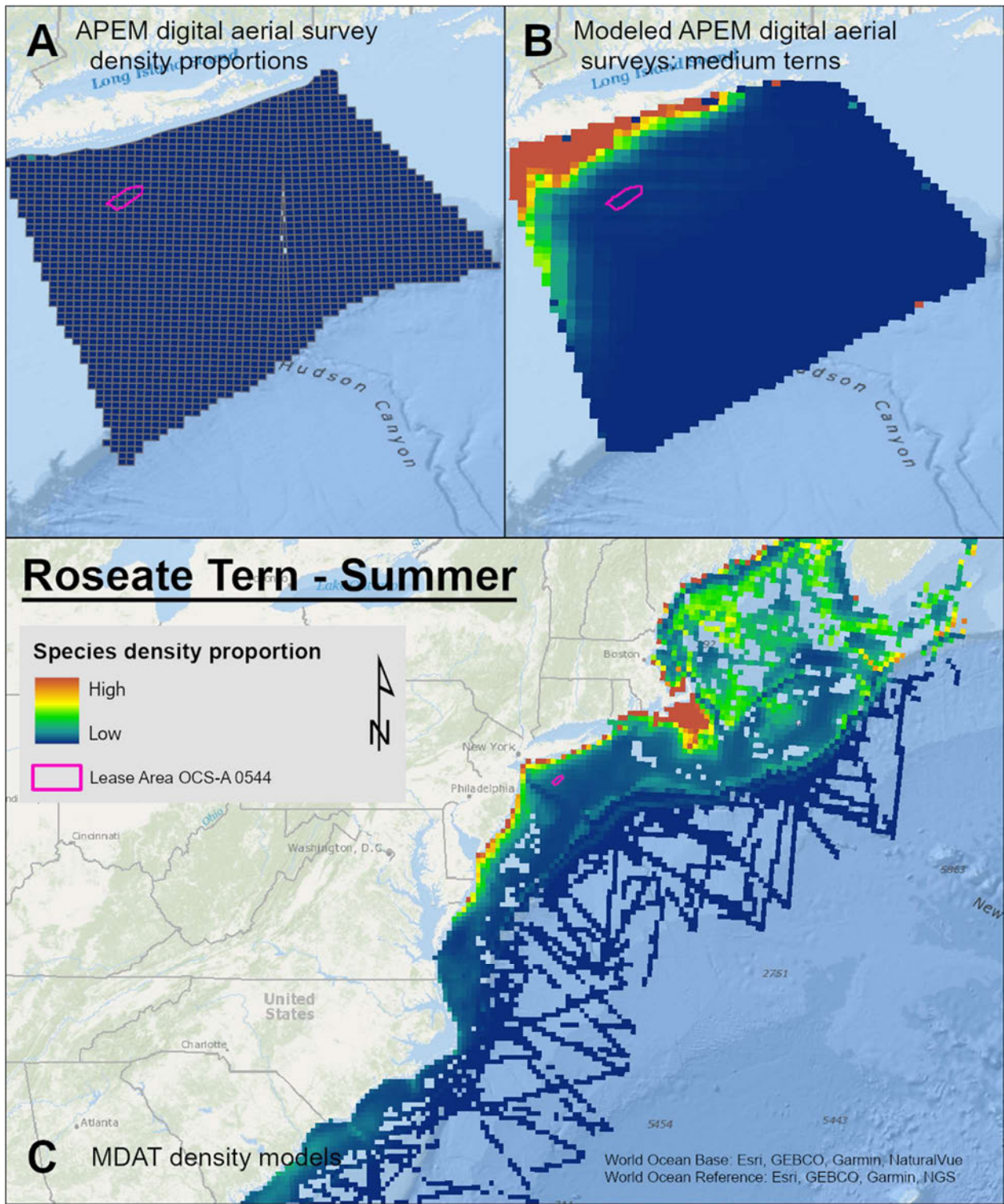
Map 126. Fall Sooty Tern density proportions in the NYSERDA APEM and Empire Wind high resolution digital aerial survey data (A), the NYSERDA APEM and Empire Wind high resolution digital aerial model outputs for medium terns in Fall (B) and, Fall Sooty Tern MDAT modeled abundance at the regional scale (C). The scale for all maps is representative of relative spatial variation in the sites within the season for each map input.



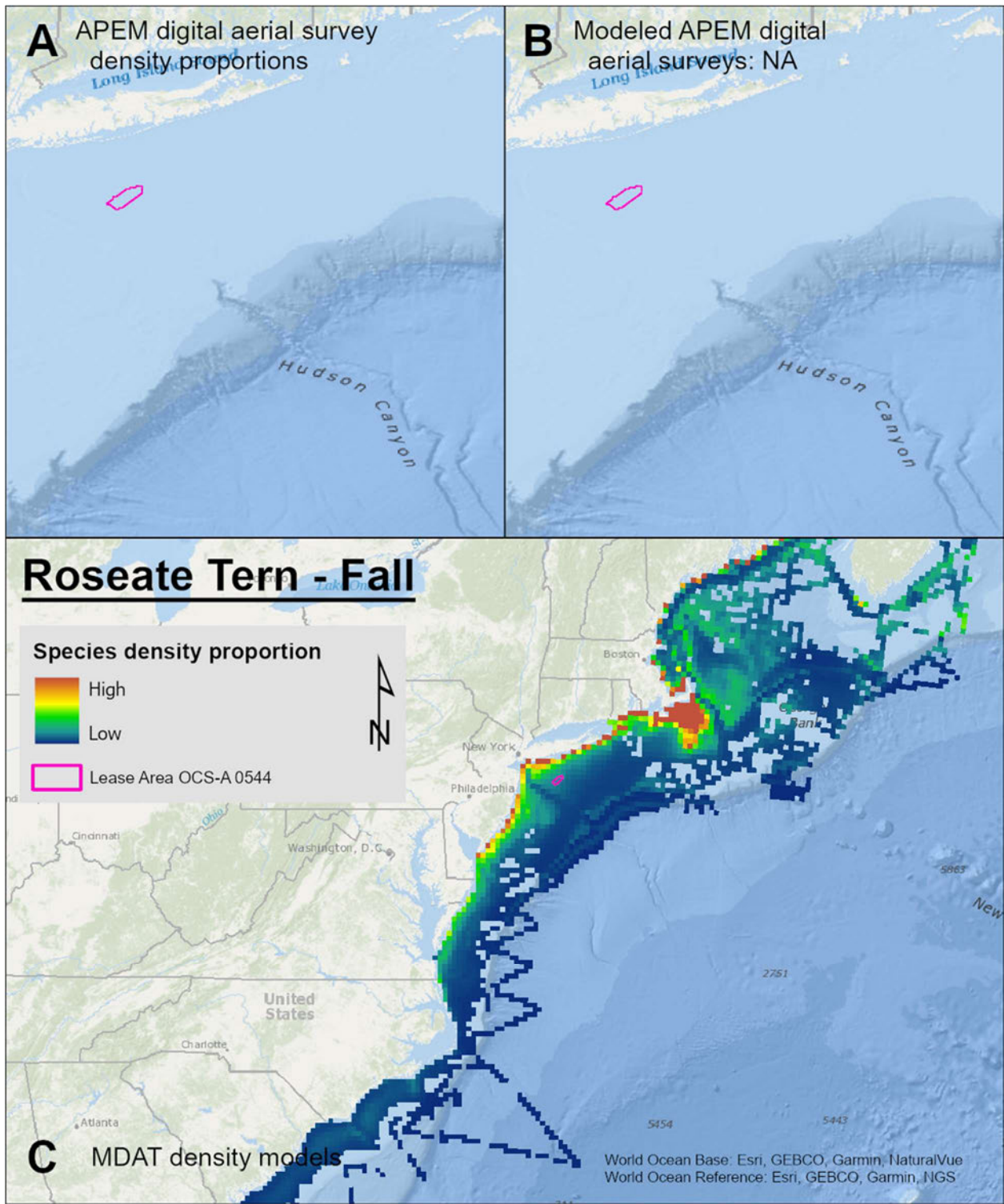
Map 127. Winter Roseate Tern density proportions in the NYSERDA APEM and Empire Wind high resolution digital aerial survey data (A), the NYSERDA APEM and Empire Wind high resolution digital aerial model outputs for medium terns in Winter (B) and, Winter Roseate Tern MDAT modeled abundance at the regional scale (C). The scale for all maps is representative of relative spatial variation in the sites within the season for each map input.



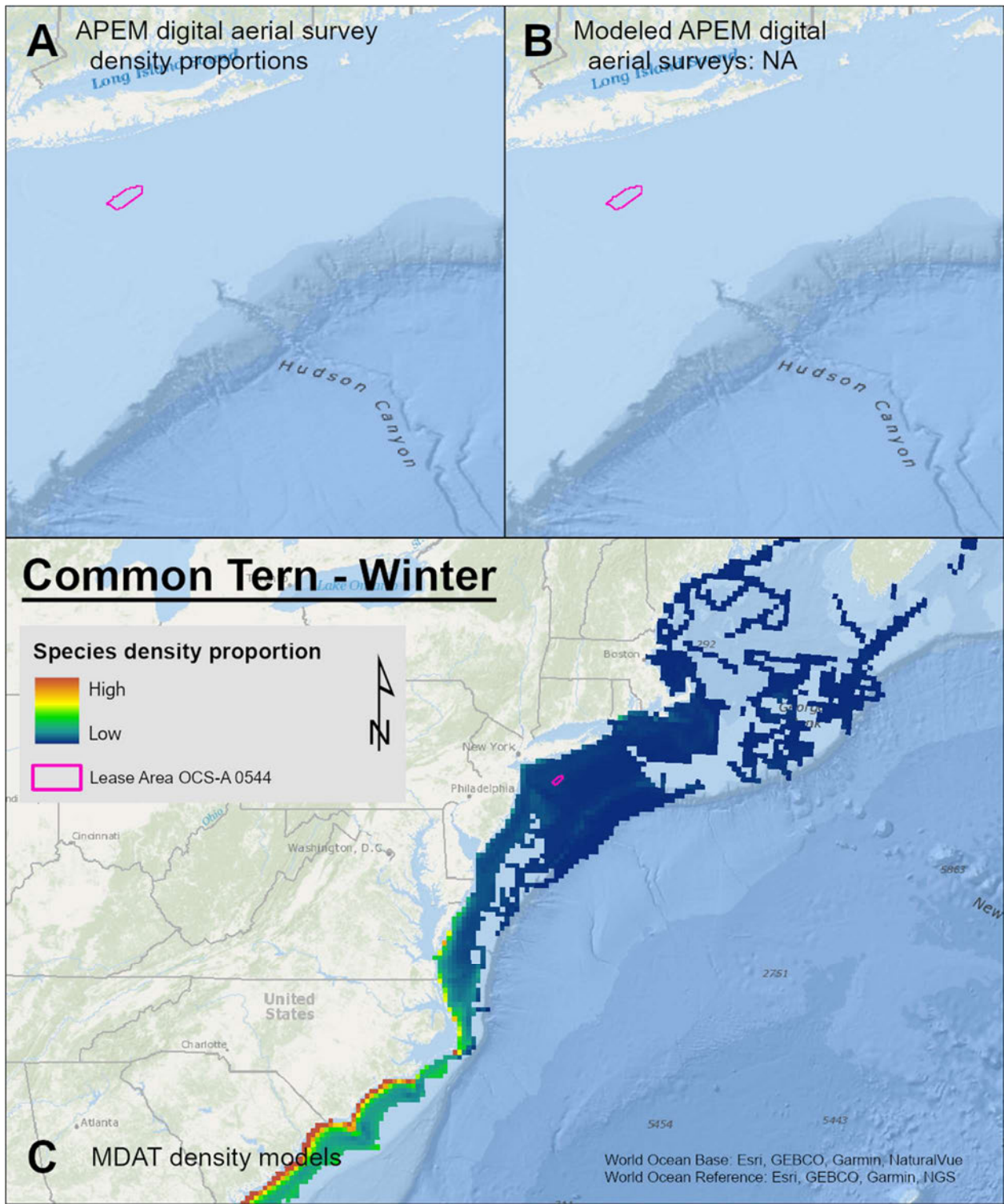
Map 128. Spring Roseate Tern density proportions in the NYSERDA APEM and Empire Wind high resolution digital aerial survey data (A), the NYSERDA APEM and Empire Wind high resolution digital aerial model outputs for medium terns in Spring (B) and, Spring Roseate Tern MDAT modeled abundance at the regional scale (C). The scale for all maps is representative of relative spatial variation in the sites within the season for each map input.



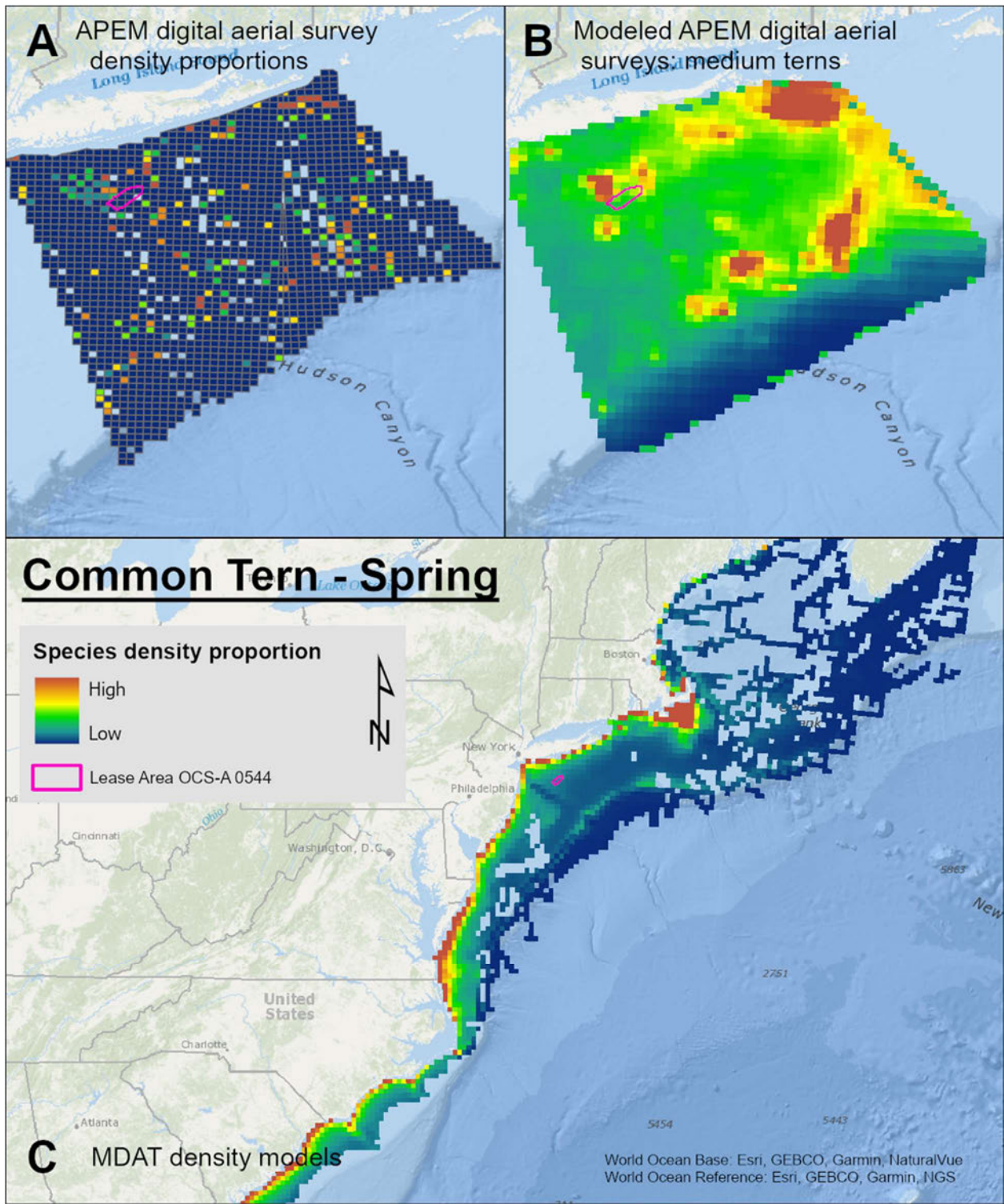
Map 129. Summer Roseate Tern density proportions in the NYSERDA APEM and Empire Wind high resolution digital aerial survey data (A), the NYSERDA APEM and Empire Wind high resolution digital aerial model outputs for medium terns in Summer (B) and, Summer Roseate Tern MDAT modeled abundance at the regional scale (C). The scale for all maps is representative of relative spatial variation in the sites within the season for each map input.



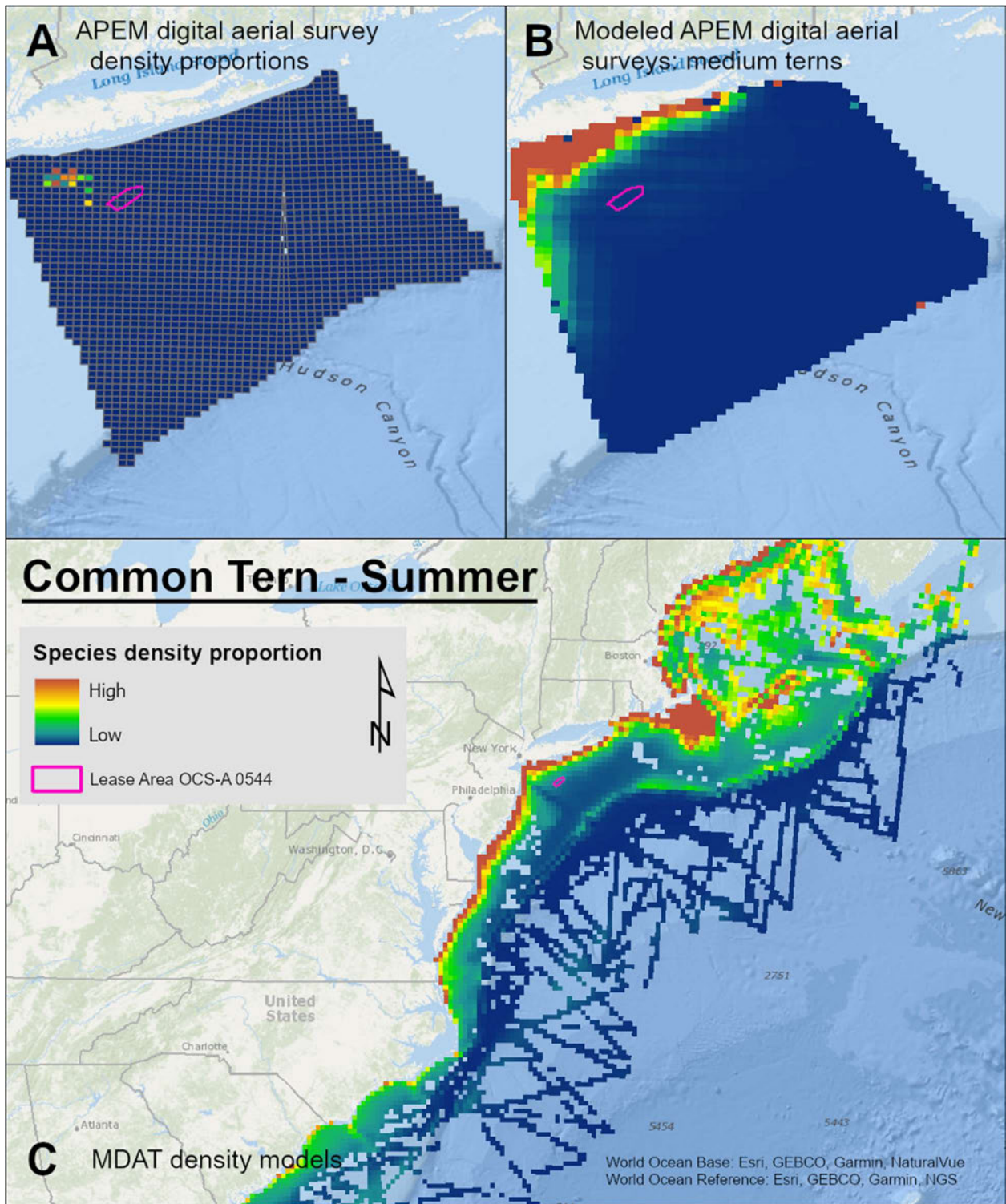
Map 130. Fall Roseate Tern density proportions in the NYSERDA APEM and Empire Wind high resolution digital aerial survey data (A), the NYSERDA APEM and Empire Wind high resolution digital aerial model outputs for medium terns in Fall (B) and, Fall Roseate Tern MDAT modeled abundance at the regional scale (C). The scale for all maps is representative of relative spatial variation in the sites within the season for each map input.



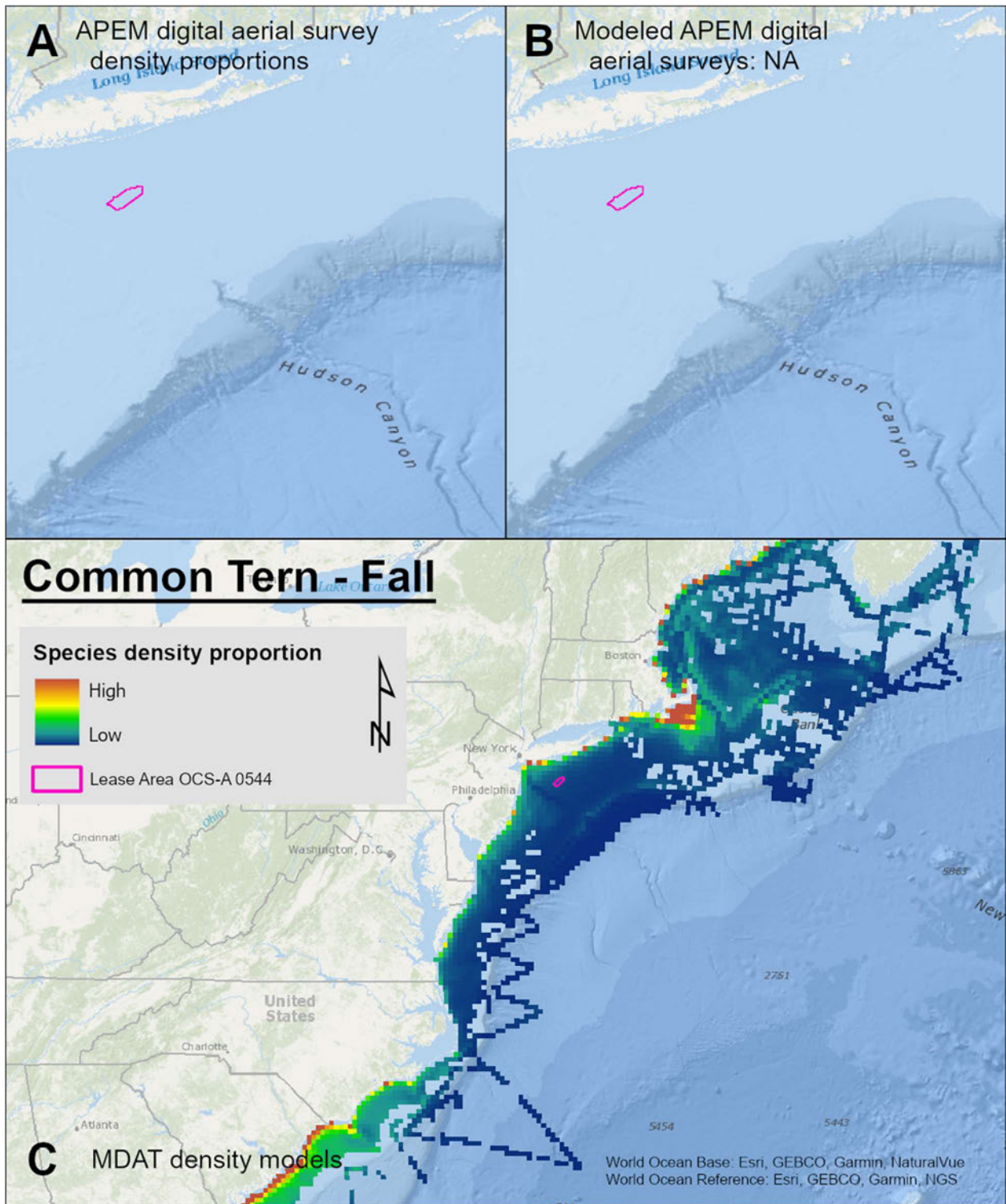
Map 131. Winter Common Tern density proportions in the NYSERDA APEM and Empire Wind high resolution digital aerial survey data (A), the NYSERDA APEM and Empire Wind high resolution digital aerial model outputs for medium terns in Winter (B) and, Winter Common Tern MDAT modeled abundance at the regional scale (C). The scale for all maps is representative of relative spatial variation in the sites within the season for each map input.



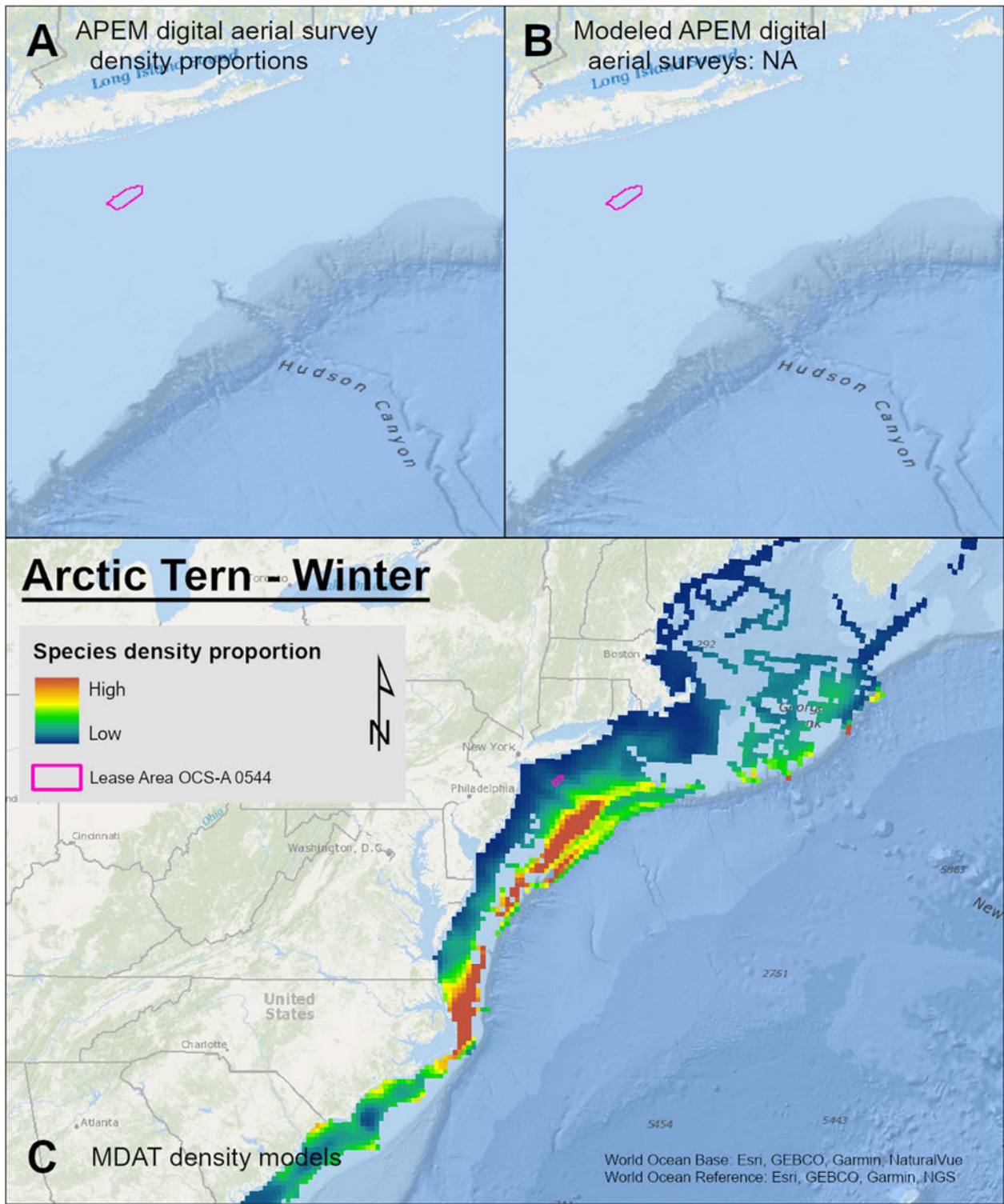
Map 132. Spring Common Tern density proportions in the NYSERDA APEM and Empire Wind high resolution digital aerial survey data (A), the NYSERDA APEM and Empire Wind high resolution digital aerial model outputs for medium terns in Spring (B) and, Spring Common Tern MDAT modeled abundance at the regional scale (C). The scale for all maps is representative of relative spatial variation in the sites within the season for each map input.



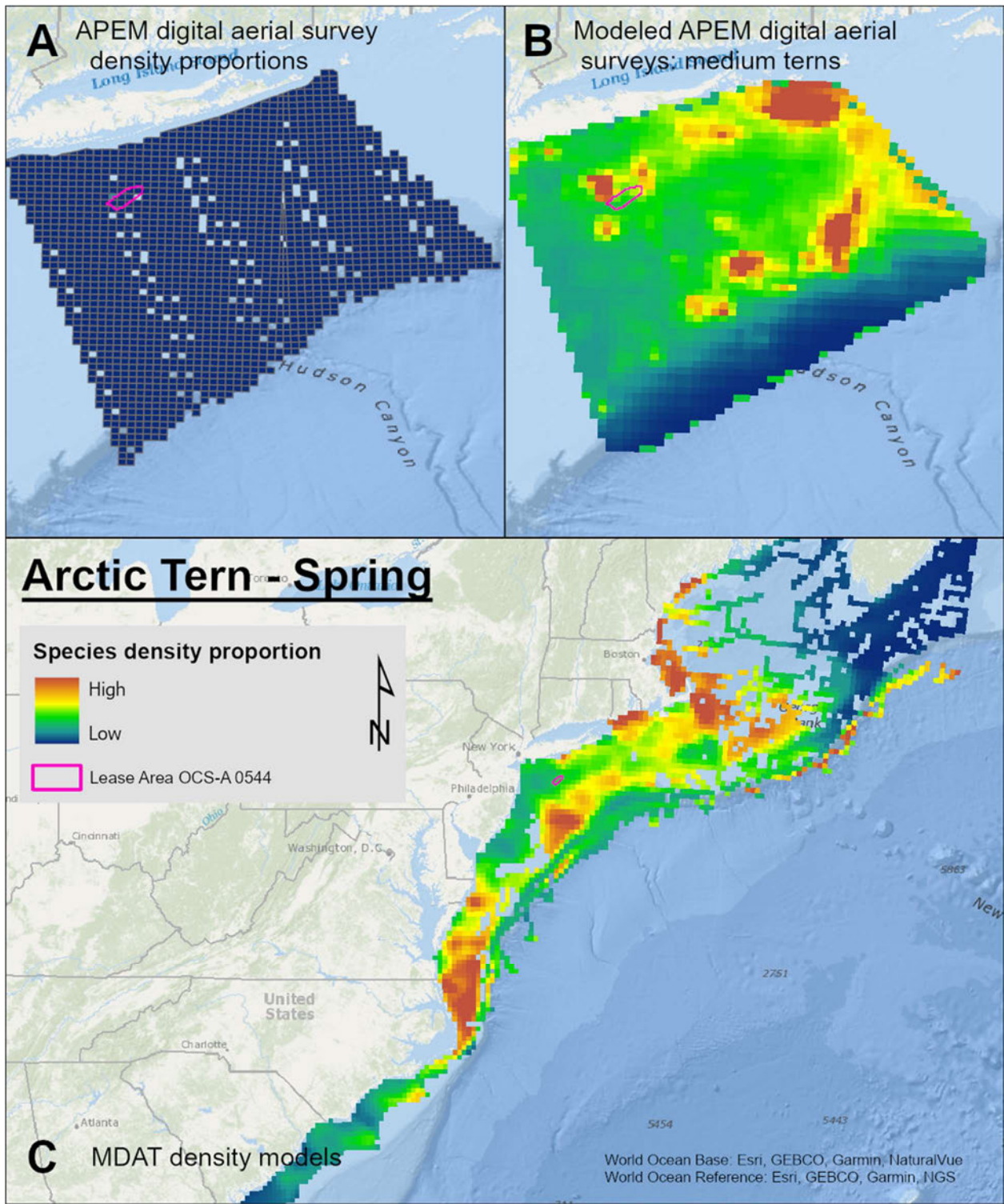
Map 133. Summer Common Tern density proportions in the NYSERDA APEM and Empire Wind high resolution digital aerial survey data (A), the NYSERDA APEM and Empire Wind high resolution digital aerial model outputs for medium terns in Summer (B) and, Summer Common Tern MDAT modeled abundance at the regional scale (C). The scale for all maps is representative of relative spatial variation in the sites within the season for each map input.



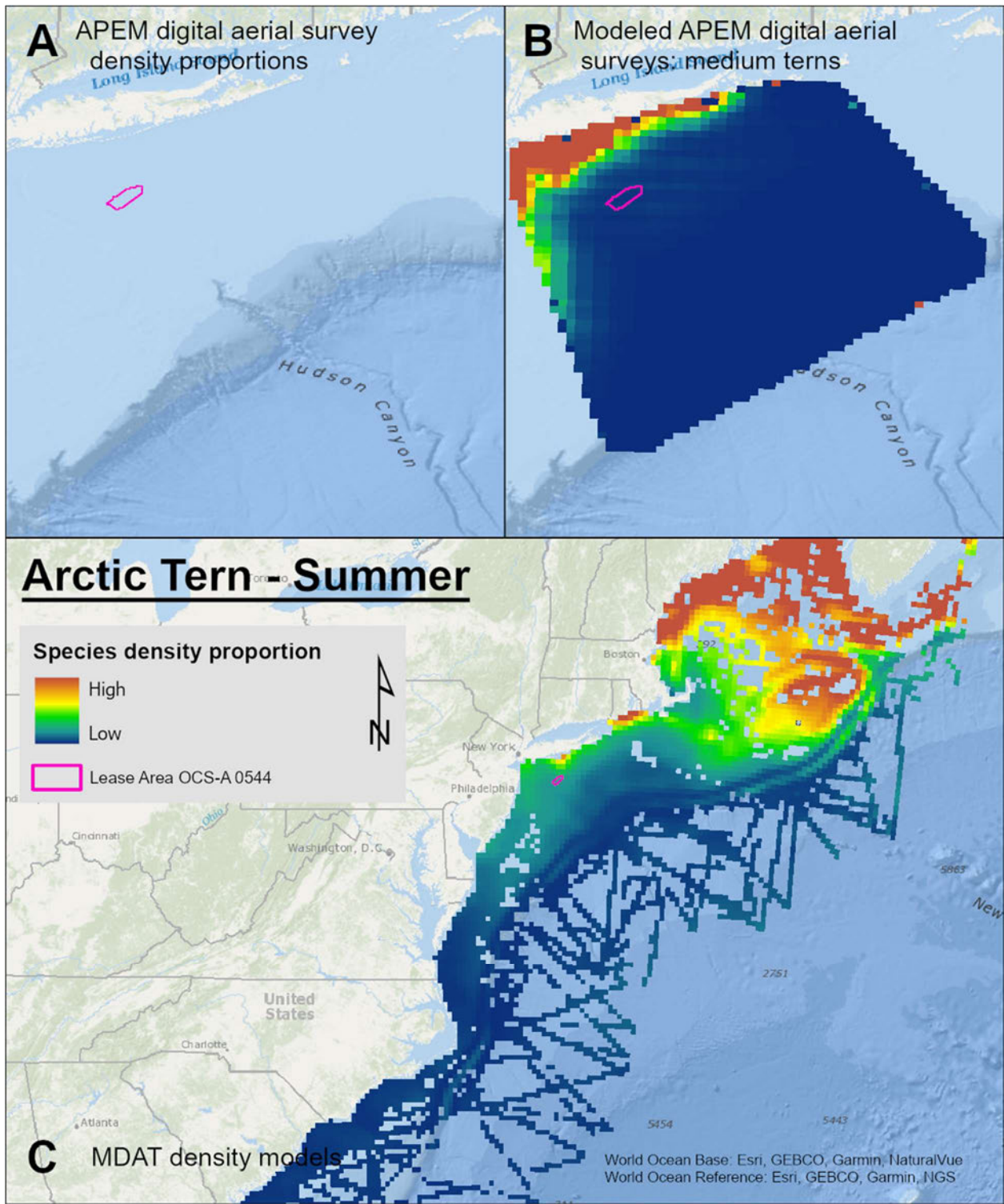
Map 134. Fall Common Tern density proportions in the NYSERDA APEM and Empire Wind high resolution digital aerial survey data (A), the NYSERDA APEM and Empire Wind high resolution digital aerial model outputs for medium terns in Fall (B) and, Fall Common Tern MDAT modeled abundance at the regional scale (C). The scale for all maps is representative of relative spatial variation in the sites within the season for each map input.



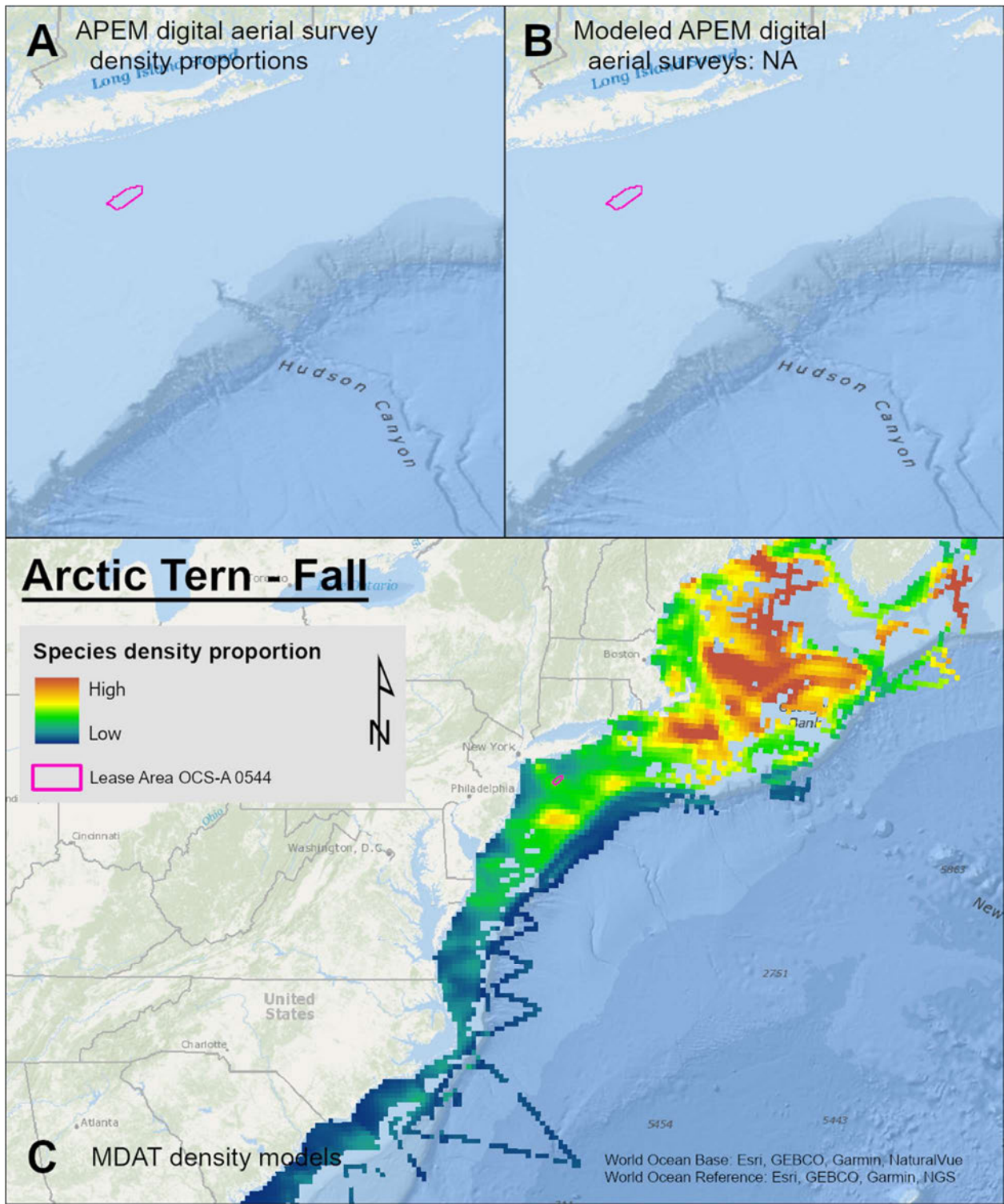
Map 135. Winter Arctic Tern density proportions in the NYSERDA APEM and Empire Wind high resolution digital aerial survey data (A), the NYSERDA APEM and Empire Wind high resolution digital aerial model outputs for medium terns in Winter (B) and, Winter Arctic Tern MDAT modeled abundance at the regional scale (C). The scale for all maps is representative of relative spatial variation in the sites within the season for each map input.



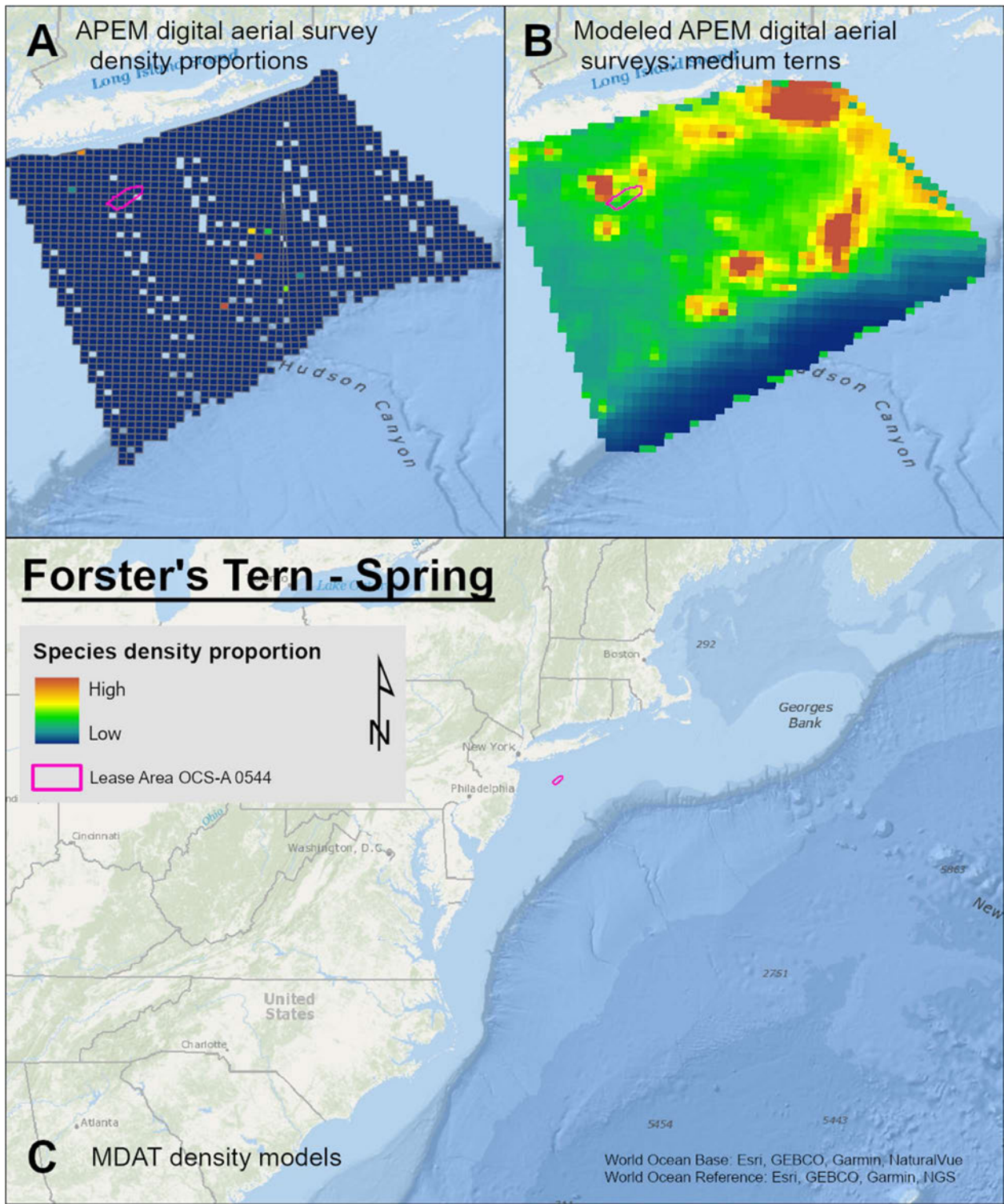
Map 136. Spring Arctic Tern density proportions in the NYSERDA APEM and Empire Wind high resolution digital aerial survey data (A), the NYSERDA APEM and Empire Wind high resolution digital aerial model outputs for medium terns in Spring (B) and, Spring Arctic Tern MDAT modeled abundance at the regional scale (C). The scale for all maps is representative of relative spatial variation in the sites within the season for each map input.



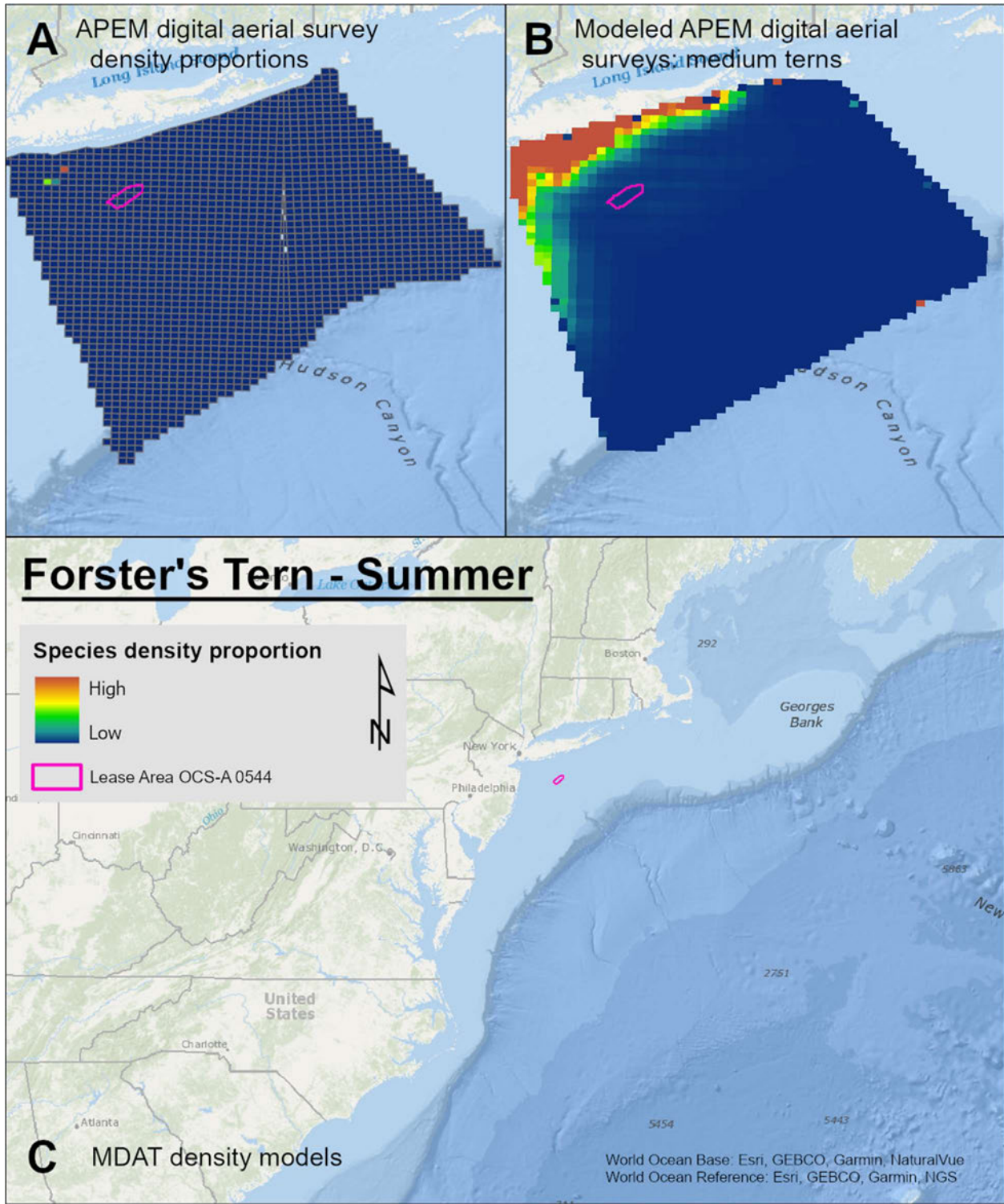
Map 137. Summer Arctic Tern density proportions in the NYSERDA APEM and Empire Wind high resolution digital aerial survey data (A), the NYSERDA APEM and Empire Wind high resolution digital aerial model outputs for medium terns in Summer (B) and, Summer Arctic Tern MDAT modeled abundance at the regional scale (C). The scale for all maps is representative of relative spatial variation in the sites within the season for each map input.



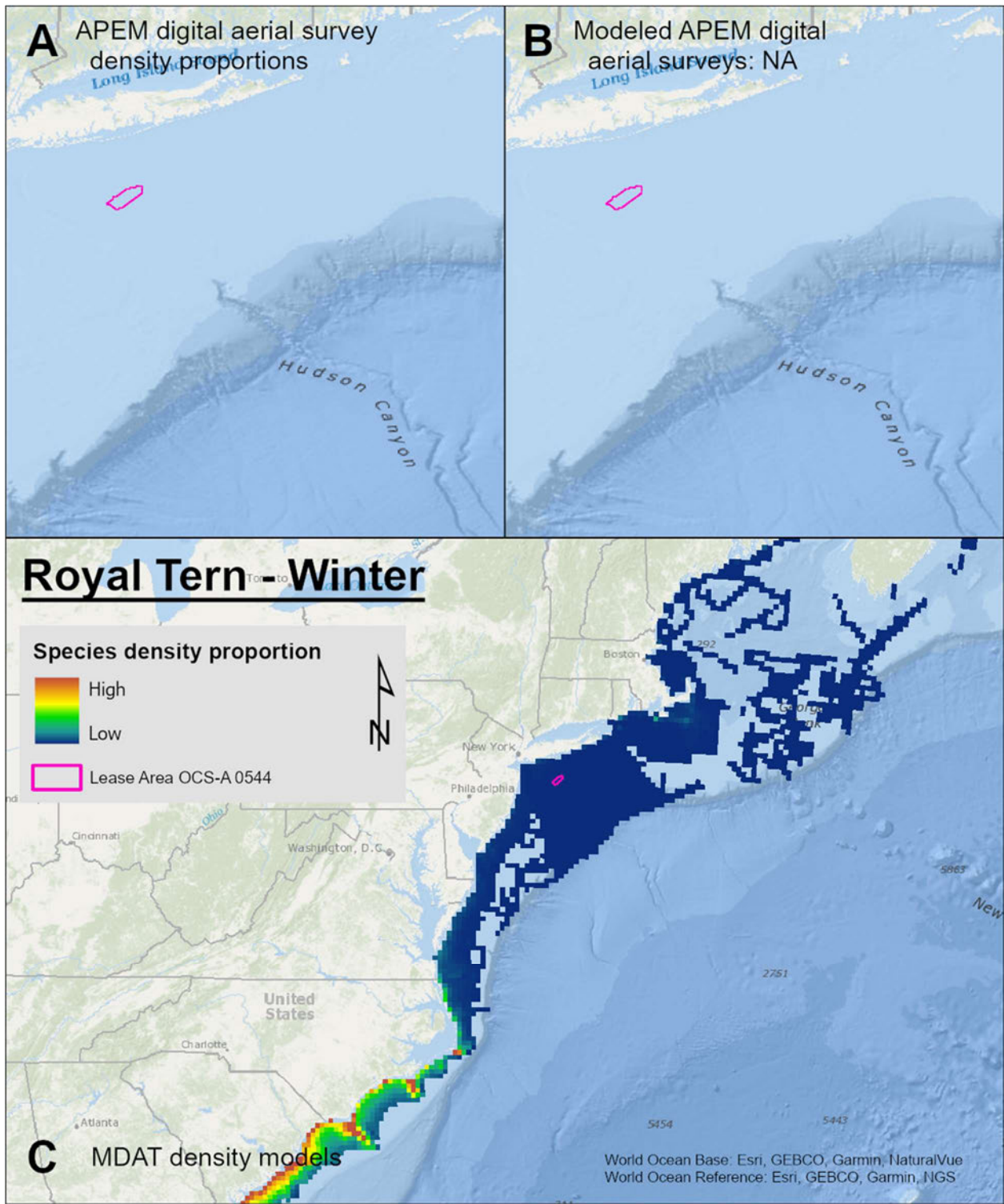
Map 138. Fall Arctic Tern density proportions in the NYSERDA APEM and Empire Wind high resolution digital aerial survey data (A), the NYSERDA APEM and Empire Wind high resolution digital aerial model outputs for medium terns in Fall (B) and, Fall Arctic Tern MDAT modeled abundance at the regional scale (C). The scale for all maps is representative of relative spatial variation in the sites within the season for each map input.



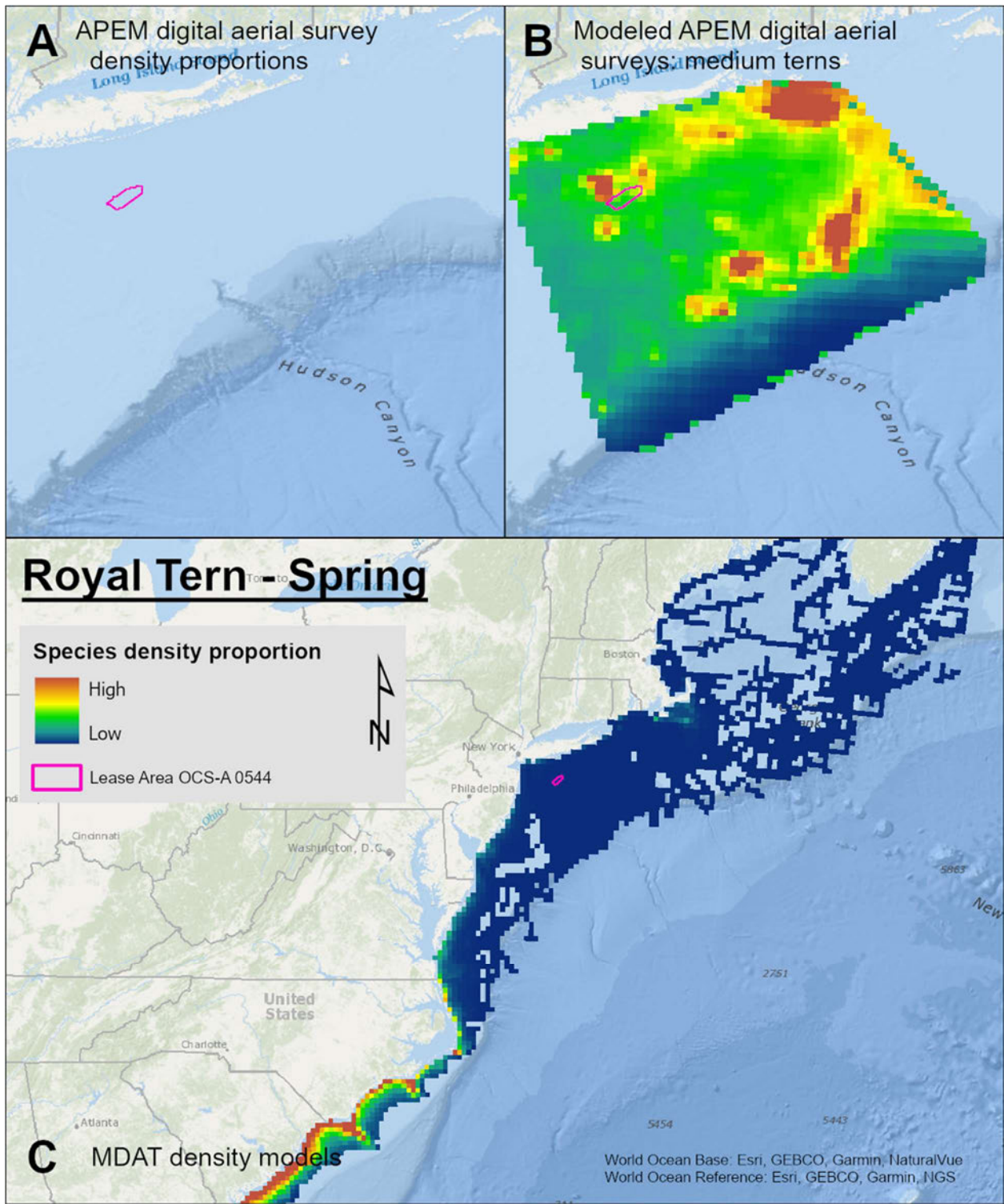
Map 139. Spring Forster's Tern density proportions in the NYSERDA APEM and Empire Wind high resolution digital aerial survey data (A), the NYSERDA APEM and Empire Wind high resolution digital aerial model outputs for medium terns in Spring (B) and, Spring Forster's Tern MDAT modeled abundance at the regional scale (C). The scale for all maps is representative of relative spatial variation in the sites within the season for each map input.



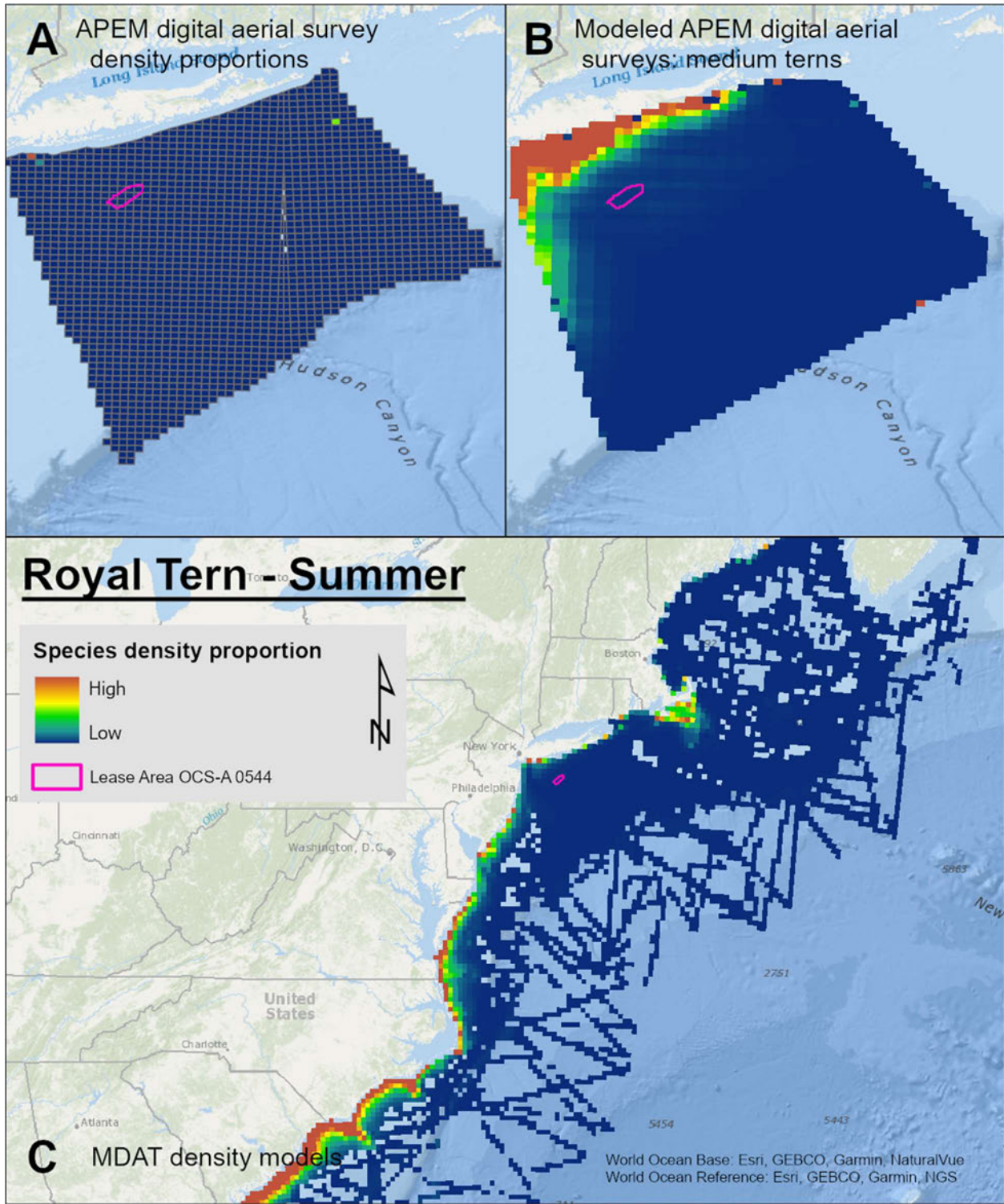
Map 140. Summer Forster's Tern density proportions in the NYSERDA APEM and Empire Wind high resolution digital aerial survey data (A), the NYSERDA APEM and Empire Wind high resolution digital aerial model outputs for medium terns in Summer (B) and, Summer Forster's Tern MDAT modeled abundance at the regional scale (C). The scale for all maps is representative of relative spatial variation in the sites within the season for each map input.



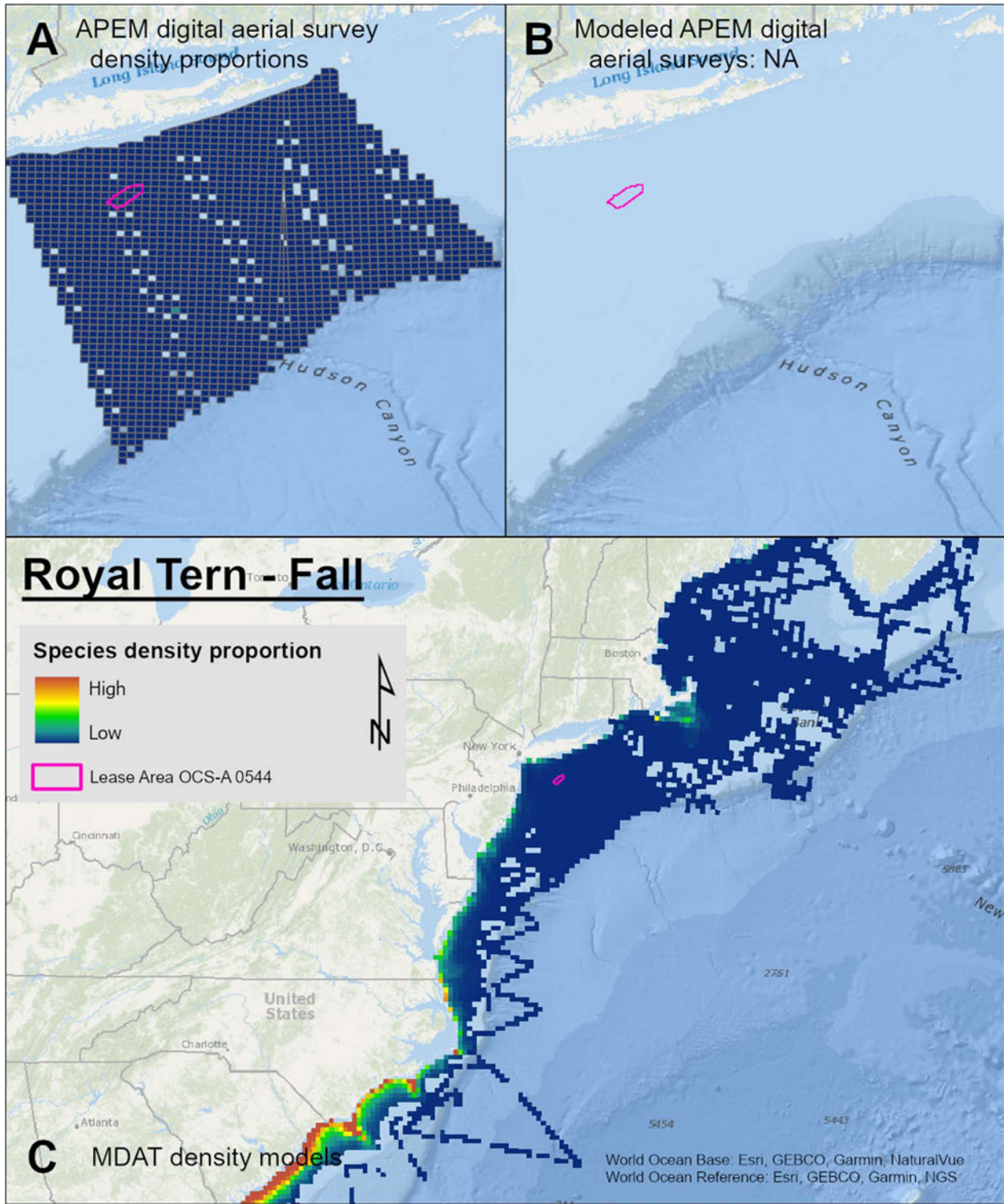
Map 141. Winter Royal Tern density proportions in the NYSERDA APEM and Empire Wind high resolution digital aerial survey data (A), the NYSERDA APEM and Empire Wind high resolution digital aerial model outputs for medium terns in Winter (B) and, Winter Royal Tern MDAT modeled abundance at the regional scale (C). The scale for all maps is representative of relative spatial variation in the sites within the season for each map input.



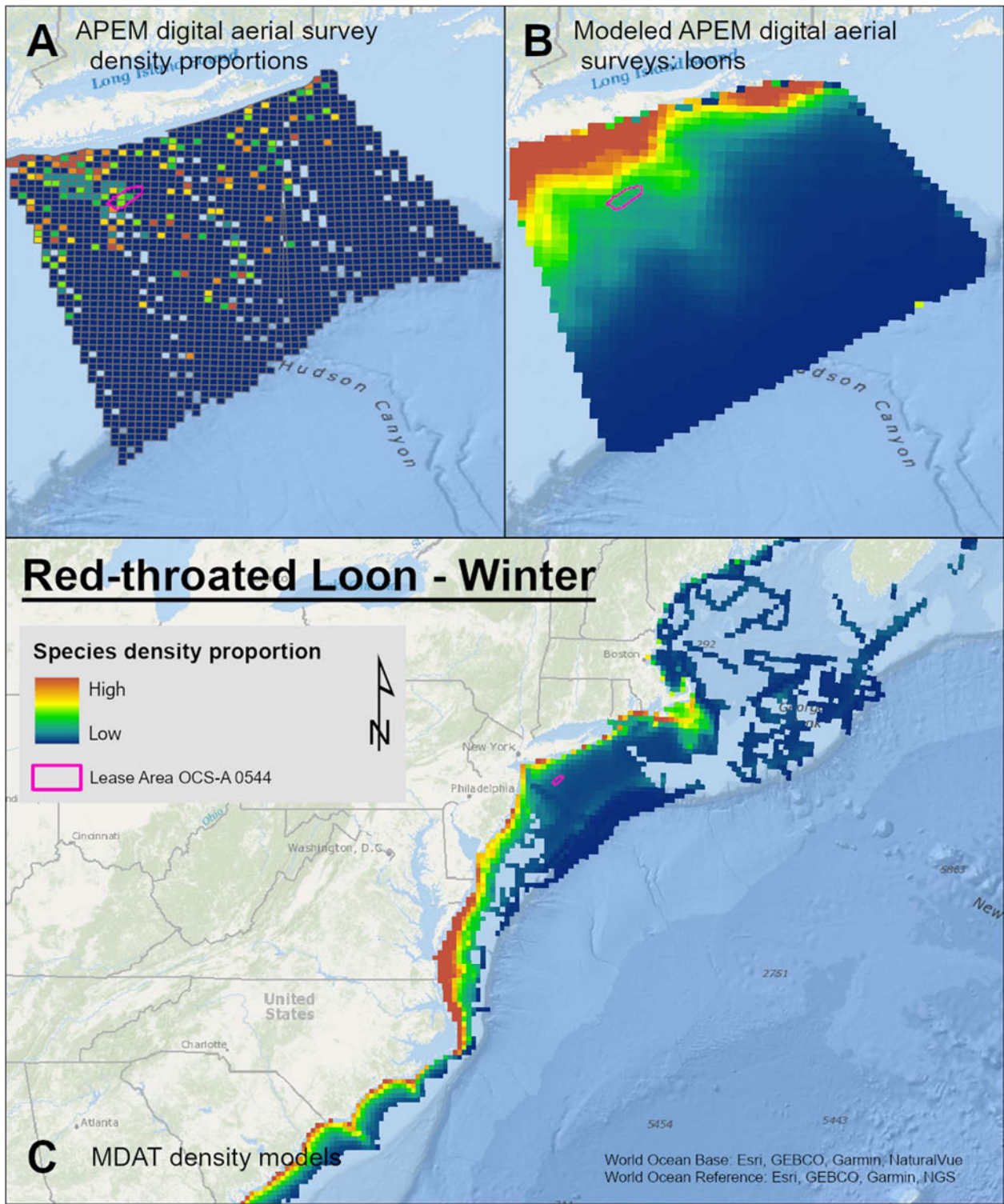
Map 142. Spring Royal Tern density proportions in the NYSERDA APEM and Empire Wind high resolution digital aerial survey data (A), the NYSERDA APEM and Empire Wind high resolution digital aerial model outputs for medium terns in Spring (B) and, Spring Royal Tern MDAT modeled abundance at the regional scale (C). The scale for all maps is representative of relative spatial variation in the sites within the season for each map input.



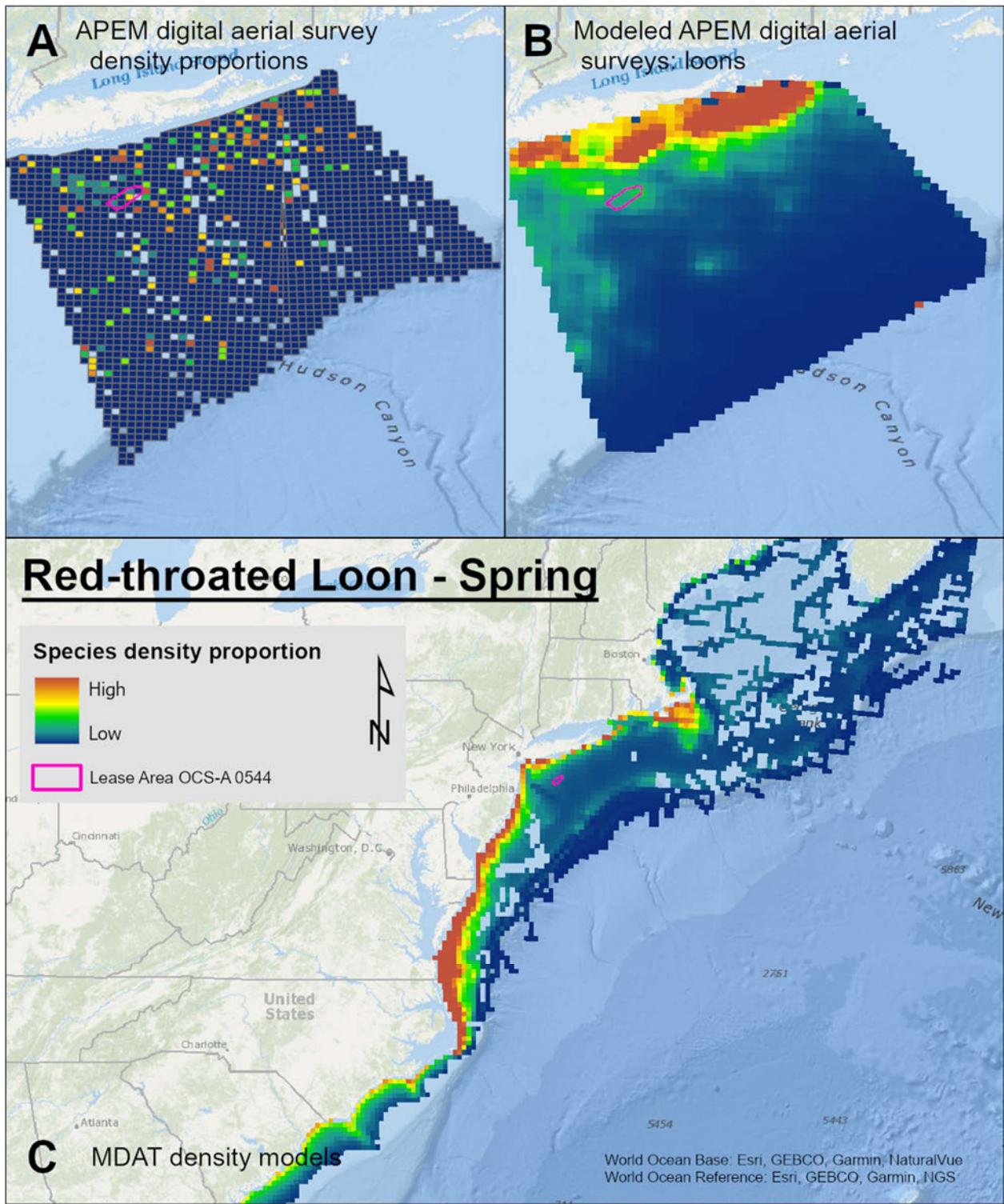
Map 143. Summer Royal Tern density proportions in the NYSERDA APEM and Empire Wind high resolution digital aerial survey data (A), the NYSERDA APEM and Empire Wind high resolution digital aerial model outputs for medium terns in Summer (B) and, Summer Royal Tern MDAT modeled abundance at the regional scale (C). The scale for all maps is representative of relative spatial variation in the sites within the season for each map input.



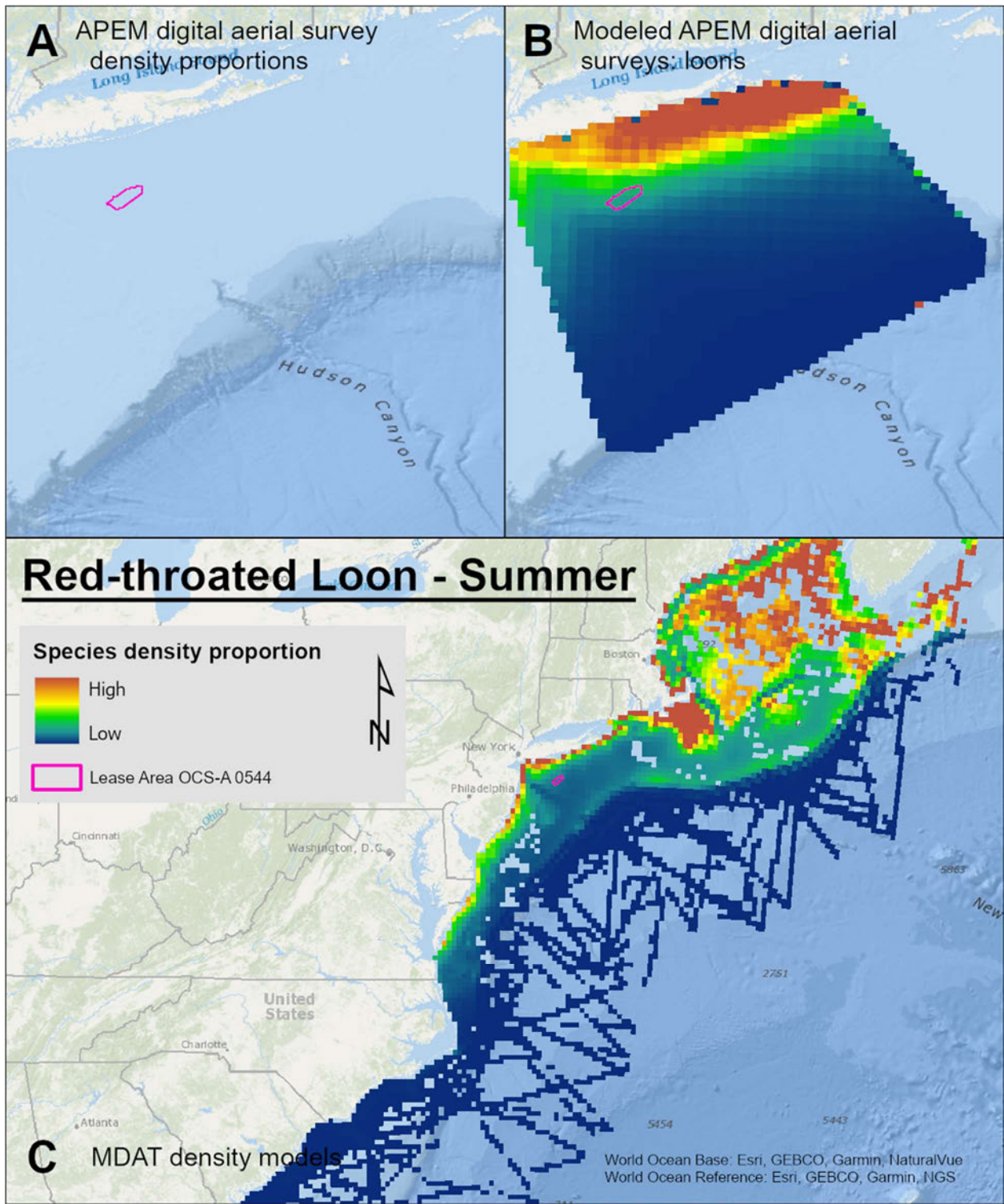
Map 144. Fall Royal Tern density proportions in the NYSERDA APEM and Empire Wind high resolution digital aerial survey data (A), the NYSERDA APEM and Empire Wind high resolution digital aerial model outputs for medium terns in Fall (B) and, Fall Royal Tern MDAT modeled abundance at the regional scale (C). The scale for all maps is representative of relative spatial variation in the sites within the season for each map input.



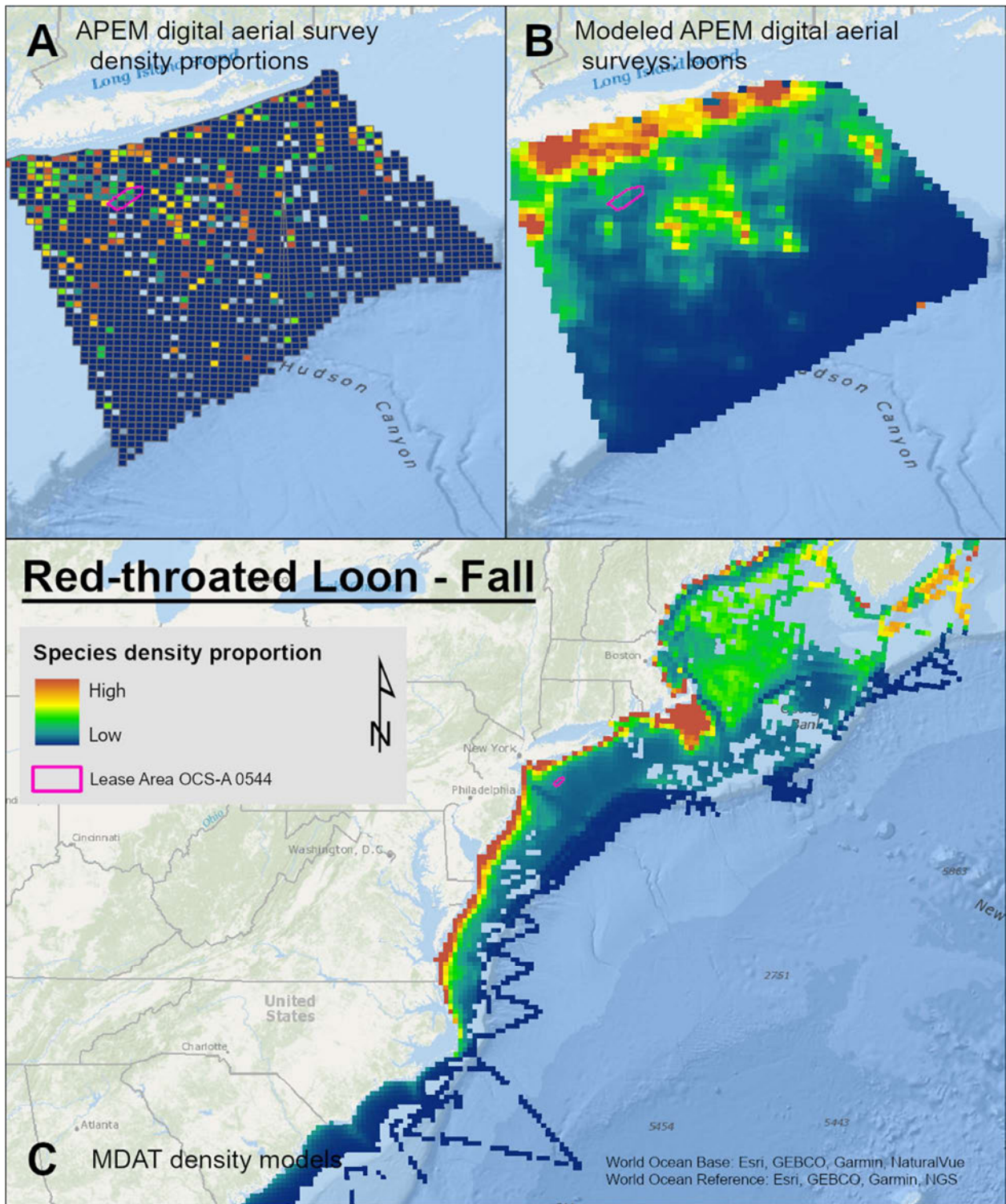
Map 145. Winter Red-throated Loon density proportions in the NYSERDA APEM and Empire Wind high resolution digital aerial survey data (A), the NYSERDA APEM and Empire Wind high resolution digital aerial model outputs for loons in Winter (B) and, Winter Red-throated Loon MDAT modeled abundance at the regional scale (C). The scale for all maps is representative of relative spatial variation in the sites within the season for each map input.



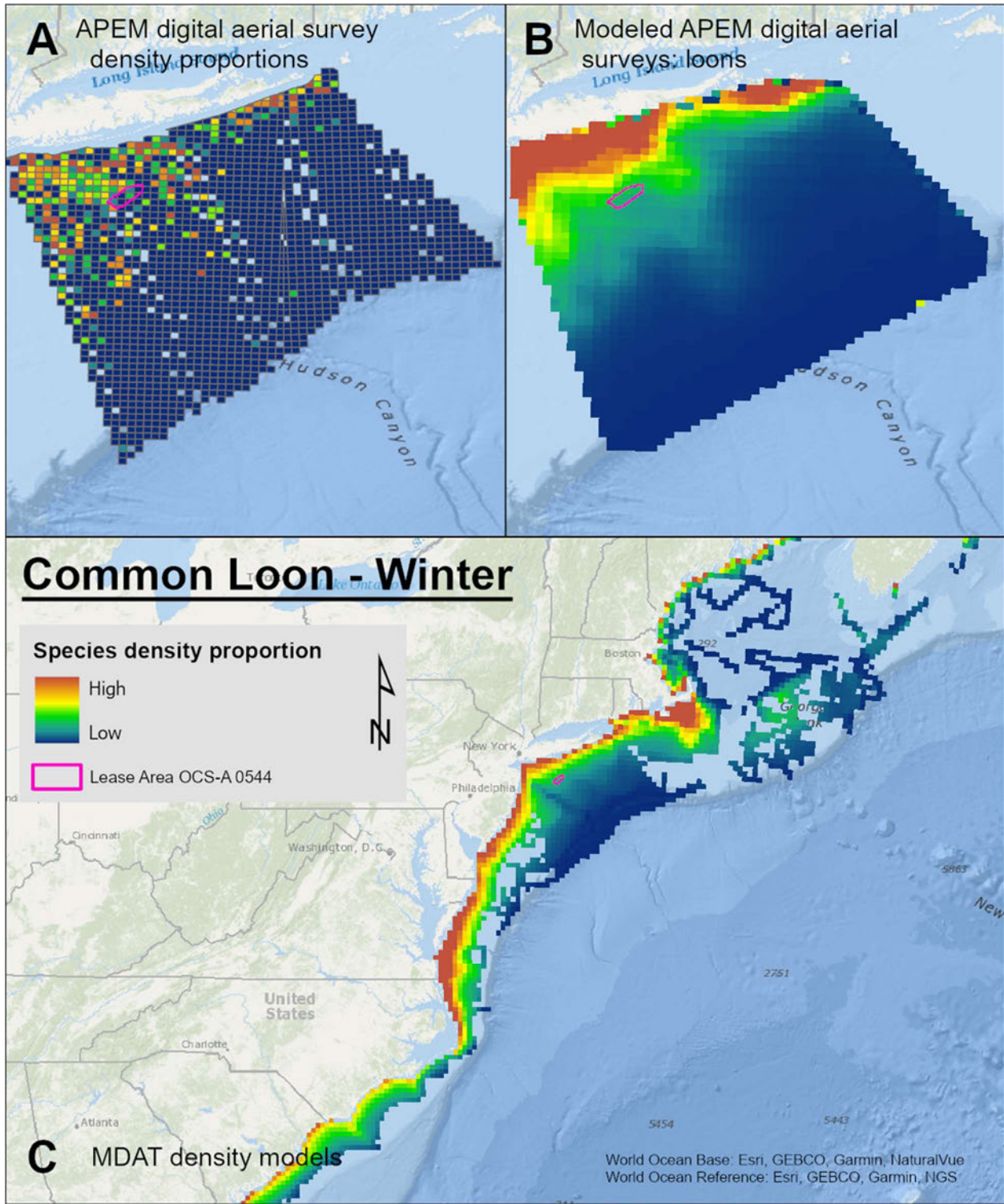
Map 146. Spring Red-throated Loon density proportions in the NYSERDA APEM and Empire Wind high resolution digital aerial survey data (A), the NYSERDA APEM and Empire Wind high resolution digital aerial model outputs for loons in Spring (B) and, Spring Red-throated Loon MDAT modeled abundance at the regional scale (C). The scale for all maps is representative of relative spatial variation in the sites within the season for each map input.



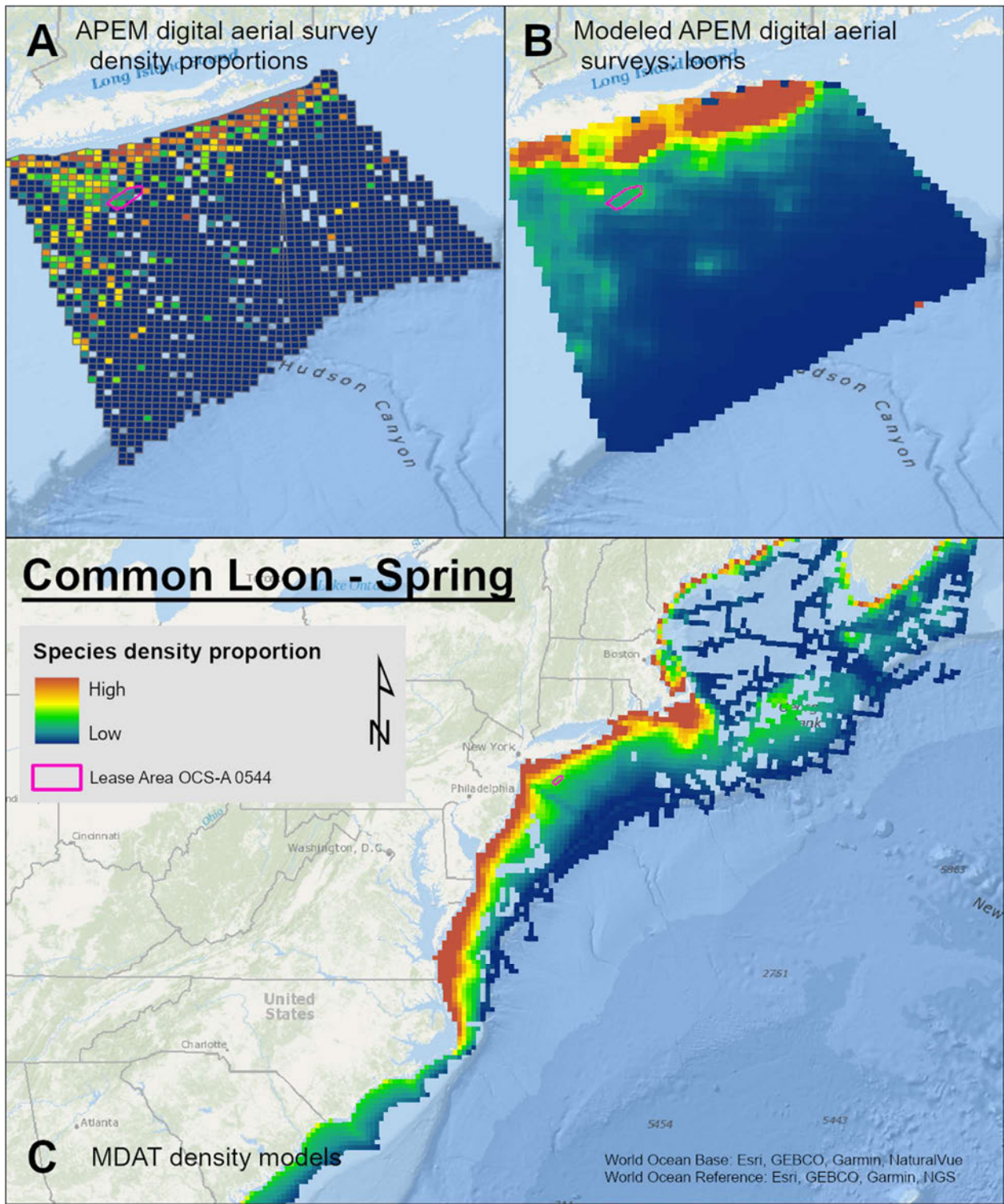
Map 147. Summer Red-throated Loon density proportions in the NYSERDA APEM and Empire Wind high resolution digital aerial survey data (A), the NYSERDA APEM and Empire Wind high resolution digital aerial model outputs for loons in Summer (B) and, Summer Red-throated Loon MDAT modeled abundance at the regional scale (C). The scale for all maps is representative of relative spatial variation in the sites within the season for each map input.



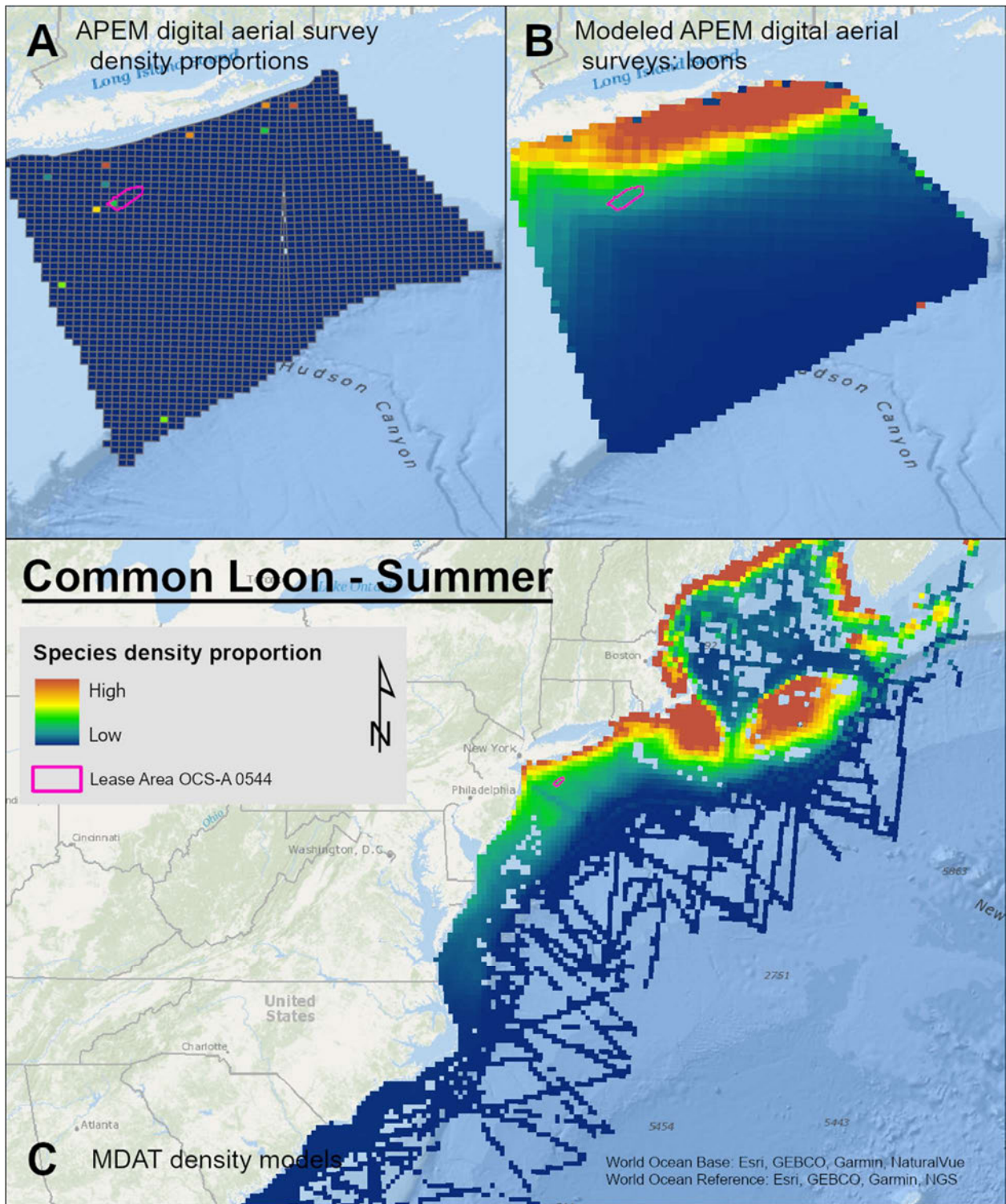
Map 148. Fall Red-throated Loon density proportions in the NYSERDA APEM and Empire Wind high resolution digital aerial survey data (A), the NYSERDA APEM and Empire Wind high resolution digital aerial model outputs for loons in Fall (B) and, Fall Red-throated Loon MDAT modeled abundance at the regional scale (C). The scale for all maps is representative of relative spatial variation in the sites within the season for each map input.



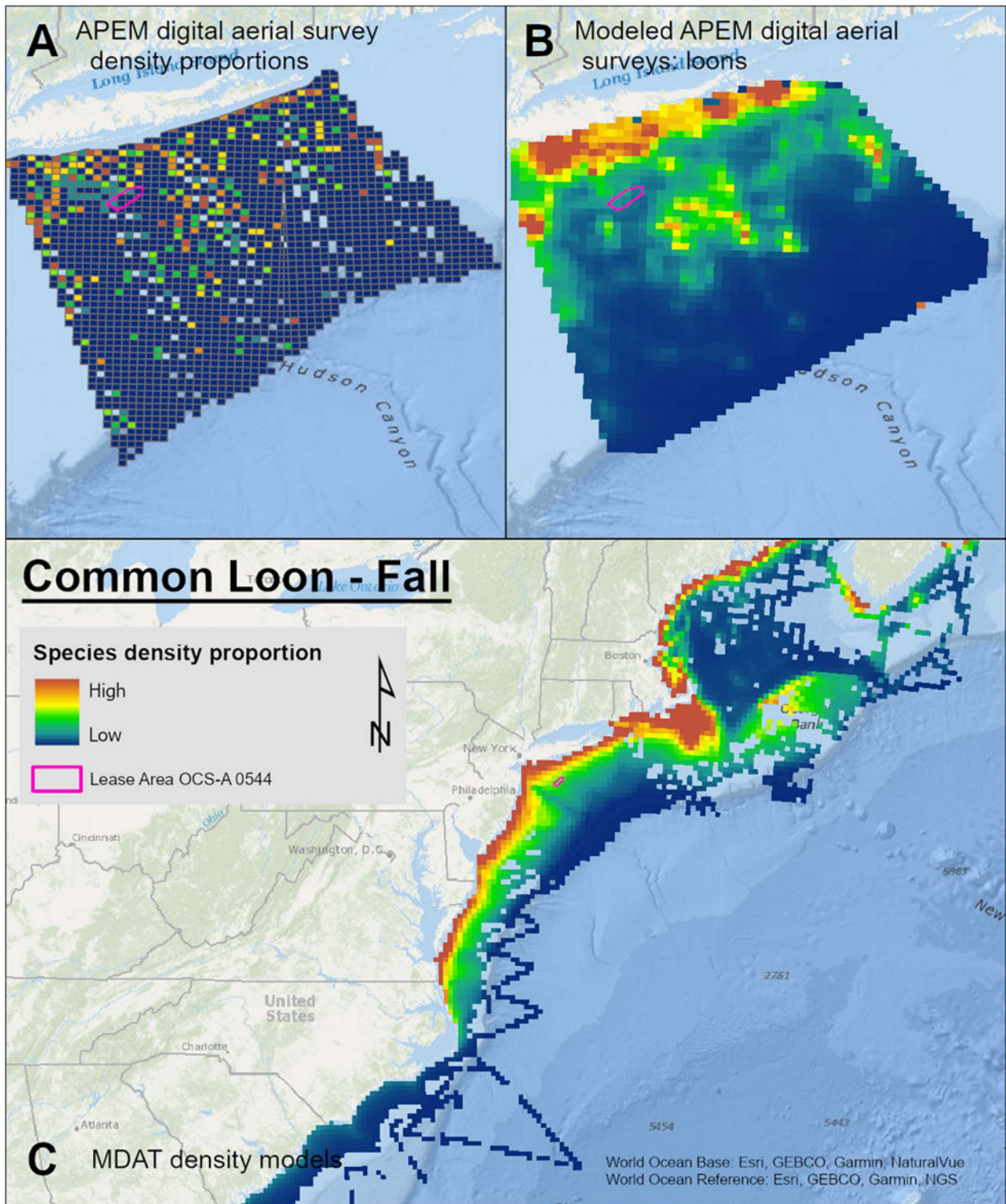
Map 149. Winter Common Loon density proportions in the NYSERDA APEM and Empire Wind high resolution digital aerial survey data (A), the NYSERDA APEM and Empire Wind high resolution digital aerial model outputs for loons in Winter (B) and, Winter Common Loon MDAT modeled abundance at the regional scale (C). The scale for all maps is representative of relative spatial variation in the sites within the season for each map input.



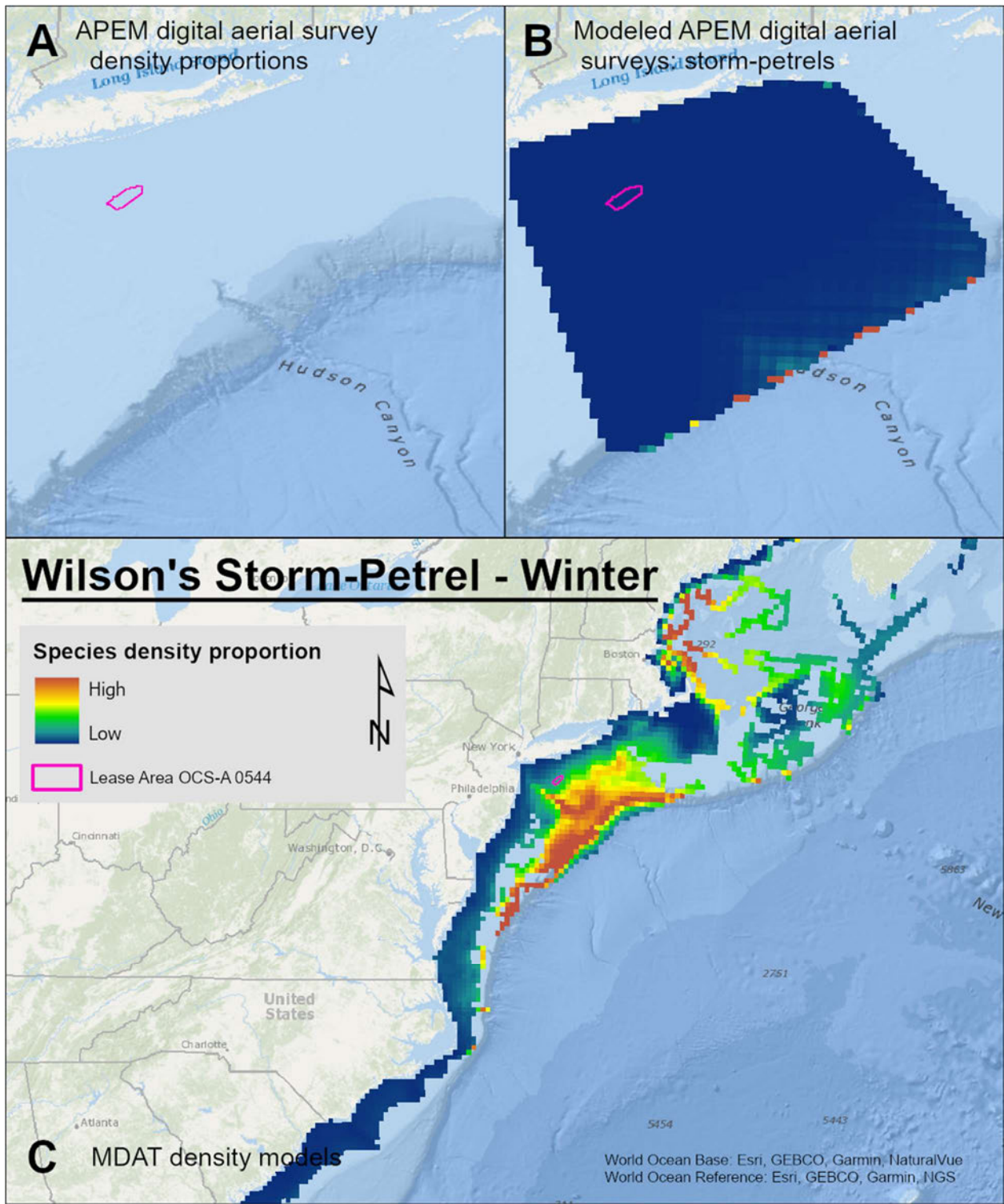
Map 150. Spring Common Loon density proportions in the NYSERDA APEM and Empire Wind high resolution digital aerial survey data (A), the NYSERDA APEM and Empire Wind high resolution digital aerial model outputs for loons in Spring (B) and, Spring Common Loon MDAT modeled abundance at the regional scale (C). The scale for all maps is representative of relative spatial variation in the sites within the season for each map input.



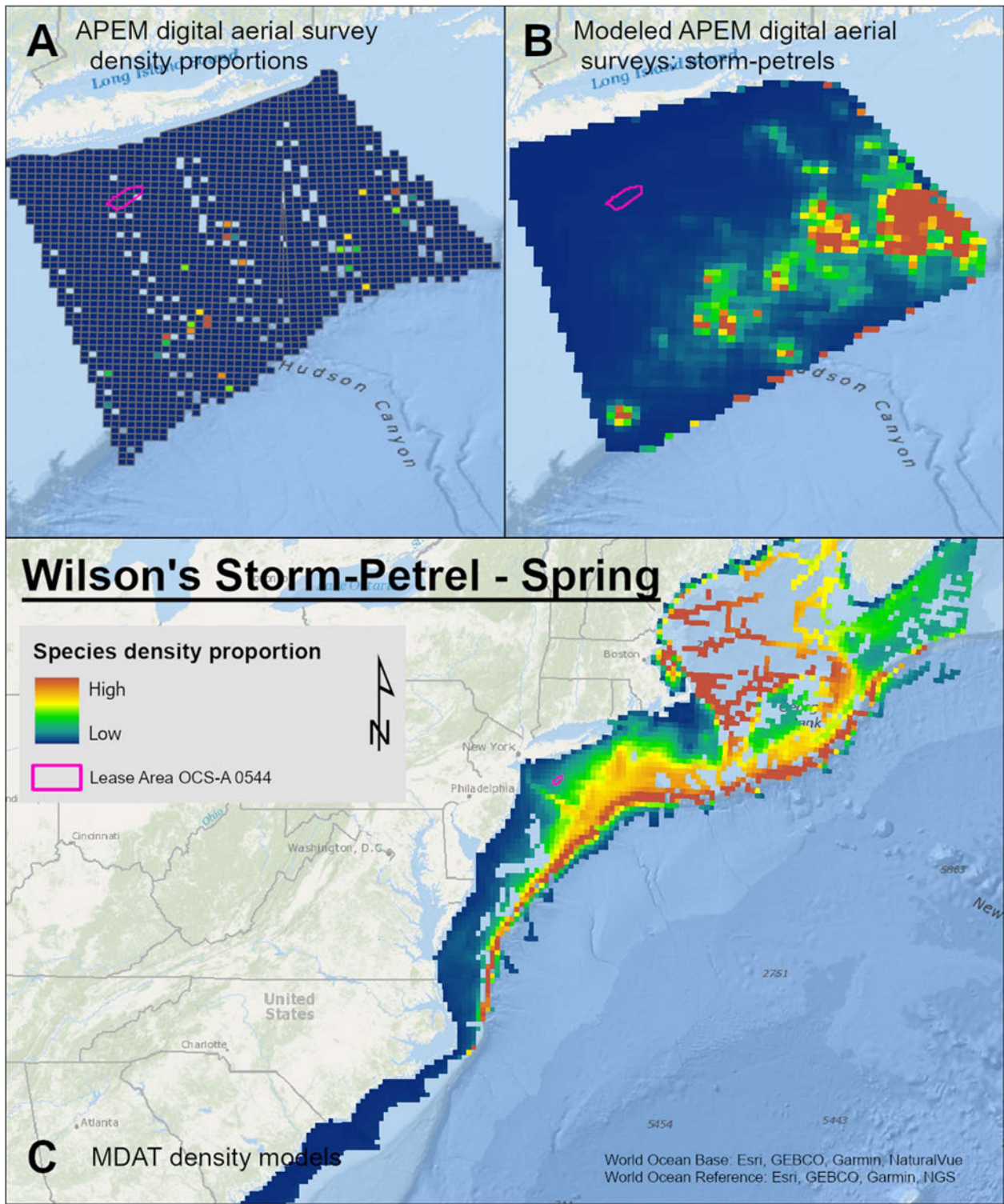
Map 151. Summer Common Loon density proportions in the NYSERDA APEM and Empire Wind high resolution digital aerial survey data (A), the NYSERDA APEM and Empire Wind high resolution digital aerial model outputs for loons in Summer (B) and, Summer Common Loon MDAT modeled abundance at the regional scale (C). The scale for all maps is representative of relative spatial variation in the sites within the season for each map input.



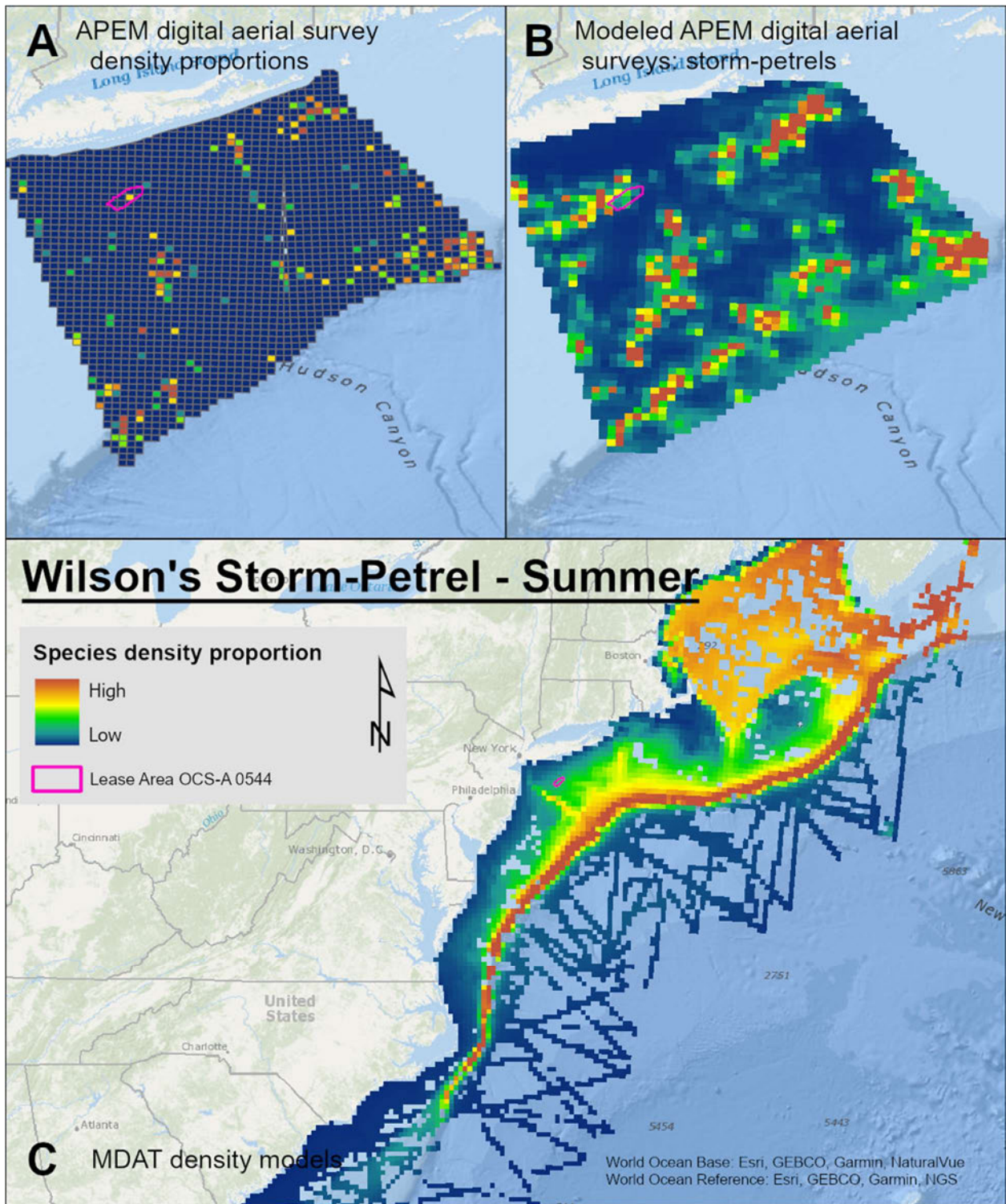
Map 152. Fall Common Loon density proportions in the NYSEDA APEM and Empire Wind high resolution digital aerial survey data (A), the NYSEDA APEM and Empire Wind high resolution digital aerial model outputs for loons in Fall (B) and, Fall Common Loon MDAT modeled abundance at the regional scale (C). The scale for all maps is representative of relative spatial variation in the sites within the season for each map input.



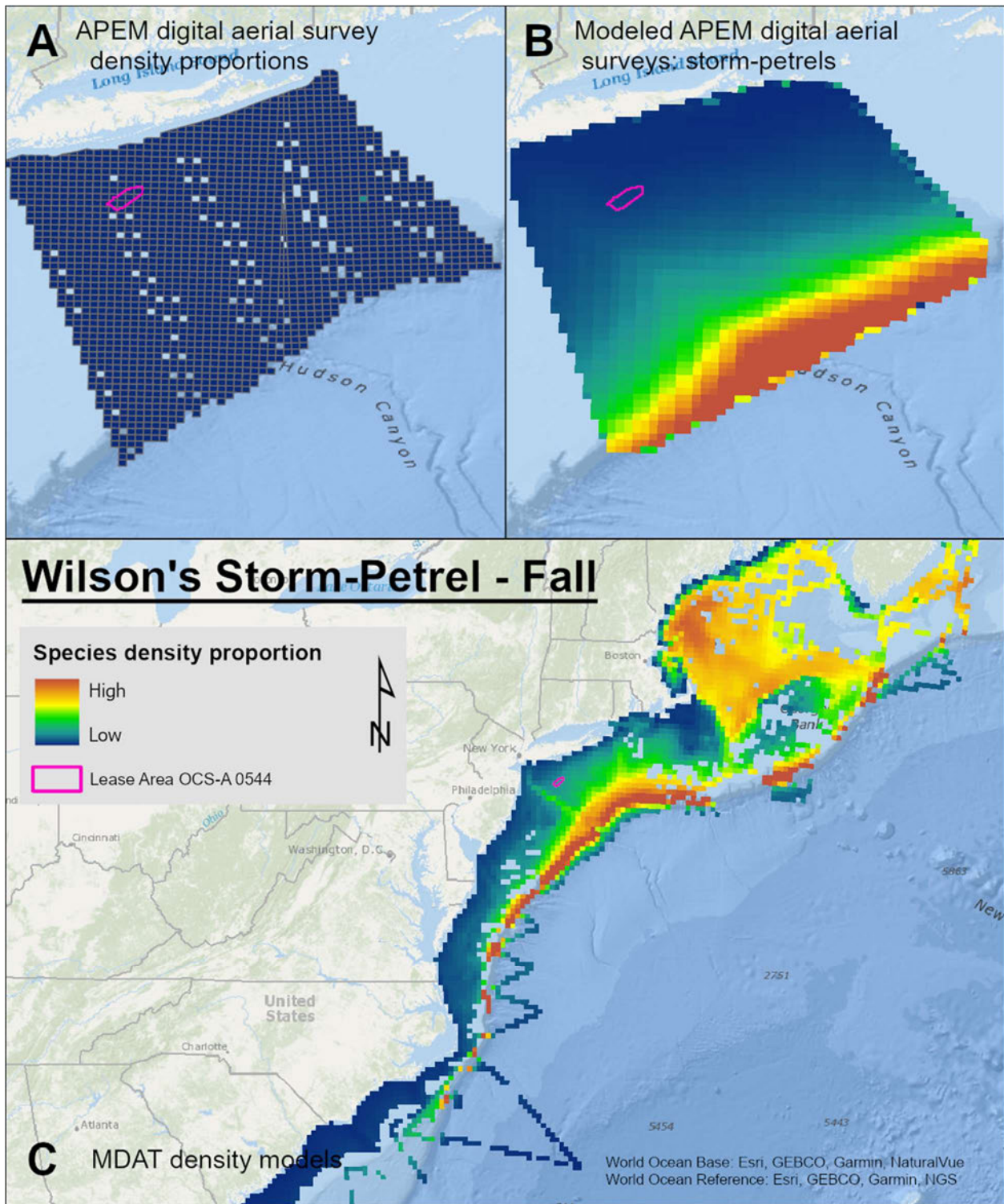
Map 153. Winter Wilson's Storm-Petrel density proportions in the NYSERDA APEM and Empire Wind high resolution digital aerial survey data (A), the NYSERDA APEM and Empire Wind high resolution digital aerial model outputs for storm-petrels in Winter (B) and, Winter Wilson's Storm-Petrel MDAT modeled abundance at the regional scale (C). The scale for all maps is representative of relative spatial variation in the sites within the season for each map input.



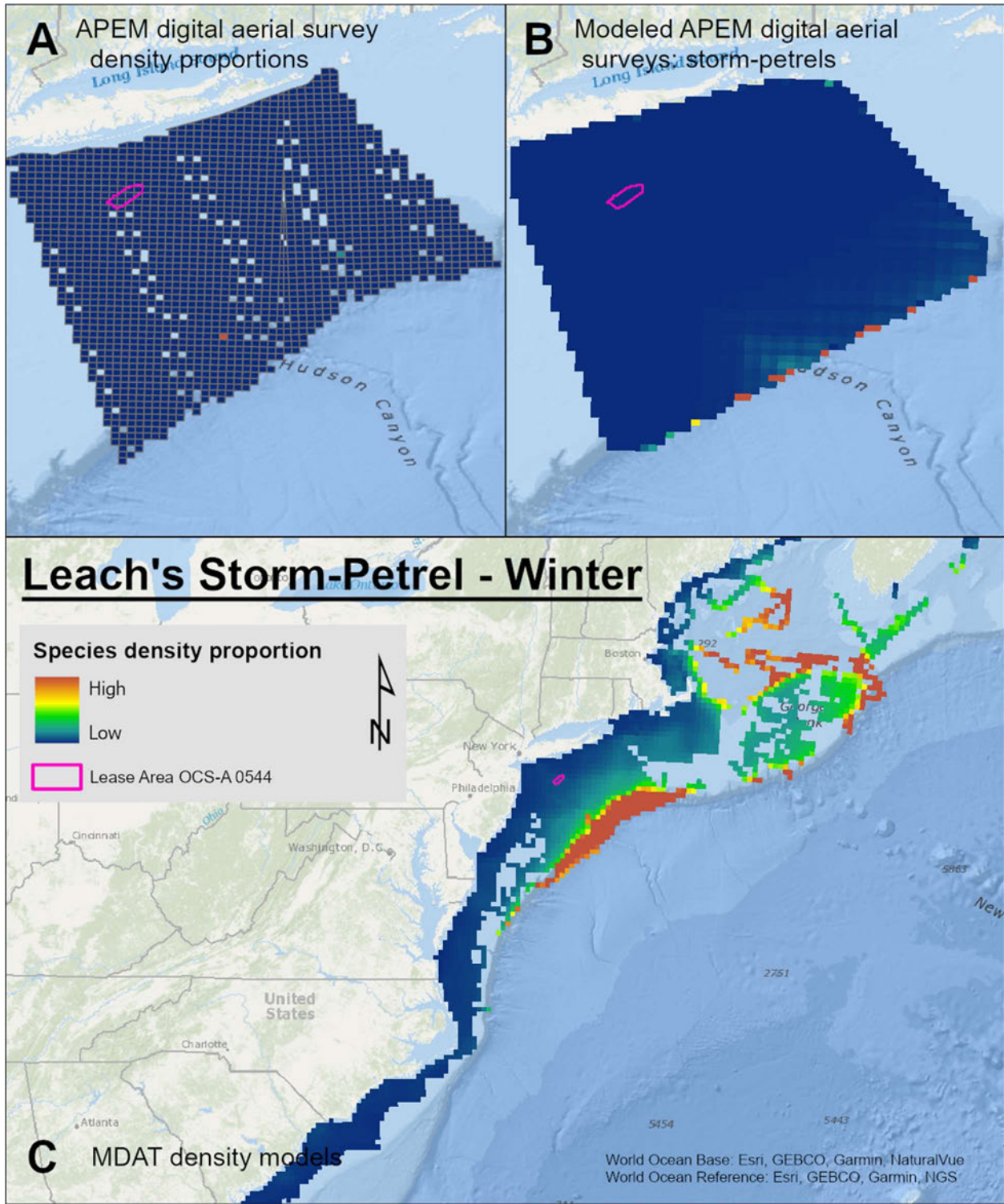
Map 154. Spring Wilson's Storm-Petrel density proportions in the NYSERDA APEM and Empire Wind high resolution digital aerial survey data (A), the NYSERDA APEM and Empire Wind high resolution digital aerial model outputs for storm-petrels in Spring (B) and, Spring Wilson's Storm-Petrel MDAT modeled abundance at the regional scale (C). The scale for all maps is representative of relative spatial variation in the sites within the season for each map input.



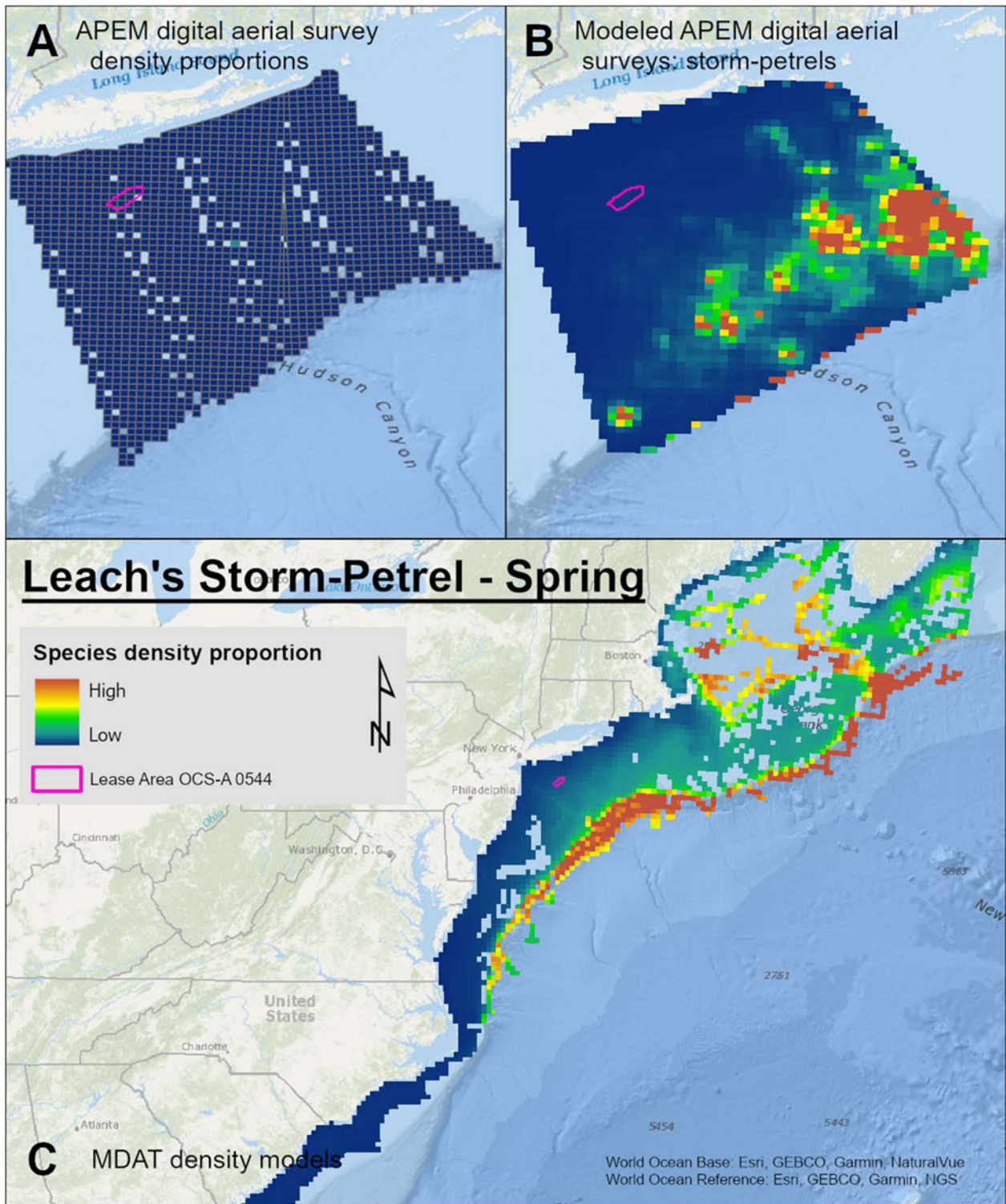
Map 155. Summer Wilson's Storm-Petrel density proportions in the NYSERDA APEM and Empire Wind high resolution digital aerial survey data (A), the NYSERDA APEM and Empire Wind high resolution digital aerial model outputs for storm-petrels in Summer (B) and, Summer Wilson's Storm-Petrel MDAT modeled abundance at the regional scale (C). The scale for all maps is representative of relative spatial variation in the sites within the season for each map input.



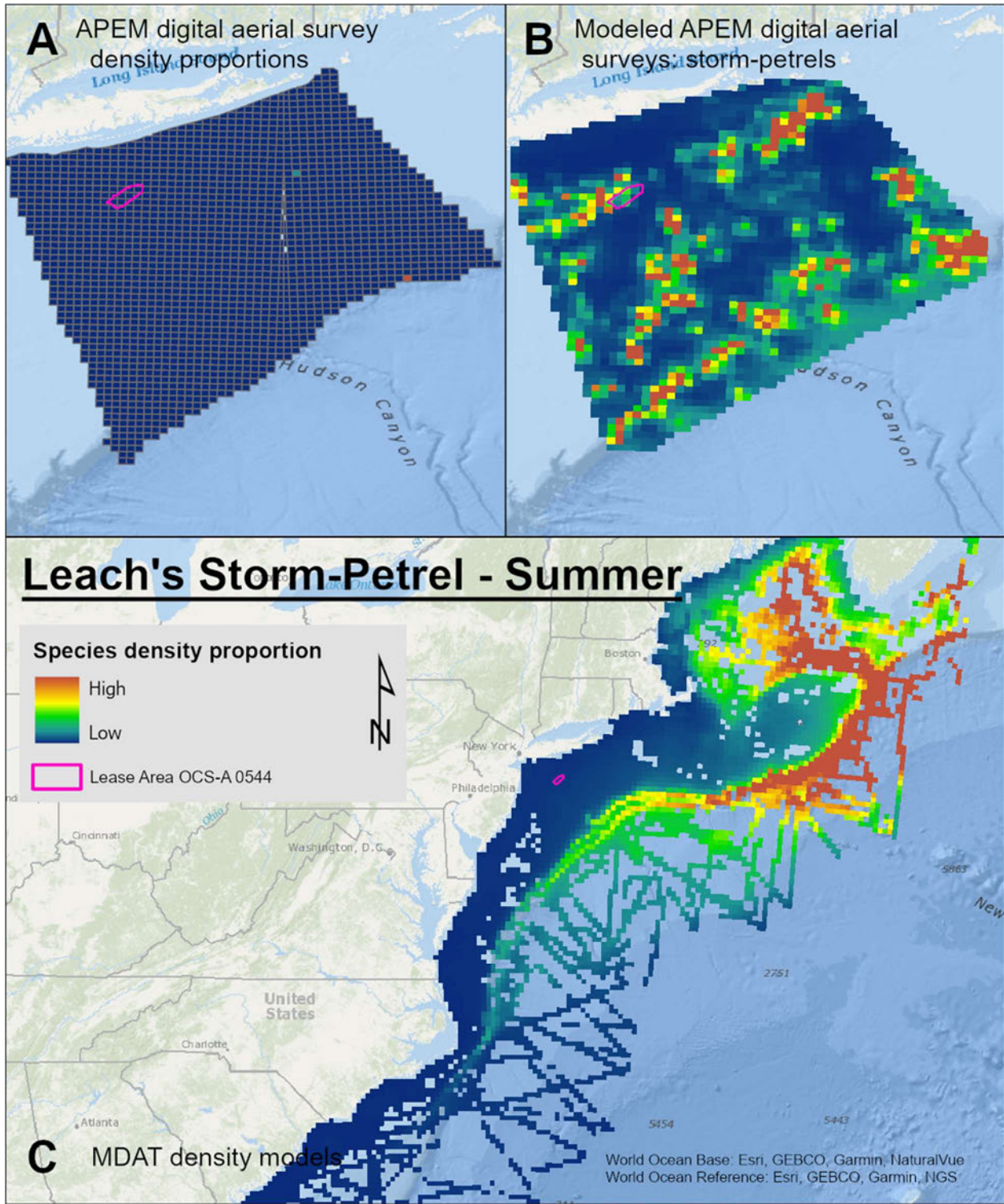
Map 156. Fall Wilson's Storm-Petrel density proportions in the NYSERDA APEM and Empire Wind high resolution digital aerial survey data (A), the NYSERDA APEM and Empire Wind high resolution digital aerial model outputs for storm-petrels in Fall (B) and, Fall Wilson's Storm-Petrel MDAT modeled abundance at the regional scale (C). The scale for all maps is representative of relative spatial variation in the sites within the season for each map input.



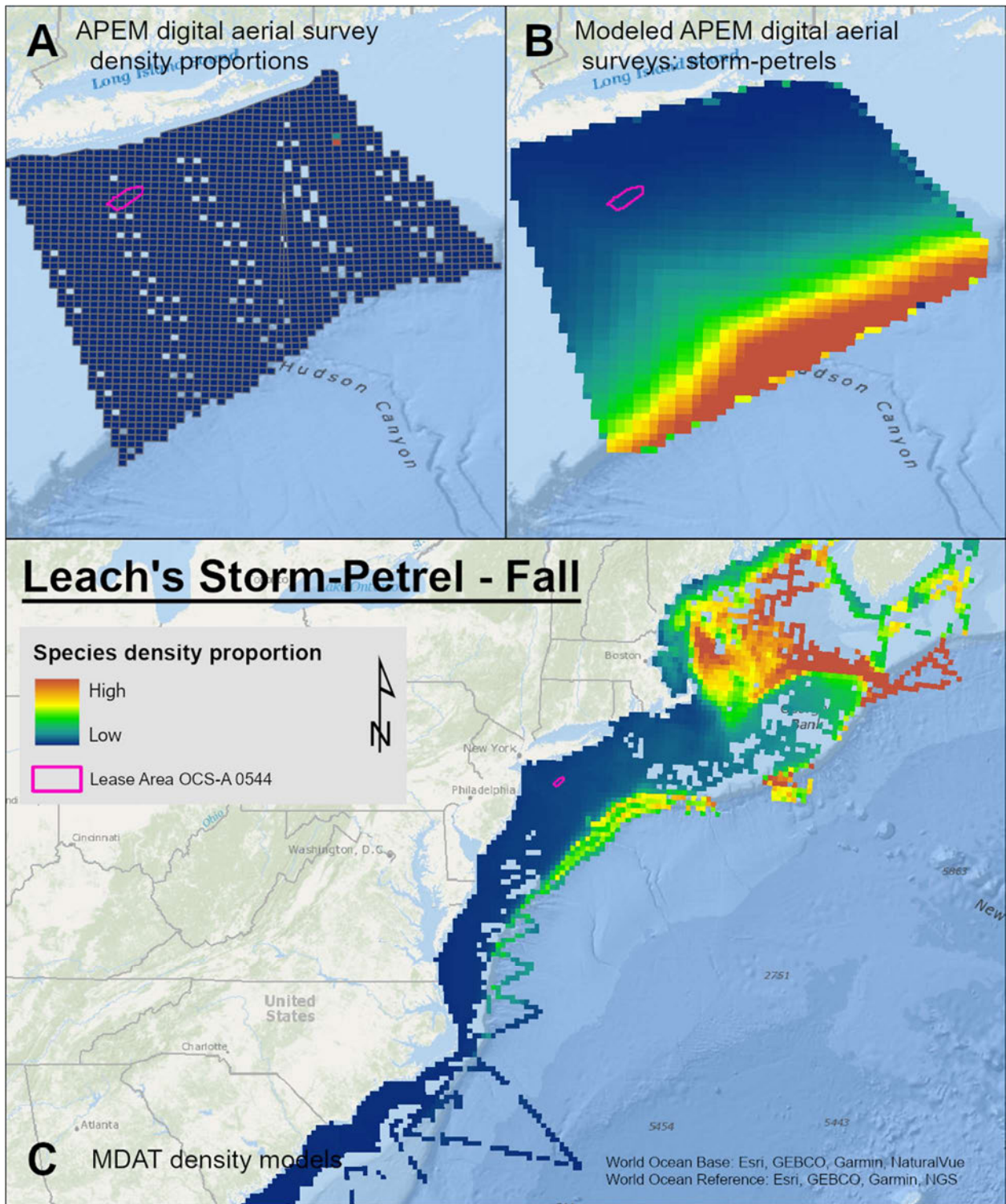
Map 157. Winter Leach's Storm-Petrel density proportions in the NYSERDA APEM and Empire Wind high resolution digital aerial survey data (A), the NYSERDA APEM and Empire Wind high resolution digital aerial model outputs for storm-petrels in Winter (B) and, Winter Leach's Storm-Petrel MDAT modeled abundance at the regional scale (C). The scale for all maps is representative of relative spatial variation in the sites within the season for each map input.



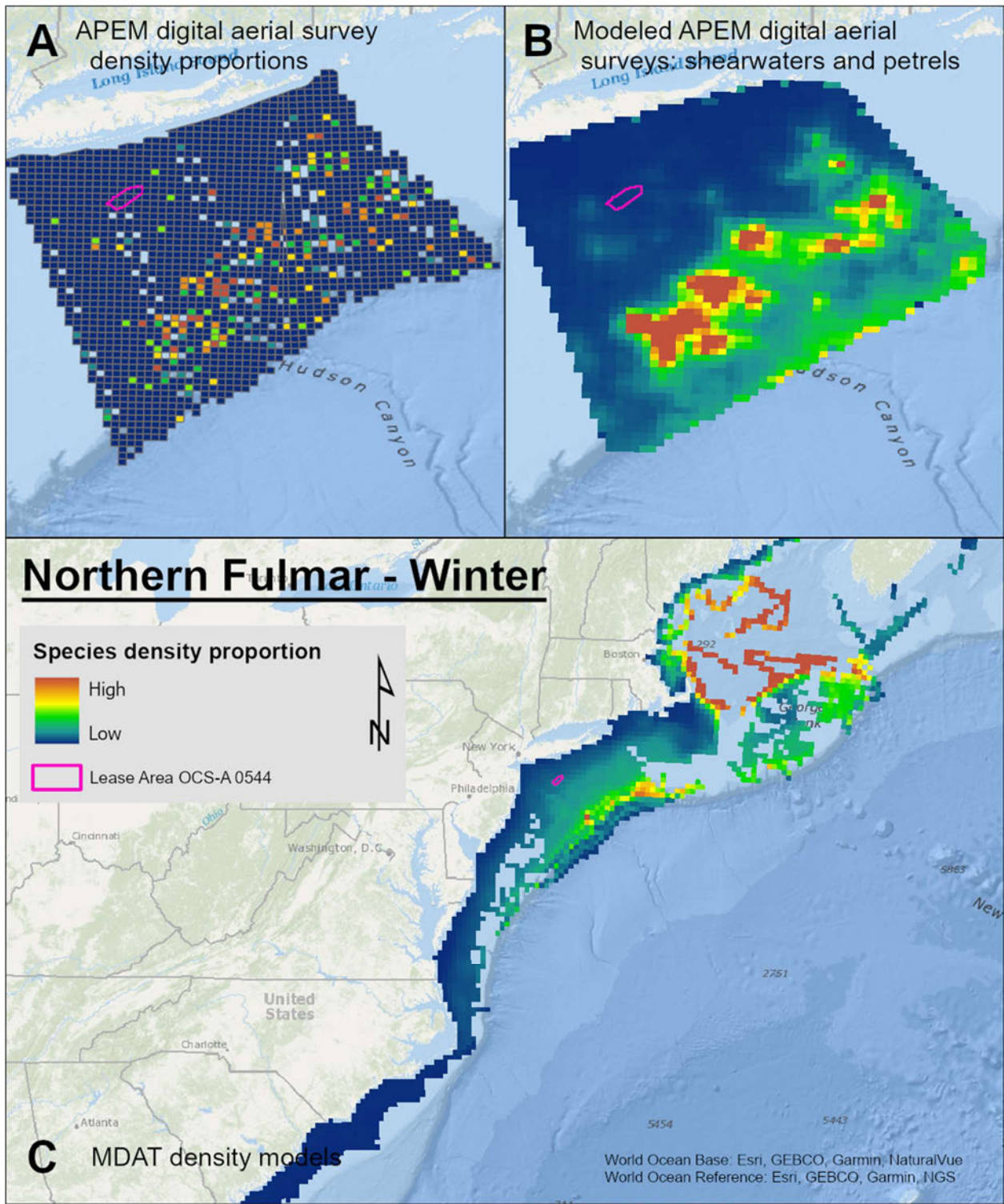
Map 158. Spring Leach's Storm-Petrel density proportions in the NYSERDA APEM and Empire Wind high resolution digital aerial survey data (A), the NYSERDA APEM and Empire Wind high resolution digital aerial model outputs for storm-petrels in Spring (B) and, Spring Leach's Storm-Petrel MDAT modeled abundance at the regional scale (C). The scale for all maps is representative of relative spatial variation in the sites within the season for each map input.



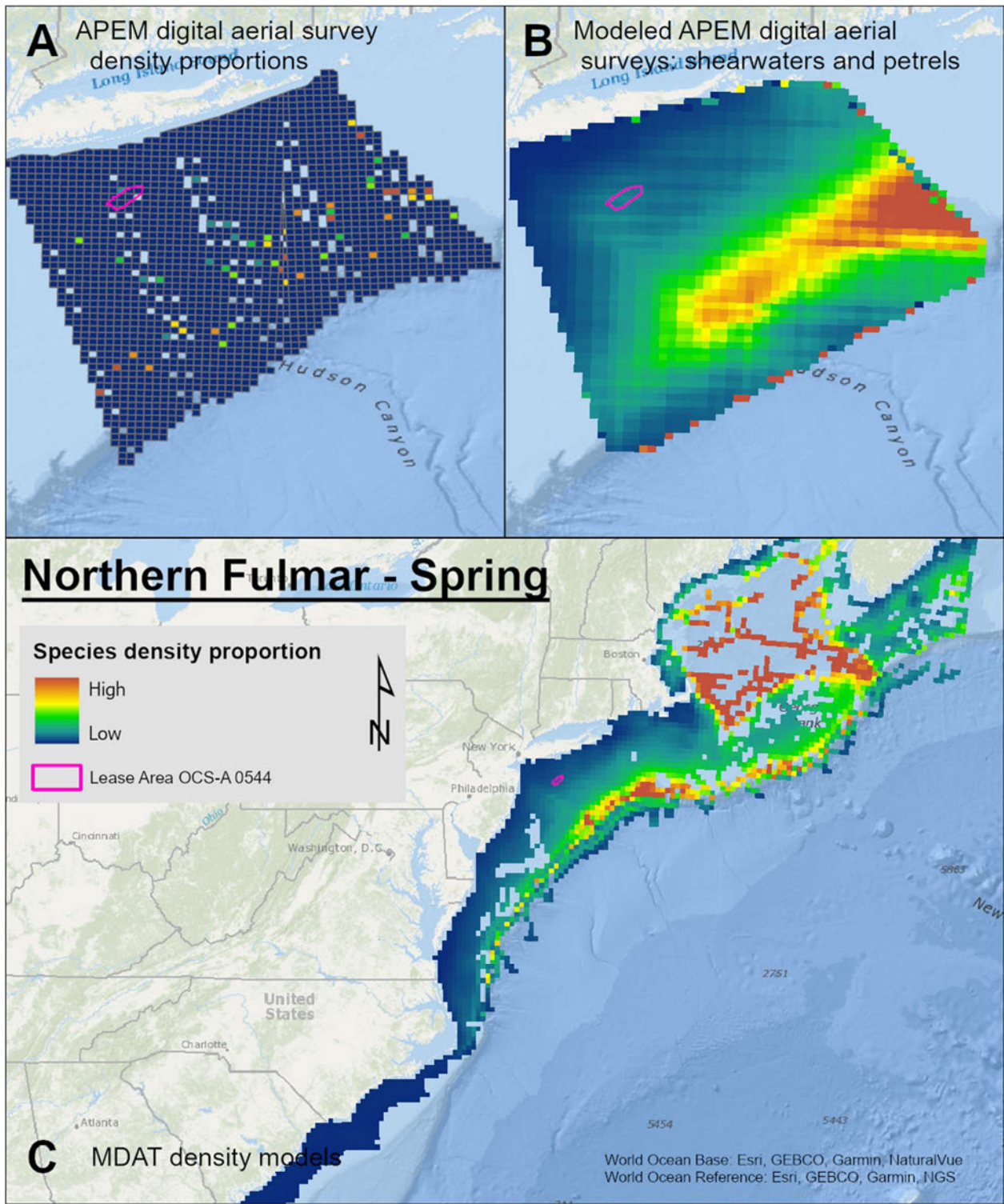
Map 159. Summer Leach's Storm-Petrel density proportions in the NYSERDA APEM and Empire Wind high resolution digital aerial survey data (A), the NYSERDA APEM and Empire Wind high resolution digital aerial model outputs for storm-petrels in Summer (B) and, Summer Leach's Storm-Petrel MDAT modeled abundance at the regional scale (C). The scale for all maps is representative of relative spatial variation in the sites within the season for each map input.



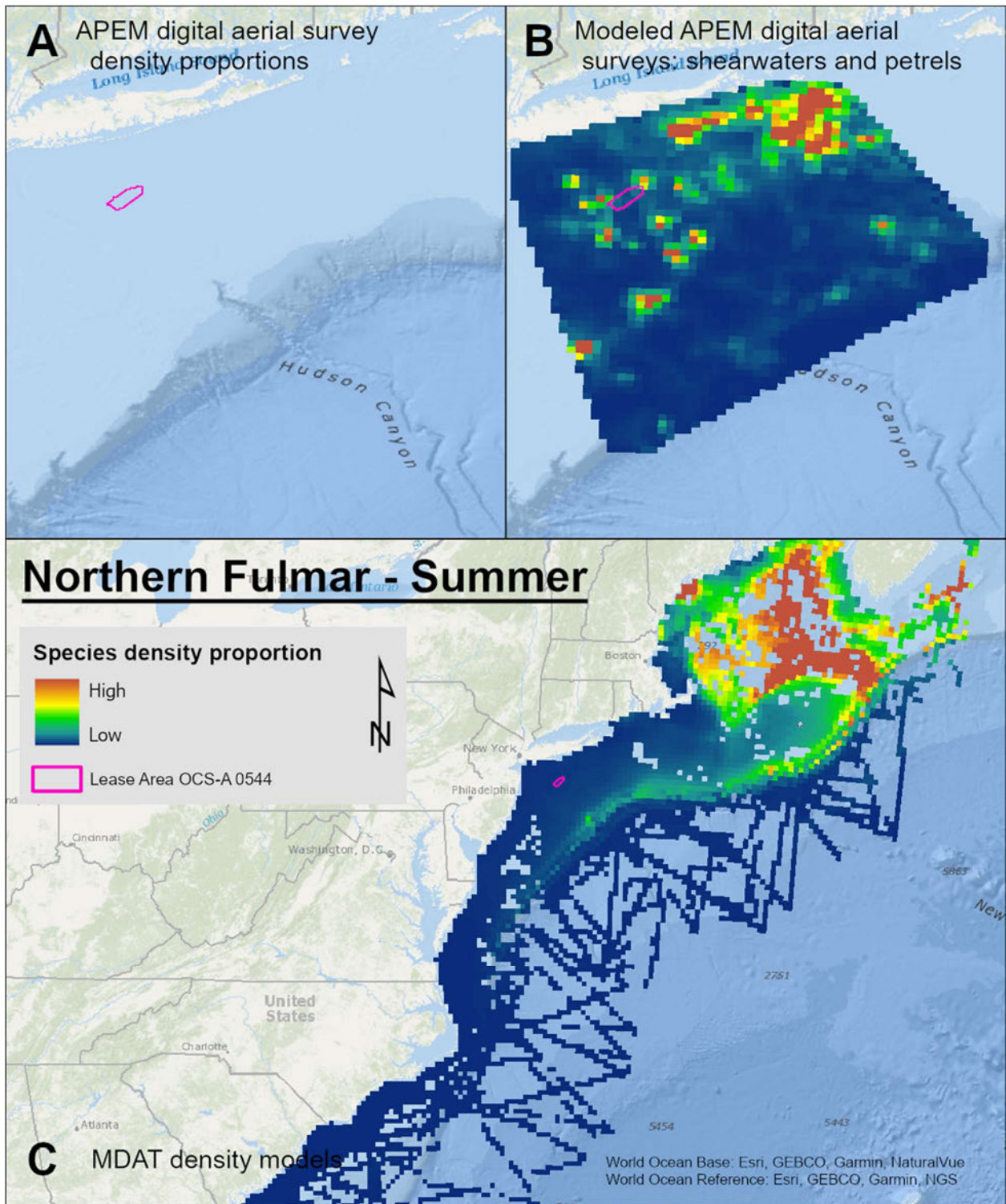
Map 160. Fall Leach's Storm-Petrel density proportions in the NYSERDA APEM and Empire Wind high resolution digital aerial survey data (A), the NYSERDA APEM and Empire Wind high resolution digital aerial model outputs for storm-petrels in Fall (B) and, Fall Leach's Storm-Petrel MDAT modeled abundance at the regional scale (C). The scale for all maps is representative of relative spatial variation in the sites within the season for each map input.



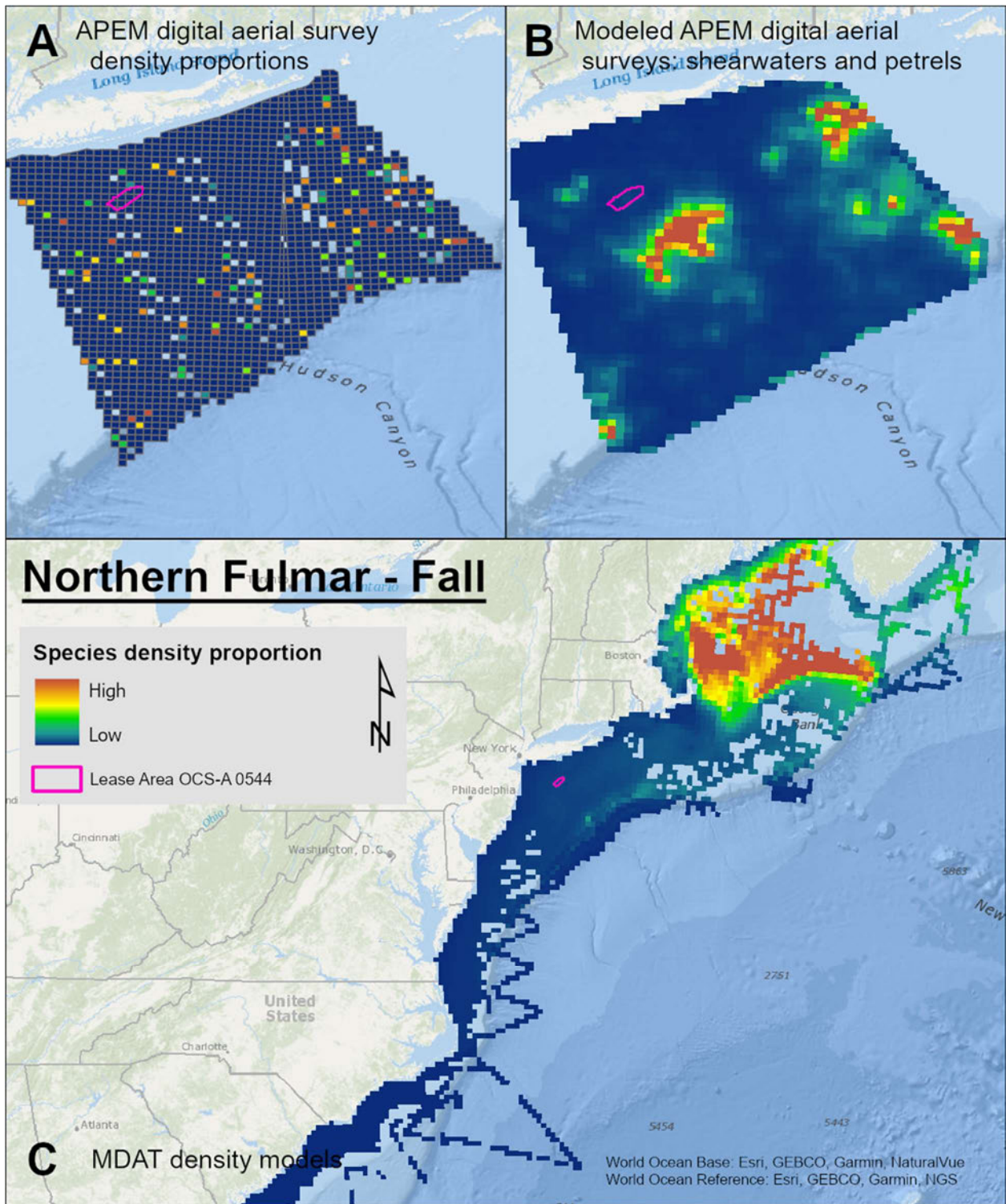
Map 161. Winter Northern Fulmar density proportions in the NYSERDA APEM and Empire Wind high resolution digital aerial survey data (A), the NYSERDA APEM and Empire Wind high resolution digital aerial model outputs for shearwaters and petrels in Winter (B) and, Winter Northern Fulmar MDAT modeled abundance at the regional scale (C). The scale for all maps is representative of relative spatial variation in the sites within the season for each map input.



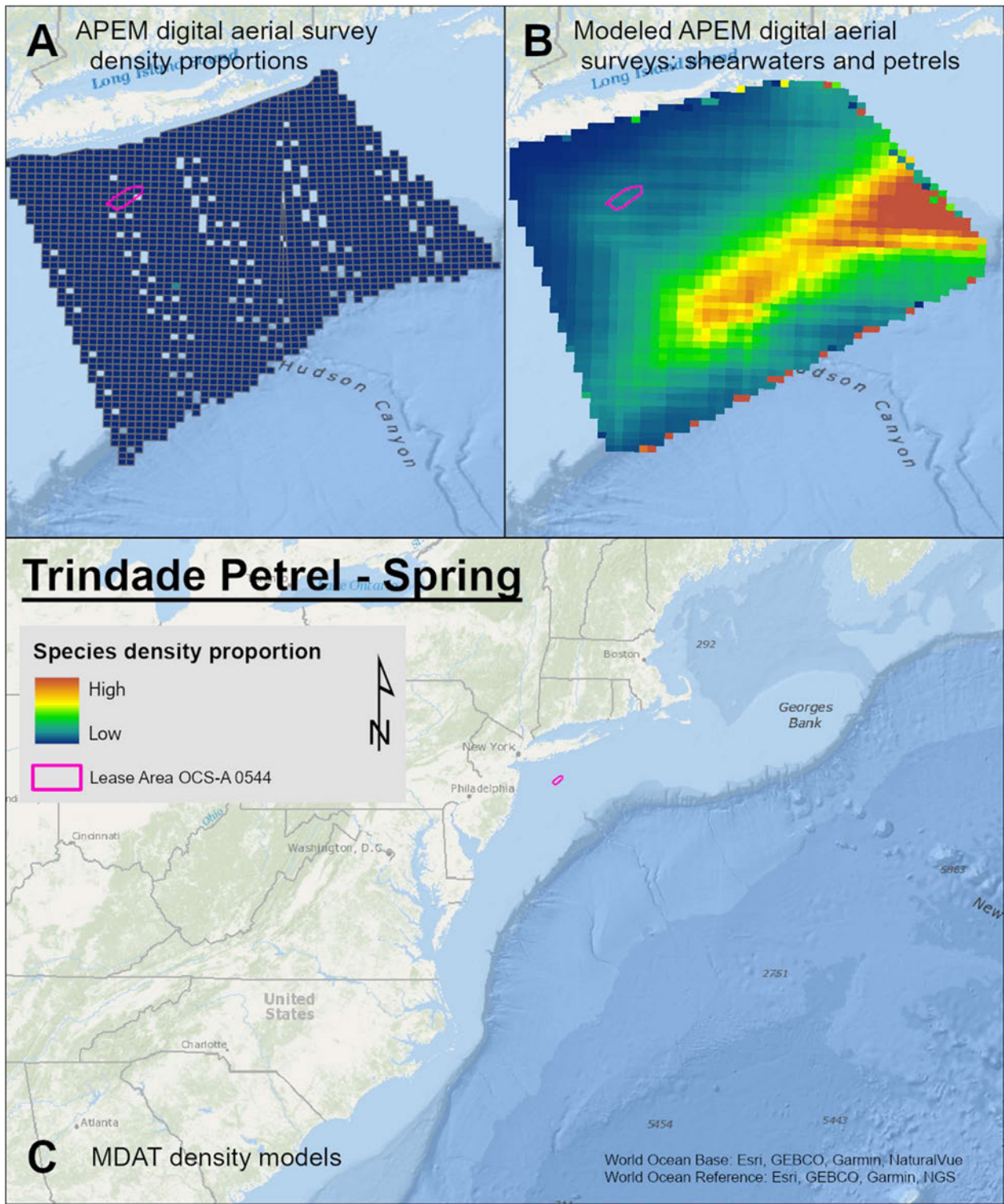
Map 162. Spring Northern Fulmar density proportions in the NYSERDA APEM and Empire Wind high resolution digital aerial survey data (A), the NYSERDA APEM and Empire Wind high resolution digital aerial model outputs for shearwaters and petrels in Spring (B) and, Spring Northern Fulmar MDAT modeled abundance at the regional scale (C). The scale for all maps is representative of relative spatial variation in the sites within the season for each map input.



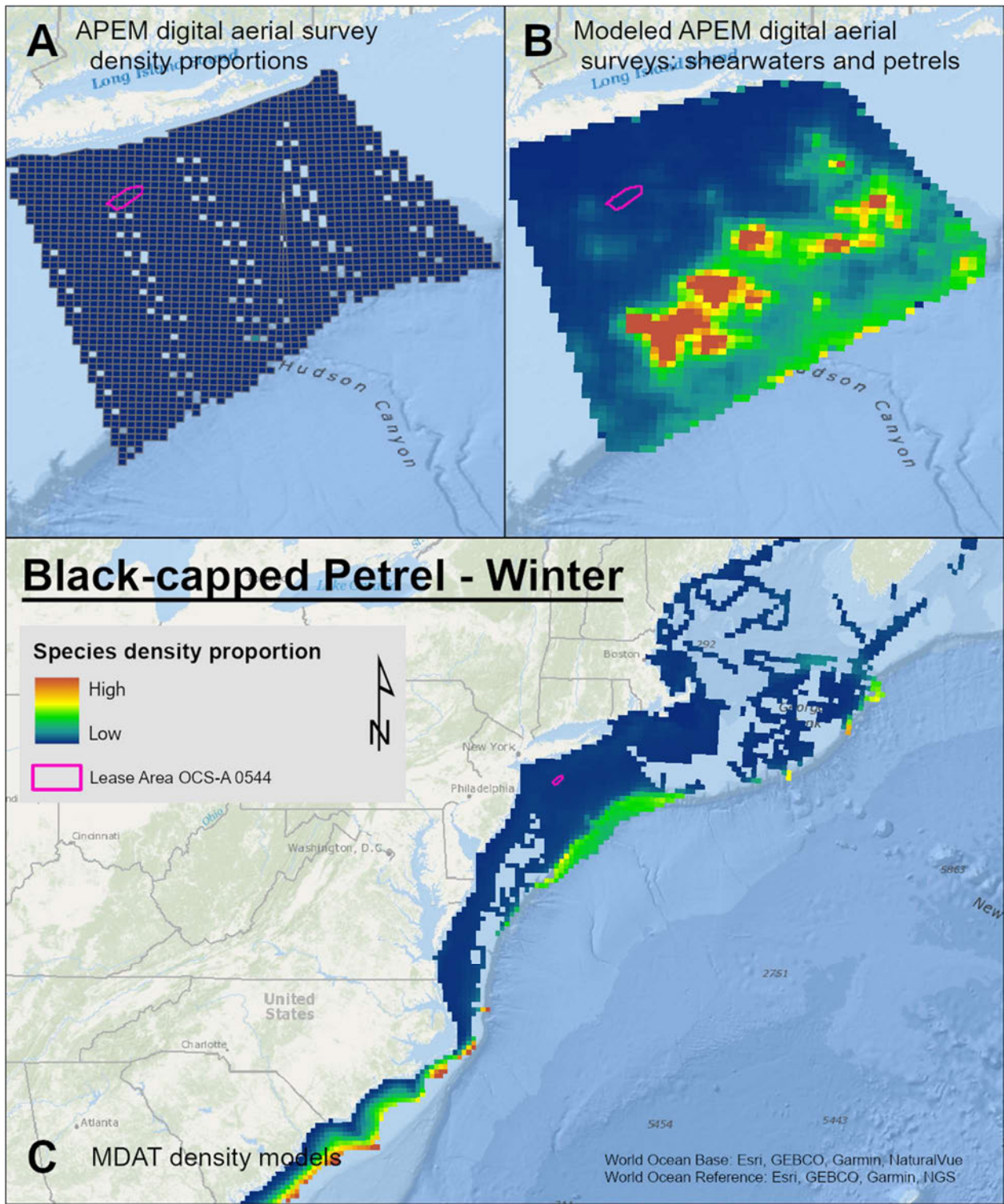
Map 163. Summer Northern Fulmar density proportions in the NYSERDA APEM and Empire Wind high resolution digital aerial survey data (A), the NYSERDA APEM and Empire Wind high resolution digital aerial model outputs for shearwaters and petrels in Summer (B) and, Summer Northern Fulmar MDAT modeled abundance at the regional scale (C). The scale for all maps is representative of relative spatial variation in the sites within the season for each map input.



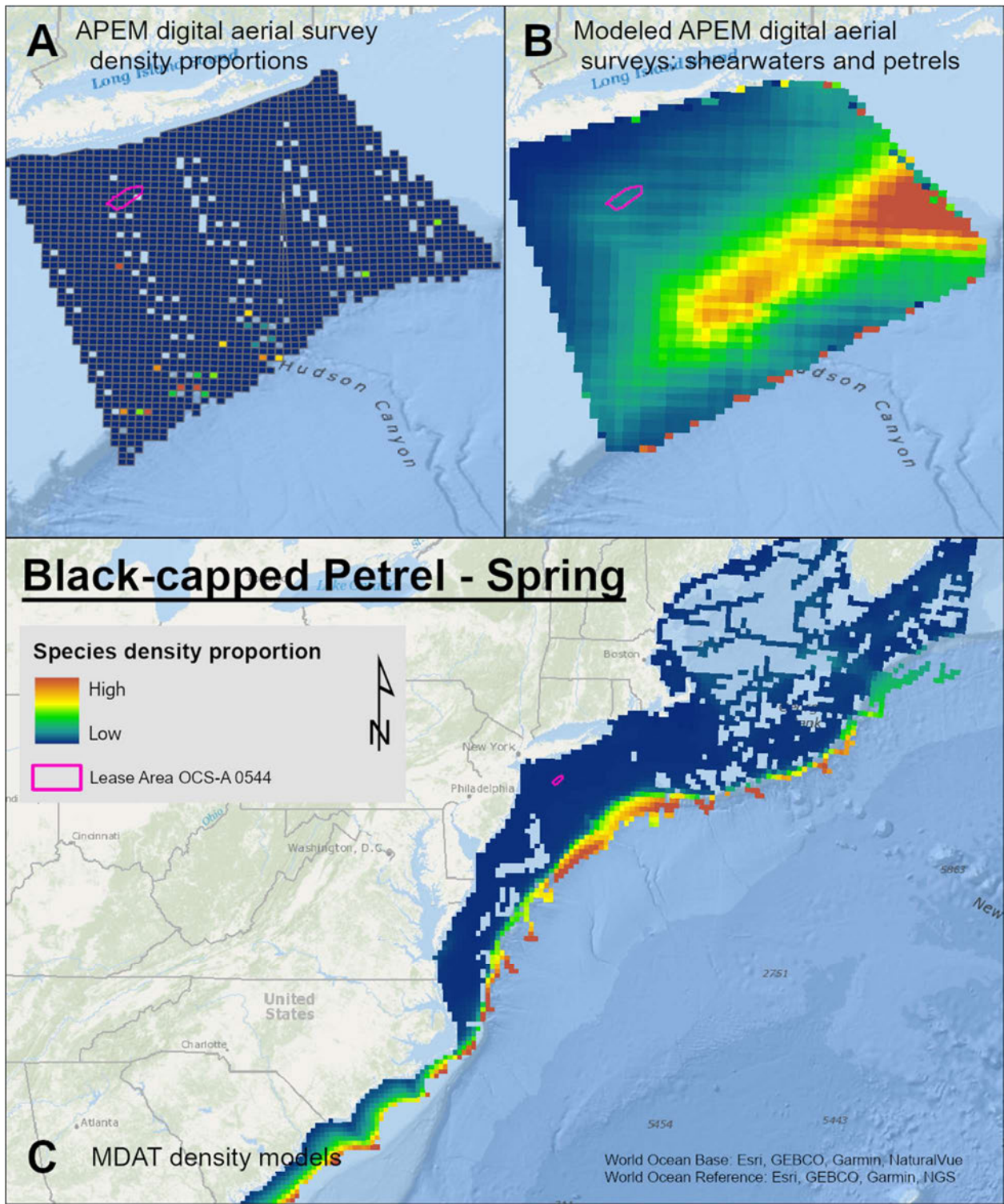
Map 164. Fall Northern Fulmar density proportions in the NYSERDA APEM and Empire Wind high resolution digital aerial survey data (A), the NYSERDA APEM and Empire Wind high resolution digital aerial model outputs for shearwaters and petrels in Fall (B) and, Fall Northern Fulmar MDAT modeled abundance at the regional scale (C). The scale for all maps is representative of relative spatial variation in the sites within the season for each map input.



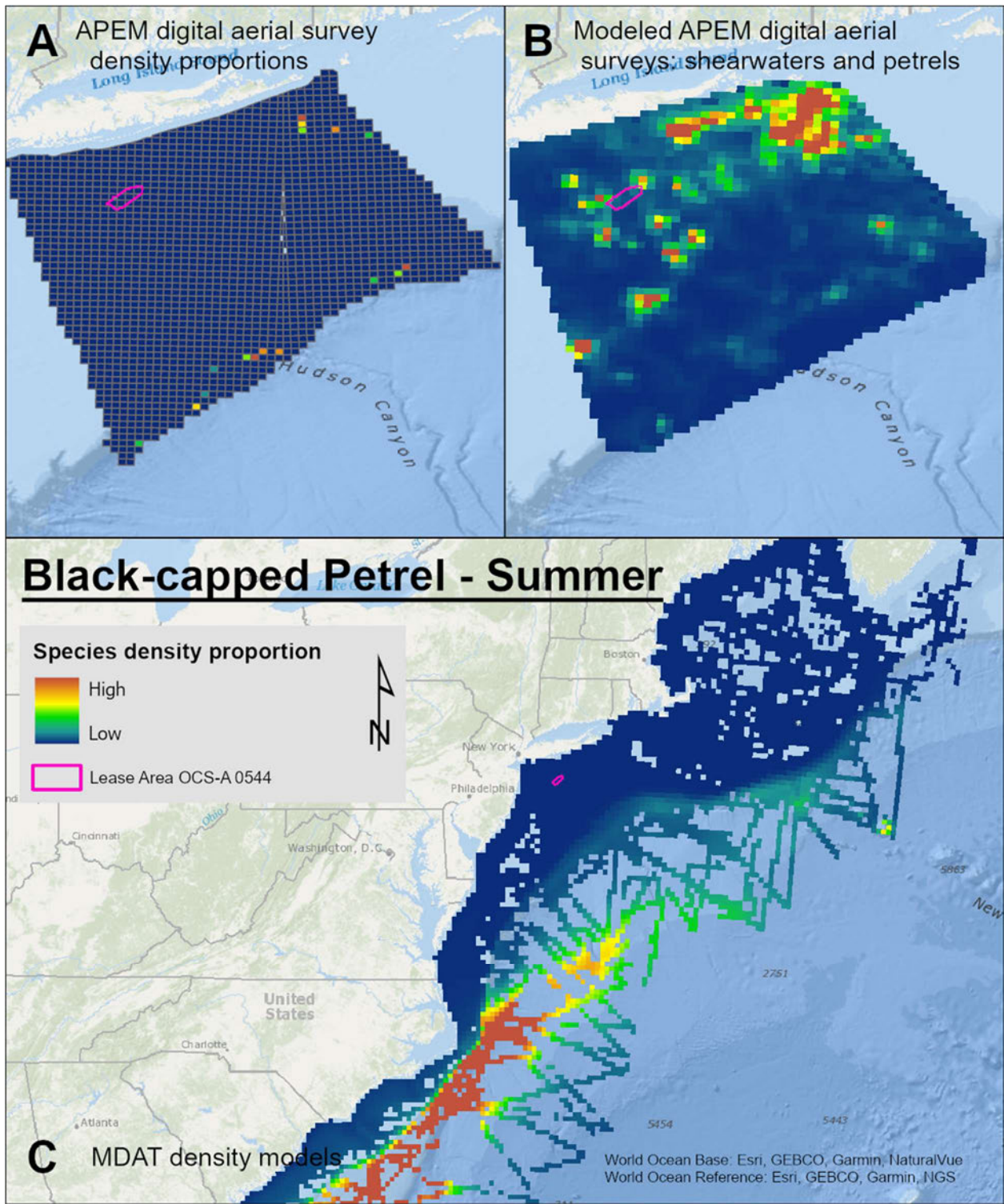
Map 165. Spring Trindade Petrel density proportions in the NYSERDA APEM and Empire Wind high resolution digital aerial survey data (A), the NYSERDA APEM and Empire Wind high resolution digital aerial model outputs for shearwaters and petrels in Spring (B) and, Spring Trindade Petrel MDAT modeled abundance at the regional scale (C). The scale for all maps is representative of relative spatial variation in the sites within the season for each map input.



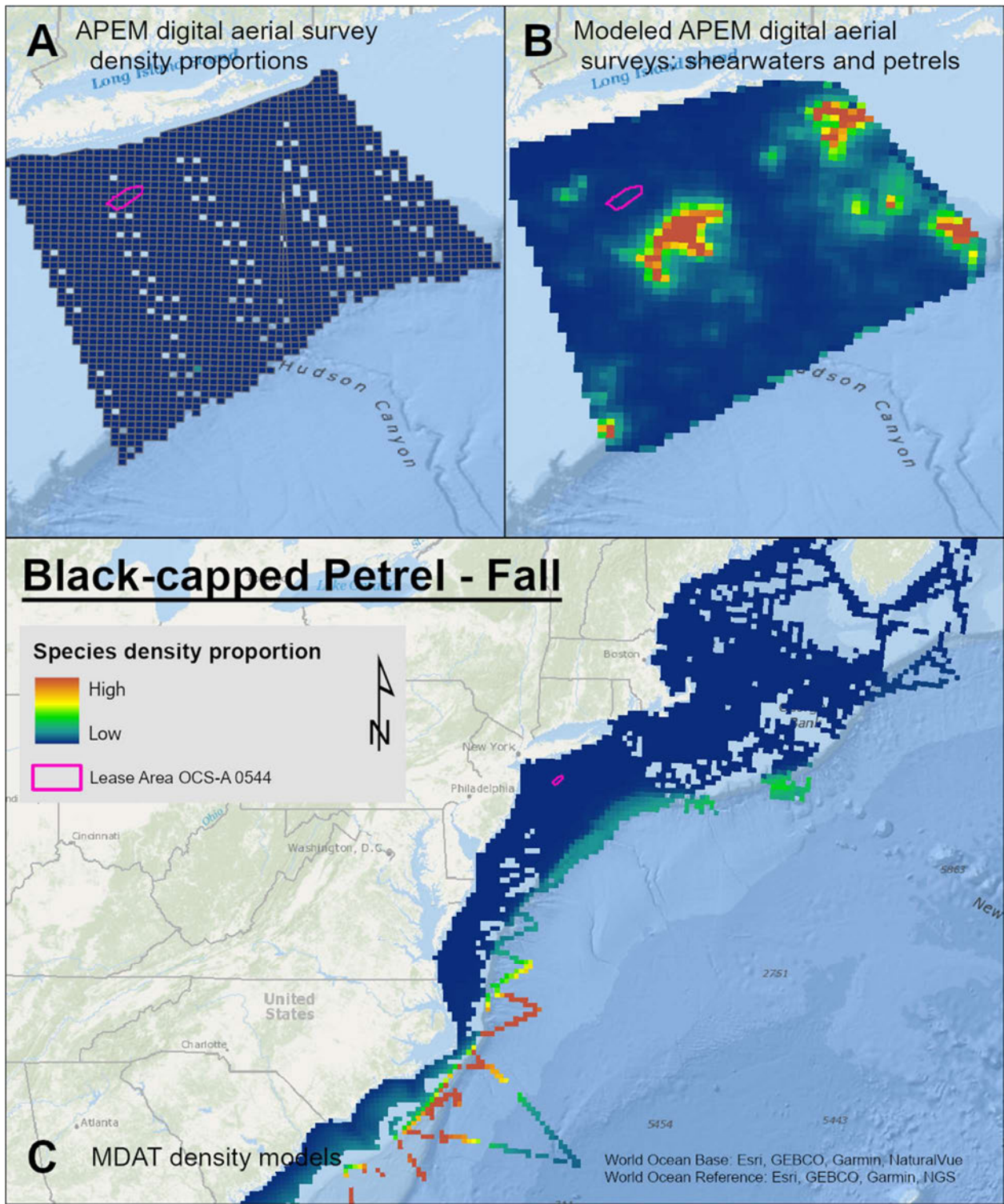
Map 166. Winter Black-capped Petrel density proportions in the NYSERDA APEM and Empire Wind high resolution digital aerial survey data (A), the NYSERDA APEM and Empire Wind high resolution digital aerial model outputs for shearwaters and petrels in Winter (B) and, Winter Black-capped Petrel MDAT modeled abundance at the regional scale (C). The scale for all maps is representative of relative spatial variation in the sites within the season for each map input.



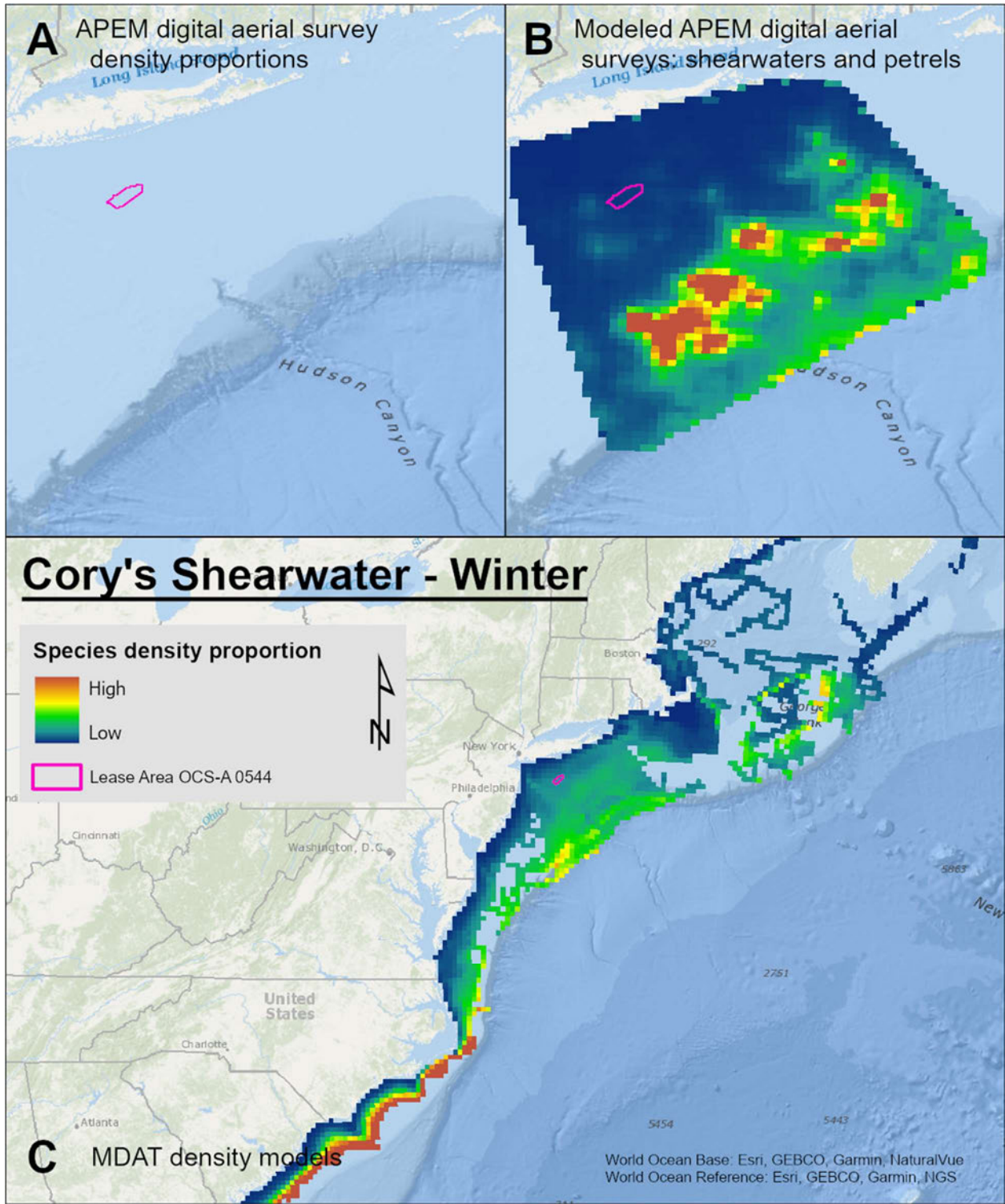
Map 167. Spring Black-capped Petrel density proportions in the NYSERDA APEM and Empire Wind high resolution digital aerial survey data (A), the NYSERDA APEM and Empire Wind high resolution digital aerial model outputs for shearwaters and petrels in Spring (B) and, Spring Black-capped Petrel MDAT modeled abundance at the regional scale (C). The scale for all maps is representative of relative spatial variation in the sites within the season for each map input.



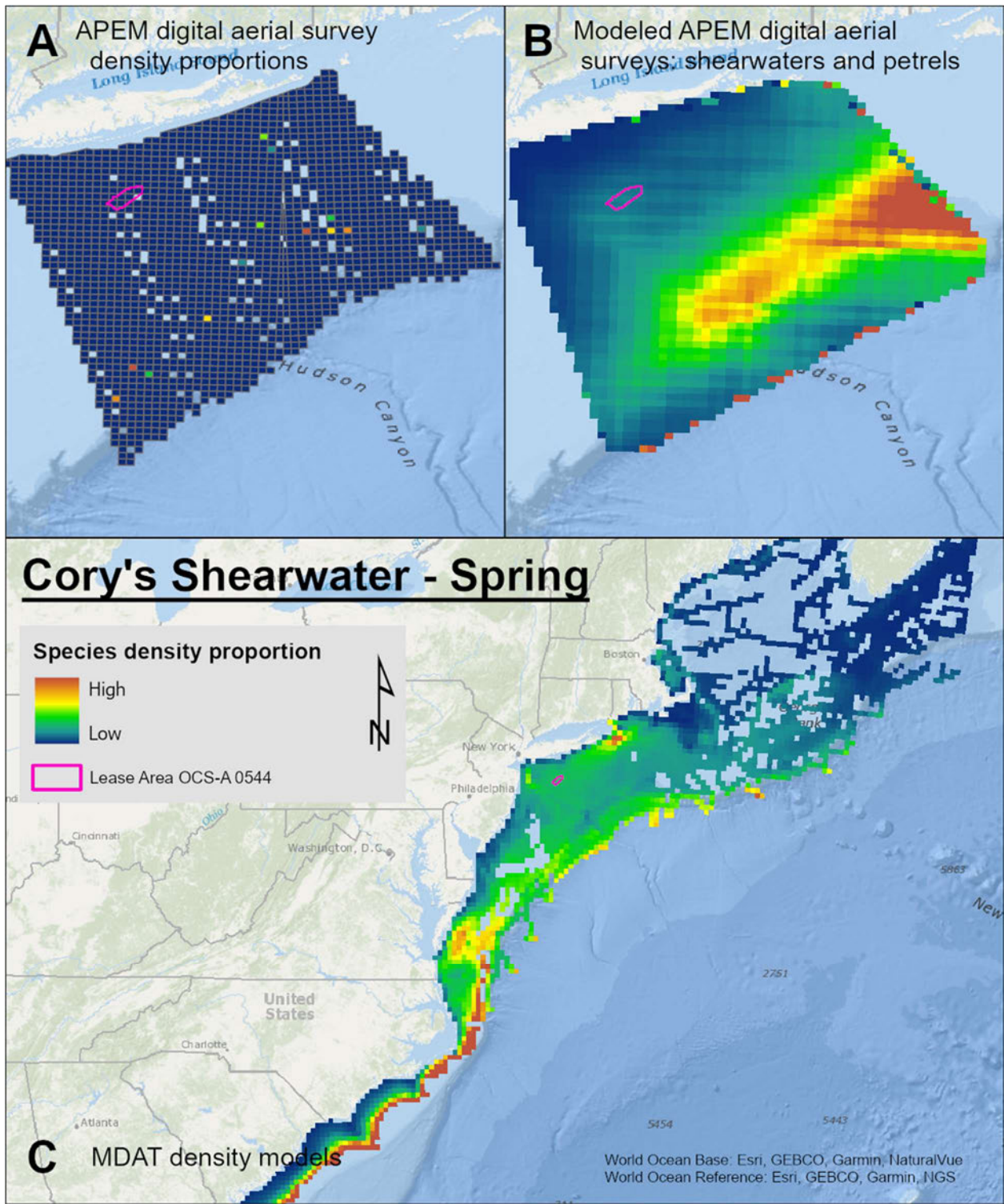
Map 168. Summer Black-capped Petrel density proportions in the NYSERDA APEM and Empire Wind high resolution digital aerial survey data (A), the NYSERDA APEM and Empire Wind high resolution digital aerial model outputs for shearwaters and petrels in Summer (B) and, Summer Black-capped Petrel MDAT modeled abundance at the regional scale (C). The scale for all maps is representative of relative spatial variation in the sites within the season for each map input.



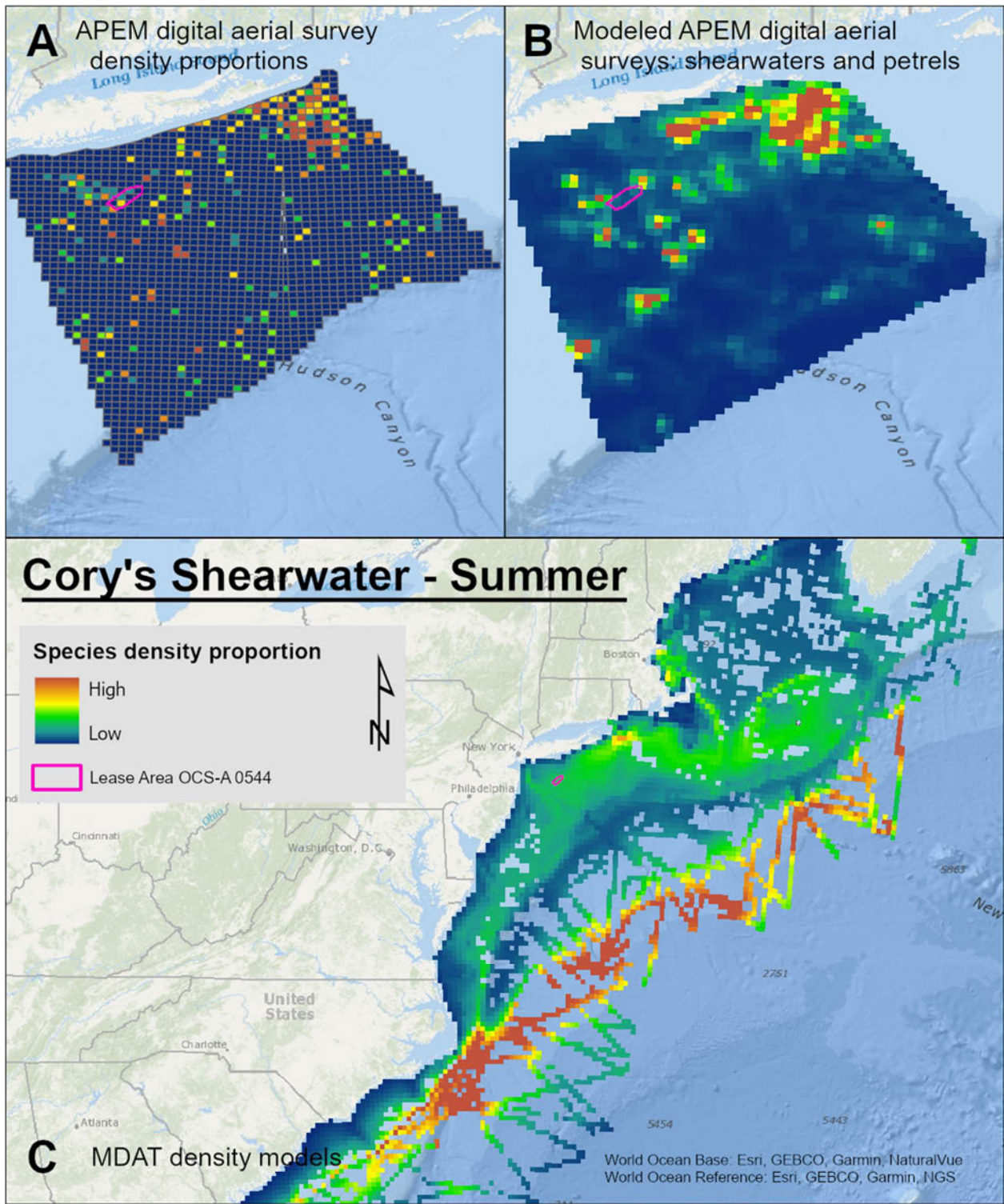
Map 169. Fall Black-capped Petrel density proportions in the NYSERDA APEM and Empire Wind high resolution digital aerial survey data (A), the NYSERDA APEM and Empire Wind high resolution digital aerial model outputs for shearwaters and petrels in Fall (B) and, Fall Black-capped Petrel MDAT modeled abundance at the regional scale (C). The scale for all maps is representative of relative spatial variation in the sites within the season for each map input.



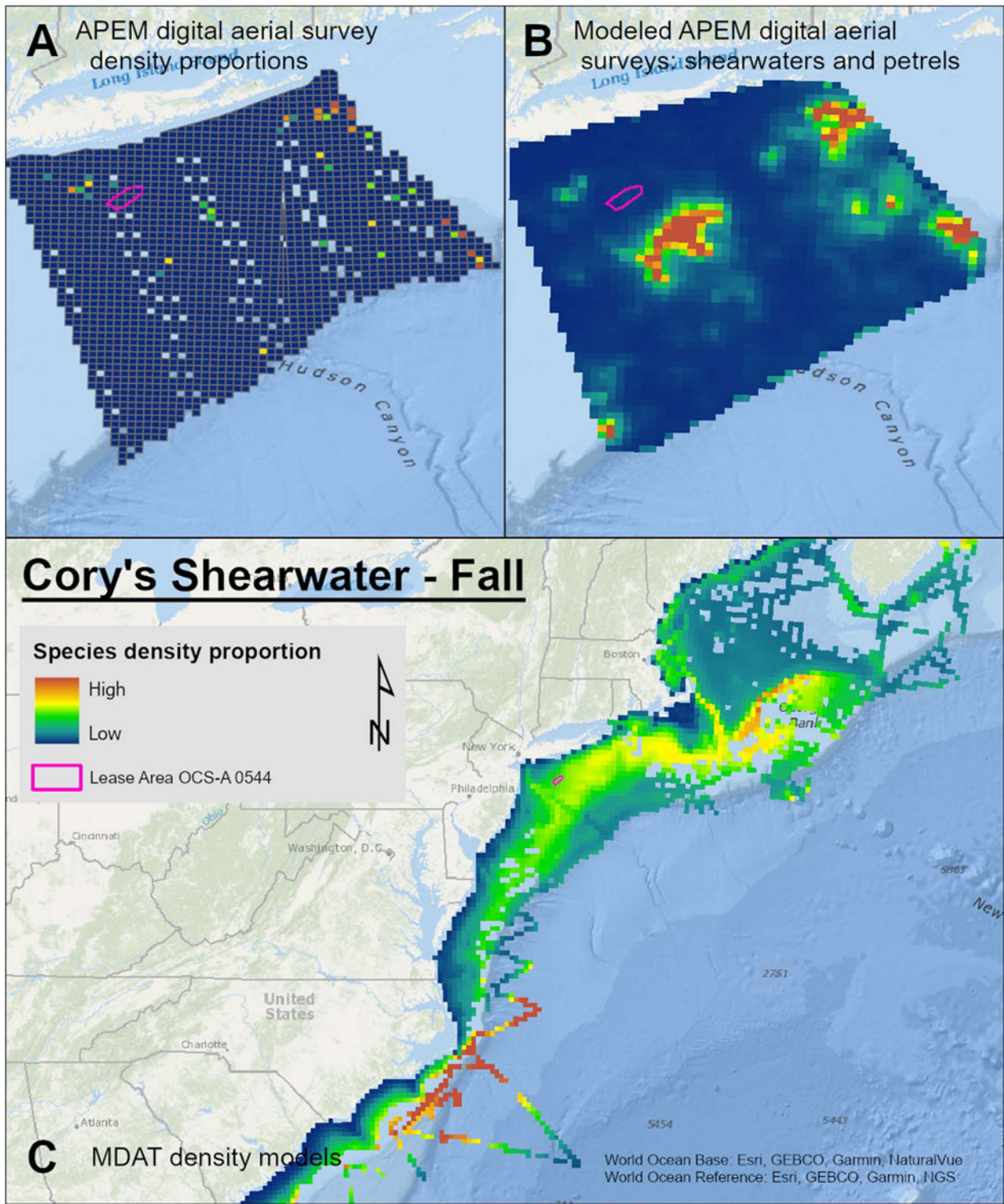
Map 170. Winter Cory's Shearwater density proportions in the NYSERDA APEM and Empire Wind high resolution digital aerial survey data (A), the NYSERDA APEM and Empire Wind high resolution digital aerial model outputs for shearwaters and petrels in Winter (B) and, Winter Cory's Shearwater MDAT modeled abundance at the regional scale (C). The scale for all maps is representative of relative spatial variation in the sites within the season for each map input.



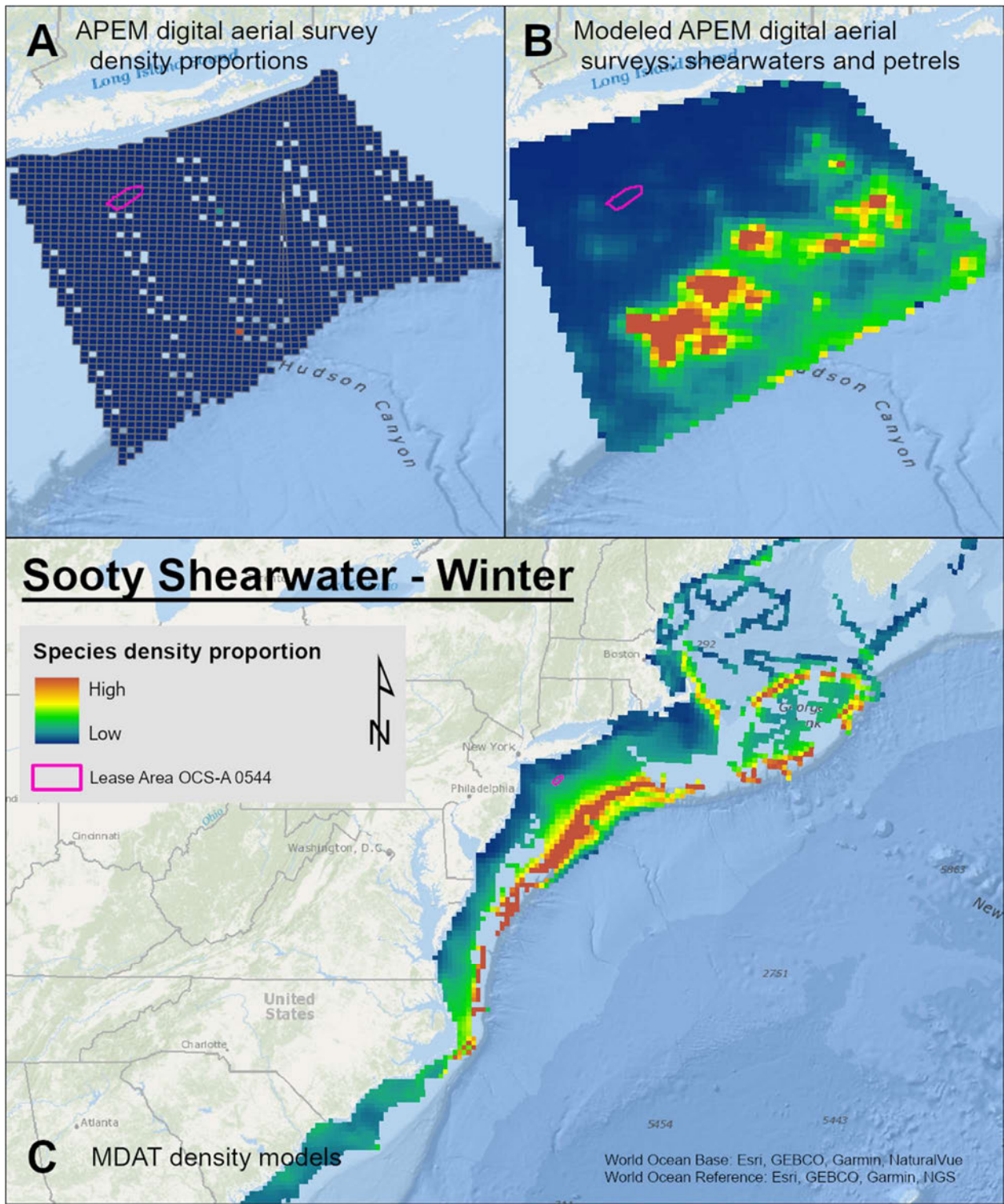
Map 171. Spring Cory's Shearwater density proportions in the NYSERDA APEM and Empire Wind high resolution digital aerial survey data (A), the NYSERDA APEM and Empire Wind high resolution digital aerial model outputs for shearwaters and petrels in Spring (B) and, Spring Cory's Shearwater MDAT modeled abundance at the regional scale (C). The scale for all maps is representative of relative spatial variation in the sites within the season for each map input.



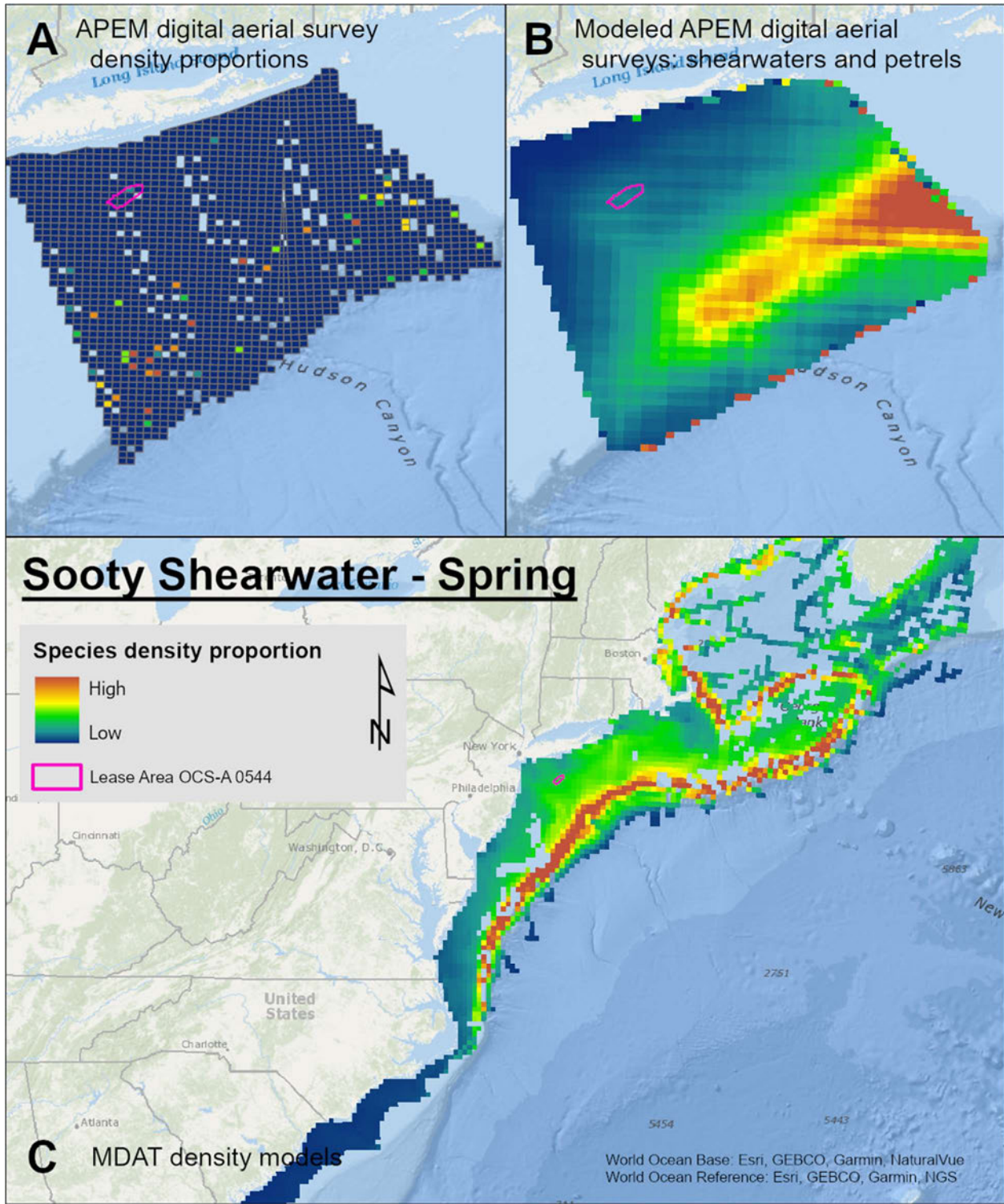
Map 172. Summer Cory's Shearwater density proportions in the NYSERDA APEM and Empire Wind high resolution digital aerial survey data (A), the NYSERDA APEM and Empire Wind high resolution digital aerial model outputs for shearwaters and petrels in Summer (B) and, Summer Cory's Shearwater MDAT modeled abundance at the regional scale (C). The scale for all maps is representative of relative spatial variation in the sites within the season for each map input.



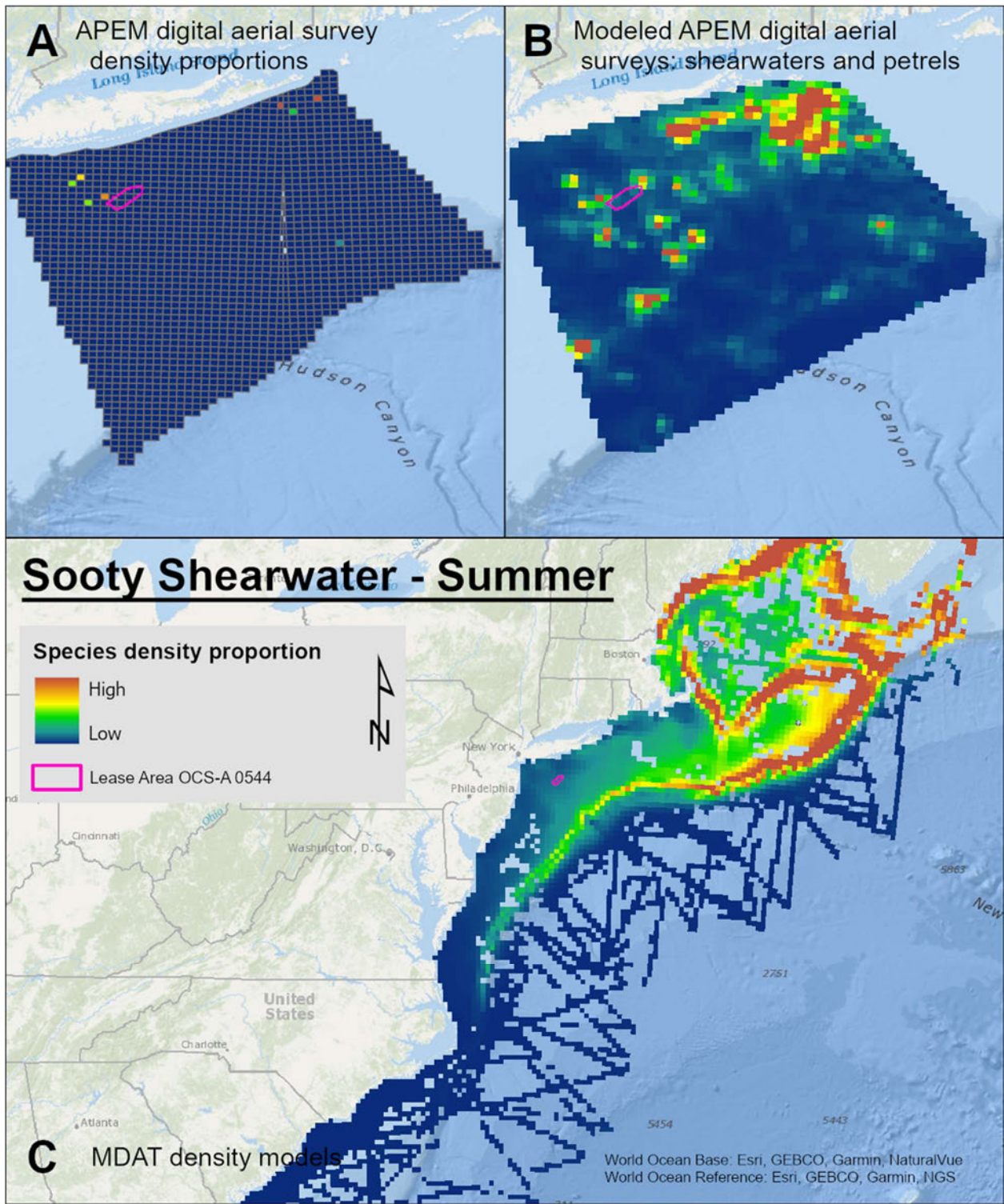
Map 173. Fall Cory's Shearwater density proportions in the NYSERDA APEM and Empire Wind high resolution digital aerial survey data (A), the NYSERDA APEM and Empire Wind high resolution digital aerial model outputs for shearwaters and petrels in Fall (B) and, Fall Cory's Shearwater MDAT modeled abundance at the regional scale (C). The scale for all maps is representative of relative spatial variation in the sites within the season for each map input.



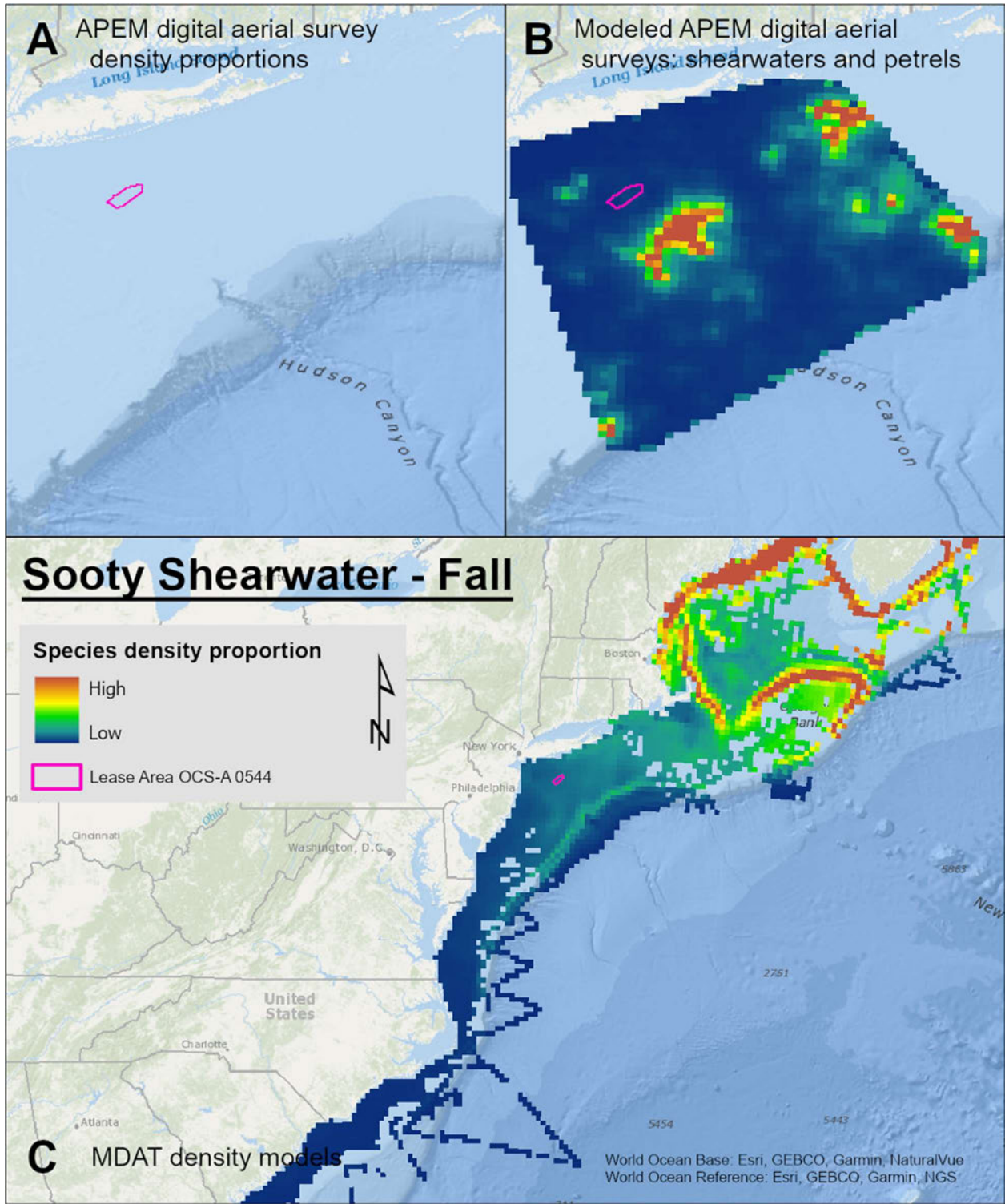
Map 174. Winter Sooty Shearwater density proportions in the NYSERDA APEM and Empire Wind high resolution digital aerial survey data (A), the NYSERDA APEM and Empire Wind high resolution digital aerial model outputs for shearwaters and petrels in Winter (B) and, Winter Sooty Shearwater MDAT modeled abundance at the regional scale (C). The scale for all maps is representative of relative spatial variation in the sites within the season for each map input.



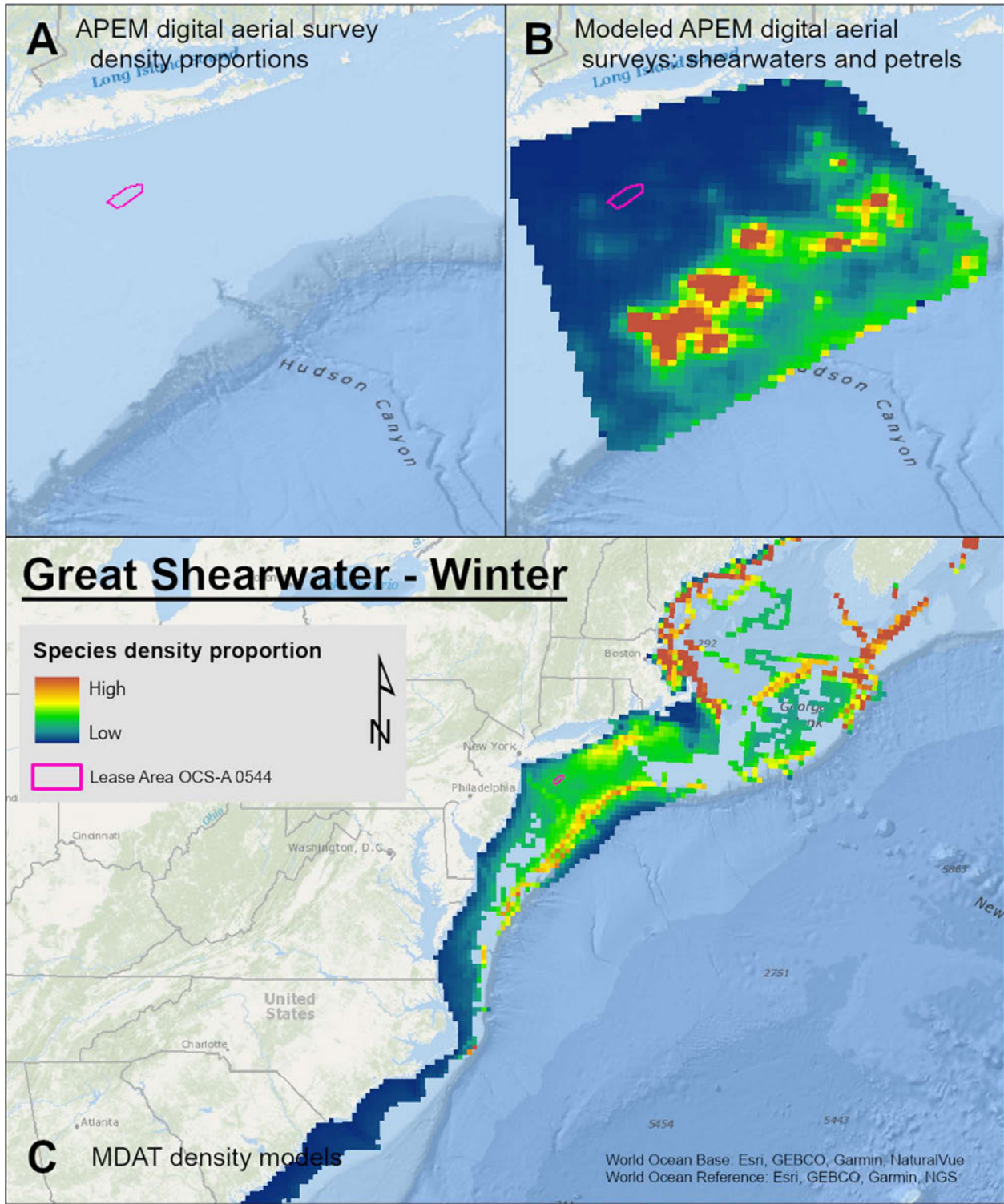
Map 175. Spring Sooty Shearwater density proportions in the NYSERDA APEM and Empire Wind high resolution digital aerial survey data (A), the NYSERDA APEM and Empire Wind high resolution digital aerial model outputs for shearwaters and petrels in Spring (B) and, Spring Sooty Shearwater MDAT modeled abundance at the regional scale (C). The scale for all maps is representative of relative spatial variation in the sites within the season for each map input.



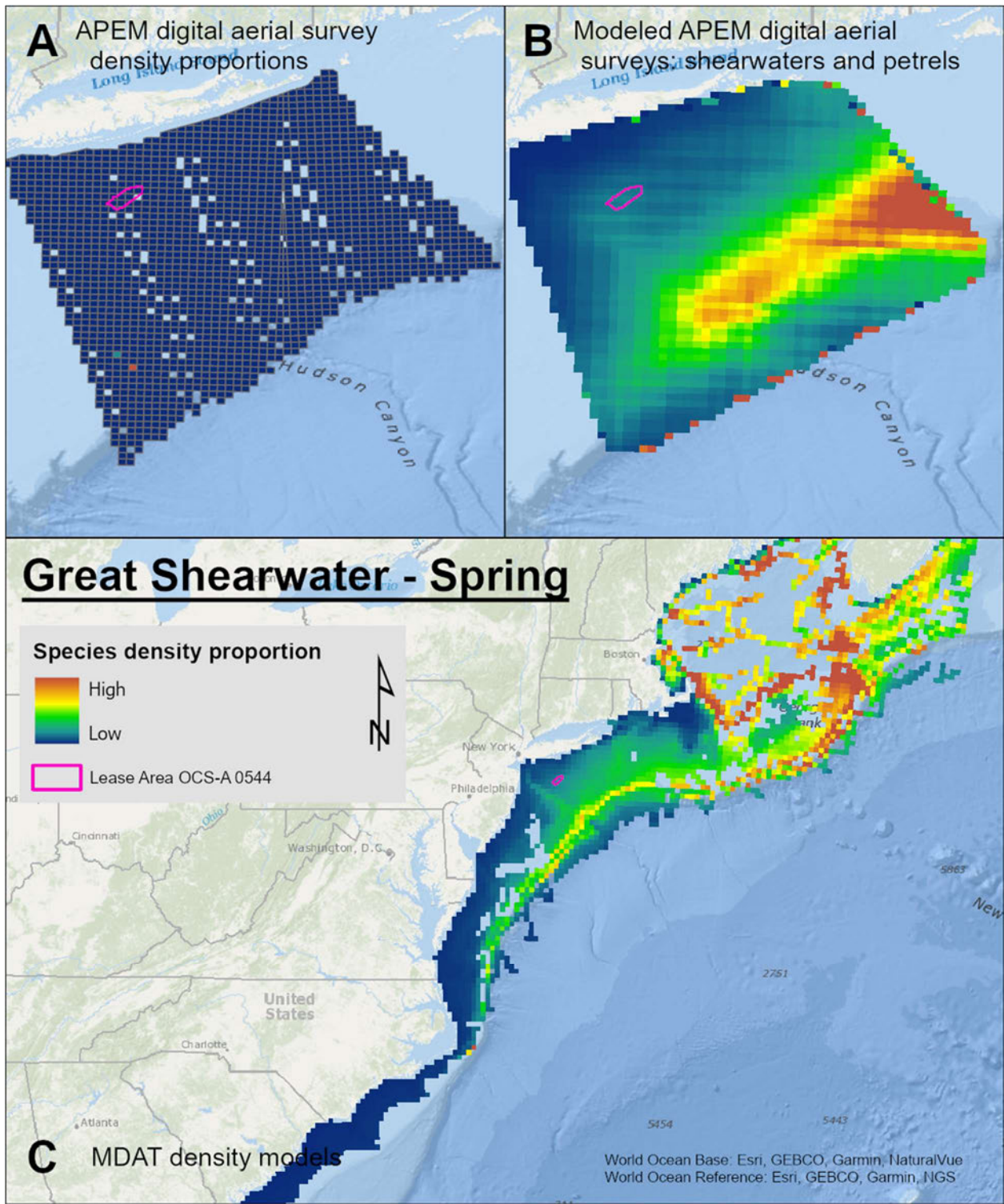
Map 176. Summer Sooty Shearwater density proportions in the NYSERDA APEM and Empire Wind high resolution digital aerial survey data (A), the NYSERDA APEM and Empire Wind high resolution digital aerial model outputs for shearwaters and petrels in Summer (B) and, Summer Sooty Shearwater MDAT modeled abundance at the regional scale (C). The scale for all maps is representative of relative spatial variation in the sites within the season for each map input.



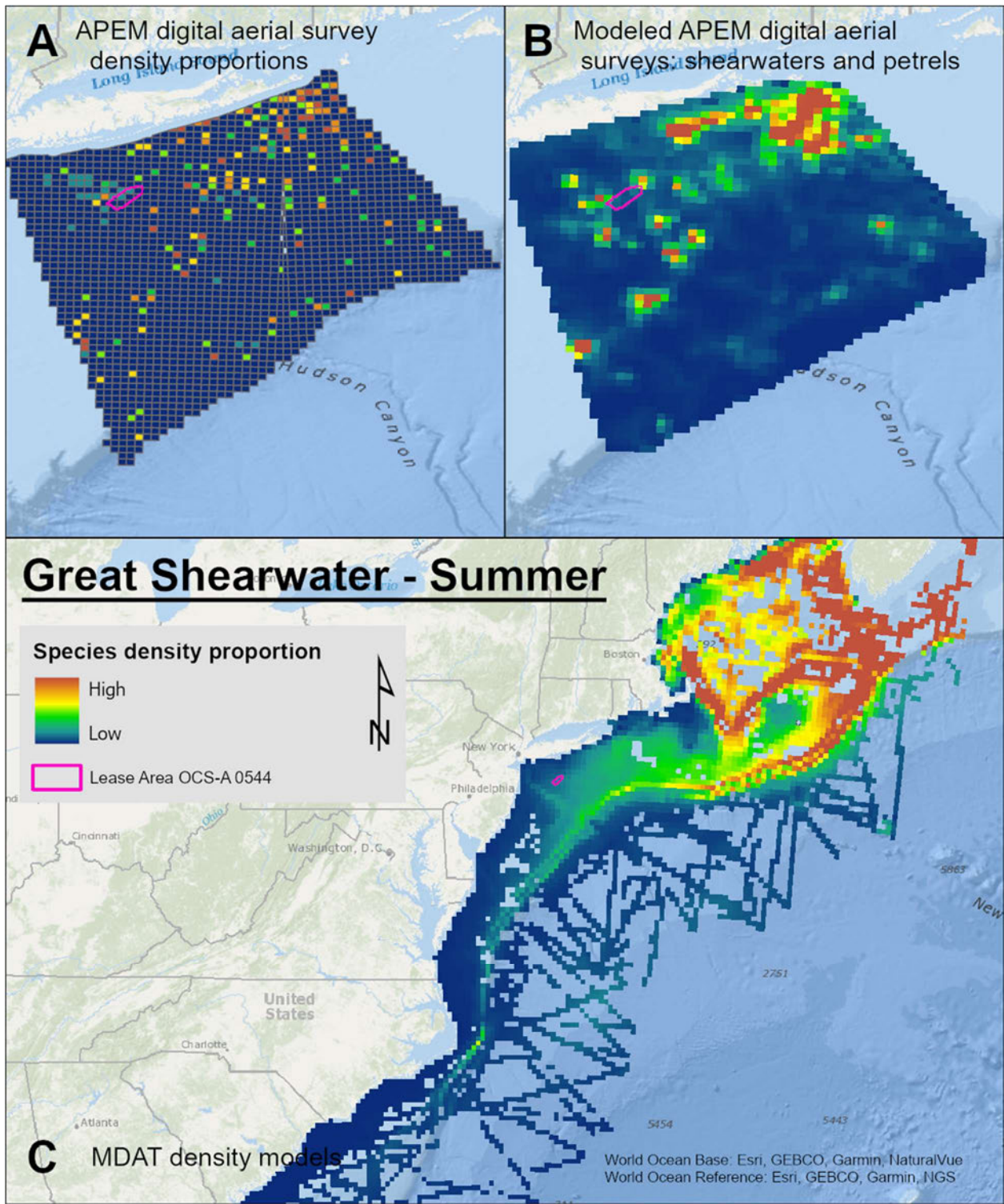
Map 177. Fall Sooty Shearwater density proportions in the NYSERDA APEM and Empire Wind high resolution digital aerial survey data (A), the NYSERDA APEM and Empire Wind high resolution digital aerial model outputs for shearwaters and petrels in Fall (B) and, Fall Sooty Shearwater MDAT modeled abundance at the regional scale (C). The scale for all maps is representative of relative spatial variation in the sites within the season for each map input.



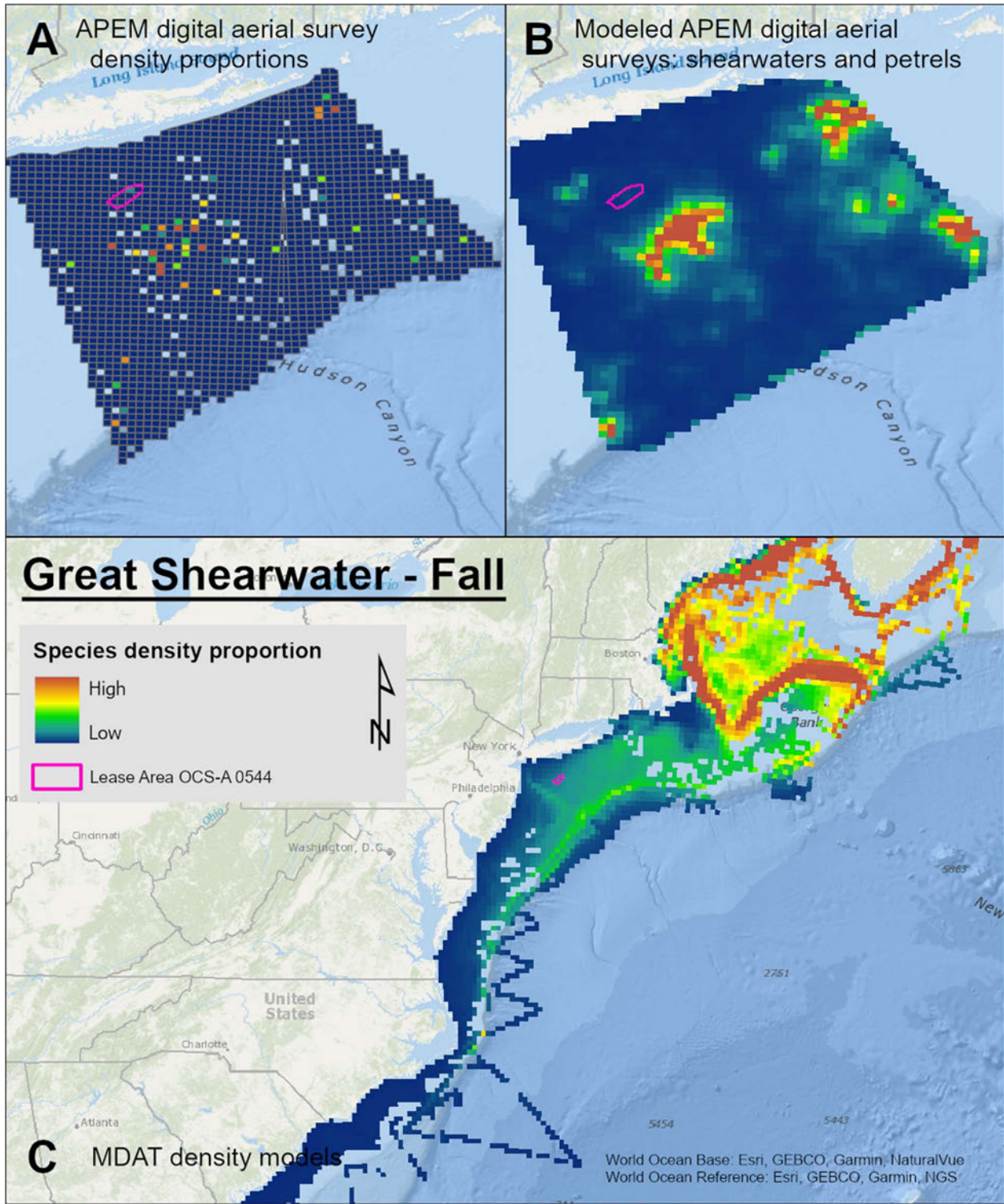
Map 178. Winter Great Shearwater density proportions in the NYSERDA APEM and Empire Wind high resolution digital aerial survey data (A), the NYSERDA APEM and Empire Wind high resolution digital aerial model outputs for shearwaters and petrels in Winter (B) and, Winter Great Shearwater MDAT modeled abundance at the regional scale (C). The scale for all maps is representative of relative spatial variation in the sites within the season for each map input.



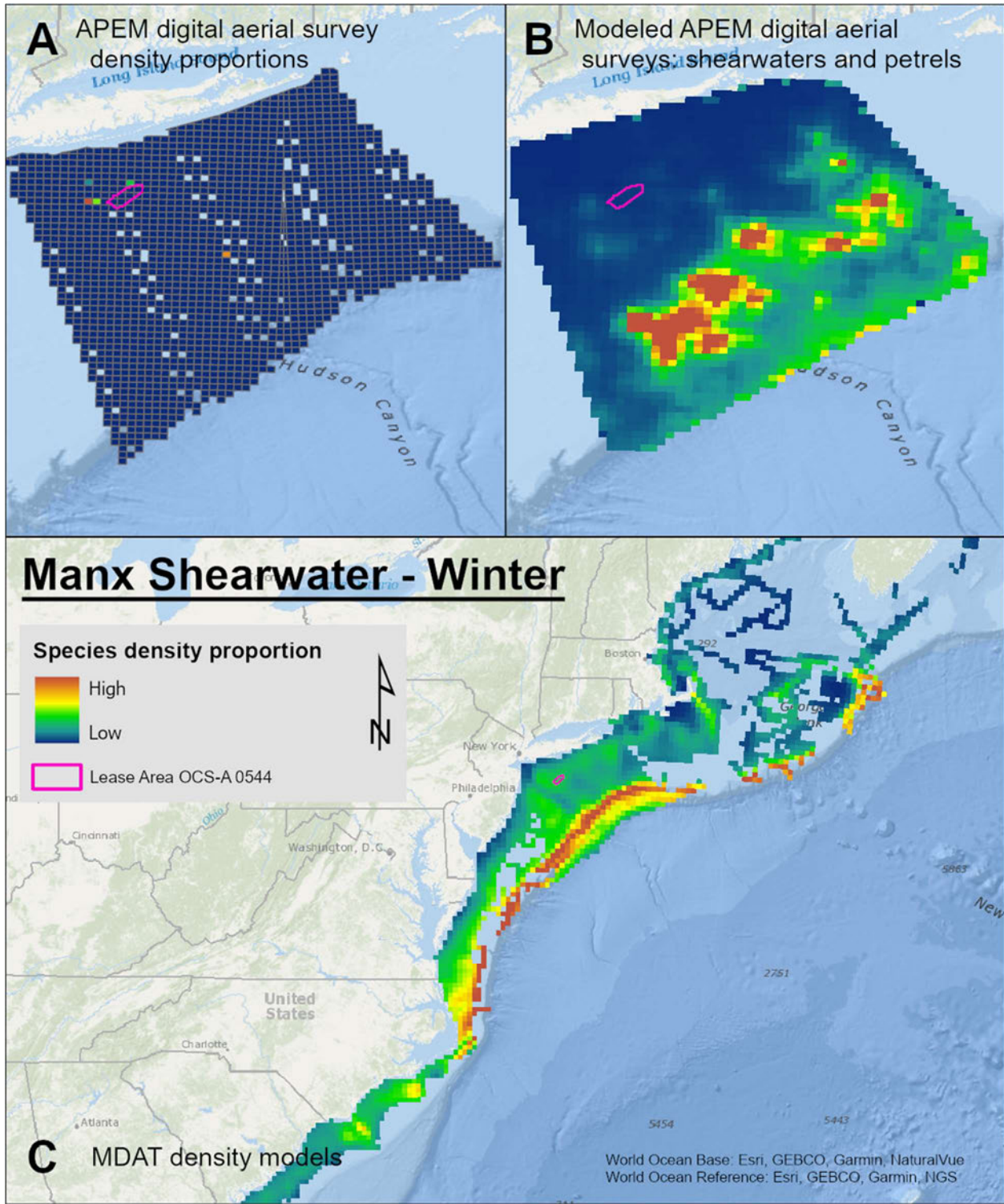
Map 179. Spring Great Shearwater density proportions in the NYSERDA APEM and Empire Wind high resolution digital aerial survey data (A), the NYSERDA APEM and Empire Wind high resolution digital aerial model outputs for shearwaters and petrels in Spring (B) and, Spring Great Shearwater MDAT modeled abundance at the regional scale (C). The scale for all maps is representative of relative spatial variation in the sites within the season for each map input.



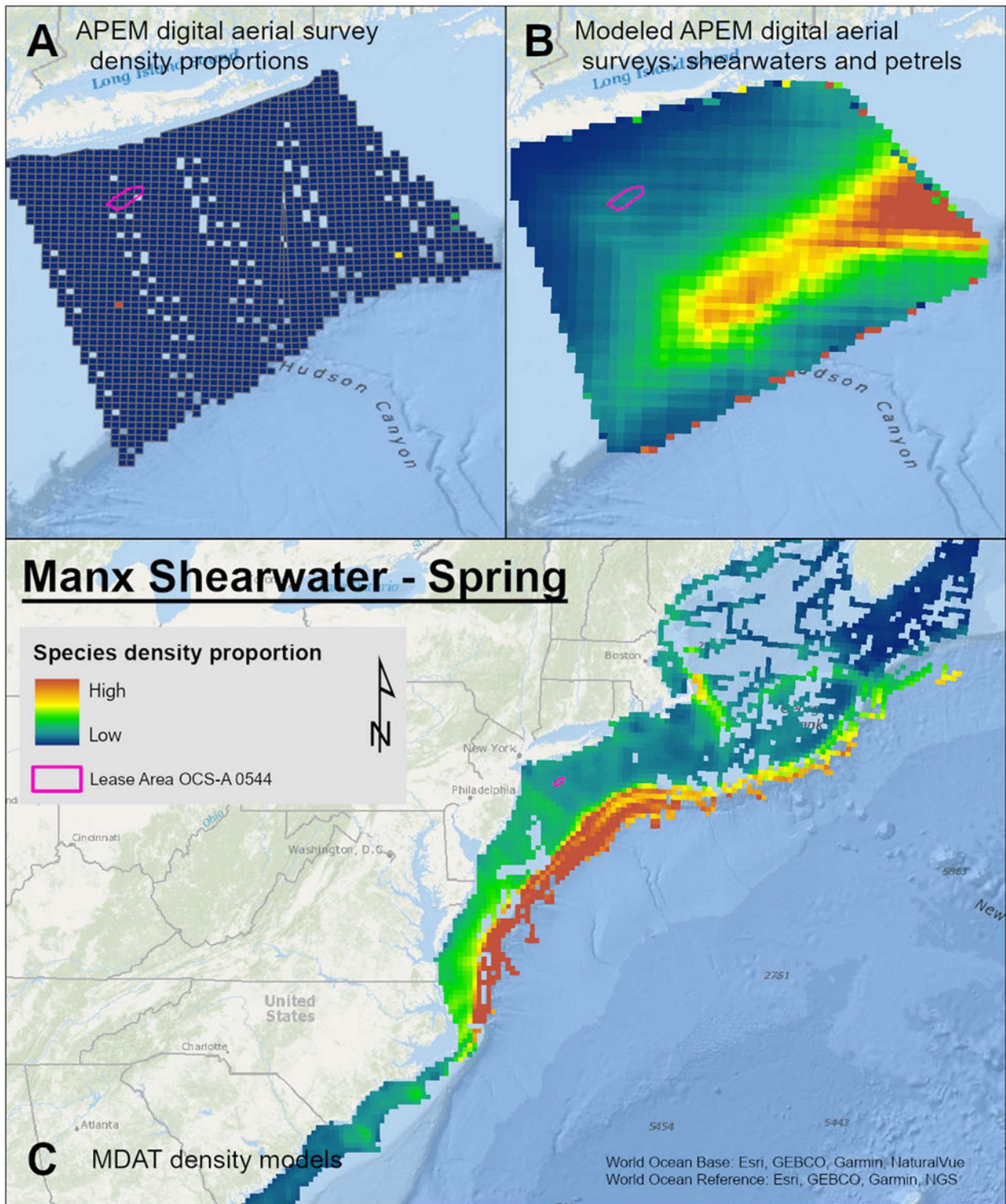
Map 180. Summer Great Shearwater density proportions in the NYSERDA APEM and Empire Wind high resolution digital aerial survey data (A), the NYSERDA APEM and Empire Wind high resolution digital aerial model outputs for shearwaters and petrels in Summer (B) and, Summer Great Shearwater MDAT modeled abundance at the regional scale (C). The scale for all maps is representative of relative spatial variation in the sites within the season for each map input.



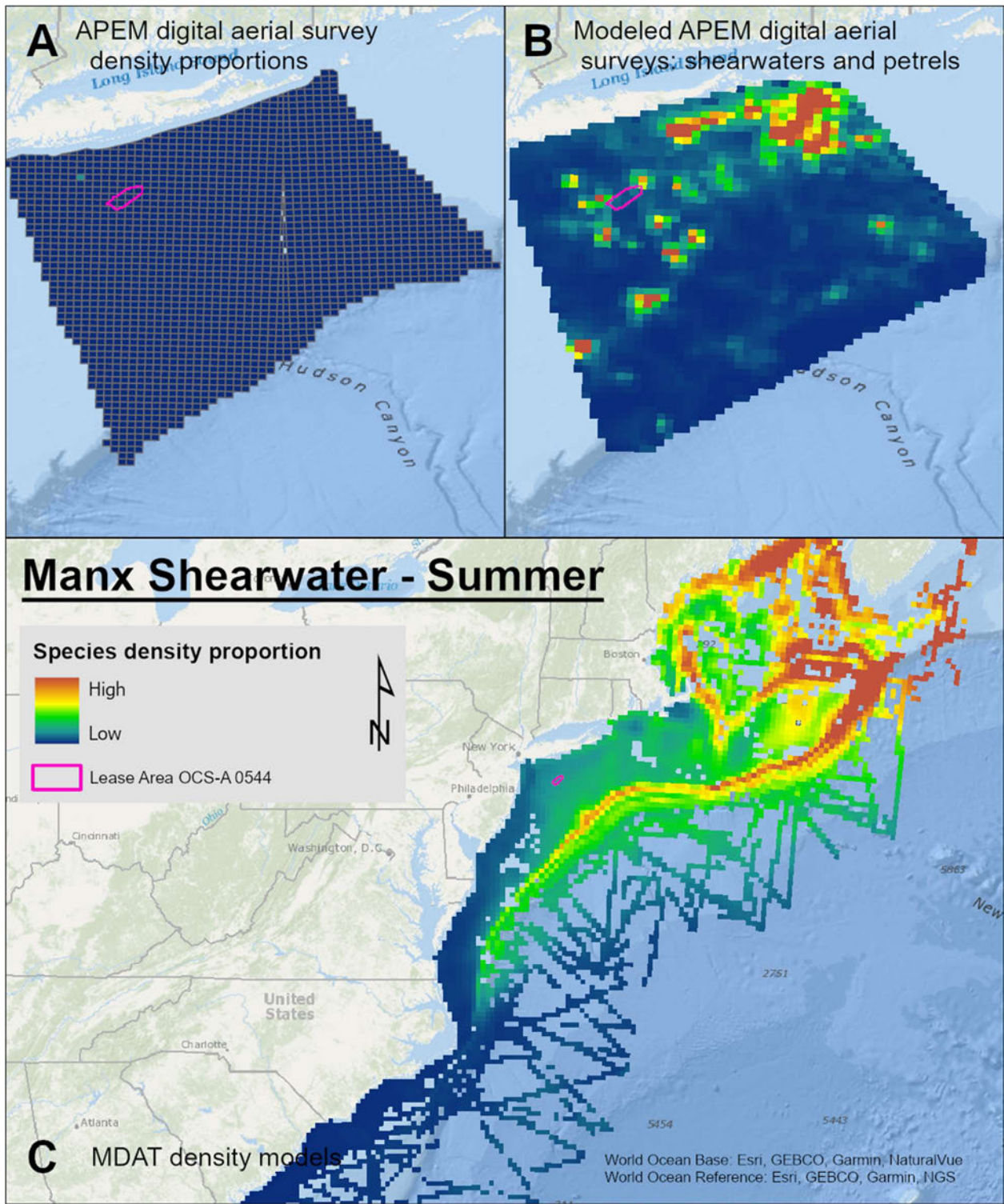
Map 181. Fall Great Shearwater density proportions in the NYSERDA APEM and Empire Wind high resolution digital aerial survey data (A), the NYSERDA APEM and Empire Wind high resolution digital aerial model outputs for shearwaters and petrels in Fall (B) and, Fall Great Shearwater MDAT modeled abundance at the regional scale (C). The scale for all maps is representative of relative spatial variation in the sites within the season for each map input.



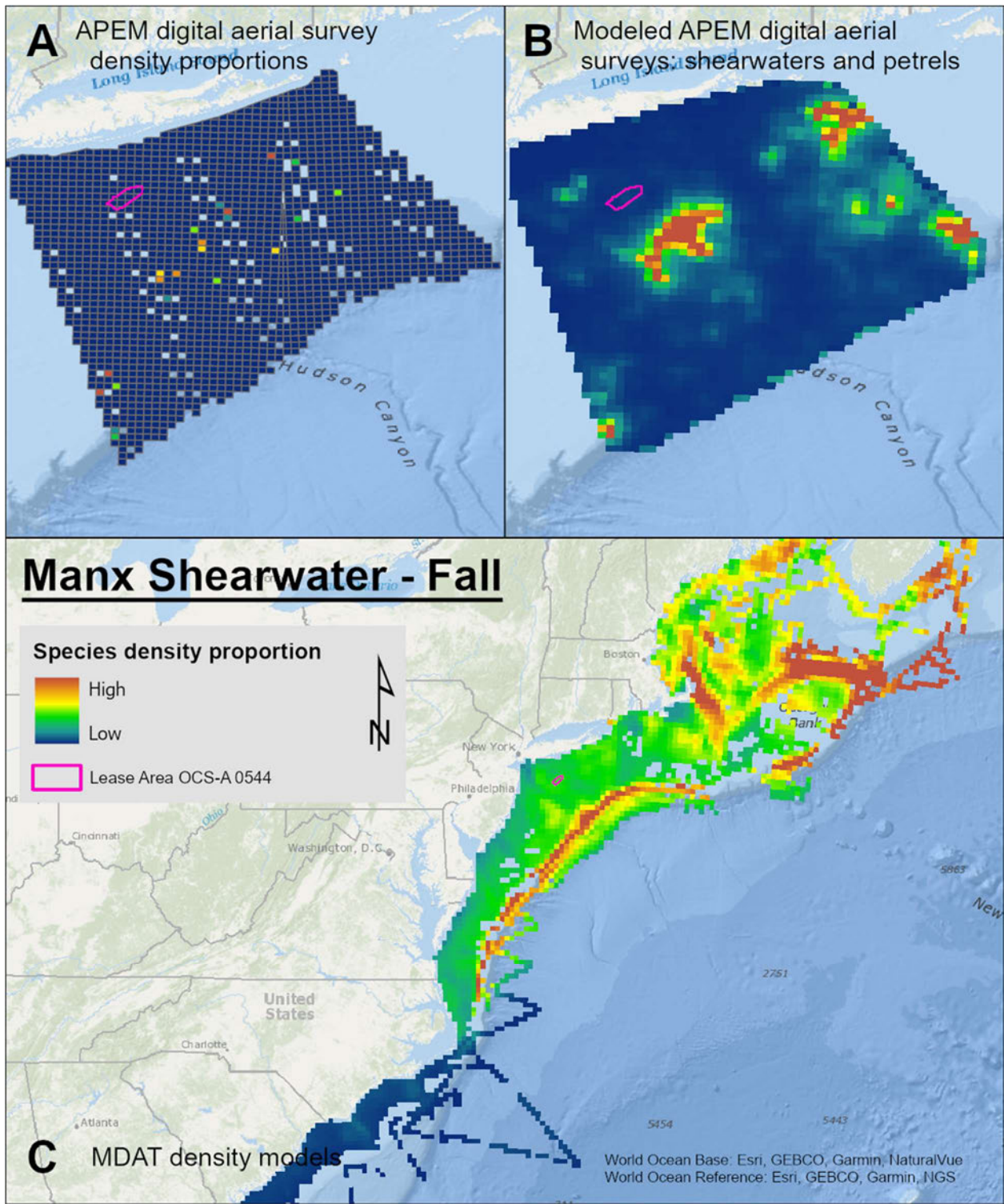
Map 182. Winter Manx Shearwater density proportions in the NYSERDA APEM and Empire Wind high resolution digital aerial survey data (A), the NYSERDA APEM and Empire Wind high resolution digital aerial model outputs for shearwaters and petrels in Winter (B) and, Winter Manx Shearwater MDAT modeled abundance at the regional scale (C). The scale for all maps is representative of relative spatial variation in the sites within the season for each map input.



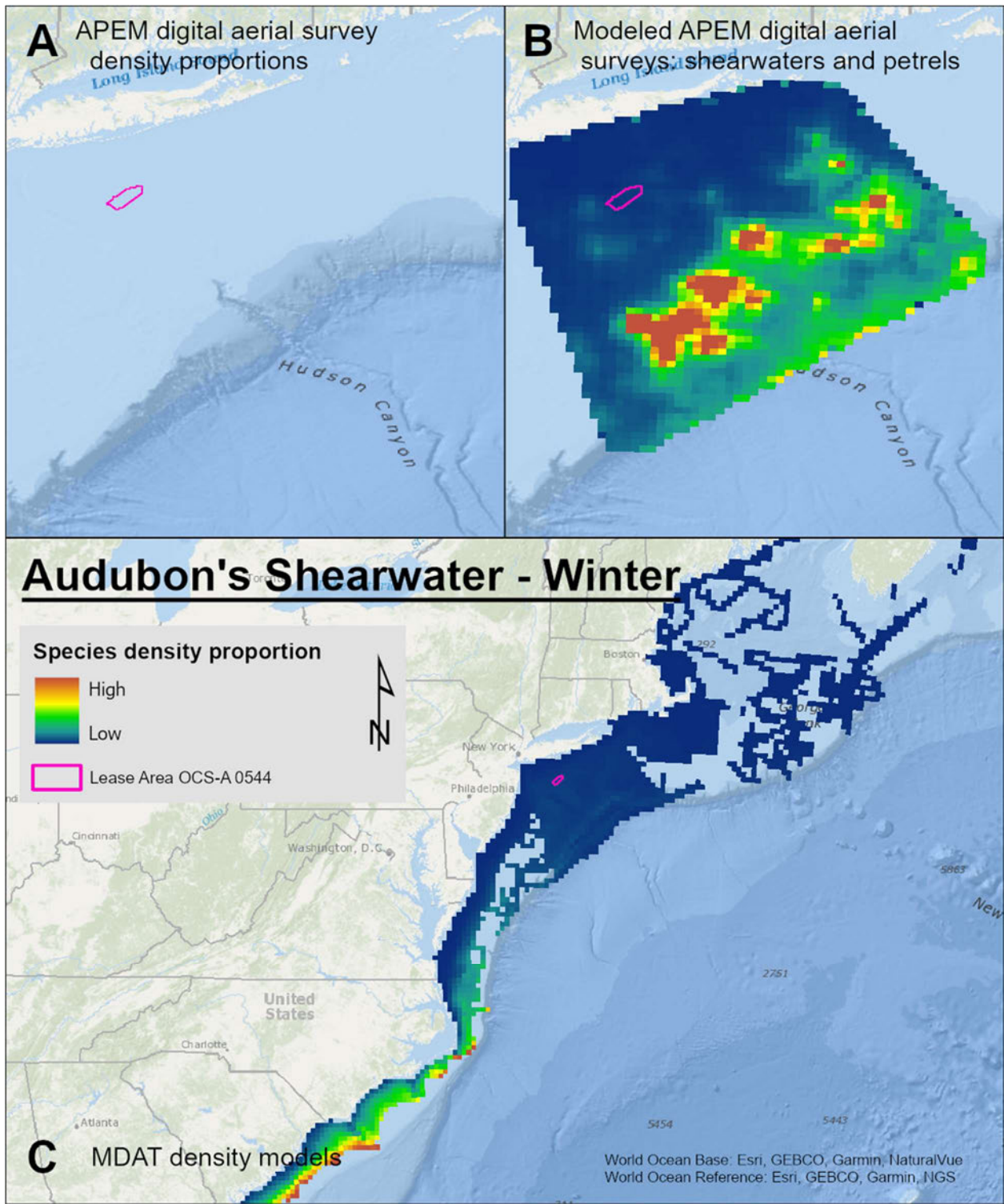
Map 183. Spring Manx Shearwater density proportions in the NYSERDA APEM and Empire Wind high resolution digital aerial survey data (A), the NYSERDA APEM and Empire Wind high resolution digital aerial model outputs for shearwaters and petrels in Spring (B) and, Spring Manx Shearwater MDAT modeled abundance at the regional scale (C). The scale for all maps is representative of relative spatial variation in the sites within the season for each map input.



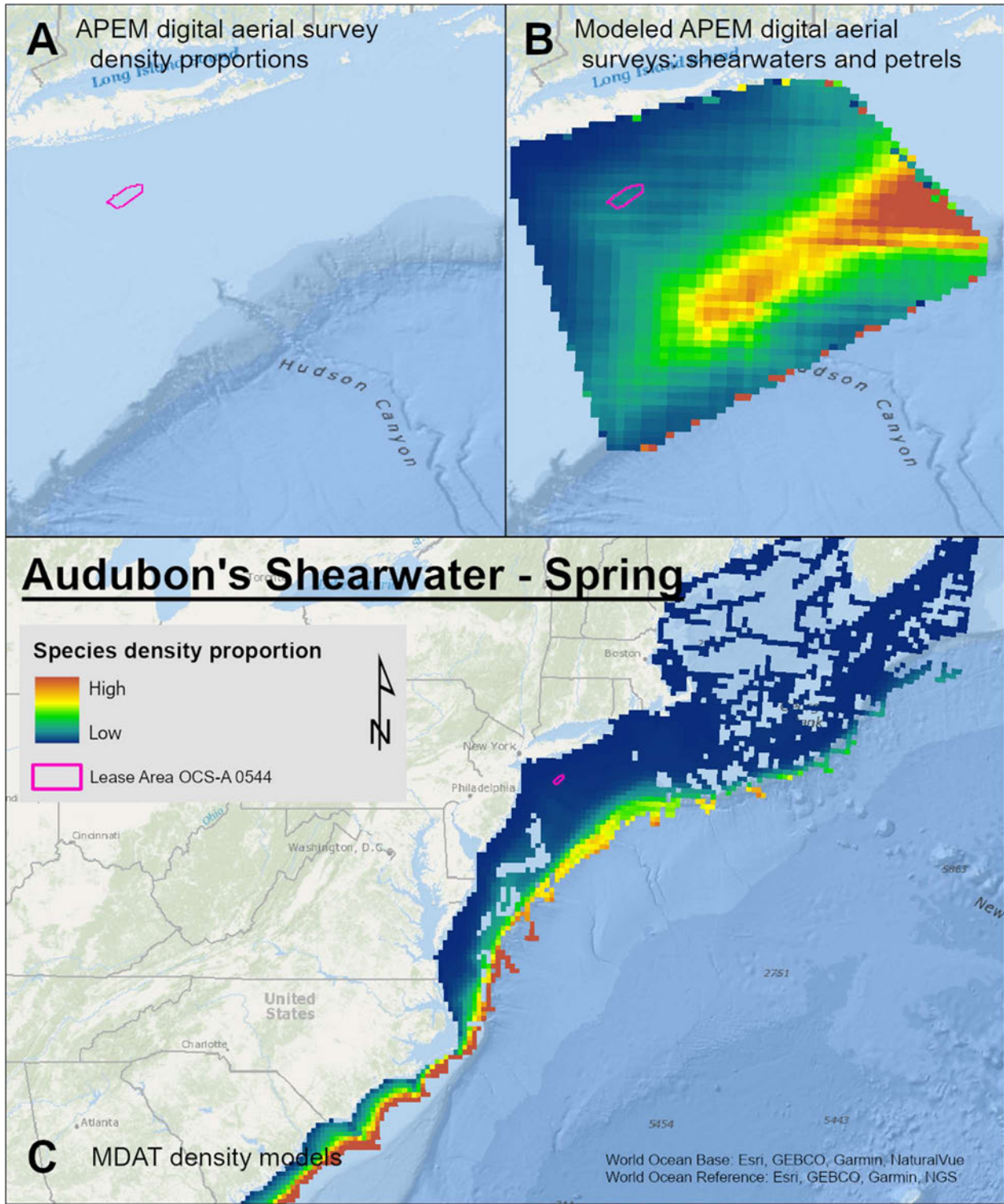
Map 184. Summer Manx Shearwater density proportions in the NYSERDA APEM and Empire Wind high resolution digital aerial survey data (A), the NYSERDA APEM and Empire Wind high resolution digital aerial model outputs for shearwaters and petrels in Summer (B) and, Summer Manx Shearwater MDAT modeled abundance at the regional scale (C). The scale for all maps is representative of relative spatial variation in the sites within the season for each map input.



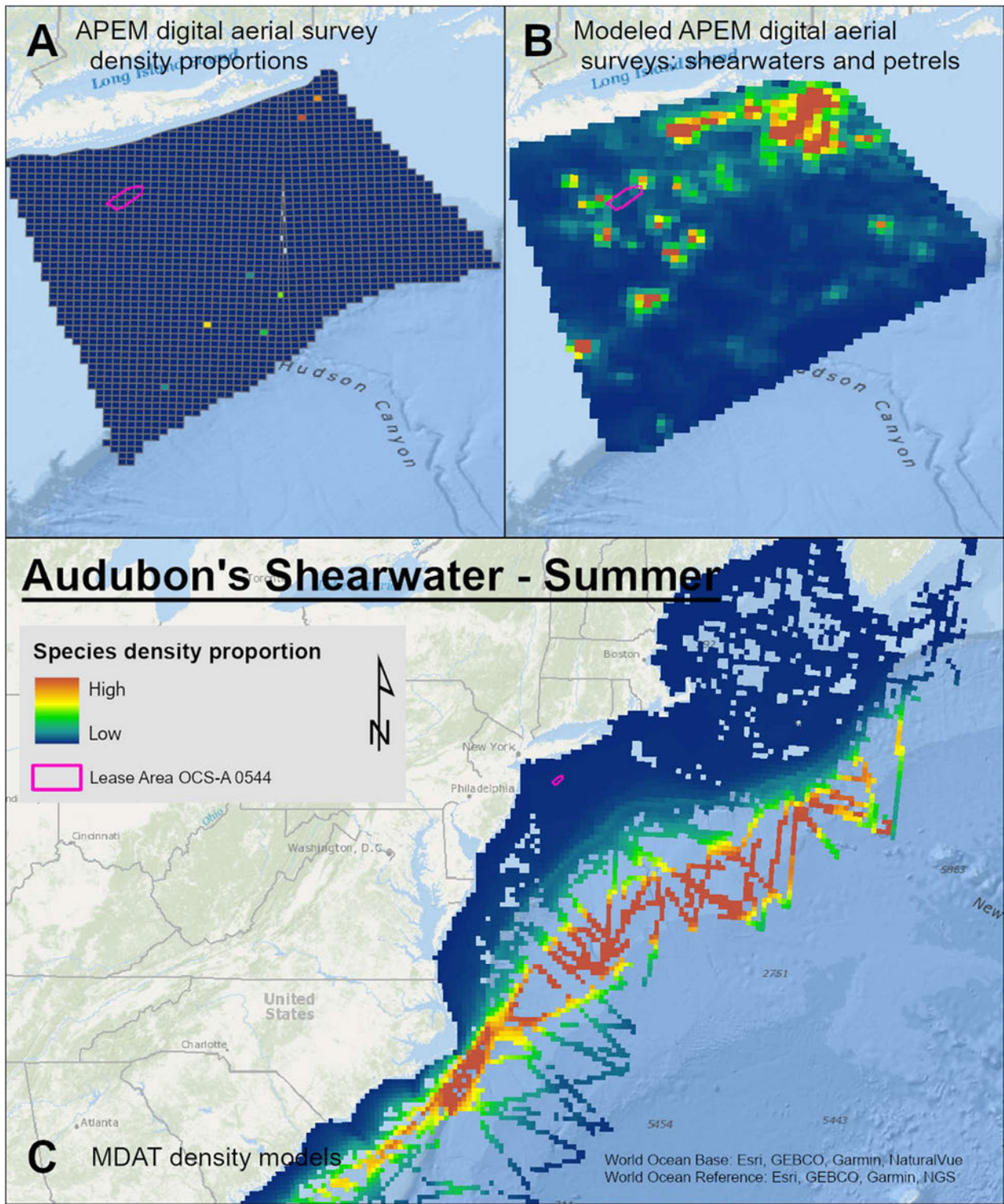
Map 185. Fall Manx Shearwater density proportions in the NYSERDA APEM and Empire Wind high resolution digital aerial survey data (A), the NYSERDA APEM and Empire Wind high resolution digital aerial model outputs for shearwaters and petrels in Fall (B) and, Fall Manx Shearwater MDAT modeled abundance at the regional scale (C). The scale for all maps is representative of relative spatial variation in the sites within the season for each map input.



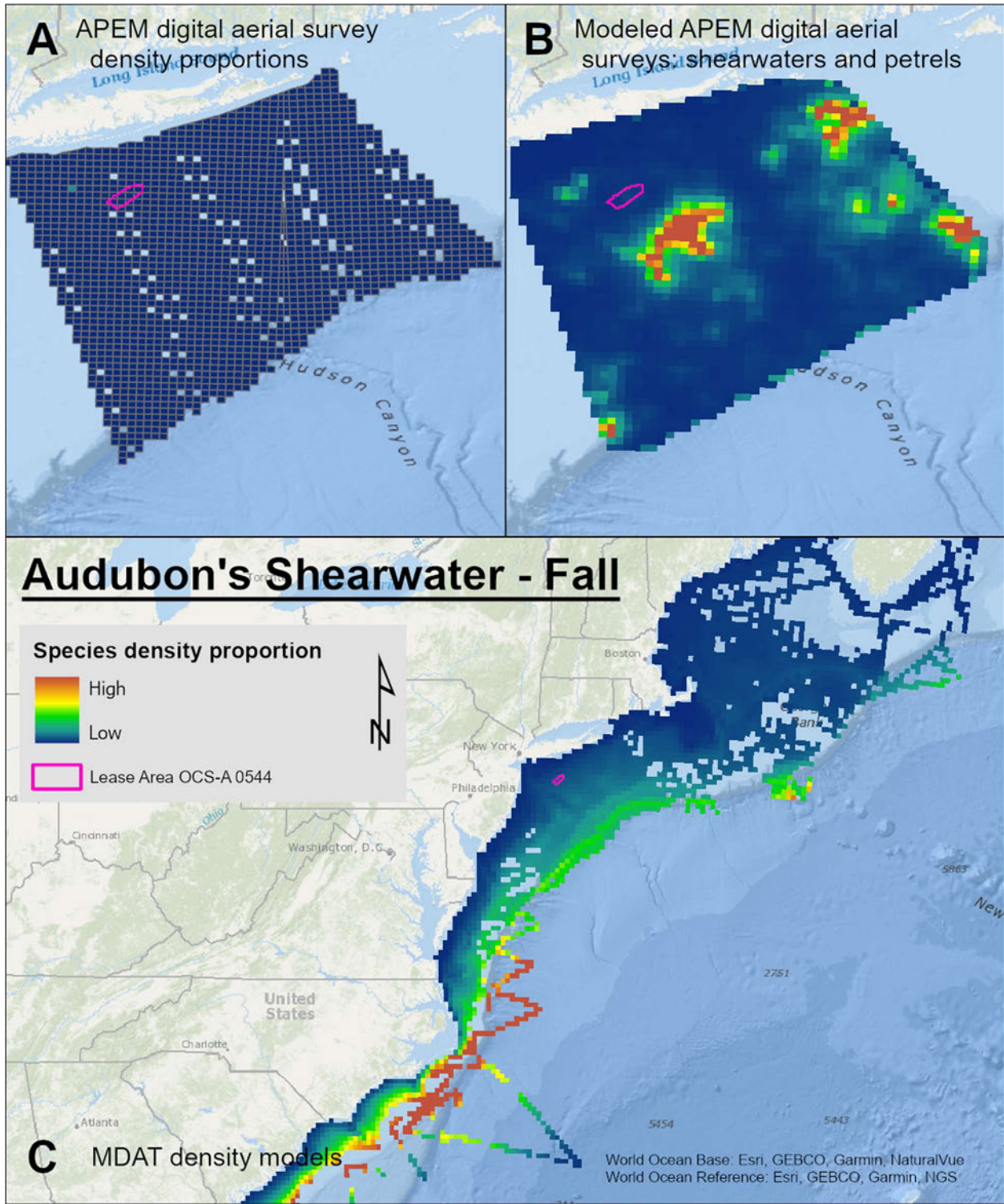
Map 186. Winter Audubon's Shearwater density proportions in the NYSERDA APEM and Empire Wind high resolution digital aerial survey data (A), the NYSERDA APEM and Empire Wind high resolution digital aerial model outputs for shearwaters and petrels in Winter (B) and, Winter Audubon's Shearwater MDAT modeled abundance at the regional scale (C). The scale for all maps is representative of relative spatial variation in the sites within the season for each map input.



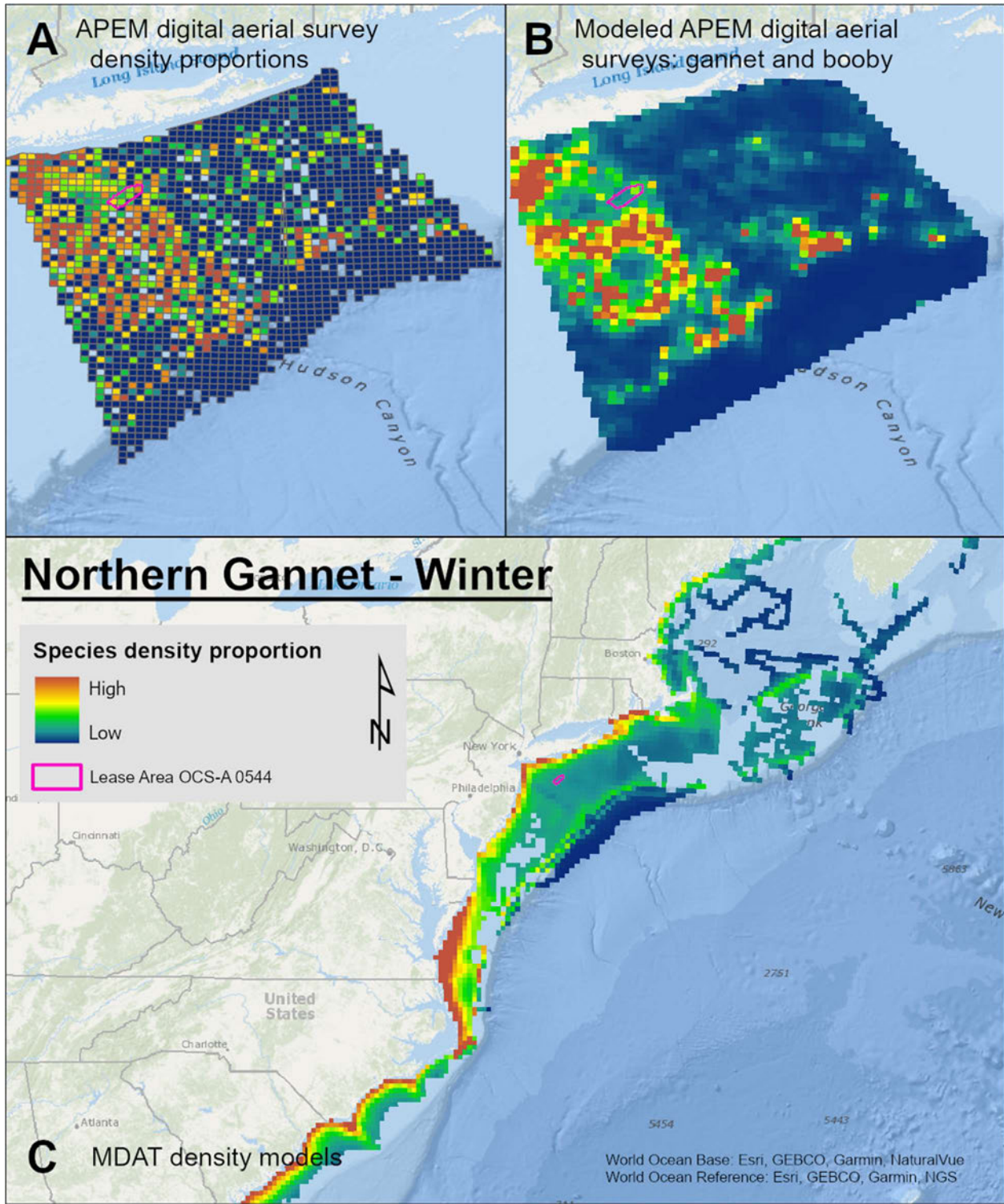
Map 187. Spring Audubon's Shearwater density proportions in the NYSEDA APEM and Empire Wind high resolution digital aerial survey data (A), the NYSEDA APEM and Empire Wind high resolution digital aerial model outputs for shearwaters and petrels in Spring (B) and, Spring Audubon's Shearwater MDAT modeled abundance at the regional scale (C). The scale for all maps is representative of relative spatial variation in the sites within the season for each map input.



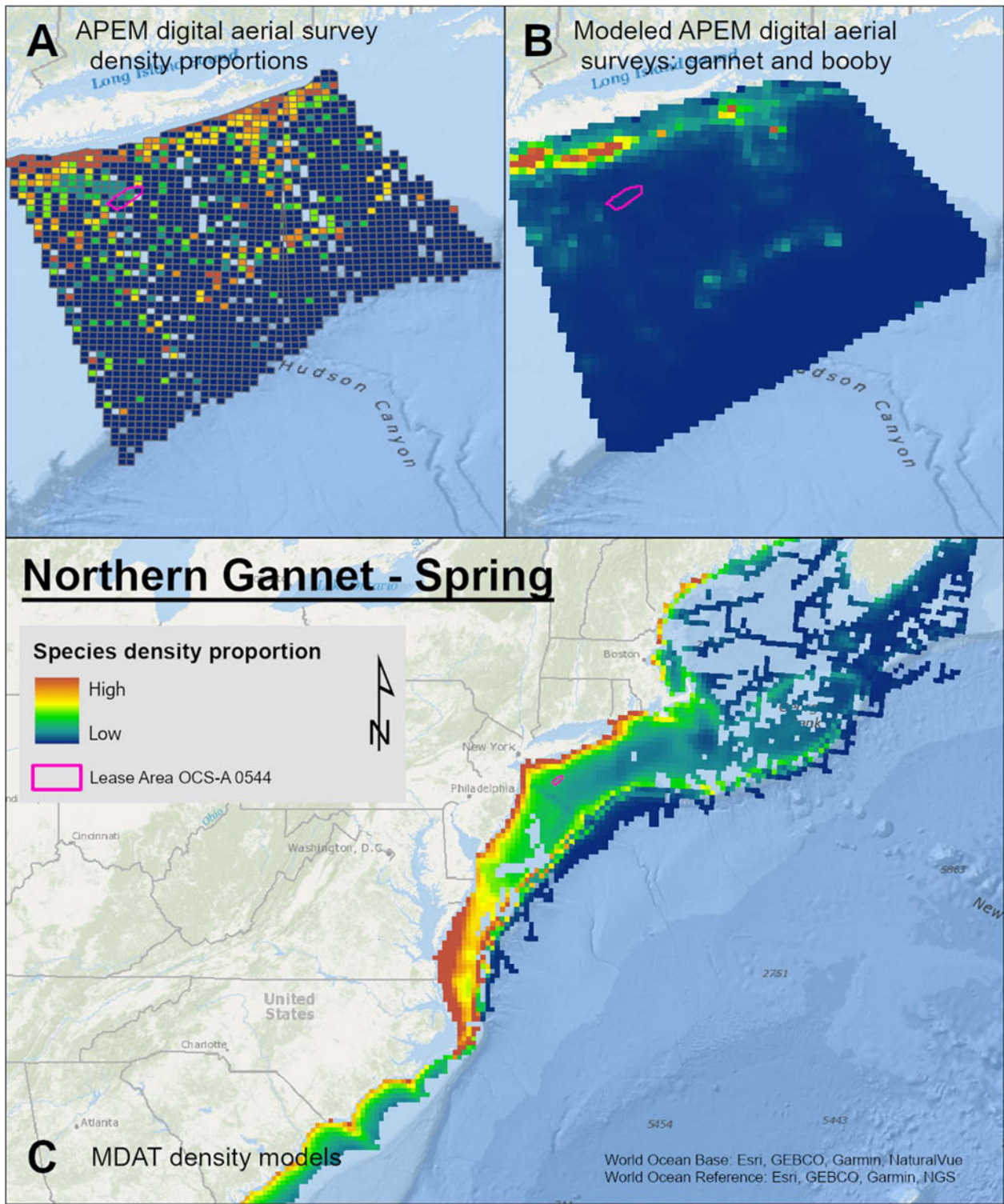
Map 188. Summer Audubon's Shearwater density proportions in the NYSERDA APEM and Empire Wind high resolution digital aerial survey data (A), the NYSERDA APEM and Empire Wind high resolution digital aerial model outputs for shearwaters and petrels in Summer (B) and, Summer Audubon's Shearwater MDAT modeled abundance at the regional scale (C). The scale for all maps is representative of relative spatial variation in the sites within the season for each map input.



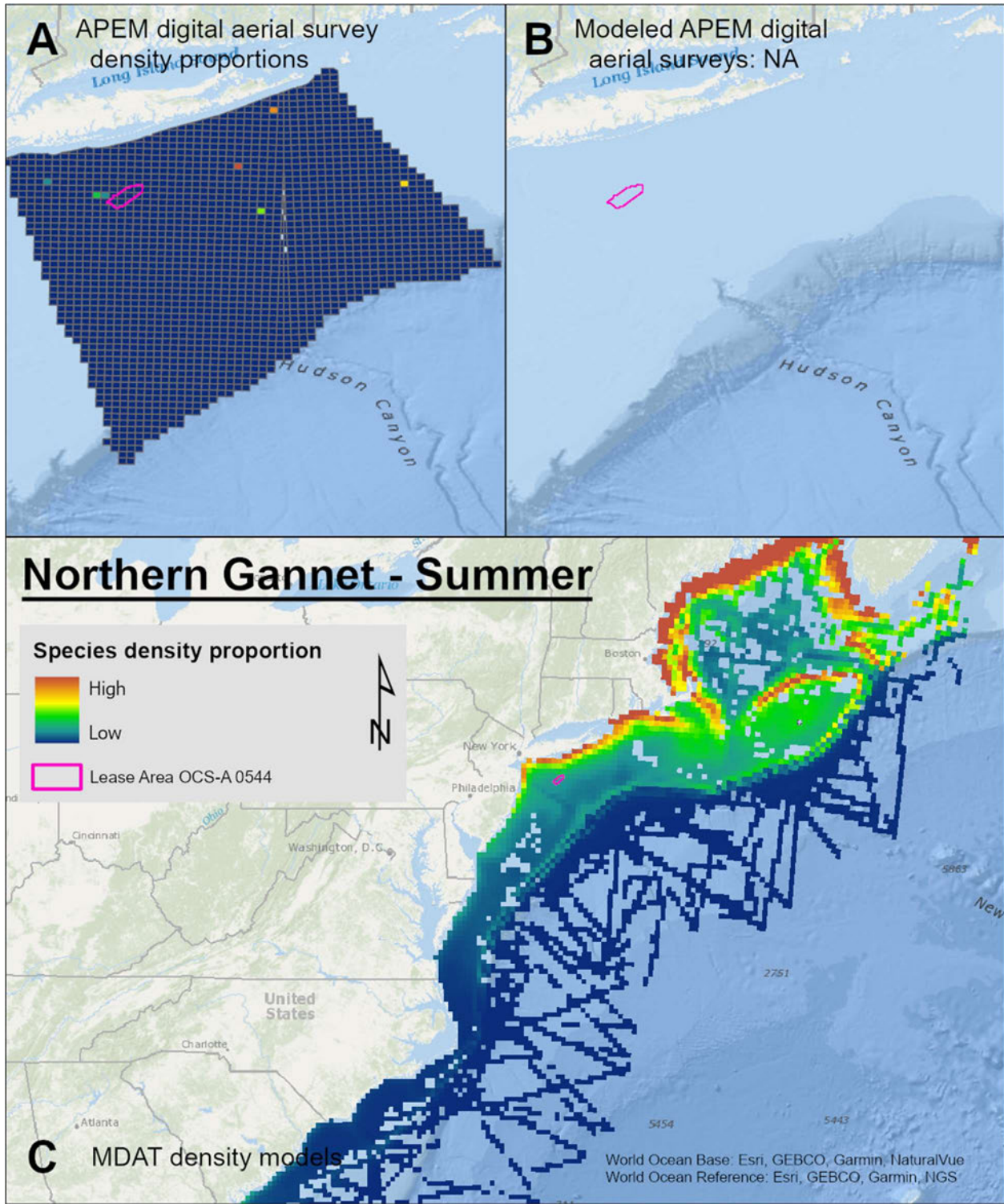
Map 189. Fall Audubon's Shearwater density proportions in the NYSERDA APEM and Empire Wind high resolution digital aerial survey data (A), the NYSERDA APEM and Empire Wind high resolution digital aerial model outputs for shearwaters and petrels in Fall (B) and, Fall Audubon's Shearwater MDAT modeled abundance at the regional scale (C). The scale for all maps is representative of relative spatial variation in the sites within the season for each map input.



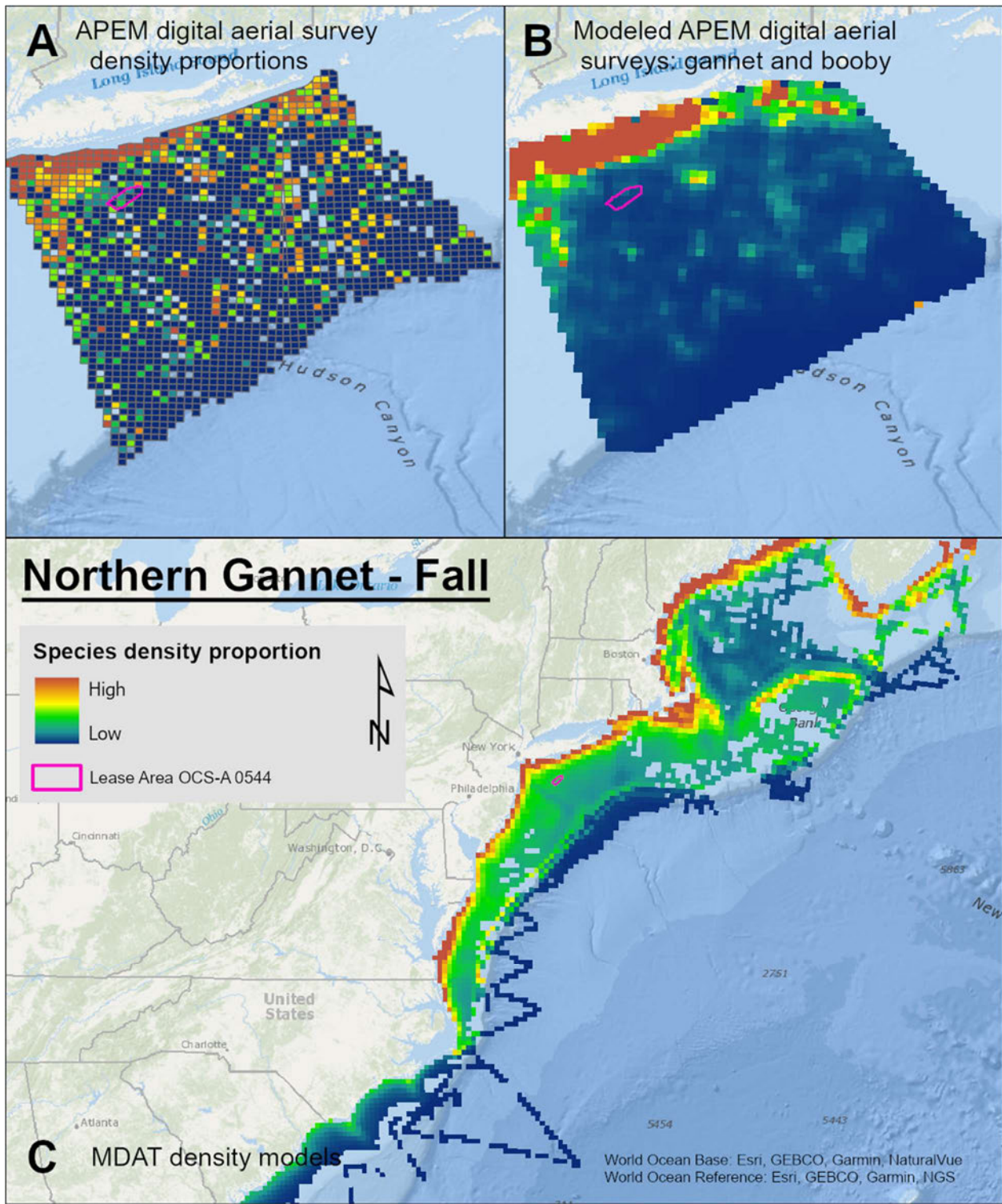
Map 190. Winter Northern Gannet density proportions in the NYSERDA APEM and Empire Wind high resolution digital aerial survey data (A), the NYSERDA APEM and Empire Wind high resolution digital aerial model outputs for gannet and booby in Winter (B) and, Winter Northern Gannet MDAT modeled abundance at the regional scale (C). The scale for all maps is representative of relative spatial variation in the sites within the season for each map input.



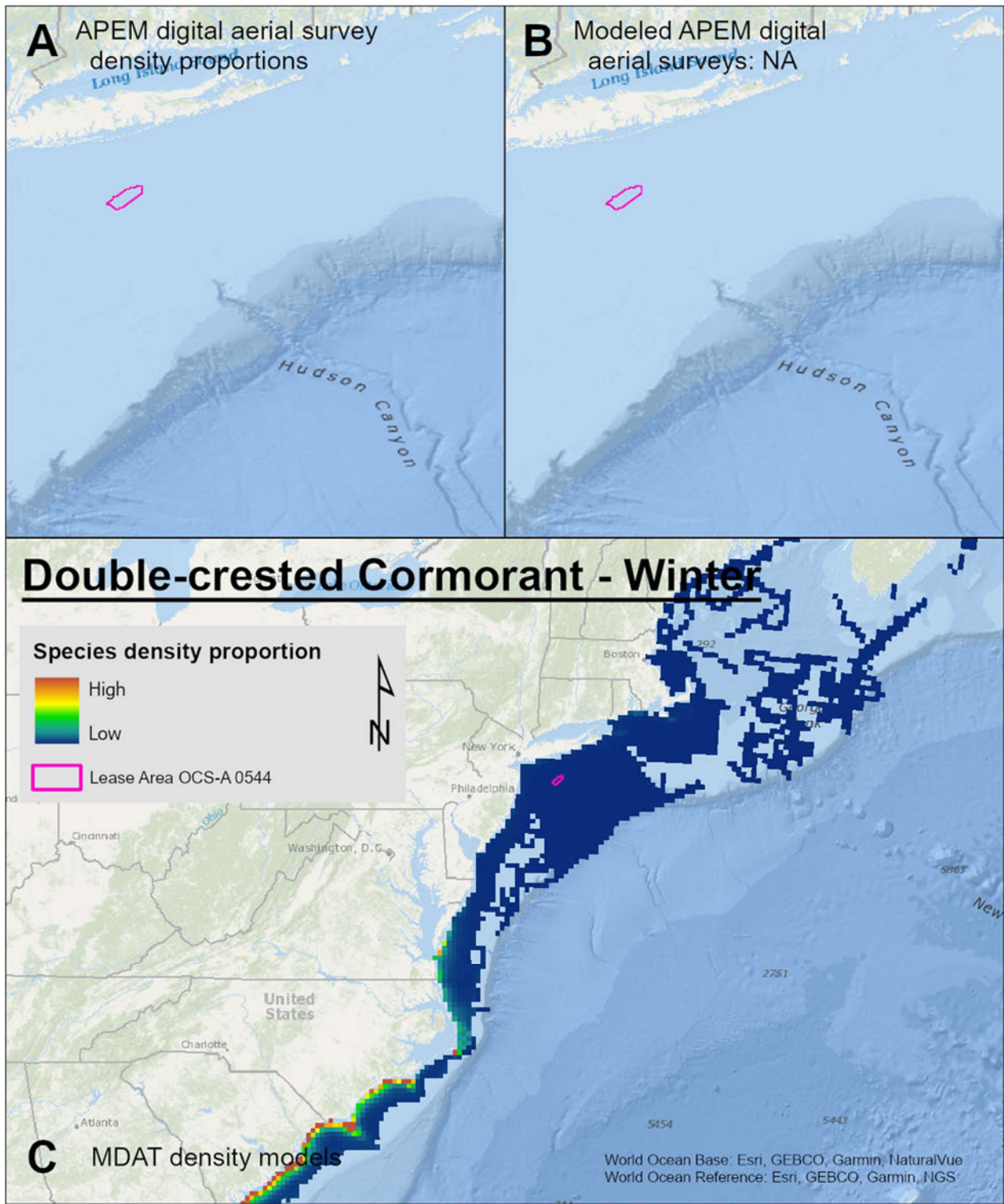
Map 191. Spring Northern Gannet density proportions in the NYSERDA APEM and Empire Wind high resolution digital aerial survey data (A), the NYSERDA APEM and Empire Wind high resolution digital aerial model outputs for gannet and booby in Spring (B) and, Spring Northern Gannet MDAT modeled abundance at the regional scale (C). The scale for all maps is representative of relative spatial variation in the sites within the season for each map input.



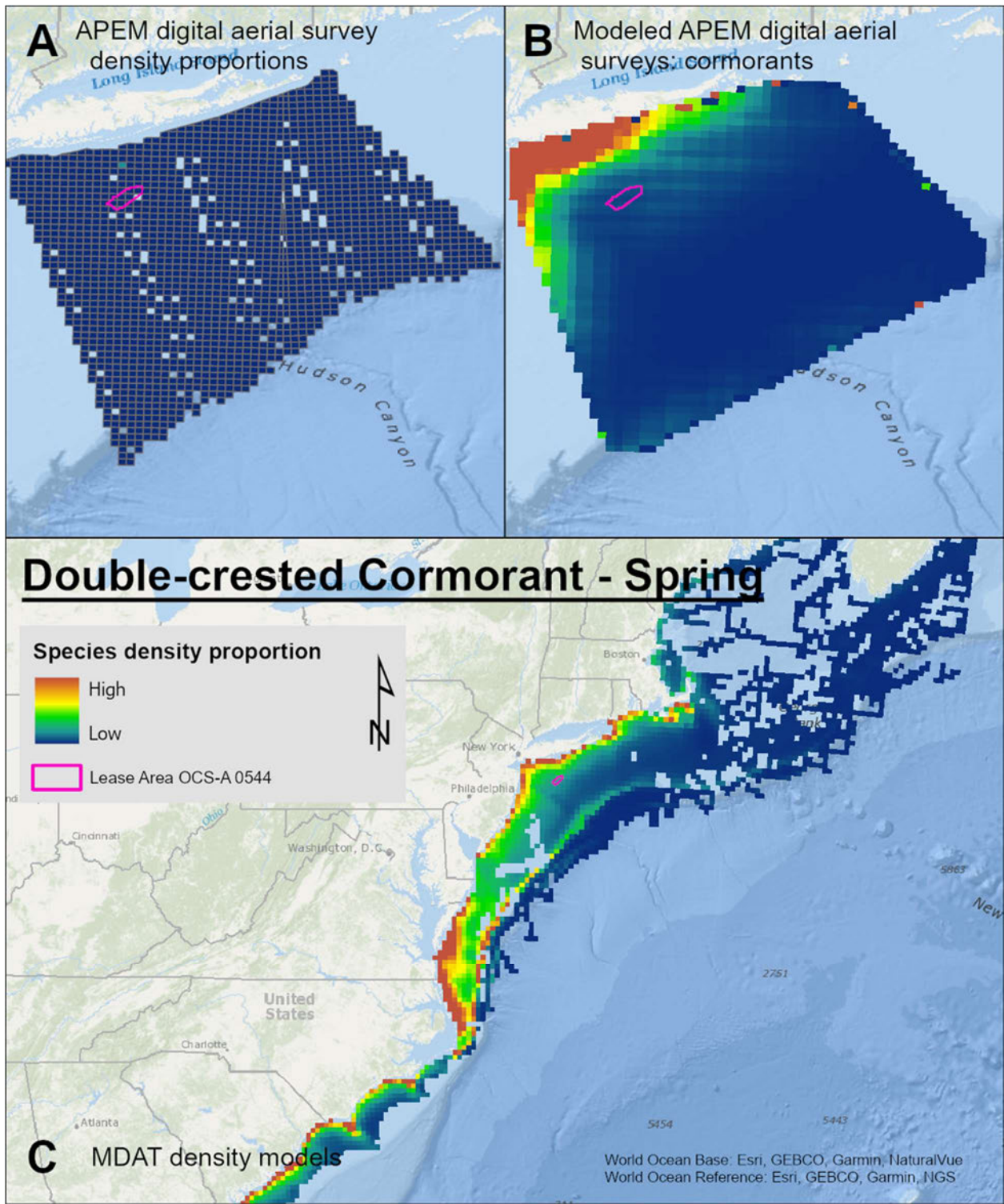
Map 192. Summer Northern Gannet density proportions in the NYSERDA APEM and Empire Wind high resolution digital aerial survey data (A), the NYSERDA APEM and Empire Wind high resolution digital aerial model outputs for gannet and booby in Summer (B) and, Summer Northern Gannet MDAT modeled abundance at the regional scale (C). The scale for all maps is representative of relative spatial variation in the sites within the season for each map input.



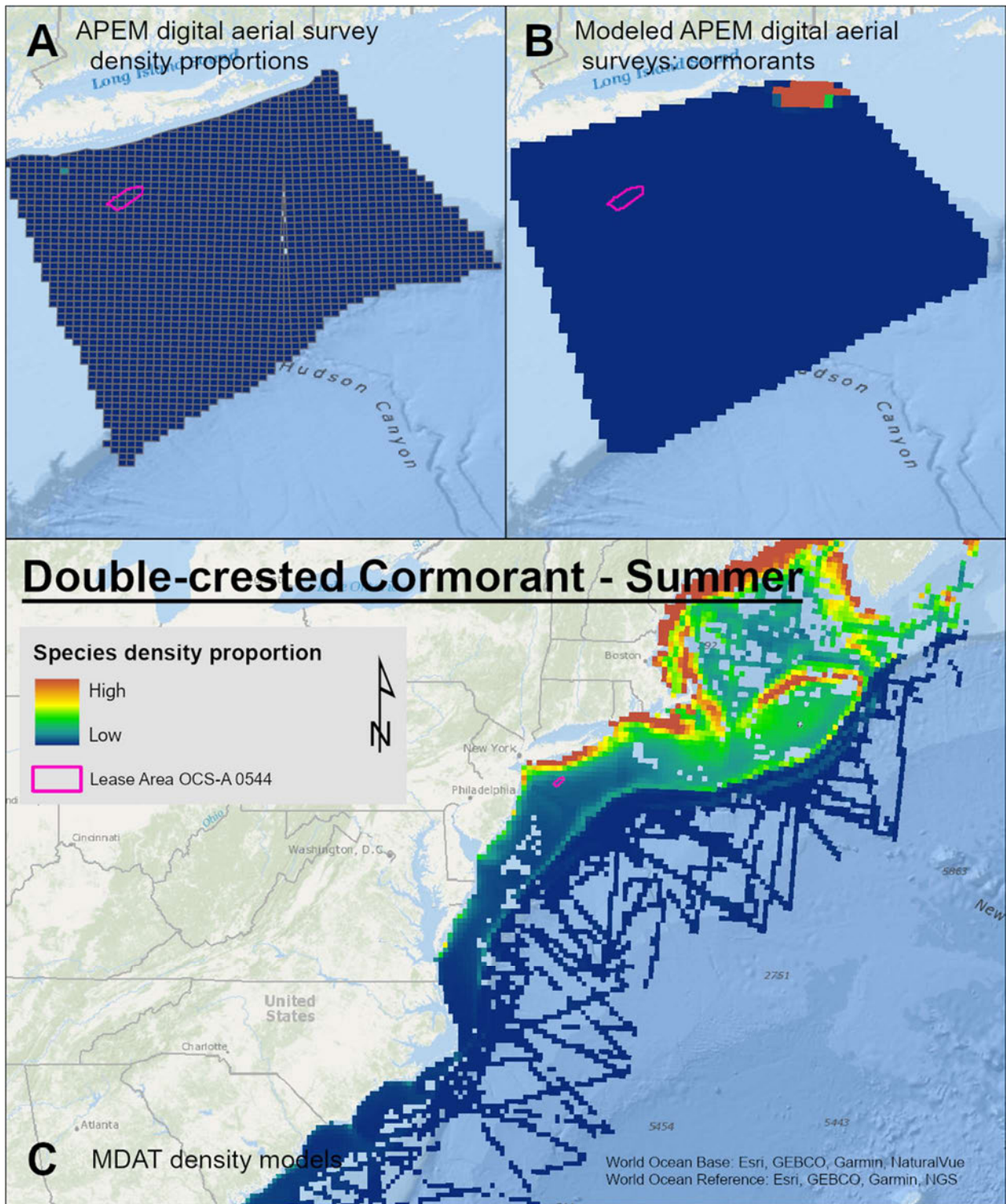
Map 193. Fall Northern Gannet density proportions in the NYSERDA APEM and Empire Wind high resolution digital aerial survey data (A), the NYSERDA APEM and Empire Wind high resolution digital aerial model outputs for gannet and booby in Fall (B) and, Fall Northern Gannet MDAT modeled abundance at the regional scale (C). The scale for all maps is representative of relative spatial variation in the sites within the season for each map input.



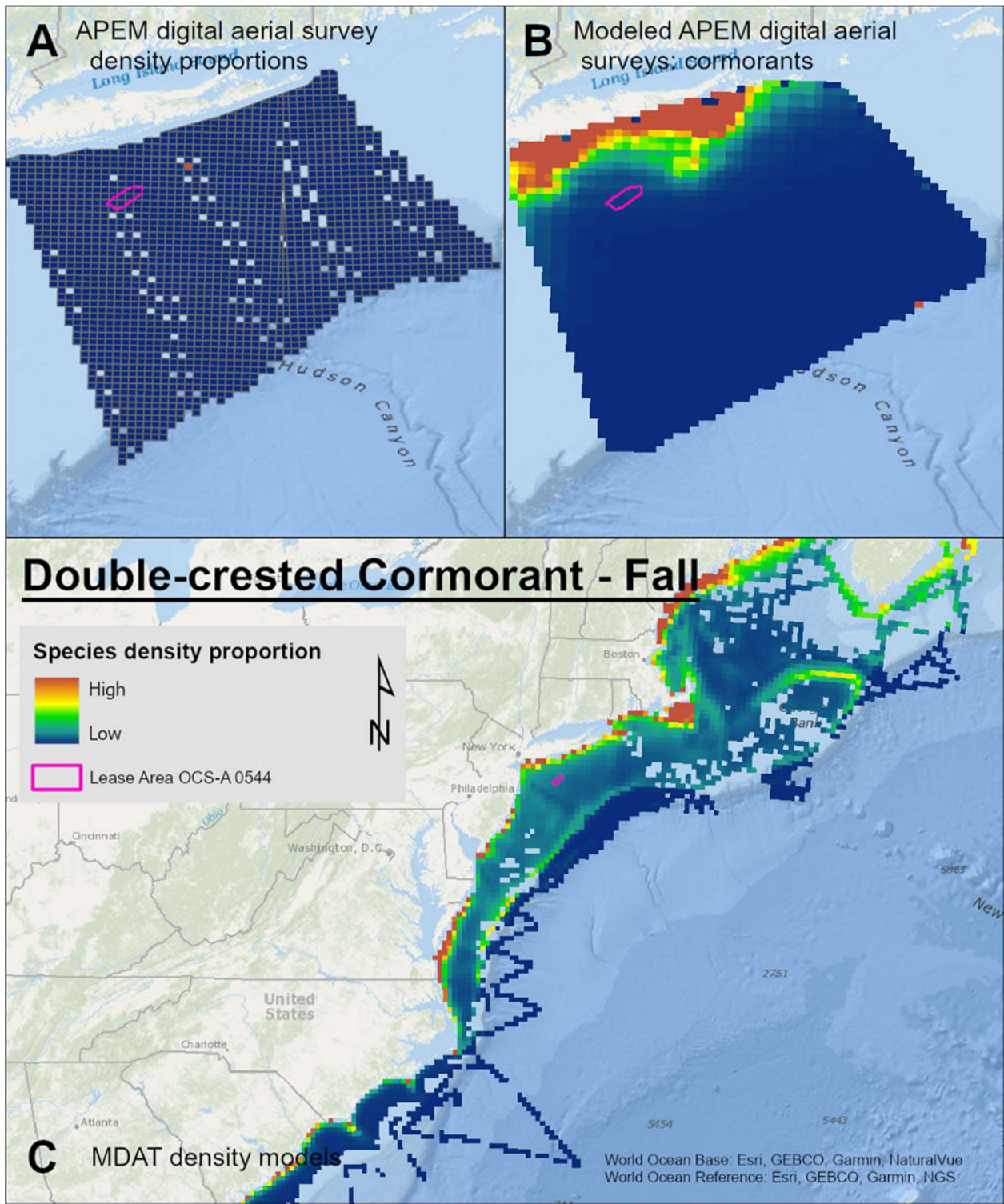
Map 194. Winter Double-crested Cormorant density proportions in the NYSERDA APEM and Empire Wind high resolution digital aerial survey data (A), the NYSERDA APEM and Empire Wind high resolution digital aerial model outputs for cormorants in Winter (B) and, Winter Double-crested Cormorant MDAT modeled abundance at the regional scale (C). The scale for all maps is representative of relative spatial variation in the sites within the season for each map input.



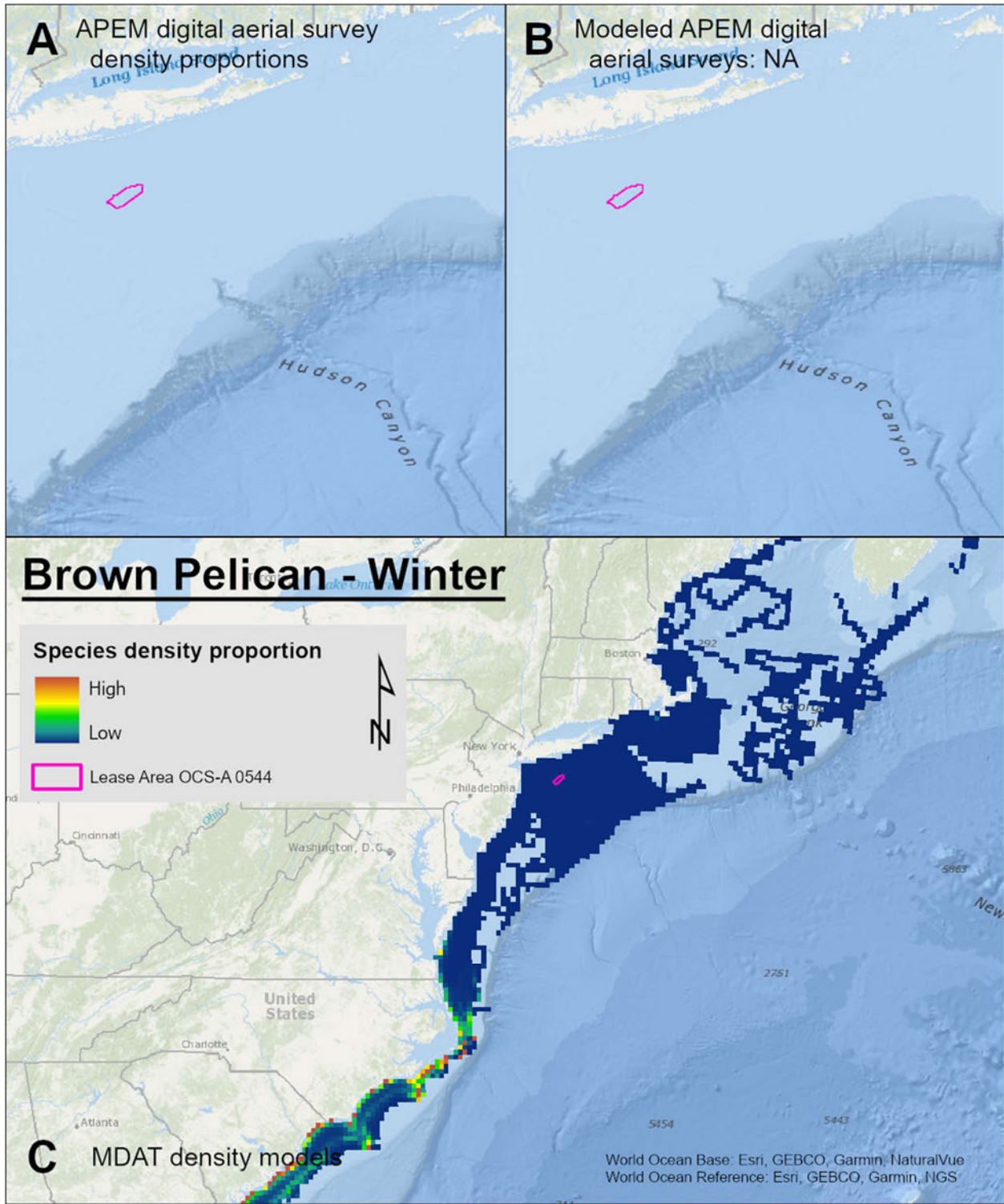
Map 195. Spring Double-crested Cormorant density proportions in the NYSERDA APEM and Empire Wind high resolution digital aerial survey data (A), the NYSERDA APEM and Empire Wind high resolution digital aerial model outputs for cormorants in Spring (B) and, Spring Double-crested Cormorant MDAT modeled abundance at the regional scale (C). The scale for all maps is representative of relative spatial variation in the sites within the season for each map input.



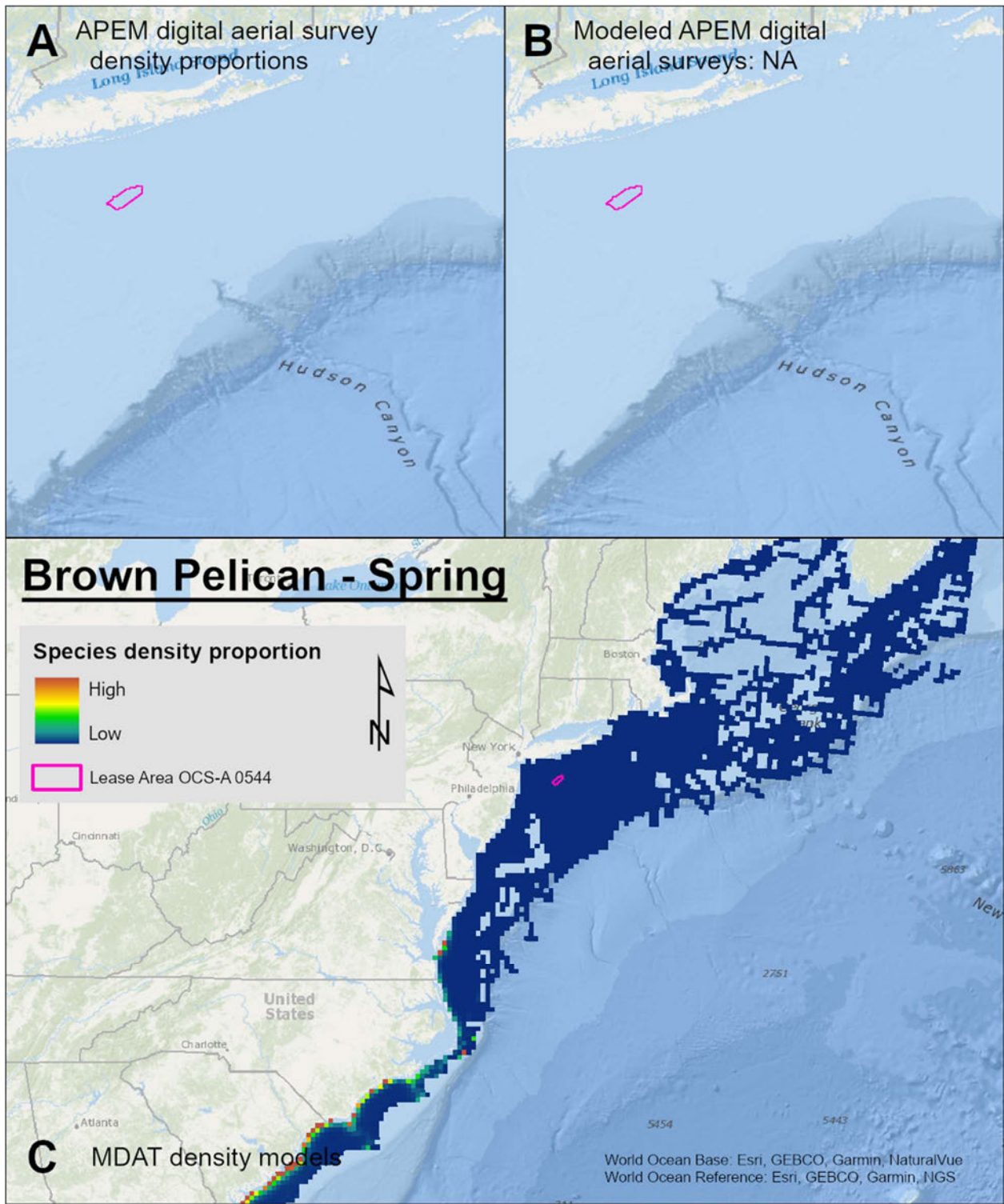
Map 196. Summer Double-crested Cormorant density proportions in the NYSERDA APEM and Empire Wind high resolution digital aerial survey data (A), the NYSERDA APEM and Empire Wind high resolution digital aerial model outputs for cormorants in Summer (B) and, Summer Double-crested Cormorant MDAT modeled abundance at the regional scale (C). The scale for all maps is representative of relative spatial variation in the sites within the season for each map input.



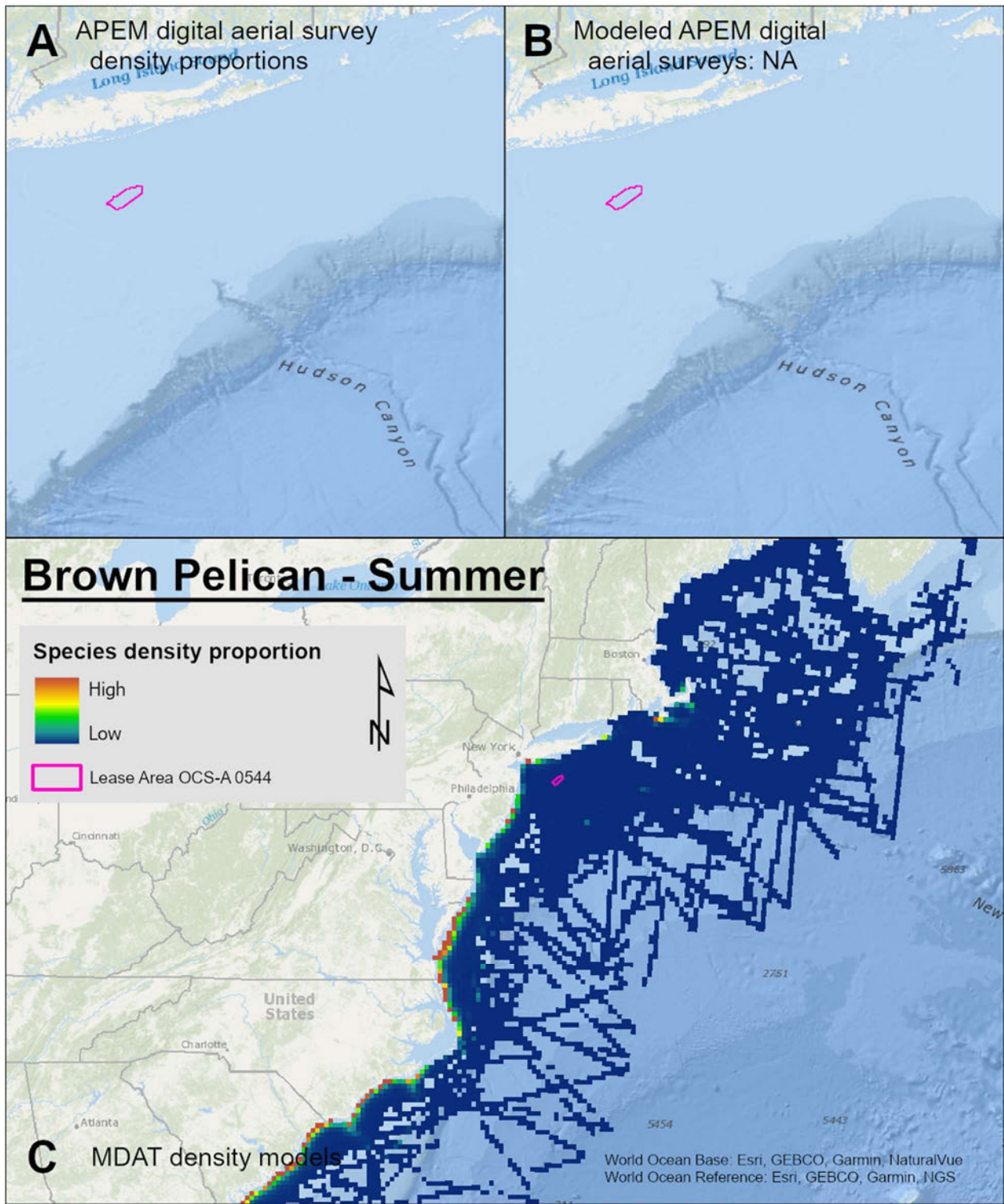
Map 197. Fall Double-crested Cormorant density proportions in the NYSERDA APEM and Empire Wind high resolution digital aerial survey data (A), the NYSERDA APEM and Empire Wind high resolution digital aerial model outputs for cormorants in Fall (B) and, Fall Double-crested Cormorant MDAT modeled abundance at the regional scale (C). The scale for all maps is representative of relative spatial variation in the sites within the season for each map input.



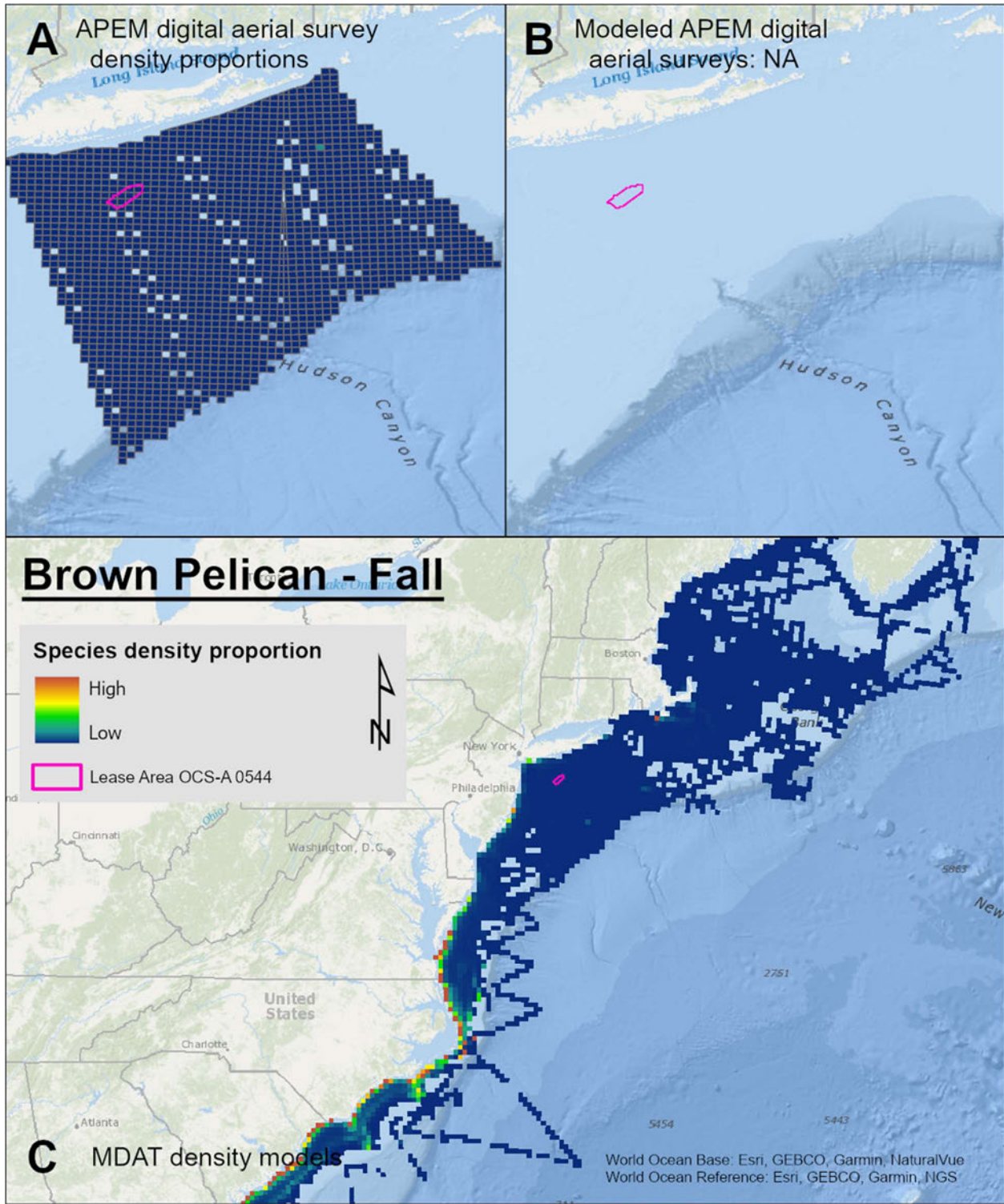
Map 198. Winter Brown Pelican density proportions in the NYSERDA APEM and Empire Wind high resolution digital aerial survey data (A), the NYSERDA APEM and Empire Wind high resolution digital aerial model outputs for pelicans in Winter (B) and, Winter Brown Pelican MDAT modeled abundance at the regional scale (C). The scale for all maps is representative of relative spatial variation in the sites within the season for each map input.



Map 199. Spring Brown Pelican density proportions in the NYSERDA APEM and Empire Wind high resolution digital aerial survey data (A), the NYSERDA APEM and Empire Wind high resolution digital aerial model outputs for pelicans in Spring (B) and, Spring Brown Pelican MDAT modeled abundance at the regional scale (C). The scale for all maps is representative of relative spatial variation in the sites within the season for each map input.



Map 200. Summer Brown Pelican density proportions in the NYSERDA APEM and Empire Wind high resolution digital aerial survey data (A), the NYSERDA APEM and Empire Wind high resolution digital aerial model outputs for pelicans in Summer (B) and, Summer Brown Pelican MDAT modeled abundance at the regional scale (C). The scale for all maps is representative of relative spatial variation in the sites within the season for each map input.



Map 201. Fall Brown Pelican density proportions in the NYSERDA APEM and Empire Wind high resolution digital aerial survey data (A), the NYSERDA APEM and Empire Wind high resolution digital aerial model outputs for pelicans in Fall (B) and, Fall Brown Pelican MDAT modeled abundance at the regional scale (C). The scale for all maps is representative of relative spatial variation in the sites within the season for each map input.